

Holocene landscape changes of the Lezha region

**A contribution to the palaeogeographies of coastal Albania and
the geoarchaeology of ancient Lissos**

Dissertation

zur

Erlangung des Doktorgrades

der Naturwissenschaften

(Dr. rer. nat.)

**dem Fachbereich Geographie
der Philipps-Universität Marburg**

vorgelegt von

Levent Uncu

aus Samsun, Türkei

Marburg/Lahn 2011

Acknowledgements

I am very grateful to have been given the chance to be one of the first researchers to conduct geoarchaeological studies in Albania – a country which had been closed to foreigners for the second half of the 20th century. My thesis supervisor Prof. Dr. Helmut Brückner (University of Cologne) played a vital role in getting me involved with the interdisciplinary archaeological project “Lissos. Urbanistik und sozio-ökonomische Strukturen einer hellenistischen Polis in Illyrien”. Not only was he leading the geoarchaeology team during fieldwork in 2006 and 2007, he also organised most of the funds for this research, such as salary, laboratory analyses and, ¹⁴C datings. Over all the past years he was a permanent source of encouragement and support for me. I am extremely grateful to him for having provided me with the opportunity to write a doctoral dissertation on this previously rather unexplored terrain in the heart of Europe.

The project is headed by Prof. Dr. Ortwin Dally and Dr. Andreas Oettel from the German Archaeological Institute (DAI), and partly funded by the German Research Foundation (DFG). I thank the DFG and the DAI Berlin for institutional and financial support, especially during fieldwork.

Dr. Andreas Oettel from the DAI Berlin gave me invaluable advice in the field. Dr. Bashkim Lahi, and Dr. Gëzim Hoxha from the Albanian Archaeological Institute in Tirana have also provided me with useful information, especially by dating pieces of ceramics which were found in our corings.

Important, detailed topographical and geological maps were given to me by Dr. Kujtim Onuzi (Institute of Geosciences, Tirana), and tectonic maps as well as associated Albanian publications came from Prof. Dr. Shyqyri Aliaj (Institute of Seismology, Tirana).

Further thanks go to Dipl.-Ing. Ursula Rübens, Technische Fachhochschule Berlin, who carried out all of the GPS measurements and always had some heartening words to say.

Dr. Mathias Handl (Marburg) examined my microfossil samples and was happy to share his knowledge and expertise with me. The encouragement from him and his family was invaluable throughout my studies. Dr. Peter Frenzel (University of Jena) kindly examined some samples from the 2008 field campaign. Palynological analyses were carried out by Dr. Maria Knipping from the University of Hohenheim.

Dr. Walter W. Jungmann as well as Mrs. Marita Budde and Mrs. Christa Günther (University of Marburg) helped me with advice and assistance in the laboratory.

Cartographers Dipl.-Ing. Christiane Enderle, Dipl.-Ing. Cordula Mann, Mr. Helge Nödler and Mrs. Gabriele Ziehr (University of Marburg) solved many a problem for me during the graphic implementation of my results and interpretations.

Dr. Manuel Fiedler and Gregor Döhner, M.A. (University of Berlin) worked on the chronological classification of ceramics during the field campaign 2007.

Very special credit must go to Anton Çuni from Lezha, who has always been a reliable and hard-working member of our team during all three field campaigns.

Katrin Boldt, Ann-Florin Grothe, Philip Ohrndorf, Mareike Rösingh, Friederike Stock (Geography students from the University of Marburg) and Klajdi Mato (Archaeology student from the University of Tirana) also assisted me in the field. Ann-Florin Grothe compiled her diploma thesis (Diplomarbeit) on the evolution of the Drini Delta.

Dipl.-Geogr. Dominik Brill (University of Marburg) was always at hand whenever the various computer programmes got the better of me. Dr. Nicole Klasen (formerly University of Marburg, now University of Cologne) provided useful advice especially at the beginning of my write-up. Prof. Dr. John C. Kraft (University of Delaware at Newark, USA) also discussed various aspects with me, and I am grateful for his insights and advice.

Kirstin Jacobson (University of Marburg) deserves a very special notice, because she patiently reviewed all of my chapters (several times) and she was always happy to discuss and advise me particularly in terms of the structure of my thesis.

Last, but by no means least, I thank my family and my partner who have always given me so much support and believed in my ability to complete this venture. I just wish my late father could have witnessed my success. He sadly passed away after the first field campaign had finished.

I offer sincere apologies in case some people who provided me with help and advice over the last few years find their names unmentioned in the above list.

Contents

Acknowledgements	ii
List of figures	x
List of photos	xiii
List of tables	xiv
1 Introduction	1
1.1 Research aims and objectives	1
1.2 Research logistics	2
2 Geographical setting of the research area	5
2.1 Location of the research area	5
2.2 Geology and tectonic setting	7
2.2.1 Tectonic setting of Albania	7
2.2.2 Geology and tectonic setting of the research area	9
2.2.2.1 <i>Jurassic ophiolitic complex</i>	10
2.2.2.2 <i>Cretaceous limestone and Cretaceous-Eocene flysch</i>	11
2.2.2.3 <i>Quaternary deposits</i>	14
2.2.3 Seismic history	16
2.3 Geomorphology	17
2.3.1 General geomorphological features of Albania	18
2.3.2 Mountains and hills around Lezha	19
2.3.3 Alluvial plains around Lezha	21
2.3.3.1 <i>Zadrime plain</i>	22
2.3.3.2 <i>Ballëdreni plain</i>	22
2.3.3.3 <i>Merqia plain</i>	23
2.3.3.4 <i>The Drini delta</i>	23
2.4 Climate	26
2.4.1 General climate pattern of Albania	27
2.4.2 Climate around Lezha	28
2.5 Hydrology	30
2.5.1 The river Drini	31
2.5.2 Lagoons in the Drini delta	34

2.5.3	Lake Kënalles	35
2.6	Pedology	36
2.7	Vegetation	38
2.7.1	General vegetation of Albania	38
2.7.2	Vegetation of the research area	39
2.7.2.1	<i>Vegetation of the highlands around Lezha</i>	40
2.7.2.2	<i>Vegetation of the coastal area</i>	40
2.7.2.3	<i>Vegetation of the Drini delta plain</i>	41
3	History of vegetation	45
3.1	Applicability of early research	45
3.2	History of vegetation in connection with climatic changes	46
3.3	Human impact on the vegetation	48
4	Historical background of Lezha and its environs	53
4.1	From the early beginnings to the end of antiquity	53
4.2	From Byzantine to modern times	56
5	History of geoarchaeological research	59
5.1	Research around the Mediterranean Sea	59
5.1.1	Research in the Western Mediterranean	59
5.1.2	Research in the Central Mediterranean	60
5.1.3	Research in the Eastern Mediterranean	61
5.2	Geoarchaeological research around the Adriatic Sea	65
5.3	Palaeoenvironmental and geoarchaeological research in Albania	69
5.4	Previous geographical and archaeological research around Lezha	72
6	Research design and methodology	76
6.1	Theoretical concepts on depositional environments	78
6.2	Field work	79
6.3	Laboratory work	80
6.3.1	Geochemical analyses	81
6.3.1.1	<i>pH value</i>	81

6.3.1.2	<i>Electric conductivity</i>	81
6.3.1.3	<i>Loss-on-ignition (LOI)</i>	82
6.3.1.4	<i>Carbonate content</i>	83
6.3.1.5	<i>Phosphate concentration</i>	84
6.3.1.6	<i>Atomic Absorption Spectrometry (AAS) measurements</i>	84
6.3.2	Dating methods	85
6.3.2.1	<i>Radiocarbon (¹⁴C-AMS) dating</i>	85
6.3.2.2	<i>Archaeological dating</i>	87
6.3.3	Palaeoecological analyses	87
6.3.3.1	<i>Macro- and microfossil examinations</i>	87
6.3.3.2	<i>Palynological analyses</i>	88
6.4	Literary Sources	88
6.5	Cartographic information	89
6.6	Satellite images	90
6.7	Graphic implementation	90
7	Results and discussion	91
7.1	Corings from the Balldreni plain	92
7.1.1	Transect A-A'	92
7.1.1.1	<i>Vibracoring LIS 39</i>	92
7.1.1.2	<i>Vibracoring LIS 26</i>	93
7.1.1.3	<i>Vibracoring LIS 40</i>	95
7.1.1.4	<i>Synopsis of transect A-A'</i>	96
7.2	Corings in the Merqia plain	98
7.2.1	Transect B-B'	98
7.2.1.1	<i>Vibracoring LIS 27</i>	98
7.2.1.2	<i>Vibracoring LIS 47</i>	101
7.2.1.3	<i>Vibracoring LIS 42</i>	103
7.2.1.4	<i>Vibracoring LIS 24</i>	104
7.2.1.5	<i>Vibracoring LIS 23</i>	105
7.2.1.6	<i>Synopsis of transect B-B'</i>	107

7.2.2 Transect C-C'	109
7.2.1.1 <i>Vibracoring LIS 48</i>	109
7.2.1.2 <i>Vibracoring LIS 52</i>	110
7.2.1.3 <i>Vibracoring LIS 25</i>	111
7.2.2.4 <i>Synopsis of transect C-C'</i>	114
7.3 Transects through the archaeological area	116
7.3.1 Transect D-D'	116
7.3.1.1 <i>Vibracoring LIS 04</i>	117
7.3.1.2 <i>Vibracoring LIS 06</i>	119
7.3.1.3 <i>Vibracoring LIS 07</i>	119
7.3.1.4 <i>Synopsis of transect D-D'</i>	120
7.3.2 Transect E-E'	121
7.3.2.1 <i>Vibracoring LIS 37</i>	122
7.3.2.2 <i>Vibracoring LIS 28</i>	123
7.3.2.3.1 <i>Vibracoring LIS 29</i>	126
7.3.2.3.2 <i>Vibracoring LIS 35</i>	129
7.3.2.4 <i>Synopsis of transect E-E'</i>	132
7.3.3 Corings around the Skanderbeg Monument	135
7.3.3.1 <i>Vibracoring LIS 03</i>	136
7.3.3.2 <i>Vibracoring LIS 05</i>	137
7.3.3.3 <i>Vibracoring LIS 02</i>	139
7.3.3.4 <i>Vibracoring LIS 38</i>	140
7.3.3.5 <i>Synopsis of the corings around the Skanderbeg Monument</i>	143
7.4 Transects across the Drini delta plain	145
7.4.1 Transect F-F'	145
7.4.1.1 <i>Vibracoring LIS 11</i>	145
7.4.1.2 <i>Vibracoring LIS 53</i>	148
7.4.1.3 <i>Vibracoring LIS 43</i>	149
7.4.1.4 <i>Vibracoring LIS 14</i>	150
7.4.1.5 <i>Vibracoring LIS 15</i>	152
7.4.1.6 <i>Vibracoring LIS 01</i>	153
7.4.1.7 <i>Synopsis of transect F-F'</i>	154

7.4.2 Corings around the Manatia alluvial fan	156
7.4.2.1 <i>Vibracoring LIS 34</i>	156
7.4.2.2 <i>Vibracoring LIS 51</i>	157
7.4.2.3 <i>Synopsis of corings LIS 51 and LIS 34</i>	159
7.4.3 Coring in the Lezha swamp	160
7.4.3.1 <i>Vibracoring LIS 09</i>	161
7.4.3.2 <i>Interpretation of coring LIS 09</i>	164
7.4.4 Transect G-G'	164
7.4.4.1 <i>Vibracoring LIS 17</i>	165
7.4.4.2 <i>Vibracoring LIS 19</i>	167
7.4.4.3 <i>Vibracoring LIS 18</i>	168
7.4.4.4 <i>Vibracoring LIS 45</i>	169
7.4.4.5 <i>Synopsis of transect G-G'</i>	170
7.4.5 Transect H-H'	172
7.4.5.1 <i>Vibracoring LIS 08</i>	172
7.4.5.2 <i>Vibracoring LIS 16</i>	174
7.4.5.3 <i>Vibracoring LIS 12</i>	175
7.4.5.4 <i>Vibracoring LIS 13</i>	177
7.4.5.5 <i>Synopsis of transect H-H'</i>	178
7.4.6 Transect I-I'	180
7.4.6.1 <i>Vibracoring LIS 30</i>	180
7.4.6.2 <i>Vibracoring LIS 46</i>	182
7.4.6.3 <i>Vibracoring LIS 08</i>	184
7.4.6.4 <i>Synopsis of transect I-I'</i>	184
7.4.7 Transect J-J'	185
7.4.7.1 <i>Vibracoring LIS 31</i>	186
7.4.7.2 <i>Vibracoring LIS 41</i>	187
7.4.7.3 <i>Vibracoring LIS 50</i>	188
7.4.7.4 <i>Synopsis of transect J-J'</i>	191
7.5 Palynological results	192
8 Palaeogeographic scenarios	196
8.1 The Holocene transgression maximum	197
8.2 4 th millennium BC (Middle Neolithic)	199
8.3 3 rd millennium BC (Late Neolithic – Chalcolithic period)	200

8.4 2 nd millennium BC (Bronze Age)	201
8.5 6 th century BC (Late Iron Age)	202
8.6 4 th century BC (Hellenistic period)	203
8.7 Around 200 AD (Roman Imperial times)	205
8.8 Discussion of harbour situation in Hellenistic to Roman times	206
8.8.1 Written sources and historical accounts	207
8.8.2 Geoarchaeological evidence	208
8.9 10 th century AD (Early Medieval times)	209
8.10 Ca. 1500 AD (Late Medieval times)	211
8.11 From 1500 AD to present	213
9 Sea level changes	219
9.1 Indicators of sea level change	219
9.2 Adriatic Sea level changes during the Holocene	222
9.3 A relative sea level curve for northern Albania	223
10 Summary	228
11 Zusammenfassung	232
12 References	236
13 Appendices	263
Appendix 1 Terminology	263
Appendix 2 Selected ISO and DIN norms	267
Appendix 3 Radiocarbon age estimates	268
Appendix 4 Macro- and microfossils as indicators of specific environmental conditions	270
Appendix 5 Geological profiles, photos and geochemical results of vibracorings	273
Appendix 6 Key to the coring profiles	329
Appendix 7 List of abbreviations	330

List of figures

- Figure 1: Location of Lezha, Albania (adapted from Mountain High Maps® Copyright © 1993, Digital Wisdom, Inc. and www.Albania.embassyhomepage.com/Albania-map.gif).
- Figure 2: Satellite image of north Albania. The research area is marked by the red box (adapted from Google Earth, access 22-12-2009).
- Figure 3: Tectonic setting of the eastern Mediterranean. Topography: Mountain High Maps® Copyright © 1993 Digital Wisdom, Inc. (slightly changed from Brückner et al., 2010, p. 162, fig. 1).
- Figure 4: Tectonic zones of Albania (Uncu 2010, based on Meço & Aliaj, 2000, fig. 4, p. 11).
- Figure 5: Southern convergent margin of the Eurasian Plate: Adriatic collision and Aegean Arc. Segments of Adriatic collision frontal thrust are noted by capital letters as follows: LU-Lezha-Ulqini, FD-Frakulla-Durresi, KS-Karaburuni-Sazani Island, LC-Lefkas-Corfu. Strike-slip faults: 1) the Gjiri i Drinit-Lezha, 2) the northern Sazani Island, 3) the Othoni Island-Dhermi, 4) Cephalonia transform fault (adapted from Aliaj, 2006, fig. 6, p. 142).
- Figure 6: Geological map of the research area (scale 1: 50,000, part of sheet: 26, Instituti Kerkimeve Gjeologjike, 2005).
- Figure 7a: Geological map with location of geological cross-sections on the delta between the Drini and Mati rivers (adapted from Fouache, 2006, fig. 54, p. 94).
- Figure 7b: Geological cross-sections of the Drini delta. For locations see fig. 7a (adapted from Fouache, 2006, fig. 55a, p. 96).
- Figure 7c: Geological cross-sections of the Drini delta. For locations see fig. 7a (adapted from Fouache, 2006, fig. 55b, p. 97).
- Figure 8: Satellite image of the research area with names of the most important places and topographic units (Google Earth, access 22-12-2009).
- Figure 9: Geomorphological map of the research area (Uncu 2010, based on Google Earth Satellite image, access 22-12-2009; topographical map of Albania, scale 1:25,000, Instituti Topografik i Ushtrisë, 1998).
- Figure 10: Beach ridges and meander belts in the Drini delta plain (slightly changed from Mathers et al., 1999, fig. 2, p. 347).
- Figure 11: Climate graph of Lezha (HMI Tirana, through pers. comm. with Mucaj, 2007).
- Figure 12: Windrose graph demonstrating prevalent wind directions at Lezha (f: frequency, s*2: mean speed) (HMI Tirana, through pers. comm. with Mucaj, 2007).
- Figure 13: Catchment area of the river Drini (excerpt taken from Diercke Weltatlas, 1994: 110).

- Figure 14: Soil map of Albania (slightly changed from Zdruli, 2005, p. 40).
- Figure 15: Vegetation zones of Albania (adapted from Markgraf, 1932, p. 91, fig. 20).
- Figure 16: Simplified pollen diagram for Sovjan, south Albania (Fouache et al., 2001, p. 82, fig. 4).
- Figure 17: Pollen diagram from the Seman Delta, Central Albania (Fouache et al., 2010, p. 126, fig. 11).
- Figure 18: Map of Lissos' surroundings (left) and first city plan of Lissos (right) (Praschniker & Schober, 1919, p. 15, fig. 22, and p. 27, fig. 39).
- Figure 19: Methods of geoarchaeology (Brückner & Gerlach, 2007, p. 59, fig. 7).
- Figure 20: Block diagram showing the typical sediment facies of a bird foot delta (Coleman, 1976 in Wright, 1985, p. 58, fig. 1-33).
- Figure 21: Location of coring sites and their arrangement in transects (Uncu 2010, based on a satellite image from Google Earth, accessed 22-12-2009).
- Figure 22: Synoptic chart of coring LIS 26.
- Figure 23: Geological transect A-A' (own research).
- Figure 24: Synoptic chart of coring LIS 27.
- Figure 25: Synoptic chart of coring LIS 47.
- Figure 26: Geological transect B-B' (own research).
- Figure 27: Synoptic chart of coring LIS 25.
- Figure 28: Geological transect C-C' (own research).
- Figure 29: Location of coring sites within the archaeological area (adapted from Rübens, 2009, unpublished).
- Figure 30: Synoptic chart of coring LIS 04.
- Figure 31: Geological transect D-D' (own research).
- Figure 32: Synoptic chart of coring LIS 37.
- Figure 33: Synoptic chart of coring LIS 28.
- Figure 34: Synoptic chart of coring LIS 29.
- Figure 35: Synoptic chart of coring LIS 35.
- Figure 36: Geological transect E-E' (own research).
- Figure 37: Synoptic chart of coring LIS 03.
- Figure 38: Synoptic chart of coring LIS 05.
- Figure 39: Synoptic chart of coring LIS 02.
- Figure 40: Synoptic chart of coring LIS 38.
- Figure 41: Geological profiles of the corings around the Skanderbeg Monument (own research).
- Figure 42: Synoptic chart of coring LIS 11.

- Figure 43: Synoptic chart of coring LIS 14.
- Figure 44: Geological transect F-F' (own research).
- Figure 45: Synoptic chart of coring LIS 51.
- Figure 46: Geological profiles of corings LIS 51 and LIS 34 (own research).
- Figure 47: Synoptic chart of coring LIS 09.
- Figure 48: Synoptic chart of coring LIS 17.
- Figure 49: Geological transect G-G' (own research).
- Figure 50: Synoptic chart of coring LIS 08.
- Figure 51: Synoptic chart of coring LIS 12.
- Figure 52: Geological transect H-H' (own research).
- Figure 53: Synoptic chart of coring LIS 30.
- Figure 54: Geological transect I-I' (own research).
- Figure 55: Synoptic chart of coring LIS 50.
- Figure 56: Geological transect J-J' (own research).
- Figure 57: Palynological data obtained from corings LIS 08, LIS 11, LIS 14, LIS 17, and LIS 18 (Uncu, 2010).
- Figure 58: Central Mediterranean coastline assumed for 18000 BP and 9000 BP, respectively (slightly changed from Shackleton et al., 1984, p. 308, fig. 1 and p. 311, fig. 4).
- Figure 59: Palaeogeographic scenario for the research area during the Holocene transgression maximum (Uncu, 2010, based on a satellite image from Google Earth, accessed 22-12-2009).
- Figure 60: Palaeogeographic scenario for the research area during the 4th millennium BC (Middle Neolithic) (Uncu, 2010, based on a satellite image from Google Earth, accessed 22-12-2009).
- Figure 61: Palaeogeographic scenario for the research area during the end of the 3rd millennium BC (Uncu, 2010, based on a satellite image from Google Earth, accessed 22-12-2009).
- Figure 62: Palaeogeographic scenario for the research area during the 6th century BC (Late Iron Age) (Uncu, 2010, based on a satellite image from Google Earth, accessed 22-12-2009).
- Figure 63: Palaeogeographic scenario for the research area during the 4th century BC Hellenistic period (Uncu, 2010, based on a satellite image from Google Earth, accessed 22-12-2009).
- Figure 64: Palaeogeographic scenario for the research area around 200 AD (Roman Imperial times) (Uncu, 2010, based on a satellite image from Google Earth, accessed 22-12-2009).
- Figure 65: Palaeogeographic scenario for the research area during the 10th century AD (Early Medieval times) (Uncu, 2010, based on a satellite image from Google Earth, accessed 22-12-2009).

- Figure 66: Palaeogeographic scenario for the research area during around 1500 AD (Late Medieval times (Uncu, 2010, based on a satellite image from Google Earth, accessed 22-12-2009).
- Figure 67: Old maps from north Albania showing the shifting river courses of the Drini [top left: map by Jode (1593) in Nopcsa 1929b, p. 665, fig. 166; top right: map by Sanson (1667) in Nopcsa, 1929b, p. 666, fig. 167; bottom left: map by Hahn & Kiepert (1867) in Nopcsa 1929b, p. 692, fig. 187; bottom right: Übersichtskarte von Mitteleuropa (1914) in Nopcsa 1929b, p. 696, fig. 189].
- Figure 68: Palaeogeographic reconstructions of sea level positions for the central Mediterranean region for the time slices 8, 6, 4 and 2 kyr BP. The red (negative) and yellow (zero and positive) contours refer to the sea level change. The ice-volume equivalent sea level (esl) values are given in metres (Lambeck et al., 2004b, p. 1593, fig. 12).
- Figure 69: Local sea level curves for the Eastern Mediterranean (Vött & Brückner, 2006, p. 15, fig. 4).
- Figure 70: Sea level curve for northern Albania. The envelope curve is based on age boxes of ¹⁴C-dated samples. Their vertical extension reflects the uncertainties of the reconstruction of sea level from the dated sample, the horizontal extension is the 1 sigma standard deviation of the ¹⁴C age estimate (own research).

List of photos

- Photo 1: View from Mali Shelbuemit over parts of the modern town of Lezha. The plateau on the right hand side is the Acropolis of Lissos (Lezha Hill). The river Drini runs across the centre of the photo from right to left. In the background on the right hand side, the town of Shengjin with its harbour can be seen situated at the small embayment. (Photo: Oettel, 2006)
- Photo 2: View from the Drini towards Lezha Hill (in the middleground, left) and Mali Shelbuemit (in the background, right). (Photo: Brückner 2007)
- Photo 3: View from the Acropolis over the Merqia plain, immediately north of Lezha. The Balldreni plain lies between the two limestone ridges Mali Rrenci (left) and Mali Kakarriqi (right). (Photo: Brückner, 2007)
- Photo 4: Military bunkers, built originally much further inland during the early 1970s, are being destroyed by the waves. (Photo: Uncu, 2007)
- Photo 5: The Drini splits into two branches at Vau Dejes (view from Rozafa Castle). It flows from the left hand side towards Lezha (central background) and as the Drinassa towards Shkodra (right foreground). (Photo: Uncu 2007)
- Photo 6: Flood event from January 1963, inundating the town of Lezha. (Photo: Pulaha & Parruca, 2006, p. 131)
- Photo 7: Lake Kënalles near Shengjin (left middle ground). View from Mali Rrenci towards the south. Also visible are the Merxhani lagoon and the Shengjin sand spit separating it from the Adriatic Sea (far right). (Photo: Oettel, 2006)
- Photo 8: Coastal erosion threatening the forests on the Shengjin sand-spit. (Photo: Uncu, 2006)
- Photo 9: Skanderbeg Monument in the archaeological ‘park’ area. (Photo: Uncu, 2007)
- Photo 10: Drilling with vibration corer Cobra mk1 in a pleasant location (Balldreni plain, LIS 26). (Photo: Brückner, 2007)
- Photo 11: Coring LIS 26. (Uncu, 2007)
- Photo 12: Coring LIS 27. (Uncu, 2007)
- Photo 13: Coring LIS 47. (Uncu, 2008)
- Photo 14: Coring LIS 25. (Uncu, 2007)
- Photo 15: Coring LIS 04. (Uncu, 2006)
- Photo 16: Coring LIS 37. (Uncu, 2007)
- Photo 17: Coring LIS 28. (Uncu, 2007)
- Photo 18: Coring LIS 29. (Uncu, 2007)
- Photo 19: Coring LIS 35. (Uncu, 2007)
- Photo 20: Coring LIS 03. (Uncu, 2006)

- Photo 21: Coring LIS 05. (Uncu, 2006)
- Photo 22: Coring LIS 02. (Uncu, 2006)
- Photo 23: Coring LIS 38. (Uncu, 2008)
- Photo 24: Coring LIS 11. (Uncu, 2006)
- Photo 25: Coring LIS 14. (Uncu, 2006)
- Photo 26: Coring LIS 51. (Uncu, 2008)
- Photo 27: Coring LIS 09. (Uncu, 2006)
- Photo 28: Coring LIS 17. (Uncu, 2006)
- Photo 29: Coring LIS 08. (Uncu, 2006)
- Photo 30: Coring LIS 12. (Uncu, 2006)
- Photo 31: Coring LIS 30. (Uncu, 2007)
- Photo 32: Coring LIS 50. (Uncu, 2008)

List of tables

- Table 1: Climate data for Lezha (temperature 1951-1990, precipitation 1951-2006). (compiled by L. Uncu, based on Mucaj, pers. comm. in 2007)
- Table 2: Annual distribution of the Drini's discharge (in m³/s). (Pano & Avdyli, 2009: 69, table 2)
- Table 3: Species composition for vegetation above 200 m altitude. (slightly changed, after Demiraj et al., 1996: 161)
- Table 4: Species composition of the coastal lowlands (up to 200 m). (slightly changed, after Demiraj et al., 1996: 161)
- Table 5: Overview of historical and archaeological periods in Albania. (L. Uncu, 2010, compiled from: Korkuti, 1983; 1988; Eggebrecht, 1988; Koch, 1989; Korkuti & Petruso, 1993; Jacques, 1995; Wilkes, 1995; Hutchings, 1996; Ceka, 2005)
- Table 6: Ancient sources with references to Lissos.
- Table 7: Macro- and microfossils found in coring LIS 09.
- Table 8: Chronology of events for cross section E-E'.
- Table 9: Lezha and its surroundings as it appears on historical maps (L. Uncu, 2010, adapted from Nopcsa, 1916, 1929b).
- Table 10: ¹⁴C age estimates used for the construction of the sea level curve in fig. 70. Institute of Physics (Physikalisches Institut) at Erlangen, University of Erlangen-Nürnberg, Germany, and the Centre of Applied Isotope Studies (CAIS), University of Georgia, Athens, USA.

1 Introduction

The coasts of Western Turkey, Greece, Italy and even Croatia have been subject to a huge variety of scientific investigations. Particularly the number of palaeogeographical and geoarchaeological projects in those countries has increased significantly over the last few decades.

Albania, however, is still a *terra incognita* for scientists in many respects, although scientific investigations already started in the middle of the 19th century. During the following one hundred or so years, several scholars visited the country and published geographic, geologic and archaeological articles or monographs (e.g., von Hahn, 1853; Evans, 1885-86; Ippen, 1907a; Praschniker & Schober, 1919; Louis, 1927; Nopcsa, 1929a).

The extreme politicisation of all aspects of life under the communist regime from 1946 to 1991 led to the isolation of Albania – first from Western Europe and later also from the rest of the world. If Albanians could carry out research at all, it was often done in collaboration with Russian scientists and the results were published in Albanian or Russian. Independent and non-political scientific research was lacking, as was the application of new technologies and advanced equipment.

Until the fall of the communist regime in 1991, Albania, together with a few African countries (e.g., Algeria, Libya), was the only country not integrated in any international scientific projects concerning the Mediterranean region. It was only then that Albania opened up to the international scientific community. In collaboration with foreign scientists and companies, the sometimes outdated Albanian geological reports and publications were re-evaluated and new research projects in different parts of the country were established.

In this context, Albania has also become an interesting area for the Earth Sciences over the last two decades. Accordingly, the number of English and French publications about Albania increased considerably since 1995 (e.g., Ciavola et al., 1999; Mathers et al., 1999; Fouache et al., 2000, 2001, 2010; for details see chapter 5.3).

From a geoarchaeological and palaeogeographic point of view, it is important to complete the picture for the evolution of the Albanian coasts throughout the Holocene and to generate data sets for comparison with other regions around the Adriatic Sea.

1.1 Research aims and objectives

The major aim of our interdisciplinary geoarchaeological and palaeogeographical research is the reconstruction of palaeo-landscapes in the Lezha region, Northern Albania, during the Holocene. The second focus is to establish the nature of man-environment interactions in the context of the ancient city of Lissos.

To achieve our overall aims, we have set the following specific research objectives:

- to determine how far the sea reached inland during the Holocene transgression maximum;
- to detect the spatial and temporal evolution of the Drini delta, with special regard to the shifts in the shoreline in prehistorical and historical times;
- to establish what effect human settlement and human activities had on the landscape, particularly in the context of the urban development of ancient Lissos;
- to find evidence for the changing harbour situation during Lissos' history;
- to construct a local relative sea level curve for Northern Albania.

1.2 Research logistics

The first German archaeological project in Albania: "*Lissos. Urbanistik und sozio-ökonomische Strukturen einer hellenistischen Polis in Illyrien*" (Lissos, urbanism and socio-economic structures of a Hellenistic polis in Illyria) began in 2006. It is part of a priority programme ('Schwerpunktprogramm' SPP 1209) called "*Die hellenistische Polis als Lebensform. Urbane Strukturen und bürgerliche Identität zwischen Tradition und Wandel*" (The Hellenistic polis as a living space – Urban structures and civic identity between tradition and innovation), funded by the German Research Foundation (DFG).

Dr. Andreas Oettel from the German Archaeological Institute (DAI Berlin) heads the archaeological project in collaboration with Dr. Gëzim Hoxha and Dr. Bashkim Lahi (both from the Albanian Institute of Archaeology in Tirana). It focuses on the urban and socio-economic development of Lissos, from the foundation of the city during the Hellenistic period until early Roman times (cf. www.dainst.de/index_772455eebb1f14a198290017f0000011_de.html).

In the recent past, Albanian archaeological projects, such as in Butrinti and Apollonia have benefited from an interdisciplinary approach, particularly the application of geo-scientific methodology. Therefore, we were asked to contribute to the success of the Lissos Project by using geoarchaeological techniques within the framework already set up by the archaeologists. After the invitation by the DAI, we started to gather information about Albania in general and the area around Lezha in particular. Due to the political isolation for 45 years, not many relevant papers, books or maps were available. Some of the scientific publications written in English, French or German are about a century old.

Throughout the first research campaign in 2006, the motto was: “Think on your feet.” A breakthrough came during a visit at the Geological Research Institute (Instituti Kerkimeve Gjeologjike) in Tirana, where a few good topographical [sheets: K-34-76-C-a (Shengjini), K-34-76-C-b (Lezha), K-34-76-C-c, K-34-76-C-d (scale 1: 25,000; published 1980) and sheets: 2978 I (Lezhë) and 2978 II (Krujë) (scale 1: 50,000; published 1998)] and geological [Harta Gjeologjike e Shqipërisë (scale: 1: 200,000; published 2002) and sheet: 26 (Lezha) (scale 1: 50,000; published 2005)] maps of the research area could be acquired. Those maps were essential in gaining a better understanding of the topographical and geological setting of the research area. Based on these maps, the planning and organisation of the field campaigns in subsequent years became much more accurate.

Field work in the Lezha region was carried out for three extended field seasons: 13 August – 10 September 2006, 14 August – 30 August 2007, and 19 July – 05 August 2008. During the first field season in 2006 the selection of our coring sites was very much led by the requests of the archaeologists who were looking for sites with great potential in terms of achieving the overall aims and objectives of their project. During the second and third campaigns, however, not just the spotting of suitable sites for coring presented us with problems, but the still unsettled political situation also created a sometimes uneasy atmosphere. The landownership was sometimes unclear; but whenever we found out who owned the land we asked for the permission to carry out our drillings. On one occasion (coring LIS 11), just at the beginning of our coring, we were suddenly confronted by a man holding a gun and commanding us to take our equipment and leave immediately. Fortunately enough, most people were just curiously inquiring what we were doing; sometimes we were even invited to drink Rakı with them (a sign of friendship). Our generally good relationship with the locals was mostly due to Anton Çuni, our excellent Albanian workman, who worked with us in each campaign and was invaluable when communicating with the local population.

For the duration of the field campaigns, we stayed at a house close to the centre of modern Lezha, together with the archaeologists, architects and geodesists. This house, hired by the DAI, is located directly next to a monument dedicated to the Albanian national hero: the Georg Kastrioti – Skanderbeg memorial place, erected in 1981 after the big earthquake of 1979.

In each of the campaigns I spent some time visiting the scientific and educational institutions in Tirana in order to collect more information and to establish some contacts with influential Albanian scientists, such as Prof. Dr. Shyqyri Aliaj (The Institute of Seismology in Tirana), Prof. Dr. Gjovalin Gruda (University of Tirana), and Prof. Dr. Salvatore Bushati (The Academy of Sciences of Albania). Thereby, I received tectonic/seismologic maps as well as relevant articles only published in Albanian journals and therefore unavailable elsewhere; I gathered information about the geomorphology of Albania in general and the recent developments of the coastline around the area of Lezha in particular. Modern climatic data was made available to me, courtesy Dr. Liri Muçaj from the Hydrometeorological Institute in Tirana.

The samples we took home at the end of each field campaign were analysed geo-physically and geo-chemically, primarily by myself, in the laboratories of the Faculty of Geography at the University of Marburg. Microfossil analysis took place in collaboration with Dr. Mathias Handl, Marburg, and Dr. Peter Frenzel, Friedrich-Schiller-Universität Jena. Material for AMS-¹⁴C dating was sent to the radiocarbon dating laboratories of the Institute of Physics at Erlangen (Physikalisches Institut der Universität Erlangen-Nürnberg), Germany, and the Centre of Applied Isotope Studies (CAIS), University of Georgia, Athens, USA.

2 Geographical setting of the research area

This chapter gives an overview of the geographical setting of the research area in terms of geology, geomorphology, climatology and hydrology as well as pedology and vegetation.

2.1 Location of the research area

Albania is a relatively small country in southeast Europe, bordering the Adriatic and Ionian Seas, respectively (fig. 1). The city of Lezha (Albanian: Lezhë) is situated in northwest Albania, on the Adriatic coast (41° 46' 55" N, 19° 38' 40" E). The city, the district and the county bear the same name. The district of Lezha (Albanian: Rrethi e Lezhës) is one of thirty-six districts of Albania; together with Kurbin and Mirdita it makes up the county of Lezha (Albanian: Qarku e Lezhës). The total area of the district of Lezha is 473 km² – a relatively small area.



Figure 1: Location of Lezha, Albania (adapted from Mountain High Maps® Copyright © 1993, Digital Wisdom, Inc. and www.Albania.embassyhomepage.com/Albania-map.gif).

The research area, encompassing the deltaic coastal plain of the Drini, is bordered by the Zadrimea plains in the north and the banks of the River Mati in the south. It reaches from the highlands of Shite-Veles Mountains in the northeast and Skanderbeg Mountain in the southeast to the Adriatic Sea in the west (fig. 2).

Being situated at the point where the river Drini passes the narrow gap between Mali Rrenci (Mount Rrenci) and Lezha Hill, which is also known as Kalaja or Acropolis of Lissos, and

enters what is now a broad coastal delta plain, Lezha (and its predecessors) has a geographically favourable position between Shkodra (45 km distance) and Tirana (70 km distance).

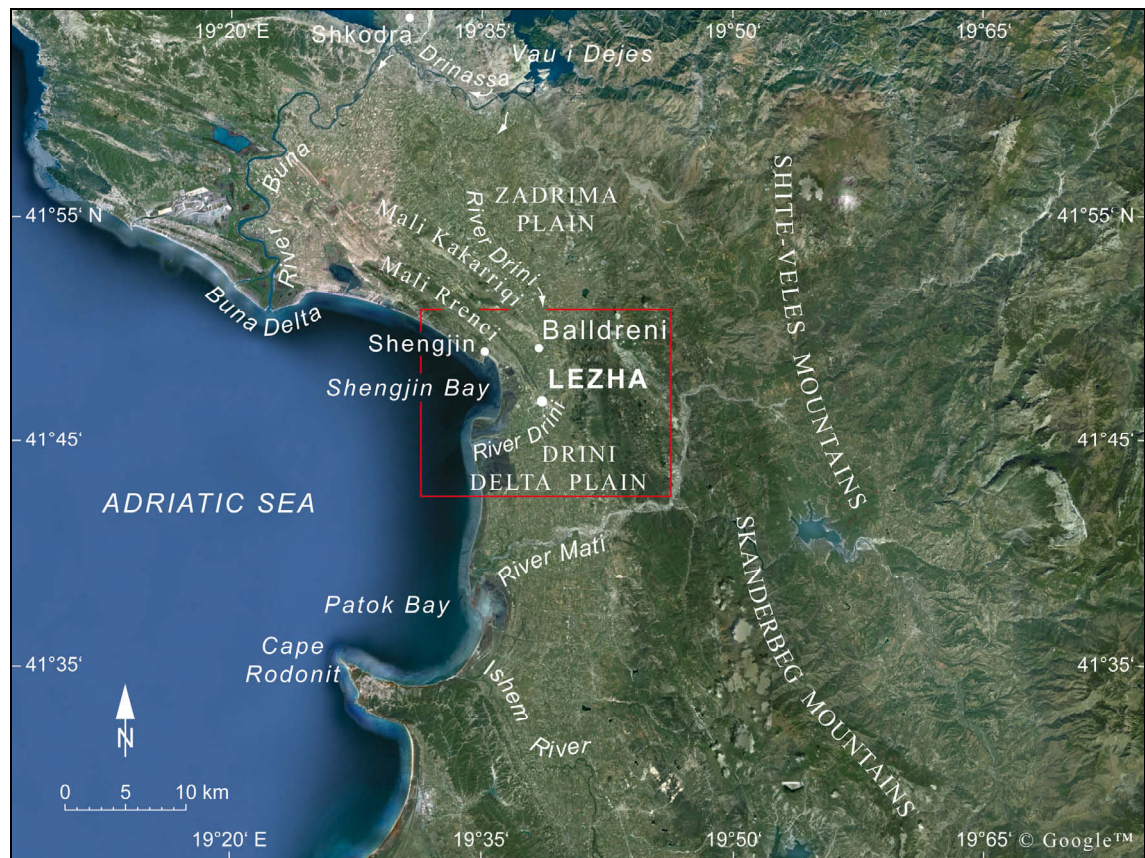


Figure 2: Satellite image of north Albania. The research area is marked by the red box (adapted from Google Earth, access 22-12-2009).

The advantages of this location can be traced back to antiquity, when the close proximity of the coastline was an added benefit. The city's harbour played a significant role in terms of military control, and important trade routes passed through this area, especially those to Shkodra and the Dalmatian seashore in the north and other regions in the south. It has also been, and still is a starting point for connecting the Adriatic Sea via Pristina (ancient Ulpiona), Nis (ancient Noissus) and the Central Balkan. The city's short connection to Shengjin, the second largest commercial and military harbour complex of Albania, located only 8 km northwest of Lezha, is still important.

The area around Lezha has been populated for more than 3,000 years, and a sizable settlement has existed there incessantly since the foundation of the city of Lissos approximately 2,400 years ago, which means that it has a long and complex settlement history. With its 25.623 inhabitants (Pulaha & Parruca, 2006), modern Lezha is one of the most important cities in northern Albania.



Photo 1: View from Mali Shelbuemit over parts of the modern town of Lezha. The plateau on the right hand side is the Acropolis of Lissos (Lezha Hill). The river Drini runs across the centre of the photo from right to left. In the background on the right hand side, the town of Shengjin with its harbour can be seen situated at the small embayment. (Photo: Oettel, 2006)

2.2 Geology and tectonic setting

After a brief summary of the general tectonic setting of Albania, the focus of this subchapter is on the geological structures and their evolution, as well as on the particular tectonic situation of the research area. An account of the seismic history is included.

2.2.1 Tectonic setting of Albania

The Albanian mountains are part of the Circum-Mediterranean Alpine orogenic belt, generally a result of the collision between the European and the African plates. Together with the Dinaric and Hellenic Mountains, they result from a continental collision between the northern segment of the southern convergent margin of the Eurasian plate and the Adriatic microplate (Anderson & Jackson, 1987: 939; Aliaj, 2006: 134). South of the Cephalonia transform fault, along the entire lineament, the continental collision changes to an active oceanic subduction of the Hellenic-Aegean Arc (Aliaj, 2006: 135) (fig. 3).

The Adriatic microplate itself is relatively stable. It includes non-seismic areas such as the Adriatic Sea floor as well as the marginal areas of the Po delta and Apulia platform. The

remaining boundary areas, however, are seismically very active (Cavazza et al., 2004; Aliaj, 2006).

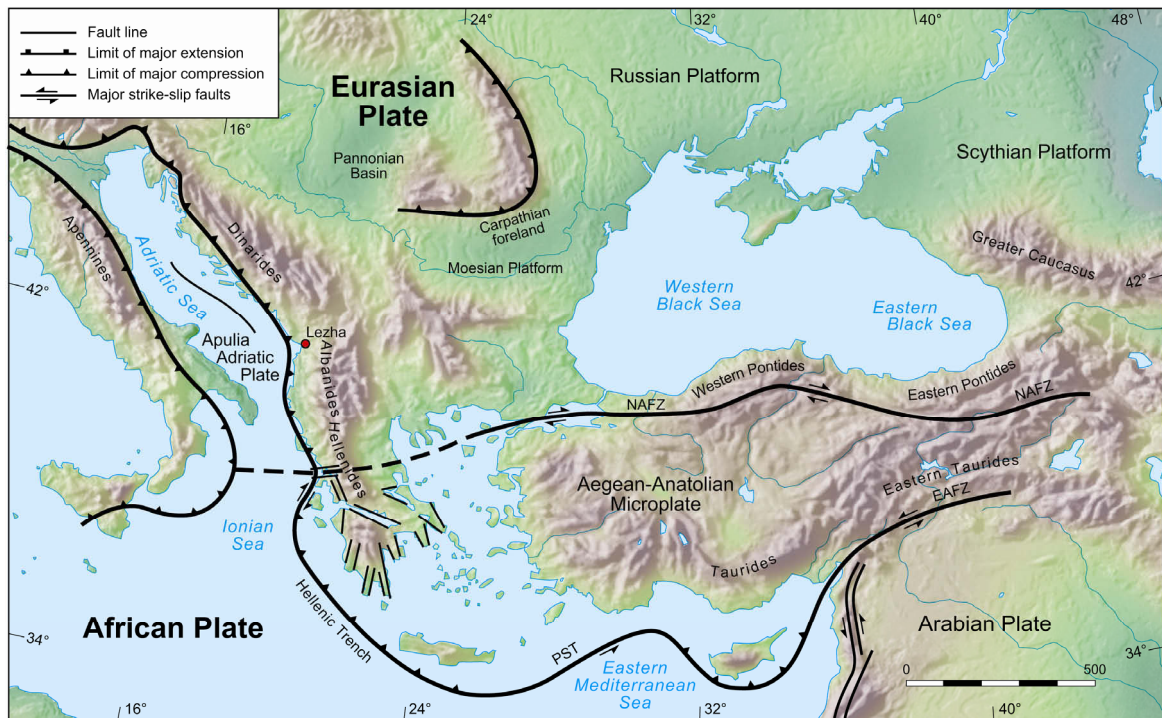


Figure 3: Tectonic setting of the eastern Mediterranean. Topography: Mountain High Maps® Copyright © 1993 Digital Wisdom, Inc. (slightly changed from Brückner et al., 2010, p. 162, fig. 1).

On the eastern edge of the Adriatic microplate, the Dinaric, Albanian and Hellenic mountains form a continuous orogenic belt, the so-called “Dinaro-Hellenic fold-and-thrust belt” (Meço & Aliaj, 2000; Cavazza et al., 2004; Muçeku et al., 2006). Structurally, the Albanian mountains occupy an important position within this fold-and-thrust belt. For this reason, the term “Albanides” is commonly used in the geological literature to describe the transition zone between the Dinarides in the north and the Hellenides in the south (fig. 3).

The northern limit of the Albanides is marked by the Shkodra-Peja lineament (or Scutari-Peč transversal tectonic structure) which extends in a SW-NE direction in North Albania (fig. 4). It has been interpreted as an important “transform fault zone” that influenced the regional tectonic evolution in the area during the entire Mesozoic and Early Tertiary (Robertson & Shallo, 2000; Meço & Aliaj, 2000). North of it, the mountain folds strike WNW-ESE and they belong to the southernmost part of the Dinarides (sensu lato) also called “Dinarides (sensu stricto)” (Aliaj, 2006: 133). South of the Shkodra-Peja lineament, the strike of the mountain folds changes to NNW-SSE where they gradually merge with the Hellenides throughout the Vlorë-Tepelana transverse flexure structure in southern Albania (Aliaj, 2006).

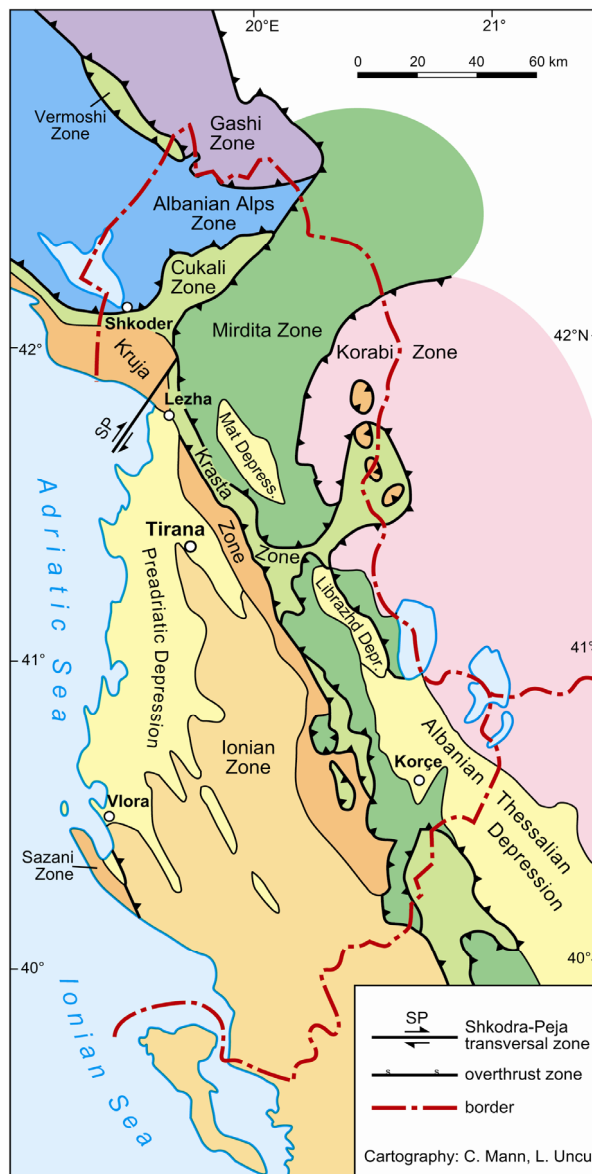


Figure 4: Tectonic zones of Albania (Uncu 2010, based on Meço & Aliaj, 2000, fig. 4, p. 11).

through Lezha divides the external units into two segments, namely the NW-trending Lezha-Ulqini and the roughly N-trending Frakulla-Durresi (fig. 5). This strike-slip fault is also responsible for the sharp change in direction of the coastline near Lezha.

In general, the research area can be divided into four main lithostratigraphic units of different age and composition: Jurassic ophiolitic series (serpentine, gabbro) with volcanic units (basalt and sedimentary rocks of volcanic origin), Cretaceous carbonate rocks, Cretaceous-Eocene flysch formations, and Quaternary deposits. These units strike almost parallel to each other, from NW to SE, because of the direction of the major tectonic lineaments of the region. They are also severely deformed and displaced by secondary faults and over-thrusts to the east of Lezha.

Structurally, the Albanides consist of the same fundamental components as the Dinaro-Hellenic orogenic belt: an external unit in the western part, ophiolitic thrust sheets in the central part and an internal complex in the eastern part (Robertson & Shallo, 2000; Muçeku et al., 2006: 539). Between the external units making up the outer margin of the Albanian orogeny, and the Adriatic off-shore, the Periadriatic foredeep basin has formed, which includes the hills and plains of western Albania (Aliaj, 2006) (fig. 4).

2.2.2 Geology and tectonic setting of the research area

The research area is situated on the border between the Periadriatic foredeep basin and the Albanian orogenic front (external units) (fig. 4), which is characterised by the occurrence of folds as well as reverse faults (including both thrusts and back-thrusts) (Aliaj, 2006: 140). The Gjiri i Drintit-Lezha strike slip fault which runs

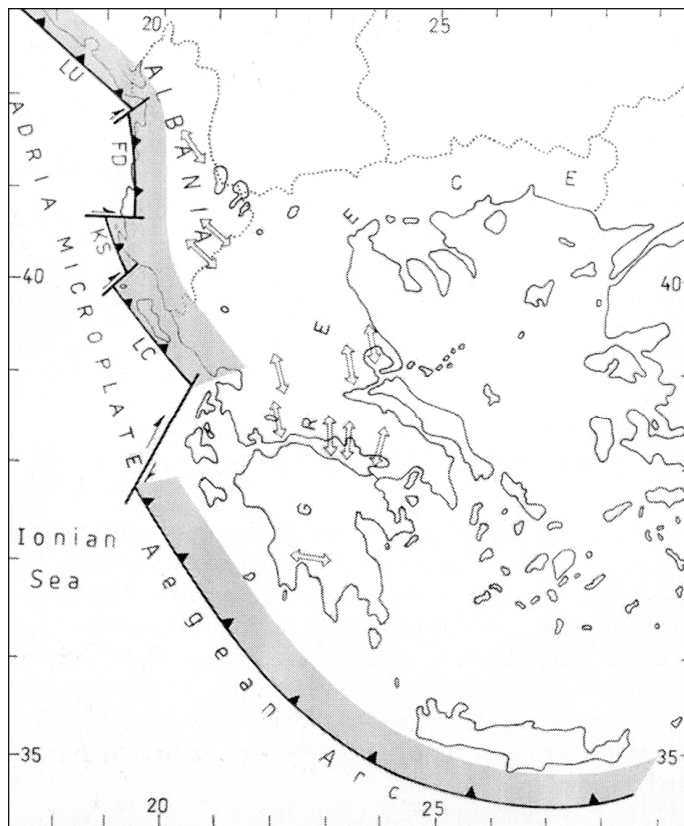


Figure 5: Southern convergent margin of the Eurasian Plate: Adriatic collision and Aegean Arc. Segments of Adriatic collision frontal thrust are noted by capital letters as follows: LU-Lezha-Ulqini, FD-Frakulla-Durresi, KS-Karaburuni-Sazani Island, LC-Lefkas-Corfu. Strike-slip faults: 1) the Gjiri i Drinit-Lezha, 2) the northern Sazani Island, 3) the Othoni Island-Dhermi, 4) Cephalonia transform fault (adapted from Aliaj, 2006, fig. 6, p. 142).

2.2.2.1 Jurassic ophiolitic complex

The ophiolitic series of the Mirdita zone occupies a large area between the External and Internal Albanides in Central Albania (fig. 4). However, some geologists argue that this series should be classified as part of the Internal Albanides (Meço & Aliaj, 2000; Nieuwland et al., 2001). Together with the ophiolites of the Dinarides-Hellenides mountain belt, the series of the Albanides make up the largest ophiolitic complex in Europe. The Mirdita zone overthrusts the Krasta zone in the west and the Cukali zone as well as the Albanian Alps zone in the north, and is itself overthrust by the Korabi zone in the east (Meço & Aliaj, 2000: 19) (fig. 4).

The Albanian ophiolites have formed within the Mirdita Ocean, the most northern part of the Mirdita-Pindos ocean which itself is the northward continuation of the Neotethys (Robertson & Shallo, 2000). The Mirdita-Pindos Ocean opened up between the Adriatic microplate and Pelagonian margin of the Eurasian plate (in the central part of the Dinaric-Hellenic orogenic system) during the Middle Triassic to Middle Jurassic (Robertson & Shallo, 2000; Beccaluva et al., 2005: 553; Muçeku et al., 2006: 542).

The lowermost part of the stratigraphical profile of the Mirdita zone is made up of Middle Triassic sedimentary rocks of volcanic origin. The next layer is an Upper Triassic to Early Jurassic limestone which exhibits a transition from pelagic to neritic conditions (Meço & Aliaj, 2000; Muçeku et al., 2006). After rifting had started in the Mirdita Ocean at the end of the Early Jurassic, the ophiolitic series formed in the slow spreading, rifted mid-ocean ridge setting during the Middle Jurassic (Shallo, 1992; Robertson & Shallo, 2000: 229; Gawlick et al., 2008: 867).

Following the intra-oceanic subduction of the Mirdita ocean towards the Late Jurassic, the ophiolitic series was covered by the regional deposition of radiolaritic-ophiolitic wildflysch (ophiolitic *mélange*) (Gawlick et al., 2008: 874). Finally, Late Jurassic shallow-water carbonate facies developed around the periphery. This shows that the Mirdita Ocean had remained partly open during the Late Jurassic; however, by the end of the Late Jurassic it had totally closed (Shallo, 1992: 682; Aliaj, 1997: 72; Schlagintweit et al., 2008: 125).

2.2.2.2 Cretaceous limestone and Cretaceous-Eocene flysch

Throughout the Cretaceous, the Mirdita zone became a shallow marine environment due to a period of marine transgressions (Aliaj, 1997). The sediments of that time make up the “External Albanides”, also known as “outer zone” of the Albanides. In the research area, they are represented by two subzones: the “Krasta-Cukali zone” and the “Kruja zone” which exhibit different lithologies (flysch and carbonate formations, respectively) and facies (pelagic and neritic, respectively), dating from the Cretaceous to the Oligocene (Meço & Aliaj, 2000).

The Krasta-Cukali zone extends belt-like between the Mirdita zone and the carbonate formation of the Kruja zone, along a narrow corridor from Central Albania to Montenegro (fig. 4). This zone consists of pelagic sediments which contain two main lithostratigraphic units (from bottom to top): Early to Late Cretaceous (Albian to Cenomanian) flysch, Late Cretaceous (Cenonian to Maastrichtian) limestones with *Globotruncana* fossils, and Late Cretaceous (Maastrichtian) to Eocene flysch (Meço & Aliaj, 2000: 18). The Cretaceous sediments of the Krasta-Cukali zone outcrop in a large area east of Lezha. The Eocene flysch formation occupies the region north of Lezha towards Shkodra, along the slopes of the Shite-Veles Mountains (fig. 6).

The Kruja zone makes up the orogenic front of the Albanides, and is situated between the Adriatic Collision zone and the Krasta-Cukali zone mentioned above. This zone also extends as a belt-like formation from southern Albania towards the coast of Montenegro (fig. 4). The Kruja zone embodies a neritic platform with two main units: a neritic carbonate formation (dolomite and dolomitised limestone) from the Late Cretaceous to the Middle Eocene, and a flysch formation from the Middle Eocene to the Oligocene (Meço & Aliaj, 2000; Aliaj, 2006).

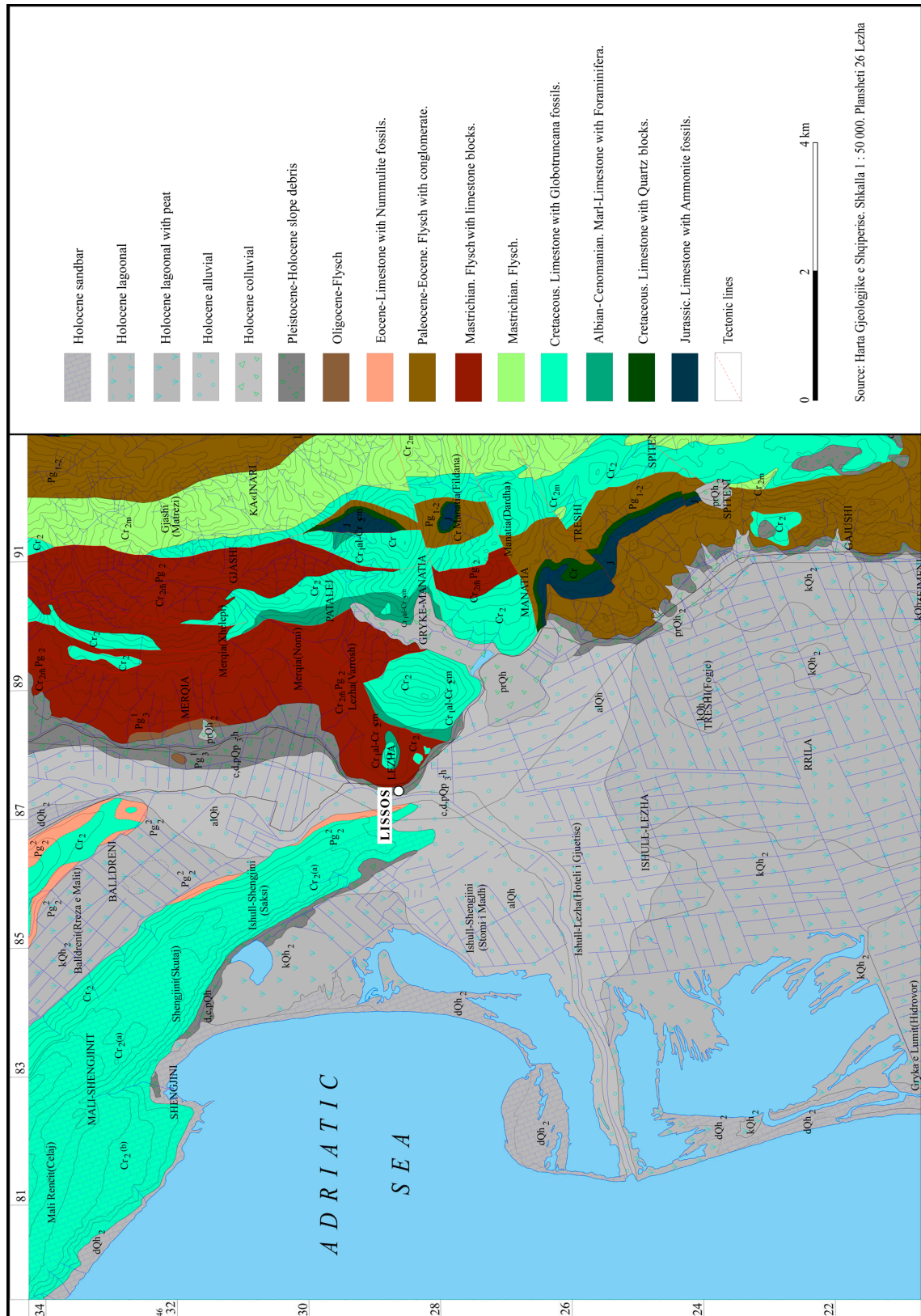


Figure 6: Geological map of the research area (scale 1: 50,000, part of sheet: 26, Instituti Kerkimeve Gjeologjike, 2005).

The sediments of the Kruja zone extend over a large area around Lezha (fig. 6). The Mali Shelbuemit (known also as Acrolissos) and the top of Lezha Hill (Kalaja with the Acropolis of Lissos) are made up of the dolomite and dolomitised limestone of the Kruja zone. The anticline

ridges of Mali Rrenci and Mali Kakarriqi northwest of Lezha are composed of Cretaceous limestone which is fringed by Eocene limestone with Nummulite fossils (Meço & Aliaj, 2000: 135). In the vicinity of Manatia south of Lezha, limestone formations occur belt-like and run from NW to SE. The Palaeocene to Eocene flysch formation of the Kruja zone outcrops at the slopes of Skanderbeg Mountain south of Manatia. A small outcrop of Oligocene flysch can be found in the slopes and a hill nearby Merqia, a town north of Lezha (fig. 6).

The Krasta basin was closed and folded at the end of the Eocene due to subduction of the Kruja platform beneath its frontal thrust (Aliaj, 1997). The folding phase of the Kruja zone coincides with the end of the Oligocene (Meço & Aliaj, 2000). As a result of these intensive tectonic deformations during the end of the Eocene and Oligocene, the ophiolitic series of the Mirdita zone and their sedimentary cover as well as the carbonate platform which had formed along the periphery were thrust and overthrust onto the zones further west, i.e. the Krasta-Cukali and the Kruja zones (Shallo, 1992: 682, Meço & Aliaj, 2000: 19).

Tectonic subsidence along the margins of the Albanian orogenic front associated with the main orogenic Alpine phases led to the formation of marine molassic basins during the Neogene. As a result of this process, a depression was formed in the west of the external structural zones, the so-called "Periadriatic foredeep basin" (Aliaj, 1997). It is regarded as a foredeep basin because of its location at the western (outer) margin of the Albanian orogeny between the Shkodra-Peja and the Vlora-Tepelana transverse structure zone (Aliaj, 2006: 140). Its seaward border extends offshore into the Adriatic Sea whereas the eastern margin developed on the folded structures of the Kruja zone (Shkupi & Aliaj, 1997: 362).

The Periadriatic basin began forming during the Middle Miocene (Serravallian) and was filled with molasse sediments from the Middle Miocene to the end of the Pliocene (Shkupi & Aliaj, 1997; Meço & Aliaj, 2000). With the onset of the "Neotectonic period" or the so-called "Pliocene revolution" at the beginning of the Pliocene, most of the Miocene sediments were weakly folded; they emerged from the sea to form hilly and mountainous structures (Aliaj, 1997). Therefore, the rivers were directed westwards thus establishing the fluvial network of the country. West of the uplifted highlands, however, marine conditions prevailed (Shkupi & Aliaj, 1997: 364).

Due to the collision between the Albanian orogene and the Adriatic microplate at the end of the Early Pleistocene, the Periadriatic foredeep basin was closed, and the Mio-Pliocene molasse deposits were heavily folded to form relatively narrow anticlines (associated with thrusts and back-thrusts) and synclines close to the coastal areas (Aliaj, 1997; Shkupi & Aliaj, 1997; Aliaj

et al., 2001). Another consequence of this compressional tectonic phase was the oblique dissection of the Pre-Quaternary structures, which in the Periadriatic offshore are buried under Quaternary marine sediments along the Adriatic shores by N-S striking faults (Shkupi & Aliaj, 1997: 362). This phenomenon is represented by the Frakulla-Durrresi segment which is separated by the Gjiri i Drini-Lezha fault from the Lezha-Ulcini segment, striking NW-SE in the research area (Aliaj, 2006: 144) (see fig. 5).

In contrast to the coastal region, the Mirdita zone, associated with the internal zone in the east of Albania, was affected by strong extensional deformations during the Pliocene-Early Pleistocene. This led to normal faulting and the formation of horsts and grabens (Aliaj et al., 2001, Aliaj, 2004, Aliaj, 2006). The graben structures are now occupied by small lake basins, alluvial plains and rivers (Aliaj et al., 2001: 314). This is also the case for the Drini River, which occupies the easternmost graben structure, flowing through three lake basins in its upper course (only Lake Ohrid persisted, the other two lakes were later uplifted and dried up).

2.2.2.3 Quaternary deposits

Since the Middle Pleistocene, the tectonics has been dominated by continued uplift in the highlands and local subsidence in the coastal areas (Aliaj, 1997). As a result of the ongoing subsidence in western Albania both graben lakes (e.g., Lake Shkodra) and graben plains (e.g., Zadrimea plain, Merqia plain) formed, and the Mio-Pliocene synclinal structures were covered by alluvial deposits of the rivers that drain the neighbouring mountains (Aliaj, 1997; Aliaj et al., 2001). The subsidence is the reason why Pleistocene marine terraces or uplifted former coastlines cannot be found along the Adriatic coasts of Albania.

Finally, the interplay between the Holocene transgression on the one side and the river alluviation on the other formed large coastal deltaic plains, the so-called “Lowland Albania” (Robinson, 1970), covering a coastal area from the mouth of the river Buna in the north to the town of Vlora in the south. The research area, made up of the Ishim, Mati and Drini deltas between Mali Rrenci and Cape Radonit in the eastern part of the Gulf of Drini forms the northernmost part of the Tirana-Ishim synclinal structure.

The drilling records from deep wells in the Drini delta plain show that the Quaternary deposits are more than 150 m thick, with a maximum of approximately 280 m in the central-western part near the Adriatic Sea (Eftimi, 1998; Fouache, 2006). These deposits are composed of intercalated layers of gravel and finer sediments such as clays and silts, which had accumulated

under a variety of environmental conditions, e.g. marine, terrestrial, and lagoonal (Fouache, 2006: 96-97; see also figs. 7a-c).

Pleistocene (or earlier?) terrestrial sediments are represented by slope debris and alluvial fans at the foot of the Shite-Veles and the Skanderbeg Mountains (fig. 6). These deposits consist of coarse gravels with clayey and sandy alternations and with a maximum thickness of ca. 100 m (Meço & Aliaj, 2000). They are mostly covered by Holocene marine-lagoonal and later floodplain deposits. Holocene marine deposits consist of sandy to silty strata.

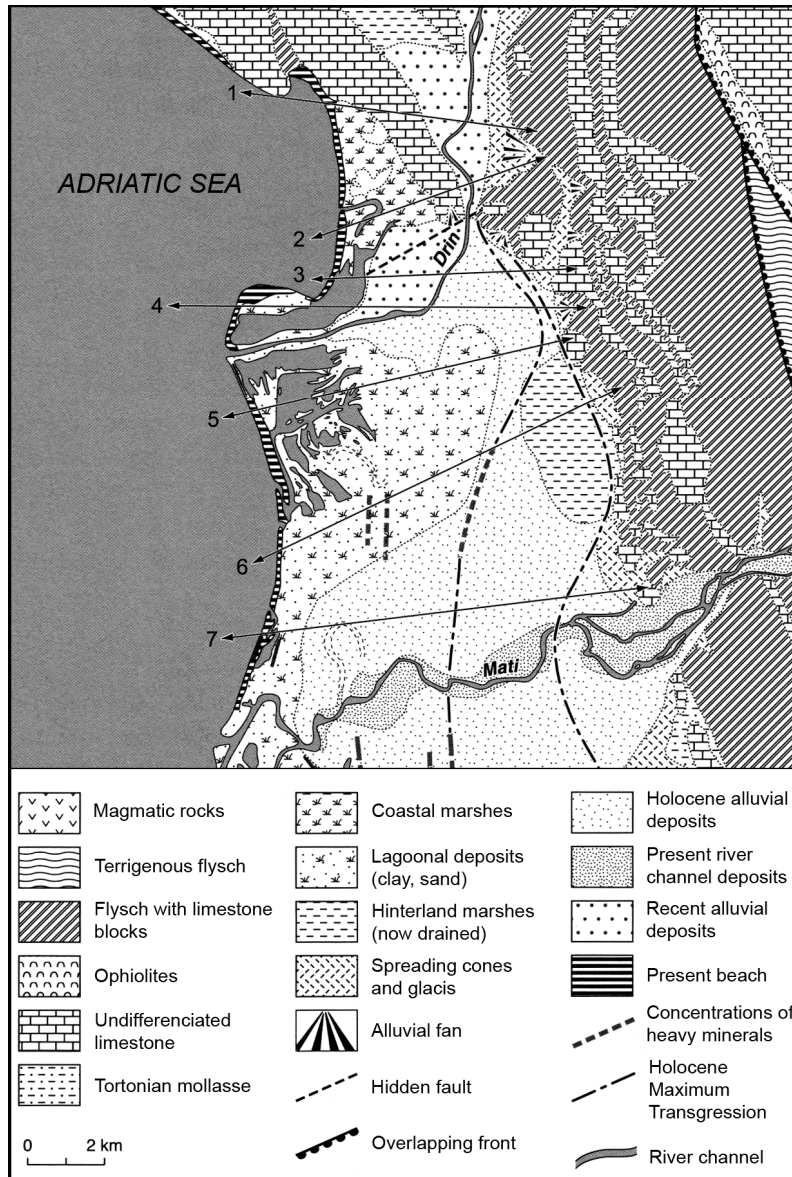


Figure 7a: Geological map with location of geological cross-sections on the delta between the Drini and Mati rivers (adapted from Fouache, 2006, fig. 54, p. 94).

7a). These deposits consist of clays, clayey silts and fine sands with intercalated peat layers. Current lagoonal-marshy deposits have developed around the Merxhani and Ceka lagoons near the Adriatic Sea.

They are widely spread below the recent marsh deposits as well as the cultivated soils of the present surface. Their maximum thickness increases towards the northern and western part of the Drini Delta (Ishull Shengjin Region) from ca. 20-25 m to ca. 40 m (fig. 7b). Obviously marine and littoral sands are also found along the coast, forming a 100-300 m wide beach.

The former lagoonal-marshy deposits can also be described in the eastern part of the Drini delta plain between Lezha and the Mati River on the one side and Lezha and the Balldrini plain on the other (fig.

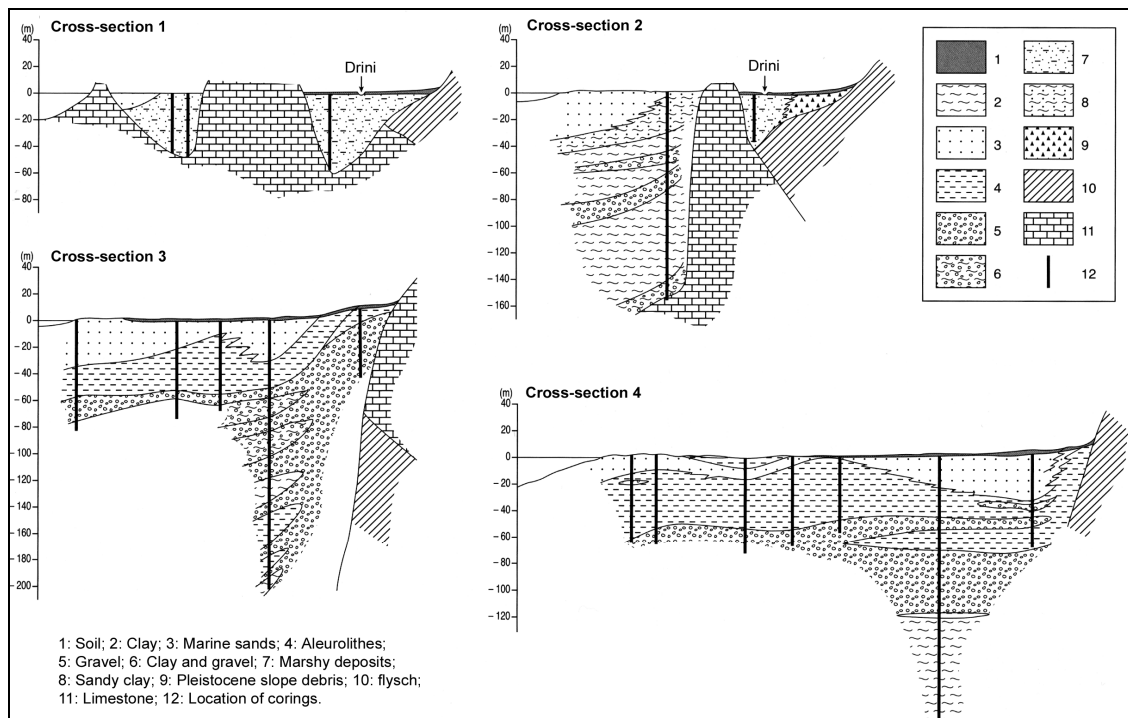


Figure 7b: Geological cross-sections of the Drini delta, for locations see fig. 7a (adapted from Fouache, 2006, fig. 55a, p. 96).

The present surface sediments of the Merqia and Zadrime plains and the Drini delta are dominated by fine sandy to silty strata which have been deposited during the flooding events of the river. In these sediments coarse material is missing because this has been accumulated by the Drini along its river bed before reaching its delta plain. Gravelly sediments are only visible within the course of the Mati River due to its torrential character and the high relief energy at short distance between mountains and sea which is very much different from the hydrologic regime and the topographic setting of the Drini (see fig. 7a).

2.2.3 Seismic history

Albania is one of the seismically active countries in Europe (Aliaj, 2004). Earthquakes are mostly of moderate size; however, many cities were devastated by strong earthquakes in their history (Kociaj & Sulstarova, 1980; Muço et al., 2002; Sulstarova et al., 2005). Most of the stronger earthquakes took place in the coastal area, triggered by movements along the plate boundary between the Eurasian plate and the Adriatic microplate (Aliaj, 2004). Beside this overregional pattern, graben systems in central and eastern Albania are also seismically active structures (Sulstarova et al., 2005).

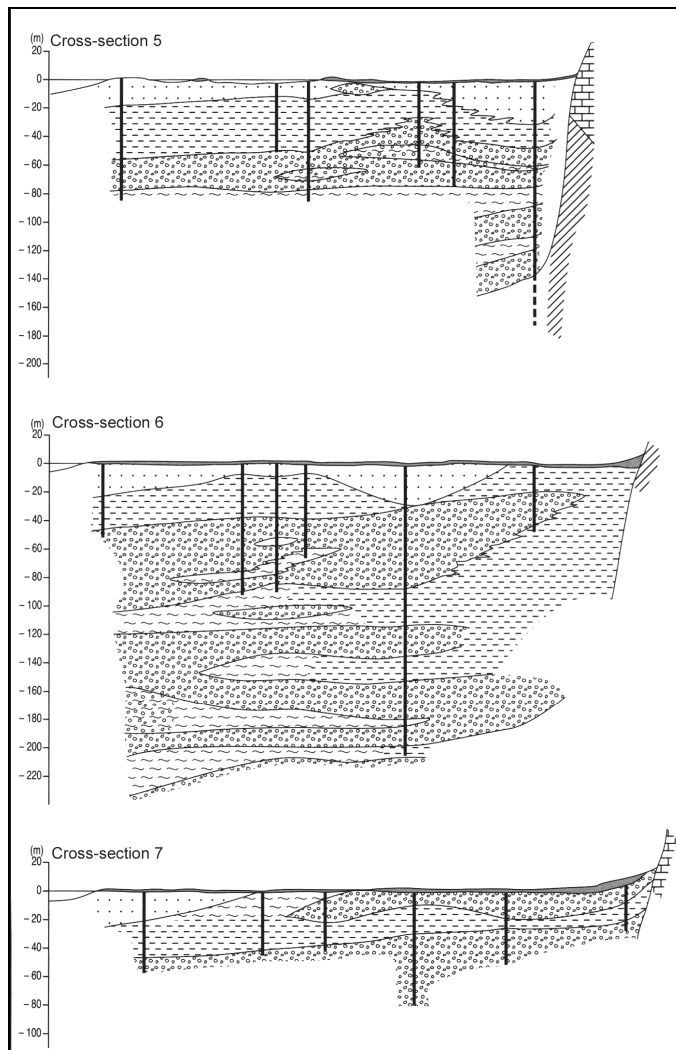


Figure 7c: Geological cross-sections of the Drini delta, for locations see fig. 7a (adapted from Fouache, 2006, fig. 55b, p. 97).

January 13, 1563 ($M_s = 6.9$); July 25, 1608 ($M_s = 7.2$); April 06, 1667 ($M_s = 7.2$); September 21, 1780 ($M_s = 6.6$); June 1, 1905 ($M_s = 6.6$) and April 15, 1979 ($M_s = 6.9$) (Aliaj, 2004: 143, Sulstarova et al., 2006). The latter one caused the destruction of the old centre of Lezha.

2.3 Geomorphology

The general geomorphological units of Albania depend to a large degree on tectonic movements. However, on a more regional scale, other factors also need to be considered, but their influence varies locally, thereby producing minor differences. The alluvial plains around Lezha are described in more detail, particularly the Drini delta plain. Human intervention plays an increasingly important role in shaping the geomorphology in the research area.

The magnitude and source analyses of present-day and historical earthquakes indicate that Lezha and its surrounding area are situated in the centre of three different seismic source zones which are called Lezha-Ulqini (LU), Periadriatic Lowland (PL) and Eastern Albanian Background (EAB), respectively (Muço et al., 2002: 282; Aliaj, 2004: 142; Sulstarova et al., 2005: 9).

Historical records show that around Lezha the most active seismic source is the Lezha-Ulqini zone, being oriented NW-SE and running parallel to the Adriatic coastal offshore (Aliaj, 2004: 143) (fig. 5). The most severe historical earthquakes triggered by this zone were recorded as follows: AD 518 (Mercalli intensity scale $M_s = 7.2$);

2.3.1 General geomorphological features of Albania

From a geomorphological point of view, Albania can be divided into five main units: (i) The Albanian Alps, exceeding 2,000 m altitude, are situated in the north; (ii) the central highlands with a less prominent relief, are located in the central part between valleys of the rivers Drini in the north and the Devoll in the south; (iii) depressions and enclosed basins in the east, including the valley of the Black Drini in the north and several lake basins in the south (e.g. Lake Ohrid and Lake Prespa or dried-up Lake Maliq in the Korça Basin); (iv) the southern highlands (Albanian Epirus), a limestone range with deep, parallel valleys, including the marginal part of the Epirus Mountains in Greece; (v) the western lowlands consist of the alluvial plains, bays and high rocky headlands (Louis, 1927: 62; Robinson, 1970: 273; Lienau & Prinzig, 1984; Lienau, 1993: 15).

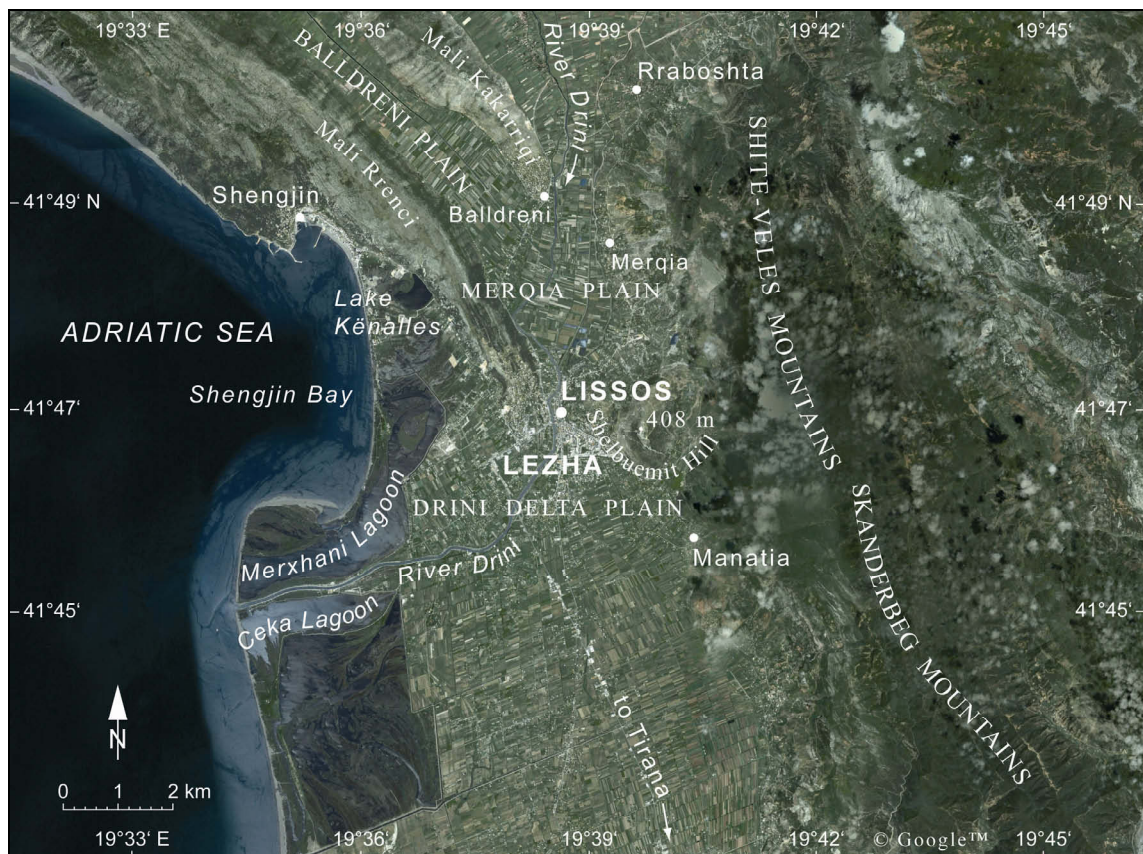


Figure 8: Satellite image of the research area with names of the most important places and topographic units (Google Earth, access 22-12-2009).

These major geomorphological divisions were formed during different phases of the neotectonic period (see chapter 2.2). On the one hand, general uplift has been a major factor in producing the mountainous relief in the central and southern parts of the country, while on the other hand, subsidence led to the formation of the large coastal and alluvial plains to the west and east of the

mountains. The border between these two domains is mostly controlled by still active fault lines.

The Albanian coastline has a total length of about 380 km (Simeoni et al., 1997: 152), and can generally be divided into two sections. The Adriatic coast from the Buna Delta to Vlora Beach (ca. 284 km) is part of the western lowlands and present mainly accumulative environments, segmented by high rocky headlands (e.g., Mali Rrenci, Cape Rodonit, Cape Durres). The research area also belongs to this section. However, the Ionian coast from Cape Stillo to the Greek border (ca. 96 km) is part of the southern highlands and consists of steep cliffs, dominated by erosive processes (Kabo et al., 1990; Gjikhuri, 1995; Qiriazzi & Sala, 1997).

2.3.2 Mountains and hills around Lezha

The research area is located on the transition zone between the central highlands and the western lowlands. The border is determined by a generally NW-SE striking lineament. The geomorphology is closely linked with local tectonics, as is clearly visible in the linear directions of the river valleys within the highlands (see figs. 2 & 9).

The mountainous relief around Lezha embodies horst-type mountain ranges. Situated to the north and east of Lezha are the Shite-Veles Mountains, also called Mirdita Highlands, and south of Lezha lies the Skanderbeg Mountain range. They are less rugged with an average altitude of approximately 500 to 700 meters. The highest peak, Mali i Veles (1,170 m a.s.l.), is located NE of Lezha. The highlands are drained by the tributaries of the Drini (Gjadri, Grykes and many small torrential streams), as well as the rivers Mati and Ishim.

The rivers in this area have a low average discharge throughout the year. However, after heavy rains, their carrying capacity increases manifold; then the sediment load becomes extremely high, also amplified by suitable lithological components in the catchment area and high-relief energy. Some authors (Milliman & Meade, 1986; Milliman & Syvitsk, 1992) mention the small Albanian rivers named above as significant with reference to the world-wide delivery of river sediment to the oceans (Meçaj, 2005a: 61). The large and pebbly torrential bed of the Mati River exemplifies the magnitude of ongoing hydrological processes (figs. 2 & 7a).

The hilly relief around Lezha marks the transition zone between the highlands and the alluvial plains. The hills present various geomorphological characteristics as a result of their lithological composition. The Mali Shelbuemit (410 m a.s.l.) and Lezha Hill (172 m a.s.l.), rising in close proximity to the centre of Lezha (see photo 2), are composed of carbonate rocks and have steep

slopes. The other hilly section, north of Lezha, is made up of flysch formations, and slopes gently from Rraboshta to Shkodra (fig. 6).



Figure 9: Geomorphological map of the research area (Uncu 2010, based on Google Earth Satellite image, access 22-12-2009; topographical map of Albania, scale 1:25,000, Instituti Topografik i Ushtrisë, 1998).

The territory of Lezha includes also the hilly ridges of Mali Rrenci (Mount Rrenci) and Mali Kakarriqi (Mount Kakarriqi) to the west and northwest of the modern town of Lezha. The highest elevations on Mali Rrenci (Mali Kolaj, 545 m a.s.l.) and Mali Kakarriqi (383 m a.s.l.) can be found close to the NW corner of the respective ridges. Mali Rrenci, bordered by the delta plains of the Drini and Buna Rivers, lies more or less parallel to the present coastline and determines the NW-SE direction of the coastline up to the town of Shengjin (fig. 9; photo 3).

The direction of the coastline changes to N-S at Shengjin, where the low-lying coasts of the Drini delta plain begin.



Photo 2: View from the Drini towards Lezha Hill (in the middleground, left) and Mali Shelbuemit (in the background, right). (Photo: Brückner, 2007)

These two ridges composed of carbonate rocks (limestone and dolomite) can be considered as the southernmost extension of the Dinaric Mountains (Meçaj, 2005a: 62). It is important to note that the SW slopes of Mali Rrenci border the “Dinaric Karst Area” (Meço & Aliaj, 2000). An undulating karst plateau has formed at the top of both ridges. Isolated limestone blocks with numerous karren and remnants of red loamy soils (*Terrae rossae*) point to an intensive karstification in earlier times. This is also confirmed by the presence of strongly deformed (palaeo-)karstic features (e.g., sinkholes) along the SW base of Mali Rrenci. Today the bottom of such sinkholes is either occupied by a lake (e.g., Lake Kënalles) or a swamp (e.g., Knetë Lezha) (see fig. 9). Karst morphodynamics around Lezha are illustrated by many karstic springs which feed the ground water and swamps of the Balldreni plain and the Drini delta. Karstic caves, today visible in the steep slopes of Mali Shelbuemit are further (palaeo-)karstic features.

2.3.3 Alluvial plains around Lezha

Large alluvial plains, which developed in the Periadriatic depression make up the second major geomorphologic component around Lezha. The alluvial plains do not just have important agricultural potential, but they can serve as geo-bio-archives for geoarchaeological research. The plains can be divided further into the flood plains to the north of Lezha, including the Zadrina, Balldreni and Merqia plains and the piedmont plain at the base of the Shite-Veles

Mountains, and the coastal plains, including the Drini delta to the south and west of Lezha (see fig. 9).

2.3.3.1 Zadrime plain

The extensive flat area between Shkodra and Merqia is known as “Zadrime plain” (fig. 2). It has a tectonic origin and has developed as a result of local subsidence at the end of the Early Pleistocene (Aliaj et al., 2001). Subsequently, the area was filled in with alluvial deposits by the rivers Drini, Gjadri and numerous other torrential streams (revmas). From a geomorphological point of view, the Zadrime plain consists essentially of two larger units. Firstly the floodplain alongside the rivers Drini and Gjadri, which is situated between the north-eastern slopes of Mali Kakarriqi and the flysch hills, and secondly the large piedmont plain, which extends from the riverside floodplain to the Shite-Veles Mountains (fig. 2).

The flysch slopes of these mountains are worn down by denudation processes as well as fluvial erosion. These processes have been operating since the Middle Pleistocene or even earlier. As a result, a piedmont plain along the base of the mountains has formed, consisting of slope debris and alluvial fan material. This plain became the marginal part of the broad coastal plain which developed during the Last Glacial Maximum, when the river mouths were located approximately some 100 km further west in comparison with the present shoreline (Mathers et al., 1999: 352). The following Holocene transgression caused partial inundation of this plain by the sea. Since the Middle Holocene, deltaic and floodplain deposits have accumulated, covering a large part of the former plain. Only outcrops of slope debris and alluvial fans along the western base of the mountains are still noticeable today.

2.3.3.2 Balldreni plain

The Balldreni plain is a prominent and geomorphologically interesting feature, formed in a narrow syncline between the hilly ridges of Mali Rrenci and Mali Kakarriqi (fig. 6 and photo 3). It extends for about 20 km in a NW-SE direction, connecting the Merqia plain in the SE with the floodplains between Shkodra and the Buna delta in the NW. The Balldreni plain has a maximum width of 1 km. The syncline is accentuated by a graben-like structure due to the tectonic activities of the area. During the Holocene maximum transgression, it became part of the sea, forming a marine corridor (cf. the so-called vallone or canale-type coast of Dalmatia) (see chapter 8.1). Marine conditions in this corridor prevailed for quite some time due to the lack of sediment input. After the deltas of the Drini and Buna rivers prograded past the corridor on both sides, the area was transformed into a lake, which later turned into a swamp, the so-

called “Balldreni swamp” (Albanian: Knetë Balldreni). The introduction of drainage measures in the 1960’s led to the conversion of the former swamp into fertile arable land, with the exception of the NW corner, where swampy conditions persisted to date.



Photo 3: View from the Acropolis over the Merqia plain, immediately north of Lezha. The Balldreni plain lies between the two limestone ridges Mali Rrenci (left) and Mali Kakarriqi (right) (Photo: Brückner, 2007).

2.3.3.3 *Merqia plain*

Geographically, the Merqia plain, located immediately to the north of Lezha (see fig. 9 and photo 3), makes up the southernmost part of the Zadrina plain. The river Drini drains the Merqia plain before entering its delta plain south of Lezha. In the NW, the Merqia plain is connected to the Balldreni plain, and in the east, an interesting, amphitheatre-like feature borders the plain. This feature indicates strong, localised subsidence tectonics. Along its base, the floodplain sediments of the Drini mask the slope debris and alluvial fans. An artificial channel in the eastern part of the plain drains the area. However, some lakes can be still seen in the central part of the plain even today.

2.3.3.4 *The Drini delta*

The other alluvial plain in the research area is the actual Drini delta, extending to the south and west of the modern town of Lezha. The Drini delta, together with the deltas of the Mati and Ishim rivers further south, forms a broad coastal plain, a zone of accumulation between the erosive sections at Mali Rrenci in the north and Cape Rodonit in the south (fig. 2). This alluvial complex has been created since ca. 6,000 years BP, and, in the process, the coastline has been shifted about 10 km to the west (Mathers et al., 1999: 349).

The Drini delta extends from the town of Lezha to the pebbly banks of the river Mati in the south and from the steep slopes of the Shite-Veles Mountains in the east to the Adriatic coast in the west. After passing the narrow gap at Lezha, the Drini River enters its delta plain and flows first southwestwards then west before debouching into the Gulf of Drini between the Merxhani and Ceka lagoons (fig. 9).

The Drini delta can be divided into two sections (fig. 9). The southern and eastern parts of the delta are called Plain of Lezha Island (Fushu i Ishull Lezha); this part is older, while the area to the north and west of the present-day river channel, called Plain of Shengjin Island (Fushu i Ishull Shengjin), is younger. Sandy coastal sediments in the western part of the Drini delta change to fine-grained floodplain sediments towards further inland. The alluvial fans and slope debris at the foot of the Shite-Veles Mountains are drowned by the floodplain sediments between the town of Manatia and the Mati River. However, the Manatia alluvial fan to the east of Lezha formed by the Grykes River, presents an exception, because it is still visible today.

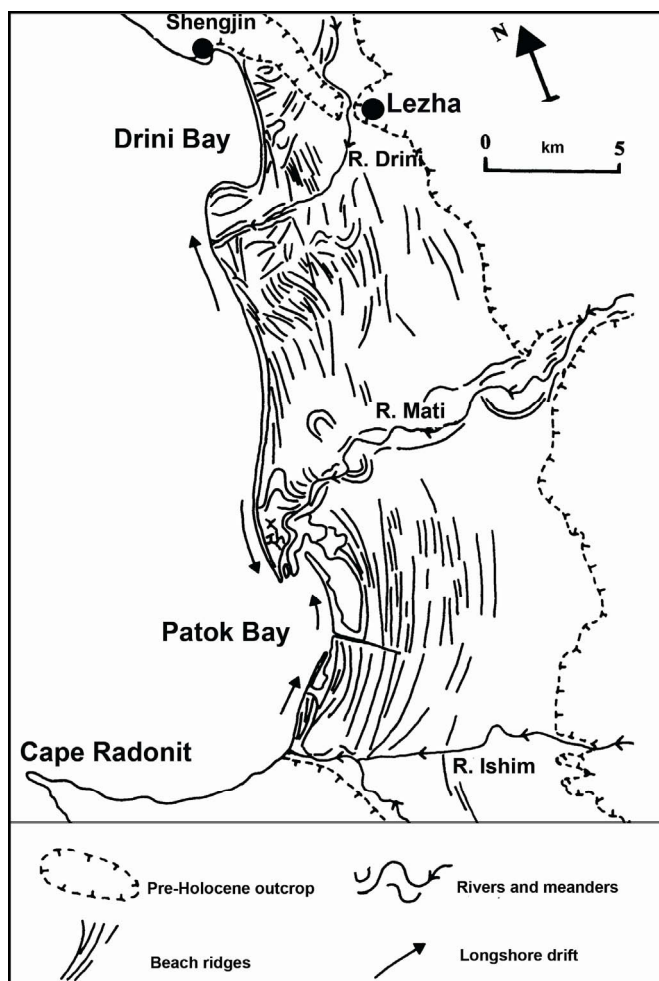


Figure 10: Beach ridges and meander belts of the Drini delta plain (slightly changed from Mathers et al., 1999, fig. 2, p. 347).

farthest inland developed as an extension of the limestone outcrop of Mali Rrenci. Clearly

During the 1960's, the delta and floodplains around Lezha were drained and several areas were transformed into arable land. Today, the Drini flows across the plain via an artificial channel, which was built for flood prevention purposes. Therefore, the original geomorphology of the Drini delta has been intensively changed. However, some former features can be clearly seen on topographic maps and satellite images (see figs. 8 & 9).

The most interesting features on the Drini delta are several belts of roughly parallel N-S aligned beach ridges (fig. 10). Such beach ridge belts are cut by abandoned meanders which had been traversing the coastal deposits (Mathers et al., 1999: 349). The beach ridge belt

noticeable in the Ishull Shengjin Region as well as south of the Drini, the central belt consists of tightly clustered beach ridges, exhibiting truncation patterns; an indication of several cycles of formation. The most westward beach ridge belt runs mostly parallel to the present-day coastline (fig. 9 & 10).

Behind the beach barrier, various coastal features have evolved: brackish lagoons (Merxhani and Ceka), marshy labyrinths (amphibic lands), and crevasse splay deposits (in Ceka lagoon) (fig. 9). In addition, two former meandering courses of the Drini can be identified within the coastal lagoons. The northern one is still visible within the Merxhani lagoon, the southern one within the Ceka lagoon (Mathers et al., 1999: 349) (figs. 8 & 9).

Another interesting landform can be made out in the north of the present mouth of the Drini: an ensemble of beach ridges alternating with swales (inter-ridge depressions) forms an island (see fig. 9). The same development is also visible at a former mouth of the Drini, about 5 km north of its present position. These features may be interpreted with the interactions between longshore drift and seasonally changing wind directions. When the longshore drift is weaker during the summer, the northwesterly winds dominate the area and cause a direction change of the movement of sediment. Thus, after many years, successive hook-shaped sand-spits form an island. It is well possible that a similar system of sand bars once evolved in the areas of Ishull Shengjin and Ishull Lezha, the literary translation of which is “Island of Shengjin” and “Island of Lezha”. Analogue examples of such a coastal feature can be found in the Baltic Sea (e.g., Island of Darß).

The outer geometry of the Drini delta used to be a result of the interaction of the quite substantial amounts of sediment supplied by the rivers Mati and Drini and the northbound longshore drift (average speed of 0.3-0.5 m/sec and a maximum of 1.5-2.0 m/sec) (Simeoni et al., 1997). The long sandy beach barrier and Shengjin spit result from this morphodynamics. Nowadays, the rather small tidal range (only 0.20-0.30 m), and the dramatically decreased sediment input caused the shape of the delta to become rounded. It may be compared, not in size but in shape, to the Rhône delta (Kelletat, 1984). Fluvially-dominated processes have been replaced by wave-dominated ones (Simeoni et al., 1997; Mather et al., 1999; Meçaj, 2005a).

Recent satellite images and geomorphological observations in the field indicate that the extent of coastal erosion has become a problem in recent times. Meçaj (2005a: 66) reports that the Drini delta plain was still advancing until 1936. From 1936 to 1957, shoreline erosion was about 50 m, at an average of 2.5 m/year (Meçaj, 2005b: 256). Re-activation of an old river course (Drinassa) by dredging in 1958 diverted much of the Drini's waters to the river Buna (Bojana);

this dramatically reduced the sediment discharge of the Drini along its natural course. As a consequence, significant erosion at the river mouth occurred from 1957 to 1998, the loss of land was more than 250 m, at an average of 6 m/year (Meçaj, 2005b).

The drowning of the military bunkers along the beach is further evidence for rapid marine erosion. Built on the Shengjin sand-spit between 1967 and the beginning of the 1970s, some of them are now damaged by waves or they are inundated (photo 4). Human induced intensive coastal erosion is also reported from other coastal areas of Albania, e.g., from the deltas of the Seman and Vjosa rivers (Boçi, 1994; Ciavola et al., 1995; Gjiknuri, 1995; Simeoni et al., 1997; Mathers et al., 1999; Fouache et al., 2001, 2010; Pano et al., 2003; Meçaj 2005a, b).

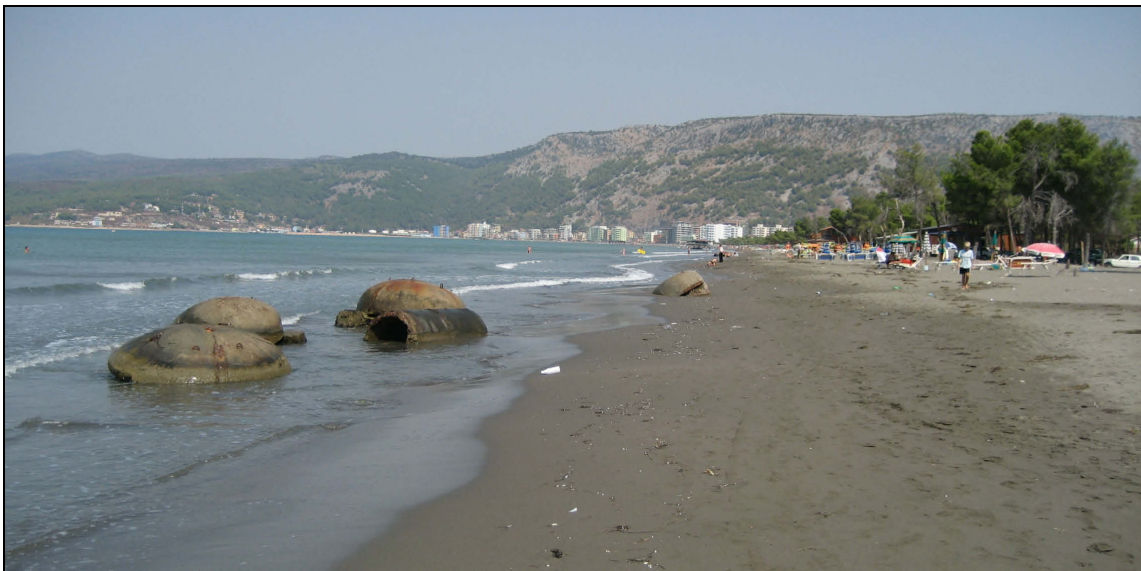


Photo 4: Military bunkers, originally built much further inland during the early 1970s, are being destroyed by the waves. (Photo: Uncu, 2007)

Reasons for this dramatic change from an accumulative coast to an erosive one are: (i) man-made diversion of much of Drini's waters in its middle course to the Buna river system in 1958; (ii) intensified human impact on the hydrological regime by building dams and associated reservoirs (starvation of the sediment budget of the delta) since the 1970s; (iii) deforestation of the coastal sand spits, particularly after the collapse of the communist regime in 1991; (iv) global sea level rise of approximately 15 cm within the last century; (v) overall subsidence tectonics of this coastal region.

2.4 Climate

The climate of the Mediterranean region results from its position in the transition area between the subtropical high pressure belt and the mid-latitude westerlies (Trigo et al., 1999: 1685).

Albania, despite being located relatively close to the centre of the Mediterranean macroclimatic zone, exhibits distinctly different climatic characteristics on a regional level.

2.4.1 General climate pattern of Albania

In summer, the area is part of the sub-tropical high pressure belt leading to hot and dry conditions, whereas in winter it is part of the mid-latitude frontal depressions resulting in mild and humid conditions (Lineau, 1984; Rother, 1993). Cyclones come from the Mediterranean Sea (especially the ones of the Gulf of Genoa) and the North Atlantic (P.m.: Polar maritime air), while anticyclones come from the Azores (T.m.: Tropical maritime air) or from Siberia (P.c.: Polar continental air) (Demiraj et al., 1996: 17). The frequency of occurrence of cyclonic and anti-cyclonic weather systems has a distinct annual pattern. The cold season is dominated by the high frequency of cyclones, as well as influences from the “Polar Front”.

Coastal Albania, however, is mainly affected by cyclones formed over the Northern Adriatic Sea as well as the Gulf of Genoa during the cold season. They are usually associated with clouds and intense frontal rain and they move in a south-easterly direction towards to Ionian Sea. They also provide ideal conditions for the development of the regional cold wind called “Bora” (Harding et al., 2009: 74). These cyclones may form throughout the year, but their intensity declines towards summer.

In contrast, anti-cyclonic conditions frequently occur during the warm season (HMI, 1975, quoted after Demiraj, 1996). For this reason, the weather conditions during the summer months are characterised by clear skies with occasional clouds and very little rain or none at all. In the transition seasons of spring and autumn, the instability of the upper atmosphere, combined with the low-level forced convection, leads to precipitation (Mustaqi, 1986, quoted after Demiraj, 1996: 17).

Due to the elongated shape of Albania and its location at the sea, the climatic conditions vary greatly from north to south as well as from west to east. The coastal lowlands have typically Mediterranean weather because of the proximity to the sea, whereas the climate of the highlands has maritime as well as continental elements (Robinson, 1970). Towards the east of the country, the climate becomes more continental.

The annual average temperature decreases markedly towards the northeast, with 16.5 °C in Vlora, 14.8 °C in Shkodra and only 7.0 °C in the northern area of the Albanian Alps (Frasheri et al., 2008: 1; Kabo, 1990: 185). In addition to latitude, other factors such as altitude and the

distance from the coast have an influence on the mean annual temperature, e.g., 10.5 °C in Korça, 10.1 °C in Puke, 36 km northeast of Lezha.

In the south of Albania, typically Mediterranean conditions prevail. However, north of Vlora where the climate becomes increasingly more humid in the north, the summer drought is reduced to only 1-2 months. The amount of precipitation increases from 1028 mm/yr in Vlora to over 2065 mm/yr in Shkodra (Kabo, 1990: 202). The Albanian Alps together with the Dinaric Alps in Montenegro are the most humid places in Europe (up to 4444 mm/year of rainfall) (Grove & Rackham, 2001: 26).

According to Köppen's climate classification, the coastal lowlands of Albania lie within the Csa climate zone (Cs: dry, warm summers and mild winters; a: average temperature of warmest month > 22 °C) (Köppen & Geiger, 1961; Straßer, 1998). Rother (1993: 27) describes this zone as "Olivenklima" (climate of the olives). In contrast, the highlands are classified as Cfb (Cf: wet, cold winters and cool summers; b: average temperature of warmest month < 22 °C) (Straßer, 1998).

2.4.2 Climate around Lezha

The climate around Lezha is typically Mediterranean with hot and dry summers and generally mild and humid winters (Demiraj et al., 1996). Climatic data for Lezha is summarised in table 1.

	Jan	Feb	Mar	Apr	May	June	July	Aug	Sep	Oct	Nov	Dec	Mean
Mean Temperature (°C)	6.8	8.1	10.5	13.7	17.9	21.3	23.9	23.7	21	17	12.2	8.3	15.4
Mean Max. Temperature (°C)	10.3	11.8	14.7	18.1	22.4	25.9	29	28.9	26	21.5	16	11.7	19.7
Mean Min. Temperature (°C)	3.3	4.3	6.3	9.4	13.4	16.7	18.8	18.5	16	12.5	8.4	4.8	11
Max. Absolute Temperature (°C) (yr)	19.8 (1977)	24 (1979)	26 (1989)	27.6 (1988)	34.8 (1968)	36.7 (1967)	38.8 (1973)	40 (1981)	35 (1987)	30.4 (1961)	24.6 (1990)	20.3 (1979)	
Min. Absolute Temperature (°C) (yr)	-10 (1963)	-6 (1985)	-5 (1987)	2.4 (1964)	6.1 (1982)	9.3 (1989)	10 (1971)	11 (1989)	7 (1974)	0.1 (1972)	-1.6 (1976)	-5.5 (1967)	
Mean Precipitation (mm)	144.8	129.6	116.6	117.3	84.1	64.7	41.6	55.7	97.8	137	177.9	157	(Total) 1324.3
Max. Absolute monthly Precipitation (mm) (yr)	494.5 (1963)	374.4 (1963)	395.1 (1969)	235.6 (1978)	267.9 (1957)	294.8 (1968)	245 (1991)	238.8 (1972)	368.7 (2002)	367.8 (1973)	468.5 (1985)	314 (2005)	
Max. Absolute Daily Precipitation (mm) (yr)	152.8 (1986)	76 (1977)	120.5 (1969)	91.5 (1962)	107.4 (1964)	160.1 (1968)	118.5 (1982)	89.7 (1968)	129.5 (1972)	116.7 (1976)	135.1 (1963)	75.8 (1960)	

Table 1: Climate data for Lezha (temperature: 1951-1990, precipitation: 1951-2006) (compiled by L. Uncu, based on Mucaj, pers. comm. in 2007).

The temperature is determined by the amount of solar radiation and the type and origin of the air masses. The annual amount of solar radiation in Lezha is around 1490 kwh/m². On the average, Lezha receives 2580 hours of sunshine annually (Mucaj, pers. comm. in 2007).

The average annual temperature is 15.4 °C in Lezha (table 1). The mean temperature during the winter is around 7 °C, whereas during the summer it is 21-24 °C. The warmest month is July (23.9 °C), the coldest January (6.8 °C). It is important to note that the difference between the highest and the lowest temperature ever recorded is 50 °C which is unusually high for a Mediterranean-type climate (40 °C on August 4, 1981; -10 °C on January 24, 1963).

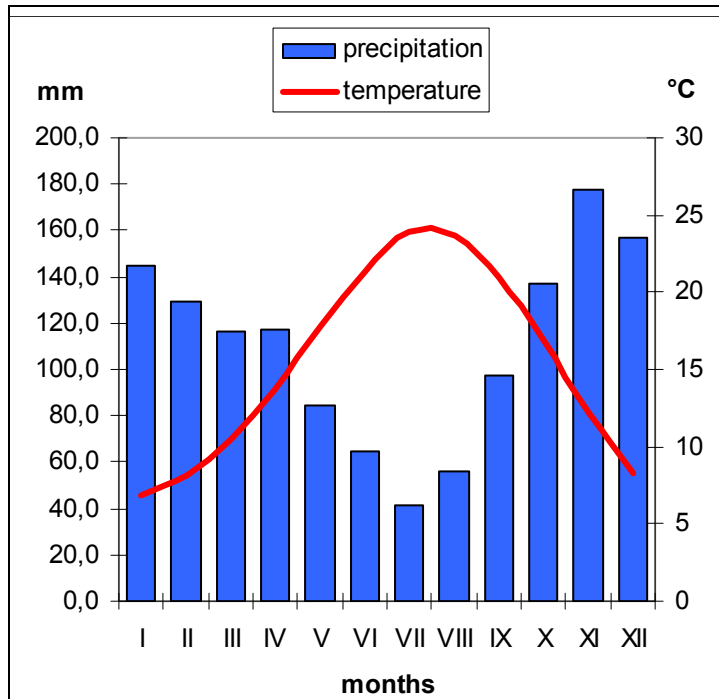


Figure 11: Climate graph of Lezha (HMI Tirana, through pers. comm. with Mucaj, 2007).

The total annual precipitation in Lezha is 1324.3 mm (for the period 1951 – 2006; table 1). However, the number of cyclones reaching this part of Albania each year fluctuates considerably, causing a great variability of the annual precipitation. For instance, the maximum annual precipitation recorded was 1904.9 mm in 1960, the minimum 737.7 mm in 2003. The higher frequency of cyclones from October to April means that then the monthly average precipitation is >100 mm in Lezha. The most humid month is November (177.9 mm), the month with the lowest precipitation is July (41.6 mm).

According to the data, Lezha may be categorised as a “Mediterranean-type rainfall regime”. The great variability of monthly and yearly precipitation, plus the majority of the rain occurring during the winter months are characteristic of this rainfall regime. The variability on a daily basis can be equally important (especially for agriculture): the highest amount of rainfall has been documented on June 10, 1968 (160.1 mm within 24 hours; quoted after Kabo, 1990: 204). Such a variability and unpredictability of the precipitation pattern causes the river regimes to be similarly erratic. Hydrologic hazards in the form of expansive floods have occurred many times throughout Lezha’s history (see chapter 2.5).

Snow is not frequent in Lezha and may be considered an extraordinary climatic event. The average number of snowy days is 1.6 (Mucaj, pers. comm. in 2007). Fog and smog are also rare phenomena in the study area.

Generally, the dominant wind direction in Lezha is north, particularly during the winter. Other relatively frequent winds blow from the east and northeast (especially during the summer) (see figs. 11 & 12). The topography has a significant effect on the wind pattern of Lezha. In the cold period, dominant continental air masses over the Balkan region initiate the flow of easterly cold air streams towards the west. The Drini valley channels these katabatic air streams, thereby changing their direction to a north-south flow of air (Martyn, 1992: 128; Rother, 1993: 30). During the summer period, anti-cyclonic weather predominates, although westerly, as well as north-westerly winds do occur during the day carrying moisture farther inland (sea breeze).

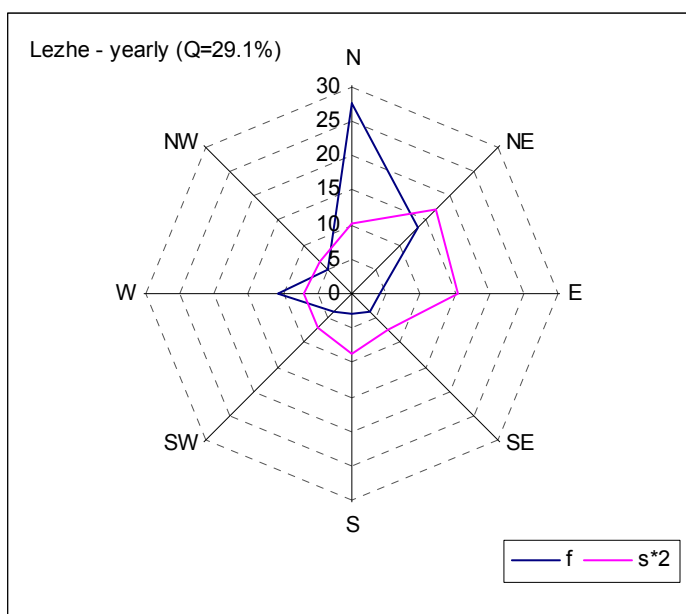


Figure 12: Windrose graph demonstrating prevalent wind directions at Lezha (f: frequency, s*2: mean speed) (HMI Tirana, through pers. comm. with Mucaj, 2007).

In Lezha, the mean wind speed is around 3.7 m/sec. Maximum speeds of up to 5.4 m/sec occur in January and minimum speeds of 2.7 m/sec are common for the summer period. Strong local winds, known as “Bora”, may occur in the winter months. The Bora is a dry and cold wind that can reach speeds of up to 25-30 m/sec (HMI, 1985, quoted after Demiraj et al., 1996: 32). This type of wind may cause serious damage to agriculture; in 1966 and 1974 it even destroyed high

tension pylons between Lezha and Laç, a town south of Lezha (Demiraj et al., 1996: 38). During the summer, the “Sirocco”, a warm wind blowing from south and south-west, brings deteriorating weather conditions (Demiraj et al., 1996: 32).

2.5 Hydrology

The main hydrological units within the research area are the Drini as the main agent controlling geomorphological processes of the delta plain, the Merxhani and Ceka lagoons on either side of the river mouth and Lake Kënalles, a freshwater lake fed by karstic springs (fig. 8).

2.5.1 The river Drini

The Drini is the longest river in Albania with a length of 283 km (Kabo et al., 1990). It has two main sources, the Black Drini (149 km) and the White Drini (139 km). The Black Drini (in Albanian: Drini i Zi) originates at Lake Ohrid (Liqeni i Ohrit) and flows through Macedonia and the eastern territories of Albania. The White Drini (Drini i Bardhë) emerges from the Žljeb Mountain in Kosovo (Kabo et al., 1990), and merges with the Black Drini near Kukës in northeastern Albania (fig. 13). At Vau i Dejës it enters the lowlands of Shkodra and splits into two distributaries. One continues to the south, passing through the plains of Zadrima. Before it reaches Lezha, it is joined by small rivers and creeks (e.g., Bushat and Gjadër) which emerge from the Shite-Veles Mountains. In Lezha this branch of the Drini enters the delta plain and finally, between the Ceka and Merxhani lagoons, it reaches the Gulf of Drini in the Adriatic Sea. In total, this distributary of the Drini, also called ‘Drini of Lezha’ (Drini i Lezhë), is 22.5 km long.



Photo 5: The Drini splits into two branches at Vau Dejës (view from Rozafa Castle). It flows from the left hand side towards Lezha (central background) and as the Drinassa towards Shkodra (right foreground) (Photo: Uncu, 2007).

The Drini and its tributaries drain large terrains in the eastern, central and northern parts of Albania and neighbouring countries. The drainage basin comprises a total area of about 14,173 km² (Kabo et al., 1990: 231). Simeoni et al. (1997: 156) compare the Drini with the Po, the main Italian river to emphasise the huge carrying capacity of the Drini. The catchment basin of the Drini is five times smaller than that of the river Po, but astonishingly, its total annual sediment load has been calculated to be 15×10^6 t/yr (Milliman & Meade, 1983: 9; Milliman & Syvitski, 1992: 529), thereby being 20 % larger than that of the Po. According to Pano et al. (1992)

(quoted in Simeoni et al. 1997: 158) about 50 % of the total freshwater input from all Albanian rivers to the Mediterranean is provided by the rivers Drini and Buna.

According to Milliman & Syvitski (1992), the Drini, just like other relatively short rivers draining into the Mediterranean had a very high sediment yield ($1200 \text{ t/km}^2/\text{yr}$) before the diversion measures and more than twice the annual runoff (325 mm/yr) of well-known North European rivers like the Loire, Seine, Elbe and Rhine (Milliman & Syvitski, 1992: 536).

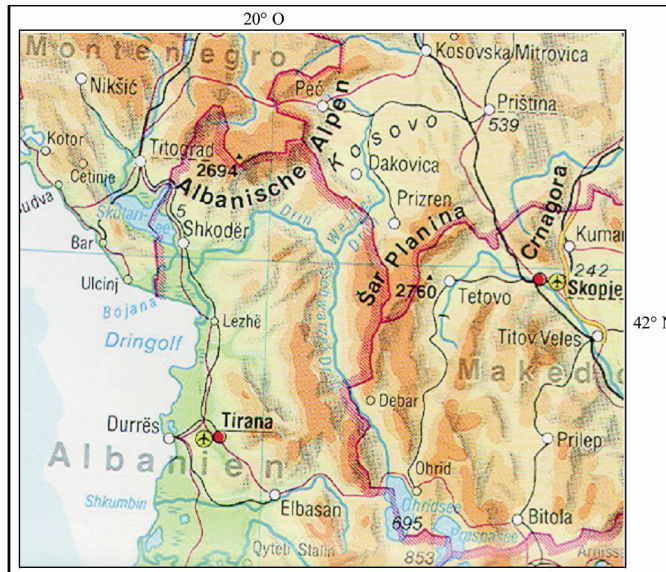


Figure 13: Catchment area of the river Drini (excerpt taken from Diercke Weltatlas, 1994: 110).

combination of the predominantly torrential river dynamics with snow melt events and the influence of the karstic hydrography.

The Drini and its tributaries are mostly fed by rainfall and snow melt from the higher mountains. Karstic springs in the northern part of the drainage area (Albanian Alps) are also an important source, particularly during the summer months. The hydraulic regime of the Drini is typically Mediterranean with seasonal variations in discharge. Therefore, the Drini is characterised by occasional enormous floods, caused by a

The annual discharge of the Drini is $12,266 \text{ m}^3/\text{s}$ (Pano & Avdyli, 2009: 69). However, due to artificial dredging and re-direction in 1958, only one third of the Drini's total discharge flows through Lezha today (table 2). The second distributary, now the main course, is called 'Great Drini' (Drini i Madh) and is connected with the river Buna (Bojana) *via* the Drinassa stream near Shkodra (photo 5). The highest discharge occurs from November to May. The average monthly flow of the Drini of Lezha is given as $351 \text{ m}^3/\text{s}$, with a minimum in August ($104 \text{ m}^3/\text{s}$) and two maxima in April ($507 \text{ m}^3/\text{s}$) and December ($501 \text{ m}^3/\text{s}$) (table 2).

	Jan	Feb	Mar	Apr	May	June	July	Aug	Sep	Oct	Nov	Dec	Annual sum
Drini of Lezha	493	459	446	507	490	293	155	104	141	228	396	501	4213
Great Drini	1067	899	850	879	861	588	322	195	210	382	770	1030	8053

Table 2: Annual distribution of the Drini's discharge (in m^3/s) (slightly changed from Pano & Avdyli, 200: 69, table 2).

Considerable fluctuations can also be observed in the amount of runoff: before greater human modifications, a low flow of 97 m³ was reported at gauge station Vau Denjs (Vau i Dejës). However, the discharge may grow up to 1,500 m³, in an extraordinary case even to 3,424 m³ (Riedel, quoted after Nopcsa, 1929a: 202).

We know from old maps and scientific reports that the Drini changed its course and the location of the river mouth many times during history (see table 9 in chapter 8.11). This phenomenon has been described scientifically for the first time by von Hahn (1853) in the mid-19th century after a major flood event. During past centuries, floods were the biggest problem for the plains of Zadrima and Lezha. Some of the most disastrous floods of the Drini recorded to date happened in 1837, 1854, 1860, 1905, 1937, 1952, 1962-1963, and 1970-1971 (Kolaneci, 2000; Pulaha & Parruca, 2006). The largest flood event occurred in January 1963 when the centre of Lezha was inundated by 1.33 m of water (Pulaha & Parruca, 2006: 130; see photo 6). Despite the regulation works on the river, the lower course of the Drini still experienced many floods during the last two decades (November 1992, August 1995, February 1998, September 2002 and January 2004).



Photo 6: Flood event from January 1963, inundating the town of Lezha (Photo: Pulaha & Parruca, 2006: 131).

The most recent extreme flood event of the Drini was reported in the first week of January 2010. However, this time it was anthropogenically induced. After long period of heavy rainfall and snow melting in the Albanian Alps the reservoirs were filled to a dangerous level and the

late opening of the dams led to flooding of the lowlands between the modern city of Shkodra and the Buna delta. Some places, e.g., Shkodra, were inundated by approx. 1 meter of water.

A similar situation occurred on the Zadrima plain some hundred years ago. Nopcsa (1929a) reports that during a moderate flood, more than a third of the Zadrima plain was inundated, and throughout the rainy winter season nearly half of it was temporarily transformed into a swamp. The big floods during the winter of 1857/58 and in November 1878 turned most of the Zadrima plain into a lake for about two weeks (Nopcsa, 1929a). Responsible for the flooding of the Zadrima plain is usually the river Gjadri as well as the Drini. The Gjadri rose up to 5 m above its normal level despite its large inundation area. This flood was seemingly not triggered through human intervention.

The flood damage potential of the Drini was partly reduced after drainage measures were introduced in the 1950s. Additionally, three dams were built along the river to harness electricity in the 1970s. These dams created big artificial lakes, with the most prominent being Lake Fierza (Liqeni i Fierzës; 73 km²) on the middle course. Lake Koman (Liqeni i Koman) and Lake Vau i Dejës (Liqeni i Vau e Dejës; 25 km²) are situated along the lower course. Nowadays, these lakes work as sediment traps – one of the main reasons why the sediment budget of the Drini delta is now negative.

2.5.2 Lagoons in the Drini delta

Two main lagoon systems exist along the coast of the Drini delta. They lie on either side of the Drini's mouth: Ceka lagoon to the south and Merxhani lagoon to the north (fig. 9). The lagoons are separated from the sea by a sand barrier system which has been shaped by longshore drift. The lagoons are permanently connected to the sea by an artificial, regularly dredged channel.

The Ceka lagoon occupies an area of 706 ha and has a mean depth of 0.3 m (max. 1 m) (Peja et al., 1996). A canal equipped with sluices connects it to the river Drini. It also receives drainage water from the river's catchment *via* pumping stations on the plain. Salt pans exist in the eastern part of the Ceka lagoon, and a protected nature reserve has been established ("Vain Reserve"). On the satellite image (fig. 8), a former river mouth and abandoned channels, semiterrestrial marshy areas as well as traces of a crevasse splay of the Drini can be observed within the lagoon.

With 338 ha, the Merxhani lagoon is significantly smaller than the Ceka lagoon. It has a mean depth of 0.5 m (max. 1.5 m) (Peja et al., 1996). The lagoon was first connected to the sea by an artificial canal in 1986. Part of this lagoon has also been set aside as protected nature reserve

(“Kune Reserve”). Again, the satellite image clearly shows preceding geomorphological features, such as a former channel of the Drini, multi-curved sand spits and marshy areas within the lagoon. Especially the northern part of the Merxhani lagoon is characterised by sandy islands and semi-terrestrial swampy environments (figs. 8 & 9).

Today, both lagoons are threatened less by natural factors such as sedimentation and siltation of the connections to the sea, but more by anthropogenic causes, particularly episodes of eutrophication, anoxia and industrial pollution (Peja et al., 1996). In the 1960s, over 2100 ha of the land around the Ceka and Merxhani lagoons were drained (Peja et al., 1996). The increased use of fertilisers (especially nitrogen and phosphorus) and pesticides caused a complete change in the hydrochemical regime and the ecological conditions of the lagoons. Before a canal for the waste water was built in 1978, the paper factory in Lezha had discharged its highly polluted water directly into the Ceka lagoon (Peja et al., 1996). After the collapse of the political system, the factory was closed. Uncontrolled development of settlements and hotels along the lagoons and on the Shengjin sand-spit has increased the domestic effluents.

2.5.3 Lake Kënalles

Although Lake Kënalles (Liqeni i Kënalles) is relatively small (lake surface area approx. 0.201 m²), it is an important hydrological feature in the research area (figs. 9). The up to 14 m deep lake is located very close to the shoreline at the base of Mali Rrenci on the road to Shengjin. The origin of the lake is tectono-karstic. It is probably a former sinkhole, which temporarily experienced lagoonal conditions when the rising sea initially flooded the depression. However, after the Shengjin sand-spit developed, fresh water influx from karstic springs dominated the further evolution of the lake. Today, a marshy landscape frames the lake (photo 7).



Photo 7: Lake Kënalles near Shengjin (left middle ground). View from Mali Rrenci towards the south. Also visible are the Merxhani lagoon and the Shengjin spit separating it from the Adriatic Sea (far right) (Photo: Oettel, 2006).

2.6 Pedology

The development of soils always depends on the interaction of several factors, e.g. underlying geology, prevailing climatic conditions, topography, vegetation etc. The research area has very variant conditions, which means that the soils are highly diverse.

To give an account of the distribution of soils in Albania proves difficult, not due of a lack of data, but because the system used differs significantly from internationally accepted ones such as the FAO soil classification (FAO-UNESCO, 1974), and the USDA Soil Taxonomy (Soil Survey Staff, 1998). The latest attempt to convert the national system of soil classification into other well-known systems was conducted in 2001, when the distribution of soils was mapped according to WRB guidelines (World Reference Base for Soil Resources) (Zdruli et al., 2003: 41). The following information of the major soil groups of the research area have been extracted from the “Soil Map of Albania” at a scale of 1: 250,000 (fig. 14).

Formed mainly during the Quaternary as a result of sea-river interaction, the soils of the coastal lowlands are commonly Fluvisols, associated with Gleysols and Histosols. To the east, in the coastal hills and highlands, the most widely spread soils are Cambisols, also associated with Leptisols, which are severely eroded in some places.

Cambisols, previously referred to as “brown soils”, commonly occur in a wide variety of environments in association with many kinds of vegetation. Pedogenic processes are evident from colour development and/or structure formation below the surface horizon. Within the research area, Cambisols are widespread on the flysch and carbonate-rich rock formations of the Shite-Veles and Skanderbeg Mountains. Naturally covered by forests, they can be very productive agriculturally, but high rates of erosion threaten any sustainable use.

Leptisols, formerly known as “Rendzinas”, are characteristic for Mediterranean environments on limestone terrain (Robinson, 1970). In the research area, they are found on limestone ridges of Mali Rrenci and Mali Kakarriqi, where the soil has been eroded to such an extent that the bedrock is very near the surface (fig. 14). Limited pedogenic development means that Leptisols are typically shallow soils, consisting of very gravely or strongly calcareous material. They are usually scarcely vegetated by shrubs and maquis elements.

In our research area, the most widespread soils are Fluvisols, which were commonly called “Alluvial soils” according to the older classification. They cover large areas in the periodically

flooded alluvial plains (Drini delta plain, Zadrina plain and Merqia plain), alluvial fans, and river valleys (fig. 14). They show layering of the sediments rather than pedogenic horizons. Their characteristics and fertility depend on the nature and sequence of the sediments and length of periods of soil formation after or between flood events. The Fluvisols in the Lezha region are generally very productive when drained.

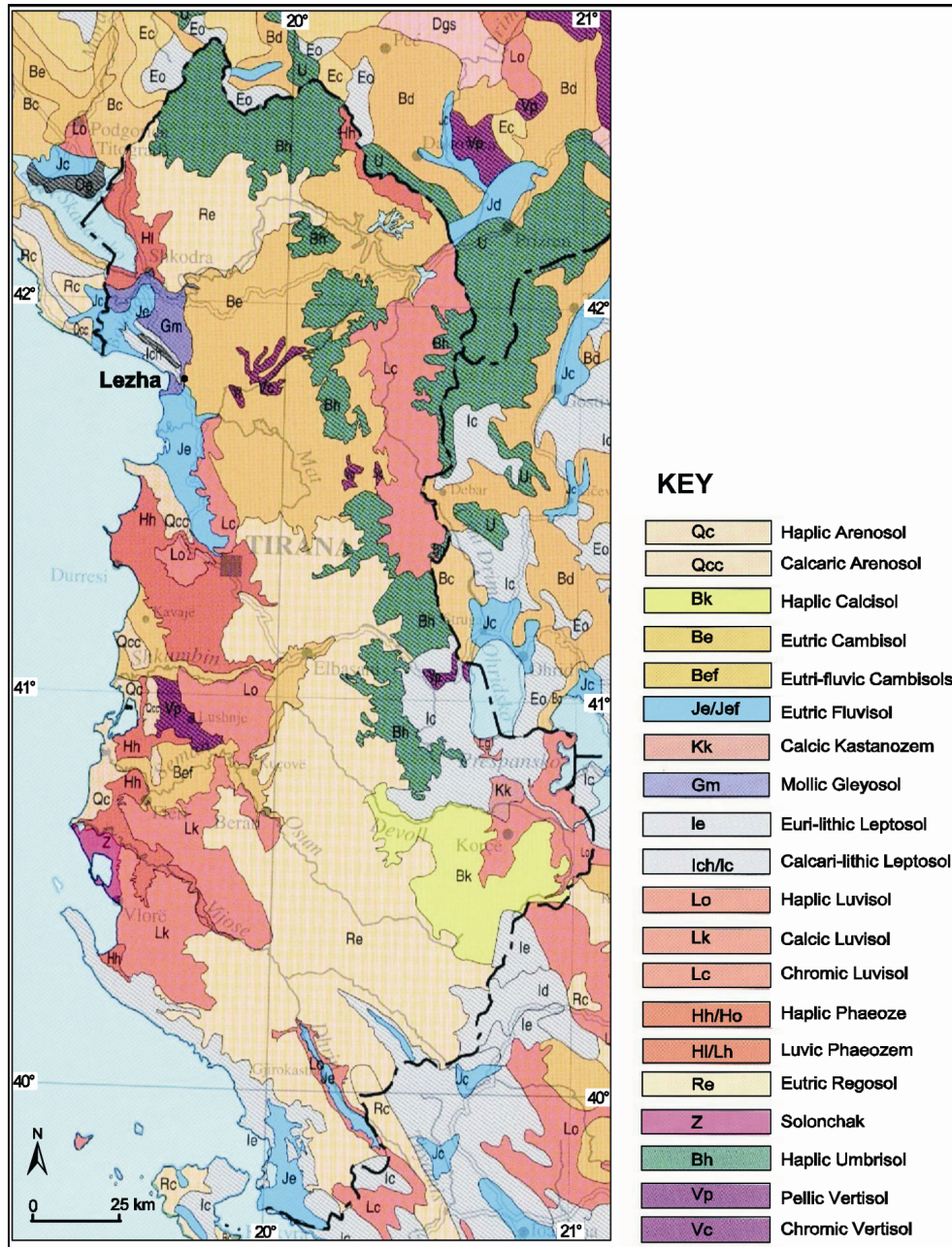


Figure 14: Soil map of Albania (slightly changed from Zdruli, 2005, p.40).

Gleysols occur mainly in swampy lowland areas (around the coastal lagoons) where the groundwater is close to the surface and the soil is saturated for long periods of time (fig. 14). In the research area, gleysols occur in the swampy areas around the Ceka and Merxhani lagoons and the Balldreni plain. Gleysols are typically bluish-grey in colour due to predominantly

reductive conditions, and are generally not well drained; they need intensive management before they can be used.

Histosols cover a relatively large area in the Balldreni plain (former swamp) between Mali Rrenci and Mali Kakarriqi, and are composed mainly of organic material (fig. 14). Their colour is usually black or very dark brown, they contain recognisable plant remains. During their development, organic matter production exceeds the rate of decomposition. Decomposition is retarded mainly by low oxygen (anaerobic) conditions, resulting in the accumulation of only partially decomposed organic matter.

The main factors limiting agricultural production around Lezha are increased salinisation, the stony nature of the soils, as well as the extremely high rates of erosion in the hinterland, caused to a large degree by overgrazing and deforestation.

2.7 Vegetation

The vegetation of an area is closely linked to the climate, topography, soils and bedrock. In the case of the Mediterranean region, another important aspect influencing the natural vegetation for many millennia is the presence and the activities of people.

2.7.1 General vegetation of Albania

The vegetation of Albania, too, has been altered by human impact to a large degree, and therefore a distinction should be made between the naturally occurring vegetation – today only small remnants of the natural vegetation still exist in the higher mountains – and the vegetation types resulting from various degrees of use and degradation through anthropogenic impacts (see chapter 3.3).

Markgraf (1932) was the first to map the vegetation patterns of Albania. He created six distinct vegetation zones, taking into account the different altitudes, as well as combining his observations with the geomorphologic classification of the country by Louis (1927) (see fig. 15). Thereby it becomes clear that the vegetation of Albania changes considerably from north to south and from east (mountains) to west (coast) (Jakucs, 1967). Particularly notable is the fact that in the south of the country Mediterranean species dominates the vegetation up to the peak of the mountains while in the north Central European species make up the vegetation, at least at higher altitudes (Markgraf 1932: 2). In principle, Markgraf's work is still applicable to date.

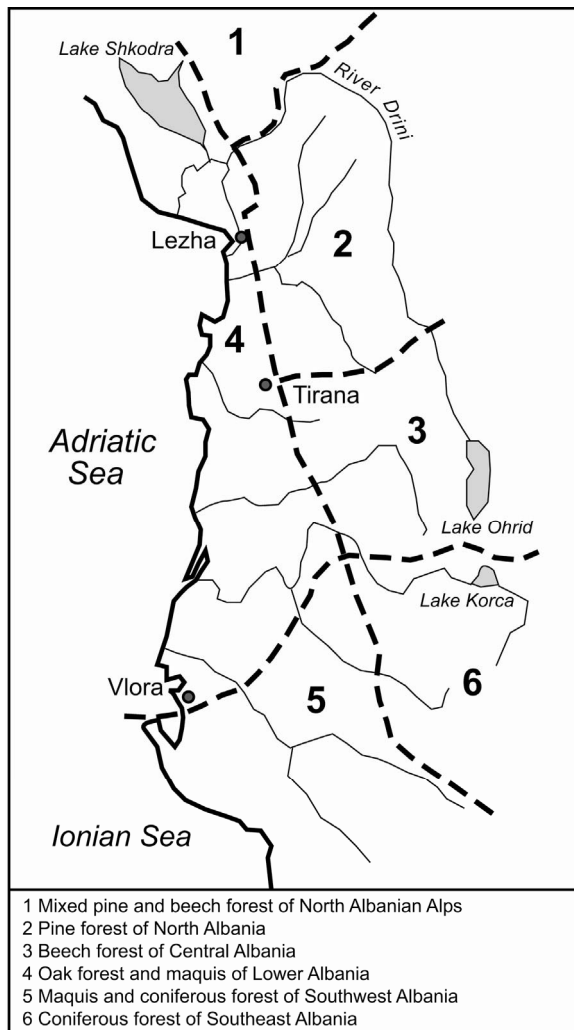


Figure 15: Vegetation zones of Albania (adapted from Markgraf, 1932, p. 91, fig. 20).

The second detailed work which also includes Albania has been done by Horvat et al. (1974). The “Vegetation Map of Southeast Europe” (scale 1:3,000,000) displays general vegetation zones and their sub-zones, characterised by special sub-alliances or associations (Horvat et al. 1974: appendix). The classification used is very closely linked to climate and geology. Horvat et al. divided North Albania into four main vegetation zones: Along the coast lowlands lies a narrow belt of the Mediterranean evergreen forest (*Orno-Quercetum* Adriatic sub-zone). Towards the east, the low-elevated hills as well as the slopes of the mountains are characterised by sub-Mediterranean deciduous forest (*Ostryo-Carpinion* Adriatic sub-zone). Oak dominated continental deciduous forest (*Quercetum petraeae* sub-zone) can be found at the slopes of the mountains farthest inland.

The vegetation at the top of these mountains is made up of Central European mountainous beech-fir forest (*Fagion moesiacum* zone) [Horvat et al., 1974: appendix (Beilage: Vegetationszonen Südosteuropas)].

2.7.2 Vegetation of the research area

Altitude plays a significant role in determining the vegetation within the research area. Therefore this subchapter is divided into two main vegetation zones according to their altitude: (i) highlands (200-1250 m), and (ii) coastal lowlands (0-200 m). The delta plain (iii) is dealt with separately due to its difference in edaphic conditions.

2.7.2.1 Vegetation of the highlands around Lezha

Demiraj et al (1996: 161) seem to agree with Horvat et al. (1974) in that they also propose the vegetation around Lezha from 200 m to 1250 m a.s.l. to be dominated by sub-Mediterranean deciduous forest, especially oak species and hornbeam (table 3). Markgraf (1932: 37) categorised this type of vegetation as *Quercus pubescens* – *Carpinus orientalis* forest. Some maquis and garrigue elements (shrubs) are common on calcareous bedrock (e.g., on Mali Rrenci and Mali Kakarriqi) as well as at lower altitudes of the Shite-Veles and Skanderbeg Mountains. However, the Mediterranean species totally disappear above 800 m. Then, the forest becomes drier, consisting of mainly pine with some oak species (up to 1200 m). Black pine (*Pinus nigra*) is indicative of serpentine bedrock, while Bosnian pine (*Pinus heldreichii*) grows typically on limestone bedrock (Markgraf, 1932: 57). Towards the east, at an increasing altitude of up to 1900 m, black pine, common beech (*Fagus sylvatica*) and silver fir (*Abies alba*) dominate the vegetation.

Latin Name	Common Name	Latin Name	Common Name
<u>Deciduous trees</u>		<u>Evergreen high shrubs</u>	
<i>Quercus petraea</i>	Sessile Oak	<i>Quercus coccifera</i>	Kermes Oak
<i>Quercus pubescens</i>	Downy Oak	<i>Juniperus oxycedrus</i>	Prickly Cedar
<i>Quercus frainetto</i>	Hungarian Oak	<i>Forsythia europaea</i>	European Forsythia
<i>Quercus cerris</i>	Turkey Oak	<i>Acer platanoides</i>	Norway Maple
<i>Quercus macrolepis</i>	Valonia Oak	<i>Ligustrum vulgare</i>	Wild Privet
<i>Quercus trojana</i>	Macedonian Oak	<i>Buxus sempervirens</i>	Common Box
<i>Carpinus orientalis</i>	Oriental Hornbeam	<i>Ilex aquifolium</i>	Holly
<i>Ostrya carpinifolia</i>	Hop Hornbeam		
<i>Fraxinus</i> sp.	Ash	<u>Climbers</u>	
<i>Acer tataricum</i>	Tartarian Maple	<i>Clematis vitalba</i>	Clematis
<i>Salix incana</i>	Willow	<i>Lonicera caprifolium</i>	Perfoliate Honeysuckle
<i>Robinia pseudoacacia</i>	Black Locust		
<i>Prunus mahaleb</i>	Rock Cherry	<u>Herbaceous perennials</u>	
<i>Corylus avellana</i>	Hazelnut	<i>Salvia officinalis</i>	Shop Sage
<u>Deciduous shrubs</u>		<i>Siderites raiseri</i>	Mountain Tea
<i>Ulmus</i> sp.	Elm	<i>Phlomis fruticosa</i>	Jerusalem Sage
<i>Colutea arborescens</i>	Bladder Senna	<i>Daphne cneorum</i>	Garland Flower
<i>Rubus</i> sp.	Blackberry		
<i>Rosa canina</i>	Dog Rose		

Table 3: Species composition for vegetation above 200 m altitude (slightly changed, after Demiraj et al., 1996: 161).

2.7.2.2 Vegetation of the coastal area

Along the Albanian coast, the vegetation is dominated by Mediterranean evergreen forest as shown on the map by Horvat et al. (1974). However, Demiraj et al. (1996) point out that the composition of species changes considerably in the Vlora Region of Central Albania. They agree that south of Vlora, evergreen forests mostly consist of sclerophyll, narrow-leaved maquis elements associated with holm oak (*Quercus ilex*) due to the dry climatic conditions. Conversely, north of Vlora, the increasing humidity causes the coastal vegetation to be

dominated by mixed broad-leaved deciduous forests with only some evergreen elements such as kermes oak (*Quercus coccifera*) (Demiraj et al., 1996).

Latin Name	Common Name	Latin Name	Common Name
<u>Deciduous trees</u>		<u>Evergreen high shrubs</u>	
<i>Quercus trojana</i>	Macedonian Oak	<i>Quercus coccifera</i>	Kermes Oak
<i>Quercus pubescens</i>	Downy Oak	<i>Laurus nobilis</i>	Bay Laurel
<i>Quercus robur</i>	Pedunculate Oak	<i>Olea europaea</i>	Olive
<i>Quercus cerris</i>	Turkey Oak	<i>Arbutus unedo</i>	Strawberry Tree
<i>Quercus macrolepis</i>	Valonia Oak	<u>Deciduous shrubs</u>	
<i>Carpinus orientalis</i>	Oriental Hornbeam	<i>Ulmus foliacea</i>	Common Elm
<i>Ostrya carpinifolia</i>	Hop Hornbeam	<i>Paliurus spina-christi</i>	Christi's Thorn
<i>Acer</i> sp.	Maple	<i>Rubus</i> sp.	Blackberry
<i>Fraxinus ornus</i>	Manna Ash	<i>Rosa</i> sp.	Wild Rose
<i>Pistacia terebinthus</i>	Turpentine Tree	<i>Punica granatum</i>	Pomgranate
<i>Amygdalus communis</i>	Almond		
<i>Pyrus</i> sp.	Pear		
<i>Cornus</i> sp.	Cornel		
<i>Cercis siliquastrum</i>	Judas Tree		
<i>Populus alba</i>	White Poplar		
<i>Alnus glutinosa</i>	Common Alder		
<i>Platanus orientalis</i>	Oriental Plane		
<i>Salix viminalis</i>	Willow		
<i>Eucalyptus camaldulensis</i>	River Red Gum		

Table 4: Species composition of the coastal lowlands (up to 200 m) (slightly changed, after Demiraj et al., 1996: 161).

Around Lezha, these typical, deciduous forests are widespread: from the Shengjin spit at sea level to the slopes of Mali Rrenci and Mali Kakarriqi, as well as on the lower slopes of the mountains and hills near Lezha (up to 200 m) (Demiraj et al., 1996: 87). The vegetation also contains occasional maquis and garrigue elements typical for evergreen forests of the Mediterranean; however, these elements are not dominant as suggested by Horvat et al. (1974). Overall, this zone as defined by Demiraj et al. (1996) is concordant with the “Macchien-Schbiljak-Stufe” of Markgraf (1932: 5), which comprises riparian forest, deciduous forest (Croatian: Šibljak) and oak forest (*Quercus pubescens*). Šibljak seems to be the transition between riparian forest and oak forest along the entire Albanian coast (Markgraf, 1932: 54). However, it is worth emphasising that on a more local scale, differences in edaphic conditions have an important influence on the vegetation type, and species assemblages can vary accordingly.

2.7.2.3 Vegetation of the Drini delta plain

It seems an impossible task to determine the natural climax vegetation of the Drini delta plain. Especially in recent times it has been subject to dramatic alterations by people. Firstly, it has been drained and used intensively for cultivation. Secondly, the small belt-like area along the coast, which had been protected during communist times, is now also threatened by uncontrolled expansion of the settlements nearby.

Today's vegetation is controlled by the artificially generated ecological conditions on the coastal plain. Edaphic factors such as alkalinity/acidity of the soils, salinity, as well as high groundwater levels and the interface between fresh- and saltwater determine the composition of plants which consist mostly of hydrophilic and halophilic species.

The large sandy island, including the Shengjin sand-spit, separating the Merxhani Lagoon from the sea is covered in riparian forest, which consists of deciduous trees, bushes, and a rich understorey flora. The dominant tree species are Common Alder (*Alnus glutinosa*), Narrow-leaved Ash (*Fraxinus angustifolia*), Field Elm (*Ulmus minor*), Pedunculate Oak (*Quercus robur*) and White Poplar (*Populus alba*) (Demiraj et al., 1996). This forest is one of the oldest nature protection areas in Albania, known also as Kune Reserve. However, the recent building activities (hotels etc.) seem to indicate that its protection status has diminished.

On the delta plain, along the banks of the river Drini and the margins of the lagoons, floral assemblages are dominated by Salt Cedar (*Tamarix* sp.) and Common Privet (*Ligustrum vulgare*) which can tolerate high salinity. Reed (*Phragmites communis*), Sea Club-rush (*Scirpus maritimus*) and Cattail (*Typha angustifolia*) can also be found (Demiraj et al., 1996).

Sandy marshes around the coastal lagoons are covered with a layer of salt during the summer due to evaporation. High salinity and the ground water table being very close to the surface cause these areas to be dominated by hydrophilic and halophilic species such as Glasswort (*Salicornia fruticosum*) and Common Sea Lavender (*Limonium vulgare*) (Demiraj et al., 1996).

Despite the slightly lower groundwater level further inland, a composition of hydrophilic species can still be observed, comprising Sea Rush (*Juncus maritimus*), Spiny Rush (*Juncus acutus*), Opposite Leaved Saltwort (*Salsola soda*), Chaste Tree (*Vitex agnus-castus*) and Salt Cedar (*Tamarix* sp.) (Demiraj et al., 1996).

The man-made forests on the Shengjin sand-spit principally consist of Mediterranean conifers, comprising Aleppo Pine (*Pinus halepensis*), Stone Pine (*Pinus pinea*) and Maritime Pine (*Pinus pinaster*) (Demiraj et al., 1996). These areas were afforested between 1971 and 1976. Today they are threatened by coastal erosion as well as salinisation of the ground water due to marine ingression (photo 8).



Photo 8: Coastal erosion threatening the forests on the Shengjin sand-spit. (Photo: Uncu, 2006)

Large floodplain forests on the delta plains of the Drini and the Mati were noted by travellers since the 19th century. Wiet (1866) described forests consisting of pines, sessile oaks, firs, beeches, elms, junipers, limes, and poplars on the plain of Berdloja between Drini and Mati. From the southern banks of the Mati to Tirana, a large forest dominated by different kinds of oak, elm and ash species was noticed by Ippen (1907a: 63). A few kilometres south of Alessio (Lezha), Nopcsa (1929a: 199) writes about a “Sumpfwald” (bog forest) in the Bregumatja plain consisting of willows, alders, oaks, ashes and poplars associated with reeds, duckweed and waterplantain. This large forest was already categorised as “Uferwald” (riparian forest) by Markgraf’s map in 1931.

Meanwhile, these forests are gone. The area was cleared, drained and transformed to arable land. Nowadays, the Drini, Balldreni, Zadrime and Merqia plains are exploited for various kinds of crops (wheat, maize, millet, barley, oat), vegetables (potatoes, beans) as well as tobacco and sun flowers. Lezha is particularly famous for its watermelon (*Citrullus lanatus*). There is no citrus plantation around Lezha due to the cold Bora winds. Also, olive and fig production is not commercially carried out in this region. Olive trees can be found as a wild form within the maquis communities. In contrast, the grape vine (*Vitis vinifera*) has been cultivated in Lezha as early as Hellenistic times.

Although the forests have largely disappeared, the name of the city, Lezha, derived from older versions such as *Lissitan*, *Lissos*, *Lisso*, *Lissum*, has survived. The etymological root of these

names is “*Lis*”, an Albanian word of Illyrian origin, meaning “oak” (Guraziu, 2006: 84) – a definite hint at what type of vegetation was once found in this area. However, the vegetation history will be discussed in much more detail in the next chapter.

3 History of vegetation

It has been known for a long time that the present-day vegetation of the Mediterranean region is the result of climatic oscillations and human impact since the Last Glacial Maximum. However, little has been published as yet about the Holocene vegetation and climatic changes in Albania.

3.1 Applicability of early research

A general overview of the vegetation history across the Balkan Peninsula was published by Willis (1994), but information from Albania was lacking. The first published data, relevant for Albania, was based on the Konispol Cave near the border to Greece during the second half of the 1990s. By measuring the magnetic susceptibility (MS) of the cave sediments, Ellwood et al. (1996; 1997) obtained information about the palaeoclimatic changes in Southern Albania between 9,000 and 3,000 BP.

The number of publications on the vegetation history of Albania as a whole increased during the last decade. Recent publications include the vegetation and climate history around Lake Maliq and the Korça Basin in SE Albania for the last 16,000 years (Denèfle et al., 2000; Fouache et al., 2001; Bordon et al., 2009). These sites are located much further inland at a higher altitude in the southeast of Albania; they do not lend themselves very easily for a comparison and connection with our research area around Lezha.

In addition, the availability of similar information for the coastal regions is rather limited. The only pollen records for coastal Albania come from the geological vibracoring taken in former lagoons around the ancient cities of Butrinti (Lane, 2004) and Apollonia (Fouache et al., 2010). However, there are two main obstacles when trying to apply the data from the two coastal sites to our research area:

(a) Lake Bufi near Butrinti is situated in the extreme south of Albania where climatic conditions (as mentioned in chapter 2.4) are very different and, therefore, the representativeness of the natural vegetation is very limited; one has to be careful when drawing conclusions applying these data to our study area.

(b) The pollen spectrum from the Seman delta near Apollonia in Central Albania, about 40 km north of Vlora, is more applicable to our research, mainly because the flora represents a transition from the genuine Mediterranean vegetation towards the south (evergreen elements, e.g., *Quercus ilex*) to sub-Mediterranean elements north of this region (deciduous ones, e.g.,

Quercus pubescens) (fig. 16). However, this pollen record is rather fragmentary and provides only general information without further comments.

3.2 History of vegetation in connection with climatic changes

Due to the lack of available data for coastal Albania, better researched locations in relatively close proximity need to be considered for this study. Research on the vegetation and climate history of the Dalmatian coast of Croatia (Central Adriatic) has been carried out by palynologists for nearly 50 years (Beug, 1961; 1967; Jahns & van den Bogaard, 1998; Jahns, 2002). Data on the vegetation history of Italy's Adriatic coast are available from coastal pollen sequences taken on the Gargano headland (Caroli & Caldara, 2007; Caldara et al., 2008), from the Tavoliere Plain (Caldara et al., 2003) and from the Lago Alimini Piccolo (Di Rita & Magri, 2009). Additional information concerning the late Quaternary to late Holocene climatic conditions was obtained from south Adriatic marine cores (Rossignol-Strick, 1992; Zonneveld, 1996; Oldfield et al., 2003; Piva et al., 2008) and coastal records from the Ionian Sea of Greece (Jahns, 2005; 2009).

The results of the studies mentioned above were integrated in the latest publication of Bordon et al. (2009), according to whom the climate and vegetation history of Albania since 16,000 BP can be divided into four climatic periods. However, their conclusions are based on data from SE Albania (Lake Maliq, ca. 800 m a.s.l.).

- (a) The Oldest Dryas (16,000 \pm 200 to 15,100 \pm 200 BP) is characterised by a cold and dry climate with an open steppe vegetation dominated by *Artemisia*, Chenopodiaceae and Poaceae (Zonneveld, 1996; Bordon et al., 2009). The steppic vegetation phase of the Last Glacial period had already been described by Bonatti (1966) for entire Northern Mediterranean.
- (b) The Bølling – Allerød interstadial (15,100 \pm 200 to 12,800 \pm 50 BP) was a temperate climatic period with deciduous forests consisting mainly of *Betula*, *Pinus* and deciduous *Quercus* associated with some steppe elements (Zonneveld, 1992: 92; Bordon et al., 2009). In contrast, Bonatti (1966) had noted a cool and humid climate with grassland (Gramineae) until 12,000 BP.
- (c) The Younger Dryas stadial (12,800 to 11,300 BP) is dominated by cold and dry climatic conditions with cold herbaceous steppe elements (*Artemisia*, Chenopodiaceae, *Hippophaë*, *Ephedra*), similar to the ones of the Oldest Dryas stadial (Denèfle et al.,

2000; Bordon et al., 2009). In contrast, Zonneveld (1992) reports the occurrence of a forest with *Pinus*, *Abies*, *Juniperus*, *Betula* in the region between 13,000 and 11,000 BP. Bonatti (1966) had noted cool humid climatic conditions and the presence of *Corylus* with grassland elements, assuming that *Corylus* preceded the establishment of the *Quercus*-dominated forest during the Post-Glacial.

- (d) Remarkably stable climatic conditions associated with a temperate deciduous oak forest is characteristic for Albania from 11,300 to 420 BP (Bordon et al., 2009). During this period, *Fagus*, *Ulmus*, *Tilia*, *Corylus*, *Carpinus*, *Fraxinus*, *Alnus*, *Betula*, *Abies*, *Pistacia* became important elements of the vegetation. Zonneveld (1996) also suggests the spreading of deciduous oak forest over the Adriatic region after 10,000 BP.

Bordon et al. (2009: 26) subdivided the last period (d) further by pointing out the occurrence of two distinct phases. The first one between 8,300 and 8,100 BP is marked by a rapid increase of steppic species (Poaceae pollens) due to colder and more arid conditions (Bordon et al., 2009). According to the authors, this is the Albanian reflection of the so-called 8.2 ka event which has been attributed to the final outburst flood of Lake Agassiz into the North Atlantic via the Hudson Strait (e.g., von Grafenstein et al., 1998; Barber et al., 1999).

The other major change in terms of vegetation according to Bordon et al. (2009) began about 1,000 BP and is still ongoing. It can probably also be attributed to human activities rather than being solely caused by climatic factors, although it is worth noting that large fluctuations in both temperature and precipitation are associated with this phase. However, the last 1,000 years are characterised by the development of cultivated taxa such as *Cerealia*-type and *Olea* sp. (Bordon et al., 2009: 26).

The last period (d) described by Bordon et al. (2009) needs to be looked at in more detail. This can be done by considering results from other locations around the Adriatic Sea and by linking developments revealed at Albanian sites to trends observed further away. It is important to be aware of the dividedness amongst researches. Such disagreement might have been caused by the variety of approaches as well as by the different localities examined.

During the first part of the Holocene (ca. 11,000-7,500 BP), except the above mentioned cold event, the climate was warmer and more humid than at present around the entire Mediterranean (Bonatti, 1966; COHMAP Members, 1988; Jalut et al., 2009). This was favourable for the spread of deciduous oak forests accompanied by other deciduous taxa. Pollen records from the

Lake Maliq also show the higher percentage of *Alnus*, *Salix*, *Fraxinus*, *Abies*, *Corylus*, *Tilia* between ca. 9,200 and 7,350 yrs BP (Denèfle et al., 2000: 426) (fig. 15).

Many pollen records from southern Europe reflect the onset of the modern Mediterranean climate from 7,500 to 5,000 BP (Magny et al., 2002; Jalut et al., 2009). This period can be considered as a transition phase from the relative humid early Holocene to increasingly arid climatic conditions (Jalut et al., 2009). In the central Mediterranean region the mid-Holocene (6,000-4,000 BP) is characterised by the spreading of oak-dominated vegetation, including both deciduous and evergreen species (Rita & Magri, 2009: 301). In fact, the dominant vegetation seems to change from deciduous broad-leaved trees to evergreen sclerophyllous taxa at lower altitudes (Jalut et al., 2000: 13). Sadori (2007: 2770) suggests that strong changes towards typically Mediterranean vegetation took place in entire Mediterranean basin with the rise of sclerophyllous taxa around 5,000-4,500 yrs BP. In the Korça Basin, *Abies*, *Carpinus orientalis/Ostrya* and *Fagus* increase, whereas *Corylus*, *Alnus* and *Salix* decrease due to drier climatic conditions around ca. 4,500 BP (Denèfle et al., 2000: 426).

The crucial transition from the mid to late Holocene (4,300-3,800 BP) is characterised by short-lived wet and dry climatic phases. Magny et al. (2009) present several pieces of evidence such as lake-level changes and volcanic eruptions from sediment sequences of Lake Accesa in Tuscany and Lake Maliq, indicating drier climatic conditions ca. 4,100-3,950 BP. A severe drought event around 4.2 ka, recorded in a cave flowstone in central western Italy (Alpi Apuane karst), has been suggested by Drysdale et al. (2006). This episode may be a reflection of the “4.2 ka event” which has been observed from Africa to Tibet, apparently causing the collapse of Old World civilisations around 4,000 BP (Weiss et al., 1993; Dalfes et al., 1997; Mayewski et al., 2004; Di Rita & Magri, 2009; Magny et al., 2009).

3.3 Human impact on the vegetation

In addition to the onset of drier climatic conditions, increasing human impact on the Mediterranean vegetation is also recorded in the different pollen records in Italian and Balkan coastal sequences (Jahns & van den Bogaard, 1998; Jahns, 2005, 2009; Caroli & Caldara, 2007; Di Rita & Magri, 2009; Colambaroli et al., 2009), in marine cores (Zonneveld, 1996; Rossignol-Strick, 1998; Oldfield et al., 2003; Piva et al., 2008), as well as inland areas of Albania (Denèfle et al., 2000; Fouache et al., 2001) and northwest Greece (Willis, 1992a, b; Lawson et al., 2004) from around 4,500 BP until today.

Forest clearances and fires for cultivation as well as overgrazing probably caused an increase of shrubs and macchia elements in the vegetation. Pollen records from Lake Maliq show that in SE Albania human impact on the natural vegetation began ca. 4,500 BP, when the first indicators of cultivation – rising percentages of *Cerealia* and *Juglans* together with Mediterranean species such as *Quercus ilex* and *Olea* spp. appeared (Denèfle et al., 2000: 426) (see fig. 16). Along coastal Albania, however, deforestation began with the foundation of Illyrian settlements (ca. 4,000 BP). Lane (2004: 43) mentions that the ratio of arboreal pollen to non-arboreal pollen shifts in favour of the latter due to increasing human impact in the Butrinti area after 3,800 BP, which meant that the natural vegetation was replaced with cultivated species. Due to the onset of the cultivation of *Olea* (Pollen zone 5) from 3,600 to 2,600 BP, Lane (2004: 43) concludes that deforestation must have taken place around Butrinti at that time. Jahns & van den Bogaard (1998) also assume extensive deforestation because of increasing pollen amounts of cultivated species (*Pinus halepensis*, *Castanea*, *Ceratonia*, *Juglans*, *Platanus*, *Punica*, as well as *Olea*, *Secale* and *Juniperus*) from the southern Dalmatian coast around 3,000 BP (1,300 cal BC) or even earlier.

During the Greek colonisation period (ca. 2,600 BP) and following Roman times, a strong human impact on the natural vegetation is well noticeable at the pollen sites from the entire Adriatic coast. The amount of grape seeds found within the archaeological layers suggests that grapes were cultivated on the slopes of the hills and mountains around Lezha during Hellenistic and Roman times. Numerous pieces of amphorae were unearthed during the Lissos excavations, pointing towards wine consumption/production. Along the Dalmatian coast, much of the forest had also been cleared for timber export or to expand the areas available as pastures or for the production of cereals during Roman times (Kranjc, 2009). These activities also triggered soil erosion, which led to a more rapid delta progradation along Mediterranean coasts (Brückner, 1986; Brückner & Hoffmann, 1992; Bintliff, 2002).

One would assume that human activities must have had a continuous impact on the natural vegetation in the whole of Albania during Byzantine and Venetian times. However, pollen analyses of the peat layers from the Drini delta show the re-establishment of deciduous forest during the 11th – 13th centuries AD (see chapter 7.5). This is supported by the existence of various types of arboreal pollen in the pollen diagram for the Seman Delta, dated to the 10th – 13th centuries AD (Fouache et al., 2010: 121) (fig. 17). This can be interpreted with the existence of more humid climatic conditions during the “Little Climatic Optimum” (between 900 and 1,200 AD) and rather less anthropogenic activities in the following “Little Ice Age”. More humid climatic conditions in the Mediterranean area may be indicated by the increasing accumulation of young alluvial deposits from the 13th to 17th centuries AD (Vita-Finzi, 1969).

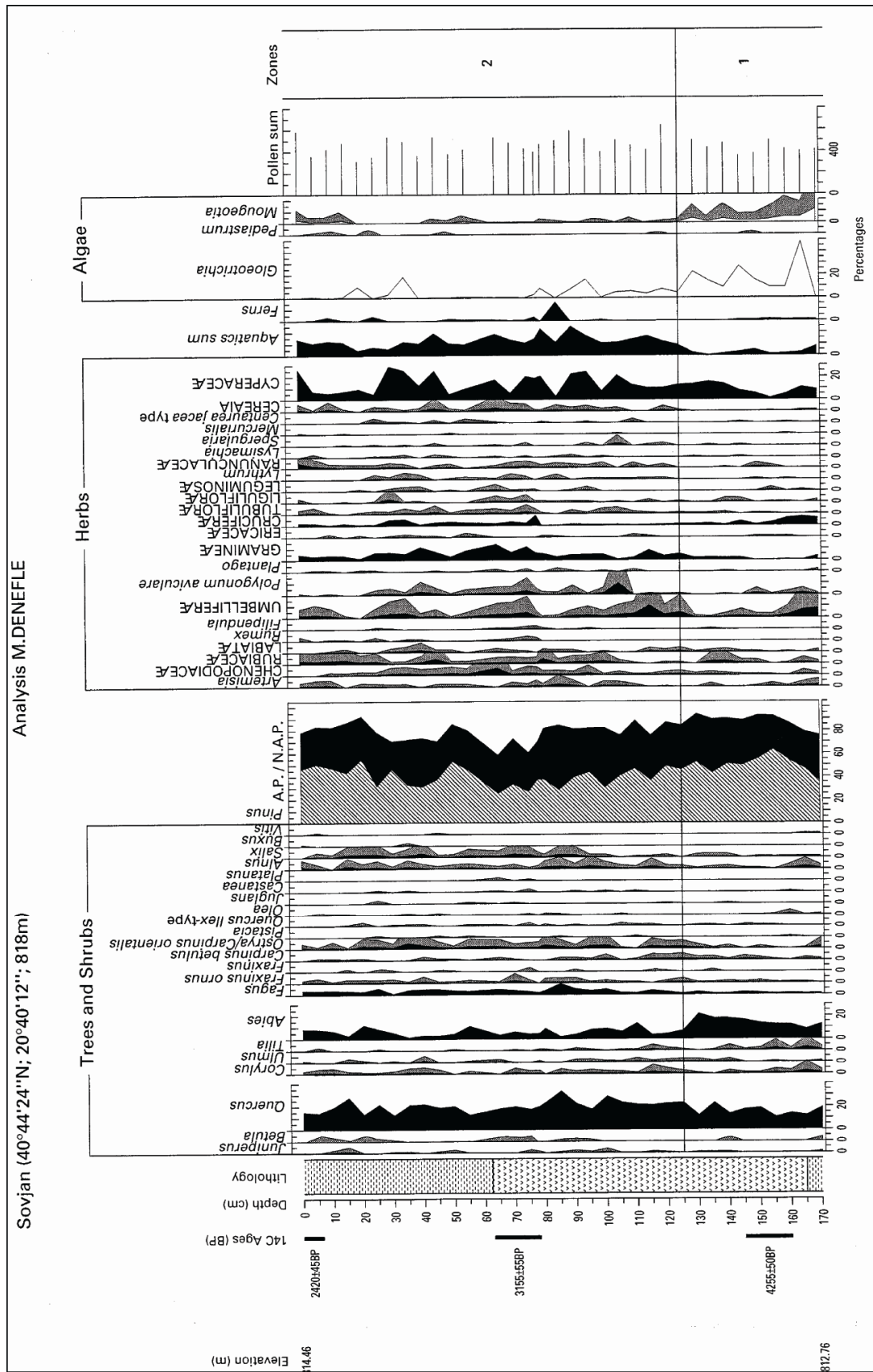


Figure 16: Simplified pollen diagram for Sovjan, southeastern Albania (Fouache et al., 2001, p. 82, fig. 4).

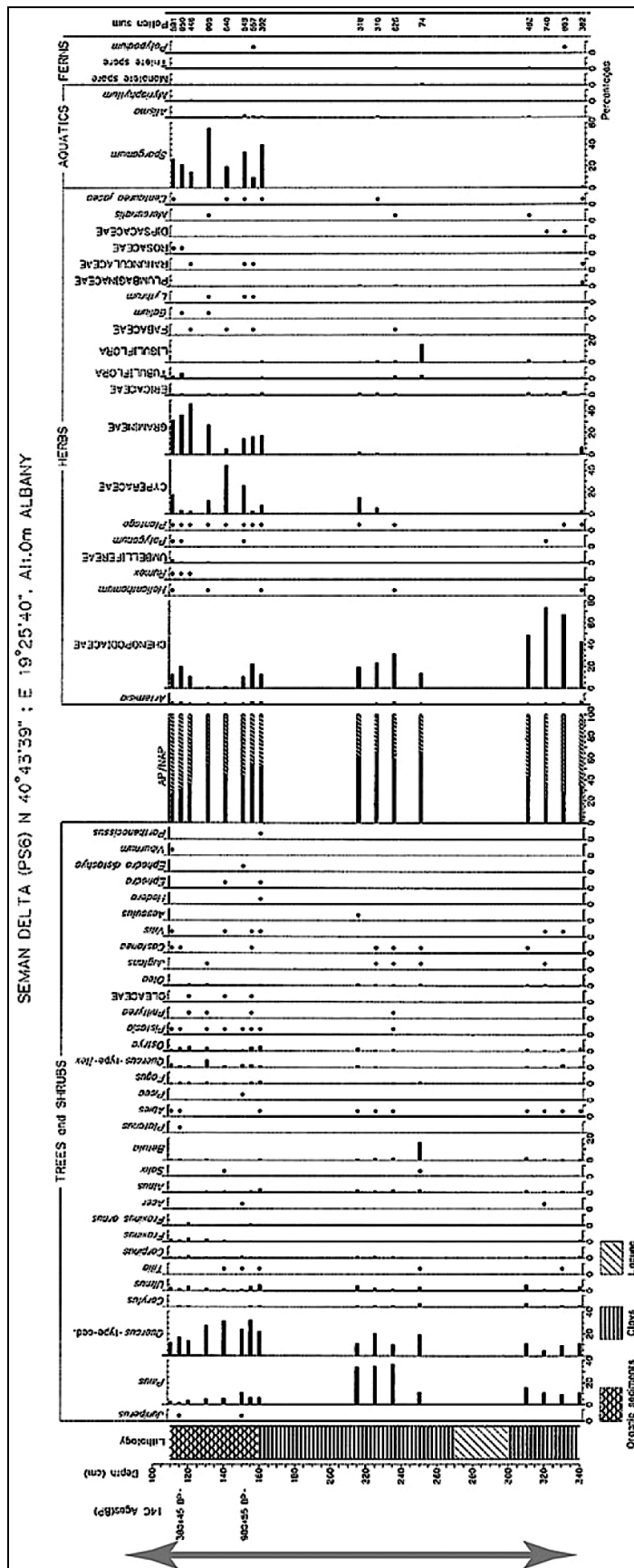


Figure 17: Pollen diagramme for the Seman delta, Central Albania (Fouache et al., 2010, p.126, fig. 11).

Historical records document that the main deforestation period in Albania began during Venetian times and most of the oak forests in the southern part of the country were cut for ship building purposes (Zdruli & Lushaj, 2001: 92). Wood was one of the most important export goods for Albania, including Lezha. However, the sources indicate the existence of expansive forests during the following centuries. In an Italian source from 1570, the vegetation of Albania is described as follows: “*Albania being everywhere very rich in all types of wood. On the coast in particular and along the rivers, it is full of forests and of wood suitable for every sort of work and for all types of vessels, big and small, as well as for large fleets.*” (cf. Elsie, 2003: 64).

After the Turkish invasion at the beginning of the 16th century, the highlands around Lezha were densely settled and utilised for economic activities such as agriculture and the raising of livestock. This must have led to dramatic

changes of the natural vegetation, though there is no palynological data available to support this idea.

The next phase of destructive deforestation in Albania was carried out by Italian companies during World War I (Bosworth, 1974). In addition, the slopes of the low-elevated coastal hills were cleared of its natural vegetation for horticulture (citrus, olive, wine etc.) during the second half of the 20th century (Demiraj et al., 1996).

The modern names of some places in coastal Albania, such as Shkozet (Albanian for: hornbeam forest) or Orikum (Albanian for: port of wood) may be evidence for the disappeared forests (Demiraj et al., 1996). Over the last decades, the few remnants of natural vegetation in the highlands of Albania have been seriously threatened by uncontrolled human activities.

4 Historical background of Lezha and its environs

Lezha, in Hellenistic times known as Lissos, was one of the earliest Illyrian settlements, together with Scodra (modern name: Shkodra, in Albanian: Shkodër) and Epidamnus (modern name: Durrës) in North Albania. During its time of prosperity, in antiquity, Lissos itself was a harbour city (see chapter 8.8). Today, the ruins of ancient Lissos are located 8 km inland at the centre of modern Lezha (Shuisky, 1985).

4.1 From the early beginnings to the end of antiquity

A late Palaeolithic dwelling at Konispol Cave (5 km away from Butrinti, southern Albania) provides the earliest records of human activities in Albania. The Neolithic and Chalcolithic periods are relatively well documented in the valleys (e.g., Black Drini) and former lake basins (e.g., dried-up Lake Maliq) in the eastern part of the country. However, neither Palaeolithic nor Neolithic and not even Chalcolithic settlements have been reported from coastal North Albania. Only some bone and flint tools have been found in a small cave at Gajtan near Shkodra, and dated to 6,000 BC (Mesolithic period) (Jacques, 1995: 4). Bronze Age settlements have been relatively well documented in Northern Albania. Many mound burials (tumuli) on the coastal hills around the Shkodra and Zadrime plains indicate that peoples spread in this area during the Bronze Age.

In the following, prehistoric human activities and historical events in the area around Lezha will be discussed. For a more general archaeological chronology of Albania as a whole, see table 5.

The earliest archaeological find in close proximity of Lezha was discovered in 1983 at Torovica, 13 km north of Lezha. It is a hoard consisting of 123 bronze axes (Andrea, 1983-84: 106), dating to the 9th century BC (early Iron Age) (Ceka, 2005: 42).

Ruins of a fortification encompassing ca. 1.5 ha and dated to the 8th century BC, indicate the existence of an early Iron Age settlement (Gajtan culture) on the ridge of Mali Shelbuemit (Koch, 1989: 140; Lissus Excavation Report, 2004: 3). However, it is not certain, whether Mali Shelbuemit had only been used as refuge in times of danger or as a permanent settlement by some Illyrian clans and tribes. In the 6th century BC, the walls of the early fortification were repaired and a second fortified settlement was built on Lezha Hill (Acropolis), which had a better position by being closer to the sea, trade routes and arable land (Koch, 1989: 140).

This coincides with the colonisation of the Adriatic east coast by Greek traders in the 6th – 5th centuries BC. The Greeks founded settlements on the Albanian coast (e.g., Apollonia,

Epidamnos) and traded with native people as far inland as the Drini valley (Beaumont, 1936; Ceka, 2005). Thus, the rather tribal economic and social structures of the Illyrian communities gradually changed towards being highly organised, with urban centres, due to the Greek influence.

Time period	Archaeol./ Historical period	Historical development and land-use
120,000-10,000 BC	Palaeolithic	Earliest records (artefacts) indicating human presence at Konispol Cave near Butrinti, South Albania.
10,000-6000 BC	Mesolithic	Some animal bones and flint tools in a cave at Gajtan near Shkodra, North Albania. Hunter / gatherer cultures.
6000-2600 BC	Neolithic	Earliest settlements on river terraces and fertile grounds near woodlands in eastern Albania (in the upper and middle parts of the Drini Valley, Korça Plain and Kukes area). Beginning of agriculture and animal husbandry.
2600-2100 BC	Chalcolithic	Rapid expansion of agriculture and animal husbandry. Mining and usage of copper. First signs of a culturally heterogeneous community (pre-Illyrian, sometimes named “Pelasgians”).
2100-1100 BC	Bronze Age	Arrival of the so-called “Steppe-peoples” with their pastoral culture and mound burials (Tumuli). In the western half of the Balkan Peninsula they were integrated by the local people to form the Proto-Illyrian ethnos. Rapid social, economic, and spiritual development. Trade contacts along the Eastern Adriatic Sea as well as with southern Italy, Greece, and along the Danube. Bronze gradually replacing copper. Foundation of fortified settlements at the top of coastal hills (e.g., in the Shkodra plain) during the transition to the Iron Age.
1100-ca.450 BC	Iron Age	Social structuring by Illyrian families forming large groups similar in race, language and culture (e.g., Labeates in Northern Albania). Commercial relations with Aegean cultures beginning in the 8 th century BC (export of wheat, wood, dairy products, silver; import of wine, tableware). Foundation of Doric colonies by Greek traders: Epidamnos in 627 BC, Butrinti ca. 600 BC, Apollonia in 588 BC.
ca. 450-167 BC	Urban phase	Foundation of a Greek-Syracuse colony at Lissos in 385/4 BC. Roman-Illyrian and Roman-Macedonian Wars on Illyrian ground (229 to 168 BC).
167 BC-395 AD	Roman times	Construction of Via Egnatia begins in 148 BC. Civil War between Caesar and Pompey (49-45 BC). From the 1 st century AD, coastal Albania becomes wine production centre and timber is harvested in the mountains on a large scale.
395-1501	Byzantine times	Politic instability due to invasions and rulers of various ethnic groups (Goths, Bulgarians, Slavs, Normans, Serbs, Turks).
1501-1912	Turkish period	After invasion of Durres in 1501, Albania becomes part of the Ottoman Empire. Important changes of the socio-economic structures and settlement patterns in entire Albania. First record of a large flooding event of Drini in 1846. Thereafter, the Drini changed its course to the Buna River. Large earthquake in Shkodra in 1905.
1912-1946	Monarchy/ Republic	End of Turkish rule in Albania. Political instability, changes between Monarchy (1914-1925; 1928-1939) and Republic (1925-1928). Strong Italian influences in political and economic life. Italian invasion during World War II.
1946-1991	Communism	The Communist Regime lead by Enver Hoxha causes isolation of the country from the “Western World”. Organisation of economic and social structures with the help of the Soviet Union and China. Severe earthquake destroys Lezha on April 15 th , 1979.
from 1991	Democracy	Albania opens up to the West. Re-organisation of economical and political structures.

Table 5: Overview of historical and archaeological periods in Albania (L. Uncu, 2010, compiled from: Korkuti, 1983, 1988; Eggebrecht, 1988; Koch, 1989; Korkuti & Petruso, 1993; Jacques, 1995; Wilkes, 1995; Hutchings, 1996; Ceka, 2005).

Arguably, the “urban phase” of Lissos began with the foundation of the city in 385/4 BC by Dionysios the Elder (Diod. Sic., 15, 13, 4), which would mean that Lissos is in fact a Greek-Syracuse colony, rather than an Illyrian settlement. However, scholars are debating whether the “Lissos” mentioned by Diodorus is actually an island off the Croatian coast (today: Issa Island) (for further discussion see Pochmarski & Hoxha, 2005). This debate is fuelled by the lack of archaeological findings (other than foundations of walls) such as ceramics, cultural artefacts and other everyday objects in Lissos. Nevertheless, it is accepted by most scientists that the aim of the colony at Lissos was to control the seaway and therefore the trading routes from the eastern

Adriatic to northwestern Greece (Praschniker & Schober, 1919: 14; Beaumont, 1936: 203; Franke, 1983; Koch, 1989; Ceka, 2005).

Archaeological research shows that the Hellenistic city was arranged on three topographic as well as societal levels: Lower City, Upper City and Acropolis (see fig. 17, chapter 5.4). At the top of the Mali Shelbuemit another fortified site called Acrolissos existed during that time (Hammond, 1988: 398). The Lower city of Lissos, extending down to the bank of the river Drini, was strongly fortified by a circuit wall, which also encompassed the Acropolis (Hammond, 1976: 520). According to Hammond (1988: 398), the city was inhabited by Illyrians, who had come from further inland. The Upper City was erected between the Lower City and the Acropolis. Archaeologists argue that Lissos was one of the most fortified cities on Illyrian territory during the late 4th century BC (Prendi & Zheku, 1971, 1972; Koch, 1989).

Another historical account about Lissos comes from the Roman historian Polybius, who is describing the Roman – Illyrian and Roman – Macedonian wars, happening on Illyrian ground from 264 to 148 BC. We learn from his chronicles, “The Histories”, that after the First Roman – Illyrian War (229-228 BC), Lissos was declared to be the southern border of navigation for Illyrian ships (Polybios, 2, 12, 3). He also provides a good description of the topography of Lissos and Acrolissos when talking about the siege of the strong fortress of the city during the First Macedonian – Roman War (215-205 BC) (Polybios, 8, 13, 14). In 213 BC, Philip V of Macedon captured Lissos, which then became an important Macedonian naval base together with Acrolissos, their stronghold on higher ground (Wilkes, 1969: 338).

At the end of the third Roman – Macedonian War (171-168 BC), the Illyrian kingdom was conquered by the Romans and transformed into a Roman province called “Illyricum” (Ceka, 2005: 153). The name of the city was transformed into a Roman version: Lissus. It was the southernmost coastal city of this province (Wilkes, 1969). After the military conquest of Macedonia in 148 BC, Illyricum was divided into the sub-provinces of Dalmatia and Macedonia. The border between these provinces was the Mati River, directly south of Lissus (Ceka, 2005: 153).

Caesar and the Senate divided the region up between themselves which led to a political restructuring of the region, and Lissus became part of the province “Illyricum” around 59 BC. Thereafter, the first groups of veterans settled in Lissus, thus becoming a “municipium” (self-governed Roman city) under the proconsulate of Caesar (Ceka, 2005: 153). During the Civil War between Caesar and Pompey (49-45 BC) Caesar controlled the city. In his book “Bellum civile”, he states that the fortification walls of Lissus had been repaired before the civil war,

which again indicates the city's military role (Bel. civ. 3, 29). Also, we learn first time from Caesar that Lissus had another harbour three miles away which was called Nymphaeum (today Shengjin), protected from the strong south-westerly winds (Bel. civ. 3, 26).

Under Augustus, a road was built to connect the "Via Egnatia" with the northern part of the eastern Adriatic, the route passing directly through Lissus, further contributing to its importance (Wilkes, 1996: 212).

However, during the first centuries AD, Lissus was hardly mentioned by ancient authors, which points towards a loss of importance for the Roman Empire. This may have been caused by the silting-up of the city's port and the formation of swampy environments around city due to the delta progradation of the Drini (for further details see chapter 8.8). Sources from Late Roman times testify Lissus' connection with two major roads, the road from Salonae *via* Ad Zizio to Dyrrachium (modern Durrës) and the road to the Black Sea, going from Lissus *via* Naissus (modern Nis in Macedonia) to Ratiaris (in Bulgaria) (Skrivanic, 1977).

4.2 From Byzantine to modern times

When the Roman Empire was divided in 395 AD, Lissus became part of the Byzantine Empire (Eastern Roman Empire). The Byzantine Period is an unstable time because Albanian territories were invaded by different peoples such as the Goths (489-535 AD), Slavic tribes (529-640 AD), Bulgars (861-1014 AD) and Normans (1081-1190 AD) (Jacques, 1995). There is not much detailed information available about their respective influences on the city. However, the castle on Lezha Hill had been repaired and new buildings had been constructed in the lower city. This shows that Lezha had again attained importance as a military base, but it had also become a centre for Christian orthodox communities during Byzantine times. In the Bishop catalogues written by Konstantin Porphyrogenetos and Anna Komnena from the 10th-12th century, the name of the city is mentioned as "Elissos" (von Hahn, 1853: 93).

Ruled by "The Principality of Arbër", a feudal state in North Albania, Lezha developed as a trade centre from 1190 to 1216 AD. This brief interlude was followed by another period of Byzantine rule, this time by the family of Michael Comnenus, despot of Epirus.

After Charles I of Anjou, King of Naples occupied Dyrrhacium (modern Durrës) in 1272, the Byzantine dominance began to decline in coastal Albania. Eventually, Lezha was controlled by the Latin Principality of Dyrrhacium. During that time, the city became a religious centre again, but this time for Roman Catholic groups. In Latin scripts from the 13th century, the name of the

city is mentioned as Lessium, other versions being Lessum and Lexium. It changed to Alexium or Alessium in the 14th century (Jireček, 1916: 123). In the documents from late Medieval times, its Latin version “Alessio” was commonly used.

Between 1346 and 1371, Lezha was occupied by the Serbian Empire. After the fall of the Serbian rule in Lezha, the native feudal family of Dukagjini created their own principality, which was called “Principality of Dukagjini”.

In 1393, Lezha was handed over by the ruling Dukagjini to the Venetian Republic (Ippen, 1907a: 60). Thereafter, it was part of the Venetian state though intermittently being attacked by the Turks. It was in this time that Gjergji Kastrioti who subsequently became known as the national hero Skanderbeg, was in charge of defending Albania against the Turks. He died in Lezha in 1468.

Alessio had developed as a trade centre throughout Medieval times because of its ideal position between the mountainous hinterland and the coastal lowlands (Duka, 2009). Under Venetian rule, the river port of Alessio played an important role as trading point for the salt and wood which was produced in Suffada (today Zufada), 8 miles (12 km) from Lezha (Jireček, 1916: 122; Bartl, 2007).

After several unsuccessful attacks, the Turks finally conquered Alessio in 1478. However, from 1501, during the war between Venetians and Turks, the city once again gained its freedom from Turkish occupation (von Hahn, 1853). This lasted only approximately 5 years. By 1506, the Ottoman Empire had taken over the entire country. This had a strong influence on the urban and cultural development of Lezha as well as the whole of Albania (Hütteroth, 2007). Under Turkish rule, the name of the city changed to Leš. The Venetian castle on Lezha hill was repaired between 1512 and 1520, indicating that Lezha was still a strategically important location (Ippen, 1907b).

From the second half of the 16th century, the economic importance of Lezha declined continuously. This happened because Shkodra rather than Lezha was being developed as the economic and cultural centre of North Albania during the period of the Ottoman Empire. The town was also largely “islamised”, with many Christian groups having to escape to either settle higher in the mountains (Mirdita Highlands) or leave for Italy (Duka, 2009).

In the 19th century, Alessio was a “Kaza” (small administrative unit) belonging to the “Sanjak of Shkodra” (larger administrative unit: district); it was inhabited only by Turks (Duka, 2009). At

the beginning of the 20th century, the population of Lezha was approximately 2000 (Ippen, 1907a). Turkish rule ended after more than 400 years in 1912 with Albania declaring its independence. By then, Lezha was only a small village.

Between the two World Wars, Shengjin, a neighbouring village further north was better suited to economic development due its direct access to the sea. The biggest military port of North Albania was constructed at Shengjin during Communist time. Since the opening-up of the country, it has also been used as commercial port.

However, after World War II, during the Communist era, Lezha was designated as capital of the district with the same name. This led to population growth and a revival of the economic importance of the city. Lezha is now an essential centre for the redistribution of agricultural products, and many trans-regionally important routes pass through the city, connecting North Albania with the South, as well as providing links to Kosovo and Montenegro. This has also led to an increased development of tourism during the last decade.

5 History of geoarchaeological research

To put this research project into context, it is necessary to be aware of the scientific investigations which have been done already. In the first section of this chapter, coastal and palaeoenvironmental studies from different parts of the Mediterranean Sea are presented. The focus will then shift to the Adriatic Sea, before concentrating on the history of research for geoarchaeological studies in Albania, particularly coastal Albania. Finally, a review of archaeological studies carried out in and around ancient Lissos will round up this chapter.

5.1 Coastal research around the Mediterranean Sea

In terms of Holocene landscape changes, the Mediterranean coasts are among the best investigated and documented coastal areas of the world. The first geoarchaeological studies started on presently land-locked coastal settlements and silted-up ancient harbours in delta plains along the coasts of Greece and Turkey. Among the earliest publications were those about the Pamissos plain in the Gulf of Messenia (Kraft et al., 1975) and the Karamenderes plain with the ancient city of Troia (Troy) (Kraft et al., 1980a). General syntheses about the Aegean coastal plains and deltas followed (Kraft et al., 1985a; Kayan, 1988, 1996b, 1999).

5.1.1 Research in the Western Mediterranean

The deltas and coastal plains which are situated along the French and Spanish coasts of the Western Mediterranean bear suitable data for geoarchaeological research. Along the southern coast of Spain, the delta of the Ebro River (Mariño, 1992; Guillén, 1997) and the coastal plains of Andalucia (Hoffmann, 1988, 1995; Brückner & Hoffmann 1992) were studied in detail. In the course of the marine transgression after the LGM, the Ebro built up an extensive submarine deltaic plain. By 8,000 yrs BP, these sediments were covered by another layer of deltaic deposits, due to the sharply decelerating sea-level rise and an increasing input from the river. Since Roman times, the Ebro has prograded its delta plain for about 26 km seawards (Mariño, 1992: 312).

The Holocene evolution of the coastal plains of the Rio Seco, Rio Verde, Rio Guadalfeo and Rio Grande de Arda on the Andalucian coast of Spain was published by Hoffmann (1988, 1995) and Brückner & Hoffmann (1992). According to those authors, the formation of these coastal plains started around 4,000 BC. In the first 3,000 or so years, the coastline shifted seawards rather slowly. During antiquity and in Medieval times, the deltas advanced a little more rapidly due to increasing erosion in the hinterland with intensive anthropogenic activities. The most

prominent deltaic progradation, however, occurred after the “Reconquista”, with the capture of Granada by the Spanish Kings in the late 15th century AD (Hoffmann, 1995).

Along the French coast, the Holocene evolution of the Rhône delta and stratigraphy of the late Holocene deposits of the ancient harbour of Marseilles have been well documented using geoarchaeological methods (Morhange et al., 2001, 2003; Rey 2009). This region is tectonically stable. The position of the archaeological remains and bio-sedimentary units from the ancient harbour of Marseilles shows that the relative sea level has risen steadily by 1.5 m during the past 5,000 years, and stabilised around 1,500 AD (Morhange et al., 2001: 319). The rate of sea level rise was calculated to be 1.5 mm/yr for the last century (Morhange et al., 2001: 327). The Petite Camargue, the western part of the Rhône delta, started prograding about 2,000 yrs BP; fluvial-dominated processes changed to wave-dominated around 1,550 AD due to climatic change and human impact (Rey et al., 2009: 284).

5.1.2 *Research in the Central Mediterranean*

The landscape evolution of the coastal plains and deltas along the Central Mediterranean area is also well studied and published. Many archaeological coastal sites along the Tyrrhenian and Ionian Sea coasts have been examined and documented.

The earliest publications come from the Basilicata region at the Ionian Sea coast of Italy (Brückner, 1982, 1983; for an overview see Brückner 1986). Brückner recognised 11 Pleistocene marine terraces (T1-T11), and estimated erosion and accumulation rates during the Quaternary. During the Holocene, and especially during historic times, the river beds were filled up by alluvial deposits due to the intense erosion from the hilly country of Lucania. Ceramic and charcoal fragments and intercalated palaeo-soils allow an estimation of the sedimentation rate in the Bràdano and Cavone valleys. According to ¹⁴C age estimates, the average sedimentation rate has been 1.8 mm/yr in the Bràdano valley since 4,150 BC, and 8.0 mm/yr in the Cavone valley since 340 BC (Brückner, 1982: 136).

A much more recent publication comes from the Luni plain, formed by the Magra River in the northern Tyrrhenian Sea (Bini et al., 2009). According to their results, the environment was dominantly swampy to marshy, enclosed by dune ridges and fluvial sand bars, before the foundation of the ancient Roman colony of Luni in 177 BC. Using archaeological remains and radiocarbon datings, the authors concluded that between 370-343 cal BC and 320-200 cal BC (1 σ), sea level was 2.2 m lower than today (Bini et al., 2009: 156).

The evolution of the Tiber river delta plain during the late Quaternary in Central Italy was studied by Bellotti et al. (2007). They suggest that the present delta area was being deeply incised by the Tiber River until 13,000 BP. During the transgression of the Tyrrhenian Sea, this deep and narrow valley formed a marine bay. From 8,000 BP to 6,000 BP, due to anthropogenic impact in Neolithic times, the Tiber River built up a bay-head delta. By 6,000 BP, the river-dominated processes changed to wave-dominated ones, and a strand-plain with two lakes developed. During the 1st and 2nd centuries AD, the most famous and important harbour of Roman times was built close to the Tiber river mouth: Ostia, the harbour of Rome (nowadays known as *Ostia antica*). In the Renaissance period, the delta began to advance once again. Therefore, the harbour silted up, and the coastal lakes dried out in the 19th century, when the landscape became similar to the one of today (Bellotti et al., 2007: 505).

Environmental changes around the ancient Greek city of Kaulonia on the Ionian coast of Calabria (Italy) were investigated and published by Stanley et al. (2007). This region is tectonically very active, and the remains of the ancient settlement of Kaulonia (dated to 700-389 BC) are now located about 7 m below p.s.l. and 300 m away from the present shoreline. The progradation of the delta must have taken place roughly between 2,500 BC and 500 BC (Greek time), before the shoreline began retreating until the present day (Stanley et al., 2007: 28).

5.1.3 *Research in the Eastern Mediterranean*

In a geoarchaeological context, the Holocene landscape evolution of the coastal and deltaic plains along the Eastern Mediterranean coast were studied in detail since the beginning of the 1990s: e.g., Nile delta (Wunderlich, 1989; Andres & Wunderlich, 1991; Wunderlich & Andres, 1991; Chen et al., 1992; Warne & Stanley, 1993; Stanley & Bernasconi, 2006), coasts of Israel (Sivan et al., 2001; 2004), ancient harbours of Tyre and Sidon, Lebanon (Marriner et al., 2005; 2006; Marriner, 2009). Additionally, studies of the coastal settlements of Western Anatolia became a highlight for interdisciplinary geoarchaeological research during this period. The maximum extent of the Holocene transgression and subsequent shifts of the shoreline were investigated around famous ancient cities such as Troia (Kraft et al., 1980a; Kayan, 1990, 1991, 1995, 1996a, 2001; Kayan et al., 2003, Kraft et al., 2003), Ephesos (Brückner, 1997b, 2005; Kraft et al., 1999, 2000, 2001, 2005a, 2007; Brückner et al. 2008), Kaunos (Riedel, 1996), Miletos (Brückner, 1996, 1997a, b, 1998; Bay, 1999; Brückner et al., 2002, 2003a, 2003b, 2006; Müllenhoff, 2005).

Palaeogeographical and -environmental changes of the coastal plains and deltas along the Aegean and Ionian coasts of Greece have also been studied intensively, using geoarchaeological

methods. The publications from Greece will be presented in the following in more detail because they are very useful in connection with this dissertation.

The palaeogeographic evolution of the Thessaloniki delta plain, formed by the Axios River, was investigated by Vouvalidis et al. (2005). According to their publication, the sea level rose from 30 m below p.s.l. around 10,000 BP, to 5 m below p.s.l. 5,000 years ago. Debris from prehistoric settlements, dating to the 4th millennium BP, was found at a depth of 4 m below p.s.l., covered by marine sediments; an indication for local tectonic subsidence. Around 500 BC, the coastline was 40 km inland from its present position. The landscape changes occurred mainly due to increasing human activities in the hinterland, causing erosion on a large scale. However, since 2300 BP, the harbour of Thessaloniki has always been protected from silting up. Evidence for this is anthropogenic debris, dating from antiquity to present times, which was found within marine deposits, rather than terrestrial ones (Vouvalidis et al., 2005: 147).

The Late Quaternary evolution of the Marathon plain was first published by Baeteman (1985). According to her palaeogeographic maps, the maximum Holocene transgression is dated to 5,000 BP, when a coastal environment developed in the area. Due to the progradation of the Haradros delta in the eastern part of the present plain, a lagoonal environment formed between 4,900 and 3,500 BP. In 490 BC, at the time of the battle of Marathon, the shoreline was still further inland in the Shinias area; that must have been where the Greeks have fought the Persians (Baeteman, 1985: 185). Today a swamp occupies this terrain.

Current publications on the evolution of the Marathon plain during the middle to late Holocene came from Pavlopoulos et al. (2003, 2006). They also found evidence for a lagoonal environment between 5,800 and 3,500 yrs BP. Later, it changed into an ephemeral lagoon (3,500-2,500 years BP) and during the last 2,500 years into a wetland area, slowly being filled in by fluvial deposits. The relative sea level in the area has risen for about 2.5-3 m since 5,500 BP. The ratio of tectonic uplift was calculated to 0.4-0.5 mm/yr between 5,500 and 1,300 BP, the one of relative sea level rise to 0.6-0.7 mm/yr for the last 2000 years (Pavlopoulos et al., 2006: 424).

The Malian coastal plain, where the River Sperchios debouches into the Gulf of Malia, was studied by Kraft et al. (1987). Due to deltaic progradation of the river, the shoreline has advanced 15 km eastwards during the last 4,500 years. Subsequent landscape changes were documented in historical records since the Battle of Thermopylae in 480 BC. The reconstructed shoreline indicates that the famous narrow passage, described by Herodotus (7, 176), indeed existed there around 480 BC (Kraft et al., 1987).

Other geoarchaeologically well documented areas in Greece are the coastal plains along the Peloponnese peninsula. The first geoarchaeological research was done in the Pamisos coastal plain in the Gulf of Messenia (Kraft et al., 1975). According to these authors the Holocene maximum transgression reached 4 km inland, because they found a palaeo-coastline at 7 to 16 m below p.s.l., which dates to 3,500 BC (late Neolithic time). Archaeological remains show that during Hellenistic/Roman times sea level was ~2 m lower than at present (Kraft et al., 1975: 1206).

The most recent investigation of the Messenia plain shows that the sea reached its maximum inland position around 3,000 BC (Engel et al., 2010). During the late 3rd millennium BC, a prominent beach ridge formed, on the top of which, at a later stage, the early Iron Age Poseidon Sanctuary of Akovitika was founded ca. 900-850 BC. Due to increasingly marshy conditions around the ceremonial site, it was abandoned around 380-350 BC (Engel et al., 2010)

The Methoni embayment, located in the extreme SW corner of the Peloponnese was studied by Kraft & Aschenbrenner (1977). At the beginning of the Neolithic period around 6,000 BC, sea level was ~20 m lower in the Methoni Bay. In the Middle Helladic period (2,100 BC), it was still 3 m lower than at present. Due to increasing wave energy, coastal cliffs retreated and the coastal settlement of Nisakouli became an island, which is now 700 m away from the present coastline (Kraft & Aschenbrenner, 1977: 43).

As for the Navarino embayment, also called “Sandy Pylos”, in the SW Peloponnes it can be shown that sea level has risen for more than 25 m since 9,500 BP when its position was still 4 km inland from the present shoreline (Kraft et al. 1980b). By Helladic times, people settled in the southern part of the alluvial plain and used the rocky part of the coast as a harbour. From Hellenistic to Roman times, the Osmanaga Lagoon formed behind a spit. Since Roman times, the landscape of the area has hardly changed (Kraft et al., 1980b: 209).

For the western Peloponnese, new insights about the connections between coastal changes and archaeological settlements in the coastal plain of Elis were published by different scientists (Büdel, 1977; Raphael, 1978; Kraft et al., 2005b). Büdel (1977) suggested that the ancient city of Olympia was buried by alluvium between 500 and 1,500 AD. He also noted that the Alpheus delta had prograded for ca. 4.5 km since antiquity (Büdel, 1977: 259). Raphael (1978: 87) noted that sea level rose to its present position around 3,500 BC and that the main alluviation phase of the Peneus River occurred during Classic Greek, Hellenistic and Roman times. According to Kraft et al. (2005b) the coastal embayment, into which the rivers Alpheios and Peneus

debouched, had been transformed into a large lagoonal environment ca. 5,500 BC (late Mesolithic-early Neolithic). The sea level rise slowed down at the beginning of the Helladic period (ca. 3,000 BC). Subsequently, coastal barrier – lagoon systems caused the siltation of the ancient coastal settlements of Kleidhi and Epitalion, both dating back to the Helladic period; they are now located 1 and 5 km inland from the present coastline, respectively (Kraft et. al, 2005b: 1).

Much is known about the coastal plains of the Epirus region, NW Greece. The late Quaternary coastal evolution of the Ambracian Gulf was studied by Poulos et al. (1995, 2005) and Jing & Rapp (2003). The latter note that the Ionian Sea intruded rapidly into the Ambracian embayment 10,000 years ago and that its level was by then 45 m lower than today. The marine transgression decelerated after 6,000 BP, reaching its maximum landward position by 4,500 BP. At the beginning of the Bronze Age, the shoreline was 12 km inland. According to Jing & Rapp (2003), sea level rose slowly until 1,500 BP (about the end of the Roman period) due to continuous subsidence. Poulos et al. (2005) report that the sea had formed a gulf which was 35-40 m below p.s.l. around 10,000 BP. Then, sea level rose 0.5 ± 0.02 cm/yr until ca. 2,000 BP, forming the present Gulf of Amvrakikos (Ambracian Gulf). During the last 2,000 years, sea level changes have stayed within a range of 1-2 m.

The palaeogeographical maps of the Acheron delta, 35 km north of Ambracian Gulf, are reconstructions based on sedimentological and paleontological analyses, as well as the interpretation of ancient written sources (Besonen, 1997; Besonen et al., 2003). Since 4,000 BP, the shoreline of the Glykes Limen has prograded ca. 6 km seawards. The Acherousian Lake was formed between the 8th century BC and 433 BC. The present landscape is a result of shifting river channels during the last 500 years (Besonen et al., 2003: 234).

Over the last few years, an important geoarchaeological project was carried out along the coastal region of Akarnania in northwestern Greece by Vött et al. (2002, 2003, 2006a, b, c, d; Schriever, 2007). The Holocene evolution of the coastal plains of Palairos, Mytikas, Astakos and the Acheloos delta plain were systematically studied. This project achieved important results for the mentioned coastal areas. Not only were the authors able to reconstruct coastal changes in terms of shoreline shifts and sea-level fluctuations, they also found evidence of extreme events such as tsunamis and earthquakes by using sedimentological, palaeontologic and archaeological analyses and radiocarbon dating. The maximum transgression of the Ionian Sea was dated to the 7th millennium BC (in Palairos), 5,900 cal BC (in Mytikas), and 5,100 cal BC (in Astakos). According to the ¹⁴C age estimates from the deposits, the progradation of the Acheloos delta started after 5,500 cal BC. Subsequent shifts of the shoreline were well

documented in the near-coast deposits around archaeological sites. The most important environmental changes occurred during Classical/Hellenistic times, Roman times and at the end of the 19th century AD. Human impact on the landscape was the main agent for the increasing alluviation.

Vött et al. (2008) suggest that at least four tsunami events, dated to 1,000 cal BC, 300 cal BC, 430 cal AD and within the time span 1,000-1,400 cal AD, occurred along the Lefkada coastal zone. They also present seven different relative sea level curves for NW Greece since the Middle Holocene. Five of them are based on data from different coastal plains (Boukka, Palairos, Mytikas, Astakos, and Elis), two of them are for the Acheloos Delta (Triardo and Etoliko). The authors calculated that in northwestern Greece the highest rate of sea level rise occurred until 5,500-5,000 cal BC (up to 12.3 m/kyr), the lowest from 4,000 to 500 cal BC (0.2-1.1 m/kyr). For the last 2,500 years, the relative sea level rise in this area has been in the order of 0.7-2.8 m/kyr.

Late Holocene geomorphological and palaeoenvironmental dynamics in the harbour of the ancient city of Oiniades, located in the Acheloos delta, were first studied by Fouache et al. (2005) and later Vött (2007b) and Vött et al. (2007). According to Fouache et al. (2005), between the 4th and 2nd millennia BC, the river Acheloos had formed its delta in the eastern and southern part of the marine embayment where the city was later founded (ca. 500 BC). The thickness of the marine sediments in this area shows that, while the harbour of the city was used, sea level was 1.6-2 m lower than at present. Due to the increasing siltation, the harbour of Oiniades was abandoned in 210 BC (Fouache et al., 2005: 300). Vött (2007b) and Vött et al. (2007b) suggest a different scenario for the progradation of the Acheloos River delta. They indicate that the delta was prograding westward around 3,000 cal yr BC (in early Helladic times), and its main distributary came close to Triardo Island around 1,300-1,000 cal BC. Therefore, lagoonal environments in necropolis bay and even in the northern embayment were suitable harbour sites until 1 AD (Vött, 2007b: 33). A river harbour existed until Late Roman to Byzantine times at the SE promontory of the former Triardo Island (Vött, 2007b: 33).

5.2 Geoarchaeological research around the Adriatic Sea

In general, when compared with other deltaic and coastal plains in the eastern part of the Mediterranean Sea, the coastlines of the Adriatic Sea have received little attention in the context of geoarchaeological research. It should be said though that the number of publications about the Adriatic coasts of Italy and Croatia, as well as Albania have increased in the last few years. An exception, however, is the Po delta, the biggest alluvial complex in the Adriatic, formed by

the Po River, and by other minor rivers emerging from the Swiss, Austrian and Dinaric Alps (Isonzo, Tagliamento, Piave, Adige, Brenta) and from the northern Apennines (Reno, Savio, Marecchia, Conca). This delta plain has been subject to geoarchaeological examination since the early 1960s.

The earliest study dealing with the eastern Po plain, using sedimentological and petrographical analyses as well as buried archaeological remains from Etruscan and Roman times, comes from Dongus (1963). The environmental changes in the former freshwater marshes (Valli dolci) and coastal swamps and lagoons (Valli salse), were reconstructed from early historical times to present. According to Dongus (1963: 220), the position of the archaeological remains (4-5 m below p.s.l.) show that the present coastal landscape of the northwestern Adriatic Sea developed as a result of the marine transgression accompanied by subsidence since post-Roman times.

Relative sea level changes in connection with archaeological references from Venice have been studied by Ammerman et al. (1999). After the LGM, the sea level rose rapidly at a rate of 12 mm/yr until 8,000 years ago; thereafter its speed decelerated. Between ca. 4,000 BC and 400 AD, relative sea level change was estimated to have been about 3.1 m, corresponding to an average rate of 0.7 mm/yr. From 400 AD to 1897, sea level rose about 1.9 m (average rate: 1.3 mm/yr). In Venice, many archaeological remains from post-Roman times were found to be buried about 2 m below the present sea level due to subsidence. According to Ammerman et al. (1999: 311), tectonic subsidence has not affected the ground level in Venice since the time of Napoleon.

Camuffo et al. (2004), however, uses the height of algae growth (particularly *Laminaria*) on the foundation of historical Venetian buildings as depicted in the “photographic paintings” (made with an optical *camera obscura* by famous Italian painters Antonio Canaletto (1697-1768) and Bernardo Bellotto (1722-1780), to calculate the submersion rate. He suggests 61±11 cm change in relative sea level for the last 300 years (Camuffo et al., 2004: 61). The authors propose three factors to be responsible for this: (1) natural causes (tectonic, sediment compaction), (2) anthropogenic activities (pumping of ground water), and (3) eustatic sea level changes in the Mediterranean. These results support those of earlier publications by Carminati & Di Donato (1999) and Carminati & Martinelli (2002). Bertoni et al (1995) proved that human impact in the form of natural gas extraction in the area by AGIP contributed a lot to the subsidence problem.

Carton et al. (2009) worked on the Holocene evolution of the coastal plain of Piave River in the east of Venice. From the LGM to about 8,000 ¹⁴C BP, alluvial sediments of the Piave River accumulated in its own valley and in the Vallona Bellunese. Since 6,000 ¹⁴C BP, these

sediments were re-mobilised and transported to the sea forming the present delta plain. Therefore, the Nervesa mega alluvial fan, innermost part of the present delta, started to develop during 4,000-3,000 ¹⁴C BP. From the Iron Age to Roman times, the river system was stable. However, between the 5th and 10th centuries AD, the coastal plain of the Piave delta prograded due to increasing human impact (Carton et al., 2009: 155).

The Holocene evolution of the Potenza coastal plain in the central part of the Adriatic coast of Italy was published by Goethals et al. (2003) and Corsi et al. (2009). During the Holocene transgression the coastline was shifted 4-5 km further inland, in comparison with the present situation. The river delta began to advance seawards about 4,000 years ago. The Potenza river reached maximum sediment loads during Roman times as well as the early Middle Ages; therefore, those periods are characterised by high rates of deposition and siltation. This meant that Roman ports such as Cupra Marittima, Torre di Palma and Martinsicuro had to be constructed at the base of the rocky cliffs. Between the 16th and 19th centuries, the shoreline migrated seawards for more than 500 m in the Marche Region. In the 20th century, coastline progression stopped due to human intervention in the form of canalisation of the rivers and the building of reservoirs; thus, sediment was trapped and did not reach the delta plain anymore (Goethals, 2003: 76; Corsi et al., 2009: 95).

The environmental changes around the ancient settlement of Coppa Nevigata in southeastern Italy were studied by Caldara et al. (2003). They document the presence of a lagoon environment including some volcanic pyroclastic layers of the Avellino eruption of Somma-Vesuvius during the middle Bronze Age. At the end of this period, the lagoon gradually diminished and the “proto-urban” phase developed with many indicators of human impact on the environment. This phase was dated between 3,000±80 yrs BP and 2,870±40 yrs BP. Subsequently, conditions changed into a salt marsh environment near the settlement during the late Bronze Age (Caldara et al., 2003: 435).

Auriemma et al. (2004) reconstructed the Holocene evolution of the coastal plains along the Apulian coast (between Bari and Taranto) in southeast Italy. This area is the most active tectonic zone along the Adriatic Sea. According to the authors, geomorphologic features (beach sequences and wave-cut platforms) and dating results indicate a higher sea level (about 1±0.5 m a.s.l.) during the Holocene transgression maximum at 7,000-7,500 BP. Buried archaeological remains suggest that sea level dropped by about 3 m until the Bronze Age. Submerged harbour structures from Egnatia indicate that it must have been around 3 m below its present level during the Roman Imperial Period. For the southern Apulian coast, a similar development has been reported by Dini et al. (2000). As an exception they proposed a sea level high stand (+1 m

p.s.l.) at around 6,000 yr BP, and a low stand (-2 m p.s.l.) during historical times (Dini et al., 2000: 43).

The Fortore river coastal plain and evolution of the Lesina Lake in the north of the Apulia region was researched by Gravina et al. (2005: 115). The authors postulate that during the maximum of the postglacial transgression (about 6,500 cal BP), sea level reached 8.5 m above its present level. [However, this figure is only possible under the assumption of a high uplift rate.] The end of this period was marked by a very arid phase between 4,800 and 4,600 BC. The Fortore river started to form its delta plain at about 3,000 years BC. Another arid period occurred between 1,700 and 1,300 BC (middle Bronze Age). During the Republican Roman Period, the Fortore river formed a cuspidate delta triggered by increasing deforestation since 400 BC. Gravina et al. (2005) also hint at three strong earthquakes approx. 664 BC, 493 AD and at the beginning of second millennium AD (1087 or 1223 AD), which may have caused tsunami events in the area. During the Little Ice Age, the delta continued to advance, accompanied by slow subsidence. The last important delta progradation occurred during the 19th and 20th centuries (Gravina et al., 2005: 115-116).

In contrast to the Italian coasts, geoarchaeological research along the Croatian coasts requires other approaches, due to the lack of large deltas and plains along the limestone coasts. Therefore, palaeoenvironmental studies gather information about the position of submerged wave-cut notches at the base of the limestone cliffs and submerged archaeological remains from Roman times (such as quarries, fish tanks, cisterns). In addition, palynological research has been carried out along the Croatian coasts since the 1960s. Some results of these studies are discussed in chapter 3.

Fouache et al. (2000) gathered data about submerged notches and archaeological remains at several sites between Porec and Zadar, as well as on the northern Dalmatian Islands (e.g., Pag, Rab, Krk, Losinj and Cres). Their observations imply that in this coastal region, about 2,000 years ago, sea level was about 0.5 m lower than today (Fouache et al., 2000: 33).

Later, this work was correlated with new geomorphological and archaeological observations from different sections of the Croatian coasts (Faivre & Fouache, 2003). The submerged notches in the Istria and Kvarner regions support the earlier publication (Faivre & Fouache, 2003: 525). South of Zadar, however, submerged archaeological remains from Roman times (1st and 2nd centuries AD) indicate that the relative sea level was at least 1.5 m lower (Faivre & Fouache, 2003: 526). Both observations suggest that tectonic subsidence must have played an important role along the Croatian coasts since Roman times.

5.3 Palaeoenvironmental and geoarchaeological research in Albania

The history of geoarchaeological and palaeoenvironmental research in Albania goes back only two decades. The first studies were carried out in connection with the interdisciplinary archaeological excavations in the Konispol Cave and at Sovjan.

Research in the Konispol Cave, located in the extreme south of Albania, close to the Greek border, was done by an American team; it gave an idea about palaeoclimatic trends for this region from ca. 9,000 to 3,000 BP. The data was gathered from cave sediments using magnetic susceptibility measurements and ^{14}C -AMS age estimates (Ellwood et al., 1993, 1996, 1997; Petruso et al., 1994; Schuldenrein, 1998, 2001).

Another area which yielded important results for Holocene palaeoenvironmental research in Albania is the now silted up Lake Maliq in the northwestern part of the Korça Basin, close to the Macedonian border. There, geoarchaeological research was carried out by a French team associated with Albanian archaeologists in the Protohistoric (Neolithic?) settlement of Sovjan, starting in the early 1990s. The sedimentological and palynological records from the boreholes in the former lake basin were used to establish a chronology for the vegetation history, climatic changes and water-level fluctuations of the last 12,000 years (Deneffe et al., 2000; Bordon et al., 2009). Also, the interaction between human activities and environmental changes are well documented from the Korça Basin (Fouache et al. 2001) (see chapter 3.3).

In contrast, the potential for geoarchaeological and palaeogeographical research of the Adriatic and Ionian coastal plains of Albania only attracted notable attention during the last decade. The first attempts for a general synthesis about the geomorphological evolution of the deltas along the Albanian coasts were undertaken by Ciavola et al. (1999) and Mathers et al. (1999). These authors used high resolution satellite images and historical data (Ciavola et al., 1999), as well as orthogonal aerial photographs at the scales of 1:10,000 and 1:25,000 (Mathers et al., 1999). Their publications focused on the delta complex of the rivers Shkumbini, Semani and Vjose (central part of Albania's coast) which had developed in a tectonically very active area under micro-tidal conditions, with high relief and torrential river regimes in the hinterland. It may serve as a model for the coastal evolution of the Adriatic coastal region of Albania. While one paper deals with the coastal changes between the Seman and Shkumbin delta plains since 1870 (Ciavola et al., 1999), the other presents a number of palaeogeographical maps showing the evolution of the area from the time of the maximum transgression around 5,000 BP up to 1986 AD (Mathers et al., 1999). It is important to note that both publications mention rapid coastal

changes in the recent past, due to human activities such as the building of hydroelectric power stations and dams, as well as the installation of drainage and irrigation systems along the floodplains and in the catchment areas of the rivers, which caused important changes in the flow regimes of the rivers.

The studies of Fouache et al. (2000, 2001, 2003, 2006, 2010) present a valuable source of information. They are the most applicable ones for our own research area, because they applied a similar methodology as was used in the context of this dissertation. Their geoarchaeological research focused on the area around the ancient city of Apollonia, situated at the border between the Vjosa delta plain and the Neogene Mallakaster hills. The excavations at Apollonia have been carried out by a French-Albanian team since 1994 and are still ongoing. The settlement was founded as a harbour city in the 7th century BC. The configuration of the coastline, west of the ancient city, is well documented not only in ancient accounts (e.g., Strabo), but also in Ottoman sources since Medieval times. Fouache et al. (2001) reconstructed the coastal evolution of the delta since 2,000 BP, using data from satellite images (SPOT, HRV 3 081-268, dated to 25 May, 1995) and various topographical maps from 1870 to 1990; they merged those with archaeological and historical information. Later, they supported their first publication (2001) with new evidence from ¹⁴C ages, heavy mineral contents, diatom studies and grain size analyses from six boreholes around Apollonia (Fouache et al., 2010).

The results of the latest publication of Fouache et al. (2010) on the deltas of the rivers Seman and Vjosa can be summarised as follows:

- (1) The research revealed the evolution of three barrier systems. The oldest ones was dated to $3,050 \pm 55$ BP (1428-1130 BC), the second one to $2,755 \pm 35$ BP (996-827 BC) and the youngest one to 605 ± 45 BP (1292-1417 AD).
- (2) Different elevations of the uppermost beach facies in the cores may indicate local tectonic movements. The beach sediments, for example, were located above present sea level in core PS2, whereas the same deposits were found 3 m and 4 m below p.s.l. in PS3.
- (3) The descriptions from ancient sources such as Strabo, Plutarch and Caesar support the existence of a river harbour leading into the lagoon and a beach barrier system at the mouth of the river Vjosa during Roman times.
- (4) A ¹⁴C date from a piece of wood (PS4) shows a westward progradation of the river Seman after the 15th century AD (340 ± 50 BP – 1443-1655 AD). For the past 500 years, the Vjosa delta has prograded westwards for about 6 km.

- (5) The delta progradation of the rivers Seman and Vjosa of the last 500 or so years are a response to neotectonic movements, climatic fluctuations (e.g., Little Ice Age) and socioeconomic changes during the Ottoman period.

Other interesting publications in the context of our own research focus on the environmental changes around the ancient city of Butrint, located in southernmost Albania (Lane, 2004; Hounslow & Chepstow-Lusty, 2004a, b). Archaeological excavations in Butrint have been carried out by an Anglo-Albanian team since 1994. The aim of the geoarchaeological research in this area was to discuss the palaeogeographical evolution of the delta plain formed by the river Pavllas. In total, 22 boreholes were drilled and subjected to sedimentological, micropalaeontological, and palynological analyses. The sediments were categorised into three depositional environments:

- alluvial topsoil composed of silty clay of reddish grey colour (floodplain);
- marsh deposits composed of silty clayey material of light grey colour (estuarine);
- limnic/marine deposits composed of clay with intercalated sand lenses of mottled bluey grey colour and with abundant fossils (marine) (Lane, 2004: 36).

The overall results of the geoarchaeological research in Butrint indicate that during the sea level highstand at ~8,000 BP, a marine embayment formed near the later city. Around 5200 BP, it began to be silt up by the river Pavllas. The continuous input of fluvial sediment caused a shift towards estuarine conditions ca. 4,300 BP. Increasing human impact on the environment in the form of extensive erosion is evident since about 4,000 BP; it can be traced in the pollen record. Sediment input reached its peak ca. 3,000 BP. The rapid siltation processes lead to the development of the Vrina deltaplain and of the remnant lakes of Butrint and Bufi. Accumulation since post-Roman times amounts to an alluvium of 1.2 m thickness. According to submerged archaeological layers from Roman and post-Roman times in Butrint, it can be inferred that relative sea level must have risen after the 5th century AD. This could have occurred due to a compaction of the sediments or because of tectonic subsidence in the area (Lane, 2004: 33). Further chronological details about the erosion and alluviation periods from 450 to 1200 AD around the area of Butrint can be found in Hounslow & Chepstow-Lusty (2004b).

In northern Albania, such detailed studies of the palaeoenvironment and geoarchaeology are lacking completely. Therefore, it is one of the main objectives of this dissertation to fill this gap. However, Fouache's work (2006), carried out in a predominantly geological context, does provide valuable information. He has produced a geologic/geomorphologic map of the large coastal plain between Lezha and Cape Rodoni (Fouache, 2006: 94). It also includes for the first

time an estimation of the course of the coastline during the Holocene transgression maximum. Importantly, he presents seven geological cross-sections between the Drini delta and the Mati river (see figs. 7a-c). However, his work is primarily descriptive rather than explanatory, and he does not give detailed information about the cores. His information originates from unpublished hydrogeological drillings, carried out by the Albanian geologist L. Dimo (Fouache, 2006: 95).

5.4 Previous geographical and archaeological research around Lezha

The earliest archaeological accounts from the Lezha area are concerned with the ancient ruins of Lissos. The Italian traveller Ciriaco d'Ancona had copied inscriptions and described monuments, which he observed in formerly Greek and Roman settlements along the Albanian coasts during his tour in 1434-35 (Jacques, 1995: 3; Ceka, 2005: 9).

Regular surveys and excavations of settlements along the Albanian coast began in the mid-1990s, for instance, in Dyrrhachion (Durrës), Apollonia, and Buthrotum (Butrint). However, any studies concerned with the settlement history of Lezha were limited to the examination of historical documents rather than ancient remains, because of inaccessibility issues: during the 18th and 19th century, the “modern town” had been built directly on top of the very old remnants.

The Acropolis (Kalaja) on Lezha Hill (see photo 1) had been subjected to several phases of modification during its history. However, this magnificent example of early military architecture, which has attracted scientists for a long time, still bears some evidence from the 6th century BC (Lissos Excavation Report, 2004). Based on ancient sources, the history and the fortification system of Lissos have been discussed in detail for more than 150 years (von Hahn, 1853; Ippen, 1907a, b; Praschniker & Schrober, 1919; Fluss, 1926; Beaumont, 1936, 1952; May, 1946; Hammond, 1968; Wilkes, 1969; Prendi & Zheku, 1971, 1972; Franke, 1983; Stylianou, 1998; Pochmarski & Hoxha, 2005).

The first scientific account about Albania was published by Johann Georg von Hahn, who was working as Austrian Consul in Greece. He is also known as the founder of modern Albanian studies. Von Hahn used ancient and historical sources to create the first detailed report about the geography of northern Albania, including the foundation and settlement history of Lissos (von Hahn, 1853). Fifty years later, Theodor Ippen, Austrian-Hungarian Consul in Shkodra, published his observations about Shkodra and the coastal lowlands of northern Albania, including Lezha, in 1907. This book contains the first thorough, contemporary description with many references about the topography and history of Lissos, citing von Hahn's previous publication (Ippen, 1907a). Austrian-Hungarian scholar Franz Baron Nopcsa wrote many

important articles about the geology, geography, archaeology and ethnology of northern Albania at the beginning of the 20th century (Nopcsa, 1905, 1911, 1912, 1925). His final synthesis and significant monograph “Geographie und Geologie Nordalbaniens” was published in 1929. In the chapter on Lissos, Nopcsa (1929a) used mainly the descriptions of the formerly mentioned scholars.

The first mapping of the ruins of ancient Lissos was done by the Austrians Camillo Praschniker and Arnold Schober, who reached northern Albania from Montenegro, and travelled as far as Fier and Berat during World War I in 1916. In their book, Praschniker & Schober (1919) present the first plans of the ruins comparing them with ancient sources (fig. 18).

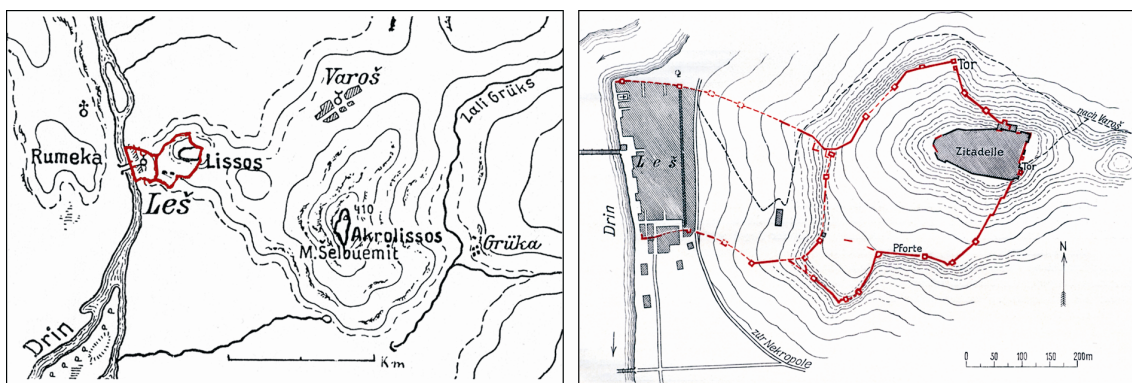


Figure 18: Map of Lissos' surroundings (left), and first city plan of Lissos (right) (Praschniker & Schober, 1919, p. 15, fig. 22, and p. 27, fig. 39).

After the achievement of this scientific milestone, it took more than 50 years before any further publication about research in Lissos became available. In the early 1970s, Albanian archaeologists Frano Prendi and Koço Zheku carried out some excavations, unearthing the West Gate (so-called Harbour Gate) and the well-known Southwest Gate, which is an excellent example of a Hellenistic gatehouse with double towers on both sides. Together with the results of their excavations, they published a detailed discussion about the fortification phases and a new plan of Lissos (Prendi & Zheku, 1971, 1972). Prendi's excavations in the Medieval castle (Acropolis, Kalaja) and in the lower part of the ancient city of Lissos were conducted in 1973 and 1977 (Andrea, 1984).

A large part of the modern 'old town' of Lezha, situated on top of the Lower City of ancient Lissos, was almost completely destroyed by an earthquake on April 15th, 1979 (Lissos Excavation Report, 2004). In the course of the clean-up efforts from 1980 to 1983, some parts of the ancient fortifications that represent the southwest corner of the Lower City were identified by Prendi (Andrea, 1984). A modern residential quarter was built in the northern part, while the southern part of the Lower City was rearranged into a National Park including a section of the ancient fortification and a memorial place for the Albania's national hero Georg

Kastrioti, better known as Skanderbeg, who was buried in Lezha in 1468. The memorial place, a protective building in the form of an ancient temple (see photo 9), encloses the ruins of a mosque (former church of St. Nicholas); it is believed to contain Skanderbeg's grave (Lissus Excavation Report, 2004: 4).

At the beginning of the new millennium, archaeological research in ancient Lissos was revitalised. In 2003, the Albanian archaeologist Gëzim Hoxha started new excavations in the Lower City by opening a trench in front of the West Gate (as the so-called Hellenistic Harbour Gate). In 2004, an Austrian team, directed by Erwin Pochmarski and Manfred Lehner (Institute of Archaeology, University of Graz) in collaboration with the Albanian archaeologists Gëzim Hoxha and Luan Përzhita (Albanian Institute of Archaeology, Tirana) carried out trial excavations in the area of the ancient town. Their investigations in the Lower City focused on two sites, known as 'Area A', directly north of the Skanderbeg Monument, in front of the Hellenistic city wall, and 'Area B', situated outside the Southwest Gate of Lissos, which had been partially excavated by Gëzim Hoxha and Frano Prendi during previous years. The results were published as a short report on the internet by Lehner & Pochmarski (Lissus Excavation Report 2004).



Photo 9: Skanderbeg Monument in the archaeological 'park' area. (Photo: Uncu, 2007)

Since 2006, the interdisciplinary archaeological project “*Urbanistik und sozio-ökonomische Strukturen einer hellenistischen Polis in Illyrien*” is carried out in ancient Lissos (see chapter 1.2). To renew the plan of the city, geodetic measurements as well as an architectural survey were conducted at the beginning of the project.

Brief reports on the progress of the current excavations can be found online (cf. www.dainst.de/index_772455eebb1f14a198290017f0000011_de.html).

6 Research design and methodology

Coastal landscapes have experienced major changes during the postglacial transgression. Around 6,000-5,000 years BC, the Holocene transgression reached a (relative) peak with the maximum landward shift of the shoreline in many areas. Due to a deceleration in sea level rise, in those areas where rivers debouched into the sea, coastal processes changed from marine-dominated to fluvial-dominated. Many rivers started to form coastal plains. Following the progradation of the river deltas, the environment around coastal settlements changed dramatically. Due to the shifting shoreline, harbours and sometimes even parts of the settlements were silted up; thus, many sites had to be abandoned. These phenomena are often well documented, both geologically (within the coastal deposits), as well as historically (in ancient documents). Therefore, the coastal sediments may serve as ideal geological and biological archives for palaeogeographic and geoarchaeological research. The combination of these studies together with information from archaeological excavations and historical sources may help to draft reconstructions of palaeogeographic scenarios spatially and chronologically, from Prehistoric times to the present.

The commonly used geoarchaeological approach (Brückner et al. 2005; revised versions cf. Brückner & Gerlach, 2007; Brückner & Vött, 2008) has been applied to the work in hand. The scheme of the research design is shown in fig. 19. A brief account of the theoretical concepts which were used as a base for deductive reasoning and environmental reconstruction is presented in section 5.1, with detailed definitions of the applied terminology in appendix 1.

As shown in fig. 19, one of the most important tools for “reading” the bio-geo-archives of a coastal setting are geological vibracoring. They can also be highly informative for archaeologists in cases where proper archaeological excavations are difficult or even impossible, e.g., due to the high water table. Therefore, geoarchaeological and palaeoenvironmental research in and around Lezha was carried out using vibracoring.

The lateral and vertical distribution patterns of sedimentary facies of the vibracores were correlated using Walther’s law of the facies correlation which is explained, among others, by Middleton (1973) and Kraft & Chrzastowski (1985). Thus, the cored sites were arranged in different cross-sections which allowed the establishment of palaeogeographic scenarios for the research area. ¹⁴C-AMS age estimates and diagnostic ceramics associated with information from literary sources gave a perspective to create a chronostratigraphic frame for the changing environmental conditions around Lezha through time.

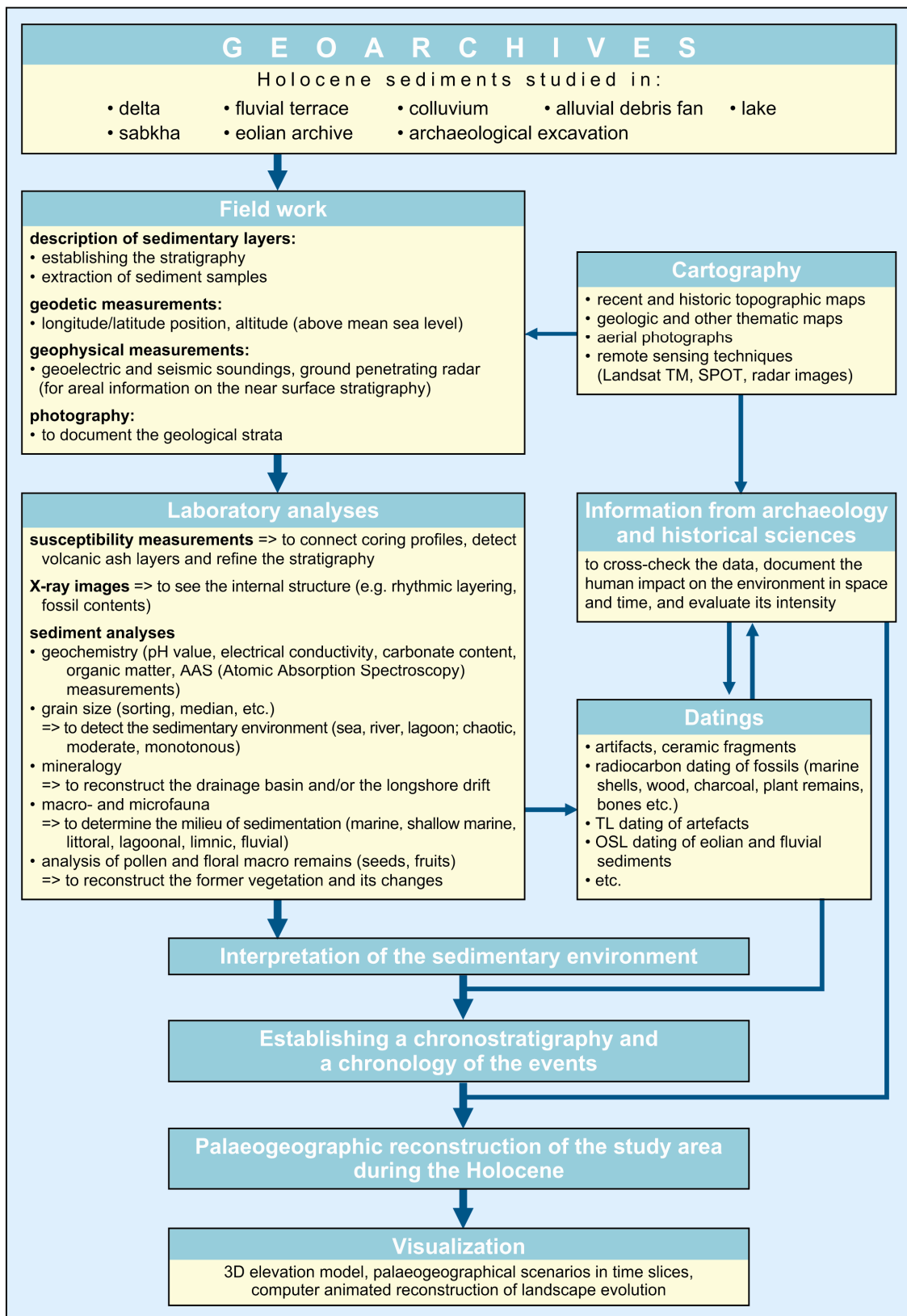


Figure 19: Methods of geoaerchaeology (Brückner & Gerlach, 2007, p. 59, fig. 7).

6.1 Theoretical concepts on depositional environments

Deltas form where rivers deposit more sediment into a large body of water, such as a lake or sea, than is removed by local currents. Deltas are progradational complexes, where fluvially derived sediments are accumulated and possibly reworked by fluvial, littoral or estuarine processes. The interaction of these processes produces a huge variety of morphologically different types of delta.

Applicable to this study is the classical concept from Gilbert (1885), who proclaimed that a delta is composed of three main sedimentary units: the topset, foreset and bottomset beds. According to him, bottomset and foreset deposits are mostly composed of monotonous fine sediments such as clays and silts. In contrast, delta topset beds are represented by a more complicated sediment pattern resulting from different depositional environments, both subaqueous and subaerial ones. Although a clear distinction between the two categories is not always possible, subaqueous environments generally include the prodelta and delta front, interdistributary bays and lagoons, as well as marine embayment- and sublittoral conditions. Subaerial environments include marshes and river channels, natural levees and flood basins, including residual lakes and swamps (Reineck & Singh, 1980). Crevasse splay sediments and various types of river channel deposits are further features which may be distinguished in sedimentary facies' analyses (see fig. 20 and appendix 1).

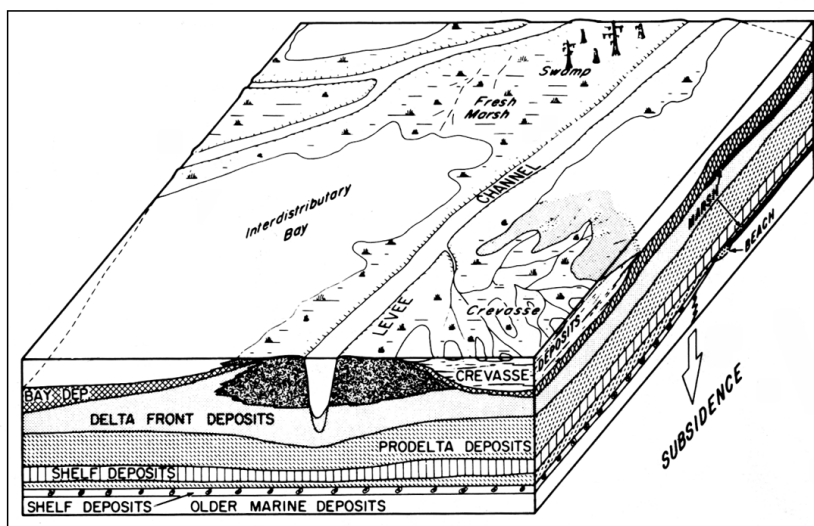


Figure 20: Block diagram showing the typical sediment facies of a bird's foot delta. (Coleman, 1976; in Wright, 1985, p. 58, fig. 1-33)

lime concretions, and content of macro- and microfauna. Such characteristics have been examined and described in detail by numerous researchers (Reineck & Singh, 1980; Davis,

The characteristics and dimensions of the deposits change vertically and laterally within the same environment. Different depositional conditions are reflected by variations in grain size, colour, structure, texture and other attributions, such as oxidation staining,

1983, 1985; Wright, 1985; Füchtbauer, 1988; McPherson et al.; Kraft & Chrzastowski, 1985; Carter & Woodroffe, 1994; Brown, 1997; Bridge, 2003; Reading, 2004).

The lack of a uniform classification makes it necessary to give at least brief definitions of the terminology used in this thesis (see also appendix 1). It has already been mentioned that it would be an impossible task to define unambiguous categories for each encountered environment, because of the enormous variety of factors involved in characterising a specific environment. Changes are often very subtle and the transition zones between differently designated environments should themselves be regarded as environments in their own rights.

6.2 Field work

During three field campaigns in 2006, 2007 and 2008, a total of 53 vibracores were retrieved in four different areas: (i) Balldreni plain (see photo 10), (ii) Merqia plain, (iii) Drini delta plain, and (iv) archaeological area. The vibration coring device Cobra mk1 of the Swedish Atlas Copco Company was used. Core diameters were 6 cm, 5 cm, 3.6 cm; maximum recovery depth was 13 m below present surface (coring LIS 25). In most cases, corings were carried out with semi-open probes. Only vibracore LIS 32, taken for pollen analysis, was retrieved using closed pipes in order to avoid any contamination with modern pollen.



Photo 10: Drilling with vibration corer Cobra mk1 in a pleasant location (Balldreni plain, LIS 26). (Photo: Brückner, 2007)

The geographical positions and altitudes of the cored sites were measured with Differential Global Positioning System (DGPS) based on the coordinate system WGS84 by Dipl.-Ing. Ursula Rübens, Technische Fachhochschule Berlin. Reference station for the measurements was

the “local point 100” with its geographical coordinates 41° 46' 58,05708" N; 19° 38' 32,38703" E in the Skanderbeg archaeological park. The “local point 100” was chosen by U. Rübens for practical reasons, and its coordinates were determined during the drilling campaign 2006 using GPS. Then, the data was transformed to be compatible with the ITRF system (International Terrestrial Reference Frame). To correct any technical errors, the results of the GPS-measured ellipsoidal heights were calculated using two different normal height models: DFHBF_DB Albanien (Finite Element Modelling, 17 Ground Control Points (GCP) from Albanian Survey by Dr. R. Jäger, Hochschule Karlsruhe) and EGG97 (European Geoid Model by Bundesamt für Kartographie und Geodäsie, U. Schirmer). In our case, the latter was used for the calculation of the altitudes because it can achieve an excellent accuracy (± 3 cm) which was needed for the reconstruction of the Holocene sea level curve.

It is important to note that the heights of some vibracoring which are located in the semiterrestrial part of the Drini delta plain (LIS 16, 31, 46, 50) and the Balldreni plain (LIS 39, 41) were measured to be below the present sea level. According to U. Rübens, this error could have arisen because each point was only measured once due to time constraints or because the distance to the reference station was too far for a better accuracy (“local point 100”). In such cases, the surface altitude was taken to be 0 m a.s.l.

In the field, each vibracore was photographed as a whole and several pictures were taken to capture details of individual sections of the core. Then a first sedimentological interpretation was given. The colours were described using the MUNSELL Soil Color Chart. Other properties of the sediments were determined using the “Bodenkundliche Kartieranleitung” (AG Boden, 2005). Grain size was identified by finger test, carbonate content was estimated with diluted HCl solution (10 %). All other diagnostic properties and features such as fossils, plant remains, charcoal, and archaeological material as well as oxidation/reduction stains were noted. Samples were taken in the laboratory for further analyses. ¹⁴C-datable organic matter (e.g., macrofossils, peat, wood, charcoal) was extracted. Archaeological artefacts were also separated from the samples to be identified by the archaeologists.

6.3 Laboratory work

Before carrying out various geochemical analyses, the sediment samples have to be prepared. The subsamples are then air-dried for about two weeks before they are carefully ground and sifted using a 2 mm sieve (Burt, 2004). The fine-grained section is then utilised for the various geochemical analyses described below.

6.3.1 Geochemical analyses

All of the sediment samples which were taken from the vibracores were analysed in the geolaboratory of the Faculty of Geography at Marburg University using standardised geochemical measurements (Schlichting et al., 1995; Barsch et al., 2000). The analyses were carried out according to standard norms of DIN (Deutsches Institut für Normung) and ISO (International Organisation of Standardization) regulations (see appendix 2).

6.3.1.1 pH value

The pH value is a measure of the acidity of a soil based on its hydrogen ion concentration. It provides a quantitative measure of the acidity or alkalinity. Thus, it helps not only to differentiate different soil types but also hints at the preservation capability of natural materials and artifacts (e.g., bone, fossils) within the deposit.

The pH value (DIN ISO 10390) is determined using a 1:5 (air-dried soil weight : volume of distilled water) soil suspension (Barsch et al., 2000: 325). An aqueous solution is achieved by stirring the mixture. The pH value is measured by means of a pH meter consisting of a glass electrode and reference calomel half-cell instrument (WTW Company Multi 340i) at 25 °C [pH (H₂O)]. Then a small amount of potassium chloride (KCl) is added to the solution and pH value is re-measured after 24 hours [pH (KCl)].

The pH value of soils ranges on a logarithmic scale from 1 to 14, where a pH value of 1-6.9 is acidic, pH 7 is neutral, and pH 7.1-14 is basic (alkaline). Lower pH values correspond with a larger number of H⁺ protons, while a higher pH is associated with a higher number of OH ions (Ellerbrock, 2000: 323).

Nearly all samples from the research area show neutral and basic (alkaline) pH values, except for the samples from vibracore LIS 27 and the upper part of vibracore LIS 09.

6.3.1.2 Electric conductivity

The electric conductivity is measured using the same aqueous solution which had been prepared for pH value measurements. It is determined at a standard temperature of 25 °C, using an electrical conductivity meter (EC meter, WTW Company Multi 340i). The EC is expressed in

microsiemens per centimetre ($\mu\text{S}/\text{cm}$) or millisiemens per centimetre (mS/cm) (DIN ISO 11265).

In coastal areas, the electric conductivity can be used as a good indicator for the saline and fresh water interface. Freshwater (fluvial, flood-plain and limnic) sediments have low conductivity values. In contrast, marine sediments are mostly characterised by a high conductivity value depending on the concentration of dissolved salts. This can also be valid for clay dominated samples. However, post-depositional salinisation due to evaporation has to be taken into account. This is especially true for near-surface samples of the delta plain.

In the research area, marine and lagoonal deposits show increased conductivity values, while low EC values within these milieus were caused by fresh water influx.

6.3.1.3 Loss-on-ignition (LOI)

The so-called loss-on-ignition (LOI) is done in order to measure the amount of organic matter within a sediment layer. In soils, organic material generally exists in the form of humus. It determines the ecological functions and properties of soils (e.g., soil structure, soil compressibility, soil colour, infiltration, cation exchange capacity, nutrient) (Höhn, 2000a: 341).

For the determination of organic matter in samples we used the basic one according to DIN 19684, T.3 (Schlichting et al., 1995: 159; Höhn, 2000a: 342; Heiri et al., 2001: 102). This method is based on sequential heating of the fine-earth fractions in a muffle furnace. 5 g of the sample are dried in the drying cabinet for 24 hours at 105 °C. Then it is annealed in the exsiccator and weighed. As second step, the sample is burnt in a muffle oven at 550 °C for 2 hours to incinerate organic matter. Thereafter, it is cooled again in an exsiccator and weighed. The weight differences between steps 1 and 2 are the loss-on-ignition, which is taken as a proxy for the organic matter of the sample (in weight percent).

A problem arises when the sample is rich in clay minerals or in sulphur, both may be the case for shallow marine or lagoonal samples. Heating up to 550 °C may lead to a desiccation of the H_2O of the crystal lattice of the clay minerals, while sulphur may be vaporized. However, the alternative method is the wet ashing with potassium dichromate ($\text{K}_2\text{Cr}_2\text{O}_7$) which is very time consuming and the waste water has to be treated as hazardous waste.

Organic content of sediments can be used as an indicator for the milieu and dynamics of deposition. It can demonstrate the evolution of a water body and may especially point out low-

energy sedimentation conditions (Müllenhoff, 2005: 51). In general, high amounts of organic matter may occur in a lake, lagoon, swamp, former river channel or an oxbow lake environment. In the study area, the organic matter content varies due to differences in the above-mentioned conditions.

6.3.1.4. Carbonate content

The carbonate content of the sediment is determined by natural conditions (carbonatic lithologies or carbonate containing fossils) and also by human activities (mortar, building materials, mining activities, fertilising).

In the field, to get an estimate of the amount of CaCO_3 , diluted hydrochloric acid (HCl 10 %) is applied to the sediment; the scale ranges from c0 (void of CaCO_3) to c5 (very high amount of CaCO_3) (cf. KA 5).

In the laboratory, the carbonate content is measured using the SCHEIBLER method (DIN ISO 10693) (Schlichting et al., 1995). 5-10 g of the sample are moistened with distilled water and diluted hydrochloric acid (10 %) is added to the sample in a calcimeter (gas-tight machine; e.g., Eijkelkamp Company, Art. no. 08.53) until all of the carbonate is converted to carbon dioxide (CO_2) according to the formula: $\text{CaCO}_3 + 2 \text{HCl} (10 \%) \rightarrow \text{CaCl}_2 + \text{H}_2\text{O} + \text{CO}_2 (\uparrow)$. The carbonate content of the sample is proportional to the measured CO_2 gas volume (volume percent). The actual atmospheric pressure and the room temperature need to be taken into account when calculating the results.

This method is semi-quantitative due to the fact that there are different carbonate sources within the sediment. It is impossible to differentiate between calcite (CaCO_3) and dolomite [$\text{CaMg}(\text{CO}_3)_2$], or between anorganic (e.g., in rocks) and organic (e.g., in fossils) carbonate (Schlichting et al., 1995: 146). However, for simplicity reasons, the overall carbonate content has been described as calcite (CaCO_3).

In the research area, the sediments usually have high carbonate contents due to the widespread occurrence of carbonatic rocks and the calcareous micro- and macrofauna. An exception is LIS 27, where the whole profile is carbonate free, probably because of the non-carbonatic flysch formations in the hinterland.

6.3.1.5 Phosphate content

The phosphate content of the sediment is often determined by the organic matter. Especially, upper soil horizons may have a high phosphate content due to both natural input (e.g., plant remains, bones, bioactivity) and various human activities (e.g., application of fertilisers, manure, grazing animals) (Crowther, 1997: 93). This kind of organic matters in the soils may remain detectable for 10^2 - 10^3 years (Crowther, 1997). Therefore, deposits of former occupation sites (e.g., shell middens, burials) also have high phosphate content (Crowther, 1997).

Phosphate in sediments consists of both inorganic (phosphate- P_i) and organic (phosphate- P_o) fractions. While it is possible to separate the two by using different analyses, in our case it was sufficient to measure the total phosphate content. 2 ml of concentrated hydrochloric acid digestion [1 g sediment and 25 ml of 37 % hydrochloric acid (HCl) is cooked at 60 °C for 2 hours; after filtration, distilled water is added to achieve a total of 50 ml solution] are mixed with 8 ml of reaction solution and 40 ml of distilled water. The reaction solution, prepared in advance, is produced by mixing 250 ml of sulphuric acid (H_2SO_4 , 25 %), 75 ml ammonium molybdate [$(NH_4)_6Mo_7O_{24} \cdot 4H_2O$], and 150 ml ascorbic acid ($C_6H_8O_6$). Then 25 ml potassium antimony (III)-oxide tartrate [$K(SbO)C_4H_4O_6 \cdot \frac{1}{2} H_2O$] are added and the solution is mixed again (Rump & Krist, 1987: 139). After 30 min of reaction the total phosphate contents of the samples were measured using a spectrophotometer, working with a wave length of 700 nm (Company Philips, PU 8620 UV/VIS/NIR). Later, the results of the measurements were calibrated using a calibration curve.

As already mentioned, a high amount of phosphate may be a good indicator for human activities. This is confirmed in the research area where high contents of phosphate were mostly observed in the cores which were done within the archaeological area. In addition, the uppermost parts of all corings as well as limnic and lagoonal sediments have high phosphate contents. The vertical variations and some high phosphate peaks in the profiles may indicate human-induced soil erosion.

6.3.1.6 Atomic Absorption Spectrometry (AAS) measurements

Atomic Absorption Spectrometry (AAS) is a method to measure the concentration of the different inorganic elements of a sediment sample (Baker & Suhr, 1982: 13), especially the alkali metal ions (e.g., K^+ , Na^+), alkaline earth metal ions (e.g., Ca^{2+} , Mg^{2+}) and heavy metal ions (e.g., $Fe^{2+/3+}$), which in turn give clues about the environmental conditions at the time of

deposition (Heinrichs, 2000; Vött et al., 2002). Due to their results, in general, high amounts of Fe, Mg and K ions may represent terrestrial facies (floodplain, fluvial, limnic) due to weathering processes and pedogenesis. In contrast, high amounts of Na and Ca ions can be considered as influence of marine conditions (Vött et al., 2002: 134; Schriever, 2007: 65).

For the digestion of the samples we used a diluted solution of concentrated hydrochloric acid digestion and distilled water in the proportion 1:100 (Schlichting et al., 1995: 138). After the sample has been transformed into a solution, it is put into the Flame-AAS where the concentration of the atoms of a given element is determined in the gas phase by measuring the intensity of the light absorbed by them when they are irradiated with electromagnetic radiation (Baker & Suhr, 1982; Höhn, 2000: 352). In our case, we measured the concentrations of K^+ , Na^+ , Ca^{2+} , Mg^{2+} and $Fe^{2+/3+}$ with a Perkin Elmer Flame-AAS A-Analyst 300. The results are expressed in g/kg.

6.3.2 Dating methods

To establish a chronostratigraphy, results from dating techniques (radiocarbon ^{14}C -AMS, OSL, diagnostic ceramics etc.) are combined with the stratigraphy of the corings, which show a succession of different environmental conditions. This is a useful tool in constructing palaeogeographic maps of the research area for different periods of time.

6.3.2.1 Radiocarbon (^{14}C -AMS) dating

Radiocarbon dating (^{14}C -AMS) is the most common method for late Pleistocene and Holocene research (Schellmann & Brückner, 2005). It works on the rate of decay of the radioactive carbon isotope 14 (^{14}C) produced by cosmic radiation in the atmosphere (Wagner, 1998; Geyh, 2005). The method is applied to organic matter, such as plants, seeds, wood, charcoal, peat, and mollusc shells. The activity of radioactive carbon in a sample can be measured either by the counting of beta particles emitted by decaying ^{14}C or by determining the $^{14}C/^{12}C$ ratio using the Accelerator Mass Spectrometry (AMS) technique (Hajdas, 2008: 7; Schellmann & Brückner, 2005: 467).

In our case, 57 samples were ^{14}C -AMS dated in two laboratories: in the AMS Laboratory of the Department of Physics, Friedrich-Alexander-University of Erlangen, and in the Center for Applied Isotope Studies (CAIS), University of Georgia, Athens, U.S.A. (see appendix 3).

The ^{14}C -AMS dating results were calibrated using the most recent on-line calibration program of Calib Rev 5.0.2 version which includes the datasets IntCal04, Marine04 and SHCal04 (M. Stuiver et al., 2006). All ages mentioned in the following chapters were calibrated; they are given as 'cal AD' or 'cal BC' (cal = calibrated years AD/BC).

Problems encountered when applying the ^{14}C -AMS dating method are the following ones: contamination, isotopic fractionation, marine reservoir effects, old wood effect and long-term variations in ^{14}C production (Wagner, 1998; Walker, 2005).

Contamination occurs in the form of additional younger or older carbon to the sample (Walker, 2005). For example, penetration of roots or younger humic acids can contaminate older horizons. E.g., the age of a peat sample can be too young due to a modern contaminant. Another kind of contamination may occur in a sample from a lake: it may be too old due to the incorporation of old carbon washed into the lake from the surrounding slopes (Walker, 2005).

Another problem for ^{14}C age estimates is the composition of the isotopic fractions of carbon (*isotope fractionation*). For instance, photosynthesis which is causing enrichment in ^{12}C and a relative depletion in ^{14}C in a growing plant can lead to an apparently older ^{14}C age (Walker, 2005). The isotopic fractionation effect can be normalised using standard ($\delta^{13}\text{C}$) values for various materials (Wagner, 1998; Walker, 2005). Our conventional ^{14}C ages were corrected for isotope fractionation by normalising to $\delta^{13}\text{C} = -25\text{‰}$ PDB, the main isotopic composition of wood (Walker, 2005: 26).

Surface waters of the sea have a higher $^{14}\text{C}/^{12}\text{C}$ ratio than the bottom waters due to an active carbon dioxide exchange with the atmosphere of the former (Wagner, 1998: 144). This phenomenon is known as the *marine reservoir effect* (ΔR). In general, for marine carbonates (e.g., mollusc shells, foraminifers, ostracods) a global ocean reservoir correction of about 400 years is applied (Reimer & McCormac, 2002; Reimer et al., 2004). In areas, where deep water rises to the surface (upwelling regions), the age correction may be much higher than the average value, in shallow seas with a fast turnover, reservoir correction may be much lower.

Wood is normally a very suitable material for ^{14}C dating. However, trees are long-living plants, some of them reaching several hundred years of age (e.g., oaks, olive trees, cedars). Therefore, wood from the same tree trunk may cover a range of several hundred years (*old wood problem*) (Wagner, 1998). The same problem may occur when using charcoal, with the added effect, that charcoal is more resistant to weathering; therefore, it can be easily re-deposited several times.

Another difficulty which was encountered during our project is the re-working of old material and subsequent incorporation into a younger stratum. This may be the case when the river erodes older strata in the hinterland and accumulates the re-worked fossils in a new delta lobe. For other examples see Stanley & Warne (1994) and Kraft et al. (2003).

6.3.2.2 Archaeological dating

Diagnostic ceramic fragments are also helpful to establish an age for a particular layer. In our case, intensive human influence is traceable in the uppermost parts of many cores within the archaeological area. The unearthed ceramic pieces date from Early Hellenistic to modern times. The ceramics were determined by Dr. Bashkim Lahi (Tirana), Dr. Manuel Fiedler (Berlin) and Gregor Döhner MA. (Berlin). In some cases, ceramic fragments of various ages were found together in the same layer (e.g., vibracorings LIS 04, LIS 06).

6.3.3 Palaeoecological analyses

The macro- and micro-organic remains such as fossils and peat layers within the sediments were examined to determine ecological characteristics of the depositional environment.

6.3.3.1 Macro- and microfossil examinations

Macro- and microfossil assemblages are used as a common tool in palaeoenvironmental and geoarchaeological research. Macrofossils include mussels (bivalvia) and snails (gastropods), microfossils foraminifers and ostracods. Due to quantitative and qualitative analyses of the fossil assemblages the sediments can be attributed to a particular milieu, and changing ecological conditions can be detected (Handl et al., 1999). Fossils can also provide suitable material for ^{14}C -AMS dating.

To carry out microfossil analysis, a subsample (approx. 10 cm³ of wet sediment) has to be taken. It is first put into solution [water and a very small amount of hydrochlorid acid (H₂O₂ 10 %)] to separate individual sediment particles. After about one day, the mixture is filtered through three sieves with a mesh-size of 400 µm, 200 µm, and 125 µm respectively, to extract micro- and macrofossils, which can later be identified under the microscope.

The fossils were mostly determined by Dr. Mathias Handl (Marburg), some samples also by Dr. Peter Frenzel (Institute of Geosciences, Friedrich-Schiller-University of Jena). For the

ecological interpretations of the identified microfossils the publication by Frenzel & Boomer (2005) was used.

In our research, the samples were poor in mollusc species (*Cerastoderma glaucum* and some others), but showed an abundant occurrence of microfossils, e.g., *Cyprideis torosa* (ostracod) and *Ammonia beccarii* (foraminifer), both indicating a brackish milieu. Ostracod and foraminifer species found in the described sediments are listed individually for each coring (see also appendix 4).

6.3.3.2. Palynological analyses

Six selected peat samples, taken during the 2006 field campaign, were palynologically analysed by Dr. Maria Knipping, University of Hohenheim, Stuttgart. These determinations were supported by ¹⁴C-AMS dates. For palynological analysis well-preserved buried peat layers were used, marking the transition zone from shallow marine or brackish to terrestrial conditions. Sample preparation was as follows: 1 cm³ of the sample was washed by wet sifting; non-organic matter was destroyed using a strong chemical digestion (for more details of the technique see Beug, 2004). After this procedure, the sample was examined with a light microscope, both qualitatively and quantitatively. Species of pollen grains were identified as arboreal and non-arboreal taxa, and their shape and texture were noted. Macro remains such as pieces of wood, seeds and leaves were also determined.

During the 2007 campaign, palynological samples were taken from buried peat layers inside and around the archaeological area of Lissos. This was supplemented by a drilling with closed pipes on the silted-up lake at the Malokaj village, close to the Buna delta. This coring (LIS 32) reached a total depth of 14 m. It will help to decipher the vegetation history of NW Albania. Work is currently under progress in cooperation with Dipl.-Biol. Michele Dinies (Berlin).

6.4 Literary sources

Ancient sources from Greek and Roman historians and geographers were used to support or verify the radiocarbon datings and the chronostratigraphic framework of the palaeogeographic scenarios. In the context of our research, the ancient sources from ca. 200 BC to 200 AD are vitally important because only a few radiocarbon dates are available for the Roman period of the research area. Therefore, the chronostratigraphical framework for the Roman times is based largely on historic accounts. The ancient sources with references to Lissos are listed in table 6.

Name	Oeuvre (reference to Lissos)	Original Name	Lifetime
Polyb	Histories, II, 12, 3; III, 16, 3; IV, 16, 6; VIII, 13,1-9; XXVIII, 8, 4	Polybius	203-120 BC
Caesar	Bellum civile, III, 26, 3; 28, 1, 2; 29, 1, 3; 40, 5, 6; 42, 4; 78, 4, 5	Gaius Iulius Caesar	100-44 BC
Diodor	The Library of History, XV, 13, 1-5; 14, 2	Diodorus Siculus	1 st cent. BC
Strabo	The Geography, VI, 2, 4; VII, 5, 8	Strabon	64/63 BC-24 AD
Livy	History of Rome, VI, XLIII, 20, 4; XLIV, 30, 6, 7	Titus Livius	59 BC-17 AD
Pliny the Elder	Natural History, III, 22-23	Gaius Plinius Secundus	23-79 AD
Lucan	The Pharsalia (De Bello Civili), V, 719	Marcus Annaeus Lucanus	39-65 AD
Plutarch	The Parallel Lives, IX, 7	Lucius Mestrius Plutarchus	46-120 AD
Appian	History of Rome: The Illyrian Wars, 7	Appianos of Alexandria	95-165 AD
Ptolemy	The Geography, II, 16, 38	Claudius Ptolemeus	2 nd cent. AD

Table 6: Ancient sources with references to Lissos (compiled by L. Uncu, 2010).

In addition to ancient sources, reports and scripts from the late medieval times also prove useful in determining the environmental conditions around Lezha. The collection of reports and traveller's impressions of the landscape around Lezha and the river Drini from the 16th and 17th century presented by Elsie (2003) was particularly valuable (see chapter 8.11).

6.5 Cartographic information

In this research project, different topographical maps – sheets: K-34-76-C-a (Shengjini), K-34-76-C-b (Lezha), K-34-76-C-c, K-34-76-C-d (published in 1980, scale 1 : 25,000) and sheets: 2978 I (Lezhë) and 2978 II (Krujë) (published in 1998, scale 1 : 50,000) – were used. These maps have been published by the Instituti Topografik i Ushtrisë in collaboration with the National Imagery and Mapping Agency (NIMA).

As well as modern maps, a number of historical maps of north Albania (middle of the 3rd century AD to the beginning of the 20th century) were also utilised. The first cartographic documentation was compiled by Franz Baron Nopcsa in 1916. Later, he republished the same paper as an appendix in his monograph “The Geology and Geography of North Albania” (Nopcsa, 1929b). These maps hold suitable information about the Drini during the last two thousand years, including changes of the river's course and its mouth, as well as the shifting of the coastline (for more detailed information see table 9).

6.6 Satellite images

The quality of the Landsat images was not adequate, partly due to their low resolution and cloud cover. For this reason, the palaeogeographic scenarios were constructed using a Google-Earth Image of North Albania from 2009 (access: 22-12-2009).

6.7 Graphic implementation

Various types of software programmes were used for graphic implementation: The geologic profiles, transects and some other illustrations were drawn with FreeHand MX 11.0.1, Macromedia. The geomorphologic map and the palaeogeographic scenarios were created using ArcGIS Desktop 9.2.0.1324, ESRI. Results from the geochemical analyses were graphically implemented with Grapher 5.0.3, Golden Software, whereas photographs and some other graphics were edited with Adobe Photoshop 7.0 and Microsoft Paint 2003.

7 Results and discussion

The research area has been divided up into four distinct sections, namely (i) the Balldreni plain, (ii) the Merqia plain, (iii) the archaeological area in Lezha, and (iv) the Drini delta plain (fig. 21 and fig. 29). In this chapter, these areas will be considered one by one, firstly discussing the individual coring profiles in detail with reference to their sedimentological characteristics and geochemical parameters (see also appendix 5 for a more detailed graphic implementation, statistical data, as well as photos of the individual corings), their contents in terms of micro- and macrofossil remains, as well as cultural material. Secondly, a synoptic view will be taken by grouping the individual coring results into geological transects. The above mentioned sediment characteristics are used to infer the depositional conditions with ^{14}C age estimates helping to establish a chronostratigraphy. An interpretation of the research area as a whole will be presented in the shape of several palaeogeographic scenarios in chapter 8, depicting the stages of coastal development and shifting river courses in the area around Lezha from the Middle Holocene until the present day.

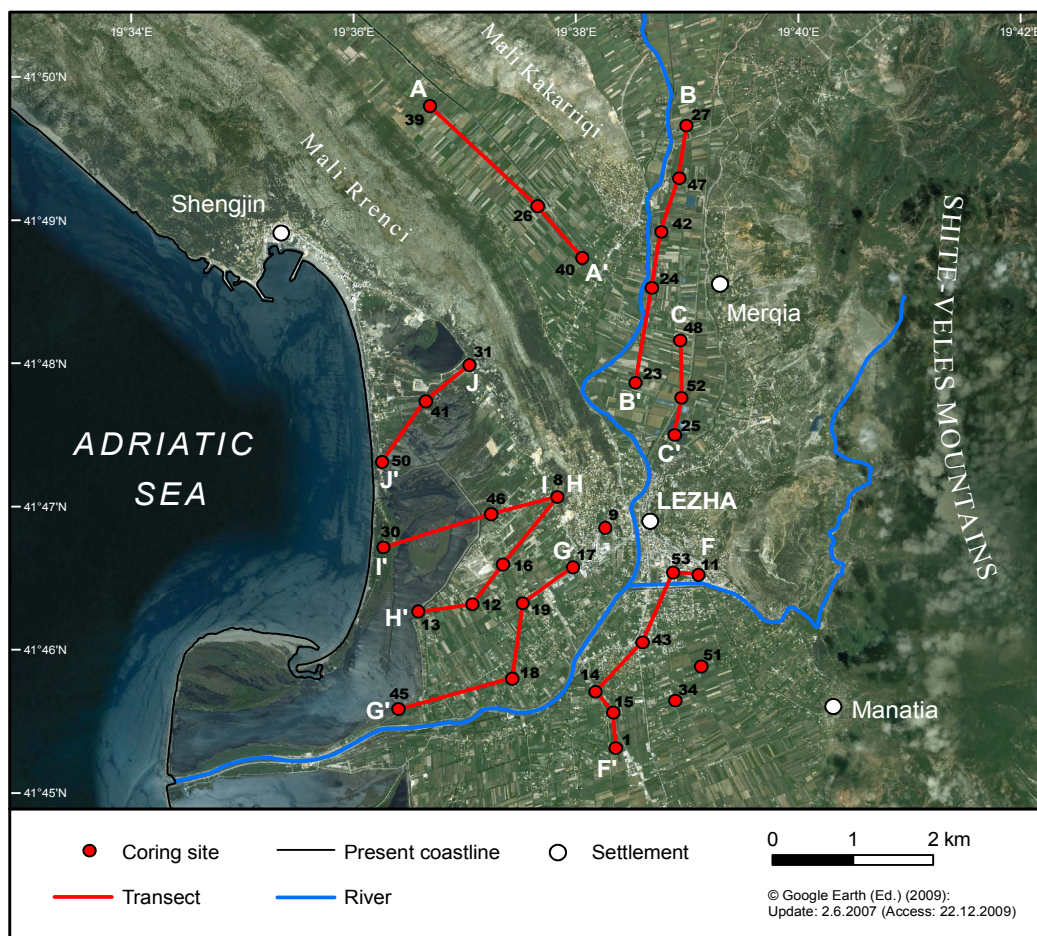


Figure 21: Location of coring sites and their arrangement in transects (Uncu, 2010, based on a satellite image from Google Earth, accessed 22-12-2009).

7.1 Corings from the Balldreni plain

The Balldreni plain lies northwest of Lezha between the limestone ridges of Mali Rrenci and Mali Kakarriqi. The coring sites are located on a former swampy area known as “Lake Balldreni”. An attempt was made to drain this lake/swamp in the 1950’s, but the clayey deposits still cause the formation of shallow lakes during the rainy season. For this reason the plain had not been settled until very recently. Even now, only a few settlements (e.g., Cella village, founded in 2002) were build on the lower western slopes of Mali Kakarriqi.

7.1.1 Transect A-A’

To be able to understand the palaeogeographic evolution of the Balldreni plain, the results from vibracoring LIS 40, LIS 26 and LIS 39 are correlated in transect A-A’, which runs across the plain from the NW to the SE. The coring sites are almost parallel to the Muratil canal, which is draining the plain (fig. 21).

7.1.1.1 Vibracoring LIS 39

LIS 39 (N 41° 49’ 50’’, E 19° 36’ 35’’, ground level at p.s.l., total length of core: 12 m) is located in the centre of the plain, 2 km NW of coring LIS 26. A synoptic view of the profile is shown in appendices 5.28.1 & 5.28.2.

The lower section of the profile begins with very dark grey, homogeneous fine sandy silt, intercalated with thin clayey and peaty layers (up to 5.87 m b.s.l.). The whole stratum is characterised by high values of electric conductivity (up to 3.95 mS/cm), abundant organic matter (up to 7.02 %), and a high amount of calcium carbonate (up to 23.45 %). The sediment contains an abundance of brackish species (macrofossil: *Cerastoderma glaucum*; ostracods: *Cyprideis torosa*; foraminifers: *Ammonia beccarii*, *Ammonia* cf. *parkinsoniana*, *Ammonia* cf. *tepida*). An increasing freshwater influx is confirmed by some oogonia (Characeae) and a few remains of a terrestrial mycorrhiza (*Cenococcum geophilum*).

From 5.87 to 3.40 m b.s.l., the section is composed of intercalated layers of silty fine sand and clayey silt. The fauna of the deposits are dominated by brackish and estuarine species (macrofossils: *Cerastoderma glaucum*, *Hydrobia* sp.; ostracod: *Cyprideis torosa*; foraminifers: *Ammonia* cf. *parkinsoniana*, *Haynesina germanica*).

These sediments are overlain by homogeneous clayey silt with an abundance of *Cerastoderma*

glaucum (up to 1.60 m b.s.l.). Grain size and fossil content indicate calm depositional dynamics under brackish conditions, possibly created by the prograding delta cutting off the direct connection between the sea and the marine corridor. Gradually, a freshwater lake had developed. The numerous oxidation stains point to semi-terrestrial conditions.

7.1.1.2 Vibracoring LIS 26

LIS 26 (N 41° 49' 07'', E 19° 37' 39'', ground level at 1.78 m a.s.l., total length of core: 10 m) is located close to the Muratil canal in the plain, 1 km NW of LIS 40. A synoptic view of the profile is shown in fig. 22, photo 11, and appendix 5.19.

The lowest part of the profile consists of very dark grey, homogeneous medium sand (up to 6.65 m b.s.l.). The mineral composition of the sediment is similar to recent coastal deposits in the Drini delta (e.g., serpentine, mica, quartz, cryzolite, pyrite). The high value of calcium carbonate (up to 23.17 %) and the ratio of $\text{Ca}^{2+}/\text{Mg}^{2+}$ (3.1) may have been caused by the carbonate bedrock and karstic sources which led to brackish conditions in a “canale-type coast”. The sediment contains brackish to shallow marine species (macrofossil: *Cerastoderma glaucum*; foraminifers: *Ammonia beccarii*, *Elphidium crispum*). The granulometry as well as the fossil content suggest a deposition in a sublittoral environment.



Photo 11: Coring LIS 26. (Uncu, 2007)

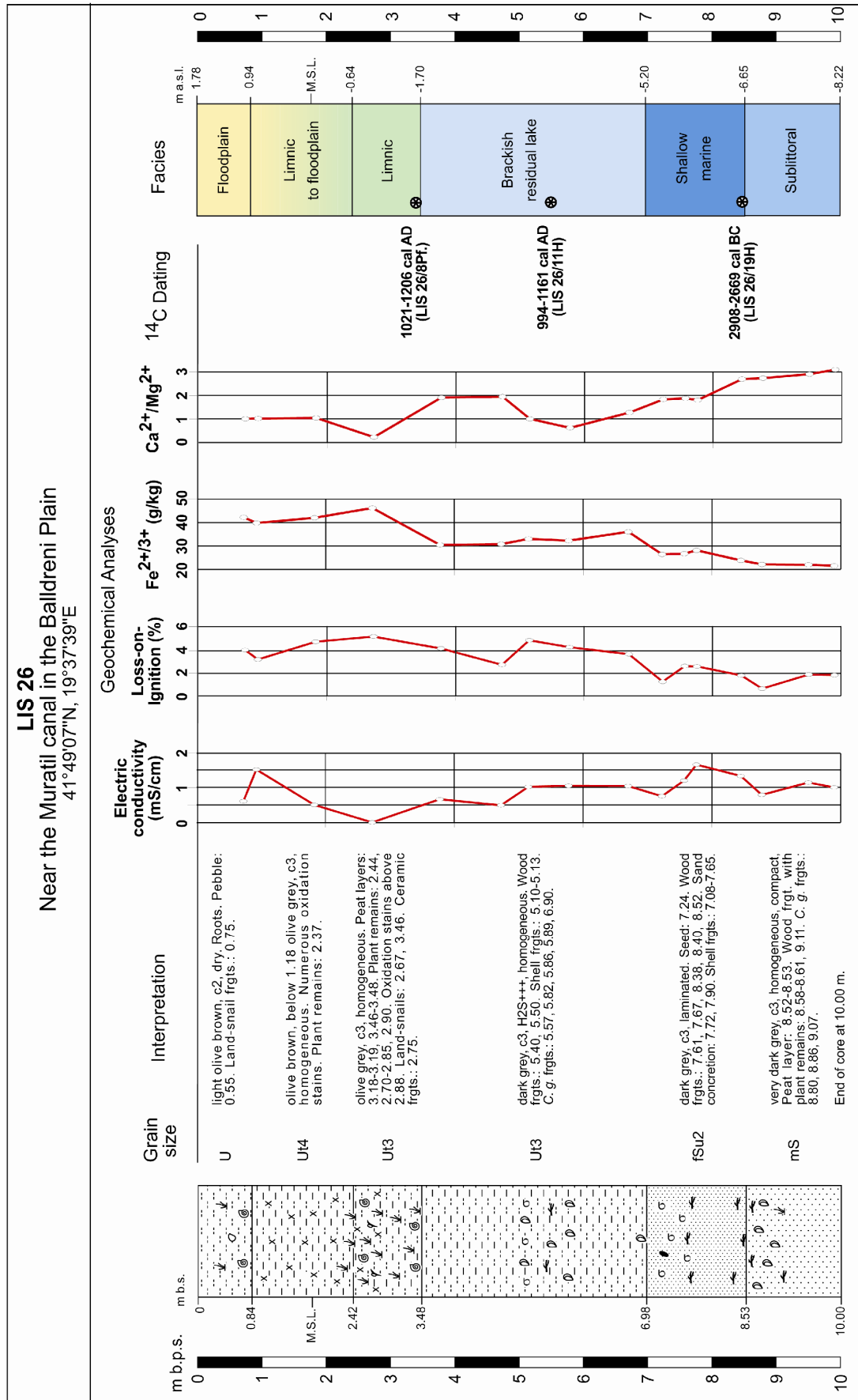


Figure 22: Synoptic chart of coring LIS 26.

The stratum is overlain by homogeneous fine sand (up to 5.20 m b.s.l.). The fossil content comprises brackish and estuarine species (macrofossils: *Cerastoderma glaucum*, *Hydrobia* sp.; ostracod: *Cyprideis torosa*; foraminifer: *Ammonia beccarii*). Many pieces of wood and a seed were transported from neighbouring slopes or from the river Drini to this location.

The middle section of the profile is made up of dark grey, clayey silt (up to 1.70 m b.s.l.). The granulometry and abundant fauna (macrofossils: *Bittium latrelleii*, *Cerastoderma glaucum*, *Hydrobia* sp., *Rissoa* cf. *labiosa*, *Tellina* sp.; ostracods: *Cyprideis torosa*, *Paracytherois* cf. *rara*; foraminifer: *Ammonia beccarii*) indicate a deposition under the calm conditions of a shallow marine/brackish environment, but affected by a strong freshwater influx. The relatively high content of organic matter (up to 4.94 %) and $\text{Fe}^{2+/3+}$ ions (36.06 g/kg) as well as the low CaCO_3 content (6.13 %) point to anaerobic conditions. The subsequent layer also consists of olive grey, clayey silt; it includes numerous plant remains and a few terrestrial gastropods. Above 1.10 m b.s.l., the sediment contains numerous oxidation stains, indicating a change to more terrestrial conditions. The stratum also contains two small unidentifiable ceramic fragments.

From 0.64 m b.s.l. to 0.94 m a.s.l., the sediment becomes more clayey with numerous oxidation stains. The colour changes from olive grey to olive brown at 0.60 m a.s.l. This stratum reflects a semi-terrestrial/swampy environment. The increased electric conductivity (2.01 mS/cm) can be interpreted by occasional intrusions of saltwater. The following light olive brown silt layer accumulated during flooding events of the Drini.

7.1.1.3 Vibracoring LIS 40

LIS 40 (N 41° 48' 45'', E 19° 38' 01'', ground level at 2.96 m a.s.l., total length of core: 12 m) is located between the towns of Lezha and Balldreni. A synoptic view of the profile is shown in appendices 5.29.1 & 5.29.2.

The lowermost part of the core is characterised by very dark grey, homogeneous, silty fine sand with many thin peat layers (up to 6.60 m b.s.l.). The latter are evidence of former coastal swamps. The fossil content (macrofossil: *Hydrobia* sp.; foraminifers: *Quinqueloculina* sp., *Siphonaperta* sp.; ostracods: *Pontocythere* sp., *Aurila woutersi*, *Cyprideis torosa*) and the ratio of $\text{Ca}^{2+}/\text{Mg}^{2+}$ (3.27) reflect a deposition under shallow marine/brackish conditions. Upwards, the fossil content becomes dominated by brackish species (foraminifers: *Ammonia* cf. *parkinsoniana* and an unidentified specimen of the Trochamminidae family).

The subsequent dark grey loamy silt with relatively high electric conductivity values (2.07-2.33 mS/cm) and abundant shell fragments indicates a change towards calm depositional conditions (up to 6.38 m b.s.l.). Homogeneous clayey silt follows with many *Cerastoderma glaucum* fragments (up to 5.20 m b.s.l.). The values of electric conductivity (1.50 mS/cm) and the fossil content suggest a deposition in an interdistributary bay environment under brackish conditions.

The following stratum is made up of intercalated layers of dark grey, silty fine sand and very dark grey clayey silt (up to 2.64 m b.s.l.). The latter contains thin peat layers and plant remains. The high electric conductivity value (2.07-2.33 mS/cm) may indicate a temporary saltwater ingress (e.g., at 3.82-3.72 m b.s.l.). The intercalations and the rich organic content suggest the continuance of the interdistributary bay milieu.

The following dark grey to olive brown pebbly sand indicates changed sedimentation dynamics. An increased freshwater input caused the electric conductivity value to decrease from 1.14 to 0.35 mS/cm. The fossil content (macrofossils: many broken pieces of *Cerastoderma glaucum*; ostracod: *Cyprideis torosa*; foraminifer: *Ammonia beccarii*) and a few oogonia specimen of Characeae suggest a deposition under brackish conditions at the mouth of the Drini.

Above 1.74 m b.s.l., the sediment consists of light grey fine sandy silt. The lime concretions and numerous oxidation stains in the uppermost part of the layer indicate a transition to seasonally wet and dry, semi-terrestrial conditions.

From 1.48 to 0.49 m b.s.l., the sediment is made up of light grey clayey silt with oxidation stains and black organic spots. This stratum was deposited under calm conditions, such as a shallow freshwater lake. Above 0.50 m b.s.l., the clay content increases and the colour changes to olive brown. The uppermost section of the core consists of clayey and fine sandy silt layers, deposited in a semi-terrestrial environment during periods of flooding.

7.1.1.4 Synopsis of transect A-A'

The lower part of all cores in this transect (fig. 23) comprises marine deposits. Core LIS 39 shows more definite signs of marine conditions than the other two cores of this transect. The dominant grain size of cores LIS 39 and LIS 40 is silty fine sand, which suggests relatively calm depositional conditions. The repeated occurrence of paralic peat layers within the marine sand may indicate a step-wise rise in sea-level, possibly triggered by co-seismic events. Two ¹⁴C age estimates from such peat lenses reveal that marine conditions existed in the second half of the

4th millennium BC [3485-3107 cal BC, peat at 7.97-8.00 m b.s.l. (LIS 39/25T); 3345-3096 cal BC, wood at 7.83 m b.s.l. (LIS 40/26H)].

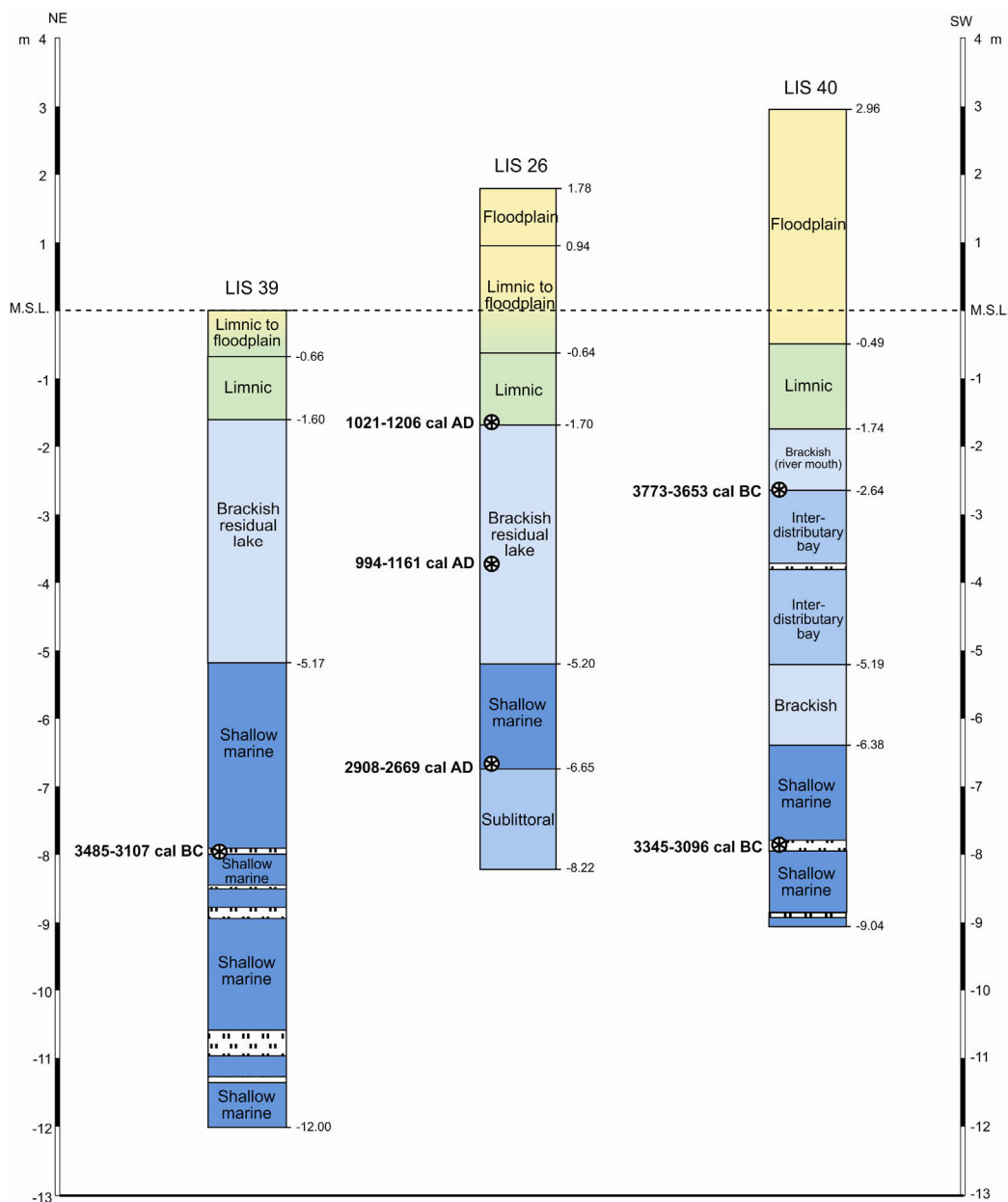


Figure 23: Geological transect A-A' (own research).

The medium sand in the lowest part of LIS 26 accumulated under sublittoral conditions. It contains numerous specimens indicative of brackish conditions (especially *Cerastoderma glaucum*) and a few estuarine gastropods (*Hydrobia* sp.) as well as many pieces of wood, which points to an important freshwater influx from the Drini. The overlying fine sandy stratum is concordant with the deposits in LIS 39 and LIS 40. The transition from sublittoral to shallow marine conditions occurred during the first half of the 3rd millennium BC [2908-2669 cal BC, wood at a depth of 6.65 m b.s.l. (LIS 26/19H)].

The shallow marine deposits are covered by clayey sediments, thereby implying a change towards calm/brackish depositional conditions. This is also confirmed by abundant *Cerastoderma glaucum* specimens within the deposits. In contrast to the relatively homogenous strata of LIS 26 and LIS 39, sandy intercalations at LIS 40 reflect an occasional sediment input by the Drini. After the delta front had passed, freshwater conditions became dominant at this coring site.

The sediments of LIS 26 suggest that brackish conditions existed much longer, even in the 11th century AD [994-1161 cal AD, wood at 3.72 m b.s.l. (LIS 26/11H)]. The change to a freshwater environment only took place during the 12th century AD [1021-1206 cal AD, plant remains at 1.69 m b.s.l. (LIS 26/8Pf.)]. Limnic conditions prevailed until the middle of the 20th century, when finally the whole area was drained and transformed to arable land.

7.2 Corings in the Merqia plain

The Merqia plain lies directly north of Lezha. It is connected to the Zadrime plain between Mali Kakarriqi and Shkodra and it also borders the Balldreni plain in the NW. The river Drini drains this large alluvial plain. Therefore, understanding the palaeogeographical changes in the Merqia plain plays a vital role in the context of the southwards progradation of the Drini delta and the development of the ancient city of Lissos.

To achieve this aim, we retrieved eight corings in total, which were then used to construct two transects, running roughly parallel to the river Drini across the Merqia plain from N to S (fig. 21).

7.2.1 Transect B-B'

This transect contains corings LIS 27, LIS 47, LIS 42, LIS 24, and LIS 23 (fig. 21), and runs from the southern Zadrime plain to the central part of the Merqia plain.

7.2.1.1 Vibracoring LIS 27

LIS 27 (N 41° 49' 44'', E 19° 39' 01'', ground level at 5.29 m a.s.l., total length of core: 11 m) is located in the southernmost part of the Zadrime plain, southwest of the town of Rraboshta. A synoptic view of the profile is shown in fig. 24, photo 12, and appendix 5.20.

The lowermost part of the core consists of angular stones and well rounded pebbles, derived

from the sandstone outcrops along the western slopes of the Shite-Veles Mountains, in a fine sandy silt matrix (up to 5.01 m b.s.l.). The brown colour of the sediment together with some oxidation stains suggests the development of a palaeosol. The subsequent black clayey silt also includes well rounded pebbles (up to 4.19 m b.s.l.). The next stratum is made up of dark greenish grey coarse sand with angular stones (up to 4.06 m b.s.l.). From the bottom of the coring to 4.06 m b.s.l., the varying grain size as well as the presence of angular and well rounded material represents the different morphodynamic phases of the evolution of an alluvial fan. The dark grey and blackish colour of the matrix shows that the sediments were deposited in a swampy (semi-terrestrial) environment.

From 4.06 to 2.21 m b.s.l., the sediment is made up of dark greenish grey fine sandy silt. This stratum is interrupted by a layer of angular stones, which again represents an alluvial fan (between 3.36 and 3.19 m b.s.l.). Two rounded ceramic fragments within the stratum (at 3.90 and at 2.47 m b.s.l.) may have been carried to this location by a stream from a prehistoric settlement in the catchment area. The granulometry and low electric conductivity values (0.06-0.09 mS/cm) point to a deposition in a limnic environment.

Above 2.21 m b.s.l., the sediment is overlain by homogeneous clayey silt with some oxidation stains and plant remains (up to 0.66 m a.s.l.). At present sea level, the colour changes from dark greenish grey to olive grey. The granulometry and geochemical results – low pH value (between 5.84 and 6.16) and high amounts of $\text{Fe}^{2+/3+}$ ions (41.75 g/kg) – suggest acidic conditions. A few pebbles within the sediment must have been deposited during flooding events.



Photo 12: Coring LIS 27. (Uncu, 2007)

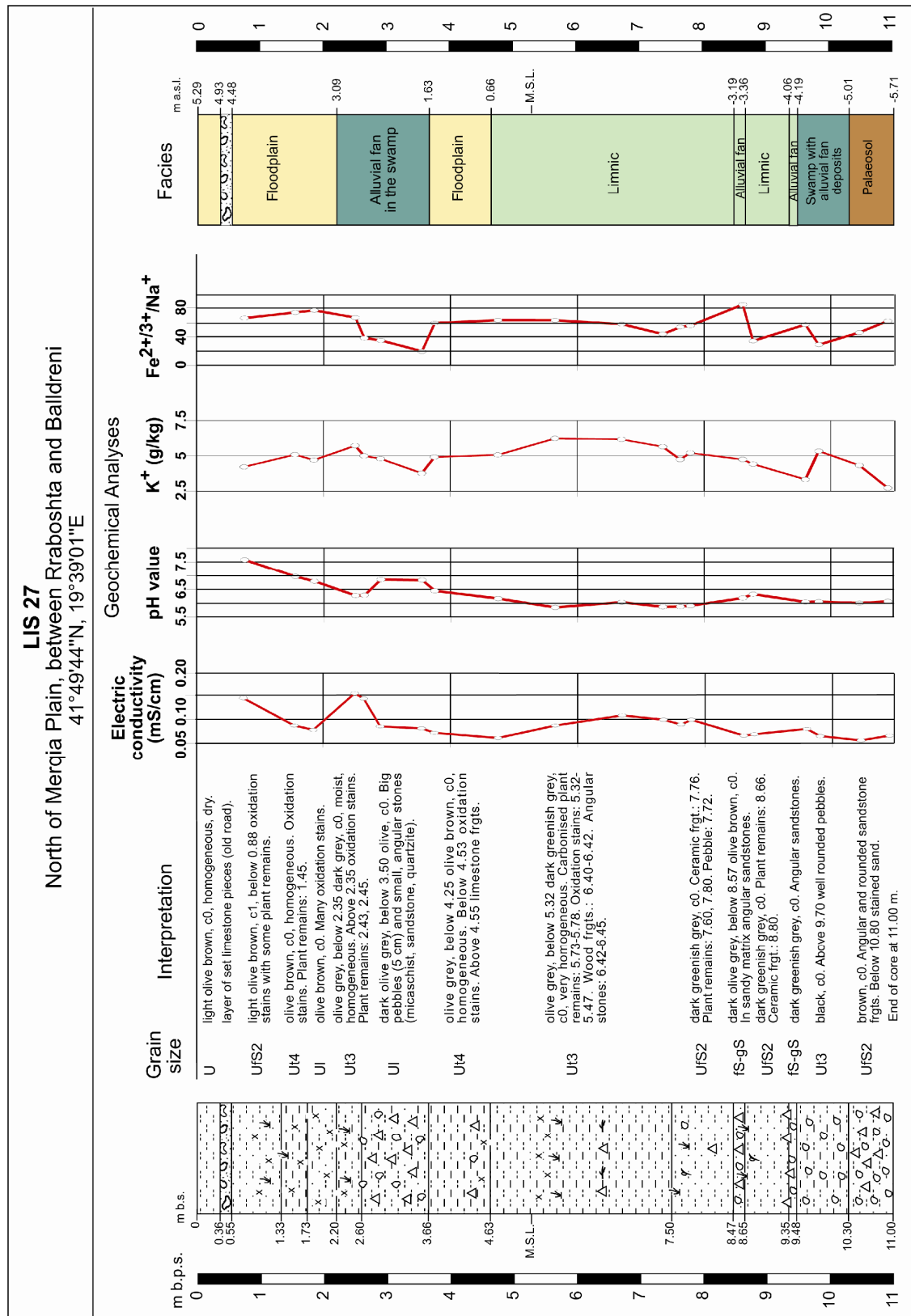


Figure 24: Synoptic chart of coring LIS 27.

From 0.66 to 1.63 m a.s.l., the clay content and oxidation stains within the sediment increase. The stream did not have enough capacity to transport a big load, which is evidenced by the presence of only two stones within this layer. Subsequent deposits are composed of pebbles

(max. 5 cm) and angular pieces of sandstone and mica-schist in a dark olive grey loamy matrix (up to 2.69 m a.s.l.). This layer can again be attributed to an alluvial fan environment.

The uppermost section of the core consists of intercalated strata of clayey, loamy and fine sandy silt with numerous oxidation stains and a few plant remains. The lack of coarser material points to calm depositional conditions in a floodplain environment up to date. A layer of set limestones (between 4.48 and 4.93 m a.s.l.) probably represents a former road.

7.2.1.2 Vibracoring LIS 47

LIS 47 (N 41° 49' 16'', E 19° 38' 57'', ground level at 3.61 m a.s.l., total length of core: 12 m) is located on the border between the Zadrime plain and the Merqia plain, 500 m northeast of the town of Balldreni. A synoptic view of the profile is shown in fig. 25, photo 13, and appendix 5.35.

The lowermost part of the profile consists of fine sandy silt with intercalated clayey layers. The geochemical results (relatively low value of electric conductivity: 1.57 mS/cm; high value of calcium carbonate: 16.21 %; high ratios of $\text{Ca}^{2+}/\text{Mg}^{2+}$: 2.55) and the fossil content (macrofossil: *Cerastoderma glaucum*; ostracod: *Cyprideis torosa*; foraminifer: *Ammonia beccarii*) suggest a deposition under brackish conditions in a marine embayment with strong freshwater input (up to 6.99 m b.s.l.).

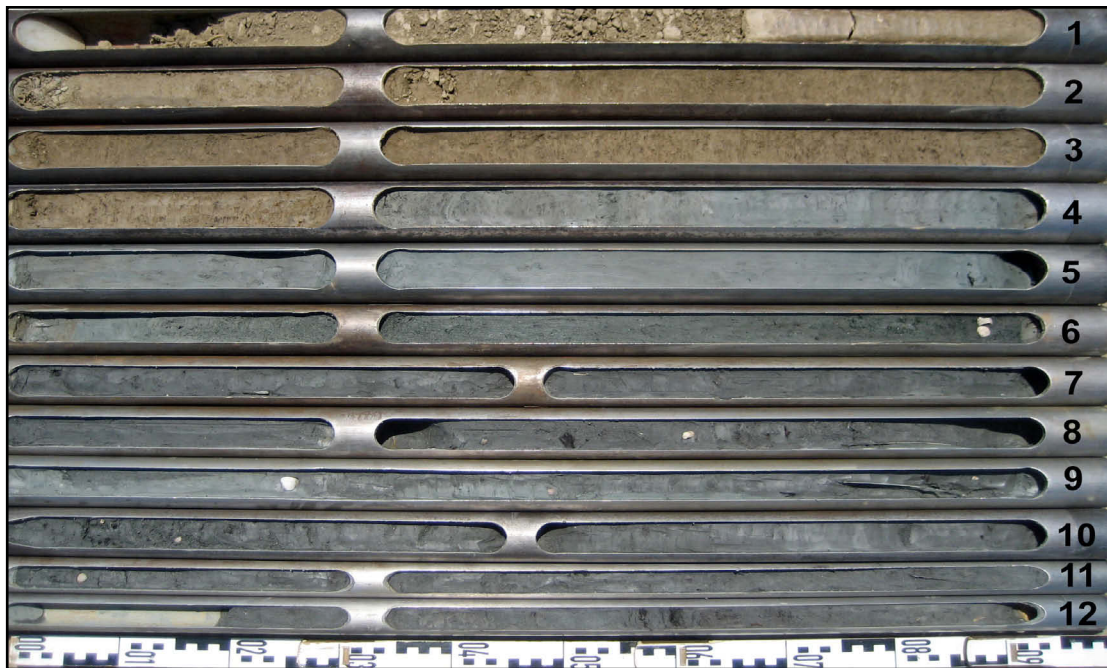


Photo 13: Coring LIS 47. (Uncu, 2008)

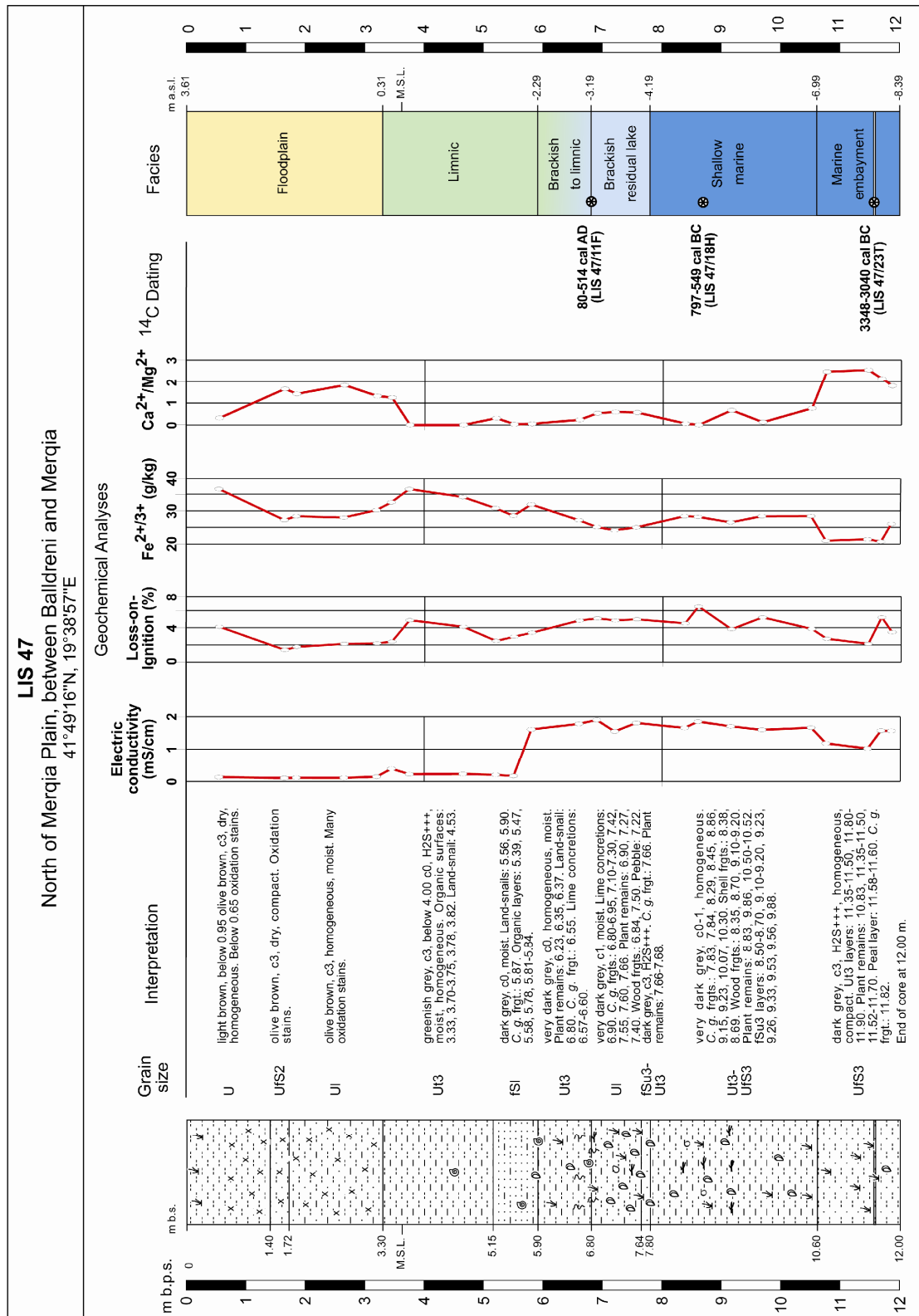


Figure 24: Synoptic chart of coring LIS 47.

These sediments are overlain by homogeneous clayey silt with numerous plant remains and pieces of wood (up to 4.03 m b.s.l.). Thin fine sandy lenses are intercalated. Geochemical analyses (low value of calcium carbonate: 1-6 %; relatively high contents of organic matter: 4-6 %) show a change towards anoxic and stagnant water conditions. The fossil fauna contains

largely salt tolerant brackish species (macrofossil: *Cerastoderma glaucum*; foraminifers: *Ammonia beccarii* cf. *tepida*, *Ammonia beccarii* cf. *parkinsoniana*; ostracods: *Cyprideis torosa*, *Cytheromorpha fuscata*). This layer is covered by homogeneous loamy silt with many specimens of *Cerastoderma glaucum* (up to 3.19 m b.s.l.).

The following stratum of clayey silt shows the first terrestrial influence: landsnails and CaCO₃ concretions. The latter indicate a seasonal variation of wet and dry conditions. The termination of the brackish conditions in the area is reflected by a *Cerastoderma glaucum* fragment at the transition to the subsequent layer of loamy fine sand (at 2.30 m b.s.l.), deposited by the Drini in a semi-terrestrial/swamp environment. The sharp decrease in the electric conductivity (from 1.61 to 0.17 mS/cm) towards the top of the layer also points to a strong freshwater influx.

From 1.55 m b.s.l. to 0.30 m a.s.l., the sediment is made up of greenish grey, clayey silt with an increasing amount of organic matter (4.88 %), which suggests a deposition under calm conditions. The high value of Fe^{2+/3+} (36.57 g/kg) and the low value of carbonate (3.42 %) indicate anoxic conditions. The uppermost part of the profile consists of fine-grained floodplain sediments with numerous oxidation stains.

7.2.1.3 Vibracoring LIS 42

LIS 42 (N 41° 48' 57'', E 19° 38' 43'', ground level at 3.93 m a.s.l., total length of core: 12 m) is located in the north of the Merqia plain, approximately 200 m east of the town of Balldreni. A synoptic view of the profile is shown in appendices 5.31.1 & 5.31.2.

The lower section of the profile is characterised by very dark grey, silty fine sands, with a few intercalated clayey layers. The latter include thin peat lenses and numerous plant remains. The poor fossil content of the sandy strata (only a few microfossils; ostracod: *Cyprideis torosa*; foraminifer: *Ammonia beccarii*) imply ecologically unsuitable conditions. The microfaunal and geochemical analyses (high calcium carbonate content: 19-21 %, electric conductivity values: 0.70-1.02 mS/cm, high ratio of Ca²⁺/Mg²⁺: 3.01) indicate a deposition under brackish conditions in a marine environment (up to 4.75 m b.s.l.).

The subsequent dark grey, clayey silt layer exhibits high values of electric conductivity (3.60 mS/cm) and organic matter (13.94 %), which, together with the lack of calcium carbonate indicate anoxic conditions in a stagnant water body such as interdistributary bay.

From 4.51 to 1.27 m b.s.l., the sediment consists of dark olive grey, medium/coarse sand with well rounded pebbles (max. size: 3 cm) and pieces of wood (1.87-1.74 m b.s.l.). The electric conductivity decreases dramatically from 3.60 to 0.08 mS/cm. The coarse grain size suggests a deposition in a river channel.

The following layers of silty fine sand (1.27-0.95 m b.s.l.), fine/medium sand (0.95 m b.s.l. to 0.40 m a.s.l.), pebbly coarse sand (0.40-1.36 m a.s.l.), loamy sand (1.36-1.56 m a.s.l.) and medium/coarse sand (1.56-2.15 m a.s.l.) reflect a variety of fluvial facies due to changing river dynamics. The uppermost part of the core is characterised by homogeneous silty and loamy floodplain sediments.

7.2.1.4 Vibracoring LIS 24

LIS 24 (N 41° 48' 36'', E 19° 38' 38'', ground level at 3.33 m a.s.l., total length of core: 11 m) is located approximately 1 km south of the town of Balldreni. A synoptic view of the profile is shown in appendices 5.17.1 & 5.17.2.

The lowermost section of the core is made up by very dark grey, homogeneous silty fine sand with some plant remains and wood fragments (up to 5.35 m b.s.l.). Grain size and geochemistry (relatively low electric conductivity: 0.77-0.86 mS/cm; high ratio of $\text{Ca}^{2+}/\text{Mg}^{2+}$: 2.98) suggest a deposition in a shallow marine environment with a strong freshwater influx.

Subsequent to several thin intercalated peat layers between 5.35 and 5.24 m b.s.l., the dominant grain size of the sediment changes from sand to loamy silt (up to 4.40 m b.s.l.). These fine-grained deposits contain abundant shallow marine to brackish species (macrofossil: *Pirenella conica*; ostracods: *Cyprideis torosa*, *Xestoleberis communis*; foraminifer: *Ammonia beccarii*) and one freshwater ostracod species (*Candona neglecta*) which may have been deposited during a flood event of the Drini. The large spectrum of the faunal composition and the increasing electric conductivity (1.44-1.70 mS/cm) suggest a change to calm depositional conditions in an interdistributary bay (estuarine environment).

From 4.40 to 3.28 m b.s.l., the sediment is dominated by dark grey, silty fine sand. A coarse sandy layer with pebbles (4.21-4.03 m b.s.l.) was deposited probably during a brief period when the river mouth was close to the coring site. The upper part of the stratum is made up of clayey lenses with numerous plant remains, showing the occasionally re-establishment of calm sedimentary conditions.

The subsequent layer of very dark grey, loamy silt contains also numerous plant remains (up to 3.07 m b.s.l.). The sediment includes abundant shallow marine to brackish species (macro fauna: *Pirenella conica*, *Rissoa* sp., *Cerastoderma glaucum*, *Scrobicularia plana*, *Pusillina* sp.; ostracods: *Cyprideis torosa*, *Xestoleberis communis*; foraminifers: *Ammonia beccarii*) and freshwater/estuarine species (macrofossils: *Hydrobia* sp., *Pisidium* sp.; ostracod: *Candona* sp.). The calcium carbonate (3.18 %) indicates a low-alkaline milieu. The granulometry and the fossil content point to a deposition in an interdistributary bay environment.

The middle section of the core is characterised by a thick medium/coarse sandy layer with pebbles (up to 0.20 m b.s.l.). The colour changes from dark olive grey to dark greyish brown (at 2.32 m b.s.l.). This body of sediment reflects deposition within a river channel. The following sandy deposits are characterised by changing grain sizes and a lack of pebbles (up to 1.46 m a.s.l.). These layers reveal temporary shifts in the depositional dynamics of the fluvial system.

The uppermost section of the profile, from 1.46 m a.s.l. to the present surface, comprises intercalations of light olive brown, loamy silt and silty sand which were deposited during flooding events of the Drini. The pebbles at the top of the layer may be interpreted as a former road.

7.2.1.5 *Vibracoring LIS 23*

LIS 23 (N 41° 47' 56'', E 19° 38' 28'', ground level at 3.20 m a.s.l., total length of core: 12 m) is located in the centre of the Merqia plain, between the towns of Lezha and Balldreni. A synoptic view of the profile is shown in appendices 5.16.1 & 5.16.2.

The lowermost part of the profile is characterised by dark grey fine sand (up to 7.80 m b.s.l.), which contains a few brackish/estuarine species (macrofossil: *Hydrobia* sp.; ostracod: *Cyprideis torosa*). Granulometry, fossil content and geochemical analyses – ratio of $\text{Ca}^{2+}/\text{Mg}^{2+}$ (2.80), electric conductivity (up to 1.82 mS/cm) – suggest a deposition under brackish conditions in a shallow marine environment with a strong freshwater influx.

The subsequent sediment is dominated by dark grey fine/medium sand; it includes many pieces of wood (up to 6.87 m b.s.l.). The coarser grain size suggests a change in the depositional dynamics from fully marine to sublittoral. The woody fragments probably derive from the neighbouring slopes. The sublittoral sands are overlain by a layer of loamy silt, indicating the re-establishment of calm sedimentation conditions at the coring site (up to 6.42 m b.s.l.).

From 6.42 to 5.10 m b.s.l., the stratum is made up of very dark grey silty fine sand with intercalated clayey silts and numerous plant remains. The sediment contains salt-tolerant species (macrofossils: *Hydrobia* sp., *Scrobicularia plana*; ostracod: *Cyprideis torosa*; foraminifers: *Ammonia beccarii*, *Elphidium crispum*). The electric conductivity (up to 1.86 mS/cm) and plant remains point to a significant freshwater influx. This layer must have been deposited in a shallow marine environment under brackish conditions.

From 5.10 to 3.01 m b.s.l., the sediment is dominated by homogeneous, very dark grey clayey silt. The fauna contains a large spectrum of species: from shallow marine/brackish ones (macrofossils: *Bittium* sp., *Cerastoderma glaucum*, *Chrysallida* sp., *Loripes lacteus*, *Pusillina* sp., *Scrobicularia plana*; ostracod: *Cyprideis torosa*; foraminifers: *Ammonia beccarii*, *Elphidium crispum*, *Quinqueloculina* sp.) to estuarine/freshwater ones (macrofauna: *Hydrobia* sp.; ostracod: *Potamocypris* cf. *fallax*). The fluctuating electric conductivity (from 2.13 to 0.95 mS/cm) and the content of calcium carbonate (from 1.18 % to 18.66 %) as well as many pieces of wood suggest temporarily strong freshwater influence. The relatively high amount of organic matter (up to 5.78 %) and lenses of organic material indicate anaerobic conditions. These characteristics indicate a change from interdistributary bay to residual lake under calm/low energy conditions.

The following layer with coarser grained sediments (fine/medium sand) reveals a strong input of terrestrial material deposited by the Drini (up to 2.37 m b.s.l.). From 2.37 to 1.60 m b.s.l., the grain size changes again to silty fine sand, intercalated with loamy silt. The results of the microfossil study (ostracod: *Candona neglecta*) and geochemical analyses – dramatically decreasing electric conductivity (from 0.95 to 0.09 mS/cm) – suggest the establishment of a limnic/freshwater environment. Some calcium carbonate concretions and numerous oxidation stains in the upper part of the deposit are proof of seasonally wet and dry conditions.

The subsequent layer is characterised by dark greenish grey, homogeneous clayey silt with some freshwater species (macrofossil: *Bithynia tentaculata*; ostracods: *Iliocypris bradyi*, *Candona neglecta*) and a few charophytes (*Characeen-oogonia*). Thin peat lenses, calcium carbonate concretions, and oxidation stains are evidence for the continuation of seasonal variations in the semi-terrestrial milieu (up to 0.13 m b.s.l.).

The uppermost section of the core is made up of olive brown, fine-grained silty sediments, deposited during flood events of the Drini. The lack of coarser material above 2.37 m b.s.l. suggests deposition within a low-energy section of the floodplain, at a time when the course of the Drini was far away from the coring site.

7.2.1.6 Synopsis of transect B-B'

LIS 27, the northernmost core of this transect (fig. 26) presents a totally different picture to the other cores and consists of terrestrial sediments throughout. The alluvial fan deposits at the lowermost part of the core are overlain by fine-grained sediment, accumulated under freshwater conditions in a limnic environment. Coarse layers in the stratum can be interpreted as the intermittent development of alluvial fan sequences.

The lowermost parts of the other cores of transect B-B' are made up of silty sand, which has accumulated in a marine embayment. However, towards the top, marine conditions became more brackish due to a strong freshwater influx by the Drini. This is shown by the increasing number of intercalated sandy and clayey layers as well as the dominance of brackish species (e.g., *Cerastoderma glaucum*, *Ammonia beccarii*, *Cyprideis torosa*), particularly in LIS 47.

Age estimates obtained from paralic peat layers, which are embedded in shallow marine strata give hints for the timing of the marine conditions in the Merqia plain. The oldest radiocarbon age, gained from a peat layer of the deepest part of LIS 42 reveals marine conditions in this area at the end of 5th millennium BC [4224-3965 cal BC, peat at 7.90-8.00 m b.s.l. (LIS 42/25T)].

Other dates from corings LIS 42, LIS 23 and LIS 47 indicate that marine conditions prevailed throughout the 4th millennium BC [3761-3643 cal BC; wood at 4.52 m b.s.l. (LIS 42/19H); 3518-3116 cal BC, wood at 7.29 m b.s.l. (LIS 23/30H) and 3348-3020 cal BC, peat at 7.98 m b.s.l. (LIS 47/23T)]. The fact that two pieces of wood of similar age were found at very different depths is evidence for tectonic movements in this area.

It is worthy to note that an another age estimate at the transition from shallow marine to brackish conditions in LIS 23 is older than the lower age estimate [4932-4691 cal BC, closed bivalve specimen (*Loripes lacteus*) at 5.20-5.25 m b.s.l. (LIS 23/24F)]. This apparent contradiction may have been caused by re-deposition of the fossil, the reservoir effect, or an error in the laboratory. Therefore, this age estimate has not been considered in our interpretation.

The brackish sediments are covered by fluvial channel deposits at coring sites LIS 42 and LIS 24. However, the northernmost and southernmost cores of this transect (LIS 47 and LIS 23) show only limited fluvial influence. Whilst at sites LIS 42 and LIS 24 the sediments turn coarser, thereby showing the proximity of a river channel, the cores of LIS 47 and LIS 23 are

characterised by silt and clay, representing calm depositional conditions. It appears as though the Drini course never reached the site of LIS 47.

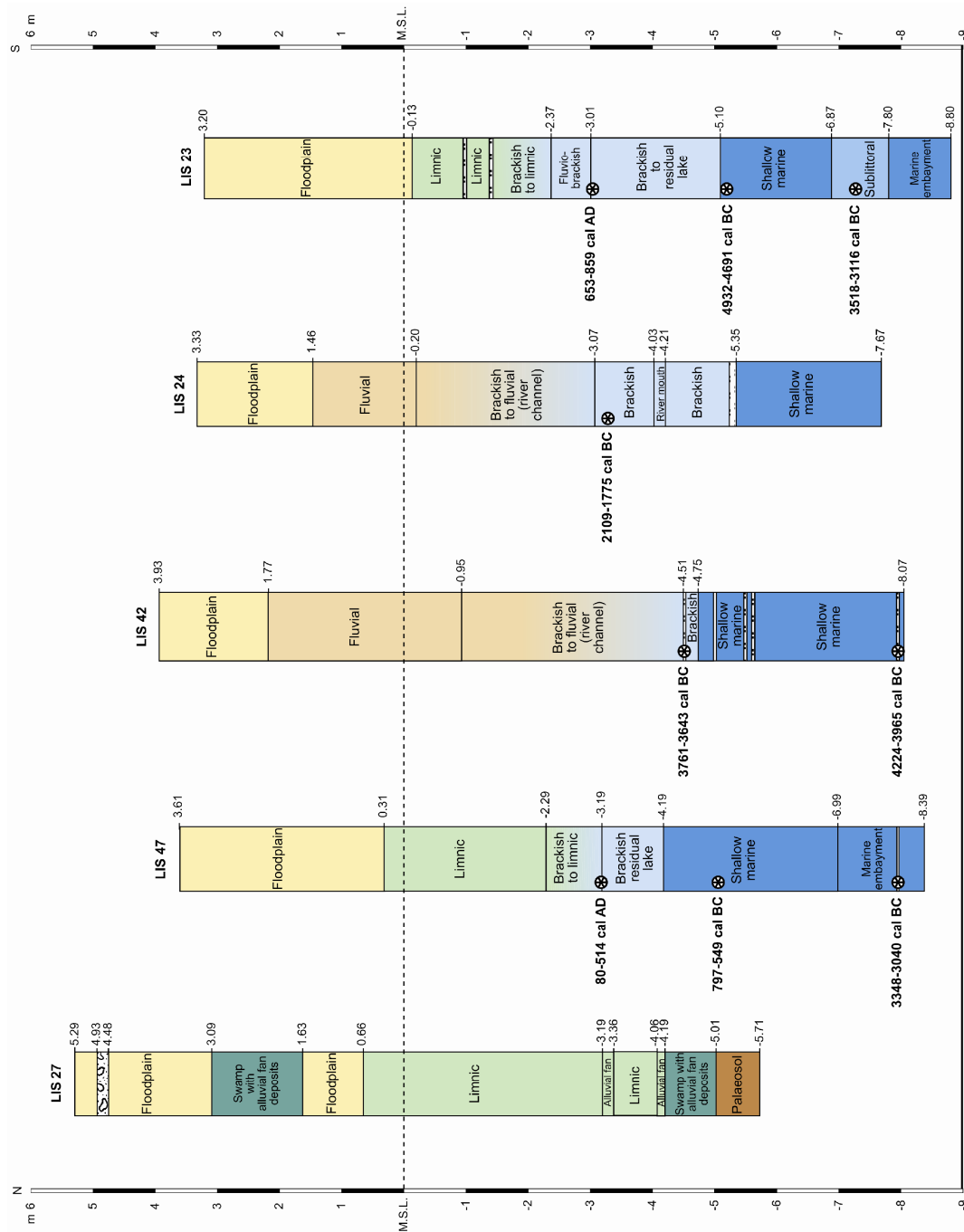


Figure 26: Geological transect B-B' (own research).

A date obtained from LIS 24 puts the change of conditions from a brackish to a river channel milieu at this coring site at the beginning of the 2nd millennium BC [2109-1775 cal BC, peat at 3.28 m b.s.l. (LIS 24/14T)]. This means that the Drini developed its delta in this area during the Middle Bronze Age.

Thick river channel deposits in the middle part of LIS 42 and LIS 24 suggest that the river meandered across these coring sites. It appears that brackish conditions prevailed for a long time at LIS 47 and LIS 23. A radiocarbon age from LIS 47 points to brackish conditions around the 8th to 6th centuries BC [797-549 cal BC, piece of wood at 5.09 m b.s.l. (LIS 47/18H)]. The change towards freshwater conditions or more precisely, the establishment of a lake at coring site LIS 47 occurred sometime between the 1st and 6th centuries AD [80-514 cal AD, marine fossil at 2.29 m b.s.l. (LIS 47/11F)]. At LIS 23, this change happened during the 7th to 9th centuries AD [653-859 AD, wood at 3.02 m b.s.l (LIS 23/19H)]. Finally, fine-grained alluvium from flooding events of the Drini covered the whole area.

7.2.2 Transect C-C'

This transect contains corings LIS 48, LIS 52 and LIS 25 (see fig. 21) and runs across the eastern part of the Merqia plain from north to south, almost parallel to the southern section of the transect B-B'.

7.2.2.1 Vibracoring LIS 48

LIS 48 (N 41° 48' 12'', E 19° 38' 54'', ground level at 2.32 m a.s.l., total length of core: 12 m) is located in the eastern part of the Merqia plain, between coring LIS 52 and the town of Merqia. A synoptic view of the profile is shown in appendices 5.36.1 & 5.36.2.

The lowermost section consists of dark grey, homogeneous fine sandy silt, covered by clayey silt (up to 6.55 m b.s.l.). The latter includes some fine sand layers, numerous plant remains as well as lenses of peat. The results from granulometry and geochemistry – high values of electric conductivity (up to 3.42 mS/cm), organic matter (10.58 %), calcium carbonate content (up to 21.98 %) and the Ca²⁺/Mg²⁺ ratio (2.66) – as well as abundant specimens of brackish ostracods (*Cyprideis torosa*) point to a deposition under brackish conditions in a low-energy marine embayment.

The subsequent very dark grey, homogeneous, fine sandy silt includes numerous thin peat lenses and pieces of wood. Due to an increasing freshwater influx, the electric conductivity (from 3.07 to 1.24 mS/cm) and the amount of organic matter (from 7.40 % to 1.08 %) decrease considerably towards the top of the layer. This also points to a change from low-wave energy to increasingly dynamic conditions.

This is confirmed by the subsequent medium/coarse sandy stratum with ample specimens of *Cyprideis torosa* (up to 5.18 m b.s.l.). These coarse deposits may have been accumulated as crevasse splay during an extreme flood event of the Drini. The following dark grey, laminated fine sand deposit indicates short temporary inputs of the river (up to 4.44 m b.s.l.) which is supported by the relatively low electric conductivity (1.45 mS/cm). High amounts of Na⁺ (16.80 g/kg) and orthophosphate (1.26 g/kg) may indicate widespread soil erosion in the hinterland.

The following dark grey, homogeneous clayey deposits contain fossils of salt-tolerant species (macrofossil: *Cerastoderma glaucum*; ostracods: *Cyprideis torosa*, *Loxoconcha stellifera*; foraminifer: *Ammonia beccarii*) in juvenile and mature forms. This layer reflects a transition to brackish-dominated conditions within a marine embayment, which developed after the southward progradation of the Drini delta (up to 2.10 m b.s.l.). The fine grain size of the subsequent layers indicates that the river course must have migrated to the west, off the coring site.

From 2.10 to 1.11 m b.s.l., the deposits consist of olive grey silty fine sand, with intercalary clayey lenses. They include a few CaCO₃ concretions and plant remains, hinting to a transition from brackish to freshwater conditions. The overlying olive grey clayey silt points to a change towards a semi-terrestrial milieu (up to 0.62 m b.s.l.). Abundant terrestrial gastropods, calcium carbonate concretions, and numerous oxidation stains reflect seasonal variations of wet and dry conditions.

The uppermost portion of the profile consists of fine-grained floodplain deposits, with silt being the dominant component. Oxidation stains are frequent in this section of the core.

7.2.2.2 Vibracoring LIS 52

LIS 52 (N 41° 47' 46'', E 19° 38' 55'', ground level at 2.31 m a.s.l., total length of core: 12 m) is located on the eastern part of the Merqia plain, between the towns of Lezha and Merqia. A synoptic view of the profile is shown in appendices 5.39.1 & 5.39.2.

Dark grey, homogeneous clayey silt makes up the lowermost part of the coring (up to 8.09 m b.s.l.). Granulometry and geochemical analyses – high values of electric conductivity (3.45 mS/cm), calcium carbonate content (16.77 %), organic matter (3.95 %) and orthophosphate (1.62 g/kg) – indicate calm depositional conditions in a low-energy marine embayment. A few freshwater bivalves (*Pisidium* sp.) and abundant brackish ostracods (*Cyprideis torosa*), found in the lower part of the stratum hint at a strong freshwater influx.

This stratum is overlain by very dark grey loamy silts, intercalated with thin fine sand lenses, containing some plant remains (up to 6.59 m b.s.l.). The relatively high value of organic matter (up to 5.33 %) and orthophosphate (1.58 g/kg) represents favourable ecological conditions. The deposits contain abundant brackish ostracods (*Cyprideis torosa*) and juvenile shell fragments, which may be explained with a rapidly changing environment.

The middle section of the profile consists of dark grey clayey silt, with intercalated thin lenses of fine sand (up to 4.54 m b.s.l.). The granulometry and the abundance of microfossils (ostracod: *Cyprideis torosa*; foraminifer: *Ammonia beccarii*) point to brackish conditions of a well protected marine embayment. This is supported by the geochemical analyses: high electric conductivity (3.40 mS/cm), calcium carbonate content (15.07 %), organic matter (5.63 %), orthophosphate (1.58 %) and a relatively high ratio of $\text{Ca}^{2+}/\text{Mg}^{2+}$ (2.37).

The subsequent layer of loamy silt contains abundant *Cerastoderma glaucum* fragments as well as terrestrial gastropods. From 3.69 to 2.04 m b.s.l., the sediment is dominated by dark grey clayey silt with numerous plant remains. The faunal content presents a large spectrum of species typical for an estuarine environment (macrofossils: *Theodoxus* sp., *Arca* sp., *Bittium reticulatum*, *Retusa* sp., *Cerastoderma glaucum*; ostracod: *Cyprideis torosa*; foraminifers: *Ammonia beccarii*, *Ammonia* cf. *tepida*, *Elphidium* sp., *Quinqueloculina* sp., *Triloculina* sp., *Haynesina germanica*). This is also supported by the geochemical analyses – high values of electric conductivity (2.45 mS/cm) and organic matter (up to 5.65 %).

The next stratum is made up of dark grey, homogeneous loamy silt (up to 1.64 m b.s.l.), probably accumulated in a semi-terrestrial environment. The high electric conductivity (2.14 mS/cm) in the uppermost part may have been caused by secondary saltwater intrusion presumably triggered by a co-seismic event.

Homogeneous clayey silt follows (up to 1.21 m a.s.l.). At 0.39 m b.s.l., the colour changes from olive grey to olive brown, marking the transition from limnic to semi-terrestrial conditions. CaCO_3 concretions and numerous oxidation stains are evidence of seasonally wet and dry conditions. Fine-grained floodplain alluvium forms the top of the profile.

7.2.2.3 *Vibracoring LIS 25*

LIS 25 (N 41° 47' 30'', E 19° 38' 39'', ground level at 2.41 m a.s.l., total length of core: 13 m) is located in a formerly swampy area, which was drained and subsequently planted with poplar

trees in the southern part of the Merqia plain. A synoptic view of the profile is shown in fig. 27, photo 14, and appendix 5.18.

The lower section of the profile is made up of very dark grey, fine sandy and loamy silts (up to 8.14 m b.s.l.), containing a rich fauna (macrofossil: *Bittium latreillii*; ostracods: *Cyprideis torosa*, *Pontocythere rubra*; foraminifer: *Ammonia beccarii*). The granulometry, fossil content, and geochemistry – high value of electric conductivity (up to 3.88 mS/cm) and ratio of $\text{Ca}^{2+}/\text{Mg}^{2+}$ (up to 2.44) – suggest brackish to shallow marine environment. A relatively high content of organic matter (up to 5.88 %) and orthophosphate (up to 1.38 g/kg) indicates calm depositional conditions.

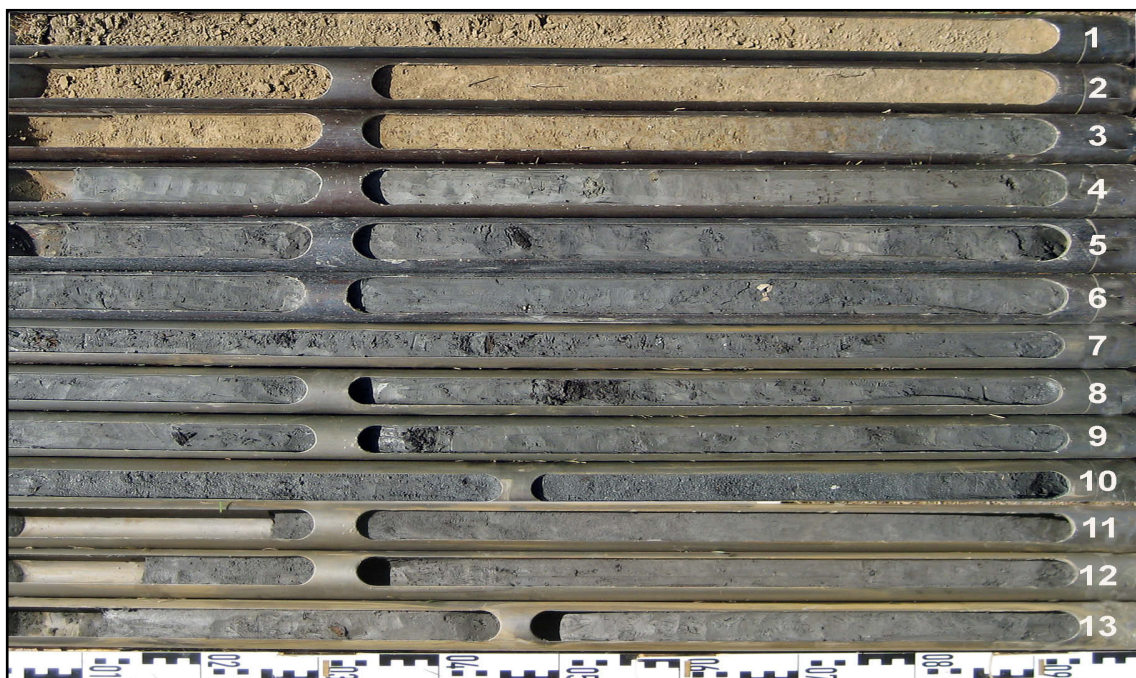


Photo 14: Coring LIS 25. (Uncu, 2007)

Then follow very dark grey, laminated fine sand (up to 6.99 m b.s.l.). The decreasing electric conductivity (0.93 mS/cm) and several pieces of wood as well as some plant remains show the influence of fluvial dynamics as part of the depositional process. The granulometry and high biodiversity (macrofossils: *Cerastoderma glaucum*, *Venus verrucosa*, *Cerithium* sp., *Bittium latreillii*, *Lucinella divaricata*, *Gibbula* sp., *Rissoa* sp., *Tricolia pullus pullus*; ostracods: *Cyprideis torosa*, *Pontocythere rubra*, *Loxoconcha stellifera*, *Cytheretta adriatica*, *Xestoleberis communis*, *Pseudocandona parallela*; foraminifers: *Ammonia beccarii*, *Quinqueloculina* cf. *venusta*) prove a deposition in a marine milieu.

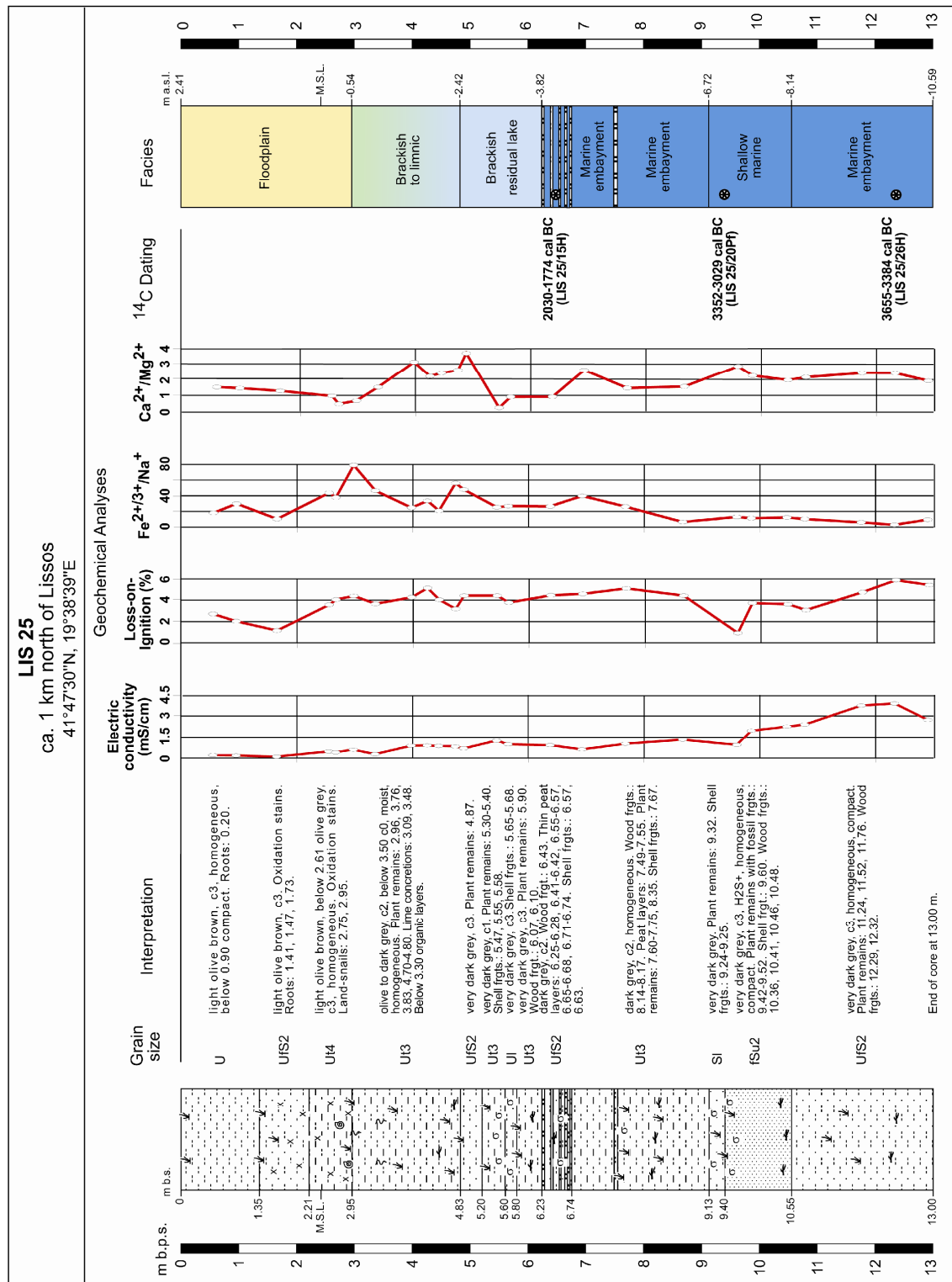


Figure 27: Synoptic chart of coring LIS 25.

The subsequent sandy layer also contains shell fragments and plant remains (up to 6.72 m b.s.l.). The relatively old age of the layer (see below) indicates that the sand cannot be of fluvial origin, by then the Drini was much further inland. Instead, the origin of the sediment is likely to have been the flysch slopes of the Shite-Veles Mountains.

The middle part of the profile consists of layered clayey silt (from 6.72 to 3.82 m b.s.l.) and fine sandy silt (up to 2.42 m b.s.l.). The latter reflect occasional sediment inputs by the river. The sediment contains pieces of wood and numerous peat lenses as well as abundant shell fragments. The fossil content is predominantly composed of brackish/shallow marine species (macrofossil: *Loripes lacteus*; ostracods: *Cyprideis torosa*, *Leptocythere bacescoi*; foraminifer: *Ammonia beccarii*). Together with the geochemistry – fluctuating values of electric conductivity (from 1.30 to 0.61 mS/cm), calcium carbonate content (from 2.06 to 17.79 %) and a high content of organic matter (up to 5.10 %) – it suggests a deposition under brackish conditions in a well-protected marine embayment with a substantial freshwater influx.

From 2.42 to 0.54 m b.s.l., the stratum is made up of olive to dark grey clayey silt, deposited in a limnic environment. The subsequent layer contains more clay (up to 0.20 m a.s.l.). At 0.32 m b.s.l., the colour changes from olive grey to olive brown. Lime concretions and numerous oxidation stains are further evidence for seasonally wet and dry conditions in a swampy environment. Additional indicators for the existence of anaerobic conditions are high values of orthophosphate (up to 2.43 %) and $\text{Fe}^{2+/3+}$ ions (50.60 g/kg).

The uppermost portion of the profile consists of light olive brown, silt-dominated floodplain sediment with numerous oxidation stains and plant roots.

7.2.2.4 Synopsis of transect C – C'

The lowermost part of all cores consists of alternating fine sandy and clayey silts, which were deposited in a marine embayment (fig. 28). The fine grain size and abundant fauna as well as some peat lenses suggest that deposition took place under low-energy conditions. A radiocarbon age from LIS 25 shows that fully marine conditions existed throughout the 4th millennium BC [3655-3384 cal BC, wood at 9.91 m b.s.l. (LIS 25/26H)]. This is supported by a dating from LIS 52 [3088-2909 cal BC, wood at 6.94 m b.s.l. (LIS 52/19H)].

Age estimates from LIS 48 and LIS 25 suggest that the transition from fully marine to brackish conditions occurred during the second half of the 4th millennium BC [3344-3095 cal BC, wood at 5.12 m b.s.l. (LIS 48/16H); 3352-3029 cal BC, plant remains at 7.01 m b.s.l. (LIS 25/20Pf)]. These results fit with the age estimates of transect B-B'.

The brackish deposits at LIS 25 and LIS 48 are interrupted by sandy layers. At LIS 48 this stratum reflects a slight fluvial influence due to the progradation of the river mouth towards the south. However, the coarse sediments at LIS 25 are likely to have originated from the nearby

slopes, because by then the Drini was quite far off this coring site.

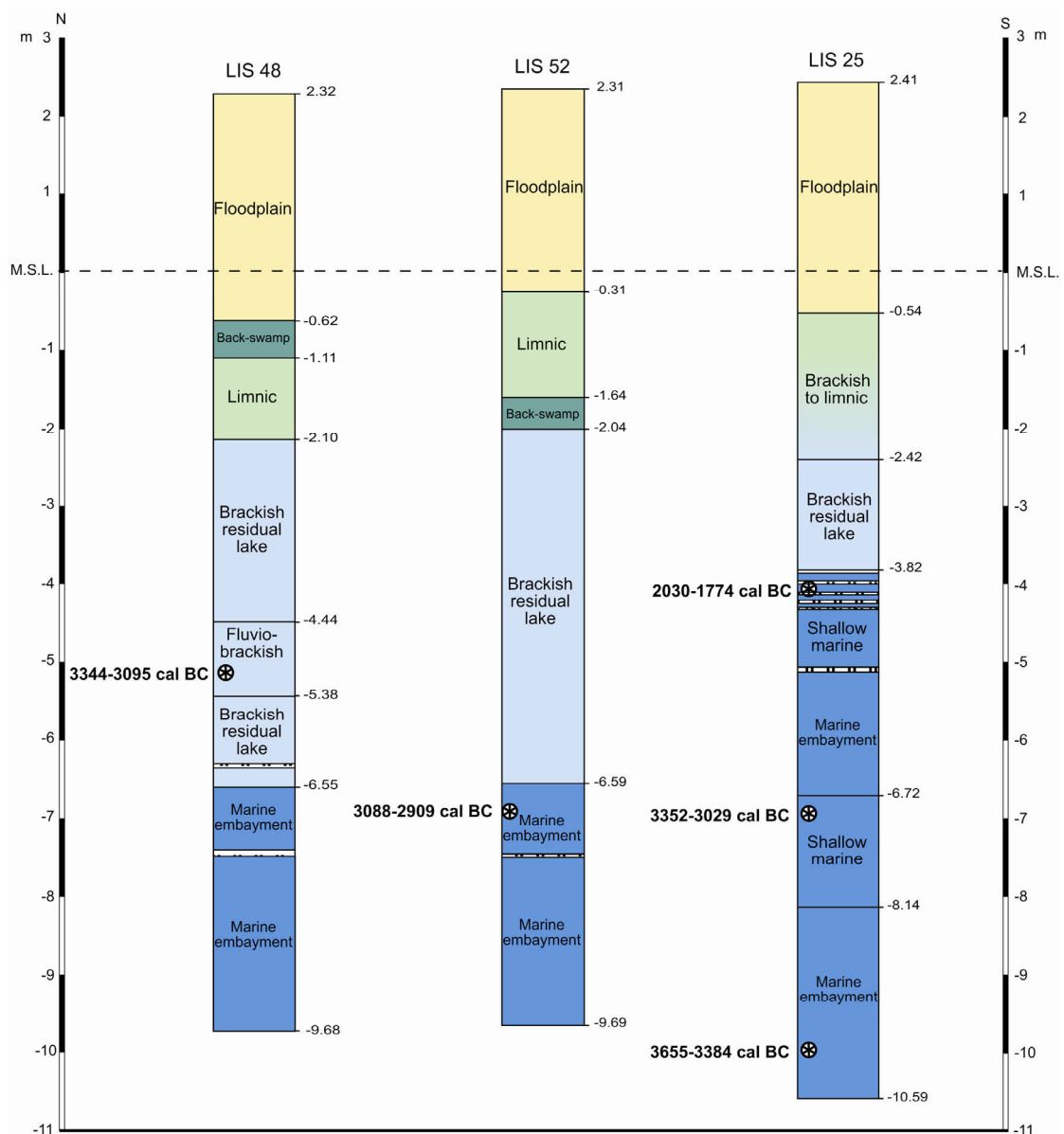


Figure 28: Geological transect C-C' (own research).

Fine grain size and numerous specimens of *Cerastoderma glaucum* within the deposits of LIS 48 and LIS 52 suggest the establishment of a brackish/lagoon-like environment, with an increasing influx of freshwater. The development of numerous peat layers at coring site LIS 25 indicates the waxing and waning of temporary coastal swamp environments during the first half of the 2nd millennium BC [2030-1774 cal BC, wood at 6.44 m b.s.l. (LIS 25/15H)]. The occurrence of some landsnails towards top of these deposits shows a change towards freshwater conditions. For this reason, subsequent sediments from all of the three cores initially reflect a limnic milieu, which then gave way to fine-grained alluvium of the Drini.

7.3 Transects through the archaeological area

The ruins of the Lower City of ancient Lissos is located at the foot of Lezha Hill (Acropolis, Kalaja) on the banks of the Drini. Overall, 17 drillings were carried out in this area to gain information about the facial build-up of the archaeological layers. In addition, we also wanted to find out more about the geographical setting of the city at the time of its foundation and operation. Profiles of the corings within the archaeological area have been linked to achieve these aims (fig. 29). Some of the cores, which are not presented here in any detail, were specifically drilled for the archaeologists (LIS 20, LIS 21, LIS 22, LIS 36, LIS 44, LIS 49). The depth of those drillings was limited to a few meters, and only floodplain deposits with archaeological material made up the cores. Therefore, these drillings did not yield valuable results in a palaeogeographical or sedimentological context.

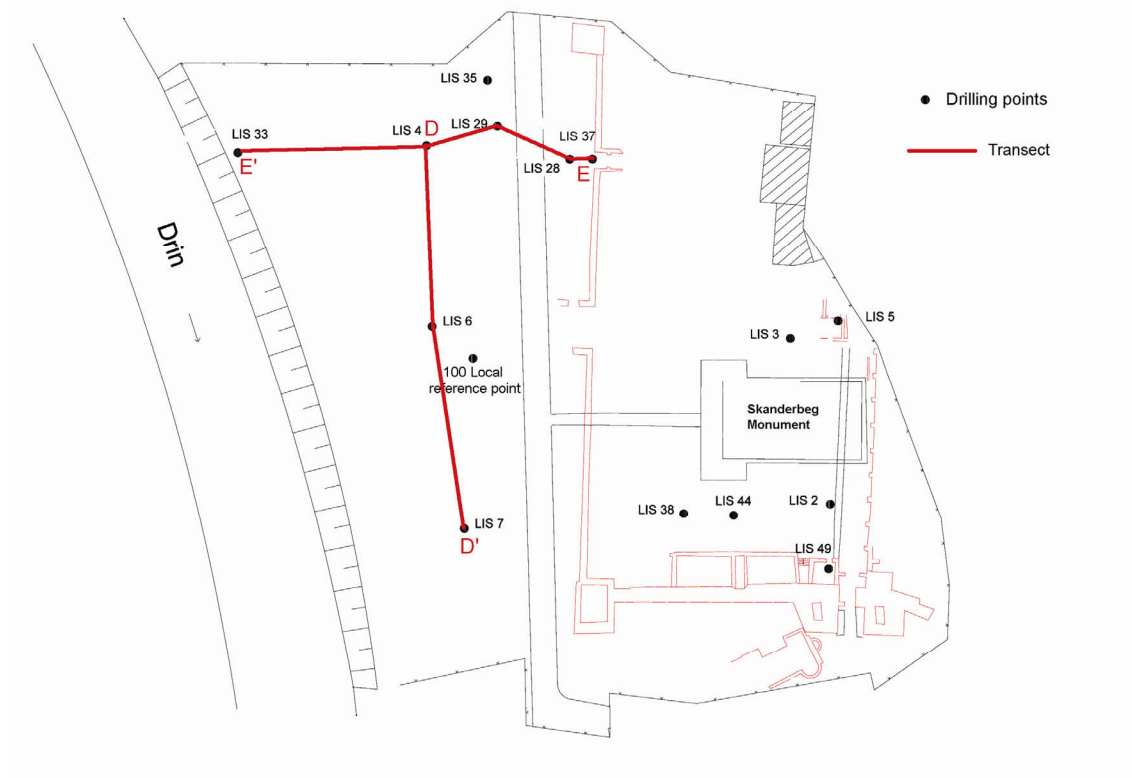


Figure 29: Location of coring sites within the archaeological area (adapted from Rübens, 2009, unpublished).

7.3.1 Transect D-D'

This transect consists of corings LIS 04, LIS 06 and LIS 07. It runs from north to south through the archaeological area between the Lower City of ancient Lissos and the Drini (see fig. 29). The aim of this transect is to identify the relationship between the river dynamics and the ancient city of Lissos.

7.3.1.1 Vibracoring LIS 04

LIS 04 (N 41° 46' 59'', E 19° 38' 31'', ground level at 3.21 m a.s.l., total length of core: 10.65 m) is located between the Hellenistic Harbour Gate and the Drini. A synoptic view of the profile is shown in fig. 30, photo 15, and appendix 5.2.

The lowermost section consists of dark olive grey, medium/coarse sand with angular stones and small pebbles, indicating sublittoral conditions (up to 6.50 m b.s.l.). The following fine sand contains some small, sub-rounded stones (up to 4.65 m b.s.l.). The grain size of the subsequent layer becomes finer and the sediment consists of silty fine sand, which indicates an increasing water depth. This shallow marine stratum is covered by dark grey, homogeneous clayey silt (between 3.65 and 3.43 m b.s.l.). The relatively high content of organic matter (6.48 %) and lack of CaCO₃ suggest a deposition under anaerobic conditions, e.g., in a backswamp.

The middle section of the core consists of medium/coarse sand with pebbles (from 3.43 to 0.24 m b.s.l.). The colour gradually changes from very dark grey to dark brown. The granulometry suggests a deposition in a river channel. The following sterile, fine/medium sand (up to 0.51 m a.s.l.) and sandy silt (up to 0.96 m a.s.l.) reflect changing fluvial dynamics.

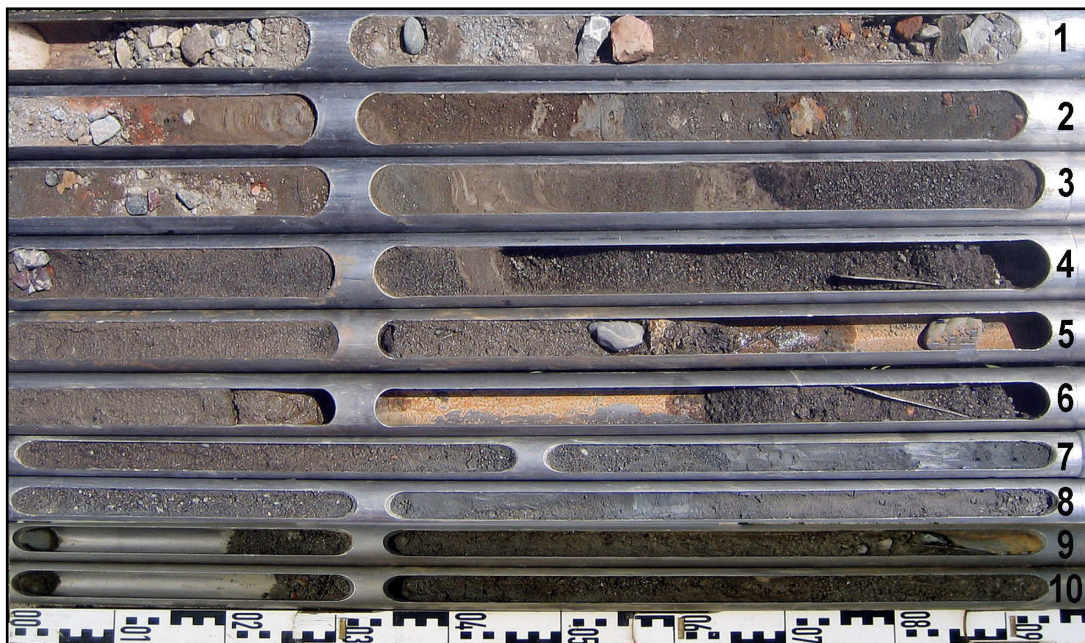


Photo 15: Coring LIS 04. (Uncu, 2006)

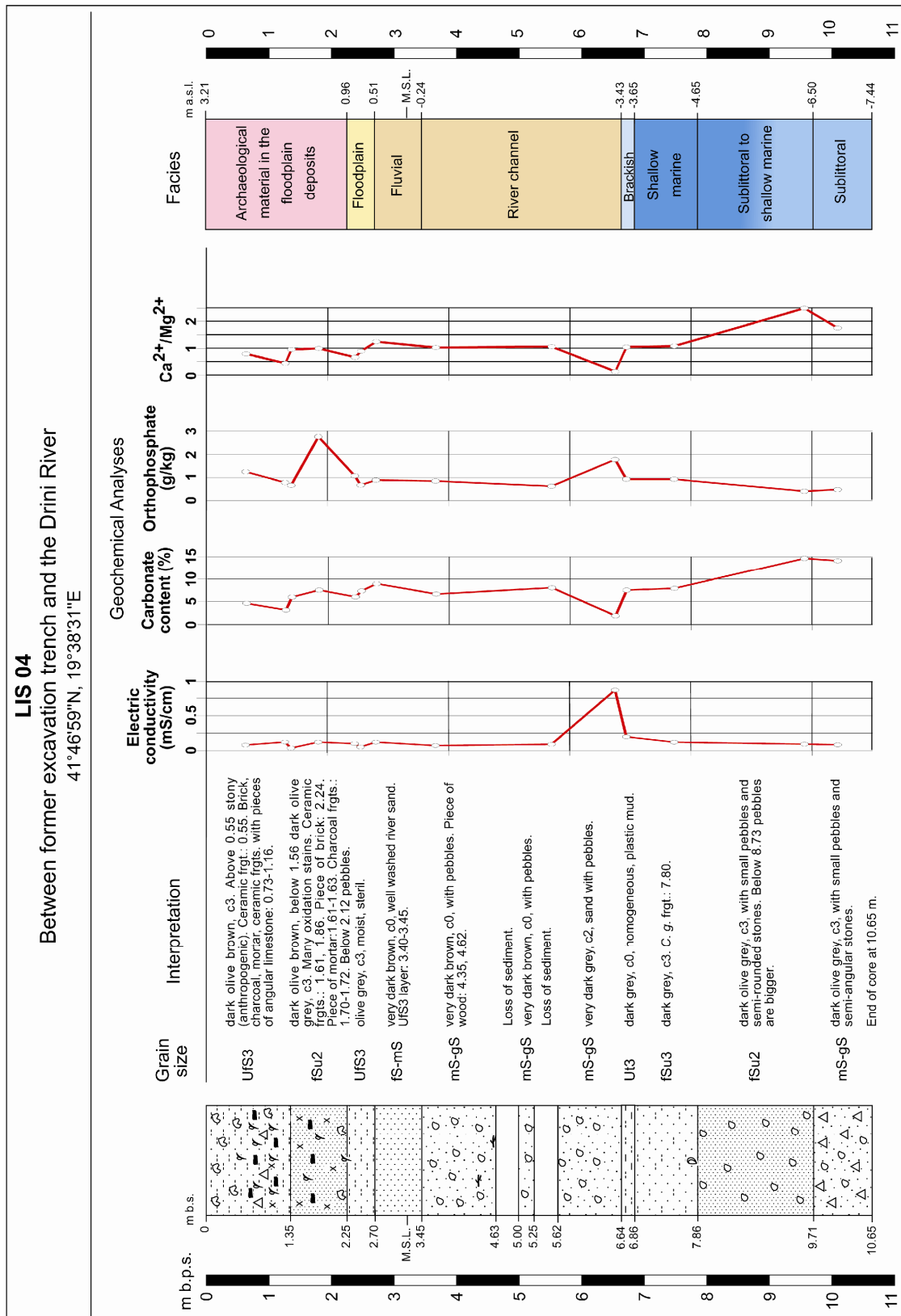


Figure 30: Synoptic chart of coring LIS 04.

The uppermost section of the core is made up of fine sands and sandy silts, deposited during flood events of the Drini. The sediment includes many ceramic fragments, pieces of charcoal and angular limestone, as well as numerous oxidation stains. The ceramic finds date from

various time periods and are intermingled with modern materials, such as waste. They must have been deposited during clean-up works and construction of the Skanderbeg Archaeological Park, which took place after the devastating earthquake in 1979. The stones at the top of the core probably also derive from this phase.

7.3.1.2 Vibracoring LIS 06

LIS 06 (N 41° 46' 58'', E 19° 38' 31'', ground level at 3.02 m a.s.l., total length of core: 8 m) is located between the Skanderbeg Monument and the Drini. A synoptic view of the profile is shown in appendix 5.3.

In the lowermost section of the core, much of the sediment was lost due to the coarse grain size and the high groundwater table (up to 1.35 m b.s.l.). The few preserved sections and the material from 1.35 m b.s.l. to 0.07 m a.s.l. consist of very dark grey, medium/coarse sand with well rounded pebbles. These river channel sediments contain one fragment of *Cerastoderma glaucum* (at 0.60 m b.s.l.).

These deposits are overlain by dark greyish brown, fine/medium sand (up to 0.62 m a.s.l.) with archaeological remains (such as ceramic and brick fragments, pieces of charcoal and angular pieces of limestone), oxidation stains and terrestrial gastropods. The following sterile layers of clayey silt and silty fine sand suggest changing depositional dynamics of the Drini.

The uppermost part of the profile (from 1.45 m a.s.l. to the present surface) is dominated by sandy silts, containing fragments of ceramics and large bricks, mortar, and charcoal, as well as many angular pieces of lime- and sandstone.

7.3.1.3 Vibracoring LIS 07

LIS 07 (N 41° 46' 56'', E 19° 38' 32'', ground level at 2.87 m a.s.l., total length of core: 8 m) is located between the Skanderbeg Monument and the Drini, south of LIS 06. A synoptic view of the profile is shown in appendix 5.4.

Much of the sediment was lost because of the high groundwater table and the coarse grain size in the lowermost part of the core (up to 2.73 m b.s.l.). The remaining sediment consists of dark grey, medium/coarse sand with some well rounded pebbles. From 2.73 m b.s.l. to present sea level, the sediment is composed of medium/coarse sand with large pebbles. These river channel deposits contain a few pieces of wood and a bone fragment (2 cm at 2.70 m b.s.l.). The angular

ceramic and brick fragments within the sediment (between 0.68 and 0.61 m b.s.l.) were dated to Hellenistic/Roman times. They must have been transported to this location from neighbouring slopes.

From the present sea level to 0.17 m a.s.l., a layer of sterile, silty sands show a change in fluvial dynamics. The subsequent medium/coarse fluvial sand contains some archaeological material, such as angular ceramic and brick fragments, pieces of charcoal and angular limestone, as well as pieces of glass and metal (up to 1.06 m a.s.l.).

The uppermost section of the profile consists of intercalations of silty sand and clayey silt with abundant archaeological material. A yellow glazed ceramic fragment (at 1.35 m a.s.l.) was dated to the 18th-19th century AD. However, modern waste (pieces of rubber and glass) within the lower portion of the stratum probably derives from the clean-up effort after the earthquake in 1979.

7.3.1.4 Synopsis of transect D-D'

The lowermost part of LIS 04 consists of sublittoral sediments mixed with slope debris, followed by an approximately 3 m thick marine deposit (see fig. 31). Such deposits can be assumed for LIS 06 and LIS 07, too; however, they are missing. Instead, coarse material of fluvial origin can be found. This could be explained if we presume that the river has eroded the marine deposits at LIS 06 and LIS 07, and replaced them with coarse, pebbly sediment, whereas LIS 04, in a more sheltered position, was not affected by the erosive power of the Drini in the same way. Coarse fluvial material was later accumulated on top of the marine deposits at LIS 04.

The middle parts of all three cores are made up of river sand and pebbles. These deposits are sterile up to the present sea level, i.e., they do not include any archaeological remains. Only LIS 07 contains a few ceramic fragments at 0.70 m b.s.l., dating to Hellenistic/Roman times.

According to the archaeologists, this coring site is the closest to the Hellenistic settlement in the Lower City of Lissos. The first archaeological remains at coring sites LIS 06 and LIS 04 are found within the fluvial sands, which have been deposited above the present sea level. The uppermost section of the cores includes abundant artefacts, dating from Hellenistic to medieval times. Originally, they were deposited in the floodplain sediments; later they were partly mixed with modern material during the construction of Archaeological Park.

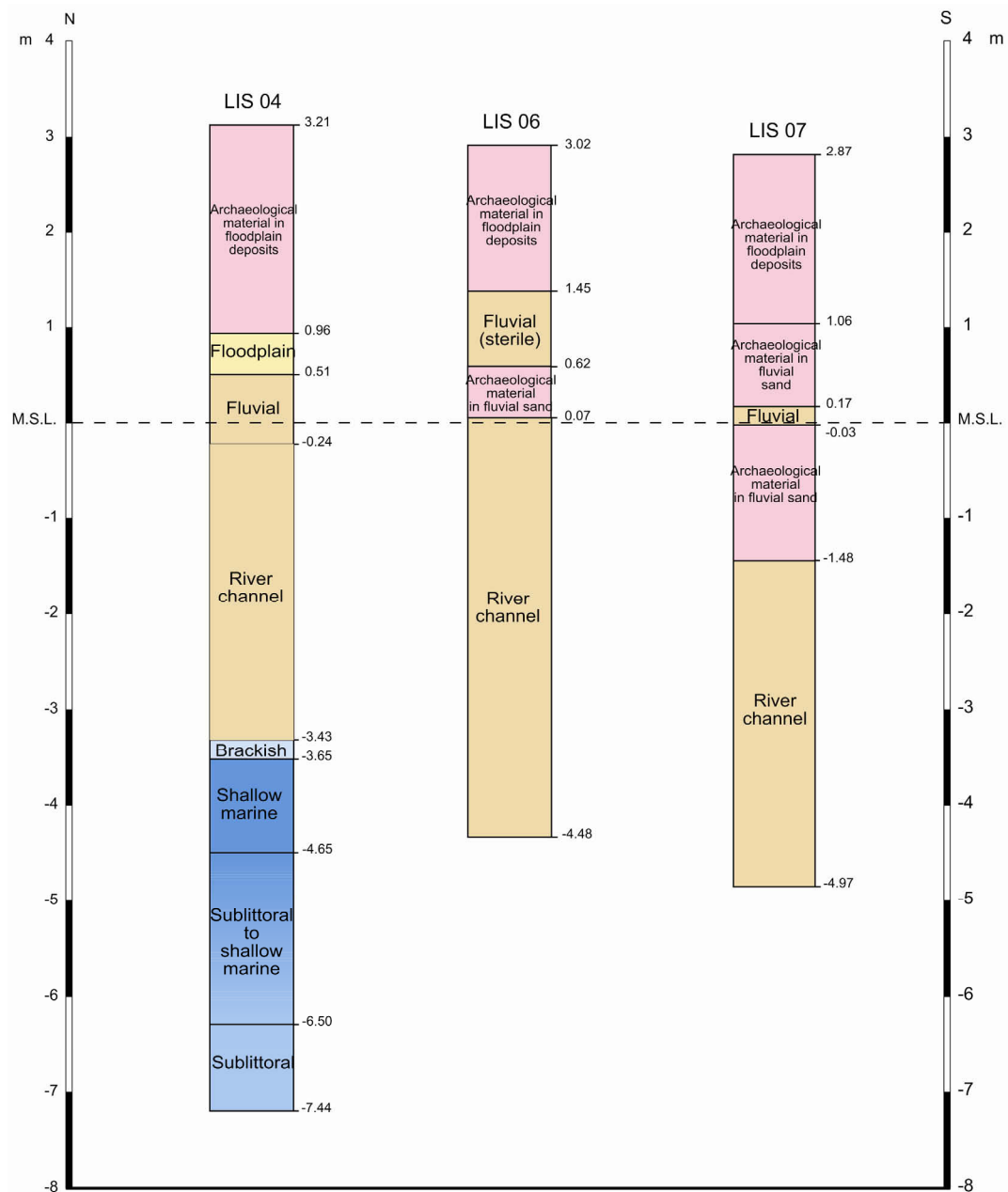


Figure 31: Geological transect D-D' (own research).

7.3.2 Transect E-E'

This east-west transect within the archaeological area contains corings LIS 37, LIS 28, LIS 29, LIS 04 and LIS 33. The transect starts in front of the Hellenistic Harbour Gate in the Lower City of Lissos (LIS 37) and continues towards the Drini (LIS 33) (fig. 29). In addition, core LIS 35 was drilled slightly north of LIS 29 and it confirmed the sediment sequence found at LIS 29. LIS 04 has already been described in detail in section 7.3.1.1. LIS 33 presumably contained only pebbles and other coarse grained material which could not be retrieved due to the coring technique.

This transect has three main aims: (1) to identify whether there has been a marine influence at this location; (2) to examine the strata before the direct human impact; (3) to document the human impact, especially with reference to the interaction of harbour activities and river dynamics throughout the past millennia.

7.3.2.1 Vibracoring LIS 37

LIS 37 (N 41° 46' 58'', E 19° 38' 31'', ground surface at 1.50 m a.s.l., total length of core: 6 m) is located in the canal at the entrance of the 'Hellenistic Harbour Gate' of Lissos. A synoptic view of the profile is shown in fig. 32 & photo 16.

The profile begins with very dark grey, loamy fine sands containing numerous plant remains and fossil fragments of shallow marine species (*Loripes lacteus*, *Corbula gibba*, *Chamelea cf. gallina*, *Hinia reticulata*) up to 3.90 m b.s.l.

Subsequently, the substrate coarsens to medium sand and later to coarse sand with rounded pebbles (up to 1.85 m b.s.l.), which indicate deposition in a river channel emerging from the slopes of Lezha Hill.

The strata are overlain by olive grey, loamy sand with pebbles and pieces of angular limestone and sandstone. The latter indicate anthropogenic input in a swampy milieu. A layer of clayey silt between 0.08 m b.s.l. and 0.33 m a.s.l. includes a ceramic fragment at 0.13 m a.s.l. The following loamy sand contains more ceramic sherds and amphora pieces of the early Hellenistic epoch. The uppermost part of the profile is composed of man-made deposits (waste material).

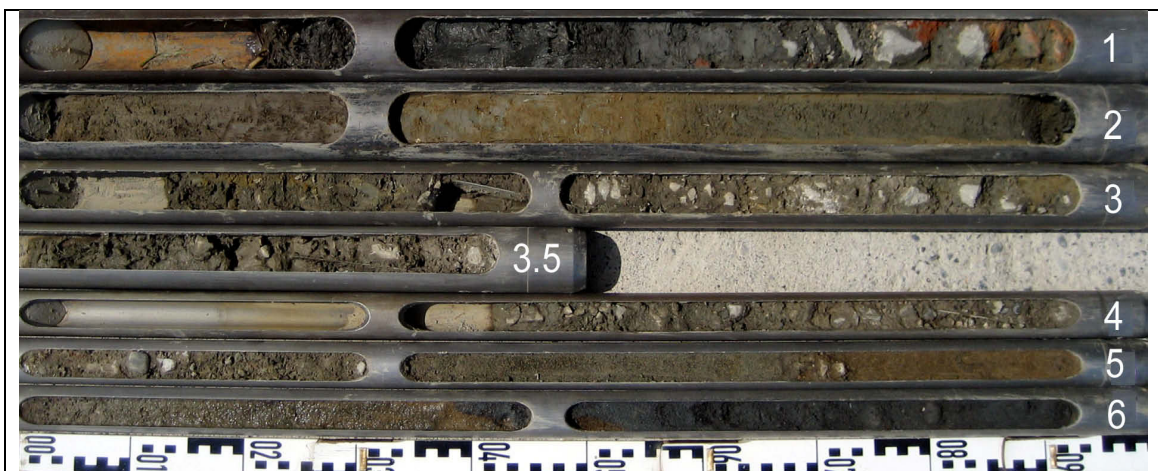


Photo 16: Coring LIS 37. (Uncu, 2007)

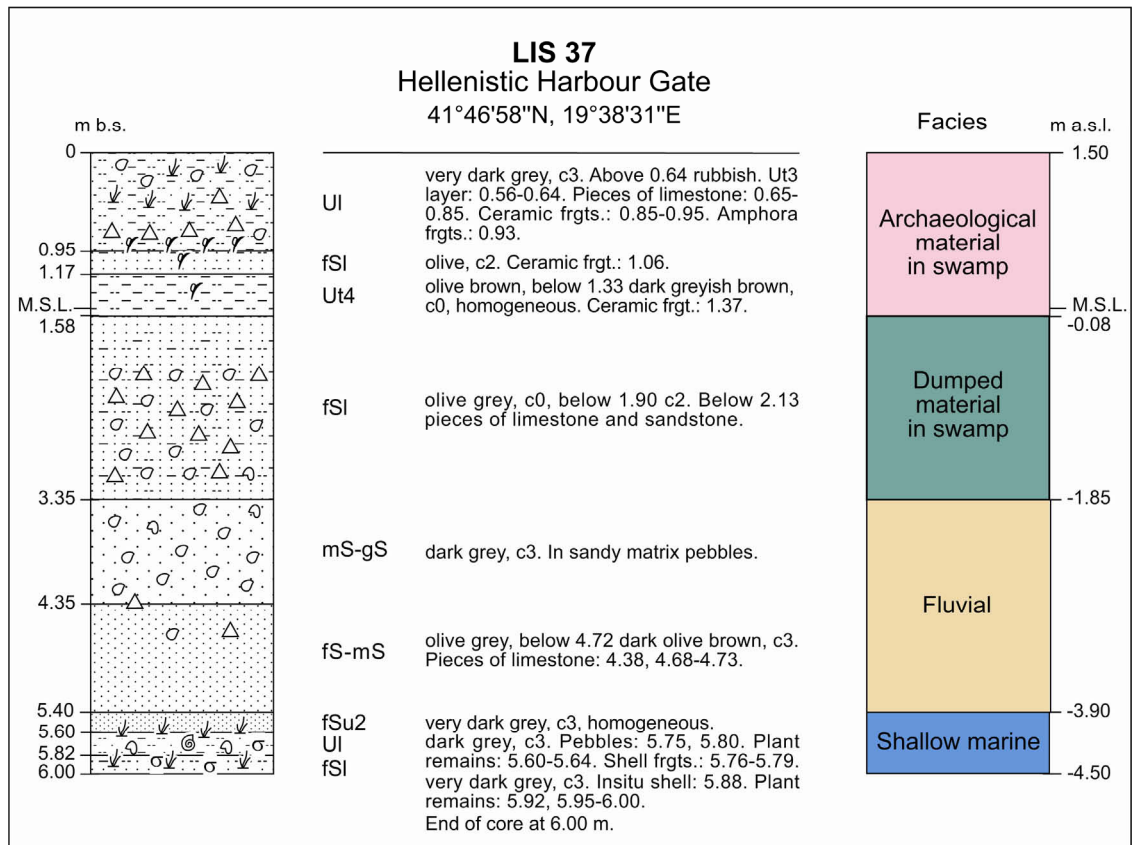


Figure 32: Synoptic chart of coring LIS 37.

7.3.2.2 Vibracoring LIS 28

LIS 28 (N 41° 46' 59'', E 19° 38' 33'', ground level at 1.48 m a.s.l., total length of core: 9 m) is located between the Hellenistic Harbour Gate and coring LIS 29. A synoptic view of the profile is shown in fig. 33, photo 17, and appendix 5.21.

The lowermost section is made up of dark olive grey medium/coarse sand with a mixture of angular stones and rounded pebbles (up to 6.07 m b.s.l.). The upper part of the section contains a few pieces of wood and a fossil fragment (*Cerastoderma glaucum*). Increasing values of electric conductivity (from 1.55 to 2.32 mS/cm) and organic matter (from 1.05 to 6.41 %) towards the very top of the section may be interpreted as a change in depositional conditions, from sublittoral to shallow marine.

From 6.07 to 4.97 m b.s.l., the sediment is dominated by very dark grey, fine sandy silt, which contains numerous plant remains and shell fragments. The fossil content (macrofossils: *Bittium latreillii*, *Cerastoderma glaucum*, *Cidaris* sp., *Hydrobia* sp., *Scrobicularia plana*; ostracods: *Aurila* sp., *Candona neglecta*, *Cyprideis torosa*, *Loxoconcha stellifera*, *Pontocythere* sp., *Xestoleberis dispar*; foraminifers: *Ammonia beccarii*, *Triloculina* sp., *Elphidium crispum*, *Quinqueloculina* sp.) points to brackish/shallow marine conditions with a significant freshwater

input. The granulometry, fossil content, as well as the values of electric conductivity (up to 1.61 mS/cm) and organic matter (up to 8.10 %) suggest sedimentation under low-energy conditions in a well-protected marine embayment. Between 4.97 and 4.30 m b.s.l., the sediment changes to loamy silt, containing an abundance of plant remains, pieces of wood and limestone fragments.



Photo 17: Coring LIS 28. (Uncu, 2007)

An abrupt change occurs at 4.30 m b.s.l., where fine sand covers shallow marine deposits discordantly. This dark yellowish brown and strongly stained sediment must have been deposited under fluvial conditions. The electric conductivity decreases dramatically from 2.34 to 0.75 mS/cm. The stratum is followed by dark olive grey fine/medium sand (up to 3.02 m b.s.l.). The coarsening of the grain size indicates high-energy dynamics.

From 3.02 to 1.07 m b.s.l., the coarse sands are overlain by dark grey loamy sand with angular and rounded pieces of limestone and sandstone. A thick layer of set limestone pieces of anthropogenic origin interrupts the stratum (between 2.52 and 2.26 m b.s.l.).

The coarse sand within the stratum of primarily loamy material, which is suggesting generally floodplain conditions, can be interpreted as residues of unusually high water levels of the river. The high value of orthophosphate (6.64 g/kg) indicates human activities in the area. The subsequent layer of loamy silt contains pieces of angular limestone and a ceramic fragment at 0.26 m b.s.l., which dates to Hellenistic times.

The uppermost part of the profile consists of a mixture of some archaeological material and very recent building site waste, which was dumped into a swampy environment.

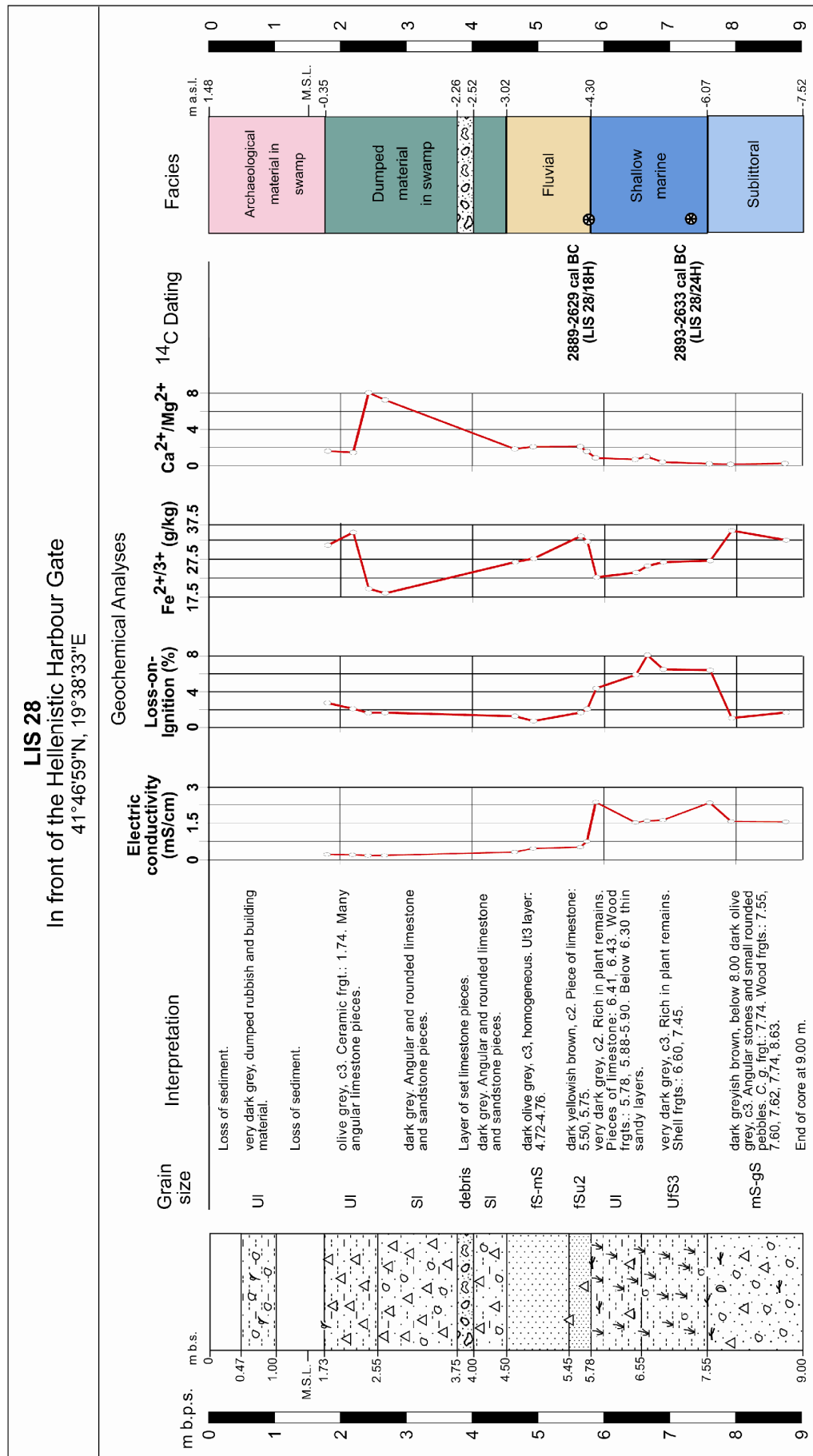


Figure 33: Synoptic chart of coring LIS 28.

7.3.2.3.1 Vibracoring LIS 29

LIS 29 (N 41° 46' 59'', E 19° 38' 32'', ground level at 1.66 m a.s.l., total length of core: 11 m) is located in the deepest part of the former archaeological trench (Hoxha Trench) between the Hellenistic Harbour Gate and the Drini, 10 m south of LIS 35. A synoptic view of the profile is shown in fig. 34, photo 18, and appendix 5.22.

The lowermost section of the profile begins with very dark grey medium/coarse sand and includes several small angular limestone fragments and rounded pebbles (up to 8.64 m b.s.l.). The electric conductivity increases upwards from 0.21 to 1.35 mS/cm. This may indicate the first marine influences at the coring site. Also, the granulometry suggests a change from littoral to sublittoral conditions.

The subsequent layer consists of very dark grey loamy silt (up to 7.76 m b.s.l.). The content of organic matter (3.66 %) numerous plant remains as well as the grain size show a deposition under calm brackish to shallow marine conditions. This interpretation is supported by the predominantly brackish to shallow marine fossil species (macrofossils: *Bittium reticulatum*, *Cidaris* sp., *Corbula gibba*, *Hydrobia* sp.; ostracods: *Cyprideis torosa*, *Pontocythere rubra*, *Aurila arborescens*; foraminifers: *Ammonia beccarii*, *Quinqueloculina* sp., *Triloculina* sp., *Elphidium crispum*).



Photo 18: Coring LIS 29. (Uncu, 2007)

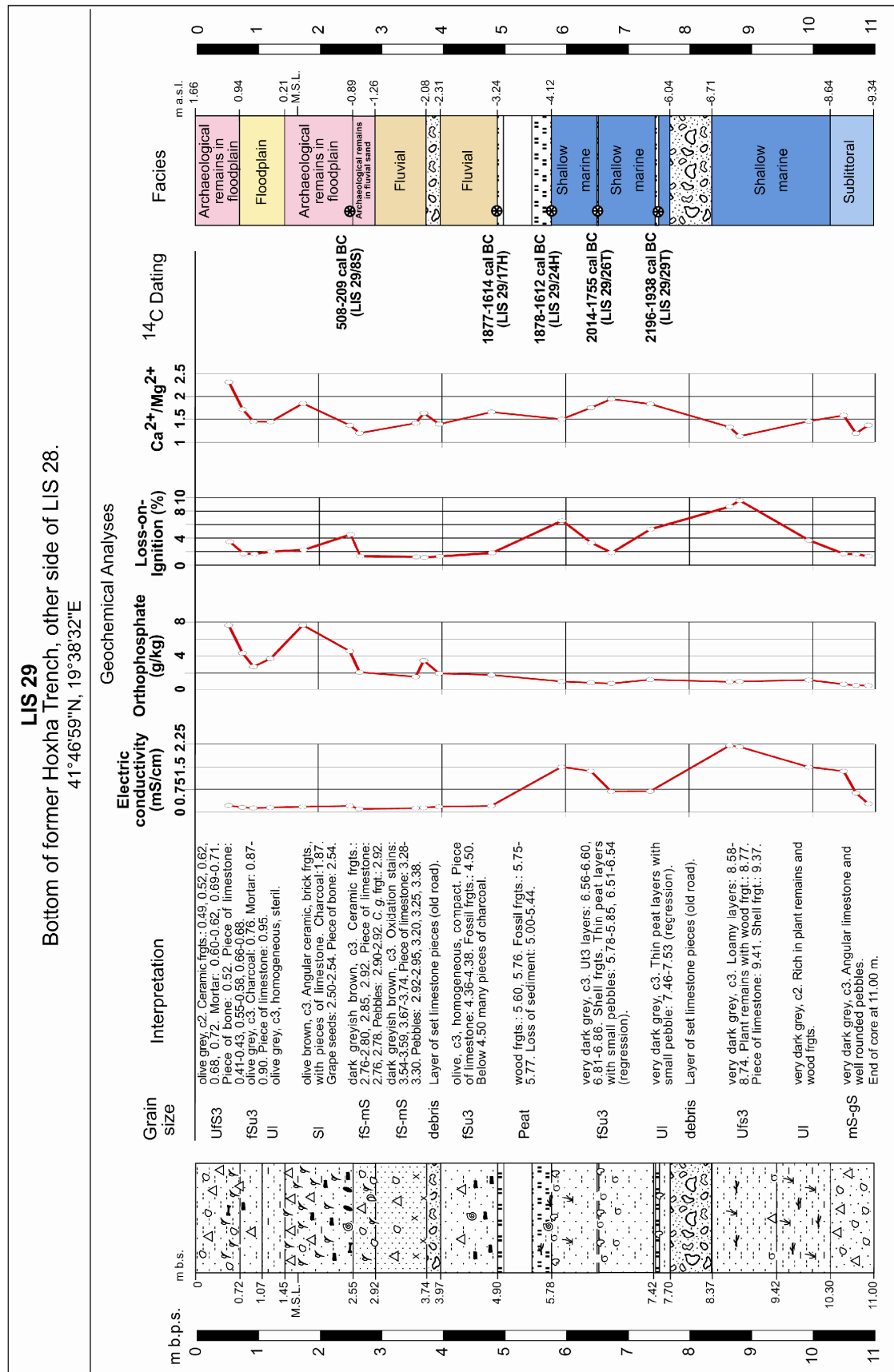


Figure 34: Synoptic chart of coring LIS 29.

Above 7.76 m b.s.l., the sediment changes to fine sandy silt with loamy intercalations. The high values of electric conductivity (2.20 mS/cm) and organic matter (9.57 %) indicate that the stratum was deposited in a well-protected shallow marine embayment. The fossil content is similar to that of the loamy strata below (macrofossil: *Cidaris* sp.; ostracod: *Xestoleberis dispar*; foraminifer: *Ammonia beccarii*, *Quinqueloculina* sp.).

From 6.71 to 6.04 m b.s.l., the shallow marine sand is overlain by a thick layer of debris, composed of angular limestone pieces in a loamy matrix. Its depth suggests that this layer may be an indication of the first noticeable anthropogenic impact around Lezha.

The limestone debris is covered by very dark grey loamy silt. At 5.76 m b.s.l., it changes to silty fine sand, with intercalated clayey and peaty layers (up to 4.12 m b.s.l.). Some of the peat layers (5.87-5.80, 4.88-4.85, 4.19-4.12 m b.s.l.) include small spherical pebbles at the bottom, which may be interpreted as local regressions in the area. The stratum shows a high biodiversity of shallow marine to brackish species (macrofossils: *Cerastoderma glaucum*, *Bittium* sp., *Mytilaster* sp., *Chrysallida* sp.; ostracods: *Cyprideis torosa*, *Pontocythere rubra*, *Loxoconcha stellifera*, *Urocytheris margaritifera*, *Cytheretta adriatica*, *Carinocythereis* sp., *Semicytherura sulcata*; foraminifers: *Ammonia beccarii*, *Elphidium crispum*, *Elphidium minutum*, *Quinqueloculina* sp., *Quinqueloculina* cf. *elegance*). The relatively high ratio of $\text{Ca}^{2+}/\text{Mg}^{2+}$ (up to 1.94) points to a deposition in a shallow marine environment as well.

A thick peat layer with fine sand lenses (between 4.12 m b.s.l. and 3.24 m b.s.l.) indicates the termination of the shallow marine conditions. The bottom as well as top of this peat layer was dated to the first half of the 2nd millennium BC [bottom: 1878-1614 cal BC, peat at 5.75-5.77 m b.s.l. (LIS 29/21T); top: 1877-1614 cal BC, wood at 4.97 m b.s.l. (LIS 29/17H)].

The subsequent olive grey, homogeneous silty sand includes many charcoal fragments and a few pieces of limestone (up to 2.31 m b.s.l.). The low electric conductivity (0.20 mS/cm) suggests deposition under fresh water conditions. However, we know that the Drini was flowing farther inland during that time and did not reach the coring site until Hellenistic times. This apparent unconformity has probably been caused by the Drini eroding the sediment which had been deposited after the first half of the 2nd millennium BC. The charcoal fragments within the sediment can be an indicator either for natural forest fires or, more likely, for human activities in the area.

From 2.31 to 2.08 m b.s.l., the alluvium is covered by another accumulation of limestone fragments. They are of anthropogenic origin, possibly placed there by people to create a passage across the swampy environment in an attempt to reach the river.

The following sediment consists of dark greyish brown, homogeneous fine/medium sand (up to 0.89 m b.s.l.), which contains many ceramic fragments – dated to Hellenistic / Roman times – as well as pieces of limestone above 1.26 m b.s.l. The high value of orthophosphate (3.46 g/kg) is indicative of human activities. Both granulometry and the very low electric conductivity (0.20 mS/sec) show that the stratum was deposited by the Drini. This is supported by the occurrence of small, well rounded pebbles within the deposits.

From 0.89 m b.s.l. to 0.21 m a.s.l., the coarse sand sections in a loamy matrix were deposited by occasional fluvial inputs into a swampy environment. The sediments include abundant archaeological material (e.g., angular sherds, pieces of limestone, piece of bone, charcoal fragments and grape seeds). The very high value of orthophosphate (7.63 g/kg) shows intensive human activities. As before, the ceramics and big amphora fragments date from Hellenistic to Roman times.

The uppermost section of the profile is made up of interfingering layers of loamy and fine sandy silt, which were deposited during flood events of the Drini. Above 0.94 m a.s.l., the floodplain sediments contain abundant archaeological material, dating from the 16th/17th century AD to modern times.

7.3.2.3.2 Vibracoring LIS 35

LIS 35 (N 41° 47' 00'', E 19° 38' 32'', ground level at 1.62 m a.s.l., total length of core: 11 m) is located in the former archaeological trench (Hoxha Trench) between the 'Hellenistic Harbour Gate' and the Drini, opposite to LIS 29. A synoptic view of the profile is shown in fig. 35, photo 19, and appendix 5.26.

The lowermost part of the profile is made up of very dark grey, compact medium/coarse sand with small pebbles (up to 8.94 m b.s.l.). The sediment contains shallow marine to brackish species (macrofossil: *Cerastoderma glaucum*; foraminifer: *Ammonia beccarii*; ostracod: *Pontocythere rubra*). The granulometry, fossil content and geochemical analyses, for instance a relatively high electric conductivity (1.18 mS/cm), point to a deposition under sublittoral conditions.

Then follows very dark grey, loamy silts with some intercalated with some clay lenses and numerous peat layers. The sediment includes common brackish to shallow marine species (macrofossils: *Corbula gibba*, *Loripes lacteus*, *Cerastoderma glaucum*; foraminifers: *Ammonia beccarii*, *Quinqueloculina* sp.; ostracods: *Cyprideis torosa*, *Loxoconcha stellifera*). Relatively high values of electric conductivity (up to 2.90 mS/cm) and organic matter (13.01 %) as well as the faunal content indicate a calm marine environment.

Above 6.88 m b.s.l., the stratum is silty fine sand with thin peat layers (from 6.19 to 6.06 m b.s.l.). It contains a rich assemblage of shallow marine to brackish species (macrofossils: *Cerastoderma glaucum*, *Bittium reticulatum*; ostracods: *Cyprideis torosa*, *Pontocythere rubra*, *Loxoconcha stellifera*, *Cytheretta adriatica*, *Xestoloberis communis*, *Uroythereis margaritifera*, *Semicytherura psila*, *Semicytherura inversa*; foraminifers: *Quinqueloculina* sp., *Ammonia beccarii*, *Elphidium crispum*). The high carbonate content (18.6 %) and the $\text{Ca}^{2+}/\text{Mg}^{2+}$ ratio (2.54) confirm the interpretation of a shallow marine environment.

The fine sand is overlain by a thick layer of angular limestone in a loamy matrix (up to 5.30 m b.s.l.), with a few oyster fragments in the uppermost part. A comparable layer was found ca. 1 m deeper at coring site LIS 29. This is likely to be a measurement error because of compaction during coring; however, local tectonics may also play a part.

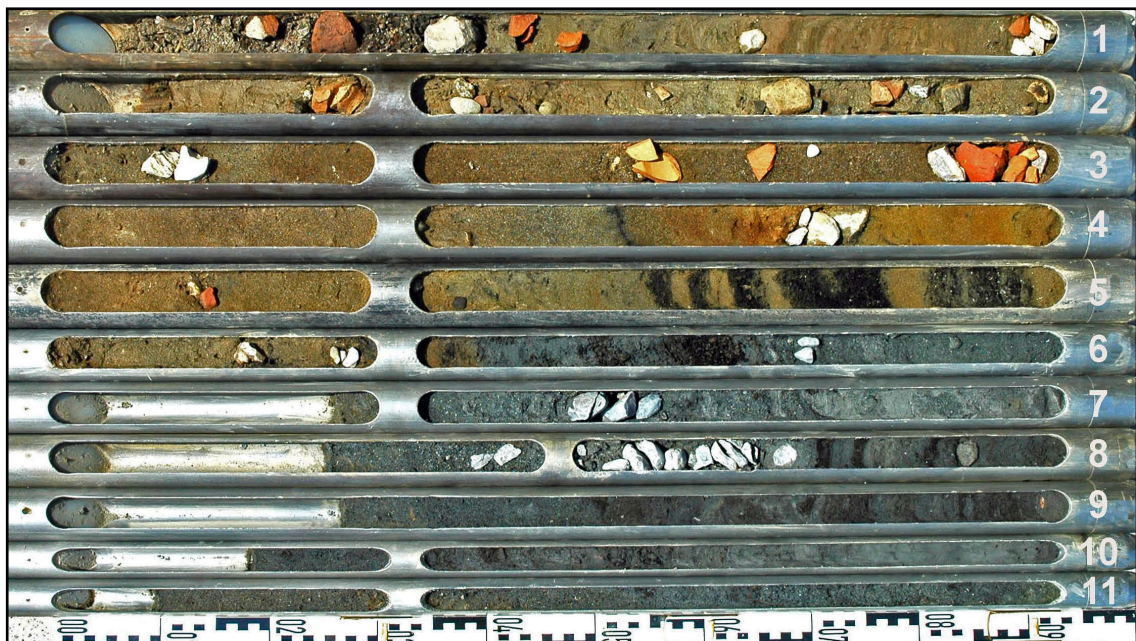


Photo 19: Coring LIS 35. (Uncu, 2007)

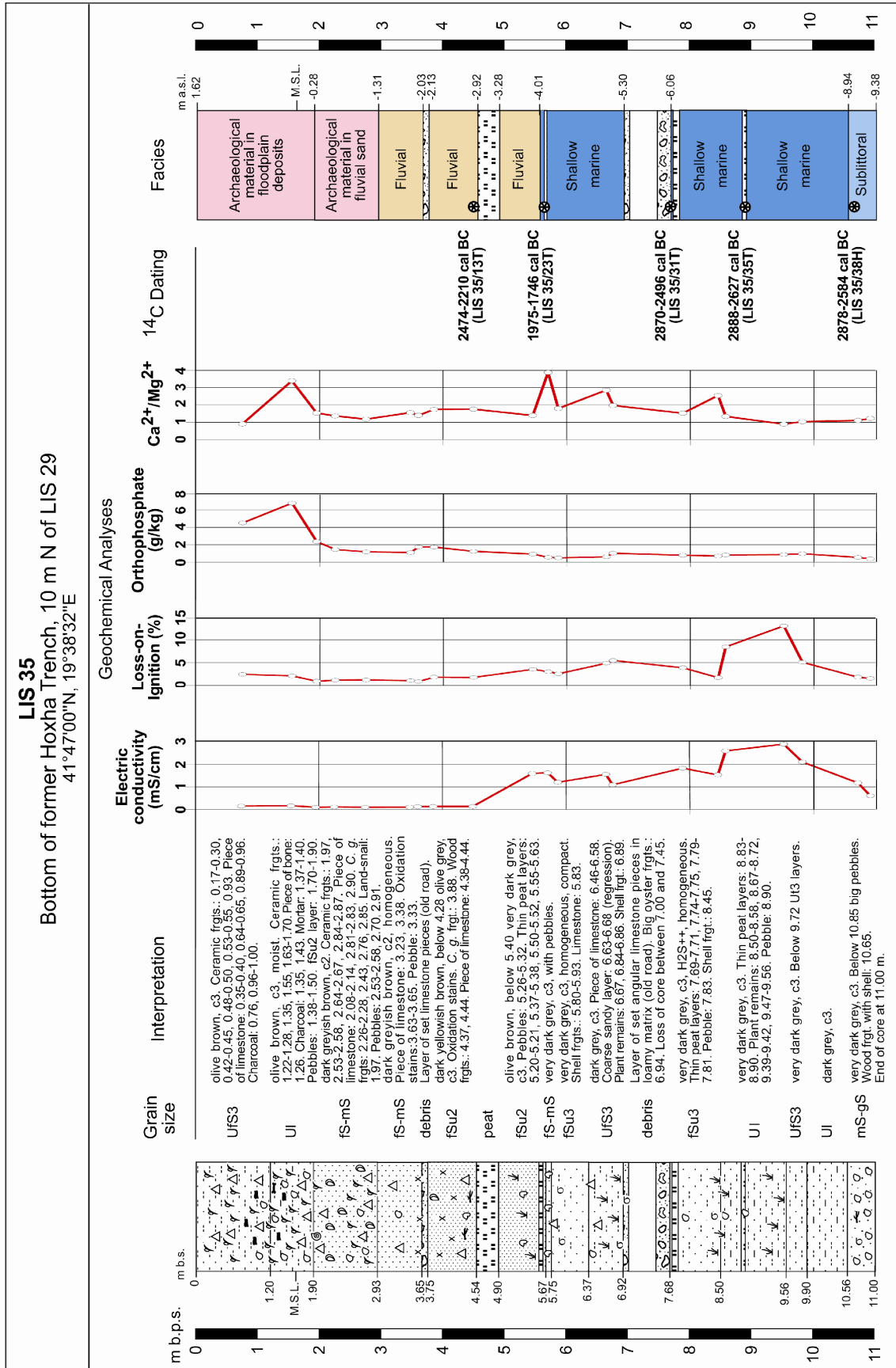


Figure 35: Synoptic chart of coring LIS 35.

The layer of limestone is covered by very dark grey, homogeneous silty fine sand with lenses of clayey silt (up to 4.05 m b.s.l.). The stratum includes numerous plant remains and peats, similar to LIS 29. Again, the peat layers with pebbles at their base (at 5.06-5.01 and 4.13-4.05 m b.s.l.) may reflect local regressions. The faunal content includes abundant shallow marine to brackish species (macrofossils: *Bittium* sp., *Mytilaster* sp., *Mytilus* sp.; ostracods: *Cyprideis torosa*, *Pontocythere rubra*, *Loxoconcha stellifera*, *Leptocythere* sp., *Urocythereis margaritifera*; foraminifers: *Ammonia beccarii*, *Elphidium minutum*, *Cibicides lobatulus*, *Quinqueloculina* sp., *Triloculina* sp.). The uppermost part reflects the continuation of a shallow marine to brackish environment (ostracods: *Cyprideis torosa*, *Semicytherura sulcata*, *Semicytherura inversa*, *Pontocythere rubra*, *Loxoconcha stellifera*, *Leptocythere* sp., *Cytheromorpha* sp.; foraminifers: *Ammonia beccarii*, *Elphidium crispum*, *Cibicides lobatulus*, *Rosalina* sp., *Quinqueloculina* sp., *Triloculina* sp.). Granulometry and results from various geochemical analyses, such as relatively high values of electric conductivity (up to 1.51 mS/cm) and calcium carbonate (16.01 %) as well as the $\text{Ca}^{2+}/\text{Mg}^{2+}$ ratio (2.86), support the milieu interpretation.

Homogeneous fine sand follows, indicating a relatively rapid sediment input. The colour changes from olive brown to olive grey, reflecting reduction conditions. A thick peat with intercalated sand lenses (3.28-2.92 m b.s.l.) must have been deposited in a back-swamp. Above the peat, the colour of the sand turns dark yellowish brown. The sediment includes numerous oxidation stains, as well as pieces of wood and limestone. The electric conductivity decreases dramatically (from 1.60 to 0.13 mS/cm), caused by fluvial input.

The stratum is overlain by a layer made up of pieces of limestone, most likely evidence of human impact (2.13-2.03 m b.s.l.). This debris is covered by dark greyish brown, homogeneous fine/medium river sand (up to 0.28 m b.s.l.). Above 1.31 m b.s.l., it contains abundant archaeological material, such as amphora fragments from Hellenistic to Roman times, pieces of angular limestone and of *Cerastoderma glaucum* fragments.

The uppermost part of the profile comprises of intercalated olive brown, loamy silt and sand layers. These floodplain deposits include charcoal, bone, limestone, and archaeological material such as ceramic fragments, dating from Hellenistic (bottom) to modern (top) times.

7.3.2.4 Synopsis of transect E-E'

The coring profiles of this transect present important stratigraphic differences, even over short distances (see fig. 32). They are very informative in terms of determining the sedimentary milieus around the ancient city of Lissos.

Rounded pebbles and angular stones in a coarse sandy matrix in the lowermost parts of the cores (LIS 28, LIS 29, LIS 35 and LIS 04) reflect deposition in a sublittoral environment. This facies represents the first marine influence in the area during the Holocene transgression maximum. Radiocarbon age estimates from LIS 28 and LIS 35 indicate that sublittoral conditions existed during the first half of the 3rd millennium BC [2893-2633 cal BC, wood at 6.14 m b.s.l. (LIS 28/24H); 2878-2584 cal BC, wood at 9.03 m b.s.l. (LIS 35/38H)]. It is important to note that the sublittoral facies of LIS 29 (and LIS 35) can be found in LIS 04 and LIS 28 as well, however two meters deeper.

The subsequent layer of silty sand in the cores LIS 29 and LIS 35 was deposited under marine/brackish conditions. The fine grain size as well as the rich faunal content of the deposits suggests accumulation in a sheltered marine embayment under low-energy conditions. Due to the continuous rise in sea level, the depth of the water increased. In this context, another radiocarbon dating from LIS 28 seems problematic. Similar to the age estimate from the older stratum, the shallow marine deposits have also been dated to the first half of the 3rd millennium BC [2889-2629 cal BC, wood at 4.41 m b.s.l. (LIS 28/18H)]. This apparently incongruous age is likely to have been caused by an error during sampling or in the laboratory.

A layer of angular limestone boulders is sandwiched within the very shallow marine deposits at LIS 29 (a similar stratum, but not as deep, occurs in LIS 35; the difference in depth may have been caused by the coring process). No evidence is available for transportation of the material from the adjacent slopes. In fact, it seems that people dumped the limestone fragments intentionally in this area – a coastal swamp-like environment – most likely in order to gain easier access to the sea. Radiocarbon ages obtained from organic matter below [2870-2496 cal BC, peat at 6.09 m b.s.l. (LIS 35/31T)] and above [2196-1938 cal BC, peat at 5.76-5.86 m b.s.l. (LIS 29/29T)] the debris layer date its formation to the second half of the 3rd millennium BC. This coincides with the establishment of fully marine conditions in other cores (e.g., Merqia plain).

Several buried peats found within the very shallow marine strata prove that between the end of the 3rd millennium BC to the first half of the 2nd millennium BC, the shoreline in close proximity of Lezha must have shifted on various occasions. Peat formation at a depth of ca. 3-4 m b.s.l. occurs in cores LIS 28 and LIS 29 (also LIS 35). It hints to a (local) regression in the area. According to ¹⁴C age estimates (see table 8), this regression dates to the Early/Middle Bronze Age, i.e., the first half of the 2nd millennium BC [1975-1746 cal BC, peat at 4.01 m b.s.l. (LIS 35/23T); 1878-1612 cal BC, peat at 4.10 m b.s.l. (LIS 29/21T)].

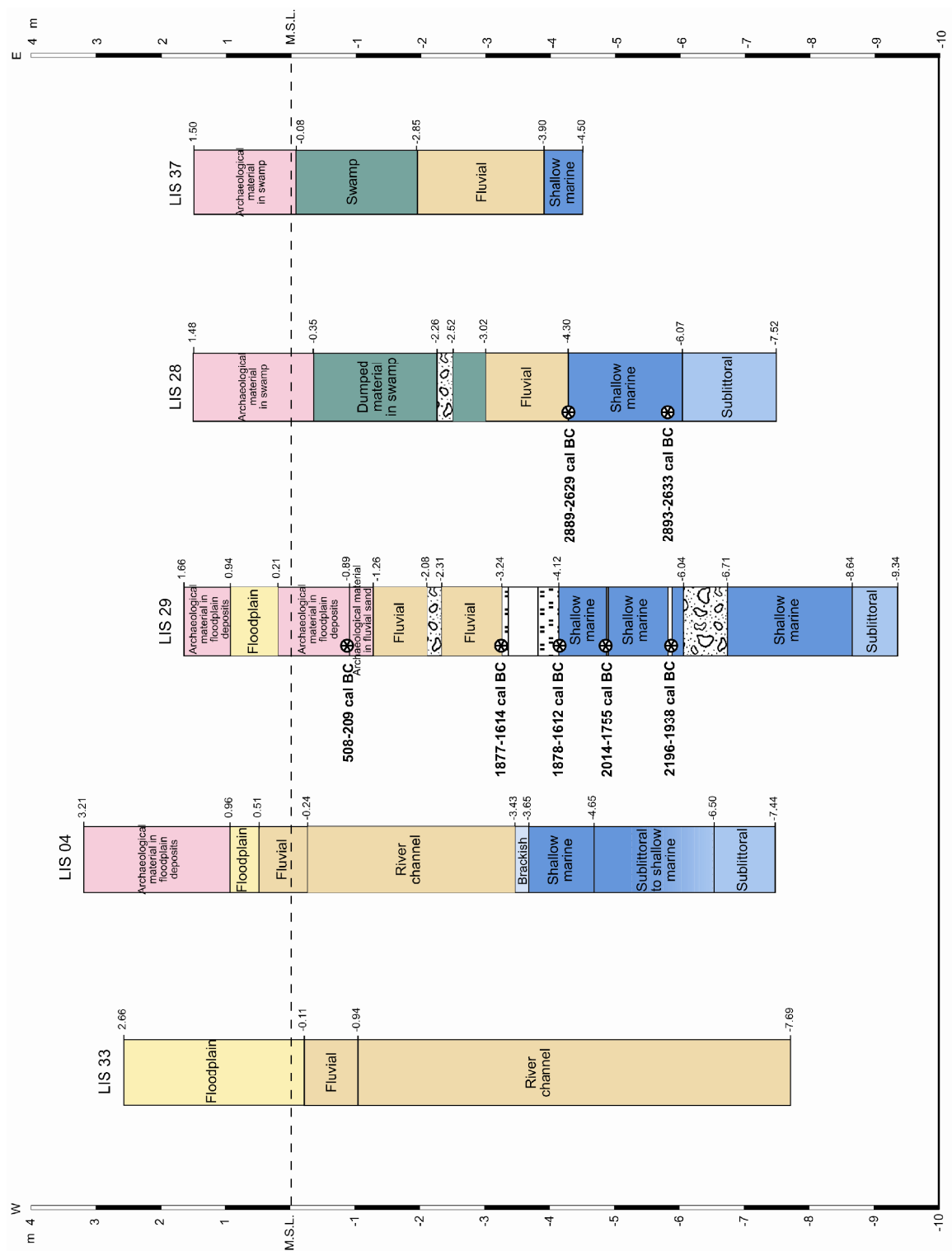


Figure 36: Geological transect E-E' (own research).

The marine deposits are discordantly overlain by fluvial sands. However, written sources, as well as results from other cores taken north of Lezha, indicate that most likely the Drini probably only passed this location at the beginning of the Hellenistic period, because ceramics of this time can be found only in deposits of the Drini. Thus, there is a gap of about 1500-2000

years in the sedimentary records. Possible explanations can be (1) dating problems with the ^{14}C samples or, more likely, (2) fluvial erosion of several meters of the marine strata.

Event	Timing
Shallow marine conditions. Numerous embedded peat layers, probably linked with co-seismic events, reflect temporary sea level fluctuations.	First half of the 3 rd millennium BC (Late Neolithic-Chalcolithic) 2878 – 2584 cal BC (LIS 35: wood, 9.03 m b.s.l.) 2888 – 2627 cal BC (LIS 35: peat, 7.21-7.28 m b.s.l.) 2893 – 2633 cal BC (LIS 28: wood, 6.14 m b.s.l.) 2870 – 2496 cal BC (LIS 35: peat, 6.09 m b.s.l.)
Local regression in the area, marked by the development of a thick peat layer.	First half of the 2 nd millennium BC (Middle Bronze Age) (between ca. 2000 and 1600 BC) 1975 – 1746 cal BC (LIS 35: peat, 4.01 m b.s.l.) 1878 – 1612 cal BC (LIS 29: peat, 4.10 m b.s.l.)

Table 8: Chronology of events for cross section E-E'.

Many pieces of charcoal within the fluvial deposits in LIS 29 may be hints for an anthropogenic influence. In cores LIS 28 and LIS 29 (also LIS 35), fluvial sands cover a second stony stratum, consisting of limestone fragments (at about 2-2.5 m b.s.l.). Again, the limestone debris was probably dumped intentionally by the inhabitants in order to gain good access to the river. The Drini must have passed very close to LIS 29, because there is a thick stratum of channel deposits in LIS 04. Towards the other side, landward of LIS 29, the cores LIS 37 and LIS 28 reflect swampy conditions. Although LIS 37 did not comprise a stony layer as found in LIS 28 and LIS 29, the fluvial/swampy deposits contain many limestone and sandstone fragments, which must have been intentionally laid down, maybe to counteract the increasingly wet conditions.

Beginning at a depth of ca. 1.30 m b.s.l., the fluvial deposits of cores LIS 29 (also LIS 35), LIS 37, and LIS 28 contain numerous archaeological remains. The ceramic and amphora fragments date to Hellenistic – Roman times. A radiocarbon age of 508-209 cal BC [grape seed at 0.84-0.88 m b.s.l. (LIS 29/8S)] fits well with information from ancient sources about the foundation of Lissos shortly before 385/4 BC (Diod. Sic., 15, 13, 1-5).

7.3.3 Corings around the Skanderbeg Monument

Four corings were carried out around the Skanderbeg Monument, two to the north and two to the south of it (see fig. 30). They were to clarify the palaeo-topography at the time of Lissos' foundation.

7.3.3.1 Vibracoring LIS 03

LIS 03 (N 41° 46' 58'', E 19° 38' 35'', ground level at 4.64 m a.s.l., total length of core: 7.40 m) is located north of the Skanderbeg Monument. A synoptic view of the profile is shown in fig. 37, photo 20.

The lowermost section of the core consists of angular stones and pebbles, embedded in an olive grey, sandy matrix (up to 2.10 m b.s.l.). This can be interpreted as former river channel deposits. The following light olive brown loamy silt includes big pieces of weathered sandstone and angular limestone (up to 0.71 m b.s.l.). From 0.71 m b.s.l. to 2.10 m a.s.l., the sediment changes to olive brown silty clay with numerous oxidation stains and small pieces of lime- and sandstone. These floodplain sediments mixed with slope debris from Lezha Hill accumulated during the pre-Holocene period.

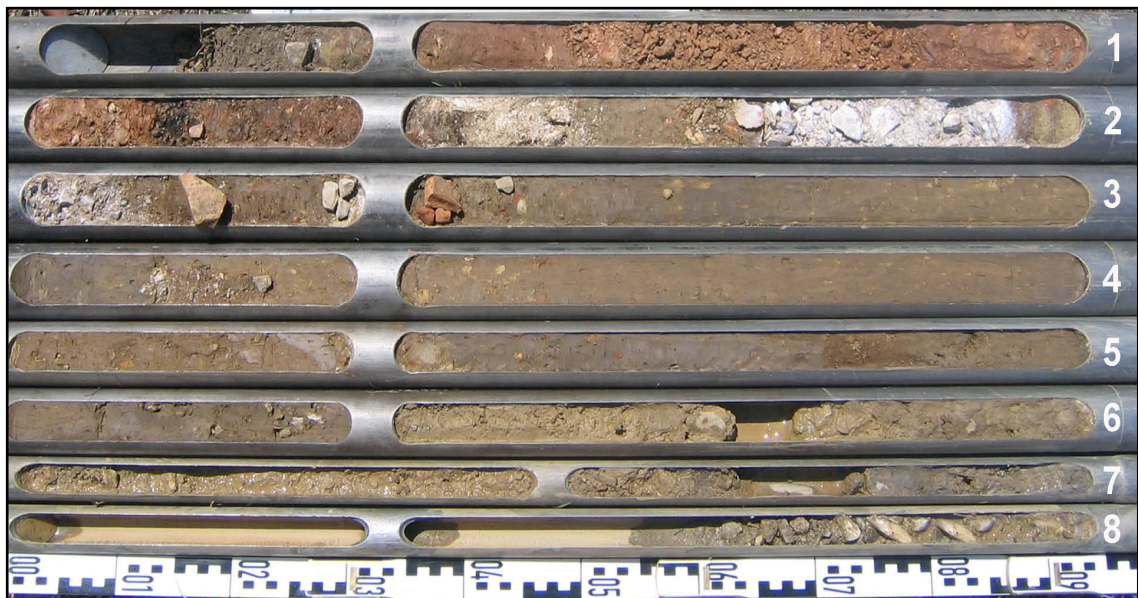


Photo 20: Coring LIS 03. (Uncu, 2006)

The uppermost section is dominated by dark yellowish brown clayey silt with abundant archaeological remains (from 2.10 m a.s.l. to the present surface). The stony layer (between 2.78 and 3.00 m a.s.l.) composed of limestone fragments can be interpreted as a former road.

Many brick fragments with mortar (3.20-3.49 m a.s.l.) and a burnt layer with many ceramics (3.49-3.52 m a.s.l.) indicate intensive human activities. The artifacts were dated to Hellenistic times at the bottom and to Roman times in the upper part. Towards the top, the abundance of archaeological material decreases, whereas small stones become more frequent.

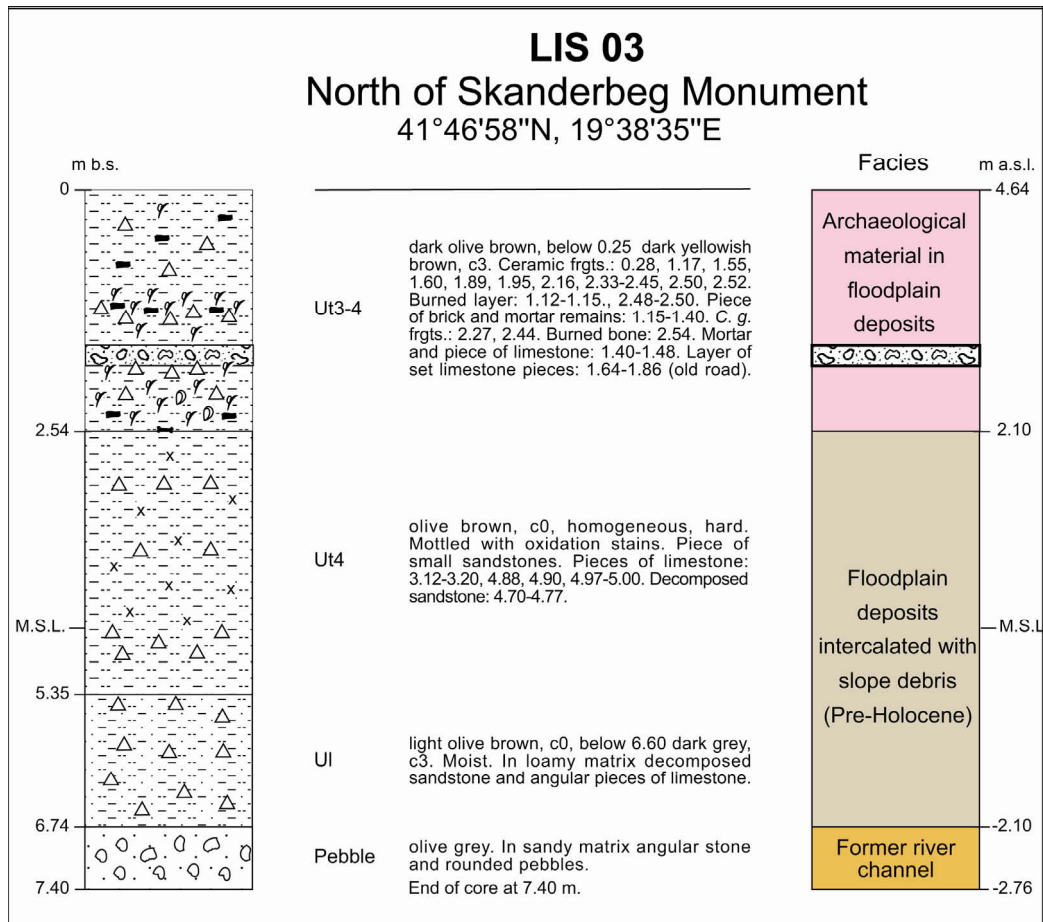


Figure 37: Synoptic chart of coring LIS 03.

7.3.3.2 Vibracoring LIS 05

LIS 05 (N 41° 46' 58'', E 19° 38' 36'', ground level at 3.82 m a.s.l., total length of core: 6 m) is located in front of the Hellenistic city wall, north of the Skanderbeg Monument. A synoptic view of the profile is shown in fig. 38, photo 21.

The lower part of the profile is composed of pale olive, silty clay with small pieces of angular sandstone. From 1.43 m b.s.l. to present sea level, the sediment is sterile. Above 0.07 m a.s.l., the clayey silt includes numerous oxidation stains and pieces of sandstone. The whole stratum suggests alternating deposition of slope debris and floodplain sediments.



Photo 21: Coring LIS 05. (Uncu, 2006)

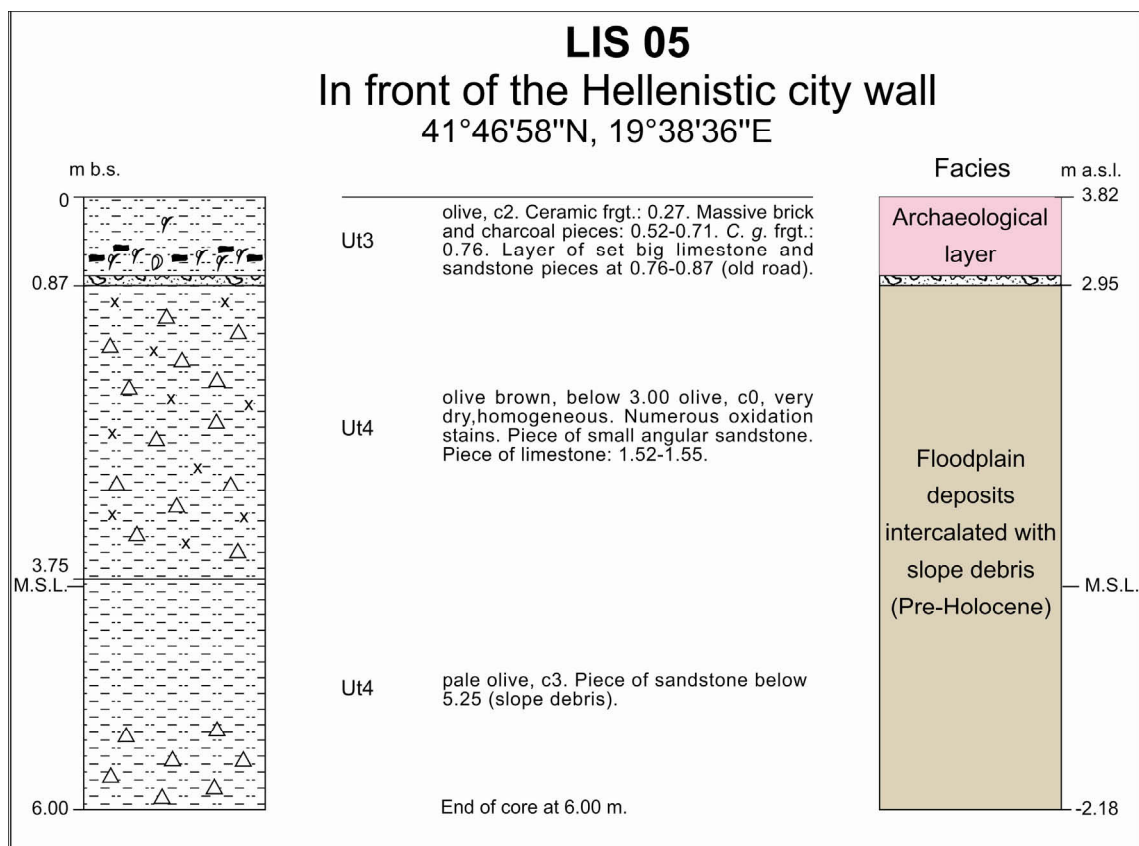


Figure 38: Synoptic chart of coring LIS 05.

A layer of large lime- and sandstone fragments between 2.95 and 3.06 m a.s.l. can be interpreted as an old road. However, no archaeological material was found below this layer, whereas a similar stony layer, located at the same depth of coring LIS 03 contained archaeological material and was dated to Roman times.

The uppermost portion of the core is made up of olive clayey silt with some archaeological remains. Between 3.11 and 3.30 m a.s.l., the stratum is interrupted by a thick brick layer with

many pieces of charcoal and shell remains (*Cerastoderma glaucum*) which also dates to Roman times.

7.3.3.3 Vibracoring LIS 02

LIS 02 (N 41° 46' 56'', E 19° 38' 36'', ground level at 3.00 m a.s.l., total length of core: 7 m) is located at the foot of the steep slope of Lezha Hill, between the Skanderbeg Monument and the Southwest Gate of Lissos. A synoptic view of the profile is shown in fig. 39, photo 22.

The lowermost part of the core consists of olive grey, clayey silt with many pieces of angular lime- and sandstone. Some oxidation staining is visible (up to 1.60 m b.s.l.). These terrestrial deposits must have been laid down during the pre-Holocene period.

The following silty, clayey stratum also contains pieces of angular lime- and sandstone (up to 1.35 m a.s.l.). The colour changes from olive grey to olive brown. Between 1.00 and 0.80 m b.s.l., a layer of set angular limestone fragments suggests an anthropogenic impact, e.g., a former road. Ceramic fragments and pieces of charcoal were found at present sea level. The upper section includes numerous oxidation stains as well as sandstone fragments. The finer sediments were deposited during flood events; the angular pieces of rock can be interpreted as slope debris from Lezha Hill.

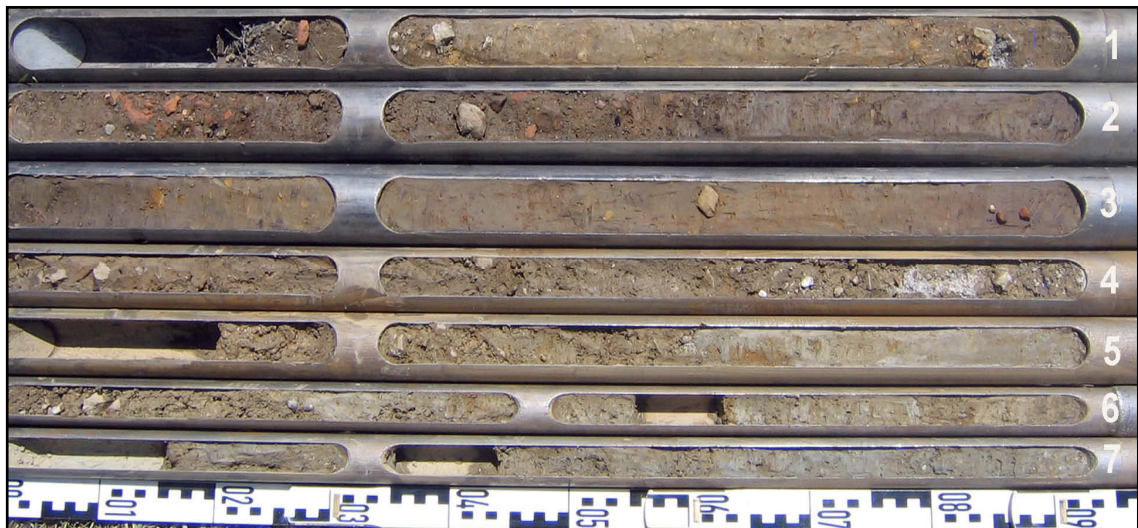


Photo 22: Coring LIS 02. (Uncu, 2006)

From 1.35 to 2.10 m a.s.l., the clayey sediment is overlain by dark olive brown, loamy silt with abundant archaeological material, such as ceramic fragments, pieces of charcoal, burnt bone, remains of mollusc shells and terrestrial gastropods as well as pieces of angular limestone. The ceramic fragments date from Hellenistic/Roman times.

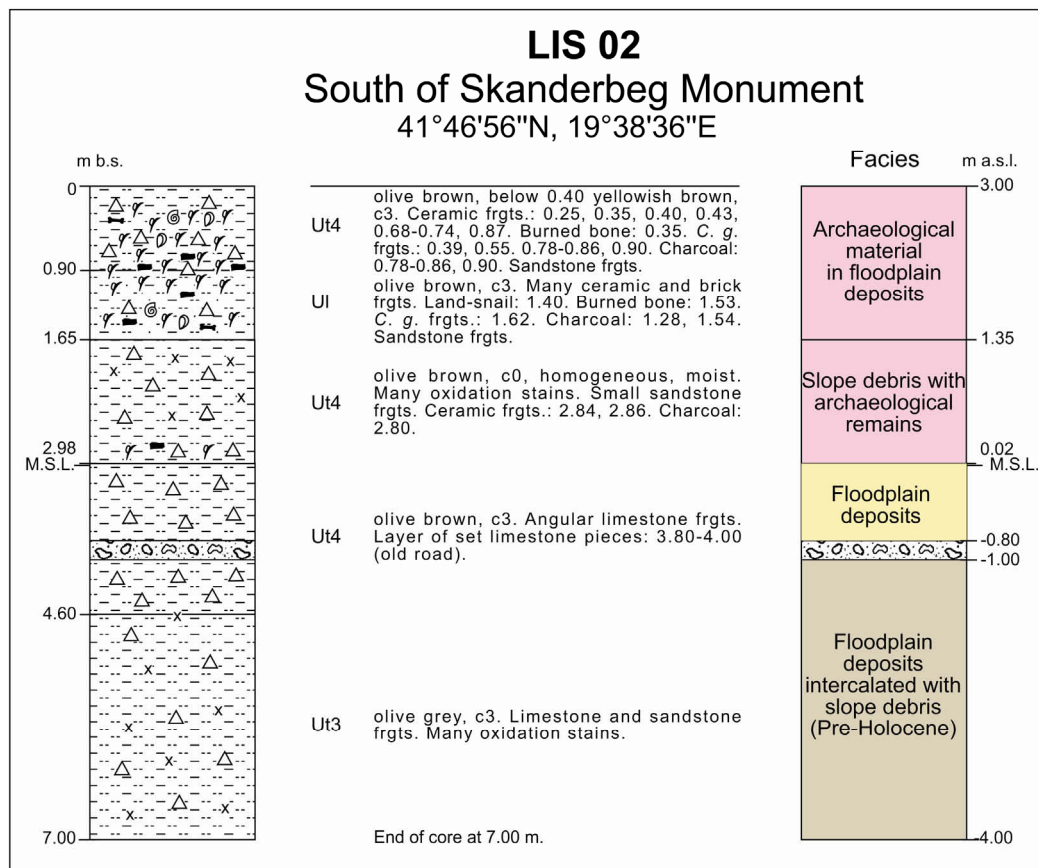


Figure 39: Synoptic chart of coring LIS 02.

The uppermost portion of the core consists of olive brown, clayey silt, deposited by the Drini during flood events. This sediment contains a lot of archaeological material as well as slope debris.

7.3.3.4 Vibracoring LIS 38

LIS 38 (N 41° 46' 56'', E 19° 38' 34'', ground level at 3.94 m a.s.l., total depth of coring: 12 m) lies in the archaeological area, southwest of the Skanderbeg monument (Excavation area E). A synoptic view of the profile is shown in fig. 40, photo 23, and appendix 5.27.

The profile starts with very dark grey, compact medium/coarse sand in a loamy matrix (up to 6.84 m b.s.l.). The upper part of this stratum contains a few small pebbles and broken shell fragments. The electric conductivity (1.15-1.61 mS/cm) and calcium carbonate content (9-17 %) are relatively high. The granulometry indicates high wave energy. Thus, the sediment was deposited in a near-shore (sublittoral) environment.

Then follow clayey silts with intercalated lenses of fine sand (up to 5.52 m b.s.l.). A facies change from dynamic sublittoral to stagnant water conditions is indicated by results from the geochemical analyses, e.g., relatively high values of organic matter (4-7 %) and $\text{Fe}^{2+/3+}$ ions (30.35 g/kg). The fossil assemblage consists of meso- to polyhaline species of a brackish/shallow marine environment (macrofossils: *Rissoa* sp., *Retusa* sp., *Cidaris* sp., many juvenile marine mollusc fragments; ostracods: *Cyprideis torosa*, *Pontocythere rubra*, *Leptocythere* sp., *Cytherura* sp., *Semicytherura* sp., *Quinqueloculina* cf. *costata*, *Basslerites berchoni*, *Haynesia germanica*; foraminifers: *Ammonia beccarii*, *Ammonia* cf. *parkinsoniana*, *Loxoconcha elliptica*, *Loxoconcha stellifera*).

The next layer consists of stratified, compact, silty fine sand which contains numerous thin intercalated peat lenses (above 5.52 m b.s.l.). The high electric conductivity (2.23 mS/cm) between these lenses may be interpreted as occasional marine ingressions due to local subsidence. The fossil content comprises meso- to polyhaline species (macrofossils: *Donax* sp., *Cerithium* sp.; ostracods: *Cyprideis torosa*, *Quinqueloculina* sp.), reflecting a shallow marine environment.

Above 3.90 m b.s.l., olive gray sandy silt dominates. Due to an increasing freshwater influx, the electric conductivity dramatically decreases from 1.52 to 0.11 mS/cm. The uppermost part of this section is concluded by a thin peat layer (at 3.56 m b.s.l.). Small pebbles at its bottom may indicate a local regression.



Photo 23: Coring LIS 38. (Uncu, 2008)

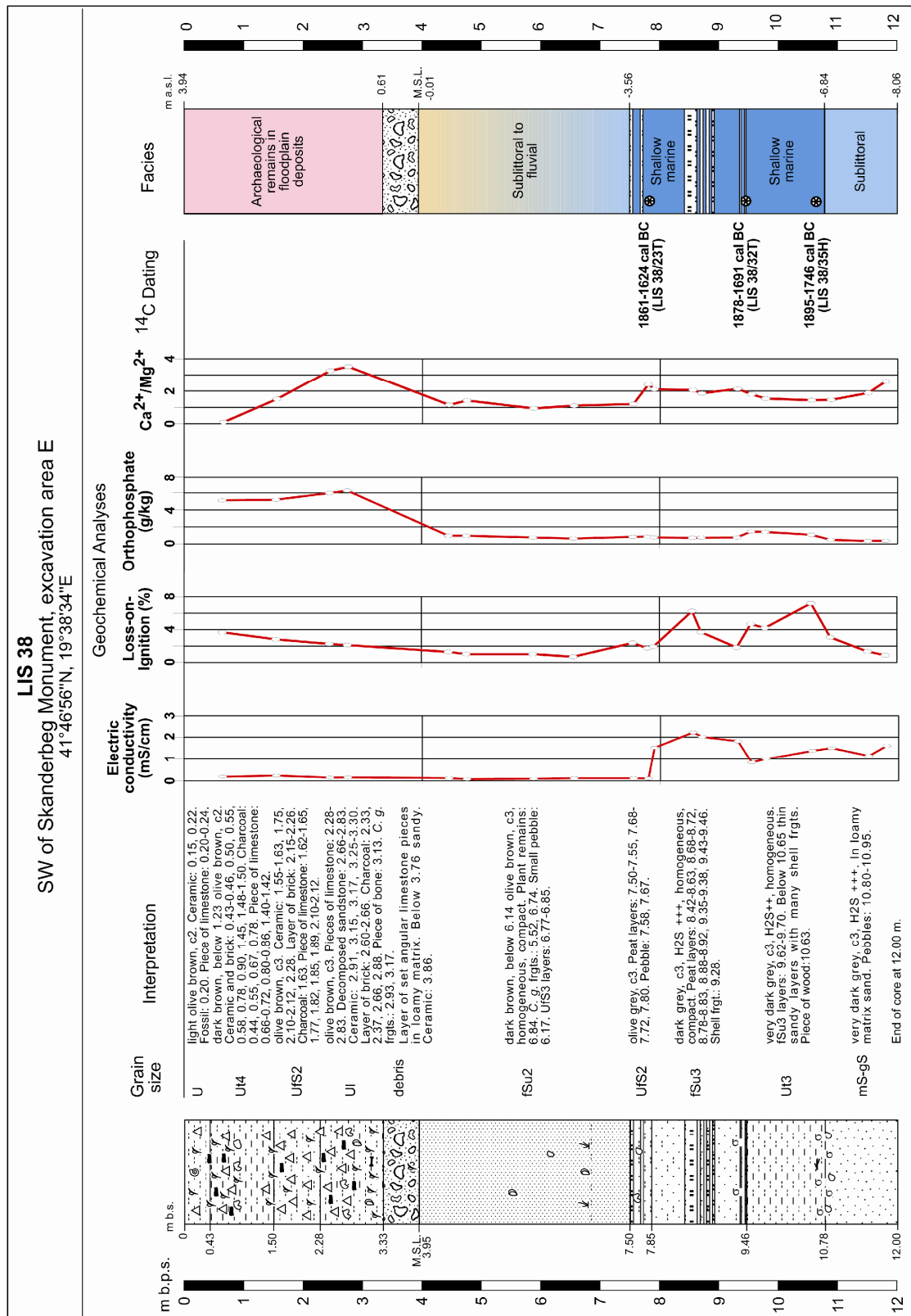


Figure 40: Synoptic chart of coring LIS 38.

A thick homogeneous fine sandy stratum makes up the middle part of the profile between 3.56 and present sea level. The colour of the deposit changes towards the top from olive brown to dark brown. Low electric conductivity (0.09 mS/cm) indicates a strong freshwater influx. The

scarceness of *Cerastoderma glaucum* fragments suggests unfavourable ecological conditions, possibly due to the rapid accumulation of sediments.

A conspicuous layer of angular limestone fragments in a loamy matrix follows (more or less at present sea level). Associated Hellenistic ceramic illustrates the first explicit human impact at this coring site. Probably settlers of Lissos laid down the limestone boulders in order to expand their settlement. Archaeological finds increase within the fine-grained floodplain sediments on top of the dumped material. The high value of orthophosphate shows intensive human activities in the area. The diagnostic ceramic finds date from the early Hellenistic to Roman times.

7.3.2.5 Synopsis of the corings around the Skanderbeg Monument

Despite all cores being in close vicinity of each other, it is intriguing how much the geomorphologic situation changes even within a short distance (see fig. 41).

Corings LIS 02, LIS 03 and LIS 05 consist largely of fine-grained floodplain sediments and include a lot of slope debris. A layer of pebbles, found only at the very bottom of LIS 03, represents a former channel of a small stream. These terrestrial sediments were accumulated as part of the formation of the large piedmont plain before the Holocene transgression took place; they date to pre-Holocene times.

The lack of marine sediment in these cores shows that the sea never reached this area at the foot of Lezha Hill, because it was a few metres above sea level during the Holocene transgression maximum. This location presented suitable conditions for a settlement around the time when the city was founded, which is also confirmed by a thick layer of archaeological remains, intercalated with slope debris in the uppermost part of all cores. The ceramics date to Hellenistic/Roman times. A set layer of angular limestone pieces found in cores LIS 03 and LIS 05 may be interpreted as an old road. The ceramic and brick fragments within this layer date to Roman times.

Coring LIS 38 shows a totally different picture compared to the other cores; however, very similar layers were found in LIS 04, LIS 29 and LIS 35 (transect E-E'). The first marine influence nearby Lezha Hill is evidenced by sublittoral sands in the lowermost part of this core. Subsequent fine-grained deposits point to a change towards a shallow marine milieu due to the increasing water depth. The fine grain size and peat layers towards the top of the marine strata indicate the existence of a well-protected marine embayment.

Radiometric dating indicates that marine conditions existed at this coring site during the first half of the 2nd millennium BC. The uppermost age [1861-1624 cal BC, peat layer at 3.86 m b.s.l. (LIS 38/23T)], reflecting a regression in the area, is congruent with age estimates obtained from LIS 29 and LIS 35. However, the other two ages have to be used with caution, because they seem to be too young [1895-1746 cal BC, wood at 6.69 m b.s.l. (LIS 38/35H); 1878-1691 cal BC, peat at 5.49-5.52 m b.s.l. (LIS 38/32T)].

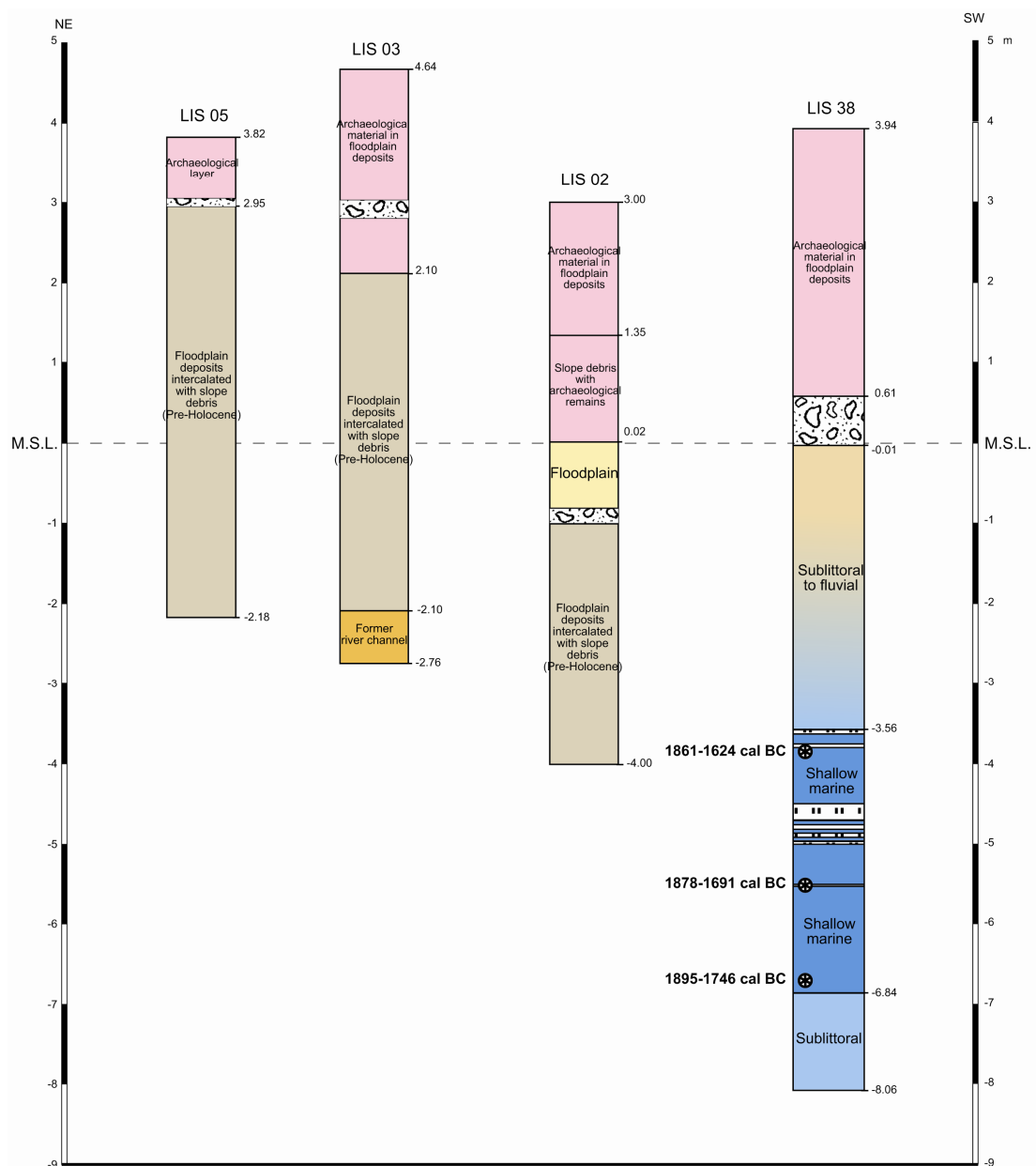


Figure 41: Geological profiles of the corings around the Skanderbeg Monument (own research).

The marine strata are covered discordantly by a thick stratum of homogeneous fine sand (ca. 3.5 m). The geochemical analyses point to a deposition under freshwater conditions. However, the origin of this sand seems problematic. Two possibilities are worth considering: (i) the sand might have been transported from the mouth of river Grykes by coastal currents and

accumulated as littoral deposits, or (ii) it must be part of a sub-aqueous levee section of the Drini.

A set of thick angular limestone fragments (ca. 0.60 m), including an early Hellenistic piece of ceramics, can be taken as evidence for an early human settlement in this area. The following floodplain sediments, accumulated during flooding events of the Drini, are very rich in archaeological material.

7.4 Corings from the Drini delta plain

The Drini delta plain begins where the Drini passes through the narrow rocky gap at Lezha. It can be divided into the older Ishull Lezha part immediately to the south of Lezha, and the later evolved Ishull Shengjin region towards the west and northwest (see fig. 21). We carried out 23 corings, grouped into five transects in order to reconstruct the delta evolution in space and time. Additionally, three of the vibracores are discussed individually (LIS 34, LIS 51, and LIS 9) because they are located in distinctly separate areas and therefore, they cannot be connected in a transect.

7.4.1 Transect F-F'

This transect is located in the Ishull Lezha region, south of Lissos. It contains corings LIS 11, LIS 53, LIS 43, LIS 14, LIS 15 and LIS 01 (see fig. 21), and runs southwest from the foot of Mali Shelbuemit to the central part of the Drini delta. The aim of this transect is to reconstruct the evolution of the oldest part of the plain.

7.4.1.1 Vibracoring LIS 11

LIS 11 (N 41° 46' 32'', E 19° 39' 05'', ground level at 3.20 m a.s.l., total length of the core: 10 m) is located at the foot of Mali Shelbuemit, close to the road from the centre of Lezha to the village of Manatia. A synoptic view of the profile is shown in fig. 42, photo 24, and appendix 5.7.

Rounded pebbles in a sandy matrix with some shell fragments make up the lowermost part of the profile (up to 6.56 m b.s.l.). The sediments contain a few marine and brackish fossil species (macrofossil: *Nucula* sp.; foraminifer: *Ammonia beccarii*). The coarse grain size and damaged tests, as well as the relatively low electric conductivity (0.72 mS/cm) indicate a deposition in a sublittoral environment with a high-energy wave climate.

The subsequent layer consists of dark grey, homogeneous silty fine sand with plant remains. Between 5.65 and 5.50 m b.s.l., the sediment contains abundant shallow marine/brackish species (macrofossils: *Alvania* sp., *Cerastoderma glaucum*, *Corbula gibba*, *Donax trunculus*, *Hinia reticulata*, *Nassarius* cf. *pygmaeus*, *Nucula* sp., *Turbonilla lacteal*, *Venus cassina*; ostracod: *Cyprideis torosa*; foraminifer: *Ammonia beccarii*). Also, the relatively high content of organic matter (up to 6.56 %) suggests favourable ecological conditions, such as a well protected marine embayment.

From 4.58 to 4.35 m b.s.l., the strata are dominated by intercalations of silty fine sand, clayey silt and fine/medium sand layers. This shows occasionally changing depositional dynamics at the coring site.

The following deposits are made up of fine/medium sand with small pebbles, pieces of wood and abundant shell fragments (up to 3.42 m b.s.l.). The latter are mostly damaged because of a high energy wave climate; only one shell fragment could be identified (*Chamelea gallina*). The granulometry and fossil content suggest a deposition in a sublittoral environment.

From 3.42 to 3.25 m b.s.l., the sand is overlain by a thick peat. A few small well-rounded limestone pebbles and brackish foraminifers (*Ammonia beccarii*) were found at the bottom of the layer. The pebbles may be taken as evidence for a (localised?) regression, which has also been observed at other coring sites within the ancient Lissos (e.g., LIS 29, LIS 35, LIS 38).



Photo 24: Coring LIS 11. (Uncu, 2006)

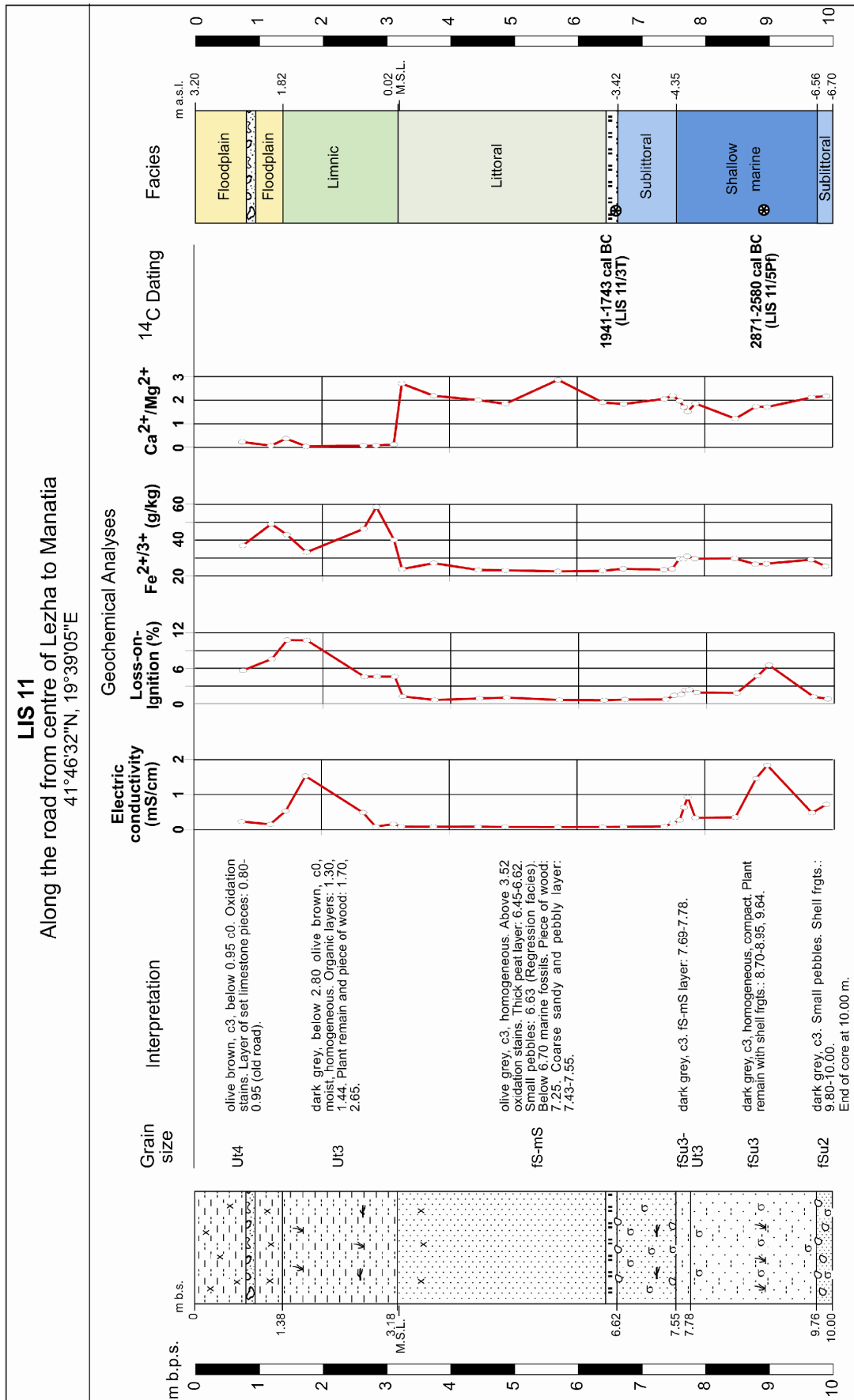


Figure 42: Synoptic chart of coring LIS 11.

On top of the peat is a homogeneous and almost sterile layer of fine/medium sand (up to 0.02 m a.s.l.). Its electric conductivity is very low (0.08 mS/cm), while the CaCO₃ content is comparatively high (up to 18.03 %). The lone presence of a few specimens of the ostracod (*Cyprideis torosa*) indicates varying temperatures and salinities. The particles of this littoral deposit – quartz, serpentine, calcite, radiolarite – are well rounded which suggests a fluvial origin. However, the coring site is located at quite a distance from the river Drini at the base of Mali Shelbuemit. Therefore, the sand rather originates from the mouth of the river Grykes in the south.

The upper section of the profile consists of fine-grained sediments. Above present sea-level, homogeneous, clayey silts dominate with numerous plant remains and a few pieces of wood (up to 1.82 m a.s.l.). The colour of the stratum changes from olive brown to dark grey due to reduction conditions. Granulometry and fossil content (ostracod: *Candonopsis* sp.) suggest a deposition under calm conditions in a freshwater pond/limnic environment. The low pH value (4.24), the high content of organic matter (10.70 %), and the lack of calcium carbonate indicate an acidic milieu.

Above 1.82 m b.s.l., the clay content increases due to the marginal position of the site, i.e., a greater distance to the high energy environment. This olive brown silty/clayey layer accumulated during flooding events of the rivers Drini and Grykes. A layer of set angular limestone pieces, situated between 2.25 and 2.40 m a.s.l., is of anthropogenic origin (a former road).

7.4.1.2 Vibracoring LIS 53

LIS 53 (N 41° 46' 35'', E 19° 38' 45'', ground level at 2.16 m a.s.l, total depth of coring: 8 m) is located in the centre of Lezha, close to the football stadium. A synoptic view of the profile is shown in appendices 5.40.1 & 5.40.2.

The lowermost part of the profile is composed of very dark grey, laminated silty fine sand (up to 4.31 m b.s.l.). It contains salt-tolerant marine species (macrofossil: *Cidaris* sp.; foraminifers: *Quinqueloculina* sp., *Elphidium* sp.) as well as wood fragments and a thin peat lens, indicating a deposition under brackish conditions in a shallow marine environment. Low values of electric conductivity (0.15-0.20 mS/cm) point to a strong freshwater influx from the river Drini.

From 4.31 to 2.54 m b.s.l., the stratum is made up of dark grey fine sand with a few pebbles. The subsequent silty fine sand includes coarse sandy lenses with small pebbles (up to 1.94 m b.s.l.). This may indicate for the proximity of the river mouth. The milieu turns more brackish in the upper part of the layer, due to an increased freshwater influx. This is confirmed by the change in fossil assemblage: several salt tolerant species in the lower part (macrofossil: echinoid spine; foraminifers: *Ammonia* cf. *parkinsoniana*, *Quinqueloculina* sp.) are replaced by just one brackish species in the upper part of the section (*Ammonia* cf. *parkinsoniana*). The following dark olive brown sand shows a shift in depositional conditions (up to 0.71 m b.s.l), because changing river dynamics are reflected in changing grain sizes. Low electric conductivity (0.03-0.13 mS/cm) also suggests that this stratum was deposited by the river Drini.

The uppermost section of the profile consists of silty to clayey deposits. The olive brown fine-grained floodplain sediment contains numerous oxidation stains and some organic matter, which may be an indication for temporarily wetter conditions in the area.

7.4.1.3 Vibracoring LIS 43

LIS 43 (N 41° 46' 04'', E 19° 38' 32'', ground level at 2.58 m a.s.l., total length of core: 12 m) is located within a building site of the SMT close to the railway (SMT: Shqipërisë Ministria e Punëve Publike dhe Transportit – Albanian Ministry of Public Works, Transport and Telecommunication). A synoptic view of the profile is shown in appendix 5.32.1 & 5.32.2.

The lower part of the core consists of dark grey silty sand intercalated with some clayey layers (up to 5.24 m b.s.l.). The grain size changes due to variable depositional dynamics. The clayey layers include organic remains and thin peat lenses, pointing to calm water conditions. The sediment contains shallow marine to brackish species (macrofossil: numerous unidentified shell fragments; foraminifers: *Quinqueloculina* sp., *Ammonia* cf. *parkinsoniana*, *Elphidium excavatum*, *Haynesina germanica*; ostracods: *Pontocythere rubra*, *Loxoconcha* sp., *Paradoxostoma* sp., *Xestoloberis* sp., *Cyprideis torosa* f. *litoralis*, *Cyprideis torosa* f. *torosa*). Relatively low values of electric conductivity (0.39-1.48 mS/cm) as well as the faunal content suggest a strong freshwater influx. These deposits must have accumulated in an interdistributary bay (e.g., an estuarine environment).

The middle section of the profile, from 5.24 to 0.20 m b.s.l., is characterised by fluvial sediments in the shape of alternating layers of sand and pebbles, partly sorted due to temporarily changing river dynamics. In addition, the geochemical results – very low electric conductivity (0.10-0.13 mS/cm) and high calcium carbonate content (up to 17.43 %) – also suggest a fluvial

origin for these deposits. At 1.55 m b.s.l., the colour turns from dark grey to dark brown. This marks the transition from brackish/estuarine to fluvial/terrestrial conditions.

Between 0.20 m b.s.l. and 1.18 m a.s.l., the grain size changes to silty fine sand. A few pebbles testify flooding events of the Drini. The colour (olive brown) and the abundance of oxidation stains indicate seasonally wet and dry semi-terrestrial conditions. The following dark olive brown fine/medium sand (up to 1.63 m a.s.l.) and silt accumulated during periods of flooding. The angular rocks at the top of the floodplain deposits are of anthropogenic origin.

7.4.1.4 Vibracoring LIS 14

LIS 14 (N 41° 45' 45'', E 19° 38' 12'', ground level at 0.94 m a.s.l., total length of core: 9 m) is located in the Ishull Lezha region near the road to Tirana opposite of the Lezha Petrol Station. A synoptic view of the profile is shown in fig. 43, photo 25, and appendix 5.10.

The lowermost part of the profile is characterised by dark grey silty sand (up to 5.71 m b.s.l.). A layer of pebbly coarse sand between 6.76 and 6.54 m b.s.l. points to the temporary nearness of the river mouth. The fossil content includes brackish/shallow marine species (macrofossil: *Cerastoderma glaucum*, *Rissoa labiosa*, *Scrobicularia cottardi*; ostracods: *Cyprideis torosa*, *Loxoconcha stellifera*; foraminifer: *Ammonia beccarii*). One freshwater ostracod species (*Candona neglecta*) was also found, which indicates an increasing fluvial influence. This is also supported by the electric conductivity value, which decreases from 1.13 to 0.38 mS/cm in the uppermost section of the layer.



Photo 25: Coring LIS 14. (Uncu, 2006)

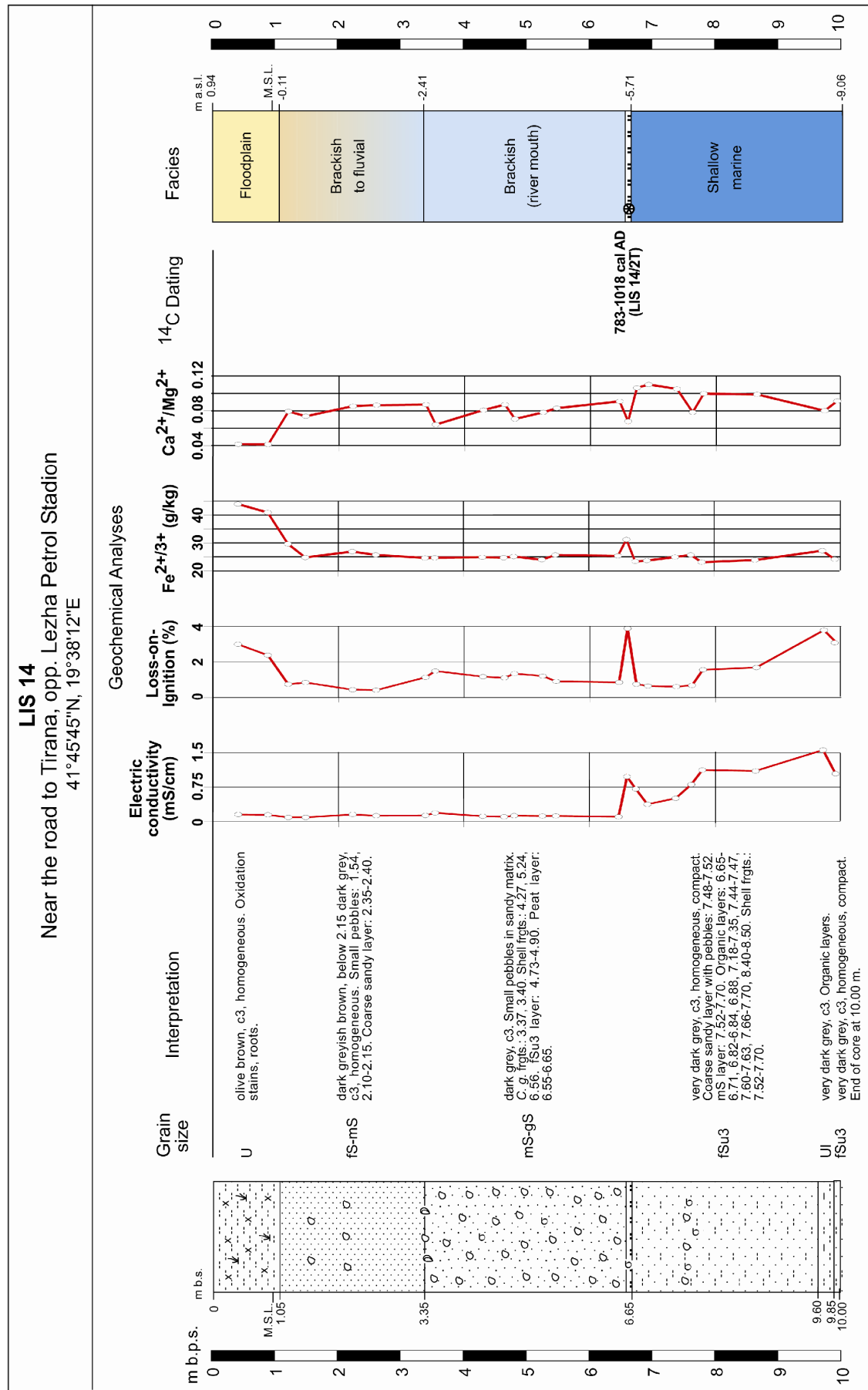


Figure 43: Synoptic chart of coring LIS 14.

The shallow marine deposits are covered by a (paralic) peat, formed in a coastal backswamp (between 5.71 and 5.61 m b.s.l.).

The middle section of the core reflects a highly dynamic depositional milieu. From 5.71 to 2.41 m b.s.l., the sediment is made up of dark grey medium/coarse sand with small pebbles. Some broken marine shell fragments and a few valves of *Cerastoderma glaucum* were found at the top. The granulometry as well as very low values of electric conductivity (between 0.10 and 0.19 mS/cm) indicate a deposition of the river mouth of a pro-deltaic environment.

Above 2.41 m b.s.l., the dominant grain size of the sediment is fine/medium sand. The stratum contains only a few small pebbly and coarse sandy intercalations, indicating temporarily changing dynamics at the river mouth. The lack of fossils can be interpreted by rapid sedimentation in a high energy milieu.

From 0.11 m b.s.l. to the present surface, the sediment consists of clayey silt with numerous oxidation stains, representing deposition in a floodplain environment.

7.4.1.5 Vibracoring LIS 15

LIS 15 (N 41° 45' 33'', E 19° 38' 19'', ground level at 1.42 m a.s.l., total length of core: 10 m) is located in the Ishull Lezha region near the road to Tirana, between LIS 01 and LIS 14. A synoptic view of the profile is shown in appendices 5.11.1 & 5.11.2.

The lowermost part of the profile consists of dark grey silty fine sand (up to 8.08 m b.s.l.). The homogeneous, compact sediment is an indication for deposition in a shallow marine environment.

From 8.08 to 5.18 m b.s.l., the sediment changes to very dark grey fine/medium sand which contains small pebbly lenses and an unidentified shell fragment. The coarse grain size and high $\text{Ca}^{2+}/\text{Mg}^{2+}$ ratio (up to 2.68) suggest deposition in a sublittoral environment.

The subsequent stratum is made up of dark grey loamy silt (up to 4.93 m b.s.l.). The fining-up grain size and the increased electric conductivity (1.57 mS/cm) together with the fauna (macrofossils: *Cerastoderma glaucum*, *Spisula* sp.; ostracod: *Cyprideis torosa*) point to a change towards brackish conditions.

The following very dark grey, silty fine sand indicates the re-establishment of shallow marine conditions in the area. The sandy layer is overlain by dark grey clayey silt (up to 3.98 m b.s.l.). The granulometry and numerous black organic spots point to low-energy depositional conditions in a lagoonal environment.

From 3.98 to 0.93 m b.s.l., the sediment consists of dark grey, loamy silt with intercalated clayey and sandy silt layers (at 2.58-2.38 m b.s.l. and at 1.88-1.58 m b.s.l.). The sediment contains only one brackish foraminifer species (*Ammonia beccarii*) in the lower section. Above 2.58 m b.s.l., plant remains increase and landsnails appear. The whole stratum reflects a transition from brackish/lagoonal to freshwater/limnic conditions.

From 0.93 m b.s.l. to the present surface, the stratum is made up of an alternation of olive brown silty sands and clayey silts with numerous oxidation spots – typical for floodplain sediments.

7.4.1.6 *Vibracoring LIS 01*

LIS 01 (N 41° 45' 26'', E 19° 38' 20'', ground level at 0.90 m a.s.l., total length of core: 9 m) is located approximately 2.7 km south of Lezha, between the towns of Ishull Lezha and Rrila. A synoptic view of the profile is shown in appendices 5.1.1 & 5.1.2.

The lowermost part of the profile is characterised by very dark grey, homogeneous, compact fine/medium sand with organic layers (up to 6.01 m b.s.l.). This stratum contains very few microfossil species, reflecting shallow marine to brackish conditions (foraminifers: *Ammonia beccarii*, *Quinqueloculina cf. striata*).

From 6.01 to 4.56 m b.s.l., homogeneous medium sand follows, with some plant remains at the bottom. The subsequent sand includes some small pebbles and shell fragments (up to 3.95 m b.s.l.). The granulometry and low electric conductivity (0.31 mS/cm) suggest fluvial deposition in a sublittoral environment.

The next stratum of silty fine sand has intercalations of numerous clayey silt layers (up to 2.15 m b.s.l.), with abundant plant remains. The sediment contains both brackish and freshwater species (ostracods: *Cyprideis torosa*, *Cytherissa lacustris*, *Candona* sp., *Pseudocandona* sp., *Darwinula* sp.; foraminifers: *Ammonia beccarii*, *Ammonia cf. parkinsoniana*). The alternating layers and the fossil content suggest the existence of a beach barrier – lagoon system in the area with a strong freshwater influx.

Above 2.15 m b.s.l., the sediment is composed of homogeneous clayey silt. The colour changes from dark grey to olive brown (at 1.60 m b.s.l.). The numerous oxidation stains, many lime concretions (1.45 to 1.40 m b.s.l.), and the microfossil content (ostracods: *Candona neglecta*, *Pseudocandona cf. parallela*) suggest a change from brackish to freshwater conditions (from a lagoonal to a limnic environment). This interpretation is supported by decreasing electric conductivity values (from 0.96 to 0.17 mS/cm).

From 0.90 to 0.45 m b.s.l., the sediment contains numerous oxidation stains and lime concretions as well as specimens of terrestrial gastropods. This is a reflection of the change from limnic to semi-terrestrial conditions. The following silt was deposited during flood events.

7.4.1.7 Synopsis of transect F-F'

The bottom layer of the most landward core, LIS 11, consists of pebbly sand and thereby represents sublittoral conditions – an indication of the Holocene transgression (see fig. 44). It is the only core of this transect where such a layer was found. Above this layer, and in the bottom section of all the other cores, the silty fine sands reflect marine conditions in the first half of the 3rd millennium BC [2871-2580 cal BC, plant remains at 5.62-5.70 m b.s.l. (LIS 11/5Pf)].

The increasing sediment input from the Grykes River in the south caused a change from fully marine to sublittoral conditions at LIS 11, and the subsequent formation of a thick peat reveals the termination of the marine environment. A ¹⁴C age from the bottom part of the paralic peat suggests that this (localised?) regression, which is indicated, occurred during the first half of the 2nd millennium BC [1941-1743 cal BC, peat at 3.41 m b.s.l. (LIS 11/3T)]. Thereafter, conditions changed first to littoral and later to fluvial ones at this coring site.

In contrast, marine conditions prevailed during Roman times at core sites LIS 53 and LIS 43. The transition from shallow marine to sublittoral conditions must have been taken place in the area between the 2nd century BC and the 2nd century AD [192-43 cal BC, peat layer at 4.51 m b.s.l. (LIS 53/13T); 23-132 cal AD, plant remains at 5.27 m b.s.l. (LIS 43/12Pf)]. These age estimates are concordant with information from ancient accounts (see chapter 4).

At LIS 14, the westernmost coring of this transect, marine conditions are gradually replaced by a fluvially dominated environment during the 9th to 10th centuries AD [783-1018 cal AD, peat at 5.61-5.71 m b.s.l. (LIS 14/2T)]. The pebbly river channel deposits accumulated up to the present sea level after one of the distributary channels of the Drini (or Grykes) had reached the coring site. The thickness of these deposits shows that the river channel had been active in the

area for a long time. Its effects can be detected at LIS 43 and LIS 53, as well (possibly also at LIS 01), but to a much lesser degree and not for the same length of time.

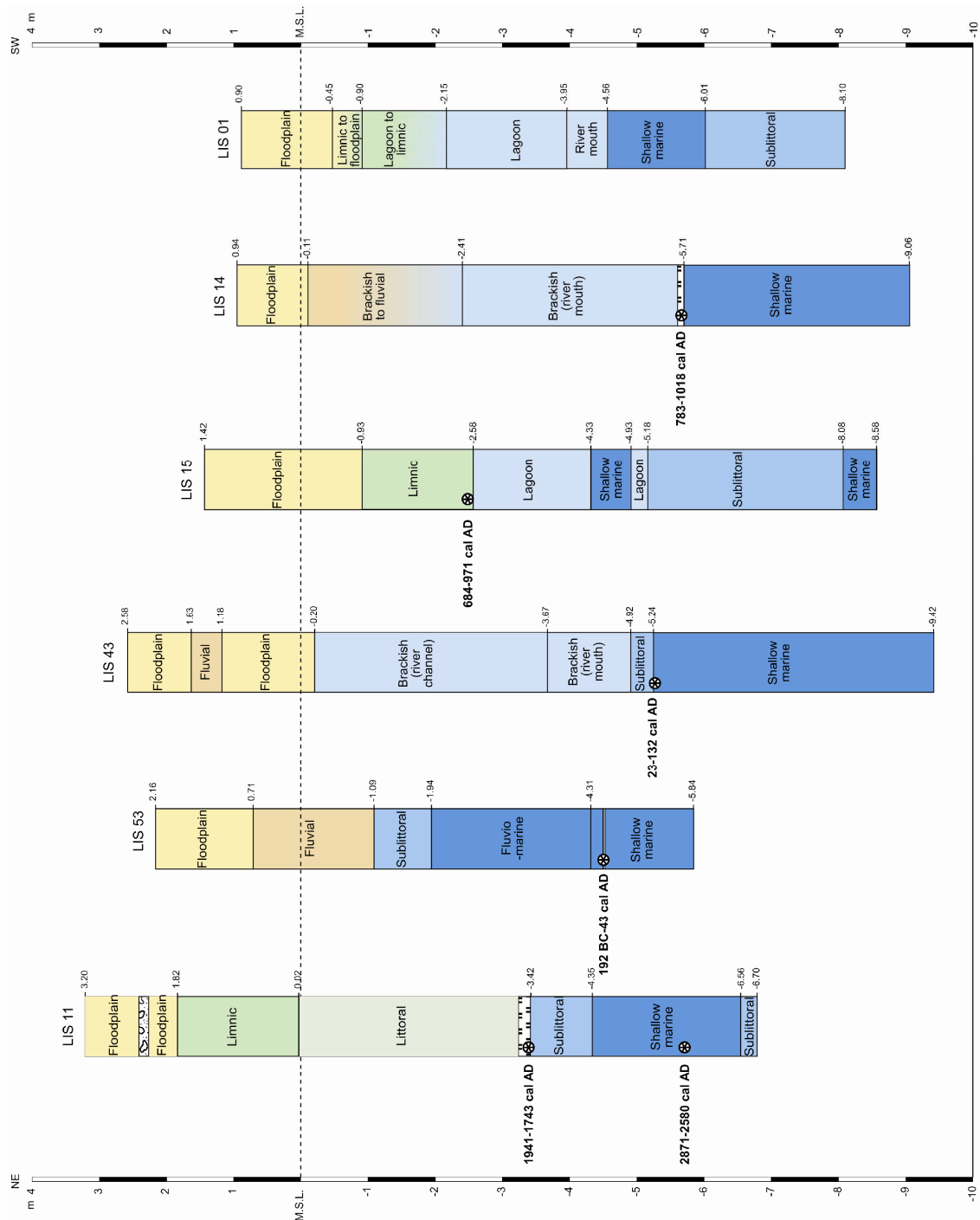


Figure 44: Geological transect F-F' (own research).

Coring LIS 15 presents a very different picture. Shallow marine conditions were followed by a sublittoral milieu and then intercalations of sandy/clayey deposits indicate the establishment of a beach barrier – lagoon system. Similar conditions developed at coring site LIS 01, after a brief period of more direct fluvial influence. The exact origin of such sandy deposits is uncertain, however. There are two possibilities for their origin: (a) a distributary of the river Grykes, or (b)

the river Mati; however, the latter flows much further south, wherefore, its material coming from this river would have had to be carried to coring site LIS 15 by the longshore drift. A radiocarbon date suggests that the brackish milieu behind the beach barrier changed to a freshwater one during the 8th to 10th centuries AD [684-971 cal AD, wood at 2.45 m b.s.l. (LIS 15/5H)].

The uppermost part of all cores is made up of alluvium, accumulated during flood events of the rivers Drini and Grykes.

7.4.2 Corings around the Manatia alluvial fan

The cores LIS 51 and LIS 34 are located at the foot of the Manatia alluvial fan in the Ishull Lezha region. The aim of these two corings was to learn about the interaction between the alluvial fan and the delta plain.

7.4.2.1 Vibracoring LIS 34

LIS 34 (N 41° 46' 45'', E 19° 36' 14'', ground level at 1.57 m a.s.l., total core length: 8 m) is located in the lower section of the Manatia alluvial fan. A synoptic view of the profile is shown in appendices 5.25.1 & 5.25.2.

The lowermost part of the profile consists of dark grey, homogeneous, compact silty fine sand (up to 4.17 m b.s.l.) with shallow marine/brackish fauna (macrofossils: *Cerastoderma glaucum*, *Chamalea gallina*; ostracods: *Pontocythere rubra*, *Cytheretta adriatica*; foraminifers: *Ammonia beccarii*, *Quinqueloculina* sp.).

From 4.17 to 3.60 m b.s.l., the stratum is made up of medium/coarse sand with pebbles. Towards the top, the grain size changes to fine/medium sand. The lowermost portion of the stratum contains broken shell fragments of shallow marine/brackish species (e.g., *Cerastoderma glaucum*) and a foraminifer specimen (*Quinqueloculina* cf. *verrusta*). The granulometry, very low electric conductivity (0.07 mS/cm), and the fossil content suggest the deposition of alluvial fan sediments by the Grykes River into a sublittoral environment.

The stratum is overlain by very dark grey silty fine sand plus some coarse sandy pebbly layers (up to 1.95 m b.s.l.). The latter can be interpreted as temporarily increasing river dynamics. The following sediment is made up of dark olive grey medium/coarse sand (up to 0.25 m a.s.l.), the lower- and uppermost portions of which contain some well rounded pebbles as well as angular

stones, indicating a temporary nearness of the river channel in an alluvial fan environment. From 0.25 to 0.82 m a.s.l., the sediment changes to olive brown fine/medium sand. This stratum was also deposited by the river. The uppermost section of the core is dominated by fine-grained floodplain sediment.

7.4.2.2 Vibracoring LIS 51

LIS 51 (N 41° 45' 57'', E 19° 39' 13'', ground level at 3.01 m a.s.l., total length of core: 10 m) is located at the foot of the Manatia alluvial fan, close to the main road to Lezha. A synoptic view of the profile is shown in fig. 45, photo 26, and appendix 5.38.

The lowermost part of the profile consists of dark grey, homogeneous, compact silty fine sand, intercalated with layers of medium/coarse sand (up to 3.24 m b.s.l.). The microfauna is dominated by shallow marine to brackish species (foraminifers: *Ammonia beccarii*, *Ammonia cf. parkinsoniana*, *Elphidium crispum*, *Quinqueloculina* sp., *Sigmoilina* sp., *Siphonaperta* sp.; ostracods: *Semicytherura* sp., *Pontocythere* sp.). The biodiversity indicates favourable environmental conditions such as a calm marine embayment. The thick coarse sandy layer (4.69-4.39 m b.s.l.) containing a wood fragment and a few small pebbles must have been deposited by the Grykes during high water levels. The low electric conductivity (0.08-0.20 mS/cm) hints at a strong freshwater influx. In the upper part of the stratum, the fauna is made up of a brackish species assemblage (*Ammonia cf. parkinsoniana*, *Haynesina germanica*, *Ammonia beccarii*).

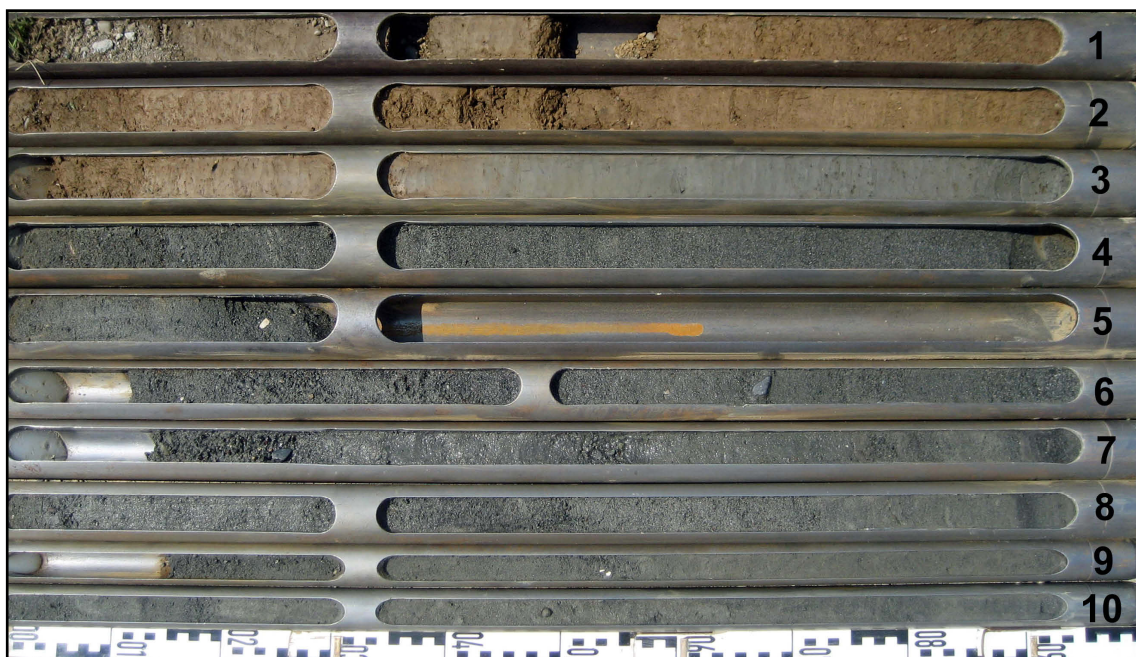


Photo 26: Coring LIS 51. (Uncu, 2008)

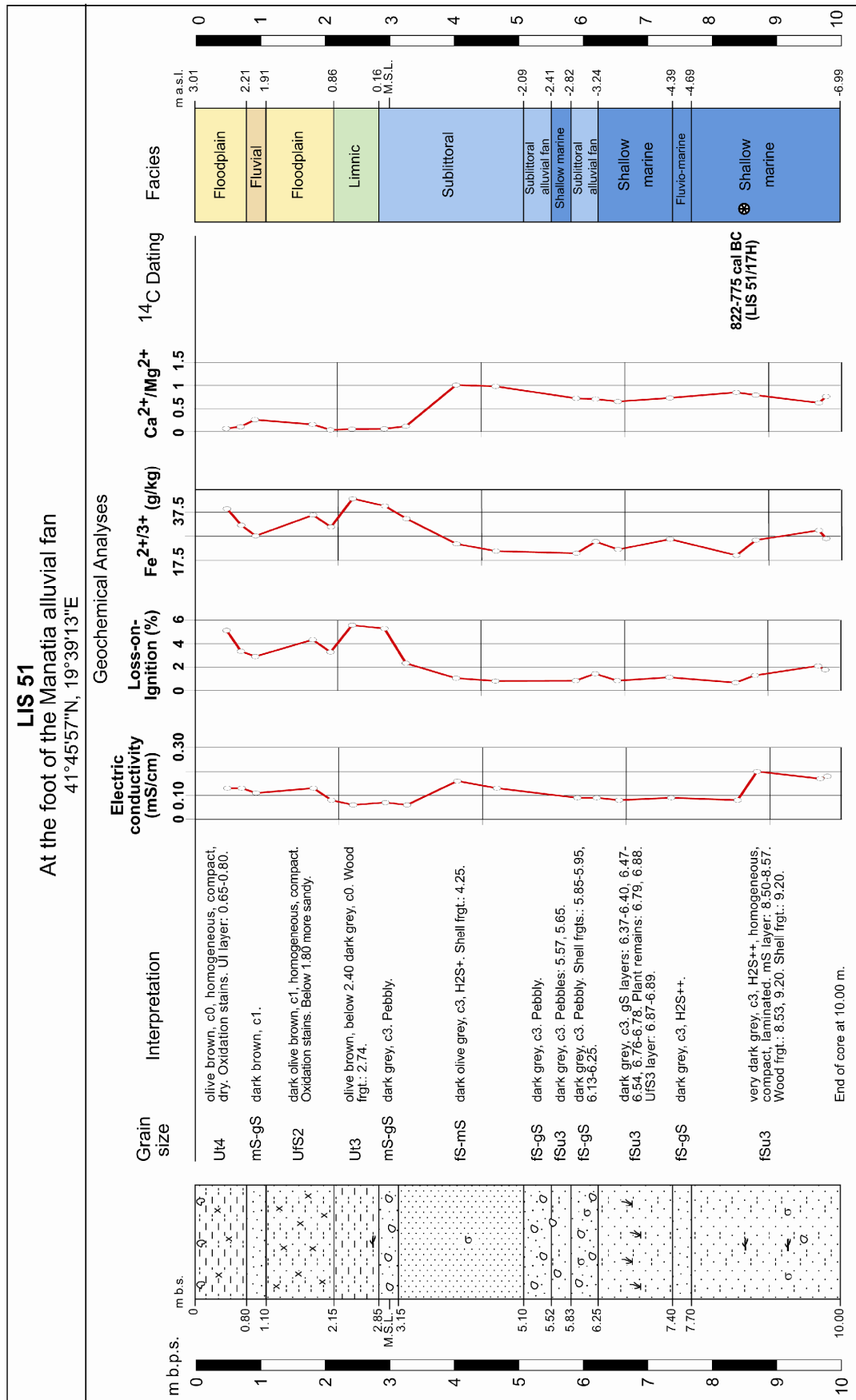


Figure 45: Synoptic chart of coring LIS 51.

The following sand with abundant pebbles (from 3.24 to 2.09 m b.s.l.) indicates that the mouth of the river Grykes was close to the coring site. The well-rounded pebbles and marine shell fragments at the bottom of this layer can be interpreted as alluvial fan material, deposited in a sublittoral setting. The intercalated layer of silty fine sand (2.82-2.51 m b.s.l.) shows a temporary re-establishment of low energy conditions. This interpretation is supported by the presence of a shallow marine to brackish microfauna (foraminifers: *Quinqueloculina* sp., *Ammonia* cf. *parkinsoniana*, *Elphidium excavatum*; ostracods: *Pontocythere* sp., *Cyprideis torosa* f. *litoralis*).

There is a loss of core between 2.09 and 1.29 m b.s.l. due to the coarseness of the material. The following layer consists of homogeneous, olive grey fine to medium sand, deposited by the Grykes in a sublittoral setting (up to 0.14 m b.s.l.). The overlying medium to coarse sand with pebbles in a silty matrix (up to 0.16 m a.s.l.) accumulated in a swampy milieu in the distal part of the Manatia alluvial fan.

The coarse sediments are overlain by silty to clayey mud with numerous organic spots and plant remains. At 0.59 m a.s.l., the colour changes from olive grey to olive brown. The fine grain size and the relatively high potassium value (3.40-3.80 g/kg) are evidence of a freshwater/limnic environment. The relatively low pH (6.08-6.46), high organic content (5.58 %) and the lack of calcium carbonate indicate anaerobic conditions.

At 0.86 m a.s.l., the limnic deposits are covered by brown, homogeneous fine sandy silt with numerous oxidation stains. These floodplain sediments include river channel deposits (medium to coarse sand, at 1.91 and 2.21 m a.s.l.), showing strong fluvial influence at the coring site. Olive brown silty/clayey floodplain deposits make up the core from 2.36 m a.s.l. to the present surface. The pieces of rock at the top are of modern anthropogenic origin.

7.4.2.3 Synopsis of corings LIS 51 and LIS 34

The lowermost part of both cores consists of silty fine sand, deposited in a shallow marine environment (see fig. 46). A ^{14}C age indicates that marine conditions still prevailed in this area around the 8th century BC [822-771 cal BC, wood at 5.52 m b.s.l. (LIS 51/17H)]. Towards the upper part of the marine deposits, the first influence of the Grykes River can be observed with coarse sands and pebbles. These deposits are of fluvial origin and have accumulated in a sublittoral environment. They are intercalated with marine sediments, reflecting temporarily changing depositional conditions. The coarse grain size of the sediment at LIS 34 suggests that

the main distributary of the Grykes stayed longer at this coring site.

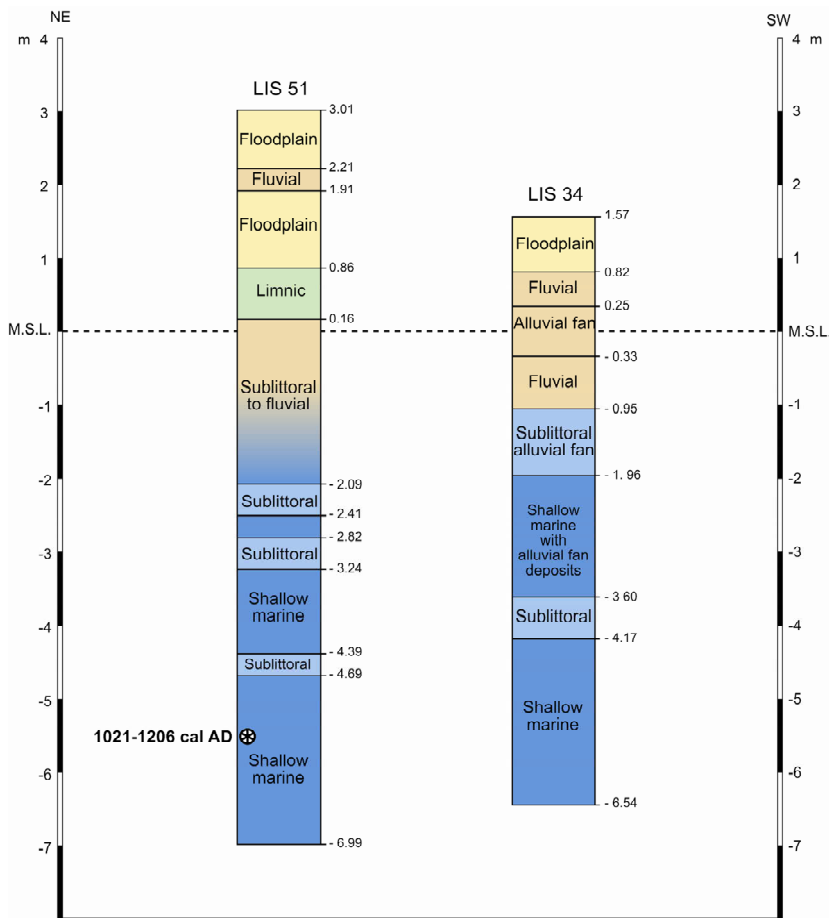


Figure 46: Corings LIS 51 and LIS 34 (own research).

Coring LIS 51 presents much finer grain sizes due to a more protected position. The last direct river channel deposits at LIS 51 can be observed around present sea level. Then the conditions turned to freshwater/limnic ones; a milieu not found at coring site LIS 34.

The uppermost part of both cores suggests a change towards a floodplain environment, with occasional fluvial influence. Meanwhile, the relatively recent canalisation of the Grykes has stopped any further alluvial fan development.

7.4.3 Coring in the Lezha swamp

The Lezha swamp (in Albanian: Kmeta Lezha) is located at the foot of the southern tip of Mali Rrenci. A coring was carried out to determine the palaeogeographic situation of this former marine embayment.

7.4.3.1 *Vibracoring LIS 09*

LIS 09 (N 41° 46' 54'', E 19° 39' 13'', ground level at 1.52 m a.s.l., total length of core: 11 m) is placed in Lezha swamp. A synoptic view of the profile is shown in fig. 47, photo 27, and appendix 5.6.

The lowermost part of the core consists of very dark grey, homogeneous clayey silt (up to 4.95 m b.s.l.). The sediment contains an abundance of marine/brackish fossils (see table 7) as well as seaweed (*Posidonia* sp.) remains. The granulometry and biodiversity indicate a deposition under calm and ecologically favourable conditions in a well protected marine embayment. This finding is supported by the results of various geochemical analyses, such as high values of electric conductivity (up to 3.78 mS/cm) and organic matter (up to 11.51 %).

Macrofossils	Foraminifera	Ostracoda
Sample LIS 09/22 (8.28-8.08 m b.s.l.)		
<i>Bittium latreillii</i> <i>Cerastoderma glaucum</i> <i>Cidaris</i> sp. <i>Donax</i> sp. <i>Gibbula</i> sp. <i>Nucula sulcata</i> <i>Rissoa</i> sp. <i>Retusa semisulcata</i> <i>Turbonilla</i> cf. <i>lactea</i>	<i>Ammonia beccarii</i> <i>Cibicides lobatulus</i> <i>Elphidium crispum</i> <i>Planorbulina mediterraneensis</i> <i>Quinqueloculina elegance</i> <i>Quinqueloculina</i> cf. <i>striata</i> <i>Rosalina globularis</i> <i>Spiroloculina depressa</i> <i>Triloculina</i> sp.	<i>Aurila</i> sp. <i>Callistocythere intricatoides</i> <i>Carinocythereis</i> cf. <i>antiquata</i> <i>Cyprideis torosa</i> <i>Loxoconcha bairdi</i> <i>Loxoconcha gibberosa</i> <i>Loxoconcha stellifera</i> <i>Paradoxostoma</i> cf. <i>fuscum</i> <i>Pontocythere rubra</i> <i>Pseudopsamocythere reniformis</i> <i>Xestoleberis communis</i>
Sample LIS 09/19 (6.03-5.85 m b.s.l.)		
<i>Cidaris</i> sp.	<i>Ammonia</i> cf. <i>parkinsoniana</i> <i>Cycloforina</i> spp. <i>Elphidium</i> sp. <i>Elphidium cuvillieri</i> <i>Elphidium excavatum</i> <i>Eponides?</i> sp. <i>Hanzawaia</i> sp. <i>Haynesina germanica</i> <i>Massilina</i> sp. <i>Quinqueloculina</i> spp. <i>Rosalina</i> spp. <i>Rotaliina</i> inc. spp. <i>Spiroloculina</i> spp. <i>Triloculina</i> sp.	<i>Aurila woutersi</i> <i>Callistocythere</i> sp. <i>Cytherois</i> sp. <i>Loxoconcha bairdi</i> <i>Pontocypris</i> sp. <i>Pontocythere</i> sp. <i>Sclerochilus</i> sp. <i>Xestoleberis</i> spp.
Sample LIS 09/17 (5.38-5.28 m b.s.l.)		
<i>Alvania mamillata</i> <i>Bittium latreillii</i> <i>Cardita</i> sp. <i>Gastrana fragilis</i> <i>Gibbula</i> sp. <i>Jujubinus</i> cf. <i>striatus</i> <i>Nucula sulcata</i> <i>Retusa semisulcata</i> <i>Rissoa variabilis</i> <i>Tricolia</i> cf. <i>tenuis</i> <i>Turbonilla</i> cf. <i>lactea</i>	<i>Ammonia beccarii</i> <i>Cibicides lobatulus</i> <i>Polimorphina</i> sp. <i>Rosalina macropora</i> <i>Spiroloculina depressa</i>	<i>Aurila arborescens</i> <i>Callistocythere</i> sp. <i>Costa batei</i> <i>Loxoconcha bairdi</i> <i>Loxoconcha gibberosa</i> <i>Loxoconcha stellifera</i> <i>Paracypris</i> sp. <i>Propontocypris</i> cf. <i>dispar</i> <i>Pseudopsamocythere reniformis</i> <i>Semicytherura paradoxa</i> <i>Xestoleberis communis</i> <i>Xestoleberis dispar</i>
Sample LIS 09/11 (4.15-4.05 m b.s.l.)		
<i>Cidaris</i> sp. <i>Irus irus</i> <i>Scrobicularia plana</i>	<i>Ammonia beccarii</i> <i>Cibicides lobatulus</i> <i>Elphidium crispum</i> <i>Elphidium minutum</i> <i>Quinqueloculina elegance</i>	<i>Loxoconcha bairdi</i> <i>Loxoconcha stellifera</i> <i>Pontocythere rubra</i> <i>Semicytherura sulcata</i> <i>Xestoleberis communis</i>

Table 7: Macro- and microfossils found in coring LIS 09 (determination by Dr. M. Handl, Marburg).

From 4.95 to 4.16 m b.s.l., the sediment is made up of very dark grey loamy silt with numerous organic remains as well as a marine/brackish fauna (see table 7). Between 4.30 to 4.28 m b.s.l., the fossil fragments have accumulated to form a layer of bio-arenite. From 4.16 to 3.98 m b.s.l., the sediment consists of very dark grey silty fine sand with a few plant remains. The fauna as well as the electric conductivity (2.46 mS/cm) suggest a deposition under brackish conditions in a shallow marine environment.

The subsequent stratum is dominated by dark grey fine/medium sand, intercalated with numerous thin peat layers (up to 0.46 m b.s.l.). The sediment contains shallow marine/brackish species (macrofossils: *Columbella rustica*, *Bittium latreillii*, *Nucula sulcata*; ostracods: *Pontocythere rubra*; foraminifers: *Ammonia beccarii*, *Quinqueloculina* sp.). However, the electric conductivity value (0.56 mS/cm) is unexpectedly low.

From 0.46 to 0.23 m b.s.l., the sandy stratum is overlain by very dark grey loamy silt, including numerous plant remains as well as terrestrial gastropods and a few estuarine/brackish species (macrofossil: *Hydrobia* sp.; ostracod: *Cyprideis torosa*). The extremely low pH value (2.96) and the decrease of carbonate content within the sediment indicate acidified lake conditions. The increasing freshwater influx can be deduced from the high value of potassium (4.10 g/kg).

The uppermost section of the core is made up of intercalations of clayey to fine sandy silts. The sediment was deposited in a swampy environment together with debris such as stones and anthropogenic material. Swampy conditions still prevail in the central part of the former marine embayment, whereas the filled-in parts indicate intensive settlement activities.

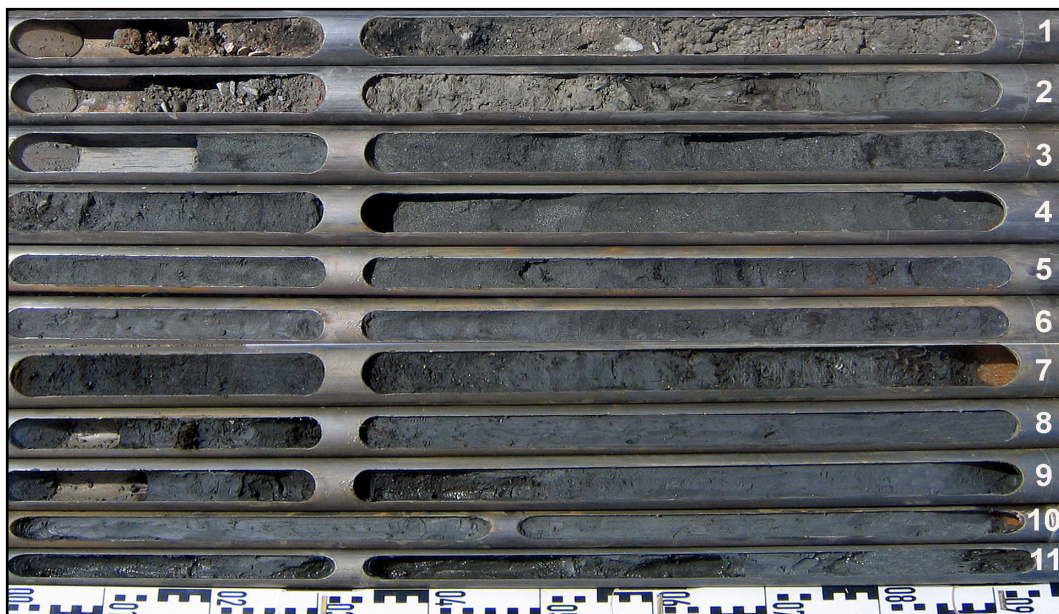


Photo 27: Coring LIS 09.

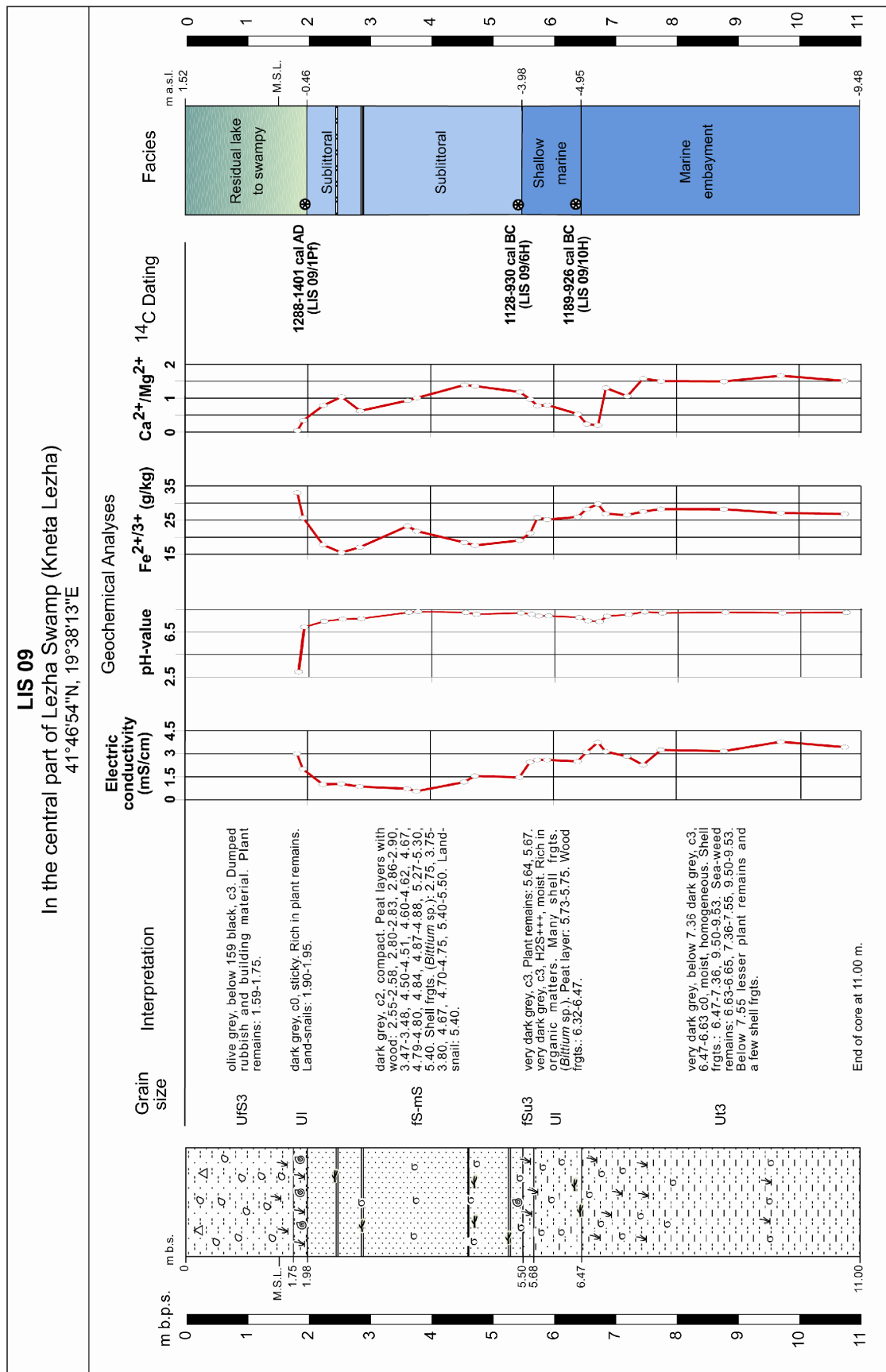


Figure 47: Synoptic chart of coring LIS 09.

7.4.3.2 Interpretation of coring LIS 09

During the Holocene transgression maximum, the area around coring site LIS 9 had undoubtedly been a well-protected marine embayment (see fig. 47). The fine grain size and the presence of seaweed indicate calm water conditions. The rich fauna in terms of quantity as well as variety is also evidence of favourable ecological conditions in the embayment. A radiocarbon age estimate proves that a marine milieu existed at least until the 11th century BC [1189-926 cal BC, wood at 4.80-4.95 m b.s.l. (LIS 09/10H)].

Fine-grained marine deposits are followed by fine/medium sand. The granulometry suggests an important change in the depositional dynamics. There are two possibilities to explain the origin of the coarse-grained deposits: (i) they can be fluvial, (ii) they were transported to this location *via* longshore drift. We know from other corings that the Drini did not reach this area at that time. Therefore, it is very likely that the sediment came from the Mati River further south, carried by the longshore drift to the coring site of LIS 09. The bottom part of these sublittoral deposits has also been dated to the 11th century BC [1128-930 cal BC, wood at 3.88-3.98 m b.s.l. (LIS 09/6H)], which causes a slight dilemma, because it would mean that about one meter of very fine-grained deposits accumulated in a very short period of time. A possible explanation is that the material in the upper layer was reworked or an error occurred in the laboratory.

The sublittoral deposits are interrupted by numerous paralic peat layers. A brackish residual lake developed after the embayment was cut off the sea before the conditions finally turned limnic in the 14th century AD [1288-1401 cal AD, plant remains at 0.38-0.43 m b.s.l. (LIS 09/1Pf)].

The age estimates confirm that this former marine embayment would have been a suitable setting for harbour activities during Hellenistic and Roman times. However, neither archaeological, nor historical sources contain any information regarding this.

7.4.4 Transect G-G'

This transect is located in the south of the Ishull Shengjin region. It runs from the foot of Mali Rrenci south-westwards to the Merxhani lagoon. It comprises corings LIS 17, LIS 18, LIS 19, and LIS 45 (see fig. 21). The aim of this transect was to reconstruct the evolution of the Drini delta in this area.

7.4.4.1 Vibracoring LIS 17

LIS 17 (N 41° 46' 39'', E 19° 38' 00'', ground level at 1.31 m a.s.l., total length of core: 10 m) is located at the foot of the south-western slopes of Mali Rrenci, approximately 1 km SW of Lezha, on the road from Lezha to Shengjin. A synoptic view of the profile is shown in fig. 48, photo 28, and appendix 5.13.

The lowermost section of the profile consists of dark grey, homogeneous silty fine sand (up to 6.39 m b.s.l.). The upper part of this stratum contains thin peat layers as well as abundant specimens of brackish microfossils (ostracod: *Cyprideis torosa*; foraminifer: *Ammonia beccarii*). The low electric conductivity (up to 0.63 mS/cm) and the brackish fauna suggest a strong freshwater influx from karstic sources.

The subsequent fine/medium sand must have been transported to this location by the longshore drift. Between 5.74 and 3.10 m b.s.l., the stratum is dominated by dark grey silty fine sand with intercalated medium sandy and loamy layers. The sediment contains marine species (macrofossil: *Bittium reticulatum*; foraminifer: *Elphidium crispum*). The variations in grain size reflect occasionally changing depositional dynamics in a shallow marine environment.

Above 3.10 m b.s.l., the silt component increases and the overall grain size becomes finer. The sediment contains thin peat layers as well as a few brackish species (macrofossil: *Cerastoderma glaucum*; ostracod: *Cyprideis torosa*), hinting at the establishment of low energy conditions such a beach barrier – lagoon system in the area.

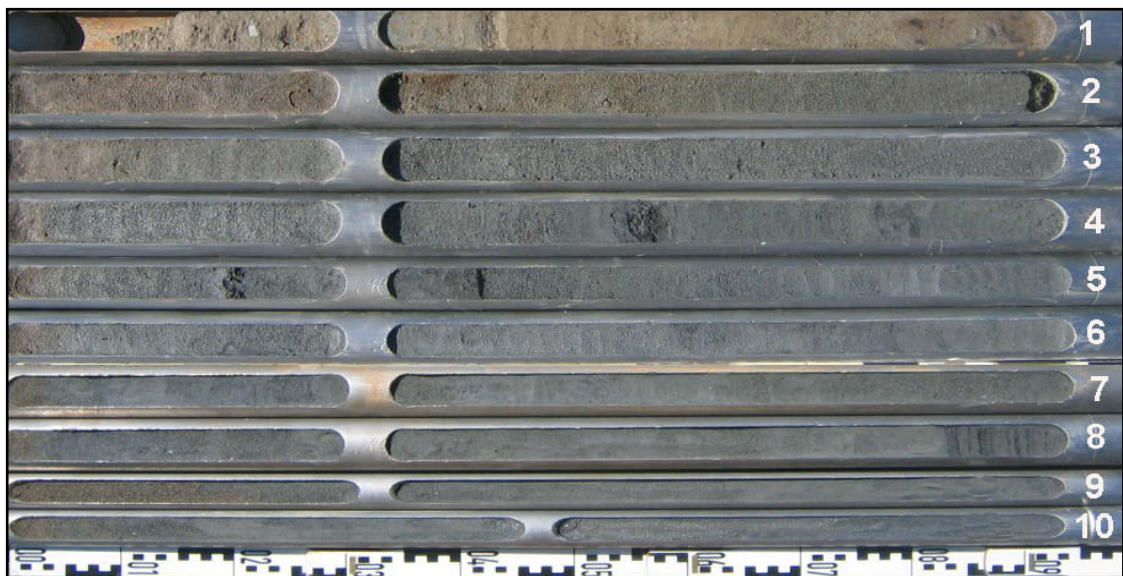


Photo 28: Coring LIS 17. (Uncu, 2006)

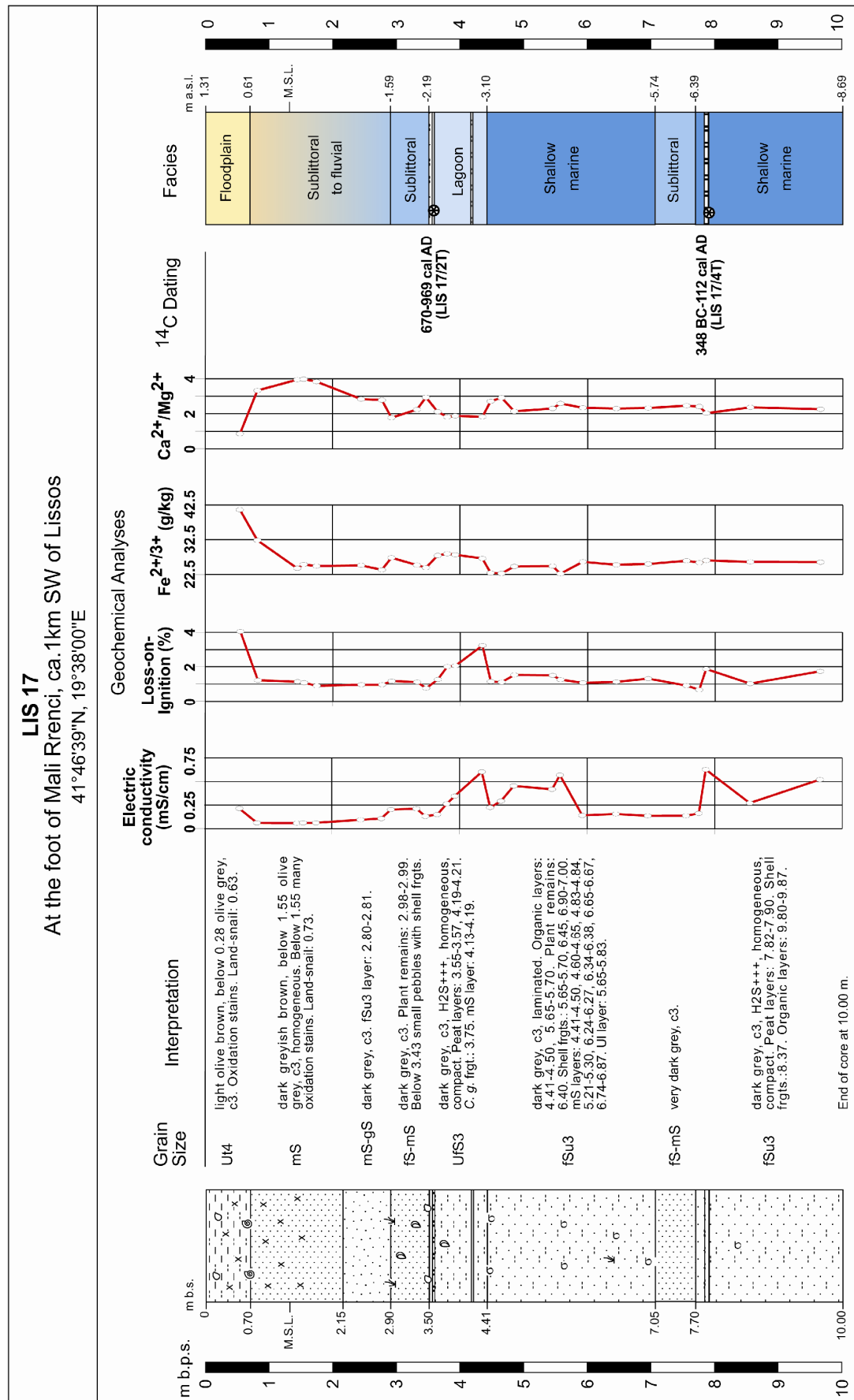


Figure 48: Synoptic chart of coring LIS 17.

From 2.19 m b.s.l. to 0.61 m a.s.l., medium sand dominates the sediment. The lower section of the stratum consists of fine/medium sand with a few small pebbles and fragments of *Cerastoderma glaucum* (up to 1.59 m b.s.l.). The following coarse sandy layer indicates an increasingly fluvial influence (up to 0.84 m b.s.l.). The subsequent, more homogeneous medium sand includes numerous oxidation stains and a land-snail specimen at the top. At 1.24 m b.s.l., the colour of the sand turns from dark grey to dark greyish brown. The granulometry and the geochemical analyses – very low value of electric conductivity (0.06 mS/cm), high content of carbonate (up to 26.41 %) – as well as the lack of fossils point to a deposition in a high-energy milieu. The whole sandy stratum reflects the change from a brackish/pro-deltaic to a freshwater/fluvial environment.

From 0.61 m a.s.l. to the present ground level, the sediment is dominated by clayey silt with a few fragments of terrestrial gastropods. The abundant oxidation stains of these floodplain sediments suggest seasonally wet and dry conditions.

7.4.4.2 *Vibracoring LIS 19*

LIS 19 (N 41° 46' 20'', E 19° 37' 41'', ground level at 1.39 m a.s.l., total length of core: 9 m) is located in the Ishull Shengjin Region, ca. 2 km SW of Lezha and at a distance of 200 m from the road to Tirana. A synoptic view of the profile is shown in appendices 5.15.1 & 5.15.2.

The lowermost part of the profile is made up of dark grey, homogeneous silty fine sand (up to 7.06 m b.s.l.). The granulometry and high electric conductivity (2.00 mS/cm) suggest a deposition in a marine environment.

The subsequent stratum consists of medium/coarse sand with small pebbles (up to 6.41 m b.s.l.). The coarse grain size, the fossil content (a few specimens of *Cerastoderma glaucum*) and the low electric conductivity (0.63 mS/cm) point to a deposition under brackish conditions in a high-energy milieu due to strong freshwater influx from the Drini.

From 6.41 to 1.11 m b.s.l., the stratum is dominated by very dark grey medium sand which includes many organic materials such as pieces of wood, plant remains and a grape seed (at 4.43 m b.s.l.). Changing river dynamics are reflected by increasingly fine sandy as well as pebbly sections towards the top. The lack of fossils and the grain size suggest high-energy dynamics.

At 1.11 m b.s.l., the sediment changes to clayey silt. The colour turns from dark grey to olive grey (at 0.36 m b.s.l.). Oxidation stains, lime concretions and plant remains are common. The

upper part of the stratum contains some terrestrial gastropods and a freshwater ostracod (*Pseudocandona parallela*). The granulometry and geochemical analyses – relatively high values of potassium ions (4.75 g/kg) and organic matter (4.47 %), low electric conductivity (0.12 mS/cm) – indicate a deposition under calmer conditions in a limnic/semi-terrestrial environment.

The uppermost section of the core consists of fine-grained floodplain sediments. Calcium carbonate concretions and numerous oxidation stains are the result of seasonally wet and dry conditions. The lack of sand in may indicate that the river was fairly distant from the coring site.

7.4.4.3 Vibracoring LIS 18

LIS 18 (N 41° 45' 51'', E 19° 37' 32'', ground level at 1.49 m a.s.l., total length of core: 9 m) is located ca. 2.5 km SW of Lezha in the Ishull Shengjin Region. A synoptic view of the profile is shown in appendices 5.14.1 & 5.14.2.

The lowermost part of the profile is dominated by dark grey, compact silty fine sand with thin clay layers (up to the 7.21 m b.s.l.). The low electric conductivity (0.65 mS/cm) and the salt-tolerant fauna (macrofossil: *Cerastoderma glaucum*; ostracods: *Cyprideis torosa*, *Loxoconcha stellifera*; foraminifer: *Ammonia beccarii*) suggest a deposition in a shallow marine/brackish environment. The existence of a temporary beach barrier – lagoon system could explain the occurrence of clayey layers.

The shallow marine deposits are followed by homogeneous, dark grey medium sand (up to 6.61 m b.s.l.). The granulometry suggests the formation of a beach barrier in a sublittoral environment. The low electric conductivity (0.17 mS/cm) may have been caused by a strong freshwater influx from the Drini.

The subsequent silty fine sand is intercalated with clayey layers, similar to the lowest part of the core. The sediment contains brackish species (macrofossil: *Lentidium* sp.; ostracods: *Cyprideis torosa*, *Pontocythere* sp.; foraminifer: *Ammonia beccarii*). Again, this may be interpreted with the development of a beach barrier – lagoon system in a shallow marine environment due to the migration of the river mouth.

The next stratum consists of homogeneous medium sand with thin peat layers (up to 4.26 m b.s.l.). The sediment contains shallow marine/brackish species (macrofossil: *Corbula gibba*; foraminifer: *Ammonia* cf. *parkinsoniana*). The grain size and fossil content indicates deposition

in a sublittoral environment. A ceramic fragment, found on top of the peat layer (at 4.71 m b.s.l.), dates from Medieval times (determination by M. Fiedler). The age discrepancy was probably caused by the coring process (transport of the ceramic fragment downwards from an upper layer).

From 4.26 m b.s.l. to present sea level, the sediment changes to medium/coarse sand with pebbles. The coarse grain size and the lack of fossils indicate high-energy depositional dynamics in a distributary channel. These deposits must have accumulated rapidly to form a pro-deltaic lobe.

Above the present sea level, the grain size becomes finer which may be explained by the migration of the river channel away from the coring site. The uppermost part of the profile is composed of olive brown, fine sandy silt with fine-grained recent floodplain sediments at the very top.

7.4.4.4 Vibracoring LIS 45

LIS 45 (N 41° 45' 37'', E 19° 36' 30'', ground level at 0.06 m a.s.l., total length of core: 10 m) is located on the landward shore of the Merxhani lagoon. A synoptic view of the profile is shown in appendices 5.33.1 & 5.33.2.

The lower portion of the profile is characterised by dark grey, laminated, silty fine sand (up to 5.76 m b.s.l.) which contains brackish/shallow marine species (macrofossil: *Cidaris* sp.; foraminifer: *Ammonia* cf. *parkinsoniana*; ostracod: *Pontocythere* sp.). Remains of terrestrial fungi (*Coenococcum geophilum*) and angiosperms (*Saponaria officinalis*) as well as a relatively high content of organic matter (2.93 %) indicate temporary semi-terrestrial conditions of a coastal swamp.

The following dark grey well sorted fine/medium sand (up to 5.37 m b.s.l.) suggests deposition in a sublittoral environment. Being part of a former spit, parallel to the present one, the sand was probably carried to this location by longshore drift.

The coarse sublittoral sand is overlain by dark grey silty fine sand, intercalated with numerous peat and a few lenses of clay (up to 0.77 m b.s.l.). Shallow marine to brackish conditions are indicated both by the microfauna (foraminifers: *Ammonia* cf. *parkinsoniana*, *Ammonia* cf. *tepida*; ostracods: *Pontocythere* sp., *Cyprideis torosa* f. *litoralis*) and the geochemical analyses: electric conductivity values (up to 5.41 mS/cm), organic content (3.84 %), calcium carbonate

content (17.56 %) and $\text{Ca}^{2+}/\text{Mg}^{2+/3+}$ ratio (up to 2.08).

The layer between 0.77 and 0.56 m b.s.l. – dark grey, silty clay – shows a change in depositional dynamics. The electric conductivity (1.76 mS/cm) decreases while the amount of organic matter (3.64 %) increases. The layer was deposited in a lagoonal environment with freshwater influx from the Drini. Olive brown silty/loamy fine sand forms the uppermost part of the profile. Numerous oxidation stains point towards semi-terrestrial conditions.

7.4.4.5 Synopsis of transect G-G'

The lowermost part of the cores is made up of silty sand, accumulated under marine conditions (see fig. 49). The thickness of the sediment suggests that fully marine conditions prevailed for a long time at coring sites LIS 17 and LIS 45. According to an age estimate from LIS 17, marine conditions existed at some time during the 4th century BC to the 2nd century AD [348 cal BC to 112 cal AD, peat at 6.51-6.59 m b.s.l. (LIS 17/4T)].

The result is concordant with the accounts of ancient authors and a radiocarbon date from LIS 43. We know from other corings that during Hellenistic / Roman times, the Drini had already passed the city of Lissos, and its delta plain was prograding into the Drini bay. It looks as though the delta prograded at first in a southerly direction and marine conditions lasted until the 8th-9th centuries AD [670-969 cal AD, peat at 2.25 m b.s.l. (LIS 17/2T)].

During the following centuries, the environment at coring site LIS 17 changed to a sublittoral and then to a fluvial one. The lack of pebbles in the whole profile confirms a river channel was never in close proximity. However, in the uppermost part of the profile, the river came closer to this site, as is indicated by coarse sand.

The marine deposits in cores LIS 18 and LIS 19 reflect sublittoral conditions during the 11th-13th centuries AD [1024-1251 cal AD, peat at 4.84-4.89 m b.s.l. (LIS 18/3T)]. In subsequent centuries, one of the distributaries of the Drini delta shifted westward to this site and deposited a thick layer of pebbly coarse-grained river channel sediments. The influence of this channel is also visible in LIS 19 in the form of pro-deltaic sand, which contains many pieces of wood and a few pebbles. A ¹⁴C age from the bottom of the stratum suggests that the Drini was forming a pro-deltaic lobe close to the coring site around the 14th century AD [1296-1430 cal AD, plant remains at 6.31-6.36 m b.s.l. (LIS 19/9Pf.)]. After the direct fluvial influence had terminated, a limnic milieu developed during the 14th century AD. Further to the west, at LIS 18, the river channel is clearly visible even today.

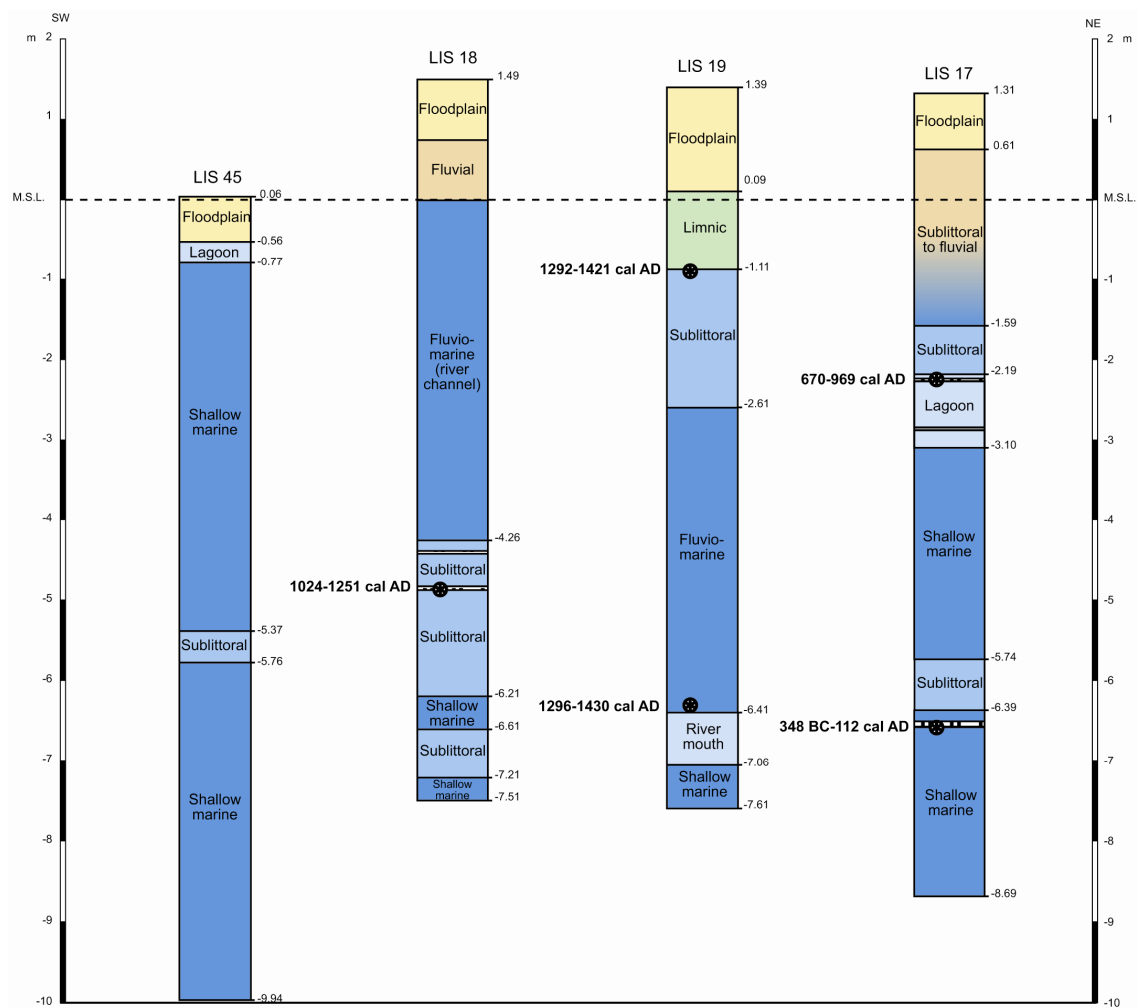


Figure 49: Geological transect G-G' (own research).

It is worth noting that another ^{14}C dating was obtained from the top of the fluvial deposits at LIS 19. However, the date acquired was quite young; approximately the 13th century AD [1292-1421 cal AD, peat at 0.88 m b.s.l. (LIS 19/1T)]. This age almost coincides with the end of the fluvial conditions in this area, and it is improbable for a thick pro-deltaic deposit to accumulate this rapidly (ca. 5.5 m in 130 years). Especially, when comparing the depth of this material with dated material at a similar depth of coring LIS 17, it becomes clear that some sort of technical error might be the best explanation for this apparent discordance. Overall, we have decided not to use this dating in our interpretation.

Conditions in LIS 45 were totally different: Nearly the whole coring profile consists of silty fine sand, indicating that shallow marine conditions prevailed until fairly recently. The fine-grained lagoonal sediment makes up only a very thin layer.

All four corings are topped by alluvium. Due to the main river channel not flowing within close proximity of these coring sites, only very fine-grained material reached the area during times of flooding.

7.4.5 Transect H-H'

This transect is located within the Ishull Shengjin Region. It is close to the border between the well-drained terrestrial part (transect G-G') and the swampy part (transect I-I') of the Drini coastal plain. It contains corings LIS 08, LIS 16, LIS 12 and LIS 13, and runs southwest from the foot of Mali Rrenci to the Merxhani lagoon (fig. 21). The aim of this transect is to reconstruct the evolution of the Drini's delta plain in this area.

7.4.5.1 Vibracoring LIS 08

LIS 08 (N 41° 47' 04'', E 19° 37' 48'', ground level at 0.92 m a.s.l., total length of core: 9 m) is located on the road from Lezha to Shengjin, at the foot of the western slope of Mali Rrenci. A synoptic view of the profile is shown in fig. 50, photo 29, and appendix 5.5.

The lower part of the profile is characterised by dark grey, homogeneous, compact silty fine sand (up to 3.01 m b.s.l.). The sediment contains thin peat layers (above 3.65 m b.s.l.) and an assemblage of shallow marine/brackish fossils (macrofossil: *Chamalea gallina*; foraminifer: *Ammonia beccarii*). The high ratio of $\text{Ca}^{2+}/\text{Mg}^{2+}$ (>2) and the low electric conductivity (0.16 mS/cm) may be interpreted with an increasing freshwater influx from karstic sources.

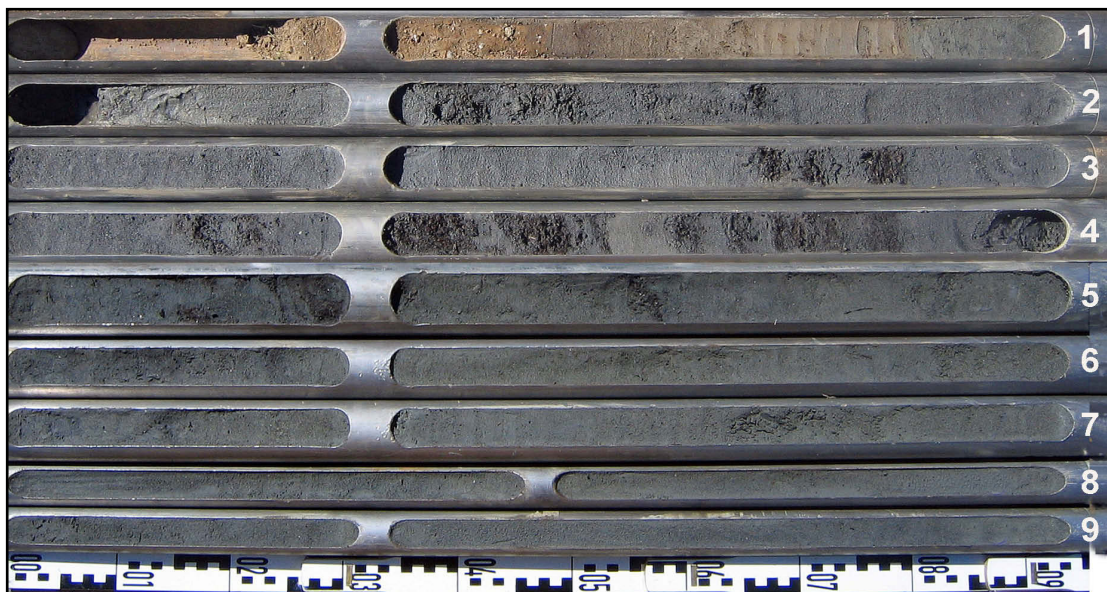


Photo 29: Coring LIS 08. (Uncu, 2006)

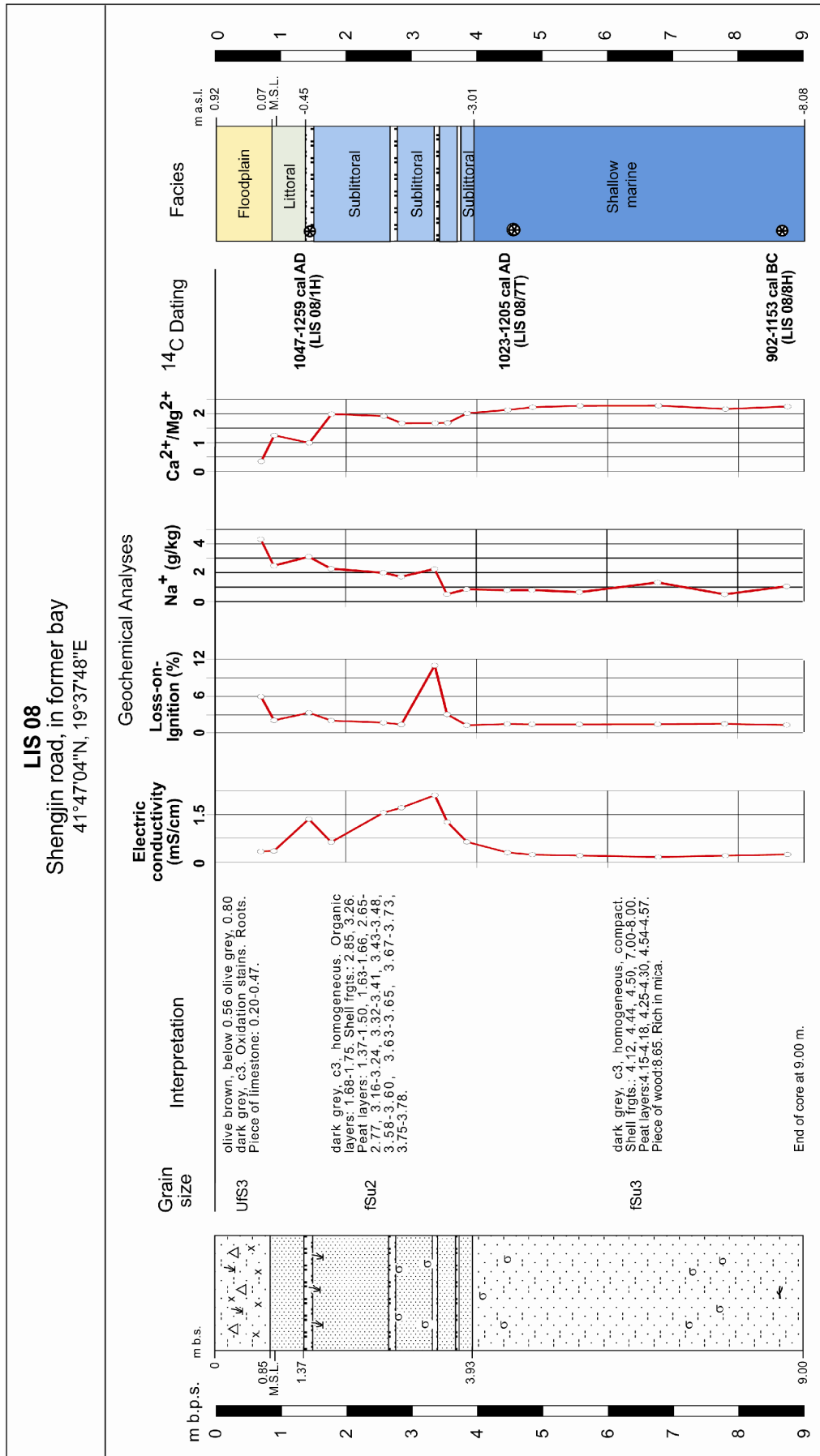


Figure 50: Synoptic chart of coring LIS 08.

The following stratum consists of dark grey, homogeneous fine sand with numerous intercalated peat layers (up to 0.07 m a.s.l.). The sediment contains a large variety of salt-tolerant species (macrofossils: *Bittium latreillii*, *Scrobicularia plana*, *Lentidium mediterraneum*, *Hydrobia* sp.; ostracod: *Cyprideis torosa*; foraminifers: *Ammonia beccarii*, *Ammonia* cf. *parkinsoniana*) and points towards a change to estuarine conditions.

The uppermost part of the core is made up of fine sandy and clayey silt with numerous oxidation stains. The colour of the sediment changes from dark grey to olive brown. The sediment was deposited in a residual lake/semi-terrestrial environment during flooding events of the Drini. The angular pieces of limestone at the top of the layer suggest recent human activities.

7.4.5.2 Vibracoring LIS 16

LIS 16 (N 41° 46' 39'', E 19° 37' 26'', ground level at -0.02 m b.s.l., total length of core: 9 m) is located in the former swampy area in the Ishull Shengjin Region between LIS 08 and LIS 12. A synoptic view of the profile is shown in appendices 5.12.1 & 5.12.2.

The lowermost section of the profile consists of very dark grey, homogeneous, compact silty fine sand (up to 8.46 m b.s.l.). The high electric conductivity (2.97 mS/cm) and the fossil content (ostracod: *Cyprideis torosa*; foraminifer: *Ammonia beccarii*) support a deposition under brackish conditions in a shallow marine environment.

From 8.46 to 7.83 m b.s.l., the sediment is made up of fine/medium sand. This layer has accumulated in a sublittoral environment, transported by longshore drift. The following silty fine sand suggests the re-establishment of shallow marine conditions.

The middle section of the core is characterised by a thick coarse sandy layer with small pebbles, a few pieces of *Cerastoderma glaucum* and wood fragments (up to 2.42 m b.s.l.). Some parts of the core were lost because of the coarse grain size. A significant decrease in electric conductivity (from 3.00 to 0.29 mS/cm) indicates a strong freshwater influx. The granulometry points to fluvial deposition within the former distributary channel of the Drini. Above 2.42 m b.s.l., the grain size becomes finer; pebbles disappear due to changing depositional dynamics (up to 2.18 m b.s.l.). The subsequent layer of silty fine sand, accumulated under brackish conditions, suggests the re-establishment of a relatively low energy milieu.

From 1.68 to 0.71 m b.s.l., the stratum is characterised by alternating layers of sandy and clayey silt. The sediment contains a few specimens of a brackish foraminifer (*Ammonia beccarii*). The decreasing electric conductivity (from 1.22 to 0.34 mS/cm) and the increasing number of oxidation stains suggest a transition from brackish/lagoonal to freshwater/limnic conditions.

The uppermost section (from 0.71 m b.s.l. to present surface) consists of olive brown clayey silt with numerous oxidation stains and a few lime concretions, indicating seasonally wet and dry conditions in a semi-terrestrial environment.

7.4.5.3 Vibracoring LIS 12

LIS 12 (N 41° 46' 22'', E 19° 37' 10'', ground level at 0.32 m a.s.l., total length of core: 10 m) is located in the Ishull Shengjin Region. A synoptic view of the profile is shown in fig. 51, photo 30, and appendix 5.8.

The lowermost part of the core is made up of dark grey silty fine sand (up to 9.28 m b.s.l.). This homogeneous sediment contains a few specimen of the marine foraminifer (*Quinqueloculina elegance*).

The subsequent layer consists of dark grey, sterile fine/medium sand, indicating changing depositional dynamics (up to 7.68 m b.s.l.). The relatively coarse sediment suggests a deposition in a sublittoral environment by longshore drift.

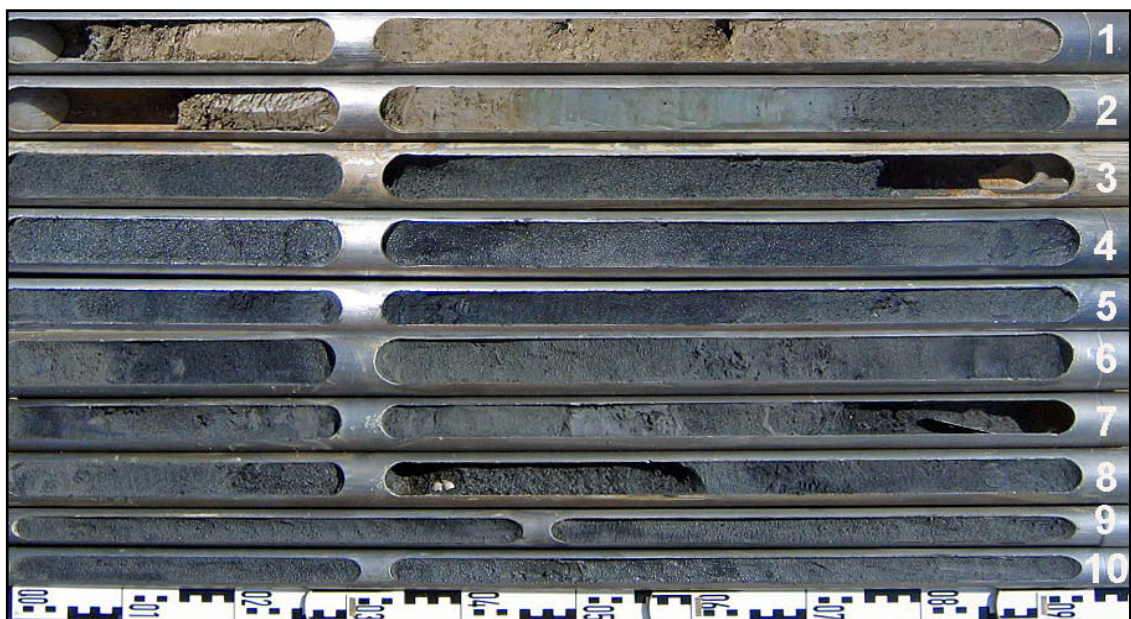


Photo 30: Coring LIS 12. (Uncu, 2006)

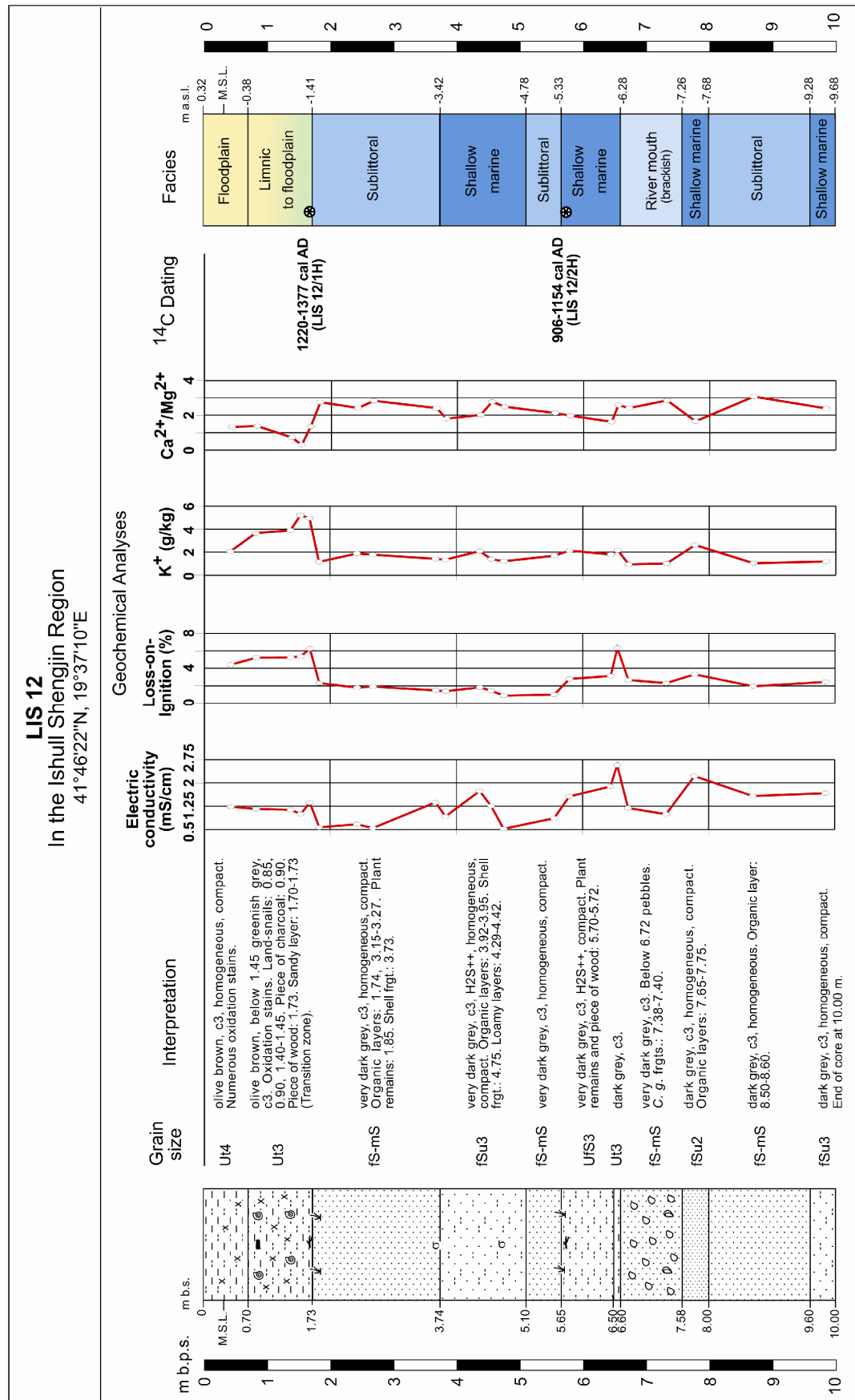


Figure 51: Synoptic chart of coring LIS 12.

From 7.68 to 7.26 m b.s.l., the dominant grain size is fine sand; thus shallow marine conditions must have returned to this location. The layer also contains some organic matter and a brackish ostracod (*Cyprideis torosa*).

The subsequent stratum made up of very dark grey fine/medium sand with small pebbles. The granulometry, fossil content (a few *Cerastoderma glaucum*), and results of the geochemical analyses – high calcium carbonate content (up to 20.25 %) and relatively low electric conductivity (0.99 mS/cm) – point to a deposition in the slightly brackish conditions of a river mouth.

The following clayey silt (from 6.28 to 6.18 m b.s.l.) reveals a calm depositional milieu, such as a lagoon behind a beach barrier system. The subsequent fine sandy silt also indicates that the conditions have prevailed for a relatively long time (up to 5.33 m b.s.l.). The fossil content is composed of brackish/marine species (foraminifers: *Ammonia* cf. *parkinsoniana*, *Loxococoncha elliptica*; ostracod: *Cyprideis torosa*).

From 5.33 to 4.78 m b.s.l., the grain size changes to a fine/medium sand. This sublittoral sediment is overlain by silty fine sand with loamy silt lenses (up to 3.42 m b.s.l.). The granulometry and the increasing $\text{Ca}^{2+}/\text{Mg}^{2+}$ ratio value (up to 2.78) indicate the re-establishment of shallow marine conditions.

The following stratum consists of homogeneous, very dark grey fine/medium sand (up to 1.41 m b.s.l.). It contains some organic layers and a few shell fragments in the lowermost part. Granulometry and the lack both in macro- and microfossils hint at a rapid deposition by the Drini into a sublittoral milieu.

From 1.41 m b.s.l. to the present surface, fine-grained sediment dominates the core. The colour gradually changes from greenish grey to light olive brown. Numerous oxidation stains as well as the faunal content (macrofossil: *Stagnicola corvus*; ostracod: *Pseudocandona parallela*) suggest a deposition under freshwater/limnic conditions in a floodplain environment.

7.4.5.4 Vibracoring LIS 13

LIS 13 (N 41° 46' 19'', E 19° 36' 38'', ground level at 0.58 m a.s.l., total length of core: 7 m) is located on the Merxhani lagoon close to the wastewater treatment plant of the former paper factory of Lezha (in Albanian: Fabrik Hidrovor). A synoptic view of the profile is shown in appendices 5.9.1 & 5.9.2.

The lower section of the core consists of very dark grey, homogeneous, compact silty fine sand (up to 3.27 m b.s.l.). The faunal content (macrofossil: *Cerastoderma glaucum*; ostracods: *Cyprideis torosa*, *Pontocythere rubra*, *Potamocypris* sp.; foraminifer: *Ammonia beccarii*) suggests a deposition in a brackish/shallow marine environment with a strong freshwater influx.

The subsequent layer is made up of dark olive grey medium/coarse sand (up to 1.92 m b.s.l.). The stratum contains a pebbly layer (between 3.27 and 3.12 m b.s.l.) and a few *Cerastoderma glaucum* fragments. The coarse grain size indicates dynamic sedimentation processes which are typical for fluvial deposition into a sublittoral milieu.

Above 1.92 m b.s.l., the grain size becomes finer. These dark greyish brown sandy layers of fluvial origin contain numerous oxidation stains. The uppermost section of the core consists of clayey silts, deposited during flooding events.

7.4.5.5 Synopsis of transect H-H'

The lowermost part all of the cores is made up of marine strata (see fig. 52). The thickness of the deposits suggests that marine conditions prevailed longer at coring sites LIS 08 and LIS 13, whereas corings LIS 16 and, though to a lesser degree LIS 12 show a strong fluvial influence, in the case of LIS 16 for a considerable length of time. The coarse-grained, pebbly sediments must have accumulated as a result of a shifting distributary of the Drini.

The river course did not pass directly over coring site LIS 13. The medium sandy layers in the middle section indicate the formation of a spit, with a lagoon developing landward of it. Today, a similar environment can be found about 1 km further west of this coring site.

A radiocarbon age estimate from LIS 12 indicates that marine conditions prevailed until the 10th-12th centuries AD [906-1154 cal AD, wood at 5.39 m b.s.l. (LIS 12/2H)]. Frequent changes of grain size can be explained by the establishment of parallel sand-bar systems similar to present-day conditions. The relatively coarse-grained sublittoral sediment in the lower part of coring LIS 12 must have been deposited by longshore drift, because the river Drini only reached the coring site during medieval times. Eventually, a large freshwater lake formed in the central part of this area (LIS 12 and LIS 16) during the 13th-14th centuries AD [1220-1377 cal AD, wood at 1.41 m b.s.l. (LIS 12/1H)].

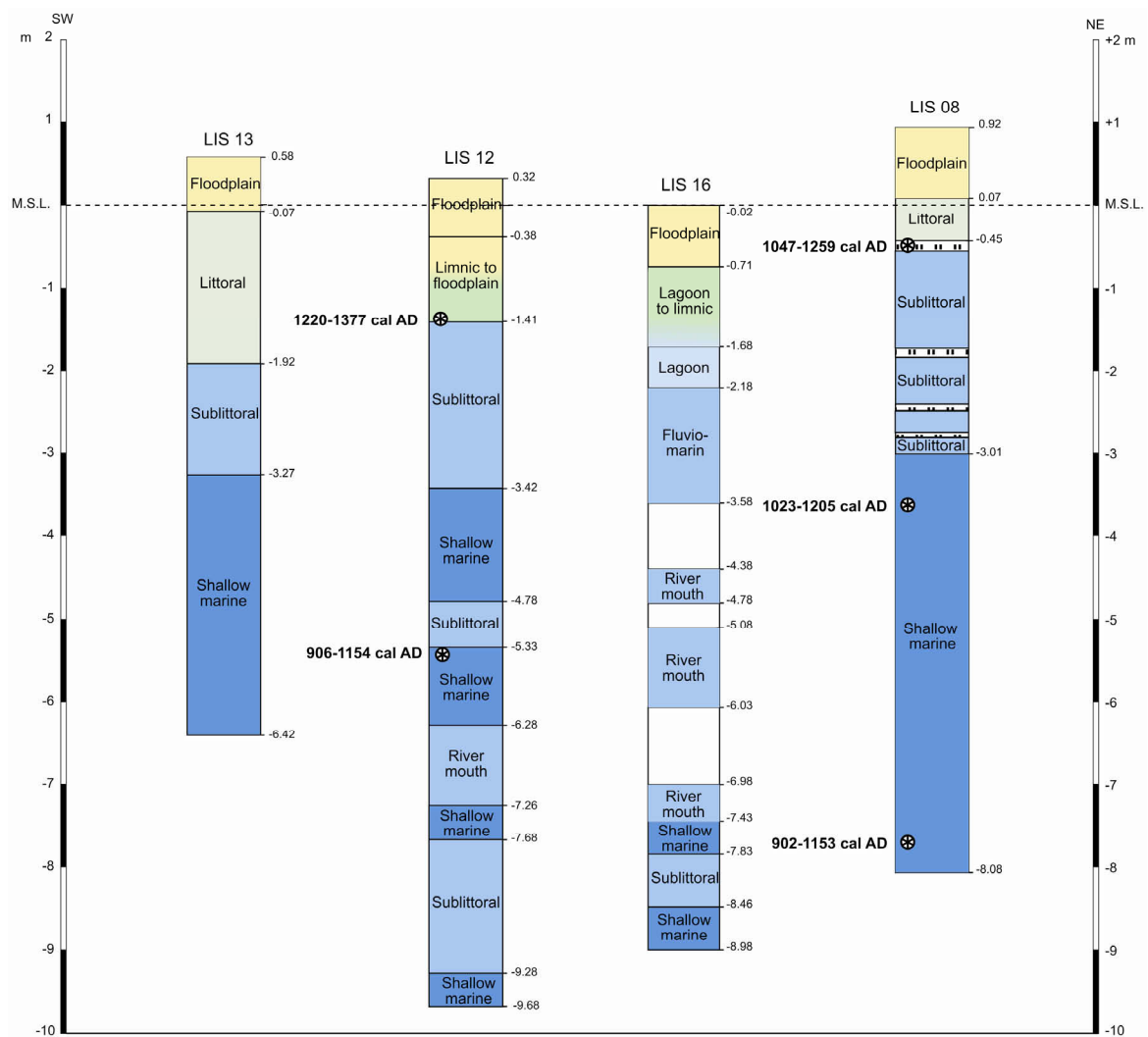


Figure 52: Geological transect H-H' (own research).

Coring site LIS 08 at the foot of Mali Rrenci is located in an unprotected former marine embayment facing the open sea and represents a very different environmental succession. Marine/brackish conditions prevailed much longer at this site, due to the lack of direct sediment input. While the Drini's delta was prograding northwards (as evidenced by river channel deposits at LIS 16), fully marine conditions gradually turned brackish in what was becoming a protected embayment at LIS 08. Two radiocarbon age estimates from the lower and upper section of the marine/brackish stratum indicate rapid sedimentation at the coring site between the 10th and 13th century AD [902-1153 cal AD wood at 7.73 m b.s.l. (LIS 08/8H) and 1023-1205 cal AD, peat at 3.62-3.65 m b.s.l. (LIS 08/7T)].

Subsequently, sublittoral sand must have accumulated as a result of local currents. Numerous buried peat layers suggest intermittent periods of swampy conditions due to temporary sea level fluctuations, probably caused by local tectonics. A piece of wood in the thickest peat layers is dated to the 12th-13th century AD [1047-1259 cal AD, wood at 0.45-0.58 m b.s.l. (LIS 08/1H)]. The uppermost part of all corings consists of fine-grained alluvium.

7.4.6 Transect I – I'

This transect is located at the edge of the swampy part of the Drini's coastal plain in the Ishull Shengjin area (fig. 21), and comprises corings LIS 30, LIS 46, and LIS 08. It runs in an easterly direction from the Shengjin sand-spit to the foot of Mali Rrenci. The aim of this transect was to reconstruct the evolution of the northernmost terrestrial part of the Drini's coastal plain.

7.4.6.1 Vibracoring LIS 30

LIS 30 (N 41° 46' 45'', E 19° 36' 14'', ground level at 0.90 m a.s.l., total length of core: 9 m) is located on the Shengjin sand-spit. A synoptic view of the profile is shown in fig. 53, photo 31, and appendix 5.23.

The lowermost part of the profile consists of very dark grey, homogeneous, compact fine sandy silt (up to 5.93 m b.s.l.). The granulometry and electric conductivity (1.94 to 2.65 mS/cm) suggest a deposition in a shallow marine environment. Between 7.85 and 7.75 m b.s.l., the clayey lenses which are containing plant remains can be interpreted as the temporary establishment of a beach barrier – lagoon system.

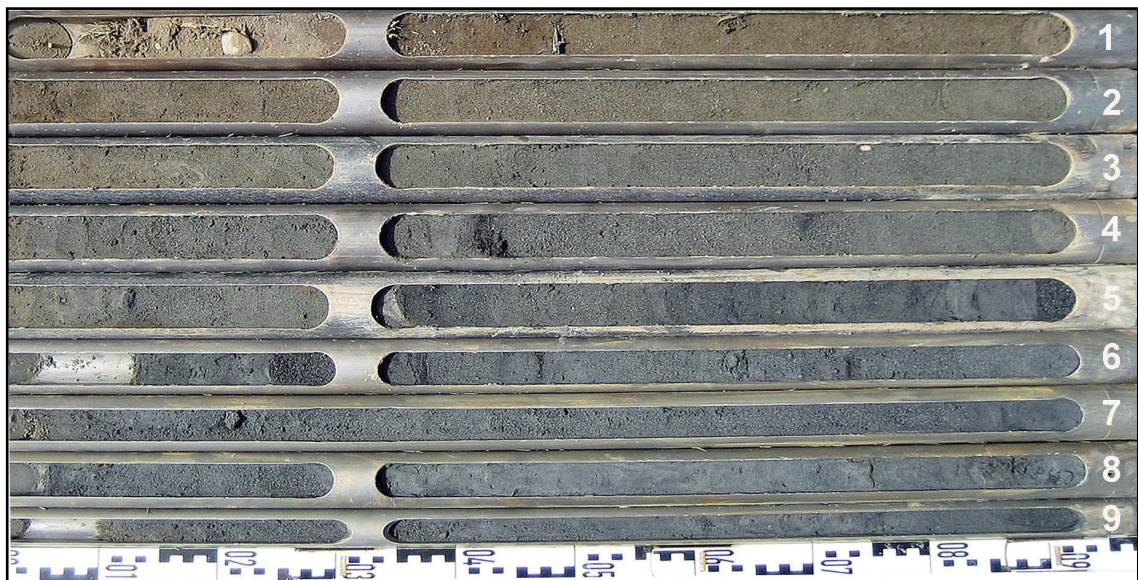


Photo 31: Coring LIS 30.

Shallow marine deposits are overlain by fine/medium sand, which has accumulated in a sublittoral environment forming the Shengjin sand-spit. They include concretions and small pebbles, which must have been transported from the river mouth to this location by the

longshore drift. The decreasing electric conductivity values (from 2.10 to 1.34 mS/cm) were probably caused by the increasing influence of freshwater.

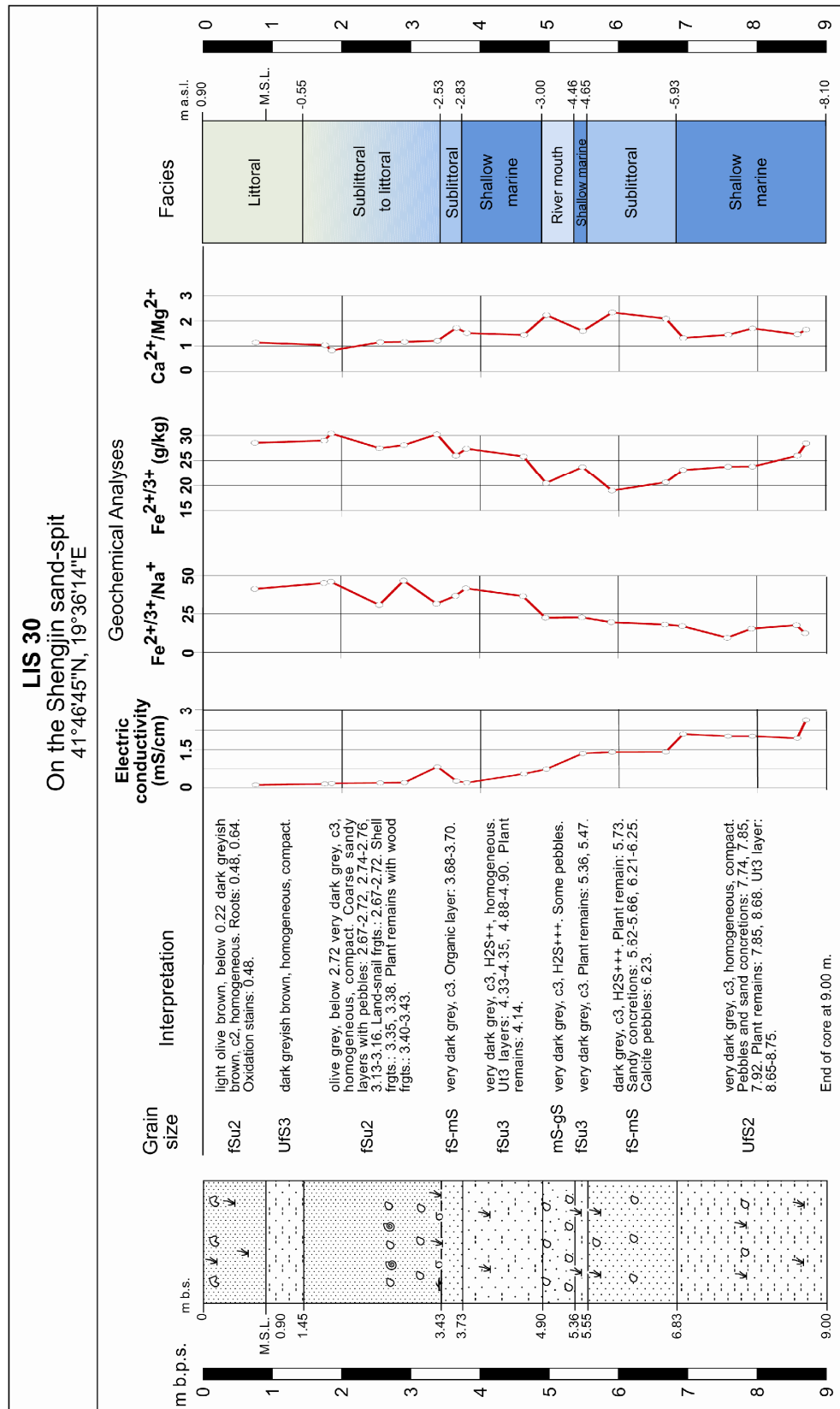


Figure 53: Synoptic chart of coring LIS 30.

The subsequent very dark grey layer of silty fine sand (from 4.65 to 4.46 m b.s.l.) includes some plant remains and implies the re-establishment of relatively calm shallow marine conditions.

From 4.46 to 3.00 m b.s.l., the stratum is dominated by medium/coarse sand with small pebbles. The grain size of the deposits points to a former channel or river mouth of the Drini being close to the coring site. A rise in freshwater influx can be deduced from the further diminished electric conductivity value (0.73 mS/cm) and an increase of the calcium carbonate content (15.21 %).

The following very dark grey silty fine sand contains a few thin clayey lenses, which may indicate the existence of a beach barrier – lagoon system in the area. This interpretation is supported by the subsequent sublittoral fine/medium sand (from 2.83 to 2.53 m b.s.l.).

The uppermost section of the profile is made up of well sorted fine sandy deposits with intercalated thin pebbly coarse sand lenses. The colour of the sediment changes from very dark grey to olive grey at 1.82 m b.s.l. The fossil content changes with the occurrence of some terrestrial gastropods between 1.82 and 1.77 m b.s.l. This sediment body is akin to the present-day beach sediment. Subsidence and compaction must have taken place to cause the occurrence of this young beach sediment at such a depth.

From 0.55 m b.s.l. to the present sea level, a dark greyish brown fine sandy silt layer represents the transition from littoral to terrestrial conditions. The subsequent fine sand forms the present-day beach on the Shengjin spit.

7.4.6.2 Vibracoring LIS 46

LIS 46 (N 41° 46' 59'', E 19° 37' 19'', ground level at 0.09 m b.s.l., total length of core: 10 m) is located in the Ishull Shengjin Region at the border between the well drained part of the Drini delta plain and the semi-terrestrial area to the north of it. A synoptic view of the profile is shown in appendices 5.34.1 & 5.34.2.

The lowermost portion of the profile is characterised by very dark grey, homogeneous silty fine sand with intercalated clayey lenses (up to 8.45 m b.s.l.). High values of electric conductivity (5.94 mS/cm) and organic content (7.14 %) point to the existence of a protected marine embayment.

The following dark grey, medium/coarse sand shows a change in depositional dynamics (up to

6.89 m b.s.l.). High electric conductivity (2.28-3.04 mS/cm) and a bigger mean grain size indicate that the strata were deposited by the Drini into a sublittoral environment. The pebbly coarse sand on top of these deposits (up to 6.62 m b.s.l.) proves that the river mouth was occasionally close to the coring site.

From 6.62 to 4.39 m b.s.l., the dominant grain size is fine sand. Shell fragments and plant remains as well as organic matter indicate ecologically favourable conditions. Lenses of pebbles and clay granules are evidence of an occasional fluvial influence (up to 5.72 m b.s.l.). High values of calcium carbonate (12.33-17.74 %) and electric conductivity (up to 3.48 mS/cm) as well as a high ratio of $\text{Ca}^{2+}/\text{Mg}^{2+/3+}$ (up to 2.42) suggest a deposition in a shallow marine embayment as well.

The following clayey layer includes very thin lenses of fine sand (up to 4.00 m b.s.l.). Geochemical parameters such as high contents of organic matter (6.36 %), orthophosphate (2.60 g/kg) and $\text{Fe}^{2+/3+}$ (45.66 g/kg), and a low value of calcium carbonate (6.93 %) reveal a deposition in a brackish (lagoonal) environment under anaerobic conditions.

From 2.86 to 1.54 m b.s.l., the dark grey, homogeneous silty fine sand is intercalated with thin peat lenses. The section contains an assemblage of shallow marine to brackish species (macrofossils: *Hydrobia* sp., *Theodoxus* sp.; foraminifers: *Ammonia* cf. *parkinsoniana*, *Haynesina germanica*; ostracods: *Cyprideis torosa* f. *litoralis*, *Loxoconcha elliptica*). A few limnic gastropod fragments and terrestrial fungal remains (*Coenococcum geophilum*) suggest a strong freshwater influx.

Above 1.54 m b.s.l., the dominant grain size changes to silt with a fine sand component and intercalary silty/clayey lenses (up to 0.86 m b.s.l.). This section also contains a few brackish microfossils (foraminifer: *Ammonia* cf. *parkinsoniana*; ostracod: *Cyprideis torosa* f. *litoralis*) and abundant oxidation stains, indicating seasonally wet and dry conditions. These fine-grained layers show that fluvial influence ceased and the area had been transformed into a semi-terrestrial environment.

The uppermost part of the profile is characterised by olive brown silty clay with oxidation stains and plant remains. The high electric conductivity (5.63 mS/cm) can be explained by strong evaporation rates during the summer season.

7.4.6.3 Vibracoring LIS 08

LIS 08 (N 41° 47' 04'', E 19° 37' 48'', ground level at 0.92 m a.s.l., total length of core: 9 m) is located at the foot of the western slope of Mali Rrenci close to the road from Lezha to Shengjin. This coring is also part of transect I-I' and has already been comprehensively described in section 7.4.5.1. A synoptic view of the profile is shown in fig. 50, and appendix 5.5.

7.4.6.4 Synopsis of transect I-I'

The lowermost part of all the cores in this transect consists of marine strata (see fig. 54). In LIS 46, the marine sand is intercalated with clayey layers, indicating temporarily beach barrier – lagoon conditions.

Subsequently, several pebbly layers, probably river mouth deposits within the marine strata in cores LIS 46 and even more distinct in LIS 30, indicate the recurring presence of a former distributary of the Drini in close vicinity. The fauna content (macrofossil: *Hydrobia* sp.; ostracod: *Cyprideis torosa*) in the sandy deposits supports the existence of estuarine/brackish conditions.

The subsequent sublittoral deposits at LIS 30 indicate the development of the Shengjin spit as a result of the enormous sediment supply by the river. At the same time, a well-protected embayment formed behind the spit, wherefore conditions became calmer at LIS 46. Much later, the milieu first changed to brackish and finally to swampy. Marine conditions at LIS 08 prevailed longer because of the lack of sediment supply. Then brackish conditions developed with some coastal peat layers (for more detailed information see transect H-H'). Finally, the whole area was continuously covered with fine-grained floodplain sediments.

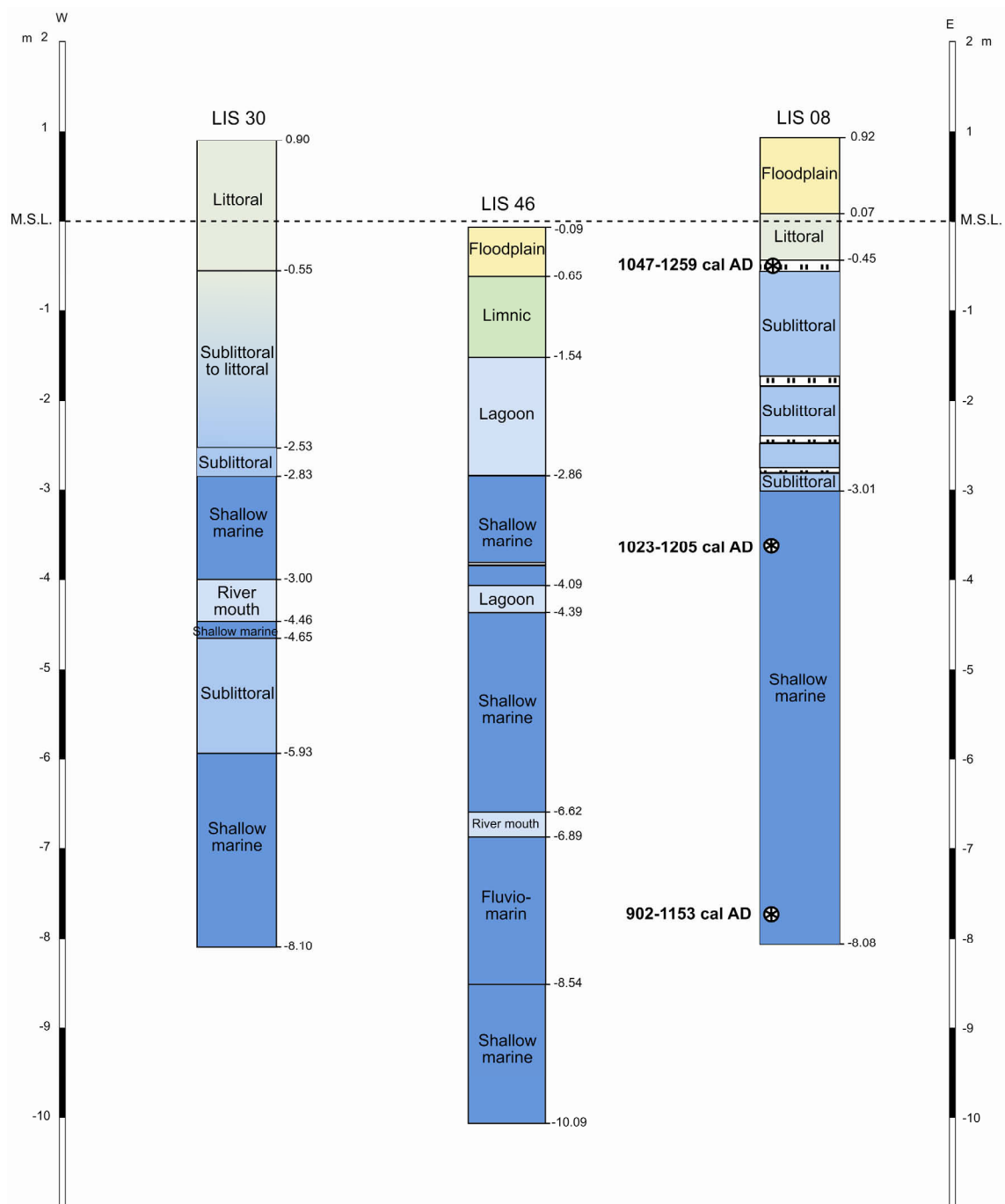


Figure 54: Geological transect I-I' (own research).

7.4.7 Transect J-J'

Transect J-J' is the northernmost one on the Drini's coastal plain, located in the centre of the swampy area between Shengjin town and the Ishull Shengjin Region. It contains corings LIS 31, LIS 41 and LIS 50, and runs southwest from the Lake Kēnalles at the foot of Mali Rrenci to the landward side of the Shengjin sand-spit (fig. 21). The aim of this transect was to reconstruct the evolution of the northernmost part of the Drini's coastal plain.

7.4.7.1 *Vibracoring LIS 31*

LIS 31 (N 41° 48' 02'', E 19° 36' 57'', ground level 0 m a.s.l., total length of core: 9 m) is located within a man-made trench at the base of Mali Rrenci close to Lake Kënalles. A synoptic view of the profile is shown in appendices 5.24.1 & 5.24.2.

The lowermost section of the profile between 9.00 and 8.25 m b.s.l. is characterised by dark grey, silty fine sand, which is overlain by fine sandy silts (up to 6.83 m b.s.l.). The latter include some loamy lenses and numerous plant remains. High values of organic matter (5.38-6.85 %) as well as abundant micro- and macro fossils (macrofossils: *Cidaris* sp., unidentified species of Mytilidae family; foraminifers: *Ammonia* cf. *parkinsoniana*, *Ammonia* cf. *tepida*, *Elphidium excavatum*, *Haynesina germanica*, *Massilina* sp., *Quinqueloculina* sp., *Triloculina* sp.; ostracods: *Carinocythereis whitei*, *Leptocythere* sp., *Pontocythere* sp., *Xestoleberis* sp., *Loxoconcha elliptica*, *Cyprideis torosa* f. *litoralis*) and terrestrial fungal remains (*Coenococcum geophilum*) point to a deposition in a comparatively stagnant marine embayment. In addition to many brackish and marine species, a few limnic ostracods (*Cycloocypris* sp., *Eucypris zenkeri*) indicate a strong freshwater influx. This is also shown by a relatively low electric conductivity (1.09-1.60 mS/cm). The freshwater probably came from submarine karstic springs rather than from the Drini.

From 6.83 to 4.76 m b.s.l., the grain size changes to silty fine sand, with intercalated layers of medium sand and numerous thin organic lenses. The faunal content is dominated by mostly brackish (meso to polyhaline) to shallow marine species (foraminifers: *Ammonia* cf. *parkinsoniana*, *Ammonia* cf. *tepida*, *Quinqueloculina* sp.; ostracods: *Cyprideis torosa* f. *litoralis*, *Leptocythere* sp., *Pontocythere* sp.). The deposit includes seeds of angiosperms (terrestrial: *Saponaria officinalis*, marine-brackish: *Ruppia maritima*) and terrestrial fungi (*Coenococcum geophilum*).

These shallow marine sands are overlain by very dark grey, homogeneous fine to medium sublittoral sand, probably carried here by longshore drift (up to 3.72 m b.s.l.). From 3.72 to 2.72 m b.s.l., the grain size is dominantly fine sand, but becoming increasingly silty, with intercalated layers of medium sand. Plant remains, organic matter and broken shell fragments as well as the grain size variations show occasional changes of environmental dynamics. The faunal content indicates a shallow marine to brackish milieu (macrofossil: *Cerastoderma glaucum*; foraminifers: *Quinqueloculina* sp., *Ammonia* cf. *parkinsoniana*; ostracods: *Pontocythere* sp., *Loxoconcha elliptica*, *Leptocythere* sp.). The subsequent layer points towards

the establishment of completely brackish conditions such as a lagoonal environment (up to 2.08 m b.s.l.).

The uppermost part of the profile comprises several thin layers of silty sand and fine/medium sand. The gradual replacement of marine shell fragments with landsnails implies increasingly terrestrial conditions. This suggests a change from a sublittoral to littoral milieu. Additionally, numerous plant remains are further indicators of a semi-terrestrial environment.

7.4.7.2 *Vibracoring LIS 41*

LIS 41 (N 41° 47' 47'', E 19° 36' 36'', ground level at 0.13 m b.s.l., total length of core: 11 m) is located in the centre of the semi-terrestrial area between coring site LIS 31 and the Shengjin sand-spit. A synoptic view of the profile is shown in appendices 5.30.1 & 5.30.2.

The lower and middle parts of the profile (11.13-4.69 m b.s.l.) consist of alternating homogeneous, compact and laminated layers of fine sandy silt and silty fine sand. The silt dominated deposits include organic remains and thin peaty lenses. The microfauna (foraminifers: *Ammonia* cf. *parkinsoniana*, *Elphidium excavatum*; ostracods: *Pontocythere* sp., *Cyprideis torosa* f. *litoralis*) points to a deposition in brackish to shallow marine milieus. A coastal peat layer between 9.58 and 9.46 m b.s.l. includes some freshwater/brackish gastropod (*Theodoxus* sp.) and ostracod (*Candona* sp.) specimens. The uppermost part of this section is dominantly brackish due to an increasing freshwater influx. This is also reflected by the decrease of electric conductivity (from 4.71 to 2.75 mS/cm) and organic matter (from 6.19 to 1.10 %), while calcium carbonate increases (from 7.77 to 13.57 %).

From 4.69 to 3.90 m b.s.l., the sediments are characterised by homogeneous, dark grey fine sand with some lenses of medium/coarse sand. The following layer of dark grey, medium/coarse sand includes small pebbles (up to 3.41 m b.s.l.). The high electric conductivity (2.10 mS/sec) of the coarse sediments may indicate a deposition in a sublittoral environment by longshore drift. A former river mouth to the west of the coring site supports this interpretation.

From 3.41 to 1.65 m b.s.l., the coarse-grained sediment changes to well-sorted, dark grey, fine/medium sand. This sublittoral stratum is overlain by a homogeneous fine sand layer which hints at a possible return of shallow marine conditions. Abundant oxidation stains (above 1.13 m b.s.l.) and organic spots, as well as several plant remains show the transition to semi-terrestrial conditions. A few foraminifers (*Ammonia* cf. *parkinsoniana*) are an indication for

occasionally slightly brackish conditions. The uppermost part of the profile (from 0.48 m b.s.l. to the present surface) is made up of a dark brown coastal peat.

7.4.7.3 Vibracoring LIS 50

LIS 50 is located on the landward side of the Shengjin sand-spit (N 41° 47' 20'', E 19° 36' 13'', ground level at 0 m a.s.l., total length of core: 9 m). A synoptic view of the profile is shown in fig. 55, photo 32, and appendix 5.37.

The lowermost section of the profile consists of dark grey, homogeneous, compact fine sandy silt (up to 8.80 m b.s.l.). The faunal content (foraminifer: *Ammonia* cf. *parkinsoniana*) and the electric conductivity (2.92 mS/cm) indicate a deposition in a brackish/shallow marine environment.

The following fine/medium sand (up to 7.85 m b.s.l) and medium/coarse sand with pebbles (up to 7.72 m b.s.l.) shows that the river mouth was nearby. This interpretation is underlined by the fact that a former river mouth can still be seen just south of the coring site.

Between 7.72 and 4.30 m b.s.l., the core consists of dark grey, homogeneous, compact silty fine sand. Thin peat layers and organic matter indicate a deposition in a low energy wave regime. Granulometry and a high electric conductivity (3.06-4.18 mS/cm) are evidence for a decreasing freshwater influx due to changing river mouth dynamics. The sediment contains mesohaline species (ostracod: *Cyprideis torosa* f. *litoralis*; foraminifers: *Ammonia* cf. *parkinsoniana*, *Elphidium crispum*). Thin peaty lenses and a high amount of organic matter show temporary shifts to semi-terrestrial conditions. It is interesting to note that the marine sand is disturbed by a layer of coarse sand and pebbles (6.63-6.45 m b.s.l.).

From 4.30 to 2.25 m b.s.l., the shallow marine sand is followed by dark grey, homogeneous fine/medium sand. Its high electric conductivity (2.82-3.87 mS/cm) indicates a deposition in a sublittoral environment. The layer is part of the Shengjin sand-spit complex. The lack of microfossils may be due to the high energy wave regime.

At 2.25 m b.s.l., the sublittoral sand is overlain by a thick peat in a silty matrix (up to 1.37 m b.s.l.). With the onset of the peat formation the CaCO₃ content decreases dramatically from 17.43 % to 0.15 % while the organic content increases from 2.28 % to 40.05 %. The pH of 6.63 indicates slightly acidic conditions. The uppermost part of the peat layer contains vermetids.

The peat is covered by homogeneous fine sand. At 0.44 m b.s.l., the colour changes from dark grey to olive brown. In this area, the sand cannot originate from a fluvial source, but from a sand bar; it was carried to this position by wind and waves. The fossil content comprises brackish to shallow marine species (foraminifers: *Ammonia beccarii*, *Ammonia* cf. *parkinsoniana*, *Elphidium crispum*, *Elphidium excavatum*, *Massilina* sp., *Quinqueloculina* sp., *Sigmoilina* sp.; ostracods: *Cyprideis torosa* f. *litoralis*, *Loxoconcha elliptica*, *Pontocythere* sp., *Semicytherura* sp.). The high electric conductivity (4.30 mS/cm) hints at a deposition in a salt marsh/lagoonal environment with marine influence of variable strength.

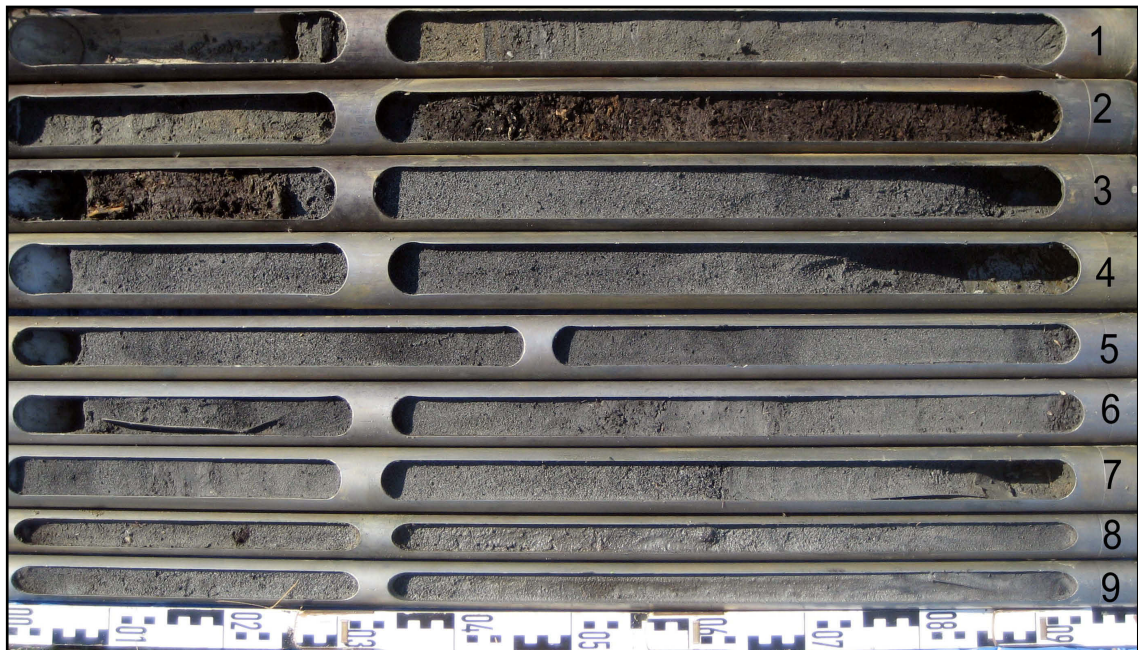


Photo 32: Coring LIS 50. (Uncu, 2008)

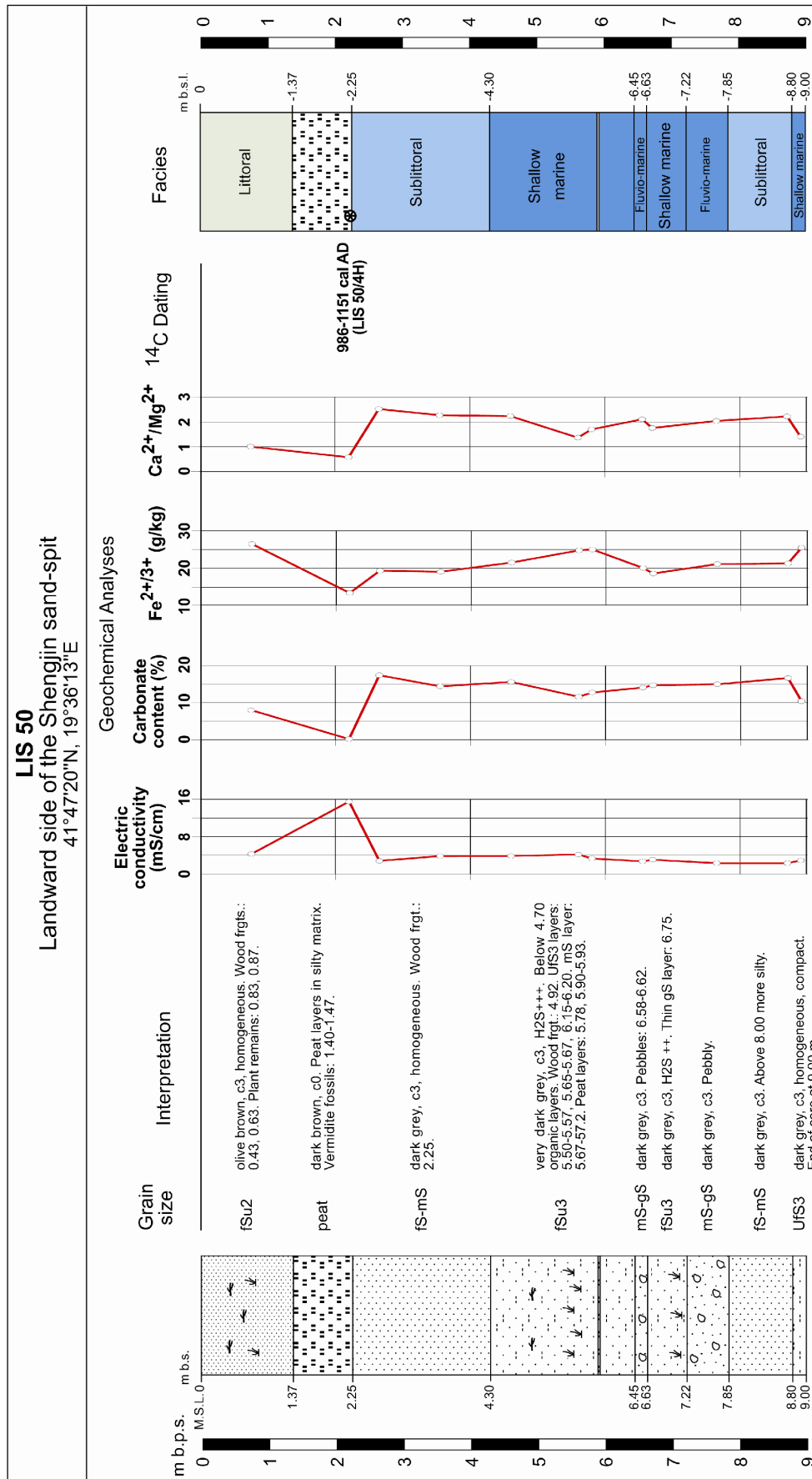


Figure 55: Synoptic chart of coring LIS 50.

8.4.7.4 Synopsis of transect J-J'

The lowermost parts of all the cores consist of shallow marine strata (see fig. 29). Marine conditions prevailed longer at LIS 31 and LIS 41. At coring site LIS 31, marine deposits are occasionally interrupted by peat layers due to its position further inland. The marine sediments of core LIS 41 point to deeper water conditions, because these deposits contain fewer plant remains than the other two cores.

Core LIS 50 represents a totally different sedimentation milieu. The marine sand at the base is intercalated with pebbly to coarse sandy strata indicating fluvial influences. Alternating layers of marine and fluvial sediments point to a continuously shifting river mouth. The thin pebbly stratum between 6.63 and 6.45 m b.s.l. signifies the final fluvial influence.

Marine conditions are replaced by a sublittoral milieu, as suggested by medium sandy deposits. The sandy strata at LIS 50 represent the formation of a beach barrier – lagoon system (starting at 4.30 m b.s.l.). The present-day Shengjin spit and the lagoonal environment protected by it have started to develop at that time. An approximately 1 m thick peat layer, formed in the back swamp of the Shengjin spit, was dated to the 10th-12th centuries AD [986-1151 cal AD, wood at 2.25 m b.s.l. (LIS 50/4H)].

During the following subsidence, the peat was covered by well sorted spit deposits. Such a thick peat layer developed much later at coring site LIS 41 because it was located at the deepest part of the lagoon. In LIS 31, at the flank of Mali Rrenci, marine conditions persisted until the 14th century AD [1301-1414 cal AD, plant remains at 5.61 m b.s.l. (LIS 31/13Pf)]. Due to the input from karstic springs, brackish conditions changed more quickly to freshwater ones at coring site LIS 31.

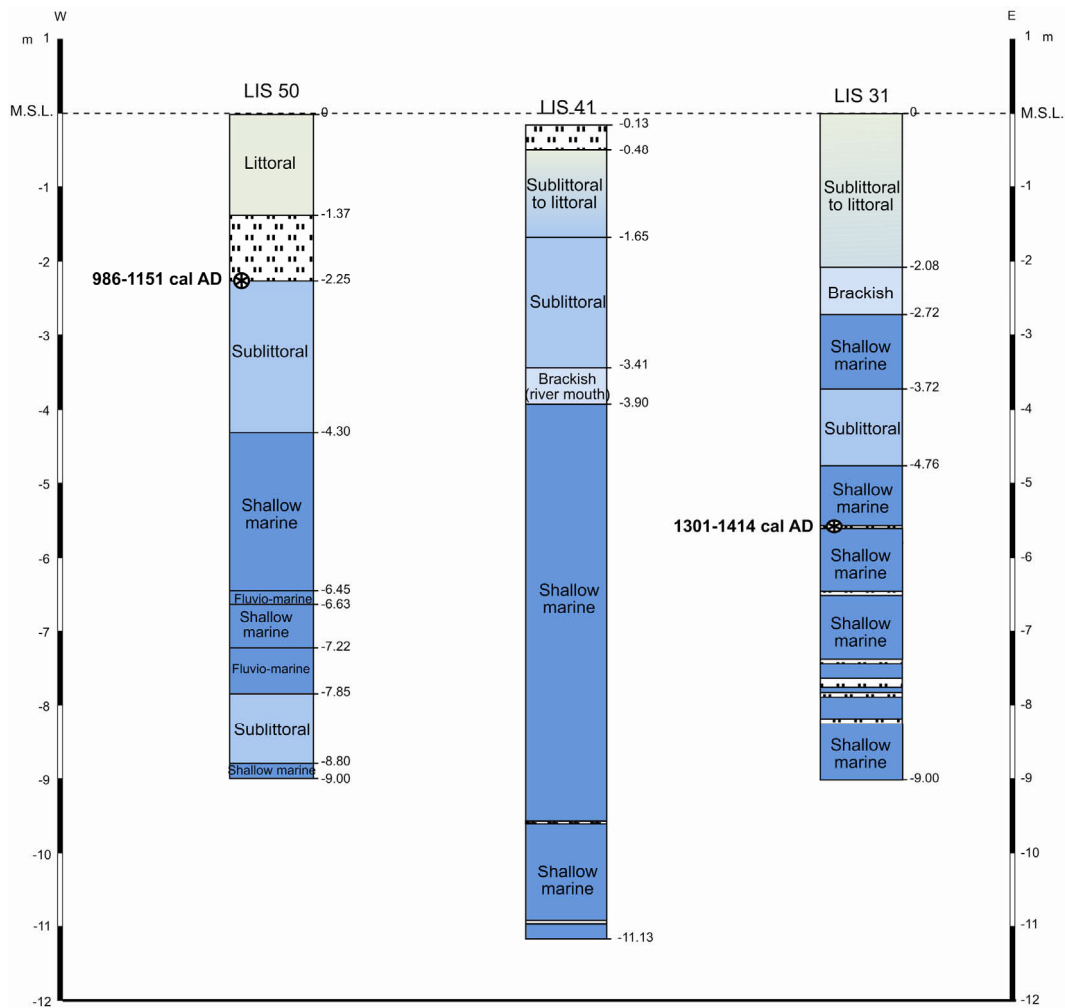


Figure 56: Geological transect J-J' (own research).

7.5 Palynological results

For a better understanding of the Holocene vegetation history around Lezha, we used the palynological results of the buried and dated peat layers, taken from several vibracorings on the Drini delta plain. The corings, which are not far from each other, were retrieved during the field campaign in 2006. Palynological results were provided by Dr. Maria Knipping (University of Hohenheim, Stuttgart).

The pollen analytical results of six peat layers give an idea on the vegetation changes around the Drini delta from the 2nd millennium BC to Medieval times (see fig. 57). These results can be correlated with the settlement history around Lezha. The pollen content of the lowermost peat layer, dated to the beginning of the 2nd millennium BC, is characterised by a greater abundance of non-arboreal pollen grains compared to arboreal pollen. The herb pollen section consists of *Ranunculus*-type (61.4 %) and lesser Cichoriaceae (15.9 %).

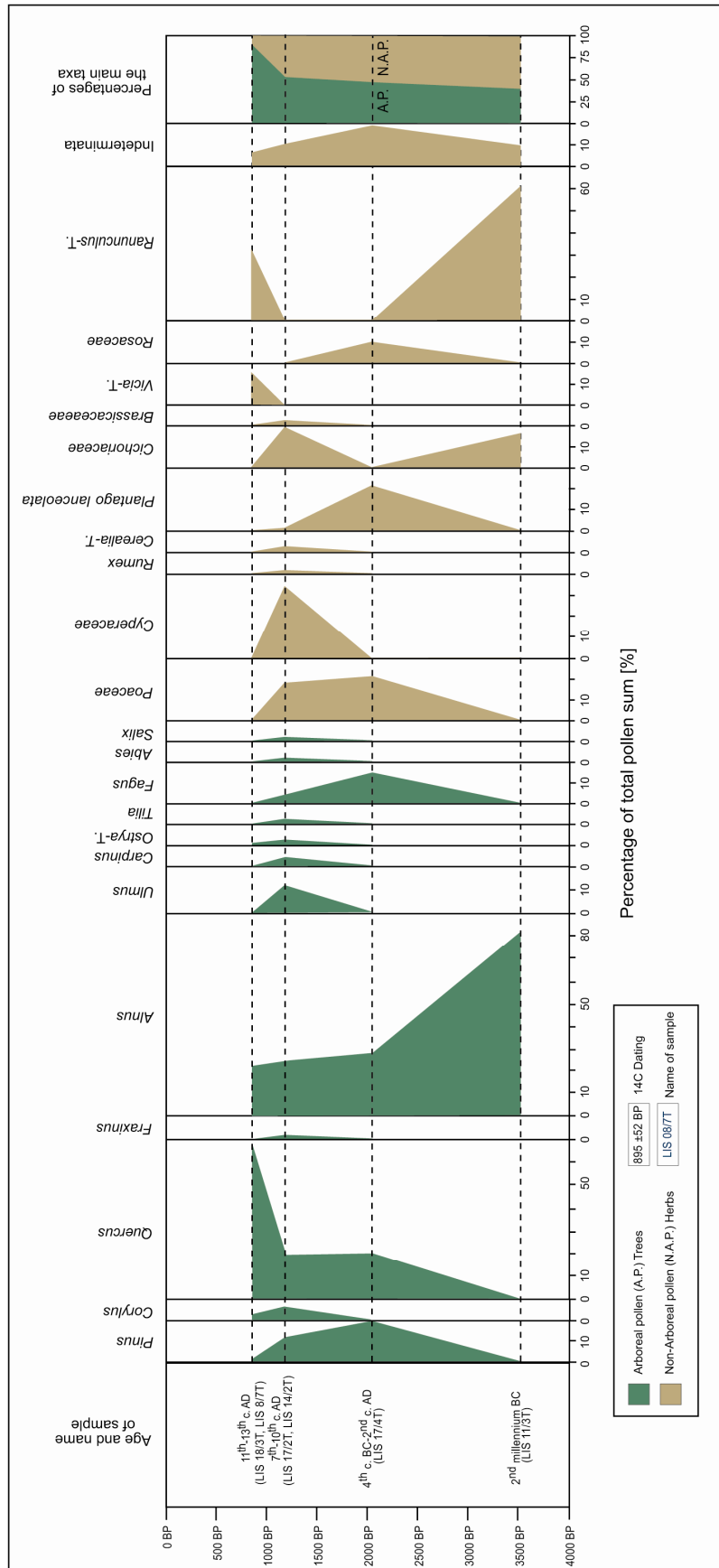


Figure 57: Synoptic palynological data obtained from corings LIS 08, LIS 11, LIS 14, LIS 17, and LIS 18. Analysed were intercalated and ¹⁴C-dated peat layers (Uncu & Knipping, 2010; unpublished).

However, these species are not representative for the whole vegetation composition; they simply indicate the existence of wetland conditions at the coring site during that time. This is supported by the dominant tree pollen being *Alnus* (82.1 %).

The percentage of arboreal pollen increases towards the Hellenistic and early Roman times. *Alnus* is still the dominant tree species, but other trees appear, namely *Pinus*, *Quercus* and *Fagus*. However, the herb pollen group, containing species such as *Plantago lanceolata*-type and Poaceae, which may indicate human activities, reaches a relatively high value (21.4 % for each species). This correlates with an intensified human impact around Lezha which began with the foundation of the ancient city of Lissos in 385/4 BC and continued into the Roman times, when the city prospered.

During the 7th to 10th centuries AD, the ratio of arboreal/non-arboreal pollen ratio changes slightly in favour of the latter, with a particularly high amount of Cyperaceae (34.1 %), Cichoriaceae (20 %) and Poaceae (18.5 %) pollen. In the sample obtained from coring LIS 17 the pollen sum is extremely low so the result may not be representative. This general decrease of pollen grains is likely to have been caused by strong degradation of the sample.

The tree pollen consists of a number of deciduous trees such as *Alnus*, *Ulmus*, *Quercus*, *Fraxinus*, *Carpinus*, *Corylus*, *Abies*, *Salix* and *Ostrya*-type. The arboreal pollen composition shows the occurrence of a floodplain forest in the area. High amount of Cichoriaceae can also indicate the presence of permanent water bodies, like ponds or shallow lakes. The existence of wet conditions is supported by the pollen of non-arboreal species (*Sparganium*-type, Cyperaceae, *Lythrum*, *Cyperus*, *Nymphaea*, *Pediastrum* and monoete spores). A few *Pinus* and *Fagus* pollen grains must have been transported from neighbouring mountains. The assemblage of tree and herb species is similar to what can be found in the near-shore wetland forest around the Merxhani lagoon even today.

In the following centuries, the arboreal pollen is dominated by *Quercus cerris*-type and *Quercus pubescence*-type (68.3 %) (LIS 18, on the central part of the delta plain) and *Alnus* (23.4 %) with a few *Corylus* (2.8 %) grains (LIS 08, close to Mali Rrenci). Both oak species are typical sub-mediterranean trees. The increasing arboreal pollen is probably an indication of the natural regeneration of forests in the region. This may have been caused by a more humid climate during the Medieval Climatic Optimum (900-1200 AD), as well as by decreasing human activities in the area. The high amount of *Alnus* pollen indicates wet conditions around Lezha. This must be connected with the deltaic evolution of the Drini in the Ishull Shengjin Region.

Some historical documents support the re-advance of forests in the Lezha region until the 16th century (see chapter 3.3). During Late Medieval times, Lezha had a river port and exported wheat, salt and wood. After the beginning of the Turkish rules in Lezha at the end of the 15th century, the settlement pattern and socio-economic structure in the region changed completely. Christian groups, who had lived along the coastal areas moved to the more mountainous highlands; therefore, the highlands were used intensively once more. Forest degradation and changed land-use patterns led to an increase of human-induced soil erosion. Thus, the Drini delta advanced fairly rapidly during post-Medieval times.

8 Palaeogeographic scenarios

The palaeo-ecological interpretation and the chronostratigraphy of the many corings described in chapter 7 are the basis for the reconstruction of the landscape evolution. Several palaeogeographic scenarios have been created, illustrating the evolution of the Drini floodplain and delta from the Holocene transgression maximum to the present.

Information from Shackleton (1984) about the coastal configuration of Northern Albania during the Late Glacial Maximum (LGM) is perfectly suited to set the scene. It is well known that the present-day coastline around the world is very dissimilar to the situation about 20,000 years ago. Many research projects indicate that the sea level was at its lowest position (approximately 120-130 m below its present level) during the Late Glacial Maximum (ca. 18,000 ¹⁴C-years BP) and coastal landscapes looked totally different, as has been shown by Shackleton et al. (1984). They used the -120 m (for 18,000 BP) and -35 m (for 9,000 BP) contour lines on the British Admiralty charts to prepare palaeogeographic maps for the position of the coastline in the central Mediterranean and Adriatic Sea (Shackleton et al., 1984: 310). Such illustrations give an idea how much the coastal landscape around Lezha has changed (fig. 58).

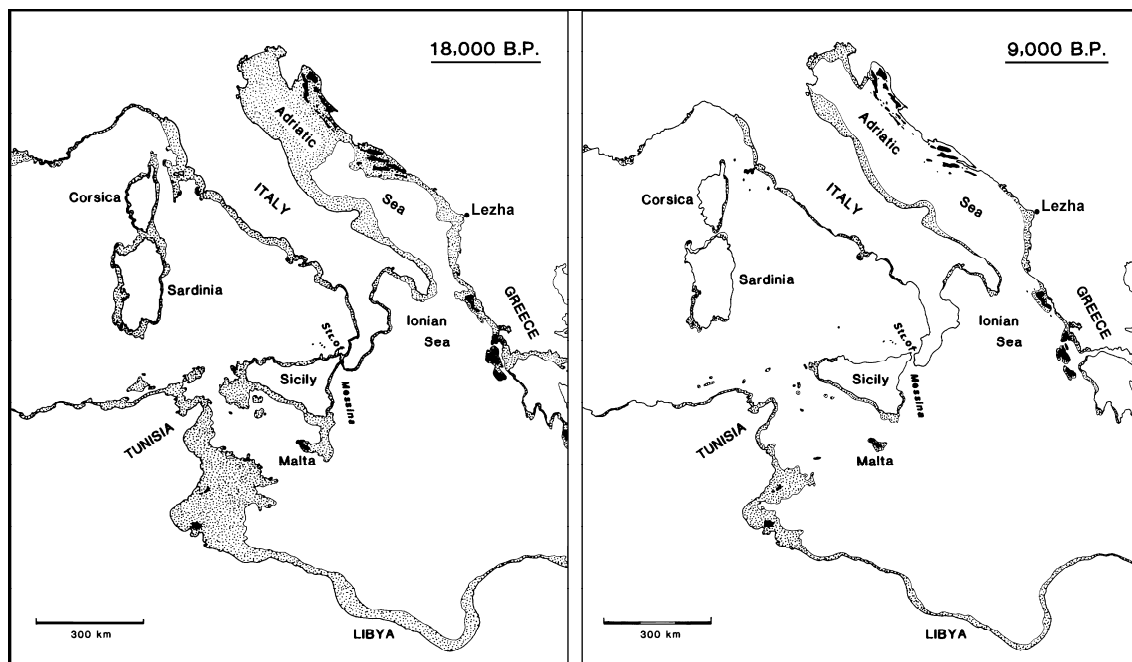


Figure 58: Central Mediterranean coastline assumed for 18,000 BP and 9,000 BP, respectively (slightly changed from Shackleton et al., 1984, p. 308, fig.1 and p. 311, fig. 4).

According to their maps, a coastal plain was fringing western Albania during the Last Glacial Maximum (Shackleton et al., 1984). It reached its largest extent in Northern Albania, in the present-day Gulf of Drini. The coastline was approximately 100 km further westwards, and the rivers Drini, Mati, Ishim and Buna were traversing this wide coastal plain (Mathers et al., 1998). Smaller streams from the highlands were forming alluvial fans along the foot of the mountains (e.g., Manatia alluvial fan). The elongated hilly ridges of Mali Rrenci and Mali Kakarriqi were overlooking the plain.

The early Holocene was characterised by global warming, causing melting of glaciers in higher latitudes and on the higher mountains. From the beginning of the Holocene transgression (ca. 15,000 BP) until ca. 9,000 BP, sea level rose rapidly, and reached 35 m below the present level. In Albania, this process led to dramatic eastward shifts of the coastline (ca. 50 km) and large parts of the former coastal plain vanished (Shackleton et al., 1984: 311).

8.1 The Holocene transgression maximum

During the following millennia, the sea level rise decelerated but continued, and the sea reached its maximum landward expansion during around 6,000-5,000 BC. Thus, the Adriatic Sea transgressed gradually eastwards consuming the former coastal plain until it reached the foot of the Shite-Veles and Skanderbeg Mountain chains east of Lezha (fig. 59).

Our research has also shown that the sea reached about 13 km further inland (as seen from the present coastline) during the peak of the Holocene transgression. The coastline must have been located somewhere in the northernmost part of the Merqia plain, between coring sites LIS 27 and LIS 47. The lowermost part of coring LIS 47 contains shallow marine/brackish deposits with abundant fossil assemblages, whereas the sediments of LIS 27 reflect fresh water conditions throughout the core, showing intercalations of alluvial fan deposits and limnic sediments, which can be interpreted as the formation of a lake.

A large marine embayment north of Lezha (today: Merqia plain) formed during the Holocene transgression maximum. This embayment was connected with the open sea in the south through the narrow rocky gap, where later Lissos was founded, and in the northwest *via* the sea corridor between Mali Rrenci and Mali Kakarriqi. However, due to these connections being rather restricted, the embayment was sheltered from high wave energy, and the sea water was mixed with fresh water resulting in brackish conditions. The abundant fauna (e.g., *Ammonia beccarii*

and *Cyprideis torosa*) of the respective deposits is largely salt tolerant, but usually typical for a brackish milieu, thereby pointing to a strong freshwater input from rivers and karstic sources.

As mentioned above, the syncline between Mali Rrenci and Mali Kakarriqi (today: Balldreni plain) was also invaded by the sea and became a marine corridor. Thus, Mali Rrenci was transformed into an island, and a “vallone or canale-type coast” formed in Northern Albania, similar to today’s Dalmatian coast. As for the ridge of Mali Kakarriqi, the situation is not yet clear. It seems that it was a peninsula because coring LIS 27 shows no marine strata; therefore, no further drillings have been carried out on the northeastern side of this hill.

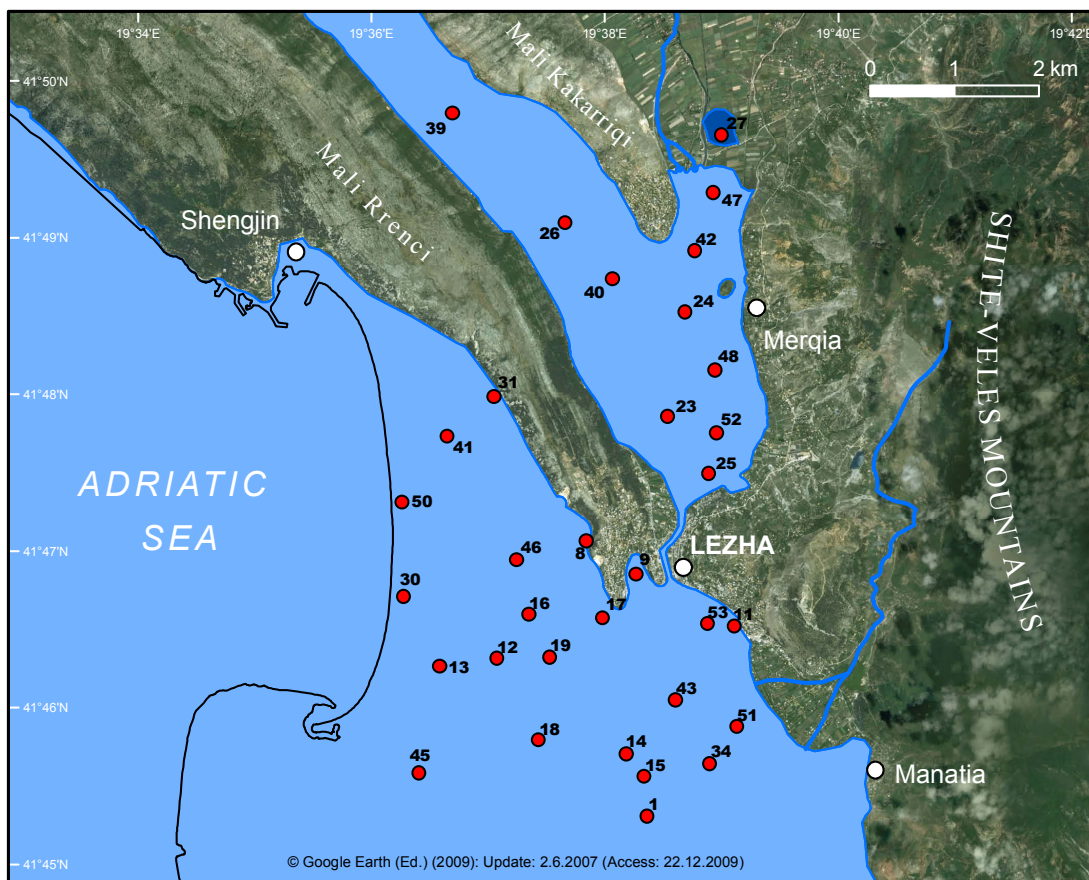


Figure 59: Palaeogeographic scenario for the research area during the Holocene transgression maximum. (Uncu, 2010, based on a satellite image from Google Earth, accessed 22-12-2009)

Several radiocarbon ages have been obtained to refine the chronology of events. The oldest one has been taken from the marine deposits of coring LIS 42 and dates to the end of the 5th / beginning of the 4th millennium BC. This age is concordant with the timing of the Holocene maximum transgression in the Mediterranean region. Other ¹⁴C datings of marine deposits in the Merqia and Balldreni plains (LIS 39, LIS 40, LIS 47; LIS 23) confirm the existence of marine conditions during the 4th to 3rd millennium BC.

The sublittoral sediments at the lowermost part of the corings at the foot of Mali Shelbuemit (LIS 11) and Lezha Hill (LIS 04, LIS 28, LIS 29, LIS 35) show that nearshore conditions change to shallow marine ones around the 3rd millennium BC. Reasons for the deepening of the water at these locations can be either co-seismic events, thereby changing the relative sea level, or the process of transgression had not yet finished.

8.2 4th millennium BC (Middle Neolithic)

Having been dominated by marine processes in the previous millennia, coastline changes begin to be controlled by fluvial action. The river Drini started to advance its delta southwards into this sheltered embayment (see fig. 60).

The first influences of the delta progradation of the Drini can be observed in coring LIS 42. A ¹⁴C dating from the boundary between marine sediments and river channel deposits shows that the main distributary of the Drini flowed east of present-day Balldreni town at the end of the 4th millennium BC. The lack of coarse sediment in coring LIS 47 can be interpreted as a lack of direct fluvial influence, thus indicating that marine conditions prevailed longer in the eastern part of the embayment.

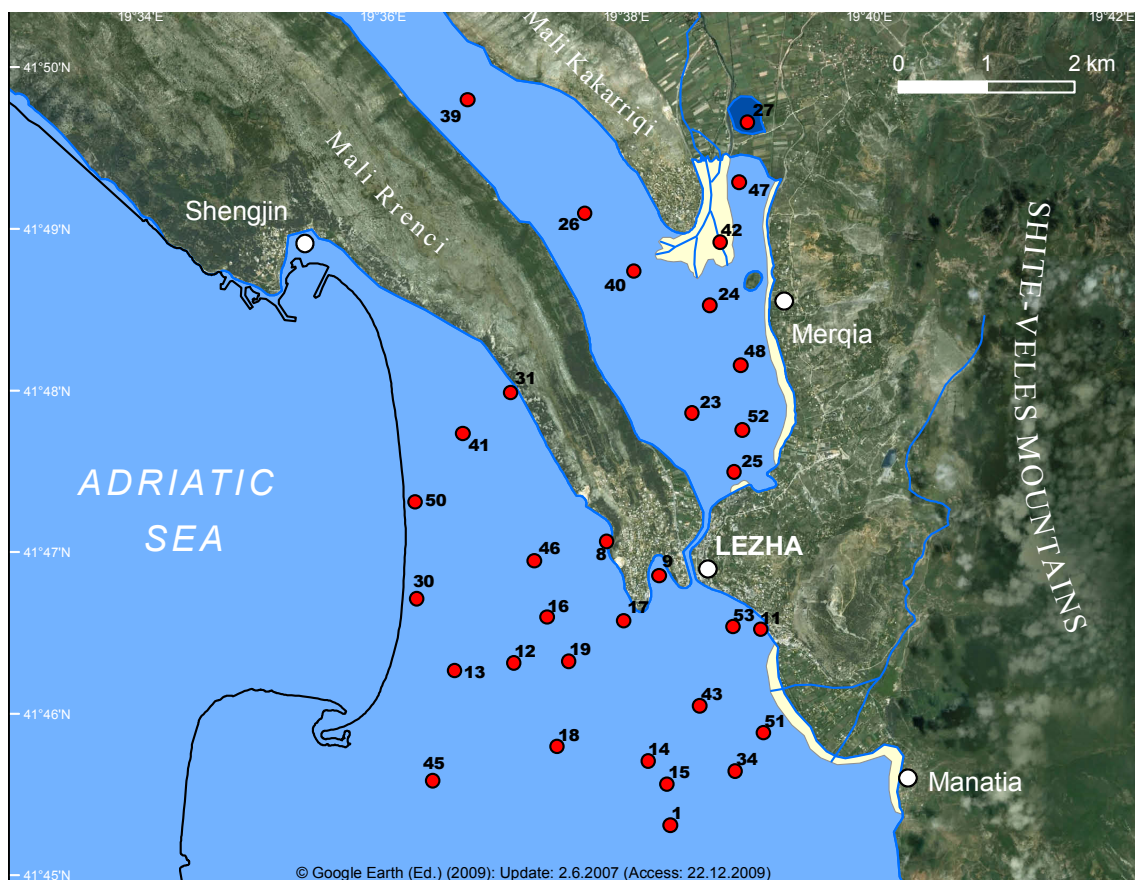


Figure 60: Palaeogeographic scenario for the research area during the 4th millennium BC (Middle Neolithic). (Uncu, 2010, based on a satellite image from Google Earth, accessed 22-12-2009)

It seems that the progradation of the Drini delta during that time coincides with the foundation of the first Neolithic settlements in the catchment area of the Black Drini, thereby hinting at an early human impact on the landscape (see chapter 4 & table 5). Interestingly, a thick sandy layer within the fine grained marine deposits at coring site LIS 25 suggests extensive erosion on the neighbouring slopes during the 4th millennium BC.

8.3 3rd millennium BC (Late Neolithic – Chalcolithic period)

Transects A-A' and B-B' present vital information for understanding the progradation of the Drini delta during the end of the 3rd millennium BC (see fig. 61). Marine deposits of coring LIS 47 indicate that the marine conditions still prevailed in the east of the early delta plain along the foot of the Shite-Veles Mountains. However, we learn from cores LIS 24 and LIS 40 that the delta of the Drini has prograded south with several distributaries, to form a Gilbert-type delta. Evidence is provided by marine to brackish facies changes with a varying freshwater input, and by the alterations of fine-grained to sandy layers with abundant brackish/shallow marine fauna, which is typical for deposition within an “interdistributary bay”.

We know that, during the first half of the 3rd millennium BC, one of the distributary channels of the Drini was advancing westwards, because we found coarse sand of fluvial origin in the lowermost part of coring LIS 26. However, this distributary changed in a southern direction before reaching this coring site.

The enormous sediment load of the Drini led to this rapid delta advance. Physical components such as easily erodable rocks in the drainage area and the hydrographic regime of the rivers caused such a volume of sediment, but it is worth considering the possible contribution of an increasing human impact on the landscape in the catchment area.

Archaeological research shows that the Drini valley was intensively inhabited since the beginning of Neolithic times (Korkuti, 1983, 1988). Neolithic people settled on old river terraces and alluvial fans as well as on the slopes of the mountains, because the valley floor and lower plains were frequently affected by flooding events (Jacques, 1995: 7). Some Neolithic settlements expanded during the Chalcolithic period due to an increasingly sedentary lifestyle, when agriculture and animal husbandry became more important. A thick layer of angular limestone pieces within the shallow marine deposits at LIS 29 and LIS 35 indicate that people were present around Lezha. The increased human impact on the ecological balance of the area may have led to degradation of the natural vegetation and thereby triggered soil erosion.

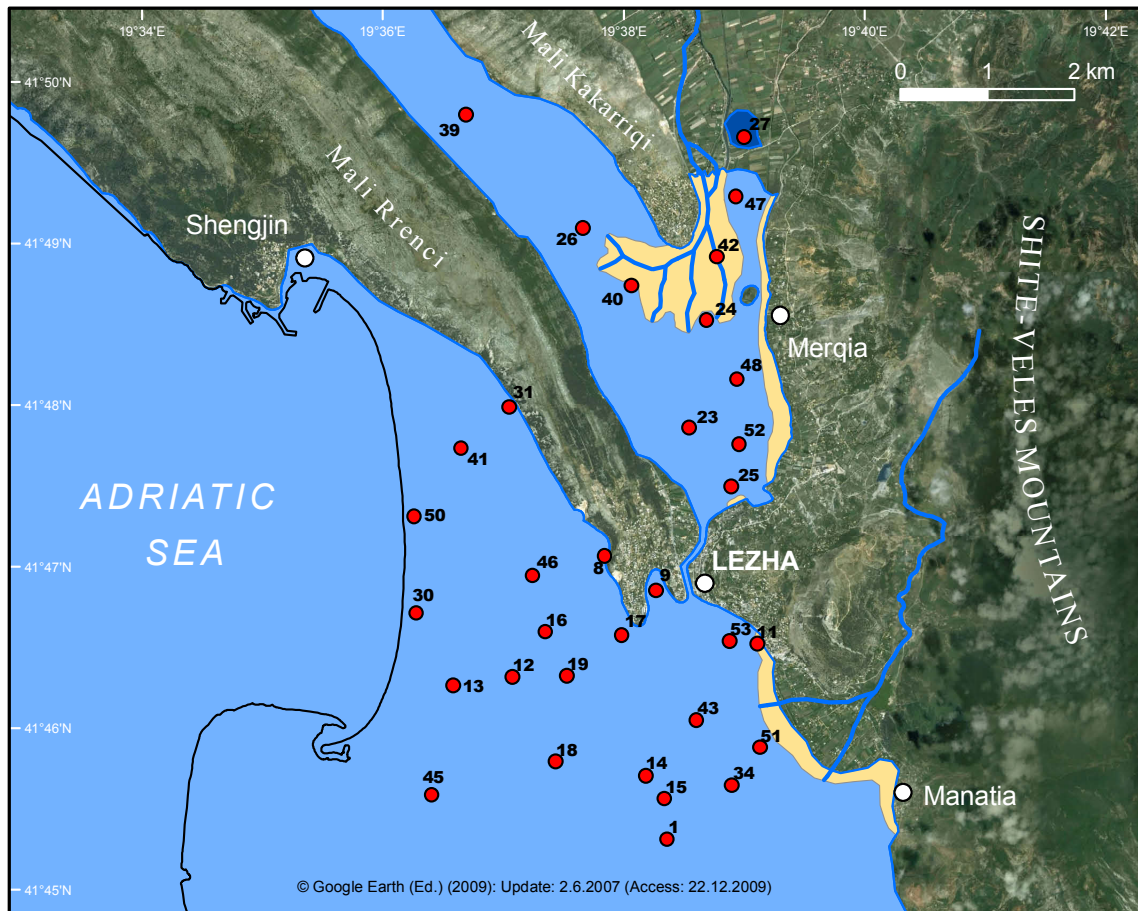


Figure 61: Palaeogeographic scenario for the research area during the end of the 3rd millennium BC (Uncu, 2010, based on a satellite image from Google Earth, accessed 22-12-2009).

8.4 2nd millennium BC (Bronze Age)

A radiocarbon age estimate from coring LIS 24 in the Merqia plain indicates that one of the distributaries of the river Drini was flowing across this site and building its delta into the marine embayment at the beginning of the Bronze Age. Marine conditions still existed in the southern part of the present-day Merqia plain as well as in the marine corridor between Mali Rrenci and Mali Kakarriqi.

Many cores around Lezha contain several paralic peat layers, indicating sea level fluctuations, which can be linked with co-seismic events in the area. A very interesting and indicative peat layer was found at a depth of ca. 3-4 m below present sea level. It was dated to the early/middle Bronze Age (see table 8). The reasons for this regression are not clear; however, it could be of climatic origin. The peat layer may represent what has been termed the late Bronze Age regression in other parts of the eastern Mediterranean Sea (Dalfes et al., 1999). It is even

assumed as one cause for the collapse of civilisations in the Old World (Weiss et al, 1993). In the case of Lezha, the final regression seems to have occurred some centuries earlier.

Rapid delta progradation has been reported from the entire Mediterranean between 1500 BC and 500 AD (for further discussions see Bintliff, 2002; Butzer, 2005). We can safely assume significant deltaic advances of the Drini during the late Bronze Age, but we do not have any radiocarbon age estimates to track the Drini river's delta development in that time. Reasons for this will have been the intensive settling of coastal hilltops and low-elevated mountains during Bronze Age, causing an increased human impact on the natural vegetation and the slopes of the highlands. Thus, human-induced erosion became the dominant factor in shaping the landscape. A similar result dating to the late Bronze Age was reported from another coastal settlement, Butrint, in Southern Albania (Lean, 2004: 45).

8.5 6th century BC (Late Iron Age)

During the Iron Age, the most noteworthy point is the rapid advance of the Drini delta (fig. 62). The delta front had already passed coring sites LIS 24 and LIS 40 and the western part of the marine embayment was largely silted up. Thus the connection of the marine embayment and the corridor between Mali Rrenci and Mali Kakarriqi was cut off in the southeast. Also, the small marine embayment along the foot of Shite-Veles Mountains was cut off. Therefore, conditions at LIS 47 changed from marine environment to that of a brackish residual lake.

The size of the marine embayment had shrunk dramatically, with only a small bay to the north of Lissos remaining. The main distributaries of the Drini must have flowed in the area between the town of Balldreni and the northeasterly slope of Mali Rrenci during that time, because no coarse fluvial sediments can be found in corings LIS 48, LIS 52, LIS 25 and LIS 23. Clarification on the exact location of the palaeo-course of the Drini during that time can only be achieved by further drillings in the western part of the Merqia plain. At this point it is worthy to note that, despite being the lowest part of the Merqia plain, the river never seem to have flowed through it. A possible explanation for this curiosity may be later local subsidence tectonics, or that the Drini kept its course within the continuously raised levees.

The reason of the rapid delta evolution can be related to increasing human activities in the area due to the changing economic structure and settlement patterns since the late Bronze Age, when the typical settlement pattern in the area was that of fortified towns on coastal hills and mountainous terrain near good pasture land, fertile fields and water resources (Korkuti, 1983: 9; Jacques, 1995). Hence, the hills and mountains close to coast between Shkoder and Lezha were

settled intensively (e.g., at Gajtan near Shkodra, at Shtoj and Nenshat between Shkodra and Lezha) (Korkuti, 1988: 6). During the 8th century BC, a fortified settlement existed on top of Mali Shelbuemit. Such intensified human activities in the highlands may have played a major role in contributing to increased erosion rates, probably by causing degradation of the natural vegetation.

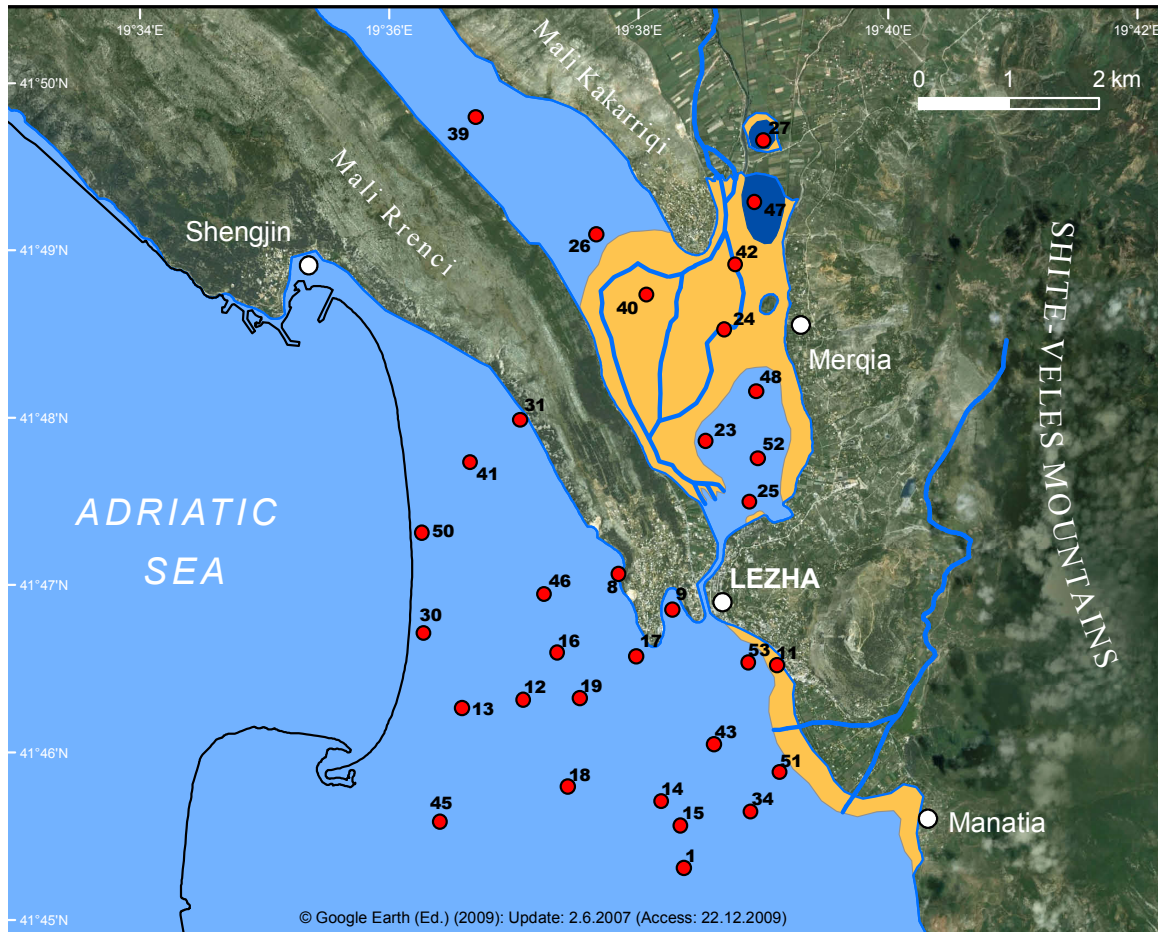


Figure 62: Palaeogeographic scenario for the research area during the Late Iron Age (6th century) (Uncu, 2010, based on a satellite image from Google Earth, accessed 22-12-2009).

8.6 4th century BC (Hellenistic period)

The palaeogeographic scenario for this period is crucial because there appears to be a slight discrepancy between ancient sources and archaeological results, particularly in terms of the harbour situation (fig. 63). By applying geoarchaeological methods, we are trying to shed light on this problem.

The transect E-E' can be used to achieve this aim. A radiocarbon age from fluvial deposits of coring LIS 29 dates to the 5th to 3rd centuries BC (508-209 cal. BC), a rather long period of time and therefore imprecise. This age estimation, obtained from a grape seed, contains the whole of the Hellenistic period, including the foundation of the city in 385/4 BC. The date together with abundant ceramic fragments points to a deposition of the fluvial sediments in front of the 'Hellenistic harbour gate' during Hellenistic to Roman times. This result is rather unsatisfactory, as it does not really solve the debate about the type and location of Lissos' harbour.

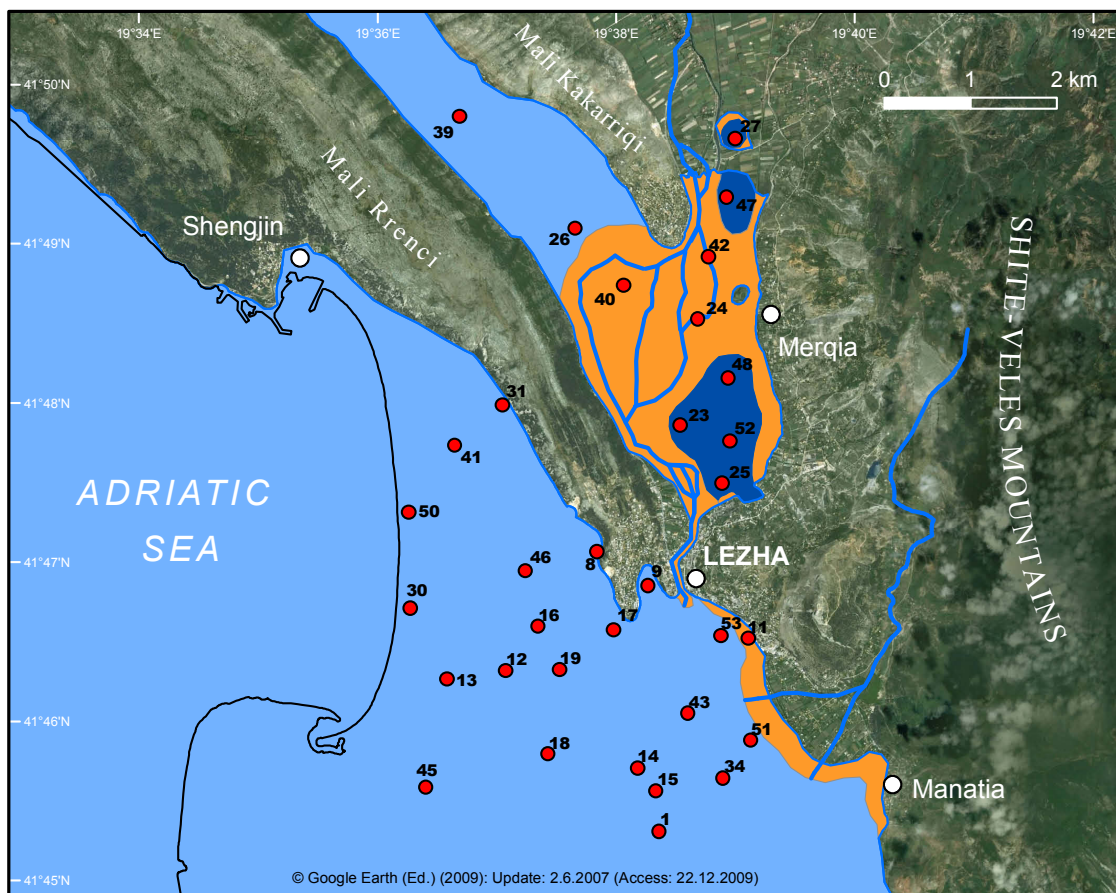


Figure 63: Palaeogeographic scenario for the research area during Hellenistic period (4th century BC) (Uncu, 2010, based on a satellite image from Google Earth, accessed 22-12-2009).

Sedimentological evidence supports the idea of the delta passing the narrow rocky gap to progress beyond Lissos possibly as early as the 4th century BC (fig. 63). Further evidence for the river having already passed the gap at Lissos in Hellenistic times comes from the core LIS 38, which is located in the SW corner of the Skanderbeg Monument. A thick cultural layer, dating from the early Hellenistic period at the base to modern times towards the top lies on top of deltaic deposits, thereby showing that the delta had already been past this point. However, the coastline must have still been very close to the Hellenistic city, and its harbour was easily

reachable *via* the river mouth from the sea. It appears as though the development of the Drini delta ceased around the time when the city was founded. This happened because the main river course of the Drini switched to join the Buna River in the north. This resulted in a crucial drop of sediment supply, halting the progradation of the delta, and probably leading to erosion along the coast similar to today.

8.7 Around 200 AD (Roman Imperial times)

The corings making up transects C-C', E-E' and G-G' as well as ancient sources help to understand the palaeo-landscapes around Lissos and the coastal configuration around the Drini delta during Roman times (fig. 64). Corings LIS 23, LIS 25, LIS 52, and LIS 48 show that directly north of Lissos, a large residual lake existed in the eastern part of the former marine embayment (similar to Lake Bafa in the Büyük Menderes delta, Turkey; cf. Brückner et al., 2006). It is noteworthy that this has not been mentioned by ancient sources. The lack of coarse sediment in this area may probably indicate that there was no direct fluvial influence. Sources from Roman times hint at a changing harbour situation of ancient Lissus during Roman times (see chapter 4; note that in Roman times the city's name was Lissus). Maybe the harbour activities in Lissus could not be sustained during the second half of the 1st century BC, due to the increased sediment load carried by the river. The change of the Drini's main course may have led to a lack of water in the harbour or downstream of it. In any case, the main harbour of the city was moved to Nymphaeum (present-day Shengjin) in 48 BC.

As just mentioned, the Drini must have changed its main course from flowing past Lissus to flowing north into the Buna River in Hellenistic to Early Roman times. It apparently switched back to its old course past Lissus during Roman Imperial times, thereby, at least in terms of discharge, making Lissus easily accessible from the sea once again. However, more water also meant more sediment, which may have caused considerable problems for navigation.

It seems that the Drini mainly developed its delta towards the south (LIS 43) during Roman Imperial times. The shoreline must have moved south by about 1.5 km beyond the narrow gap at Lissus during the second half of the 1st century AD. However, marine conditions still existed in the embayment where coring LIS 09 was taken, nearby the city (today: Lezha swamp). Coring LIS 53 suggests that marine conditions also existed between the eastern edge of the newly developed delta plain and the Manatia alluvial fan during the first half of the 1st century AD.

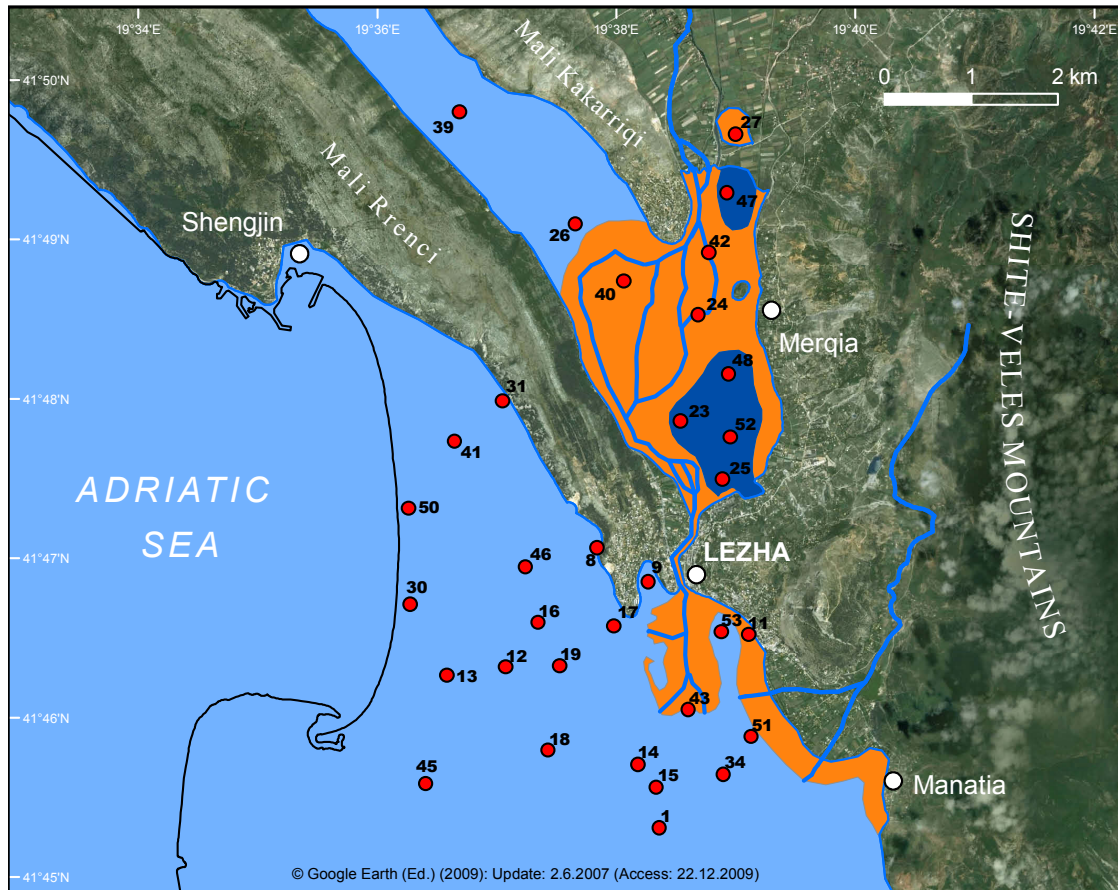


Figure 64: Palaeogeographic scenario for the research area around 200 AD (Roman Imperial times) (Uncu, 2010, based on a satellite image from Google Earth, accessed 22-12-2009).

During Roman times the landscape changes around Lezha were not only caused by natural agents such as changing river courses, but also by intensive human impact. The forests of the Drini valley and the highlands were one of the most important timber sources for Roman ship building. The slopes of the coastal hills were used for wine production (see chapter 3.3). Both these factors led to widespread forest clearances; thus, human-induced erosion resulted in a rapid delta development.

8.8 Discussion of harbour situation in Hellenistic to Roman times

In the early 1970s, Albanian archaeologists unearthed foundation stones of one of the main gates to the lower city of Lissos (Prendi & Zheku, 1972). Since this gate faces west, i.e. the direction of the present course of the Drini, the archaeologists called it “West Gate” or “Hellenistic Harbour Gate”, although there has not yet been any definite proof that it was indeed a gate to the city’s harbour. The apparent discrepancies between archaeological evidence and

historical sources concerning the harbour situation may be solved by using geoarchaeological data from our studies.

8.8.1 Written sources and historical accounts

There are several references, direct and indirect ones, depicting Lissos as a harbour city (May, 1946: 54; Wilkes, 1969; Pochmarski & Hoxha, 2005: 248). However, it is not yet clear for archaeologists and historians alike, whether Lissos's harbour was a seaport or a river harbour. Von Hahn (1853) discussed this problem by using the descriptions of ancient authors. In subsequent debates, scholars developed their arguments mainly based on Hahn's comments (Ippen, 1907a; Praschniker & Schoeber, 1919; Nopcsa, 1929a; May, 1946). It seems as though different authors have interpreted available primary sources from Roman times (e.g., Caesar's *Bellum Civile*) as well as von Hahn's contribution in various ways. For example, some say that according to Julius Caesar, Lissus was a seaport (Praschniker & Schoeber, 1919: 17), while others state that Caesar made a clear distinction between the port at Shengjin (Nymphaeum) and the one at Lissus (May, 1946: 54). Therefore, particular care must be taken when evaluating secondary sources, and preference should be given to the original historical accounts (or their direct translations).

In only two references do we find the name Lissos mentioned as being a naval base on the Adriatic Sea. The first reference comes from Greek historian Diodorus Siculus, who describes of the foundation of Lissos by "Syracusans" (Diod. Sic., 15, 13, 5). The other one comes from historian Polybios, who states that during the First Roman-Macedonian War, Philip V of Macedon captured Lissus, thereby obtaining a naval base in 213 BC (Polybios, Histories, 8, 13).

We have more detailed information about the harbour situation of Lissos during Roman times. Caesar notes in his *Bellum civile* that during the Civil War between himself and Pompey, both pontons (*pontones* = a type of Gallic ships) and large vessels (*naves onearariae*) were left at Lissus in 48 BC (*Bel. Civ.*, 3, 29, 3; cf. 3, 40, 5), thereby implying that the port must have had a certain size to be able to give refuge to such an amount of vessels. He mentions also the name of Nymphaeum as a perfectly safe harbour (*tutissimus portus*) at three Roman miles (ca. 4.5 km) away from Lissus (*Bel. Civ.*, 3, 26, 9). When comparing his remarks with Pliny the Elder's, it becomes clear that 'Nymphaeum' must be present-day Shengjin (Pliny, *N. H.*, 3, XXIII).

Von Hahn (1853) believes that Caesar regarded Lissus and Nymphaeum as two distinct harbours. According to him, Lissus's harbour must have been big enough for battle ships and at

a short distance to the south of the city; its definite site was probably later buried by alluvium of the Drini (von Hahn, 1853: 93).

Appian (*Bel. Civ.*, 5, 65) describes “a second city lay south of Scodra at Lissus near the mouth of the Drilo, where an impressive circuit of walls protected the citadel and the harbour on the river” (Wilkes, 1969: 184), and in so doing he supports the theory of distinctly different harbour sites: one on the river at/near Lissus (earlier), and one at Shengjin (seaport, later).

However, Wilkes (1969: 498), interpreting May’s accounts (1946), states that a river harbour at Lissus could not have existed in Roman times, because the main discharge of the Drini flowed north, into the Buna river. This interpretation is supported by the accounts of other authors. Strabo reports that the river Drilo (ancient name for Drini) was navigable for a certain distance inland towards the east as far as the Dardanian country (today: area in Macedonia) (*Geography*, 7, 5, 7, 316). Livy also states that the Oriundes (probably: Drini) was connected with the Barbanna river (probably: Buna) (Livy, *The history of Rome*, 6. 44. 31).

The primary sources seem to indicate that, during the second half of the 1st century BC and beginning of the 1st century AD, the Drini River was further away from Lissus, using the course near Shkodra before reaching the sea. This means that there could not have been enough water for navigation upstream to Lissus. At this point, the harbour discussion encounters a new problem: Was the harbour shifted to Nymphaeum because of the silting-up of the port at Lissus, or because of a lack of water? The chronological order of events – i.e. when did the Drini change its course so dramatically, and at what time, seen in relation to the previous occurrence, was the harbour then shifted – also needs to be answered.

8.8.2 Geoarchaeological evidence

Our geoarchaeological research results can hopefully contribute to a solution for this debate. The transect E-E’, carried out between the Hellenistic Harbour Gate and the Drini River, as well as other corings in the lower city helped to clarify the situation of Lissos’s harbour during Hellenistic and Roman times (see chapter 7.4.2).

First it can be stated that marine conditions occurred in this area during the Holocene transgression maximum. The sediments in the lower part of all cores indicate the existence of a marine embayment around Lezha during that time. Our corings in the Merqia plain suggest that marine conditions prevailed during the Neolithic and entire Iron Age.

Sedimentological analyses and radiocarbon dates indicate that the connection with the sea had ceased to exist in the 4th century BC, approximately at the time when Lissos was founded. This option would cause a disagreement with the ancient sources. However, the lack of any Hellenistic (or earlier) ceramic fragments or cultural remains within the marine deposits can only be interpreted in two ways: (i) large parts of the marine deposits which would have contained Hellenistic or earlier ceramics were eroded by the Drini, or (ii) the river Drini had already passed the narrow gap between Mali Rrenci and the Lower City of Lissos before Hellenistic times. The latter argument would also point to the existence of a river harbour and explain why we found cultural remains from Hellenistic and Roman times only within the fluvial deposits.

Transect E-E' gives further proof of the palaeo-topography for why settlers would have chosen this area as harbour location. A promontory, extending towards the west was protecting these coring sites from direct influence of the Drini. This promontory can also be seen on the first archaeological plan of Lissos (Praschniker & Schoeber, 1919). In fact, one of the major gates of Lissos was built there because of its easy accessibility from the sea *via* the river course.

8.9 10th century AD (Early Medieval times)

During late Antiquity and early Medieval times, the landscape around Lezha changed considerably (fig. 65). The lake in the north of the Merqia Plain (coring site LIS 47) had already turned from brackish to freshwater during late Antiquity. In the corridor between Mali Rrenci and Mali Kakarriqi, however, brackish conditions prevailed during the early Medieval period.

The large brackish residual lake directly north of Lissos still existed during the first centuries of the early Medieval period. A coarse sandy layer at coring LIS 23 indicates a short-time influence of the Drini around the 8th century AD. There is no dating from other cores in the eastern part of the Merqia plain, but the increasing numbers of land-snails towards the top of the brackish sediment (ca. 2 m b.s.l.) suggest that the brackish conditions changed to freshwater in the whole area around the 8th century AD.

The delta evolution of the Drini can be explained with the help of the transect G-G'. During late Antiquity and early Medieval times, one of the (main?) distributaries of the Drini was flowing across coring site LIS 43. It seems that the conditions in the marine embayment between the Drini delta and Shite-Veles Mountains changed to brackish due to occasional freshwater input by the Grykes River, which is also forming the Manatia alluvial fan. Some thin pebbly layers in coring LIS 53 support this idea. However, the coarse grain size in coring LIS 34 suggests that

the main channel of the Grykes was in the central part of the alluvial fan. Periodical influence of the Grykes River can also be seen at LIS 01, the coring site farthest away from the Drini.

Thick river channel deposits in core LIS 14 were probably deposited by a distributary of the Drini. This channel might be the southwestern continuation of the river course detected in core LIS 43. A ^{14}C age estimate shows that the river channel reached coring site LIS 14 around the 9th century. Another radiocarbon dating from LIS 15 suggests that brackish conditions changed to freshwater during the 9th-10th centuries. The fine grain size and fossil content in core LIS 15 suggest the establishment of lagoonal (brackish) conditions between the previously mentioned distributaries of the Drini and Grykes rivers.

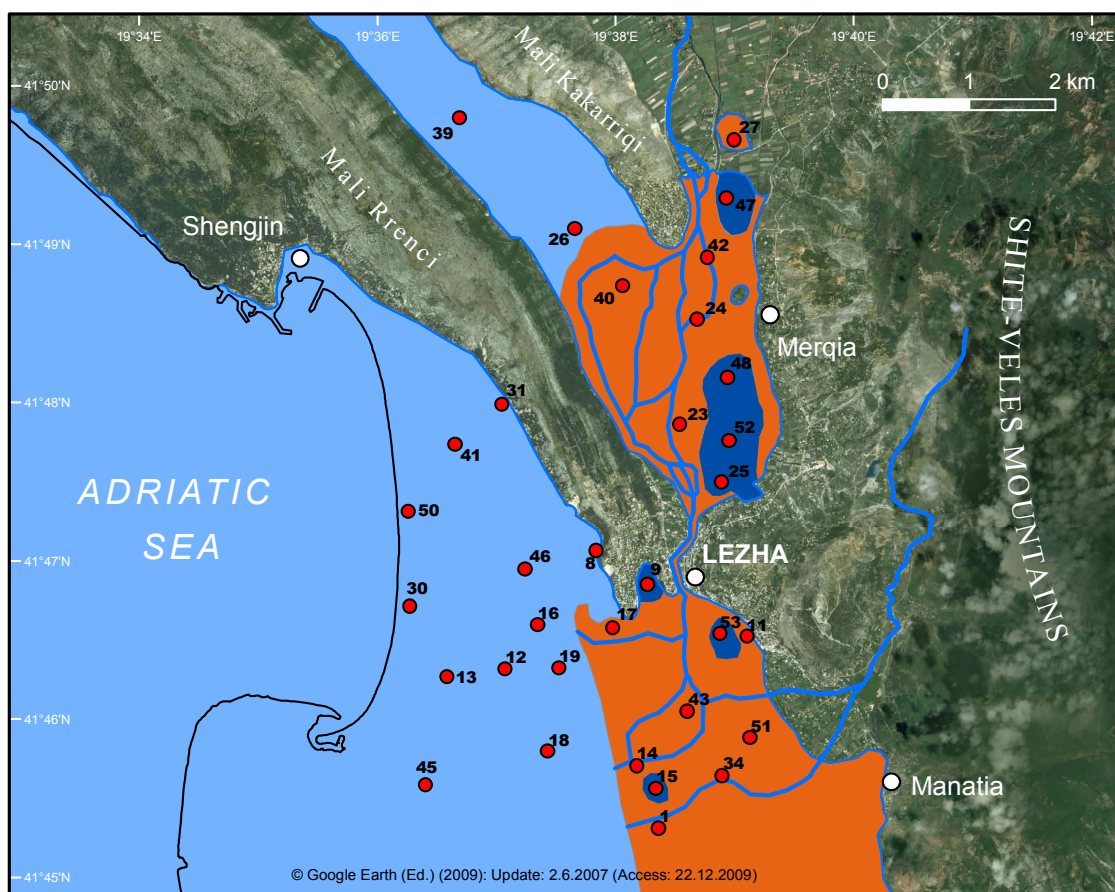


Figure 65: Palaeogeographic scenario for the research area during the 10th century AD (Early Medieval times) (Uncu, 2010, based on a satellite image from Google Earth, accessed 22-12-2009).

It seems that a beach barrier – lagoon system similar to the present-day coastal configuration must have developed during the 8th-9th centuries AD. This is supported by another ^{14}C age estimate taken from the coring at the foot of Mali Rrenci (LIS 17), which indicates the environmental change from shallow marine to sublittoral conditions during the 8th-9th centuries. This would mean that, during early Medieval times, the delta evolution of the Drini was largely

controlled by longshore drift and sediment supply from other rivers, e.g., the Mati River in the south.

We do not have detailed historical accounts about the situation of the city and its harbour during early Medieval times. The harbour in the city was still reachable from the sea *via* the river, but it seems that the city lost its military and commercial importance during that time. This may be connected with the political instability and most likely the establishment of large swampy environments around the city. Thus, malaria and other diseases may have become a big problem.

8.10 Ca. 1500 AD (Late Medieval times)

The sedimentological analyses and the radiocarbon age estimates obtained from the corings in the Ishull Shengjin Region show that significant changes in the landscape occurred between the 10th and 15th centuries (fig. 66).

The residual lakes at coring site LIS 47 and directly north of Lissos still existed throughout this period. The former marine corridor between Mali Rrenci and Mali Kakarriqi evolved into a freshwater lake during 11th-12th centuries due to the strong freshwater input by karstic sources.

The sublittoral sands found in LIS 12 and LIS 18 suggest the establishment of a beach barrier – lagoon system around the 11th century. However, thick river channel deposits from coring LIS 18 indicate that one of the distributaries of the Drini reached this location around the 12th century or later.

Another interesting dating comes from the bottom of a buried paralic peat layer at coring LIS 50. It suggests that the peat began to form on the landward side of a beach – barrier system during the 11th-12th centuries. This means that the present-day Shengjin sand spit must have formed during that time. Pebbly layers in the lowermost part of this core indicate that a palaeo-channel of the Drini was not far away, depositing large amounts of sediment. It appears most likely that, north of this coring site, a multi-curved spit system, such as the one which can be observed at the mouth of the Drini today, developed.

Thick river channel deposits in the middle part of the cores LIS 16 and LIS 46 support the theory of a palaeo-channel in this region, but there are no age estimates available. Traces of this channel are visible on satellite images even today.

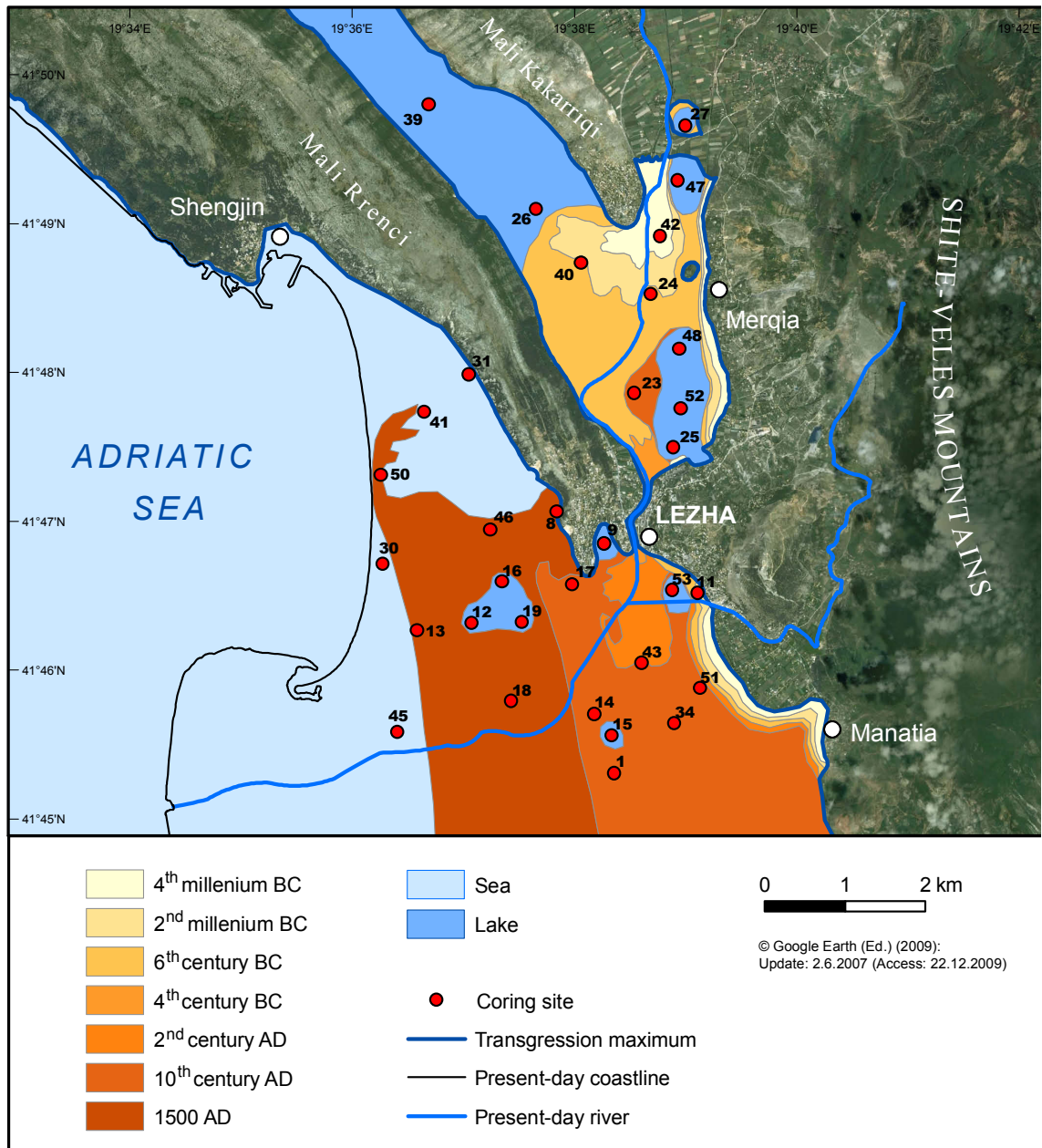


Figure 66: Palaeogeographic scenario for the research area during around 1500 AD (Late Medieval times) (Uncu, 2010, based on a satellite image from Google Earth, accessed 22-12-2009).

Marine conditions at the southwestern foot of Mali Rrenci changed from sub-littoral to coastal swamp with the formation of a thick peat layer in the mid-13th century (as shown in LIS 8). LIS 31, the northernmost coring location in the Ishull Shengjin Region indicates that marine conditions prevailed until the 14th or 15th century AD.

Results from the sedimentological and microfaunal analyses point to the establishment of a large freshwater lake at coring sites LIS 19, LIS 12 and LIS 16 around the 14th century. Brackish conditions in the Lezha swamp (LIS 09) seem to have lasted a little longer, before it, too, turned to freshwater/limnic, probably due to karstic sources.

It seems that the deltaic development was rapid during medieval times. This can be explained with the continuous socio-economic instability since early Medieval times. Especially, political insecurity and invasions led to migration of the people to the safer highlands, which were previously forested areas. These population movements and changing land use pattern must have been the major reason for increased soil erosion and therefore the high sedimentation rates during that time.

Importantly, due to the rapidly advancing delta of the Drini, Alessio (by then the contemporary name for Lezha) seems to be further and further away from the coastline. Many documents from the medieval times talk about the city serving as a river harbour for transportation from the sea to the interior, whereas Shengjin is mentioned as the sea harbour of Alessio and Shkodra (von Hahn, 1853). The fact that the harbour in Shengjin has been mentioned far more often in the records and maps (e.g., “*portus Medue*” of 1336, “*Miedua, portus Alesii*” in the records from Republic of Ragusa of 1414, “*Medoca*” on the map of Italian Benincasa of 1476 and San Giovanni di Medua) indicates that it became the most important harbour for the traders (Jireček, 1916).

8.11 From 1500 AD to present

Despite no dating being available for the following centuries, the landscape changes around Lezha and the river Drini can be traced using information from cartographic sources, as well as reports and documents from travellers since the 16th century. Elsie (2003) published a number of historical texts about Medieval Albania which contain descriptions about the landscape around Lezha, its harbour situation and the delta development of the Drini River. Nopcsa (1916, 1929b) published a comprehensive collection of maps of North Albania, thereby making important information concerning coastline changes and shifting river courses available (see table 9).

The present-day Drini delta is divided into two sections: Ishull Lezha (Island of Lezha) and Ishull Shengjin (Island of Shengjin). The names may appear strange because one does not see any islands today. However, the existence of a big island (approximately 13 km²), situated some

kilometres south of Lezha, is described in Venetian documents from the beginning of the 16th century. When the Turks captured Lezha in 1478, some people escaped to this island and settled there until the Venetian rulers handed over this island to the Turks in 1506 (Kabo, 1988: 15).

Date	Author and source	Description of Lezha and its surroundings
1318	The Portolan of Petrus Vesconte	The Drini flows through Alessio (medieval name for Lezha) before reaching the sea. By then, there is no connection with the Bojana anymore.
1545	Valvassorius Vadaginus “Totius Graeciae description”	The mouth of the Drini was north of Alessio (Lezha). However, this book may not be too reliable, because Scutari (Shkodra) is erroneously placed south of the Drini.
1548	Mattioli & Gastaldi, Atlas of Ptolemy, Venice	The Drini with two branches debouching into the gulf south of Alessio.
1560	G. Gastaldi, Carta della Graecia	The author shows a settlement between the two branches close to the sea; however, he does not name it.
1571	Camotio, Isole e fortessa, Venezia	The map depicts a large lake which is named “Paluda Charigi” (Charigi Swamps) between the Mali Rrenci and the Mali Kakarriqi. This lake (present-day Balldreni plain) is fed by two small lakes in the west and it was connected with the Drini through the swamps in the SE.
1589	The Mercator Atlas	It shows a deep marine indentation, reaching north of Alessio .
1593	C. Jode, Speculum Orbis terrarum, Antwerpen	The first to show a connection between the Lake Scutari (Shkodra) and the Drini <i>via</i> the “Barbana” river.
1667	Sanson, Cartes generales, Paris	The Drilo (Drini) flowing due south, passing Lissos (Lezha). There is no connection with Lake Scodra (Shkodra) any more. The Barbana is shown north of Lake Scodra (Shkodra).
1691	Coronelli, Atlante Veneto	The shoreline is placed south of Alessio (Lezha), the city itself is situated between the Drini (? , no name is given) and another river, the lower course of which is flowing parallel to it east of Alessio (River Gyrikes?).
1707	De L’Isle, Atlas	It shows no connection between Lake Skutari and Buna (no name is given) on the one hand and the river Drin (Drini) on the other. The Drin (Drini) is featured with two distributaries west of Alessio (Lezha) for the first time.
ca. 1718	Manuscript of das Bergland von Alessio, Kriegsarchiv, Wien	The Drini has two distributaries flowing through Alessio: One of them to the west and the other one in a southern direction.
1740	Seutter, Novus Atlas, Augsburg	The Gulf of Drini is depicted larger than before and the sea is shown close to Alessio.
1744	Homan-Hasius, Atlas Compidarius	Same as Seutter’s atlas.
1762	D’Anville, Atlas	The Drini has two river mouths close to Alessio.
1793	Maire, Carte generale, Wien, 2 nd edition	The Drini debouches into the sea <i>via</i> Alessio, and Lake Balldrini has a connection with the river Bojana (Buna).
1801	Chanlaire, Atlas	The Drini has many small distributaries at its mouth and is connected with the river Mati.
1812	Riedel, Generalkarte	The Drini has one mouth south of Alessio.
1822	Lapie, Turquie d’Europe	The Drini flows through Alessio and has one river mouth.
1867	Hahn & Kiepert, “Reise durch die Gebiete des Drini und Vardar”, Wien	The map shows a main river channel direction to Alessio. The Drini reaches to the sea in two arms starting from Alessio. The connection between the Drini and the Bojana Rivers <i>via</i> the Barbana junction is shown for the first time in this map.
1897	K. Hassert, Reiseweg von Dr. Hassert in Ober-Albanien	The Drini debouches into the sea from Alessio. It has a connection with the river Bojana <i>via</i> Drinasa (Barbana junction).
1899	Türkische Generalkarte von Mitteleuropa (scale 1:300,000)	The Drini has two mouths and is connected with the Bojana (Buna) <i>via</i> the Barbana junction. The Kneti Balldrini (Balldreni swamp) has a connection with the Bojana from the NW.
1914	Übersichtskarte von Mitteleuropa (scale 1: 75,000)	The main course of the Drini joins the river Bojana (Buna).

Table 9: Lezha and its surroundings as it appears on historical maps (L. Uncu, 2010, adapted from Nopcsa, 1916, 1929b).

The youngest part of the Drini delta was advancing westwards in the following centuries. However, former Drini courses towards the north and southwest were still temporarily active. It seems that the Drini carried enough sediment to continue its delta progradation during the Turkish period. Socio-economic changes (e.g., migration of the Christian groups from coastal areas to the highlands in the hinterland) and more intensive human activities (e.g., foundation of so-called çiftliks, i.e., large farms) probably led to widespread soil erosion within the Drini's catchment area.

Historical accounts and maps both indicate that the Drini was debouching into the sea near Lezha during the 16th century. The oldest map of Mattioli & Gastaldi of 1548 shows the river mouth in the south of Lezha with two branches. There was also a settlement between the two distributaries.

The existence of two main branches of the Drini is also reported by Anonymous in 1570. This report describes that the town of Alessio (Lezha) is situated on the banks of the Drino (Drini) River, three miles (ca. 4.5 km) from the sea, and flows westwards into the sea in two outlets, above four miles from one another (cf. Elsie, 2003). We learn also about the existence of two harbours in the north of Lezha, because Elsie (2003: 59) writes “... *at the upper outlet of the said river, to the north, there are two harbours, one called S. Zuanne della Medoa (St. John of Medua / Shengjin) three miles north of the said outlet, and the other called Sacca (Saka) which is to the south*“. This port called “Sacca” must be present-day Lake Kënalles on the road to Shengjin.

The two branches and the landscape of the Drini delta plain were described by the Venetian ambassador Lorenzo Bernardo in 1591 as follows: “...*below Lezha, it [Drini] divides into two navigable channels which flow into the sea at the gulf called Lodrino after the river, one being three miles from the other. The two branches form an island with fair and fertile fields which is said to have been the site of Lezha when it was ruled by our lords of Venice who sent the lord inspectors.The river flows slowly and has low banks, part of which for a mile and a half towards the sea are marshy and covered in reeds. At other parts, the boats can be hauled by ropes, as is done elsewhere, if one removes the logs in the way, which for the most part are from willow trees* (Elsie, 2003: 71-72).

Lorenzo Bernardo's description of the landscape in the southern part of Lezha can be supporting evidence for the marine indentation shown on the Mercator Atlas from 1589. He wrote that “...*outside of Lezha, we took the road southwards and about half a mile further on, we came upon water which was flooding the road at many points because the land is lower here. They*

said that there is always water here and it reaches the height of a horse's knees. We continued onwards for about a mile and entered a pleasant and not very dense forest of mostly ash and poplar trees" (Elsie, 2003: 72). The ingression can be an indication for co-seismic subsidence in the area, however, it is too vague and no further evidence exists so far.



Figure 67: Old maps from north Albania showing the shifting river courses of the Drini [top left: map by Jode (1593) in Nopcsa 1929b, p. 665, fig. 166; top right: map by Sanson (1667) in Nopcsa, 1929b, p. 666, fig. 167; bottom left: map by Hahn & Kiepert (1867) in Nopcsa 1929b, p. 692, fig. 187; bottom right: Übersichtskarte von Mitteleuropa (1914) in Nopcsa 1929b, p. 696, fig. 189].

C. Jode's map from 1593 shows for the first time a connection between Lake Scutari (Lake Shkodra) and the Drini River via the "Barbanna" (see fig. 67). However, Italian Mario Bizzi, Archbishop of Bari visited Albania in 1610 and reports that the river was flowing into the sea near Lezha with two branches, forming an island with of all sorts of trees (Elsie, 2003: 89). This suggests that the Drini had been changing its course continuously.

The torrential discharge characteristics of the Drini were described by the Albanian Bishop Frang Bardhi in 1641. He wrote that “*The river Drin causes just as much damage to the people of the flat land of Zadrima as the Turks, because, stemming from the border with Serbia, it flows down, making its way through the mountains of Dukagjini and Pult in the Albanian highlands. From time to time it overflows, in the winter from the great amount of precipitation and in spring from the melting of ice and snow in the mountains. It flows precipitously with great force into the valley and fields of Zadrima, covering them completely. Then it continues down through the valley, touching the walls of the ancient city of Lezha and enters the Adriatic Sea, two miles away from the town, taking with it the fertile land and soil of the said fields. At the present moment, it has left its ancient bed in the valley of As... (?) on the western side of the diocese of Shkodra, and has entered the territory of Zadrima where it has destroyed over 150 houses of the faithful and of the infidels at Upper and Lower Mietti (Mjeda), and at the ford of Dagno (Deja), a ruined town, which will be referred to below. It has laid waste to over twenty thousand ploughing days of valuable land, which produces annually every type of fruit on could imagine and every plant and seed. Now the land is covered in sand and mud, to the great detriment of its owners and cultivators.*” (Elsie, 2003: 183-184).

It seems that the Drini had several dramatic flooding events between the end of the 16th and the first half of the 17th century. This is possibly a reflection of the humid and wet climatic conditions in the European part of the Mediterranean during the Little Ice Age. Extreme floods and rapid delta progradation have been well documented in the records from the western to the central Mediterranean during this time (Grove, 2001).

The historical sources show that the Drini was again flowing in a southerly direction after 1660. In his book “*Seyahatname*”, Turkish traveller Evliya Çelebi of 1662, wrote that the Drini flows into the sea near the Sincivan Limanı (Port of Shengjin) (Dankoff & Elsie, 2000: 29). The map from Sanson (1667) supports Çelebi’s accounts; no connection with the Barbanna is shown on his map (see fig. 67).

It is interesting to see that the mouth of the Drini was mapped with few distributaries in the south of Lezha during the entire 17th until the middle of the 19th century. It was during that time when the river must have flown in a predominantly westerly direction. Von Hahn (1853: 94) reports that ships carrying 40-50 tons were able to navigate a further 3 hours upstream from Les (Lezha). This means that the main course of the Drini was still flowing through Lezha.

Due to the splitting up of the river into two distributary branches at Vau Dejes in the winter of 1858/59, and the associated reduction in discharge, the Drini lost importance as a transport route to Lezha (Ippen, 1907a: 53). This situation was mapped in 1867 by von Hahn & Kiepert (fig. 67). The Drini used mainly the distributary flowing towards the Buna River in the north until the end of the 19th century, when a Turkish military map from 1899 shows that the main river course had shifted back again to the south.

It seems that the Drini kept its course through Lezha until 1958, when it was artificially connected with the Buna *via* the Drinassa. Since that time, two thirds of its water is flowing down to the Buna and only one third through Lezha. Therefore, the delta development has changed dramatically after the end-1950s. The formerly river-controlled delta progradation is replaced by a wave-dominated one with the result of a receding coastline due to the lack of sediment supply. The latter is caused by: diversion of the Drini to the Buna catchment in 1958; building of reservoirs which trap the sediment; secular sea-level rise; compaction of delta sediments; subsidence tectonics. For further detailed information on the present-day situation, see the respective passage in the geomorphology section (chapter 2.3.3.4).

9 Relative sea level changes

The shoreline is the triple interface between ocean, land and atmosphere. Its position is interdependent with sea level, varying considerably both in time and space during the Earth's history. The Quaternary period is known particularly for fluctuating sea levels worldwide. Causes and consequences of sea level fluctuations have been discussed by many scientists, first with applied field methods and later also with theoretical modelling (e.g., Tooley & Shennan, 1987; Pirazzoli, 1991, 1996). The results of these discussions show that the sea level is controlled by many factors, including eustasy, isostasy, and tectonics. However, at a regional scale, research indicates that the sea level depends mainly on local, possibly small-scale tectonic processes (subsidence, uplift, tilting) and sediment compaction (Pirazzoli, 1996; Lambeck et al., 2004b; Brückner et al., 2010).

During LGM, approximately 21,500 yrs BP (= 18,000 ^{14}C -years BP), worldwide sea levels reached a lowstand at around 90-150 m below its present level (Shackleton, 1987; Fairbanks, 1989; Stanley 1995; Pirazzoli, 1991, 1996). The mean sea level of the Mediterranean Sea was about 120 m (± 20 m) below its present position (Pirazzoli, 1991). Around 18,000 yrs BP, the sea level first started rising at a rate of 5 mm/yr (Perissoratis & Conispoliatis, 2003: 146); due to a general warming trend between 15,000 and 8,000 yrs BP, it rose more rapidly, though with some oscillations such as the Younger Dryas cold period (12,800 to 11,500 years ago). Since ca. 8,000 yrs BP, sea level has largely kept its position, although some sea level reconstructions exhibit small falls or a continuous slow rise during the middle to late Holocene. Major oscillation, directed by climatic and tectonic processes, should be recorded in coastal geoarchives with a fair resolution, such as deltas and floodplains.

9.1 Indicators of sea level change

Former sea level positions are determined by using biological, geomorphological, and archaeological indicators in the field (van de Plassche, 1986; Pirazzoli, 1991, 1996, 2005b; Kelletat, 2005a; Brückner et al., 2010).

(a) Biological indicators include both bio-erosional notches and bio-construction features (Laborel, 1986; Laborel & Laborel-Deguen, 1994, 2005; Morhange et al., 2005; Pirazzoli, 2005b). Specific microfaunal records from buried paralic peats and from salt marshes are also useful for the determination of former sea levels (van de Plassche, 1986; Pirazzoli, 1991; Gehrels, 2005; Marriner & Morhange, 2006). In some places, submerged forests, mangroves,

and diatom assemblages can be used as sea level indicators as well (Heyworth, 1986; Pirazzoli, 1991: 15).

(b) Some geomorphological features are preserved on hard rock, such as tidal notches, benches, abrasional platforms and terraces, pools, and sea caves. They are excellent erosional indicators, not only for sea level but also for local tectonics (Pirazzoli, 2005b: 836). Depositional indicators are tidal flats, marine terraces, beaches and beachrock (Pirazzoli, 2005b).

An excellent indicator for neotectonics is the so-called MIS 5.5 marine terrace which is said to be at an elevation of ca. 4 m a.s.l. glacio-eustatically at a tectonically “stable” coast (cf. Pirazzoli, 1991). The MIS 5.5 terrace (~125 kyr BP) occurs in many places on the Tyrrhenian side of Italy, often at altitudes of 4 to 10 m (max.: 175 m in Southern Calabria), and at 4 to 30 m a.p.s.l. in Apulia (Egnazia). In cores from the central northern Adriatic, beach sands, attributed to MIS 5.5 terrace were found at depths of 100 to 120 m b.p.s.l. (Amorosi et al., 1999; Lambeck et al., 2004a). As for Albania, the situation is totally different: no MIS 5.5 terrace has ever been detected along the Adriatic coastline of Albania; this is strong evidence that the coasts of the eastern Adriatic are subject to continuous subsidence.

(c) Sedimentological indicators can be determined using data from geological corings as well as geomorphological observations. The topset/foreset contact of a Gilbert type delta, the top of a lagoonal sediment body in a totally filled-in lagoon and a river-mouth terrace can indicate a former sea level (Brückner et al., 2010).

(d) Archaeological indicators such as harbour installations, Roman fish ponds, drowned architectural remains, and information from historical sources suggesting tectonic movements (uplift, submerged features) have been used for many years (Flemming, 1978; Flemming & Webb, 1986; Blackman, 1973, 2005).

The above mentioned sea level indicators are combined with data obtained using modern dating methods, such as radiocarbon (^{14}C), electron-spin resonance (ESR) and uranium series (TIMS U/Th), as well as data sets from gauge stations and remote sensing techniques (satellite geodesy), in order to establish a chronostratigraphy.

In addition to direct measurements, numeric models are used to generate retrospective reconstructions of former sea level fluctuations (Lambeck & Johnstone, 1995; Lambeck et al., 2004a, b; Lambeck & Purcell, 2005). Lambeck & Purcell (2005) developed their predictive model for the central Mediterranean using the sum of global (eustatic) and local factors (glacio-

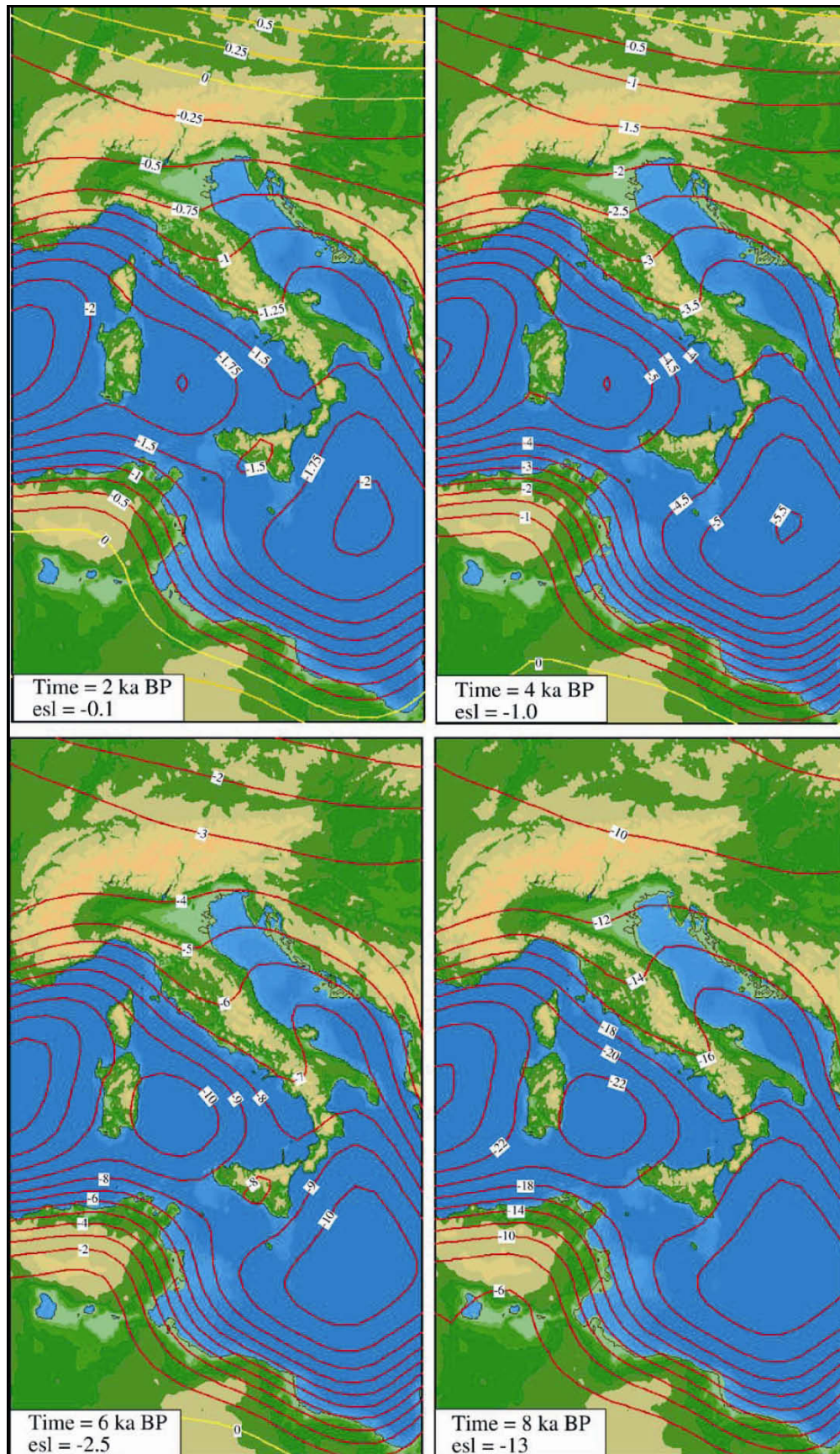


Figure 68: Palaeogeographic reconstructions of sea level positions for the central Mediterranean region for the time slices 8, 6, 4 and 2 ka BP. The red (negative) and yellow (zero and positive) contours refer to the sea level change. The ice-volume equivalent sea level (esl) values are given in metres (Lambeck et al., 2004b, p. 1593, fig. 12).

hydro-isostatic, tectonic). Lambeck et al. (2004b) calculated the position of the sea level of the Mediterranean for eight different epochs: 20, 16, 12, 10, 8, 6, 4 and 2 ka BP (see fig. 68).

9.2 Adriatic sea level changes during the Holocene

Late Quaternary sea level changes in the Mediterranean region with relative sea level curves from different locations are summarised in Pirazzoli (1987, 1991, 1996). Kelletat (2005a) recently published an idealised curve, originally derived from southern Greece and Crete, using different sea level indicators. However, as Pirazzoli (1991: 89) noted correctly, despite research on Holocene sea level changes along the Mediterranean having been numerous, the Adriatic coasts and some sections of the African coasts (e.g., Libya and Algeria) are only insufficiently explored. No sea level curve covering the Holocene period has yet been established for coastal Albania, partly due to the fact that research had been impossible until 1991.

The level of the Adriatic Sea is controlled by the sea level of the Mediterranean, which itself is closely connected to the world's oceans. The Adriatic Sea has a micro-tidal regime (Storms et al., 2008), which is beneficial to palaeo-sea level research. However, the variety of geological and environmental settings along the Adriatic coasts means that different factors have controlled relative sea level changes, e.g., local tectonics, sediment loading and compaction, as well as glacio-eustatic changes (Storms et al., 2008: 1109; Antonioli et al., 2009). Amorosi et al. (1999; cited by Storms et al., 2008) report an MIS 5.5 (Eemian) shoreline (ca. 125 ka BP) 60 km south of the recent Po delta at a depth of 120 m b.s.l. In this case, the combination of subsidence and compaction would result in an average sea level rise of ca. 1 m/ka.

The whole of the eastern Adriatic coast is subject to subsidence, resulting in a so-called "canale/vallone type coast", which is defined as a submerged folded mountain complex, where the ridges of the anticlines are above the water, often forming coast-parallel elongated islands, while the synclines are inundated, forming waterways like straight channels. Further definite proof for the subsidence trend are flooded speleothems (Surić et al., 2005) and underwater tidal notches (Fouache et al., 2000; Faivre & Fouache, 2003), as well as submerged archaeological sites along the coasts of Croatia (Fouache et al., 2000). For more detailed results from Fouache et al. (2000) and Faivre & Fouache (2003) see chapter 5.2.

The most current publication dealing with the Adriatic coast of Croatia gives an idea about former sea level positions, using submerged speleothems from different elevations as well as marine biogenic overgrowth (Surić et al., 2005). According to the ^{14}C ages from the islands of Pag, Brač, and Rogoznica, relative sea level was (i) -36 m at the Pleistocene/Holocene boundary

(10,185 cal BP); (ii) -34 m at 9,160 cal BP; (iii) -23 m (7,920 cal BP). These conclusions are based on the assumption that no tectonic adjustment of the coast has taken place (Surić et al., 2005: 174). The results suggest a rapid sea level rise during the early Holocene.

9.3 A relative sea level curve for northern Albania

The insufficient field observations in terms of palaeo-sea level indicators and the lack of data concerning measurements of local tectonics and subsidence rates along Albania's coasts have so far prevented the establishment of a sea level curve. In contrast to the Croatian and Italian coasts along the Adriatic Sea, two important types of palaeo-sea level indicators, namely geomorphological features (e.g., mostly submerged marine terraces, tidal notches, speleothems) and submerged archaeological remains from Roman times, are not found along Albanian coasts. However, it is worth mentioning that detailed coastal research along the coasts of Albanian started only about 10 years ago; therefore, many potential indicators may not yet have been unearthed or discovered.

Sample	Lab. Code	Depth (b.s.)	Depth (b.s.l.)	Material	$\delta^{13}\text{C}$ (‰)	14C Age (BP)	Calibrated Age (range $\pm 1\sigma$)
LIS 08/1H	Erl-10588	1.37-1.50	0.45-0.58	wood	-27.4	860 \pm 34 BP	1047-1259 cal AD
LIS 09/1Pf	Erl-10591	1.90-1.95	0.38-0.43	plant remains	-26.6	623 \pm 37 BP	1288-1401 cal AD
LIS 11/3T	Erl-10594	6.61	3.41	peat	-27.6	3512 \pm 39 BP	1941-1743 cal BC
LIS 24/14T	Erl-12042	6.61	3.28	peat	-26.5	3580 \pm 42 BP	2109-1775 cal BC
LIS 25/15H	Erl-12043	6.44	4.03	wood	-22.7	3569 \pm 42 BP	2030-1774 cal BC
LIS 28/24H	Erl-12050	7.62	6.14	wood	-23.6	4185 \pm 42 BP	2893-2633 cal BC
LIS 29/21T	Erl-12053	5.76	4.10	peat	-22.2	3409 \pm 42 BP	1878-1612 cal BC
LIS 35/23T	Erl-12057	5.63	4.01	peat	-23.4	3531 \pm 42 BP	1975-1746 cal BC
LIS 35/31T	Erl-12058	7.70	6.09	peat	-24.8	4096 \pm 42 BP	2870-2496 cal BC
LIS 38/23T	4163	7.80	3.86	peat	-26.1	3406 \pm 29 BP	1861-1624 cal BC
LIS 39/25T	4166	7.97-8.00	7.97-8.00	peat	-23.2	4560 \pm 28 BP	3485-3107 cal BC
LIS 40/26H	4168	10.79	7.83	wood	-26	4497 \pm 29 BP	3345-3096 cal BC
LIS 47/23T	4174	11.59	7.98	peat	-23.7	4490 \pm 29 BP	3348-3040 cal BC

Table 10: ^{14}C age estimates used for the construction of the sea level curve in fig. 70. Institute of Physics (Physikalisches Institut) at Erlangen, University of Erlangen-Nürnberg, Germany, and the Centre of Applied Isotope Studies (CAIS), University of Georgia, Athens, USA.

From the data of recent predictive modelling (Lambeck et al., 2004a; Lambeck & Purcell, 2005) it can be deduced that during the LGM (20 kyr BP), relative sea level was ca. 125-120 m below its present position along Albanian coasts. After a gradual rise, sea level reached -100 m around 16 kyr BP, then -50 to -45 m around 12 kyr BP, and -40 to -35 m at the Pleistocene/Holocene boundary (ca. 10 kyr BP). Holocene sea levels are calculated as -14 to -12 m around 8 kyr BP, -5 to -4 m around 6 kyr BP, -3 to -2.5 m around 4 kyr BP, and -1 to -0.75 m around 2 kyr BP (Lambeck et al., 2004a; see also fig. 68). In essence, their model proposes a continuous sea level rise since 20 kyr BP, though at different rates, reaching its highest position only recently. Detailed observations in NW Greece support this model prediction (Vött, 2007).

In general, it is difficult to find suitable (and datable) palaeo-sea level indicators for the study area. In total we used 13 ^{14}C -dated buried coastal peats and anthropogenic debris from our geological corings have been used to establish a chronology for relative sea level changes in North Albania (see table 10). However, the lack of data concerning the effects and rates of tectonic subsidence, sediment compaction, as well as the technical problems which occurred during the vibracoring process, such as compaction and loss of sediment, mean that the findings should only be regarded as indicating a trend. The curve definitely needs to be refined.

The application of coastal peats as a marker of palaeo-sea levels is complicated (Brückner et al., 2005, 2010; Vött, 2007). Coastal peat layers represent lagoons and marshy environments which are separated from the sea by a beach barrier system or river branches (Brückner et al., 2010: 14). Their characteristics reflect relative sea level changes at the time of formation. E.g., a slowly rising sea level leads to mounting peat formation while a fall in sea level results in erosion and disturbance of their formation (Vött, 2007: 897). In any case, if they are to be used for an estimation of the palaeo-sea level, it is important to accurately note the thickness of each peat layer, as well as the sampling depth. Vött (2007: 899) believes the sea level to have been slightly lower than the peat layer at the time of formation. For thin peat layers (<10 cm), he suggests an uncertainty bandwidth of 25 cm for the palaeo-sea level. Brückner et al. (2010: 14) also propose a palaeo-sea level within a range of 20-50 cm below sampling depth. A factor that can decrease the precision of the outcome markedly and which therefore needs to be accounted for is the fact that peat is susceptible to significant degrees of post-depositional compaction (Vött, 2007: 899). Brückner et al. (2010: 14) assume compaction estimation as being 25 cm for those samples which are covered by thick sediments.

Unfortunately, no datable buried archaeological remains are available in the research area. However, a layer of seemingly anthropogenically set thick limestone pieces, found within shallow marine deposits at coring sites LIS 29 and LIS 35, may be used as an indicator for a former sea level, because it appears quite certain that this stone layer was intentionally dumped by people in order to reach the sea more easily (see chapters 7.4.2. and 8.2). The lack of diagnostic ceramics means that a time frame for the formation of this layer can only be provided by ^{14}C age estimates obtained from directly below [2870-2496 cal BC (LIS 35/31T)] as well as above [1975-1746 cal BC (LIS 35/23T)] the layer in question (so-called “sandwich dating”).

The compilation of Vött (2007) and the discussion in Brückner et al. (2010) show that generally two types of sea level curve are published for the Holocene in the Mediterranean: those that show a transgression peak around 6-5 kyr BP and a later regression for about 2-4 m (e.g., Crete,

the Karamenderes area, the Büyük Menderes area), and those that show a constant sea level rise, reaching its peak very recently (e.g., NW Greece) (see fig. 69). Such substantial differences within a limited geographical area illustrate how important it is to realise that local tectonics can often overprint the glacio-eustatic signal.

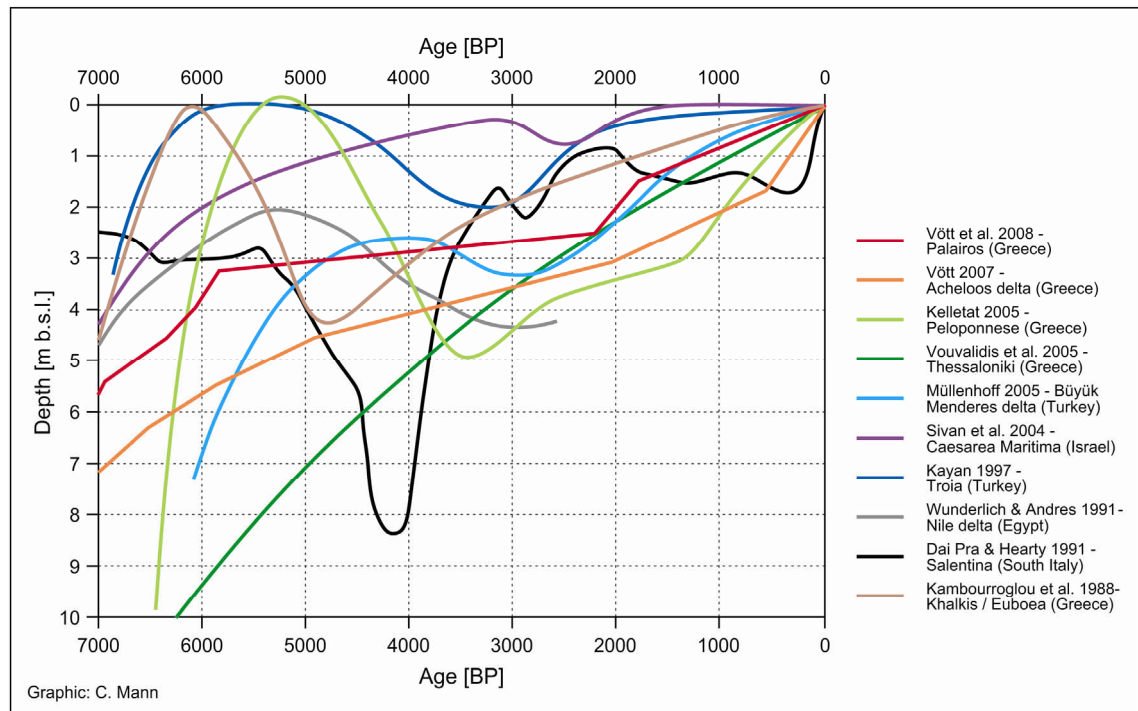


Figure 69: Local sea level curves for the Eastern Mediterranean. (Vött & Brückner, 2006a: p. 15, fig. 4)

The sea level curve for research area (fig. 70) indicates that the sea level has risen continuously (though at various rates) throughout the Holocene. It shows that between 3,500 and 3,000 cal BC mean palaeo-sea level was ca. 8 m below its present position, i.e., during a time when in other parts of the Mediterranean the maximum Holocene transgression is postulated with a peak around present sea level (cf. Brückner et al., 2010; cf. fig. 69). Along the coasts of the research area sea level reached its present position only recently (and is still rising).

The ^{14}C age estimates indicate a rapid sea level rise from 2,900 to 2,500 cal BC, when it reached approximately 6 m b.s.l. The depth of the anthropogenic debris at coring site LIS 29 (6.09 and 6.71 m b.s.l.) and the associated radiocarbon dating from the overlying marine sediments, suggesting that it must have been dumped there prior to 2,200 cal BC, also fit into the general picture, proposing a palaeo-sea level in the research area of about 6-7 m b.s.l. when late Neolithic/Chalcolithic people lived around Lezha.

The marine sediments from this period contain numerous embedded peat layers, which are reflecting temporary sea level fluctuations and co-seismic events around Lezha. The reasons for

these fluctuations are not clear; however, they can be linked with short-time climatic oscillations or local tectonic activities. Research by Mayewski et al. (2004) seems to indicate warm and dry climatic conditions in the southern Adriatic during the entire Chalcolithic period.

The sedimentological records and radiocarbon ages from the corings around Lezha reveal that numerous coastal peats developed between 2,100 and 1,600 cal BC. These peat layers may be a local reflection of the commonly known climatic oscillations, including the “4.2 kyr event” (for more details see chapter 3.3). In our research area a relatively thick peat layer between about 3 and 4 m b.s.l. marks a sea level at the beginning of 2nd millennium BC. Lambeck et al. (2004a) suggest a 2.5-3 m lower sea level than presently for this time period. However, our relative sea level curve shows that sea level was 3.5-4 m lower than today during the early Bronze Age (fig. 70). This palaeo-sea level also coincides with the transition from Chalcolithic to Bronze Age cultures in Albania. The depth differences are best explained by local tectonics. This is all the more likely since the research area is exactly at the tectonically controlled boundary between the NW-SE stretching mountain ranges bordering the Adriatic Sea to the east, and the N-S stretching coast which runs south and finds its extension in NW Greece.

The sea level seems to have risen more or less continuously during the following centuries. However, due to the lack of radiocarbon age estimates, this is only a hypothesis. A layer of set limestone fragments below an archaeological layer dated to Hellenistic times at corings LIS 28 and LIS 29 may date to the late Iron Age/early Hellenistic times. This layer lies between sublittoral and fluvial deposits at ~2 m b.s.l. We know from our corings that during that time the mouth of the Drini was close to Lissos. The anthropogenic stone setting may therefore serve as palaeo-sea level indicator. This is supported by our relative sea level curve (fig. 70).

We know from submerged archaeological remains along the coasts of Croatia that there the relative sea level was at least 1.5 m lower during Roman Imperial times (1st and 2nd centuries AD) (Faivre & Fouache, 2003: 526). Our curve suggests sea levels to have been about 1.5 m lower in early Roman times and about 1 m lower in Roman Imperial times. Unfortunately, the lack of archaeological evidence means that such data cannot contribute to refining our calculations. However, our relative sea level estimates seem to match the prediction of Lambeck et al. (2004b). During the following millennium, sea level rose relatively slowly, reaching 0.50 m b.s.l. only during the 11th century. From there it rose with a few small-scale oscillations, to its present position.

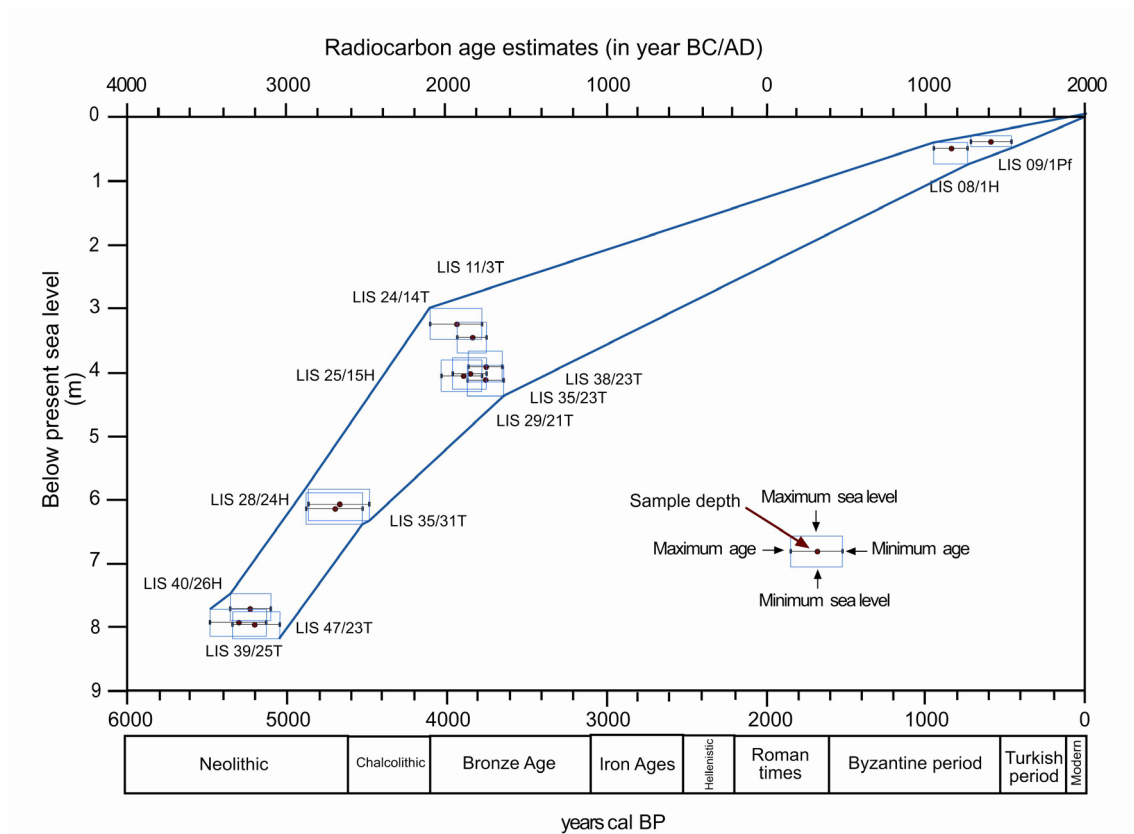


Figure 70: Sea level curve for Northern Albania. The envelope curve is based on age boxes of ^{14}C -dated samples. Their vertical extension reflects the uncertainties of the reconstruction of sea level from the dated sample, the horizontal extension is the 1 sigma standard deviation of the ^{14}C age estimate (own research).

In general, our sea level curve for the North Albanian coast can be classified to belong into the second group of relative sea level curves, representing the idea of a continuously rising sea level since the middle Holocene. It is in accordance with Vött's (2007) results for NW Greece (that curve is part of fig. 69).

10 Summary

This is the first time that detailed interdisciplinary research has been carried out along the coasts of Northern Albania. The delta progradation of the river Drini was the focus in an attempt to reconstruct the palaeoenvironmental evolution throughout the Holocene. Our geoarchaeological study comprises 53 vibracoring, obtained in the archaeological area and on the alluvial plains surrounding Lezha, 57 radiocarbon age estimates and several age determinations by diagnostic ceramics. Together with information from historical sources and maps, the results of geochemical, microfossil, and palynological analyses have been combined to create palaeogeographic landscape scenarios for the region around Lezha, beginning with the maximum extent of the Holocene marine transgression. Further scenarios have been generated for the following periods: 4th millennium BC (Middle Neolithic), 2nd millennium BC (beginning of Bronze Age), 6th century BC (Late Iron Age), 4th century BC (Hellenistic times), 2nd century AD (Roman Imperial times), 10th century AD (Early Medieval times) and 1500 AD.

The first dramatic changes date back to approximately 5,000-6,000 years ago, when the Adriatic Sea had inundated the broad piedmont plain at the foot of Shite-Veles and Skanderbeg Mountains. Our research shows that the sea had transgressed through the narrow gap between Mali Rrenci and Lezha Hill (Kalaja). During the peak of the transgression, the geological syncline between Mali Rrenci and Mali Kakarriqi was covered by the sea (the area of today's Balldreni plain), transforming the mountain ridge of Mali Rrenci into an island, parallel to the coast. This "canale-type" coast is nowadays typical for the Dalmatian coast further north.

According to our data, the sea reached its maximum inland position north of the town of Balldreni (between coring sites LIS 27 and LIS 47), thus creating a marine embayment. Although it was connected with the open sea *via* the narrow gap where Lissos was later founded, and the marine corridor between the limestone ridges of Mali Rrenci and Mali Kakarriqi, which was linked to the Buna delta further north, the embayment had a low energy wave climate, protected from high waves and the northbound longshore drift.

The river Drini began to deposit its delta sediments into this marine embayment after the peak of the Holocene transgression. At first, the formation and progradation of the delta was dominated by fluvial processes. Radiocarbon age estimates indicate that the Drini prograded south with several distributaries, forming a Gilbert-type delta during the 4th and 2nd millennium BC. It seems that the progradation of the Drini delta was controlled by both natural processes and human impact. The river and its tributaries carried large amounts of sediment, mainly due easily erodible rocks (flysch and Neogen formations) in parts of their drainage basin. The

expansion of settlements within the catchment area of the (Black) Drini during Neolithic and Chalcolithic times caused probably increasingly human-induced erosion. The first direct sign of anthropogenic activities around Lezha is a thick layer of angular limestone pieces within the marine sediments (in vibracoring LIS 29 and LIS 35), most likely dumped by Late Neolithic or Chalcolithic people, who tried to gain easier access to the sea.

During the Bronze and Iron Ages, the most noteworthy point is the rapid advance of the delta, in the progress of which the marine corridor between Mali Rrenci and Mali Kakarriqi was cut off in the southeast. Archaeological evidence, *inter alia* from Mali Shelbuemit, points to a change in settlement pattern, and an increasing number of hilltop settlements along the coast suggest an intensified human impact on the natural environment.

During the 5th and 4th centuries BC, the marine embayment had ceased to exist, with only a small residual lake to the north of Lissos remaining. The corings within the archaeological area show that the Drini had already prograded past the narrow gap between Mali Rrenci and Lezha Hill when the city was founded in 385/4 BC. Archaeological remains such as ceramics, charcoal, and grape seeds were found within the fluvial deposits of the Drini, none within the marine sediments. Our corings show that the so-called Hellenistic city was partly founded on deltaic sand.

Subsequent delta evolution was very slow around Lezha, because the Drini's previously smaller branch towards the Buna delta became the main river course, diverting much of its sediment. However, Julius Caesar (*Bel. civ.* 3, 29, 9) states that the main harbour of Lissus moved to Shengjin in 48 BC, which leaves us to assume that the main course of the Drini must have occasionally shifted back to its branch past Lissus, thereby also depositing large amounts of sediment, prograding its delta, and turning Lissos harbour into a river port. An age estimate indicates that the delta of the Drini had progressed for ~ 1.5 km beyond the narrow gorge during the 1st century AD (coring LIS 43), suggesting a complete reactivation of the river branch past Lissus (as the city was called in Roman times). The following delta growth was controlled by the northbound longshore drift, forming a series of beach barrier – lagoon systems. The majority of the sediment supply probably came from the Mati river further south.

During Medieval times, especially after the 10th century, environmental conditions changed considerably around Lezha. Pollen records show a significant increase of arboreal pollen (oak and alder), which reflects natural reforestation around Lezha – a possible manifestation of the “Medieval Climatic Optimum”. Radiocarbon ages suggest rapid delta advance northwards in the Ishull Shengjin region during the 10th to 12th centuries. The previously brackish conditions

between Mali Rrenci and Mali Kakarriqi changed to a freshwater milieu during the 11th to 12th centuries, and a continuous, strong fluvial input led to the transformation of former lagoons to freshwater lakes during the 13th and 14th centuries, e.g., in the Ishull Shengjin region, and it appears as though malaria became a big problem.

During the following centuries, historical documents play an essential role when attempting to establish a chronology for the growth of the Drini delta. A connection between the Drini and Buna rivers is attested in 1593 AD. It seems that the westernmost part of the delta developed rapidly after the main river course had changed its direction in the 17th century AD. This can be explained on the one hand by the humid climatic conditions during the Little Ice Age, and on the other hand by increasing human impact on the natural environment in the highlands due to changing settlement patterns during the Turkish period. Although Lezha seemed to be quite far away from the coastline, it had a river harbour, and the river was navigable even further upstream, at least until the middle of the 19th century.

Extensive swampy environments, especially the Balldreni and Merqia plains and the Drini delta, as well as frequent flooding events have limited settlement expansion in the region. However, this problem was partly solved by the introduction of drainage measures in the 1950s and by the diversion of the main course of the Drini towards the Buna in 1958. Further human interventions, e.g., the building of dams and hydro power plants in the catchments of the Drini and Mati rivers, resulted in a vastly reduced sediment supply. This in course led to the dominance of erosion processes over accumulation along the coast. Nowadays, there is strong evidence for a continued sea level rise and coastal erosion.

Another aim of this thesis was to generate a locally valid sea level curve. Based on ¹⁴C-dated sea level indicators (mostly paralic peat) and some archaeological evidence, the first Holocene sea level curve for Albania is presented. It shows that during the time of the maximum transgression around 5,000-6,000 cal BP, sea level was still ca. 8 m below its present position. According to our evidence, it has been rising continuously since then. The shape of this curve is very similar to the sea level curves reconstructed for coastal areas further south in NW Greece (cf. Vött, 2007).

Geoarchaeology works interdisciplinary and means to solve specific questions encountered during archaeological investigations. With our findings, we were able to add valuable information, to the still on-going excavations in Lezha. Our scenarios provide a detailed idea about the changing geographical situation of Lissos and help to put information from ancient documents into context, as well as offering a much more confined chronological framework. It

is clear by now that Lissos never hosted a sea port, because the delta had already prograded past the location when Lissos was founded in the early 4th century BC. The sea harbour was close-by; however, its proper location has not yet been detected. It is reasonable to argue that it was in the place still called Knetá Lezha (Lezha swamp) to date. We know from Julius Caesar that Shengjin became the sea harbour of Lissos in 48 BC. However, the city always had a functional river harbour until the middle of the 19th century.

Overall, it can be said that the coastal configuration in the research area results from both natural factors such as shifting river courses, continuous general and local tectonic movements, and extreme climatic conditions, as well as human impact in the form of deforestation, and engineering works. It is noteworthy that the delta development in this area is much more complex than it first appeared; for example, that the Drini delta has been formed by both the Drini as well as the Mati river, and that the Drini has also played an important role in building up the Buna delta.

The overriding aim of this dissertation was to establish a chronological framework for the coastal evolution in this region. The gaps in terms of chronology which appear in our scenarios would need to be filled by further palaeoenvironmental studies in the large alluvial plains around Shkodra and the Buna delta further north.

11 Zusammenfassung

Im Rahmen der vorliegenden Arbeit wurden erstmalig detaillierte, interdisziplinäre Studien an der Nordküste Albaniens durchgeführt. Der Fokus der Untersuchungen liegt auf der raumzeitlichen Genese des Drinideltas, um damit die paläoökologische Entwicklung des Gebietes während des Holozäns zu rekonstruieren. Die geoarchäologische Studie umfasst 53 Sedimentbohrungen innerhalb des archäologischen Ausgrabungsareals von Lezha und auf den alluvialen Flächen in deren Umkreis. 57 Proben wurden AMS-¹⁴C datiert; weitere Altersabschätzungen gehen auf die zeitliche Einordnung von Keramikfragmenten zurück. Zusammen mit Informationen aus historischen Quellen und Karten konnten die Ergebnisse geochemischer, palynologischer und mikrofaunistischer Analysen dazu verwendet werden, paläogeographische Landschaftsszenarien – beginnend mit der maximalen Ausdehnung der holozänen marinen Transgression – für das küstennahe Gebiet um Lezha zu erstellen. Weitere Szenarien liegen für die folgenden Epochen vor: 4. Jahrtausend v. Chr. (mittleres Neolithikum), 2. Jahrtausend v. Chr. (am Anfang der Bronzezeit), 6. Jahrhundert v. Chr. (späte Eisenzeit), 4. Jahrhundert v. Chr. (hellenistische Epoche), 2. Jahrhundert n. Chr. (römische Kaiserzeit), 10. Jahrhundert n. Chr. (frühes Mittelalter) und 1500 n. Chr.

Die ersten größeren Veränderungen ereigneten sich vor 5000-6000 Jahren, als das Adriatische Meer das ausgedehnte Pediment am Gebirgsfuß des Shite-Veles- und des Skanderberg-Gebirges überschwemmte. Unsere Forschungen zeigen, dass die Meerestransgression durch die schmale Öffnung zwischen Mali Rrenci und Lezha Hill (Kalaja) erfolgte. Während der maximalen Transgression war die geologische Synklinale zwischen Mali Rrenci und Mali Kakarriqi marin geflutet (die heutige Balldreni Ebene), so dass der Gebirgszug Mali Rrenci zu einer parallel zur Küste verlaufenden Insel wurde. Diese Form der Canale-Küste ist heute noch typisch für die Küste des weiter im Norden gelegenen Dalmatien.

Gemäß unseren Daten erreichte das Meer seine maximale landeinwärtige Ausdehnung nördlich der Stadt Balldreni (zwischen den Bohrungen LIS 27 und LIS 47), wo sich eine Meeresbucht bildete. Sie war über eine schmale Öffnung, an der später die Stadt Lissos gegründet wurde, und die Senke zwischen den Kalksteinhängen der Gebirgszüge Mali Rrenci und Mali Kakarriqi, die eine Verbindung zu dem weiter nördlich gelegenen Bunadelta darstellt, mit dem offenen Meer verbunden. In diesem Meeresarm herrschte ein niedrig-energetisches Milieu mit Schutz vor hohen Wellen und der nach Norden gerichteten Küstenströmung.

Nachdem die holozäne Meeresingression ihr Maximum erreicht hatte, begann der Fluss Drini die marine Bucht allmählich mit seinen Sedimenten zu verfüllen. Zunächst wurden die Bildung

und der Vorbau des Deltakörpers von fluvialen Prozessen dominiert. Radiokohlenstoffalter deuten darauf hin, dass sich das Delta zwischen dem 4. und 2. Jahrtausend v. Chr. in Form eines Gilbert-Typ-Deltas durch mehrere, verzweigte Mündungsarme, nach Süden vorbaute. Wahrscheinlich wurde dieser Prozess sowohl natürlich als auch anthropogen gesteuert. Der Drini und seine Nebenflüsse erodierten bereits damals große Mengen an Sediment in ihrem aus Flysch und neogenen Gesteinen bestehenden Einzugsgebiet. Bereits während des Neolithikums und Chalkolithikums führte offenbar die Siedlungsausdehnung im Einzugsgebiet des (Schwarzen) Drini zu einer Zunahme der anthropogen bedingten Erosion. Das erste definitive Anzeichen für menschliche Eingriffe rund um Lezha ist eine mächtige Schicht aus kantigen Kalksteinfragmenten in den marinen Sedimenten der Bohrungen LIS 23 und LIS 35. Sie sind wahrscheinlich das Resultat künstlicher Aufschüttung durch die im Spätneolithikum oder Chalkolithikum lebenden Menschen, um einen besseren Zugang zum Meer zu gewährleisten. Während des 4. Jahrtausends v. Chr. war die marine Bucht bis auf einen kleinen Restsee nördlich von Lissos verlandet.

In der Bronze- und Eisenzeit stellt der schnelle Deltavorbau des Drini und die damit verbundene Unterbrechung der Meeresverbindung zwischen Mali Rrenci and Mali Kakarriqi im Südosten die bedeutendste Veränderung dar. Archäologische Funde, unter anderem auf dem Bergrücken des Mali Shelbuemit, deuten eine Veränderung der Siedlungsstruktur an. Insbesondere die steigende Anzahl an auf Bergrücken liegenden Siedlungen ist ein Indikator für den zunehmenden Einfluss des Menschen auf den Naturraum.

Die Bohrungen im archäologischen Bereich von Lezha zeigen, dass die Deltafront des Drini die Engstelle zwischen Mali Rrenci und Lezha Hill bereits passiert hatte, als die Stadt 385/4 v. Chr. gegründet wurde. Archäologische Funde wie Keramik, Holzkohle und Traubenkerne wurden in den fluvialen Ablagerungen des Drini, nicht aber in marinen Sedimenten gefunden. Weiterhin zeigt LIS 38, dass die sogenannte Hellenistische Stadt zum Teil auf Deltasanden errichtet wurde.

Die folgende Deltaentwicklung rund um Lezha ging sehr langsam voran, da der einstmalig schmalere Driniarm in Richtung des Bunadeltas zum Hauptfluss wurde und den Großteil der Sedimente abführte. Durch Julius Caesar (*Bel. Civ.* 3, 26, 9) ist belegt, dass der Haupthafen von Lissus 48 v. Chr. nach Shengjin verlegt wurde. Das legt die Vermutung nahe, dass sich der Hauptarm des Drini zeitweise zurück nach Lissus verlagert haben muss, wobei große Mengen an Sediment abgelagert, das Delta vorgebaut, und der ehemalige Seehafen von Lissus in einen Flusshafen umgewandelt wurde. Durch eine ¹⁴C-Datierung (aus LIS 43) ist belegt, dass sich die Deltafront des Drini gegen Ende des 1. Jh. n. Chr. bereits etwa 1,5 km jenseits des schmalen

Durchlasses befand, was auf eine vollständige Reaktivierung des durch Lissus (wie die Stadt in römischer Zeit genannt wurde) führenden Flussarms schließen lässt. Das anschließende Deltawachstum wurde von der nach Norden gerichteten Küstenlängsströmung kontrolliert. Dadurch kam es zur Bildung von Strandwall-Lagunen Systemen. Deren größter Anteil an Sedimenten stammte wahrscheinlich aus dem weiter südlich mündenden Fluss Mati.

Während des Mittelalters, vor allem nach dem 10. Jh. n. Chr., veränderten sich die Umweltbedingungen rund um Lezha erheblich. Pollendiagramme zeigen einen signifikanten Anstieg des Baumpollenanteils (Eiche und Erle), der die natürliche Wiederbewaldung rund um Lezha – möglicherweise Ausdruck des „Mittelalterlichen Klimaoptimums“ – widerspiegelt. Radiokohlenstoffalter deuten auf einen schnellen, nach Norden in Richtung der Ishull Region gerichteten Deltavorbau zwischen dem 10. und 12. Jh. n. Chr. hin. Die vormals brackischen Ablagerungsbedingungen zwischen Mali Rrenci und Mali Kakarriqi gingen während des 11. und 12. Jh. n. Chr. in Süßwassersedimentation über. Außerdem führte der kontinuierliche Eintrag fluvialer Sedimente während des 13. und 14. Jh. n. Chr. zu einer Aussüßung ehemaliger Lagunen (z. B. in der Ishull Shengjin Region). Auch scheint Malaria zu einem großen Problem geworden zu sein.

Für die Rekonstruktion der zeitlichen Entwicklung des Drinideltas in den folgenden Jahrhunderten, spielen historische Dokumente eine übergeordnete Rolle. Eine Verbindung zwischen den Flüssen Drini und Buna ist für 1593 n. Chr. belegt. Der westlichste Teil des Deltas scheint sich besonders schnell entwickelt zu haben, nachdem der Hauptarm seine Richtung im 17. Jh. n. Chr. veränderte. Dies kann einerseits durch die feuchten Bedingungen während der Kleinen Eiszeit erklärt werden. Andererseits trug auch der steigende Einfluss des Menschen auf die Umwelt in den höher gelegenen Gebieten dazu bei; er ist auf sich verändernde Siedlungsmuster während der türkischen Epoche zurückzuführen. Obwohl Lezha relativ weit von der Küste entfernt lag, hatte die Stadt einen Flusshafen und der Fluss war auch weiter stromaufwärts noch mindestens bis zur Mitte des 19. Jh. n. Chr. schiffbar.

Ausgedehnte Sumpfflächen, vor allem im Bereich der Ebenen von Balldreni und Merqia sowie im Drinidelta, und das häufige Auftreten von Überschwemmungen ließen nur eine begrenzte Siedlungsausdehnung in der Region zu. Dieses Problem wurde jedoch teilweise durch die Entwässerungsmaßnahmen der 1950er Jahre sowie die Umleitung des Drini-Hauptarms in den Fluss Buna im Jahr 1958 gelöst. Weitere Eingriffe, z. B. der Bau von Dämmen und Wasserkraftwerken im Einzugsgebiet von Drini und Mati, resultierten in einer deutlich reduzierten Sedimentfracht, was zur Dominanz der Erosions- über die Akkumulationsprozesse

entlang der Küste führte. Heutzutage gibt es deutliche Anzeichen für einen steigenden Meeresspiegel und für massive Küstenerosion.

Ein weiteres Ziel der Doktorarbeit war die Erstellung einer lokalen Meeresspiegelkurve. Basierend auf ¹⁴C-datierten Meeresspiegelindikatoren (vor allem paralische Torfe) und mittels archäologischer Belege wurde die erste holozäne Meeresspiegelkurve für Albanien rekonstruiert. Sie zeigt, dass der Meeresspiegel während der maximalen marinen Transgression um 5000-6000 cal BP noch bei etwa -8 m lag und dann kontinuierlich auf sein heutiges Niveau gestiegen ist. Damit zeigt sich eine ähnliche Meeresspiegelkurve, wie sie aus dem südwärts anschließenden Akarnanien bekannt ist (vgl. Vött, 2007).

Unter geoarchäologischen Gesichtspunkten lässt sich festhalten, dass die o.g. Befunde wertvolle Informationen für die paläogeographische Situation und die Chronologie der Landschaftsveränderungen im Bereich der antiken Stadt Lissos liefern. So wurde z.B. die Hafenfrage dahingehend geklärt, dass wir erstmals zeigen konnten, dass im Gebiet der späteren Siedlung bis etwa zur Mitte des 1. Jahrtausends v. Chr. noch marine Verhältnisse herrschten. Danach baute sich in diesem Bereich das Drinidelta vor, so dass zur Zeit der Stadtgründung von Lissos der direkte Anschluss ans Meer verloren gegangen war. Der Seehafen von Lissos war ab 48 v. Chr. das nordwestlich von Lissos gelegene Shengjin. Lissos selbst hatte aber immer einen Flusshafen, der bis zur Mitte des 19. Jh. belegt ist.

Zusammenfassend kann festgestellt werden, dass die Küstengenese des Forschungsgebietes sowohl von natürlichen Faktoren, wie sich verändernden Flussläufen, regionaler und lokaler Tektonik und extremen Klimabedingungen, als auch von anthropogenen Einflüssen in Form von Entwaldung und Ingenieurbauten geprägt wurde. Es muss erwähnt werden, dass die Entwicklung des Deltas in diesem Gebiet sehr viel komplexer verlief, als es zunächst den Anschein hatte. Zum Beispiel wurde das Delta von den Flüssen Drini und Mati geformt und der Drini spielte auch beim Vorbau des Bunadeltas eine wichtige Rolle.

Das vorrangige Ziel dieser Dissertation war es, eine Chronologie der Küstenveränderungen im Gebiet von Lissos zu erstellen. Die in den vorgestellten Szenarien verbleibenden zeitlichen Lücken können nur durch weitere paläogeographische Studien in den großen alluvialen Flächen rund um Shkodra und im weiter nördlich gelegenen Bunadelta geklärt werden.

12 References

- AG BODEN (2005): *Bodenkundliche Kartieranleitung*, 5. verbesserte und erweiterte Auflage (KA5). Schweizerbart'sche Verlagsbuchhandlung. Hannover. 5. Aufl. Stuttgart.
- ALIAJ, S. (1996): Neotectonics and seismotectonics of Drini fault zone (Eastern Albania). *The Albanian Journal of Natural & Technical Sciences*, 1: 81-92.
- ALIAJ, S. (1997): Alpine geological evolution of Albania. *The Albanian Journal of Natural & Technical Sciences*, 3: 69-81.
- ALIAJ, S. (2004): Seismic source zones in Albania. *The Albanian Journal of Natural & Technical Sciences*, 16: 133-147.
- ALIAJ, S. (2006): The Albanian Orogen: Convergence zone between Eurasia and the Adria Microplate. In: PINTER, N., GRENERCZY, G., WEBER, J., STEIN, S. & D. MEDAK (eds.) – *The Adria Microplate: GPS Geodesy, Tectonics and Hazards*. Springer: 133-149.
- ALIAJ, S., BALDASSARRE, G. & D. SHKUPI (2001): Quaternary subsidence zones in Albania: some case studies. *Bulletin of Engineering Geology and Environment*, 59: 313-318.
- AMMERMAN, A. J., MCCLENNEN, C. E., DE MIN, M. & R. HOUSLEY (1999): Sea-level change and the archaeology of early Venice. *Antiquity*, 73: 303-312.
- AMOROSI, A., COLALONGA, M. L. & F. FUSCO (1999): Glacio-Eustatic control of continental-shallow marine cyclicity from late Quaternary deposits of southeastern Po plain, northern Italy. *Quaternary Research*, 52 (1): 1-13.
- ANDERSON, H. & J. JACKSON (1987): Active tectonics of the Adriatic Region. *Geophysical Journal of the Royal Astronomical Society*, 91: 937-983.
- ANDREA, Z. (1984): Archaeology in Albania, 1973-83. *Archaeological Reports*, 30: 102-119.
- ANDRES, W. & J. WUNDERLICH (1991): Late Pleistocene and Holocene evolution of the eastern Nile Delta and comparisons with the western delta. In: BRÜCKNER, H. & U. RADTKE (Hrsg.) – *Von der Nordsee bis zum Indischen Ozean. Ergebnisse der 8. Jahrestagung des Arbeitskreises „Geographie der Meere und Küsten“*. *Erdkundliches Wissen*, 105. Stuttgart: 121-130.
- ANTONIOLI, F., FERRANTI, L., FONTANA, A., AMOROSI, A., BONDESAN, A., BRAITENBERG, C., DUTTON, A., FONTOLAN, G., FURLANI, S., LAMBECK, K., MASTRONUZZI, G., MONACO, C., SPADA, G. & P. STOCCHI (2009): Holocene relative sea-level changes and vertical movements along the Italian and Istrian coastlines. *Quaternary International*, 206 (1-2): 102-133.
- AURIEMMA, R., MASTRONUZZI, G. & P. SANSÒ (2004): Middle to Late Holocene relative sea-level changes recorded on the coast of Apulia (Italy) (Variations relatives du niveau marin pendant l'Holocène moyen et supérieur le long des côtes méridionales des Pouilles (Italie)). *Géomorphologie: relief, processus, environnement*, n°1: 19-34.

-
- BAETEMAN, C. (1985): Late Holocene geology of the Marathon plain (Greece). *Journal of Coastal Research*, 1 (2): 173-185.
 - BARBER, D. C., DYKE, A., HILLAIRE-MARCEL, C., JENNINGS, A. E., ANDREWS, J. T., KERWIN, M. W., BILODEAU, G., MCNEELY, SOUTHON, J., MOREHEAD, M. D. & J.-M. GAGNON (1999): Forcing of the cold event of 8,200 years ago by catastrophic drainage of Laurentide lakes. *Nature*, 400: 344-348.
 - BARSCH, H., BILLWITZ, K. & H.-R. BORK (Hrsg.) (2000): *Arbeitsmethoden in Physiogeographie und Geoökologie*. Klett – Perthes. Gotha, Stuttgart.
 - BARTL, P. (1995): *Albanien: Vom Mittelalter bis zum Gegenwart*. Ost- und Südeuropa Geschichte der Länder und Völker. Verlag Friedrich Pustet. Regensburg.
 - BARTL, P. (2007): *Albania Sacra: Geistliche Visitationsberichte aus Albanien 1: Diözese Alessio*. Harrassowitz Verlag. Wiesbaden.
 - BAY, B. (1999): *Geoarchäologie, anthropogene Bodenerosion und Deltavorbau im Büyük Menderes Delta (SW-Türkei)*. GCA-Verlag. Bochum.
 - BEAUMONT, R. L. (1936): Greek Influence in the Adriatic Sea before the Fourth century B. C. *The Journal of Hellenistic Studies*, 56, Part 2: 159-204.
 - BEAUMONT, R. L. (1952): Corinth, Ambracia, Apollonia. *The Journal of Hellenistic Studies*, 72: 62-73.
 - BECCALUVA, L., COLTORTI, M., SACCANI, E. & F. SIENA (2005): Magma generation and crustal accretion as evidenced by supra-subduction ophiolites of the Albanide-Hellenide Subpelagonian zone. *The Islandic Arc*, 14: 551-563.
 - BELLOTTI, P., CALDERONI, G., CARBONI, M. A., DI BELLA, L., TORTORA, P., VALERI, P. & V. ZERNITSKAYA (2007): Late Quaternary landscape evolution of the Tiber River delta plain (Central Italy): new evidence from pollen data, biostratigraphy and ¹⁴C dating. *Zeitschrift für Geomorphologie, N. F.*, 51 (4). Berlin, Stuttgart: 505-534.
 - BERTONI, W., BRIGHENTI, G., GAMBOLATI, G., GATTO, P., RICCERI, G. & F. VUILLERMIN (1995): Land subsidence due to gas production in the on- and off-shore natural gas fields of the Ravenna area, Italy. In: *Land Subsidence. Proceedings of the Fifth International Symposium on Land Subsidence (The Hague, October 1995)*. IAHS Publications, No. 234: 13-20.
 - BESONEN, M., RAPP, G. & Z. JING (2003): The Lower Acheron River Valley: Ancient accounts and the changing landscape. In: WISEMAN, J. & K. ZACHOS (eds.) – *Landscape Archaeology in Southern Epirus, Greece 1*. *Hesperia Suppl.*, 32:199-263.
 - BEUG, H.-J. (1961): Beiträge zur postglazialen Floren- und Vegetationsgeschichte in Süddalmatien: Der See 'Malo Jezero' auf Mljet, 1, 2. *Flora*, 150: 600-656.
 - BEUG, H.-J. (1967): On the Forest History of the Dalmatian Coast. *Review of Palaeobotany and Palynology*, 2: 271-279.

-
- BEUG, H.-J. (2004): Leitfaden der Pollenbestimmung für Mitteleuropa und angrenzende Gebiete. Dr. Friedrich Pfeil Verlag. München.
 - BINTLIFF, J. (2002): Time, process and catastrophism in the study of Mediterranean alluvial history: a review. *World Archaeology*, 33 (3): 417-435.
 - BLACKMAN, D. J. (1973): Evidence of sea level change in ancient harbours and coastal installations. In: BLACKMAN, D. J. (ed.) – *Marine Archaeology*. Colston Papers 23. Bristol: 115-139.
 - BLACKMAN, D. J. (2005): Archaeological evidence for sea level changes. In: FOUACHE, É. & K. PAVLOPOULOS (eds.) – *Sea Level Changes in Eastern Mediterranean during Holocene – Indicators and Human Impacts*. *Zeitschrift für Geomorphologie*, N. F., Suppl.-vol. 137. Berlin, Stuttgart: 61-70.
 - BOÇI, E. (1994): Evoluzione e problematiche ambientali del litorale Albanese. *Bolletino della Società Geologica Italiana*, 113: 7-14.
 - BONATTI, E. (1966): North Mediterranean climate during the Last Würm Glaciation. *Nature*, 209. No: 5027: 984-985.
 - BORDON, A., PEYRON, O., LÉZINE, A.-M., BREWER, S. & É. FOUACHE (2009): Pollen-inferred Late-Glacial and Holocene climate in southern Balkans (Lake Maliq). *Quaternary International*, 200 (1-2): 19-30.
 - BOSWORTH, R. J. B. (1975): The Albanian Forests of Signor Giacomo Vismara: A case study of Italian Economic Imperialism during the Foreign Ministry of Antonino di San Giuliano. *The Historical Journal*, XVIII (3): 571-586.
 - BRIDGE, J. S. (2003): *Rivers and Floodplains: Forms, Processes, and Sedimentary Record*. Blackwell Science Ltd. Cornwall.
 - BROWN, A. G. (1997): *Alluvial Geoarchaeology: Floodplain archaeology and environmental change*. Cambridge Manuals in Archaeology. Cambridge University Press. Cambridge.
 - BRÜCKNER, H. (1982): Ausmaß von Erosion und Akkumulation im Verlauf des Quartärs in der Basilicata (Süditalien). In: BARSCH, D. (ed.) – *Experimente und Messungen in der Geomorphologie*. *Zeitschrift für Geomorphologie*, N. F., Suppl.-Bd. 43. Berlin, Stuttgart: 121-137.
 - BRÜCKNER, H. (1983): Holozäne Bodenbildungen in den Alluvionen süditalienischer Flüsse. *Zeitschrift für Geomorphologie*, N. F., Suppl.-Bd. 48. Berlin, Stuttgart: 99-116.
 - BRÜCKNER, H. (1986): Man's impact on the evolution of the physical environment in the Mediterranean region in historical times. *GeoJournal*, 13 (1): 7-17.
 - BRÜCKNER, H. (1990): Changes in the Mediterranean ecosystem during Antiquity. A geomorphological approach: as seen in two examples. In: BOTTEMA, S., ENTJES-NIEBORG, G. & W. VAN ZEIST (eds.) – *Man's role in the shaping of the Eastern Mediterranean landscape*. Rotterdam, Brookfield: 127-137.

-
- BRÜCKNER, H. (1996): Geoarchäologie an der türkischen Agäisküste. Landschaftswandel im Spiegel geologischer und archäologischer Zeugnisse. *Geographische Rundschau*, 48 (10): 568-574.
 - BRÜCKNER, H. (1997a): Geoarchäologische Forschungen in der Westtürkei. Das Beispiel Ephesos. In: BREUER, T. (Hrsg.) – *Geographische Forschung im Mittelmeerraum und in der Neuen Welt*. Passauer Schriften zur Geographie, 15. Passau: 39-51.
 - BRÜCKNER, H. (1997b): Coastal changes in western Turkey – Rapid delta progradation in historical times. In: BRIAND, F. & A. MALDONADO (eds.) – *Transformation and evolution of the Mediterranean coastline*. CIESM Science Series, no: 3. (Bulletin de l'Institut océanographique, numéro special 18. Musée océanographique, Monaco). Monaco: 63-74.
 - BRÜCKNER, H. (1998): Coastal research and geoarchaeology in the Mediterranean region. In: KELLETAT, D. (Hrsg.) – *German Geographical Coastal Research: The Last Decade*. Tübingen: 235-257.
 - BRÜCKNER, H. (2003): Delta evolution and culture. Aspects of geoarchaeological research in Miletus and Priene. In: WAGNER, G. A., PERNICKA, E. & H.-P. UERPMANN (eds.) – *Troia and the Troad: Scientific Approaches*. Springer-Series: Natural Science in Archaeology. Berlin: 121-144.
 - BRÜCKNER, H. (2005): Holocene shoreline displacements and their consequences for human societies: the example of Ephesus in western Turkey. *Zeitschrift für Geomorphologie*, N. F., Suppl.-vol. 137. Berlin, Stuttgart: 11-22.
 - BRÜCKNER, H. & R. GERLACH (2007): Geoarchäologie. In: GEBHARDT, H., GLASER, R., RADTKE, U. & P. REUBER (Hrsg.) – *Geographie – Physische Geographie und Humangeographie*. Elsevier, München: 513-516.
 - BRÜCKNER, H. & G. HOFFMANN (1992): Human-induced erosion processes in Mediterranean countries, evidences from archaeology, pedology and geology. *Geo-Öko plus*, 3: 97-110.
 - BRÜCKNER, H., KELTERBAUM, D., MARUNCHAK, O., POROTOV, A. & A. VÖTT (2010): The Holocene sea level story since 7500 BP – Lessons from the Eastern Mediterranean, the Black and the Azov Seas. *Quaternary International*, 225 (2): 160-179.
 - BRÜCKNER, H., MÜLLENHOFF, M., GEHRELS, R., HERDA, A., KNIPPING, M. & A. VÖTT (2006): From archipelago to floodplain – geographical and ecological changes in Miletus and its environs during the past six millennia (Western Anatolia, Turkey). *Zeitschrift für Geomorphologie*, N. F., Suppl.-vol. 142. Berlin, Stuttgart: 63-83.
 - BRÜCKNER, H. & A. VÖTT (2008): Geoarchäologie – eine interdisziplinäre Wissenschaft par excellence. In: KULKE, E. & H. POPP (Hrsg.) – *Umgang mit Risiken. Katastrophen - Destabilisierung - Sicherheit*. Tagungsband Deutscher Geographentag 2007 Bayreuth. Herausgegeben im Auftrag der Deutschen Gesellschaft für Geographie. Bayreuth, Berlin: 181-202.

-
- BRÜCKNER, H., VÖTT, A., SCHRIVER, M. & M. HANDL (2005): Holocene delta progradation in the eastern Mediterranean. *Méditerranée*, 1. 2: 95-106.
 - BURT, R. (ed.) (2004): Soil Survey Laboratory Methods Manual. Soil Survey Investigations Report No. 42. Version 4.0. Unites States Department of Agriculture Natural Resources Conservation Service.
 - BUTZER, K. W. (2005): Environmental history in the Mediterranean world: cross-disciplinary investigation of cause-and-effect for degradation and soil erosion. *Journal of Archaeological Science*, 32 (12): 1773-1800.
 - BÜDEL, J. (1977): Mediterrane Flußtätigkeit seit der Frühantike (Aufbau und Verschüttung Olympias). In: BÜDEL, J. (Hrsg.) – *Klima-Geomorphologie. Arbeit aus der Kommission für Geomorphologie der Bayerischen Akademie der Wissenschaften*, 1. Berlin, Stuttgart: 259-265.
 - CAESAR (1869): *Commentariorum (Libri III de Bello Civili) – Caesar’s Commentaries on the Gallic and Civil Wars*. Translated by W. A. DEVITTE & W. S. BOHN. Harper & Brothers. New York.
 - CALDARA, M., CAZZELLA, A., FIORENTINO, G., LOPEZ, R., MAGRI, D., MOSCOLINO, M., NARCISI, B. & O. SIMONE (2003): The relationship between the Coppa Navigata settlement and the wetland area during the Bronze Age (south-eastern Italy). In: FOUACHE, É. (ed.) – *The Mediterranean World, Environment and History. IAG Working Group on Geo-archaeology Symposium Proceedings: Environmental Dynamics and History in Mediterranean Areas*. Paris, Universite de Paris-Sorbonne, 24-26 avril 2002. Elsevier: 429-437.
 - CALDARA, M., CAROLI, I. & O. SIMONE (2008): Holocene evolution and sea-level changes in the Battaglia basin area (eastern Gargano coast, Apulia, Italy). *Quaternary International*, 183 (1): 102-114.
 - CAMUFFO, D., STURARO, G. & E. PAGAN (2004): Sinking of Venice over the last three centuries: input from Canaletto’s paintings and early photographs. In: CIESM (Commission Internationale pour l’Exploration Scientifique de la mer Méditerranée) – *Human records of recent geological evolution in the Mediterranean Basin – historical and archaeological evidence (Santorini, Greece, 22-25 October 2003)*. CIESM Workshop Monographs, 24. Monaco: 57-62.
 - CARMINATI, E. & G. DI DONATO (1999): Separating natural and anthropogenic vertical movements in fast subsiding areas: The Po Plain (N. Italy) case. *Geophysical Research Letters*, 26 (15): 2291–2294.
 - CARMINATI, E. & G. MARTINELLI (2002): Subsidence rates in the Po Plain, northern Italy: the relative impact of natural and anthropogenic causation. *Engineering Geology*, 66 (3/4): 241-255.

-
- CAROLI, I. & M. CALDARA (2007): Vegetation history of Lago Battaglia (eastern Gargano coast, Apulia, Italy) during the middle-late Holocene. *Vegetation History and Archaeobotany*, 16 (4): 317-327.
 - CARTER, R. W. G. & C. D. WOODROFFE (1994): *Coastal Evolution: Late Quaternary shoreline dynamics*. Cambridge University Press. Cambridge.
 - CARTON, A., BONDESAN, A., FONTANA, A., MENEGHEL, M., MIOLA, A., MOZZI, P., PRIMON, S. & N. SURIAN (2009): Geomorphological evolution and sediment transfer in the Piave River system (northeastern Italy) since the Last Glacial Maximum (Evolution géomorphologique et transfert sédimentaire dans le bassin du Piave (Italie nord-orientale) depuis le Dernier Maximum Glaciaire). *Géomorphologie: relief, processus, environnement*, n°3: 155-174.
 - CAVAZZA, W., ROURE, F., SPAKMAN, W., STAMPFLI, G. M. & P. A. ZIEGLER (2004): *The TRANSMED Atlas – The Mediterranean Region from Crust to Mantle. Geological and geophysical framework of the Mediterranean and the surrounding areas*. Springer-Verlag Berlin, Heidelberg.
 - CEKA, N. (2005): *The Illyrians to the Albanians*. Publishing House Migjeni. Tirana.
 - CIAVOLA, P., MANTOVANI, F., SIMEONI U. & U. TESSARI (1999): Relation between river dynamics and coastal changes in Albania: an assessment integrating satellite imagery with historical data. *International Journal of Remote Sensing*, 20 (3): 561-584.
 - COHMAP MEMBERS (1988): Climatic changes of the last 18,000 years: Observations and Model simulations. *Science*, 241: 1043-1052.
 - COLOMBAROLI, D., TINNER W., VAN LEEUWEN, J., NOTI R., VESCOVI, E., VANNIÈRE B., MAGNY, M., SCHMIDT, R. & H. BUGMANN (2009): Response of broadleaved evergreen Mediterranean forest vegetation to fire disturbance during the Holocene: insights from the peri-Adriatic region. *Journal of Biogeography*, 36: 314-326.
 - CORSI, C., DE DAPPER, M. & F. VERMEULEN (2009): River-bed changing in the lower Potenza Valley (mid-Adriatic Italy): A geo-archaeological approach to historical documents. In: PAVLOPOULOS, K. (ed.) – *Palaeo-environmental dynamics and archaeological sites*. *Zeitschrift für Geomorphologie*, N. F., 53. Suppl.-Issue, 1. Berlin, Stuttgart: 83-98.
 - CROWTHER, J. (1997): Soil Phosphate Surveys: Critical Approaches to Sampling, Analysis and Interpretation. *Archaeological Prospection*, 4: 93-102.
 - CUNDY, A. (2005): Recent rapid sea-level change in the eastern Mediterranean and the coastal sedimentary records. In: FOUACHE, É. & K. PAVLOPOULOS (eds.) – *Sea Level Changes in Eastern Mediterranean during Holocene – Indicators and Human Impacts*. *Zeitschrift für Geomorphologie*, N. F., Suppl.-vol. 137. Berlin, Stuttgart: 29-35.
 - DALFES, H. N., KUKLA, G. & H. WEISS (eds.) (1997): *Third millennium BC climatic change and Old World collapse*. NATO ASI Series I: Global Environmental Change. Vol. 49. Springer-Verlag. Berlin.

-
- DANKOFF, R. & R. ELSIE (2000): Evliya Çelebi in Albania and Adjacent Regions (Kosovo, Montenegro, Ohrid). In: KREISER, K. (ed.) – Evliya Çelebi's Book of Travels, Land and people of the Ottoman Empire in the seventeenth century. Vol.: V. Brill. Leiden, Boston, Köln.
 - DAVIS, R. A. (1983): Depositional systems: A genetic approach to sedimentary geology. Prentice-Hall, New Jersey.
 - DAVIS, R. A. (ed.) (1985): Coastal Sedimentary Environments (2nd revised, expanded ed.). Springer-Verlag. New York, Berlin, Heidelberg, Tokyo.
 - DENÈFLE, M., LÉZINE, A-M., FOUACHE, É. & J.-J. DUFAURE (2000): A 12,000-Year Pollen record from Lake Maliq, Albania. *Quaternary Research*, 54 (3): 423-432.
 - DEMIRAJ, E. (ed.) (1996): Implications of climate change for the Albanian coast – Implications du changement climatique pour la zone côtière d'Albanie. MAP Technical Reports Series No. 98. UNEP. Athens.
 - DEWIS, J. & F. FREITAS (1970): Physical and Chemical Methods of Soil and Water Analysis. Soils Bulletin 10. Food and Agriculture Organization of the United Nations. Rome.
 - DINI, M., MASTRONUZZI, G. & P. SANSÒ (2000): The effects of relative sea level changes on the coastal morphology of southern Apulia (Italy) during the Holocene. In: SLAYMAKER, O. (ed.) – Geomorphology, Human Activity and Global Environmental Change. John Wiley & Sons. Chichester: 43-65.
 - DIORORUS SICULUS (1967): The Library of History. Loeb Classical Library. 12 Volumes. Translated by C. H. OLDFATHER. Harvard University Press.
 - DI RITA, F. & D. MAGRI (2009): Drought, deforestation and Mediterranean evergreen vegetation development in the central Mediterranean: a 5500 year record from Lago Alimini Piccolo, Apulia, south east Italy. *The Holocene*, 19 (2): 295-306.
 - DONGUS, H. (1963): Die Entwicklung der östlichen Po-Ebene seit frühgeschichtlicher Zeit. *Erdkunde*, XVII: 205-222.
 - DRYSDALE, R., ZANCHETTA, G., HELLSTROM, J., MAAS, R., FALICK, A., PICKETT, M., CARTWRIGHT, I. & L. PICCINI (2006): Late Holocene drought responsible for the collapse of Old World civilizations is recorded in an Italian cave flowstone. *Geology*, 34 (2): 101-104.
 - DUKA, F. (2009): Coast and Hinterland in the Albanian Lands (16th-18th centuries). In: ORTALLI, G. & O. J. SCHMITT (Hrsg.) – *Balceni occidentali, Adriatico e Venezia fra XIII e XVIII secolo / Der westliche Balkan, der Adriaum und Venedig (13.-18. Jahrhundert)* Österreichische Akademie der Wissenschaften Philosophisch-Historische Klasse, Istituto Veneto di Scienze, Lettere ed Arti, Schriften der Balkan-Kommission, 50. Venezia, Wien: 261-270.

-
- DUMAS, B., GUÉRÉMY, P. & J. RAFFY (2005): Evidence for sea-level oscillations by the “characteristic thickness” of marine deposits from raised terraces of Southern Calabria, Italy. *Quaternary Science Reviews*, 24 (18-19): 2120-2136.
 - EFTIMI, R. (1998): The management of Kune-Vain lagoon system. Geological and hydrogeological conditions. Environmental Centre for Administration and Technology (ECAT) (unpublished report). Tirana.
 - ELLERBROCK, R. H. (2000): Der pH-Wert von Boden und Wasser. In: BARSCH, H., BILLWITZ, K. & H.-R. BORG (Hrsg.) – *Arbeitsmethoden in Physiogeographie und Geoökologie*. Klett – Perthes. Gotha, Stuttgart: 322-328.
 - ELSIE, R. (2003): Early Albania. A Reader of Historical Texts, 11th-17th Centuries. *Balkanologische Veröffentlichungen Osteuropa-Institut der Freien Universität Berlin*. Band 39. Harrassowitz Verlag. Wiesbaden.
 - ELLWOOD, B. B., HARROLD, F. B., PETRUSO, K. M. & M. KORKUTI (1993): Electrical resistivity surveys as indicators of site potential: examples from a rockshelter in southwestern France and a cave in southern Albania. *Geoarchaeology: An International Journal*, 8: 217-227.
 - ELLWOOD, B. B., PETRUSO, K. M., HARROLD, F. B. & M. KORKUTI (1996): Paleoclimate Characterization and Intra-Site Correlation Using Magnetic Susceptibility Measurements: An Example from Konispol Cave, Albania. *Journal of Field Archaeology*, 23 (3): 263-271.
 - ELLWOOD, B. B., PETRUSO, K. M. & F. B. HARROLD (1997): High-resolution Paleoclimatic Trends for the Holocene Identified Using Magnetic Susceptibility Data from Archaeological Excavations in Caves. *Journal of Archaeological Science*, 24 (6): 569-573.
 - ENGEL, M., KNIPPING, M., BRÜCKNER, H., KIDERLEN, M. & J. C. KRAFT (2009): Reconstructing middle to late Holocene palaeogeographies of the lower Messenian plain (southwestern Peloponnese, Greece): Coastline migration, vegetation history and sea level change. *Palaeogeography, Palaeoclimatology, Palaeoecology*, 284 (3-4): 257-270.
 - EVANS, A. (1885-86): *Antiquarian Researches in Illyricum, 1885 I & II 1886. Vol 48 and III & IV. Vol 49.* Archaeologia Society of Antiquaries, London. Reprint: (2006): *Ancient Illyria: An Archaeological Exploration*. I. B. Tauris & Co. Ltd.
 - FAIRBANKS, R. G. (1989): A 17,000-year glacio-eustatic sea level record: influence of glacial melting rates on the younger Dryas event and deep ocean circulation. *Nature*, 342: 637-642.
 - FAIVRE, S. & É. FOUACHE (2003): Some tectonic influences on the Croatian shoreline evolution in the last 2000 years. *Zeitschrift für Geomorphologie, N. F.*, 47 (4). Berlin, Stuttgart: 521-537
 - FAO-UNESCO (1974): *Soil Map of the World, 1:5,000,000. Vol.1, Legend.* UNESCO, Paris.
 - FLEMMING, N. C. (1978): Holocene eustatic changes and coastal tectonics in the northeast Mediterranean, Implications for models of crustal consumption. *Philosophical Transactions Royal Society London*, 289: 405-458.

-
- FLEMMING, N. C. & C. O. WEBB (1986): Tectonic and eustatic coastal changes during the last 10,000 years derived from archaeological data. In: OZER, A. & C. VITA-FINZI (eds.) – Dating Mediterranean Shorelines. *Zeitschrift für Geomorphologie, Suppl.-Bd. 62*. Berlin, Stuttgart: 1-29.
 - FOUACHE, É. (2002): Dynamiques paléo-environnementales en Albanie à l'Holocène. In: TOUCHAIS, G. & J. RENARD (eds.) – L'Albanie dans l'Europe Préhistorique: Actes du Colloque de Lorient, 8-10 Juin 2000. *Bulletin de Correspondance Hellénique, Suppl. 42*: 3-20.
 - FOUACHE, É. (2006): 10 000 ans d'évolution des paysages en Adriatique et en Méditerranée orientale (Géomorphologie, Paléoenvironnements, Histoire). *Travaux de la Maison de l'orient et de la méditerranée, N° 45*. Jean Pouilloux, Lyon.
 - FOUACHE, É., FAIVRE, S., DUFAURE, J.-J., KOVACIC, V. & F. TASSAUX (2000): New observations on the evolution of the Croatian shoreline between Poreč and Zadar over the past 2000 years. In: PFEFFER, K.-H. (ed.) – *Holocene Geomorphology. Zeitschrift für Geomorphologie, N. F., Suppl.-Bd. 122*. Berlin, Stuttgart: 33-46.
 - FOUACHE, É., GRUDA, G., MUCAJ, S. & P. NIKOLLI (2001): Recent geomorphological evolution of the deltas of the Rivers Seman and Vjosa, Albania. *Earth Surface Processes and Landforms, 26 (7)*: 793-802.
 - FOUACHE, É., DUFAURE, J.-J., DENÈFLE, M., LÈZINE, A.-M., LÈRA, P., PRENDI, F. & G. TOUCHAIS (2001): Man and environment around lake Maliq (southern Albania) during the Late Holocene. *Vegetation History and Archaeobotany, 10 (2)*: 79-86.
 - FOUACHE, É., VELLA, C., DIMO, L., GRUDA, G., DENÈFLE, M., MONNIER, O., HOTYAT, M. & E. HUTH (2003): The progradation of the Albanian deltaic plains (Drin, Mati, Seman and Vjosa Deltas): A matter of the last 500 Years? – In: XVI INQUA Congress, Paper No: 76-2, *Holocene in the Mediterranean and Black Sea Regions (Posters)*. Geological Society of America. Abstracts with Programs: 208.
 - FOUACHE, É., DELONGEVILLE, R., KUNESCH, S., SUC, J.-P., SUBALLY, D., PRIEUR, A. & P. LOZOUET (2005): The environmental setting of the harbour of the Classical Site of Oeniades on the Acheloos Delta, Greece. *Geoarchaeology: An International Journal, 20 (3)*: 285-302.
 - FOUACHE, É., DESRUELLES, S., MAGNY, M., BORDON, A., OBERWEILER, C., COUSSOT, C., TOUCHAIS, G., LERA, P., LÈZINE, A.-M., FADIN, L. & R. ROGER (2010a): Palaeogeographical reconstructions of Lake Maliq (Korça Basin, Albania) between 14,000 BP and 2,000 BP. *Journal of Archaeological Science, 37 (3)*: 525-535.
 - FOUACHE, É., VELLA, C., DIMO, L., GRUDA, G., MUGNIER, J.-L., DENÈFLE, M., MONNIER, O., HOTYAT, M. & E. HUTH (2010b): Shoreline reconstruction since the Middle Holocene in the vicinity of the ancient city of Apollonia (Albania, Seman and Vjosa deltas). *Quaternary International, 216 (1-2)*: 118-128.

- FRANKE, P. R. (1983): Albanien im Altertum. – In: Albanien im Altertum. Antike Welt (Sondernummer): 11-65.
- FRASHERI, A., PANO, N. & F. HOXHA (2008): Impact of the climate change in Albanian Adriatic littoral. BALWOIS 2010 – Ohrid, Republic of Macedonia – 25-29 May 2008. [www.balwois.com/balwois/administration/full_paper/ffp-1644.pdf (access: 07.12.2010)].
- FRENZEL, P. & I. BOOMER (2005): The use of ostracods from marginal-marine, brackish waters as bioindicators of environmental change and Quaternary palaeoenvironmental analysis – a review. *Palaeogeography, Palaeoclimatology, Palaeoecology*, 225 (1-4): 68-92.
- FÜCHTBAUER, H. (Hrsg.) (1988): Sedimente und Sedimentgesteine. 4. Aufl. (Sediment-Petrologie, II). E. Schweizerbart'sche Verlagsbuchhandlung. Stuttgart.
- GAWLICK, H.-J., FRISCH, W., HOXHA, L., DUMITRICA, P., KRYSZYN, L., LEIN, R., MISSONI, S. & F. SCHLAGINTWEIT (2008): Mirdita Zone ophiolites and associated sediments in Albania reveal Neotethys Ocean origin. *International Journal of Earth Sciences (Geologische Rundschau)*, 97: 865-881.
- GEYH, M. A. (2005): Handbuch der physikalischen und chemischen Altersbestimmung. Wissenschaftliche Buchgesellschaft. Darmstadt.
- GILBERT, G. K. (1885): The topographic features of lake shore. U. S. Geological Survey, 5th Annual Report: 69-123.
- GJIKNURI, L. (1995): The Albanian sea-coast: problems and perspectives. In: BRIAND, F. (ed.) – Les mers tributaires de Méditerranée – Mediterranean tributary seas. *Bulletin de l'Institut océanographique, Monaco, Numéro spécial 15, CIESM Science Series n°1. Monaco*: 187-201.
- GOETHALS, T., DE DAPPER, M. & B.-M. DE VliegHER (2003): The Holocene evolution of the coastal plain in the Potenza River basin and some geo-archaeological aspects of this study area. In: VERMEULEN, F. (ed.) – The Potenza Valley Survey: Preliminary Report on Field Campaign 2002: 71-106. *BABesch 78*: 76-79.
- GRAVINA, A., MASTRONUZZI, G. & P. SANSÒ (2005): Historical and prehistorical evolution of the Fortore River coastal plain and the Lesina Lake area (Southern Italy) (Évolution holocène de la plaine littorale du Fortore et de la lagune de Lesina (Italie du Sud). *Méditerranée*, N°1.2: 107-117.
- GROTHE, A.-F. (2009): Die Entwicklung des Drin-Deltas – ein Beitrag zur Genese der Küste Nordwest-Albaniens. Diplomarbeit (unpublished). Fachbereich Geographie der Philipps-Universität. Marburg.
- GROVE, A. T. (2001): The „Little Ice Age“, and its geomorphological consequences in the Mediterranean Europe. *Climatic Change*, 48: 121-136.
- GROVE, A. T. & O. RACKHAM (2001): The Nature of Mediterranean Europe: An Ecological History. Yale University Press. New Haven & London.

-
- GUILLÉN, J. & A. PALANQUES (1997): A historical perspective of the morphological evolution in the Lower Ebro River. *Environmental Geology*, 30 (3/4): 174-180.
 - GURAZIU, F. (2006): Tourism in Shkodër, Northern Albania. The Italian-Albanian Friendship Association with seat in Florence and Shkodër in collaboration with Florence Municipality.
 - HAHN, J. G. VON (1853): *Albanische Studien*. Aus der kaiserlich-königlichen Hof- und Staatsdruckerei. Wien.
 - HAJDAS, I. (2008): Radiocarbon dating and its applications in Quaternary studies. In: PREUSSER, F., HAJDAS, I. & S. IVY-OCHS (Guest eds.) – Recent progress in Quaternary dating methods. *Eiszeitalter und Gegenwart (Quaternary Science Journal)*, 57 (1-2): 2-24.
 - HAMMOND, N. G. L. (1968): Illyris, Rome and Macedon in 229-205 B.C. *The Journal of Roman Studies*, Vol. 58, Parts 1 and 2: 1-21.
 - HAMMOND, N. G. L. (1976): Lissos (Lesh). In: R. STILLWELL (ed.) – *The Princeton Encyclopedia of Classical Sites*. Princeton University Press. Princeton, New Jersey: 520.
 - HAMMOND, N. G. L. (1988): The reigns of Philip V and Perseus. In: HAMMOND, N. G. L. & F. W. WALBANK (eds.) – *A history of Macedonia: 336-167 B.C.* Vol: III. Oxford University Press. Oxford: 367-428.
 - HANDL, M., MOSTAFAWI, N. & H. BRÜCKNER (1999): Ostracodenforschung als Werkzeug der Paläogeographie. In: BRÜCKNER, H. (Hrsg.) – *Dynamik, Datierung, Ökologie und Management von Küsten*. Beiträge der 16. Jahrestagung des Arbeitskreises „Geographie der Meere und Küsten“ 21.-23. Mai 1998, Marburg. *Marburger Geographische Schriften*, 134. Marburg: 116-153.
 - HARDING, A. E., PALUTIKOF, J. & T. HOLT, (2009): The Climate System. – In: WOODWARD, J. C. (ed.) – *The Physical Geography of the Mediterranean*. Oxford University Press. Oxford: 69-88.
 - HEIRI, O., LOTTER, A. F. & G. LEMCKE (2001): Loss-on-ignition as a method for estimating organic and carbonate content in sediments: reproducibility and comparability of results. *Journal of Paleolimnology*, 25: 101-110.
 - HEYWORTH, A. (1986): Submerged forests as sea-level indicators. In: VAN DE PLASSCHE, O. (ed.) – *Sea-level research: a manual for the collection and evaluation of data*. Geo Books. Norwich: 401-412.
 - HOFFMANN, G. (1988): Holozänstratigraphie und Küstenlinienverlagerung an der andalusischen Mittelmeerküste. *Berichte aus dem Fachbereich Geowissenschaften der Universität Bremen*, 2. Bremen.
 - HOFFMANN, G. (1995): Natürliche und anthropogene Einflüsse auf das holozäne Erosions- und Sedimentationsgeschehen an der andalusischen Mittelmeerküste. *Geoökodynamik*, 16: 197-210.

-
- HOFRICHTER, R. (Hrsg.) (2001): *Das Mittelmeer. Fauna, Flora, Ökologie. 1: Allgemeiner Teil.* Heidelberg, Berlin.
 - HORVAT, I., GLAVAČ, V. & H. ELLENBERG (1974): *Vegetation Südosteuropas. Geobotanica Selecta, IV.* Gustav Fischer Verlag. Stuttgart.
 - HOUNSLOW, M. W. & A. CHEPSTOW-LUSTY (2004a): Holocene environmental change at Butrint: a preliminary evaluation of alluvial sediments using archaeomagnetic dating. In: HODGES, R., BOWDEN, W. & K. LAKO (eds.) – *Byzantine Butrint: excavations and surveys 1994 – 99.* Oxbow Books. Oxford: 396-397.
 - HOUNSLOW, M. W. & A. CHEPSTOW-LUSTY (2004b): A record of soil loss from Butrint, southern Albania, using mineral magnetism indicators and charcoal (AD 450 to 1200). *The Holocene*, 14 (3): 321-333.
 - HÖHN, A. (2000a): Organische Substanz in Boden und Wasser. In: BARSCH, H., BILLWITZ, K. & H.-R. BORG (Hrsg.) – *Arbeitsmethoden in Physiogeographie und Geoökologie.* Klett – Perthes. Gotha, Stuttgart: 340-352.
 - HÖHN, A. (2000b): Atomabsorptionsspektroskopie (AAS). In: BARSCH, H., BILLWITZ, K. & H.-R. BORG (Hrsg.) – *Arbeitsmethoden in Physiogeographie und Geoökologie.* Klett – Perthes. Gotha, Stuttgart: 352-361.
 - HUTCHINGS, R. (1996): *Historical Dictionary of Albania.* European Historical Dictionaries, No: 12. The Scarecrow Press, Inc. Lanham, Md., and London.
 - HÜTTEROTH, W.-D. (2006): Ecology of Ottoman lands. In: FAROQHI, S. N. (ed.) – *The Cambridge History of Turkey. The Later Ottoman Empire, 1603-1839. Vol. 3.* Cambridge University Press. Cambridge: 18-43.
 - IPPEN, T. A. (1907a): Skutari und die nordalbanische Küstenebene. Zur Kunde der Balkanhalbinsel, Reisen und Beobachtungen. Heft: 5. Sarajevo.
 - IPPEN, T. A. (1907b): Denkmäler verschiedener Altersstufen in Albanien. *Wissenschaftliche Mitteilungen aus Bosnien und der Herzegowina, Zehnter Bd.* Adolf Holzhausen. Wien: 1-70.
 - JACQUES, E. E. (1995): *The Albanians: An ethnic history from prehistoric times to the present* (reprinted from 1908 edition). McFarland & Company, Inc. Publishers.
 - JAHNS, S. (2005): The Holocene history of vegetation and settlement at the coastal site of Lake Voulkaria in Akarnania, Western Greece. *Vegetation History and Archaeobotany*, 14 (1): 55-66.
 - JAHNS, S. (2009): The Holocene History of Vegetation and Environment of Northern Akarnania, Western Greece. In: MATTERN T. & A. VÖTT (Hrsg.) – *Mensch und Umwelt im Spiegel der Zeit, Aspekte geoarchäologischer Forschungen im östlichen Mittelmeergebiet.* Philippika. Marburger altertumskundliche Abhandlungen I. Harrassowitz Verlag. Wiesbaden: 5-26.

-
- JAHNS, S. & C. VAN DEN BOGAARD (1998): New palynological and tephrostratigraphical investigations of two salt lagoons on the island of Mljet, south Dalmatia, Croatia. *Vegetation History and Archaeobotany*, 7 (4): 219-234.
 - JALUT, G., DEBOUBAT, J. J., FONTUGNE, M. & T. OTTO (2009): Holocene circum-Mediterranean vegetation changes: climate forcing and human impact. *Quaternary International*, 200 (1-2): 4-18.
 - JAKUCS, P. (1967): Mikroklimatische Untersuchungen im Berührungsgebiet der mediterranen und submediterranen Vegetation Albaniens. *Archive für Naturschutz und Landschaftsforschungen*, Band: 7. Berlin: 3-29.
 - JING, Z. & G. RAPP (2003): The coastal evolution of the Ambracian embayment and its relationship to archaeological settings. In: WISEMAN, J. & K. ZACHOS (eds.) – *Landscape Archaeology in Southern Epirus, Greece 1. Hesperia Suppl.*, 32: 157-198.
 - JIREČEK, K. (1916): Skutari und sein Gebiet im Mittelalter. In: THALLÓCZY, L. VON (Zusammengestellt). *Illyrisch-Albanische Forschungen*, I. Band. Verlag von Duncker & Humblot. München und Leipzig: 91-124.
 - KABO, M. (1988): Disa karakteristika gjeomorfologjike të bregdetit shqiptar të Adriatikut dhe të dinamikës së sotme të tij. *Studime Gjeografike*, 3: 5-35.
 - KABO, M. (ed.) (1990-91): *Gjeografia Fizike e Shqipërisë (Physical Geography of Albania)*. Vols. I & II. Akademia e Shkencave e rps të Shqipërisë, The Albanian Academy of Sciences, Qendra e Studimeve Gjeografike (Centre of Geographical Studies). Tirana. (in Albanian).
 - KAYAN, İ. (1988): Late Holocene sea-level changes on the Western Anatolian coasts. *Palaeogeography, Palaeoclimatology, Palaeoecology*, 68 (2-4): 205-218.
 - KAYAN, İ. (1991): Holocene geomorphic evolution of the Beşik plain and changing environment of ancient man. *Studia Troica*, 1: 79-92.
 - KAYAN, İ. (1995): The Troia Bay and supposed harbour sites in the Bronze Age. *Studia Troica*, 5: 211-235.
 - KAYAN, İ. (1996): Holocene stratigraphy of the Karamenderes-Dümrek plain and archaeological material in the alluvial sediments to the north of the Troia Ridge. *Studia Troica*, 6: 239-249.
 - KAYAN, İ. (1997): Bronze Age regression and change of sedimentation on the Aegean coastal plains of Anatolia (Turkey). In: DALFES, N. H., KUKLA, G. & H. WEISS (eds.) – *Third Millennium BC Climate Change and Old World Collapse. NATO ASI Series*, 1, 49. Berlin, Heidelberg: 431-450.
 - KAYAN, İ. (1999): Holocene stratigraphy and geomorphological evolution of the Aegean coastal plains of Anatolia. *Quaternary Science Reviews*, 18 (4-5): 541-548.

-
- KAYAN, İ. (2001): Die troianische Landschaft. Geomorphologische und paläogeographische Rekonstruktion der Alluvialebenen. In: Troia – Traum und Wirklichkeit. Archäologisches Landesmuseum Baden-Württemberg u.a. Stuttgart: 541-548.
 - KAYAN, İ., ÖNER, E., UNCU, L., HOCAOĞLU, B. & S. VARDAR (2003): Geoarchaeological interpretations of the “Troian Bay”. In: WAGNER, G. A., PERNICKA, E. & H.-P. UERPMANN (eds.) – Troia and the Troad, Scientific Approaches. Springer-Series: Natural Sciences in Archaeology. Berlin: 379-401.
 - KELLETAT, D. (1975): Eine eustatische Kurve für das jüngere Holozän, konstruiert nach Zeugnissen früherer Meeresspiegelstände im östlichen Mittelmeergebiet. Neues Jahrbuch für Geologie und Paläontologie, Monatshefte, 6: 360-374.
 - KELLETAT, D. (1984): Deltaforschung. Erträge der Forschung, 214. Darmstadt.
 - KELLETAT, D. (2005a): A Holocene sea level curve for the Eastern Mediterranean from multiple indicators. In: FOUACHE, É. & K. PAVLOPOULOS (eds.) – Sea level changes in Eastern Mediterranean during Holocene – Indicators and Human Impacts. Zeitschrift für Geomorphologie, N. F. Suppl.-vol. 137. Berlin, Stuttgart: 1-9.
 - KELLETAT, D. (2005b): Dalmatian Coasts. In: SCHWARTZ, M. L. (ed.) – Encyclopedia of Coastal Science. Springer. Dordrecht: 356-357.
 - KOCH, G. (1989): Albanien: Kunst, Kultur im Land der Skipetaren. Dumont Verlag. Köln.
 - KOCIAJ, S. & E. SULSTAROVA (1980): The earthquake of June 1, 1905, Shkodra, Albania; intensity distribution and macroseismic epicentre. Tectonophysics, 67: 319-332.
 - KÖPPEN & GEIGER (1961): Klima der Erde. Darmstadt.
 - KORKUTI, M. (1983): Geschichte und Kultur Albanien in vorgeschichtlicher Zeit. In: FRANKE, P. P. (ed.) – Albanien im Altertum. Antike Welt (Sondernummer): 3-11.
 - KORKUTI, M. (1988): Illyrien in der Vorgeschichte. In: EGGBRECHT, A. (ed.) – Albanien, Schätze aus dem Land der Skipetaren. Verlag Philipp von Zabern, Mainz: 7-31.
 - KORKUTI, M. & K. M. PETRUSO (1993): Archaeology in Albania. American Journal of Archaeology, 97 (4): 703-743.
 - KRAFT, J. C., RAPP, G. & S. E. ASCHENBRENNER (1975): Late Holocene paleogeography of the Gulf of Messenia, Greece, and its relationships to archaeological settings and coastal changes. Geological Society of American Bulletin, 86: 1191-1208.
 - KRAFT, J. C. & S. E. ASCHENBRENNER (1977): Palaeogeographic reconstructions in the Methoni Embayment in Greece. Journal of Field Archaeology, 4 (1): 19-44.
 - KRAFT, J. C., KAYAN, İ. & O. EROL (1980a): Geomorphic reconstructions in the environs of ancient Troy. Science, 209: 776-782.
 - KRAFT, J. C., RAPP, G. & S. E. ASCHENBRENNER (1980b): Late Holocene palaeogeomorphic reconstructions in the area of the Bay of Navarino: Sandy Pylos. Journal of Archaeological Science, 7 (3): 187-210.

-
- KRAFT, J. C. & M. J. CHRZASTOWSKI (1985): Coastal stratigraphic sequences. In: DAVIS, R. A. (ed.) – Coastal Sedimentary Environments (2nd revised, expanded ed.). Springer. New York, Berlin, Heidelberg, Tokyo: 625-663.
 - KRAFT, J. C., RAPP, G. R., SZEMLER, G. J., TZIAVOS, C. & E. W. KASE (1987): The pass at Thermopylae, Greece. *Journal of Field Archaeology*, 14: 181-198.
 - KRAFT, J. C., KAYAN, İ., BRÜCKNER, H. & G. RAPP (2000): A geologic analysis of ancient landscapes and the harbours of Ephesus and the Artemision in Anatolia. *Jahreshefte des Österreichischen Archäologischen Institutes in Wien*, 69: 175-233.
 - KRAFT, J. C., KAYAN, İ. & H. BRÜCKNER (2001): The geological and palaeogeographical environs of the Artemision. In: MUSS, U. (Hrsg.): *Der Kosmos der Artemis von Ephesos*. Österreichisches Archäologisches Institut, Sonderschriften, 37. Wien: 123-133.
 - KRAFT, J. C., RAPP, G. (RIP), KAYAN, İ. & J. V. LUCE (2003): Harbour areas at ancient Troy. Sedimentology and geomorphology complement Homer's *Iliad*. *Geology*, 31 (2): 163-166.
 - KRAFT, J. C., KAYAN, İ. & H. BRÜCKNER (2005a): The sea under the ancient city of Ephesus. In: BRANDT, B., GASSNER, V. & S. LADSTÄTTER (Hrsg.) – *Synergia*. Festschrift für F. Krinzinger, Bd.: 1. Wien: 147-156.
 - KRAFT, J. C., RAPP, G. R., GIFFORD, J. A. & S. E. ASCHENBRENNER (2005b): Coastal change and archaeological settings in Elis. *Hesperia*, 74: 1-39.
 - KRAFT, J. C., BRÜCKNER, H., KAYAN, İ. & H. ENGELMANN (2007): The Geographies of Ancient Ephesus and the Artemision in Anatolia. *Geoarchaeology: An International Journal*, 22 (1): 121-149.
 - KRANJC, A. (2009): History of deforestation and reforestation in the Dinaric Karst. *Geographical Research*, 47 (1): 15-23.
 - LABOREL, J. (1986): Vermetid gastropods as sea-level indicators. In: VAN DE PLASSCHE, O. (ed.) – *Sea-level research: a manual for the collection and evaluation of data*. Geo Books. Norwich: 281-310.
 - LABOREL, J. & F. LABOREL-DEGUEN (1994): Biological indicators of relative sea-level variation and co-seismic displacements in the Mediterranean area. *Journal of Coastal Research*, 10 (2): 395-415.
 - LABOREL, J. & F. LABOREL-DEGUEN (2005): Sea-level indicators, biologic. In: SCHWARTZ, M. (ed.) – *Encyclopedia of Coastal Science*. Springer. Dordrecht: 833-834.
 - LAMBECK, K., ANTONIOLI, F., PURCELL, A. & S. SILENZI (2004a): Sea-level change along the Italian coast for the past 10,000 yr. *Quaternary Science Reviews*, 23 (14-15): 1567-1598.
 - LAMBECK, K., ANZIDEI, M., ANTONIOLI, F., BENINI, A. & A. ESPOSITO (2004b): Sea level in Roman time in the Central Mediterranean and implications for recent change. *Earth and Planetary Science Letters*, 224 (3-4): 563-575.

-
- LAMBECK, K. & P. JOHNSTONE (1995): Land subsidence and sea-level change: contributions from the melting of the last great ice sheets and isostatic adjustment of the Earth. In: BARENDT, F. B. J., BROUWER, F. J. J. & F. H. SCHRODER (eds.) – Land Subsidence. Proceedings of the 5th International Symposium on Land Subsidence. A. A. Balkema. Rotterdam: 3-18.
 - LAMBECK, K. & A. PURCELL (2005): Sea-level change in the Mediterranean Sea since the LGM: model predictions for tectonically stable areas. *Quaternary Science Reviews*, 24 (18-19): 1969-1988.
 - LANE, A. (2004): The environs of Butrint 1: The 1995-96 environmental survey. In: HODGES, R., BOWDEN, W. & K. LAKO (eds.) – Byzantine Butrint: excavations and surveys 1994 – 99. Oxbow Books. Oxford: 27-46.
 - LAURITZEN, S.-E., (2005): Reconstructing Holocene climate records from speleothems. In: MACKAY, A., BATTARBEE, R., BIRKS, J. & F. OLDFIELD (eds.) – Global Change in the Holocene. Hodder Arnold. New York: 242-263.
 - LAWSON, I., FROGLEY, M., BRYANT, C., PREECE, R. & P. TZEDAKIS (2004): The Lateglacial and Holocene environmental history of the Ioannina Basin, north-west Greece. *Quaternary Science Reviews*, 23 (14-15): 1599-1625.
 - LIENAU, C. (1993): Geographische Grundlagen. In: GROTHUSEN, K.-D. (Hrsg.) – Albanien. Südosteuropa-Handbuch. Band VII. Vandenhoeck & Ruprecht. Göttingen: 1-25.
 - LIENAU, C. & G. PRINZING (Hrsg.) (1984): Beiträge zur Geographie und Geschichte Albaniens. Berichte aus dem Arbeitsgebiet Entwicklungsforschung am Institut für Geographie Münster, Heft 12.
 - LISSUS EXCAVATION REPORT (2004):
[http://www.uni-graz.at/klar1www_excavation_report_2004.pdf (access: 07.12.2010)].
 - LIVY (1905): The History of Rome. Translated and revised by C. ROBERTS. Everyman's Library. J. M. Dent & Sons Ltd. London.
 - LONG, A. (2003): The coastal strip, sea-level change, coastal evolution and land-ocean correlation. *Progress in Physical Geography*, 27 (3): 423-434.
 - LOUIS, H. (1927): Albanien. Eine Landeskunde vornehmlich auf Grund eigener Reisen. Stuttgart.
 - MACKAY, A., BATTARBEE, R., BIRKS, J. & F. OLDFIELD (eds.) (2005): Global Change in the Holocene. Hodder Arnold. New York.
 - MAGNY, M., MIRAMONT, C. & O. SIVAN (2002): Assessment of the impact of climate and anthropogenic factors on Holocene Mediterranean vegetation in Europe on the basis of palaeohydrological records. *Palaeogeography, Palaeoclimatology, Palaeoecology*, 186 (1-2): 47-59.

-
- MAGNY, M., VANNIÈRE, B., ZANCHETTA, G., FOUACHE, É., TOUCHAIS, G., PETRIKA, L., COUSSOT, C., WALTER-SIMONNET, A.-V., & F. ARNAUD (2009): Possible complexity of the climatic event around 4300-3800 cal. BP in the central and western Mediterranean. *The Holocene*, 19 (6): 823-833.
 - MARIÑO, M. G. (1992): Implications of climatic change on the Ebro Delta. In: JEFTIC, L., MILLIMAN, J. D. & G. SESTINI (eds.) – *Climatic change and the Mediterranean: environmental and societal impacts of climatic change and sea-level rise in the Mediterranean Region*. Edward Arnold: 304-327.
 - MARKGRAF, F. (1932): *Pflanzengeographie von Albanien. Ihre Bedeutung für Vegetation und Flora der Mittelmeerländer*. Bibliotheca Botanica, Heft 105. Stuttgart.
 - MARRINER, N. (2009): *Geoarchaeology of Lebanon's ancient harbours*. British Archaeological Reports (BAR). International Series, 1953. Archaeopress.
 - MARRINER, N., MORHANGE, C., BOUDAGHER-FADEL, M., BOURCIER, M. & P. CARBONEL (2005): *Geoarchaeology of Tyre's ancient northern harbour, Phoenicia*. *Journal of Archaeological Science*, 32 (9): 1302-1327.
 - MARRINER, N., MORHANGE, C. & C. DOUMET-SERHAL (2006): *Geoarchaeology of Sidon's ancient harbours, Phoenicia*. *Journal of Archaeological Science*, 33 (11): 1514-1535.
 - MARTYN, D. (1992): *Climates of the World*. *Developments in Atmospheric Science*, 18. Elsevier.
 - MATHERS, S., BREW, D. S. & R. S. ARTHURTON (1999): Rapid Holocene evolution and neotectonics of the Albanian Adriatic coastline. *Journal of Coastal Research*, 15 (2): 345-354.
 - MAY, J. M. F. (1946): *Macedonia and Illyria (217-167 B.C.)*. *The Journal of Roman Studies*, 36 (1 & 2): 48-56.
 - MAYEWSKI, P. A., ROHLING, E. E., STAGER, J. C., KARLÉN, W., MAASCH, K. A., MEEKER, L. D., MEYERSON, E. A., GASSE, F., VAN KREVELD, S., HOLMGREN, K., LEE-THORP, J., ROSQVIST, G., RACK, F., STAUBWASSER, M., SCHNEIDER, R. R. & E. J. STEIG (2004): Holocene climate variability. *Quaternary Research*, 62 (3): 243-255.
 - MCPHERSON, J. G., SHANMUGAM, G. & R. J. MOIOLA (1988): Fan deltas and braid deltas: conceptual problems. In: NEMEC, W. & R. J. STEEL (eds.) – *Fan Deltas: Sedimentology and Tectonic Settings*. Blackie and Son: 14-22.
 - MEÇAJ, N. (2005a): River deltas: Their morphology and the accompanying dynamic evolution of the Adriatic and Ionian Coasts of Albania. *Zeitschrift für Geomorphologie, Suppl.-vol.*: 141. Berlin-Stuttgart: 59-73.
 - MEÇAJ, N. (2005b): Protection of the littorals of the Kune – Vain Lagoons, by using eco-techniques to manage coastal erosion. In: GUTIÉRREZ, F., GUTIÉRREZ, M., DESIR, G., GUERRERO, J., LUCHA, P., CINTA, M. & J. M. GARCIA-RUIZ (eds.) – *Sixth International Conference on Geomorphology, Zaragoza, September 7-11, 2005*. Abstracts vol.: 256.

-
- MEÇO, S. & S. ALIAJ (2000): Geology of Albania. Beiträge zur Regionalen Geologie der Erde. Band. 28. Gebrüder Borntraeger. Berlin, Stuttgart.
 - MIDDLETON, G. V. (1973): Johannes Walther's Law of the Correlation of Facies. Geological Society of America Bulletin, 84: 979-988.
 - MILLIMAN, J. D. & R. H. MEADE (1983): World-wide delivery of river sediment to the oceans. The Journal of Geology, 91 (1): 1-21.
 - MILLIMAN, J. D. & J. P. M. SYVITSKI (1992): Geomorphic/tectonic control of sediment discharge to the oceans: The importance of small mountainous rivers. The Journal of Geology, 100 (5): 525-544.
 - MORHANGE, C., LABOREL, J. & A. HESNARD (2001): Changes of relative sea level during the past 5000 years in the ancient harbor of Marseilles, Southern France. Palaeogeography, Palaeoclimatology, Palaeoecology, 166 (3-4): 319-329.
 - MORHANGE, C., BLANC, F., SCHMITT-MERCURY, S., BOURCIER, M., CARBONEL, P., OBERLIN, C., PRONE, A., VIVENT, D. & A. HESNARD (2003): Stratigraphy and late-Holocene deposits of the ancient harbour of Marseilles, southern France. The Holocene, 13 (4): 593-604.
 - MUÇEKU, B., MASCLE, G.H. & A. TASHKO (2006): First results of fission-track thermochronology in the Albanides. In: ROBERTSON, A. H. F. & D. MOUNTRAKIS (eds.) – Tectonic Development of the Eastern Mediterranean Region. Geological Society, London, Special Publications, 260: 539-556.
 - MUÇO, B., VACCARI, F., PANZA, G. & N. KUKA (2002) : Seismic zonation in Albania using a deterministic approach. Tectonophysics, 344: 277-288.
 - MÜLLENHOFF, M. (2005): Geoarchäologische, sedimentologische und morphodynamische Untersuchungen im Mündungsgebiet des Büyük Menderes (Mäander), Westtürkei. Marburger Geographische Schriften, 141. Marburg.
 - MUNSELL Soil Color Charts (2000) Revised Washable Edition.
 - MURRAY, J. (2006): Ecology and Applications of Benthic Foraminifera. Cambridge University Press. Cambridge.
 - NEMEC, W. & R. J. STEEL (eds.) (1988): Fan Deltas: Sedimentology and Tectonic Settings. Blackie and Son.
 - NIEUWLAND, D. A., OUDMAYER, B. C. & U. VALBONA (2001): The tectonic development of Albania: explanation and prediction of structural styles. Marine and Petroleum Geology, 18 (1): 161-177.
 - NOPCSA, F. B. VON (1905): Zur Geologie von Nordalbanien. Jahrbuch der kaiserlich-königlichen Geologischen Reichsanstalt, Band: LV. Wien: 85-152.
 - NOPCSA, F. B. VON (1911): Zur Stratigraphie und Tektonik des Vilajets Skutari in Nordalbanien. Jahrbuch der kaiserlich-königlichen Geologischen Reichsanstalt, Band: LXI. Wien: 229-284.

-
- NOPCSA, F. B. VON (1912): Beiträge zur Vorgeschichte und Ethnologie Nordalbaniens. Wissenschaftliche Mitteilungen aus Bosnien und der Herzegowina. Zwölfter Band. Wien: 168-253.
 - NOPCSA, F. B. VON (1916): Zur Geschichte der Kartographie Nordalbaniens. Mitteilungen der kaiserlich-königlichen Geographischen Gesellschaft in Wien, Bd.: 59. Wien: 520-585.
 - NOPCSA, F. B. VON (1925): Albanien. Bauten, Trachten und Geräte Nordalbaniens. De Gruyter, Berlin & Leipzig.
 - NOPCSA, F. B. VON (1929a): Geologie und Geographie Nordalbaniens. *Geologica Hungarica. Fasciculi ad illustrandum notionem geologicam et palaeontologicam Regni Hungaricae. Series Geologica. Tomus III.* Budapest: 7-620.
 - NOPCSA, F. B. VON (1929b): Zur Geschichte der okzidentalen Kartographie Nordalbaniens. *Geologica Hungarica. Fasciculi ad illustrandum notionem geologicam et palaeontologicam Regni Hungaricae. Series Geologica. Tomus III.* Budapest: 651-703.
 - NOPCSA, F. B. VON (1932): Topographie und Stammesorganisation in Nordalbanien. In: Festschrift für Carl Uhlig. Zu seinem sechzigsten Geburtstag von seinen Freunden und Schülern dargebracht. Verlag der Hohenloheschen Buchhandlung F. Rau. Öhringen: 295-305.
 - OLDFIELD, F., ASIOLI, A., ACCORSI, C. A., MERCURI, A. M., JUGGINS, S., LANGONE, L., ROLPH, T., TRINCARDI, F., WOLFF, G., GIBBS, Z., VIGLIOTTI, L., FRAGNANI, M., VAN DER POST, K. & N. BRANCH (2003): A high resolution late Holocene palaeoenvironmental record from the central Adriatic Sea. *Quaternary Science Reviews*, 22 (2-4): 319-342.
 - PANO, N., FRASHERI, A., SIMEONI, U. & N. FRASHERI (2006): Outlook on seawaters dynamics and geological setting factors for the Albanian Adriatic coastline developments. *The Albanian Journal of Natural and Technical Sciences*, XI (19-20): 152-166.
 - PANO, N. & B. AVDYLI (2009): A method to estimate Buna River discharge, Albania. *Hydrology Days 2009*: 66-72.
 - PASKOFF, R. (1985): Les côtes d'Albanie: Aspects géomorphologiques. *Bulletin de l'Association de Géographes Français*, 2: 77-83.
 - PAVLOPOULOS, K., KARKANAS, P., TRIANTAPHYLLOU, M. & E. KARYMBALIS (2003): Climate and sea-level changes recorded during late Holocene in the coastal plain of Marathon, Greece. In: FOUACHE, É. (ed.) – *The Mediterranean World, Environment and History. I. A. G. Working Group on Geo-archaeology Symposium Proceedings. Environmental dynamics and history in Mediterranean areas.* Paris, Université de Paris-Sorbonne, 24-26 avril 2002. Elsevier: 453-465.
 - PAVLOPOULOS, K., KARKANAS, P., TRIANTAPHYLLOU, M., KARYMBALIS, E., TSOUROU, T. & N. PALYVOS (2006): Paleoenvironmental evolution of the coastal plain of Marathon, Greece, during the late Holocene: depositional environment, climate, and sea-level changes. *Journal of Coastal Research*, 22 (2): 424-438.

-
- PERISSORATIS, C. & N. CONISPOLIATIS (2003): The impacts of sea-level changes during latest Pleistocene and Holocene times on the morphology of the Ionian and Aegean seas (SE Alpine Europe). *Marine Geology*, 196 (3-4): 145-156.
 - PEJA, N., VASO, A., MIHO, A., RAKAJ, N. & A. J. CRIVELLI (1996): Characteristics of Albanian lagoons and their fisheries. *Fisheries Research*, 27: 215-225.
 - PETRUSO, K. M., ELLWOOD, B. B., HARROLD, F. B. & M. KORKUTI (1994): Radiocarbon and archaeomagnetic dates from Konispol Cave, Albania. *Antiquity*, 68: 335-339.
 - PIRAZZOLI, P. A. (1986): Marine notches. In: VAN DE PLASSCHE, O. (ed.) – *Sea-level research: a manual for the collection and evaluation of data*. Geo Books. Norwich: 361-400.
 - PIRAZZOLI, P. A. (1987): Sea-level changes in the Mediterranean. In: TOOLEY, M. J. & I. SHENNAN (eds.) – *Sea-level Changes*. The Institute of British Geographers, Special Publications Series 20. Basil Blackwell Ltd. Oxford: 152-181.
 - PIRAZZOLI, P. A. (1991): *World Atlas of Holocene Sea-level Changes*. Oceanography Series, 58. Elsevier, Amsterdam, London, New York, Tokyo.
 - PIRAZZOLI, P. A. (1996): *Sea-level Changes: the Last 20 000 Years*. John Wiley & Sons Ltd. Chichester.
 - PIRAZZOLI, P. A. (2005a): A review of possible eustatic, isostatic and tectonic contributions in eight late-Holocene relative sea-level histories from the Mediterranean Sea. *Quaternary Science Reviews*, 24 (18-19): 1989-2001.
 - PIRAZZOLI, P. A. (2005b): Sea-level indicators, geomorphic. In: SCHWARTZ, M. (ed.) – *Encyclopedia of Coastal Science*. Springer: 836-838.
 - PIVA, A., ASIOLI, A., TRINCARDI, F., SCHNEIDER, R. R. & L. VIGLIOTTI (2008): Late-Holocene climate variability in the Adriatic Sea (Central Mediterranean). *The Holocene*, 18 (1): 153-167.
 - PLINIUS (1999): *Natural History (Naturalis historiae)*. Translated by H. RACKHAM. The Loeb Classical Library, 352. Cambridge, London.
 - POCHMARSKI, E. & G. HOXHA (2005): *Lissos: Quellen und Stadtgeschichte*. *Römisches Österreich*, 28: 243-251.
 - POLYBIUS (1922): *The Histories*. Loeb Classical Library. Translated by W. R. PATON. New York: G. P. Putnam's Sons.
 - POULOS, S. E., KAPSIMALIS, V., TZIAVOS, C., PAVLAKIS, P., LEIVADITIS, G. & M. COLLINS (2005): Sea-level stands and Holocene geomorphological evolution of the northern deltaic margin of Amvrakikos Gulf (western Greece). In: FOUACHE, É. & K. PAVLOPOULOS (eds.) – *Sea Level Changes in Eastern Mediterranean during Holocene – Indicators and Human Impacts*. *Zeitschrift für Geomorphologie*, N. F., Suppl.-vol. 137. Berlin, Stuttgart: 125-145.

-
- PRASCHNIKER, C. & A. SCHÖBER (1919): Archäologische Forschungen in Albanien und Montenegro. Akademie der Wissenschaften in Wien. Schriften der Balkankommission, Antiquarische Abteilung, Heft VIII, Wien.
 - PRENDI, F. & K. ZHEKU (1971): Qyteti ilir i Lisit, origjina dhe sistemi i fortifikimit të tij. Studime Historike. Tirana: 155-205.
 - PRENDI, F. & K. ZHEKU (1972): La ville illyrienne de Lissus. Son origine et son système de fortifications. Iliria II. Tirana: 215-244.
 - PULAHA, S. & A. PARRUCA (2006): Lezha dhe Shëngjini: Vështrim historiko-geografik. Shtëpia Botuese ILAR. Tirana.
 - QIRIAZI, P. & S. SALA (1997): Geomorphologic peculiarities of the Albanian Adriatic coastline. The Albanian Journal of Natural & Technical Sciences, 3: 59-68.
 - READING, H. G. (ed.) (1996): Sedimentary Environments: Processes, Facies and Stratigraphy (Reprinted from 3rd ed.). Blackwell Science.
 - REIMER, P. J. & F. G. MCCORMAC (2002): Marine radiocarbon reservoir corrections for the Mediterranean and Aegean Seas. Radiocarbon, 44 (1): 159-166.
 - REIMER, R. W., BAILLIE, M. G. L., BARD, E., BAYLISS, A., BECK, J. W., BERTRAND, C. J. H., BLACKWELL, P. G., BUCK, C. E., BURR, G. S., CUTLER, K. B., DAMON, P. E., EDWARDS, R. L., FAIRBANKS, R. G., FRIEDRICH, M., GUILDERSON, T. P., HOGG, A. G., HUGHEN, K. A., KROMER, B., MCCORMAC, G., MANNING, S., RAMSEY, C. B., REIMER, R. W., REMMELE, S., SOUTHON, J. R., STUIVER, M., TALAMO, S., TAYLOR, F. W., VAN DER PLICHT, J. & C. E. WEYHENMEYER (2004): IntCal04 terrestrial radiocarbon age calibration, 0-26 cal kyr BP. Radiocarbon, 46: 1029-1058.
 - REINECK, H.-E. & I. B. SINGH (1980): Depositional sedimentary environments. With reference to terrigenous clastics (2nd rev. and updated ed.). Springer-Verlag. Berlin, Heidelberg, New York.
 - REY, T., LEFEVRE, D. & C. VELLA (2009): Deltaic plain development and environmental changes in the Petite Camargue, Rhône Delta, France, in the past 2000 years. Quaternary Research, 71 (3): 284-294.
 - RIEDEL, H. (1996): Die holozäne Entwicklung des Dalyan-Deltas (Südwest-Türkei). Marburger Geographische Schriften, 130. Marburg.
 - ROBERTSON, A. & M. SHALLO (2000): Mesozoic-Tertiary tectonic evolution of Albania in its regional Eastern Mediterranean context. Tectonophysics, 316: 197-254.
 - ROBINSON, H. (1970): The Mediterranean lands. Advanced Level Geography Series, 2. University Tutorial Press Ltd. London.
 - ROSSIGNOL-STRICK, M., PLANCHAIS, N., PATERNE, M. & D. DUZER (1992): Vegetation dynamics and climate during the deglaciation in the south Adriatic basin from a marine record. Quaternary Science Reviews, 11 (4): 415-423.

-
- ROTHER, K. (1993): *Der Mittelmeerraum. Ein geographischer Überblick.* Teubner. Stuttgart.
 - RUMP, H. H. & KRIST, H. (1987): *Laborhandbuch für die Untersuchung von Wasser, Abwasser und Boden. (2. korrigierte Auflage).* Deutsche Gesellschaft für Technische Zusammenarbeit (GTZ) GmbH (Hrsg.). Wiley-VCH. Weinheim, New York.
 - SADORI, G. & (2006): Pollen records, Postglacial/Southern Europe. In: ELIAS, S. A. (ed.) – *Encyclopedia of Quaternary Science.* Elsevier: 2763-2773.
 - SCHEFFER, F. & P. SCHACHTSCHABEL (2002): *Lehrbuch der Bodenkunde (15th Auflage).* Spektrum Akademischer Verlag. Heidelberg.
 - SCHELLMANN, G. & H. BRÜCKNER (2005): Geochronology. In: SCHWARTZ, G. (ed.) – *Encyclopedia of Coastal Sciences.* Springer: Dordrecht: 467-472.
 - SCHLAGINTWEIT, F., GAWLICK, H.-J., MISSONI, S., HOXHA, L. LEIN R. & W. FRISCH (2008): The eroded Late Jurassic Kurbnesh carbonate platform in the Mirdita Ophiolite Zone of Albania and its bearing on the Jurassic orogeny of the Neotethys realm. *Swiss Journal of Geosciences*, 101: 125-138.
 - SCHLICHTING, E., BLUME, H.-P. & K. STAHR (1995): *Bodenkundliches Praktikum: eine Einführung in pedologisches Arbeiten für Ökologen, insbesondere Land- und Forstwirte und für Geowissenschaftler (2., neubearbeitete Auflage).* Pareys Studentexte 81. Blackwell Wissenschafts-Verlag. Berlin, Wien.
 - SCHRIEVER, A. (2007): *Die Entwicklung des Acheloos-Deltas. Eine paläogeographisch-geoarchäologische Untersuchung zum holozänen Küstenwandel in Nordwest Griechenland.* Dissertation (unpublished). Fachbereich Geographie der Philipps-Universität. Marburg.
 - SCHULDENREIN, J. (1998): Konispol Cave, Southern Albania, and correlations with Aegean caves occupied in the Late Quaternary. *Geoarchaeology: An International Journal*, 13 (5): 501-526.
 - SCHULDENREIN, J. (2001): Stratigraphy, Sedimentology, and Site Formation at Konispol Cave, Southwest Albania. *Geoarchaeology: An International Journal*, 16 (5): 559-602.
 - SHACKLETON, J. C., VAN ANDEL, T. H. & C. N. RUNNELS (1984): Coastal Paleogeography of the Central and Western Mediterranean during the Last 125,000 Years and its Archaeological Implications. *Journal of Field Archaeology*, 11 (3): 307-314.
 - SHALLO, M. (1992): Geological evolution of the Albanian ophiolites and their platform periphery. *Geologische Rundschau*, 81 (3): 681-694.
 - SHKUPI, D. & S. ALIAJ (1997): PreAdriatic depression, Albania: some geologic and engineering-geological features and Adriatic shoreline shifting. *Engineering Geology and Environment*, 1: 361-366.
 - SHUISKY, Y. (1985): Albania. In: BIRD, E. C. F. & M. L. SCHWARTZ (eds.) – *The World's Coastline.* Van Nostrand Reinhold Company. New York: 43-44.

-
- SIMEONI, U., PANO, N. & P. CIAVOLA (1997): The coastline of Albania: morphology, evolution and coastal management issues. In: BRIAND, F. (ed.) – Transformations and evolution of the Mediterranean coastline. Bulletin de l'Institut océanographique, Spécial N°: 18. CIESM Science Series n°3. Monaco: 151-168.
 - SIVAN, D., WADOWINSKI, S., LAMBECK, K., GALILI, E. & A. RABAN (2001): Holocene sea-level changes along the Mediterranean coast of Israel, based on archaeological observations and numerical model. *Palaeogeography, Palaeoclimatology, Palaeoecology*, 167 (1-2): 101-117.
 - SIVAN, D., LAMBECK, K., TOUEG, R., RABAN, A., PORATH, Y. & B. SHIRMAN (2004): Ancient coastal wells of Caesarea Maritima, Israel, an indicator for relative sea level changes during the last 2000 years. *Earth and Planetary Science Letters*, 222 (1): 315-330.
 - SKRIVANIC, G. (1977): Roman roads and settlements in the Balkans. In: CARTER, F. W. (ed.) – *An Historical Geography of the Balkans*. Academic Press. London: 115-145.
 - SOIL ATLAS OF EUROPA (2000): European Soil Bureau Network, European Commission.
 - SOIL SURVEY STAFF (1998): *Keys to Soil Taxonomy*. US Department of Agriculture, Natural Resource, Conservation Service (8th ed.). Washington DC.
 - STANLEY, J.-D. (1997): Mediterranean deltas. Subsidence as a major control of relative sea-levels rise. In: BRIAND, F. (ed.) – Transformations and evolution of the Mediterranean coastline. Bulletin de l'Institut océanographique, Spécial N°: 18. CIESM Science Series n°3. Monaco: 35-62.
 - STANLEY, J.-D. (2001): Dating modern deltas. Progress, problems, and prognostics. *Annual Review of Earth and Planetary Sciences*, 29: 257-294.
 - STANLEY, J.-D. & A. G. WARNE (1994): Worldwide initiation of Holocene marine deltas by deceleration of sea-level rise. *Science*, 265: 228-231.
 - STANLEY, J.-D., BERNASCONI, M. P., TOTH, T., MARIOTTINI, S. & M. T. IANNELLI (2007): Coast of Ancient Kaulonia (Calabria, Italy): Its submergence, lateral shifts, and use as a major source of construction material. *Journal of Coastal Research*, 23 (1): 15-32.
 - STORMS, J. E. A., WELTJE, G. J., TERRA, G. J., CATTANEO, A. & F. TRINCARDI (2008): Coastal dynamics under conditions of rapid sea-level rise: Late Pleistocene to Early Holocene evolution of barrier – lagoon systems on the northern Adriatic shelf (Italy). *Quaternary Science Reviews*, 27 (9-10): 1107-1123.
 - STRÄBER, M. (1998): *Klimadiagramme zur Köppenschen Klimaklassifikation*. Klett-Perthes. Gotha, Stuttgart.
 - STUIVER, M. & P.J. REIMER (1993): Extended ¹⁴C database and revised CALIB radiocarbon calibration program. *Radiocarbon*, 35: 215-230.
 - STUIVER, M., REIMER, P. J. & R. REIMER (2006): CALIB Radiocarbon Calibration Programm. [URL: <http://radiocarbon.pa.qub.ac.uk/calib/> (access: 20.04.2009)].

-
- STYLIANOU, P. J. (1998): A historical commentary on Diodorus Siculus Book 15. Oxford Classical Monographs. Oxford.
 - SULSTAROVA, E. (1997): The seismic faults in Albania. *The Journal of Natural & Technical Sciences*, 2 (2): 91-100.
 - SULSTAROVA, E. & S. ALIAJ (2001): Seismic hazard assessment in Albania. *Albanian Journal of Natural & Technical Sciences*, 6 (10): 89-100.
 - SULSTAROVA, E., ALIAJ, S., MUÇO, B. & L. DUNI (2005): Recent achievements in seismic hazards assessment in Albania. *The Journal of Natural & Technical Sciences*, 18 (2): 3-15.
 - SURIĆ, M., JURAČIĆ, M., HORVATINČIĆ, N. & I. KRAJKAR-BRONIĆ (2005): Late Pleistocene-Holocene sea-level rise and the pattern of coastal karst inundation: records from submerged speleothems along the Eastern Adriatic Coast (Croatia). *Marine Geology*, 214 (1-3): 163-175.
 - TOOLEY, M. J. (1987): Sea-level studies. In: TOOLEY, M. J. & I. SHENNAN (eds.) – *Sea-level changes*. The Institute of British Geographers, Special Publications Series 20. Basil Blackwell Ltd. Oxford: 1-24.
 - TOOLEY, M. J. & I. SHENNAN (eds.) (1987): *Sea-level changes*. The Institute of British Geographers, Special Publications Series 20. Basil Blackwell Ltd. Oxford.
 - VAN DE PLASSCHE, O. (ed.) (1986): *Sea-level research: a manual for the collection and evaluation of data*. Geo Books. Norwich.
 - VITA-FINZI, C. (1969): *The Mediterranean valleys, geological changes in historical times*. Cambridge University Press. Cambridge.
 - VON GRAFENSTEIN, U., ERLLENKEUSER, H., BRAUER, A., JOUZEL, J. & S. J. JOHNSEN (1999): A mid-European decadal isotope-climate record from 15,500 to 5,000 years BP. *Science*, 284: 1654-1657.
 - VOVALIDIS, K. G., SYRIDES, G. E. & K. S. ALBANAKIS (2005): Holocene morphology of the Thessaloniki Bay: Impact of sea level rise. In: FOUACHE, É. & K. PAVLOPOULOS (eds.) – *Sea Level Changes in Eastern Mediterranean during Holocene – Indicators and Human Impacts*. *Zeitschrift für Geomorphologie, N. F., Suppl.-vol. 137*. Berlin, Stuttgart: 147-158.
 - VÖTT, A. (2007a): Relative sea level changes and regional tectonic evolution of seven coastal areas in NW Greece since the mid-Holocene. *Quaternary Science Reviews*, 26 (7-8): 894-919.
 - VÖTT, A. (2007b): Silting up Oiniadai's harbours (Acheloos River delta, NW Greece) – geoarchaeological implications of late Holocene landscape changes. *Géomorphologie: relief, processus, environnement*, n°: 1 : 19-36.
 - VÖTT, A., HANDL, M. & H. BRÜCKNER (2002): Rekonstruktion holozäner Umweltbedingungen in Akarnanien (Nordwestgriechenland) mittels Diskriminanzanalyse von geochemischen Daten. *Geologica et Palaeontologica*, 36: 123-147.

-
- VÖTT, A., BRÜCKNER, H. & M. HANDL (2003): Holocene environmental changes in coastal Akarnania (northwestern Greece). In: DASCHKEIT, A. & H. STERR (Hrsg.) – Aktuelle Ergebnisse der Küstenforschung. 20. AMK-Tagung Kiel, 30.05.-01.06.2002. Berichte aus dem Forschungs- und Technologiezentrum Westküste der Universität Kiel, 28. Büsum: 117-132.
 - VÖTT, A. & H. BRÜCKNER (2006a): Versunkene Häfen im Mittelmeerraum. In: EITEL, B. (ed.) – Geoarchäologie. Geographische Rundschau, 58 (4): 12-21.
 - VÖTT, A., BRÜCKNER, H., HANDL, M. & A. SCHRIEVER (2006b): Holocene palaeogeographies and the geoarchaeological setting of the Mytikas coastal plain (Akarnania, NW Greece). Zeitschrift für Geomorphologie, N. F., Suppl.-Bd: 142. Berlin, Stuttgart: 85-108.
 - VÖTT, A., BRÜCKNER, H., HANDL, M. & A. SCHRIEVER (2006c): Holocene palaeogeographies of the Astakos coastal plain (Akarnania, NW Greece). Palaeogeography, Palaeoclimatology, Palaeoecology, 239 (1-2): 126-146.
 - VÖTT, A., BRÜCKNER, H., SCHRIEVER, A., LUTHER, J., HANDL, M. & K. VAN DER BORG (2006d): Holocene palaeogeographies of the Palairos coastal plain (Akarnania, Northwest Greece) and their geoarchaeological implications. Geoarchaeology: An International Journal, 21 (7): 649-664.
 - VÖTT, A., SCHRIEVER, A., HANDL, M. & H. BRÜCKNER (2007a): Holocene palaeogeographies of the central Acheloos River delta (NW Greece) in the vicinity of the ancient seaport of Oiniadai. Geodinamica Acta, 20 (4): 241-256.
 - VÖTT, A., SCHRIEVER, A., HANDL, M. & H. BRÜCKNER (2007b): Holocene palaeogeographies of the eastern Acheloos River delta and the Lagoon of Etoliko (NW Greece). Journal of Coastal Research, 23 (4): 1042-1066.
 - VÖTT, A., BRÜCKNER, H., MAY, M., LANG, F., HERD, R. & S. BROCKMÜLLER (2008): Strong tsunami impact on the Bay of Aghios Nikolaos and its environs (NW Greece) during Classical-Hellenistic times. Quaternary International, 181 (1): 105-122.
 - WAGNER, G. A. (1998): Age Determination of Young Rocks and Artifacts. – Physical and Chemical Clocks in Quaternary Geology and Archaeology. Springer-Verlag. Berlin, Heidelberg, New York.
 - WALKER, M. (2005): Quaternary Dating Methods. John Wiley & Sons. Chichester.
 - WEISS, H., COURTY, M.-A., WETTERSTROM, W., GUICHARD, F., SENIOR, L., MEADOW, R. & A. CURNOW (1993): The genesis and collapse of third millennium North Mesopotamian Civilization. Science, 261: 995-1004.
 - WELLS, L. E. (2001): Archaeological sediments in coastal environments. In: STEIN, J. K. & W. R. FARRAND (eds.) – Sediments in Archaeological Context. The University of Utah Press: 149-182.

-
- WIET, E. (1866): Le diocèse d'Alessio et la Mirdite: extrait d'un mémoire de M. Wiet, Consul de France à Scutari. *Bulletin de la Société de Géographie*: 271-288. Paris. (Reprinted in: P. BARTL: *Albania Sacra: Geistliche Visitationsberichte aus Albanien*, 1. Diözese Alessio. Herausgegeben und bearbeitet von Peter Bartl. *Albanische Forschungen*, Band 26, 1 (Wiesbaden: Harrassowitz, 2007): 390-400.
 - WILKES, J. J. (1969): *Dalmatia. History of the Provinces of the Roman Empire*. Routledge & Kegan Paul. London.
 - WILLIS, K. J. (1992a): The late Quaternary vegetational history of north-west Greece. I. Lake Gramousti. *New Phytologist*, 121: 101-117.
 - WILLIS, K. J. (1992b): The late Quaternary vegetational history of north-west Greece. II. Rezina marsh. *New Phytologist*, 121: 119-138.
 - WILLIS, K. J. (1994): The vegetational history of the Balkans. *Quaternary Science Reviews*, 13 (8): 769-788.
 - WRIGHT, L. D. (1985): River deltas. In: DAVIS, R. A. (ed.) – *Coastal Sedimentary Environments* (2nd rev. ed.). Springer-Verlag. New York, Berlin, Heidelberg, Tokyo: 1-76.
 - ZDRULI, P. & S. LUSHAJ (2001): The status of soil survey in Albania and some of its major environmental findings. In: ZDRULI, P., STEDUTO, P., LACIRIGNOLA, C. & L. MONTANARELLA (eds.) – *Soil resources of Southern and Eastern Mediterranean countries. Options Méditerranéennes: Serie: B. Etudes et Recherches*. No: 34. CIHEAM-IAMB. Paris: 69-97.
 - ZDRULI, P., LUSHAJ, S., PEZZUTO, A., FANELLI, D., D'AMICO, O., FILOMENO, O., DE SANTIS, S., TODOROVIC, M., NERILLI, E., DEDAJ, K. & B. SEFERI (2003): Preparing a georeferenced soil database for Albania at scale 1:250,000 using the European Soil Bureau Manual of Procedures 1.1. In: ZDRULI, P., STEDUTO, P. & S. KAPUR (eds.) – *Options Méditerranéennes. Serie: A: Mediterranean Seminars*, No: 50. CIHEAM. Paris: 135-144.
 - ZDRULI, P. (2005): Soil Survey in Albania. In: JONES, R. J. A., HOUŠKOVA, B., BULLOCK, P. & L. MONTANARELLA (eds.) – *Soil Resources of Europe* (second ed.). European Soil Bureau Research Report No. 9. EUR 20559 EN. Luxembourg: 39-45.
 - ZONNEVELD, K. A. F. (1996): Palaeoclimatic reconstruction of the last deglaciation (18-8 ka B.P.) in the Adriatic Sea region; a land-sea correlation based on palynological evidence. *Palaeogeography, Palaeoclimatology, Palaeoecology*, 122 (1-4): 89-116.

MAPS

Topographical maps:

In this research project, different scale topographical maps were used [prepared and published by the Instituti Topografik i Ushtrisë in collaboration with the National Imagery and Mapping Agency (NIMA)]:

- scale 1 : 25,000; sheets: K-34-76-C-a (Shengjini), K-34-76-C-b (Lezha), K-34-76-C-c, K-34-76-C-d (all published in 1980).
- scale 1 : 50,000; sheets: 2978 I (Lezhë) and 2978 II (Krujë) (all published in 1998).

Geological maps

- scale 1 : 50,000, Harta Gjeologjike e Shqipërisë Sheet: 26 (Lezha) with an explanation by K. Onuzi published by Instituti Kerkimeve Gjeologjike in Tirana in 2005.
- scale 1 : 200,000, Harta Gjeologjike e Shqipërisë (The Geological Map of Albania) (3 sheets). Published by Republika e Shqipërisë, Ministria e Industrisë dhe Energjitikës and Ministria e Arsimit dhe Shkencës in collaboration with the Instituti i Kerkimeve Gjeologjike (A. Xhomo, A. Kodra, Ll. Dimo), Instituti i Naftës dhe Gazit Fier (Z. Xhafa et al.), Fakulteti i Gjeologjisë dhe Minierave (M. Shallo et al.) in 2002.

Other Maps

- scale 1 : 200,000, Harta Hidrogjeologjike e RPS të Shqipërisë (The Hydrogeological Map of Albania) (3 sheets). Published by Ministria e Industrisë dhe e Minierave in 1985.
- scale 1 : 200,000, Harta Metalogjenike e Shqipërisë (The Metallogenic Map of Albania) (3 sheets). Published by Republika e Shqipërisë, Ministria e Ekonomisë Publike dhe Privatizimit and Ministria e Arsimit dhe Shkencës in the collaboration with the Universiteti Politeknik i Tiranës, Instituti i Kerkimeve Gjeologjike and Fakulteti i Gjeologjisë dhe Minierave in 1999.
- scale 1 : 200,000, Harta e Rrezikut Gjeologjik të Shqipërisë (The Geohazard Map of Albania) (3 sheets). Published by Ministria e Industrisë dhe Energjetikës Sherbimi Gjeologjik Shqiptar in 2000.
- scale 1 : 500,000, Seismotectonic Map of Albania (1 sheet). Compiled by S. Aliaj, E. Sulstarova, B. Muço & S. Koçiu, and published by Academy of Sciences Seismological Institute in Tirana in 2000.
- scale: 1 : 2,200,000, Soil Atlas of Europe, Plate: 15, p. 71. Published by European Soil Bureau Network, European Commission, 2005. 128 p.

13 Appendices

Appendix 1: Terminology

Coastal environments develop at the land/sea interface, which is sometimes even described as a “triple interface”, integrating the atmosphere (Wells, 2001). Many different types of environments and geomorphological features develop depending on the respectively dominating factors. The following amalgamation of definitions and characteristics has been compiled using Reineck & Singh (1980), Davis (1983, 1985), Wright (1985), Füchtbauer (1988), Kraft & Chrzastowski (1985), Carter & Woodroffe (1994), Brown (1997), Bridge (2003), and Reading (2004). The terminology used in the chapters of this book is based on these definitions.

Marine environments and features

Marine embayments are characterised by generally low wave energy, which means that fine grained material, such as silt and clay, is accumulated. Such calm conditions are ecologically ideal and the micro- and macrofauna as well as -flora thrives, resulting in fairly high contents of organic matter within the deposits.

The subaqueous, seaward part of a coastal environment has been termed *sublittoral*, sometimes referred to as the *foreshore*. The *littoral zone* or the *beach* is where waves and longshore currents are distributing the material, mostly sands or pebbles, which has been supplied by rivers or by cliff erosion. Its sorting is very good due to the continuous wave action. In littoral deposits, shell fragments and microfossils are commonly found, with the tests and valves of the organisms usually rounded or broken, showing signs of reworking due to the high wave energy. Finer grained material (silt, clay) is carried on in suspension, being deposited further offshore as *shallow marine* sediments.

Typical representatives of secondary coasts are *barriers* and *sand spits*. Sediment-laden rivers debouch into the sea, releasing their load, which is then reworked and transported by waves and longshore currents along the coast. Another source is cliffs that are eroded. These deposits are composed of well-sorted sands, showing mostly low-angle bedding. Some fine pebbly and coarse sandy lenses are common. The sediment includes heavy minerals, damaged shell fragments and pieces of rounded wood.

The *prodelta* or *delta front slope* environment represents the subaqueous seaward progradation of a delta system. Prodelta sediment consists of stratified, fine-grained mud (clays, silty clays), revealing very thin lamination, both in colour and grain size. The fossil content is frequently composed of marine as well as brackish species depending on the amount of freshwater influx. Bioturbation occurs regularly. Prodeltaic sediment (in a Gilbert-type delta: foreset beds) is overlain by coarser delta front sediments (topset beds).

Delta front environments and features

Delta front environments develop where the river mouth and marine processes meet. Typical features are distributaries, distributary mouth bars and interdistributary bays.

Distributaries are channels which branch off the main river course to disperse the sediment-laden waters into a marine embayment. Seawards, they broaden and become shallower. The deposits of such distributary channels are typically composed of sands and silts. However, during times of low discharge, even very fine particles may settle to form clayey layers. The deposits also display cross and current ripple bedding, scour and fill structures and erosion surfaces. Due to the inconsistent nature of the fluvial dynamics, marine or terrestrial fossils are rarely found.

Interdistributary bays are shallow water bodies directly connected with the open sea. They are formed between the natural levees of two distributaries during progradation of a bird-foot type delta. These environments represent low wave energy and a slow rate of sedimentation. Deposits are dominated by fine-grained clayey silts, intercalated with sandy layers, derived from crevasse splay during flooding events. Ecologically, interdistributary bays display ideal conditions for sea weeds (*Posidonia oceanica*) and other salt-tolerant plants, as well as micro- and macrofauna, resulting in rich fossil contents (both marine and brackish species) and bioturbation structures.

A *lagoon* is a coastal water body which has a restricted connection with the open sea, being separated from it by a barrier or sand spit. In general, lagoons are quite shallow and are characterised by a very low energy wave climate. Therefore, deposits are mainly composed of clayey and silty mud; sandy layers may have accumulated during storms, levee breaches or tsunami events. Sometimes, lagoons can be rapidly filled in with sand if a distributary arm of the river changes course. The water quality may show seasonal changes from brackish to hypersaline conditions, depending on rainfall and fluvial freshwater input on the one hand, and evaporation rates and sea water intrusion on the other hand. A lagoon environment harbours a

specific kind of fauna, which has to be able to adapt according to four stress factors which may vary considerably: temperature, salinity, turbidity and content of oxygen. Species indicative of a lagoon are *Cerastoderma glaucum* (macrofauna) and *Cyprideis torosa* (ostracod, microfauna). The shells are commonly very thin due to poor calcification. Biodiversity is low, while the number of specimens can be very high.

Salt marshes, sometimes referred to as *backswamps*, are typical for the *backshore* environment. They develop along the margins of lagoons or interdistributary bays, commonly represented by *mud flats* or *salt marsh* deposits with *peat* formations. These deposits are made up of homogeneous clayey silty mud, with a high content of organic matter. In general, plant remains are well preserved due to good embedding in the sediment under low content of oxygen. The microfossil content of the sediments is generally rich. Dependent from the ecological conditions brackish or limnic gastropods (e.g., *Hydrobia* sp.) occur.

Fluvial environments and features

Fluvial deposition occurs within river channels, on levees, and on the floodplain. Drainage basin characteristics as well as (seasonal) changes in rainfall control the amount and rate of river discharge. Generally, coarse sediment indicates close proximity to highly dynamic river channels, whereas fine-grained deposits are associated with floodplain deposition further away from the river course.

River channel deposits accumulate at the bottom of the river channel. They are composed of coarse sediment such as pebbles in a coarse sandy matrix. Boulders which can only be transported by the river during times of flood, wood and clay pebbles are common in the deposits. Fine-grained material cannot settle due to the high energy conditions. Fining-upwards sequences may indicate the former existence of a *point bar*. *Abandoned river channels*, such as *oxbow lakes* are characterised by slow siltation rates. The subsequently developing silty-clayey deposits are rich in organic matter such as plant remains and freshwater fossils.

Natural levees frame the active river channel and grade into flood basin sediments. They form as wedge-shaped ridges during times of flooding, when the water levels are very high. Levee deposits are made up of sand, becoming finer laterally, away from the river channel. Plant remains, oxidation stains and iron concretions are common.

Crevasse splay deposits represent temporary breaches of a levee, where the sediment-laden water bursts into the adjacent floodplain or backswamp during flood events. They display

alluvial fan-like features in the flood basin. Sand and, occasionally, pebbles are characteristic for crevasse splay deposits. Drifted plant remains and terrestrial fossils are common.

Floodplains, sometimes also called *flood basins*, comprise flat, low-lying areas adjacent to the river channel, separated from it by natural levees. Repeated flooding events result in often very thick deposits, consisting mostly of fine-grained material such as silt and clay. Individual sequences are fining- upwards, and with increasing distance away from the river channel, the sediment also becomes finer. Coarse intercalations point towards crevasse splay sediment. Plant remains and terrestrial/freshwater fossils are common. The surface layers may include carbonate concretions, iron and manganese oxidation stains due to seasonally changing groundwater levels. Thus, floodplains represent a complex assemblage of fluvial environments resulting from alternating phases of deposition and erosion processes.

Remnants of shifting river courses such as oxbow lakes can be observed on the floodplain. Often, these poorly drained areas develop into *swamps* or *bogs* with abundant peat growth. The sediment consists of very fine silts and clays with a high content of organic matter. The common colour of such deposits is dark gray to black. They represent suitable ecological conditions for freshwater species.

Floodplain lakes typically form in the most low-lying and wettest parts of the floodplain. They are (seasonal) extensive, shallow stagnant bodies of freshwater. The usually stratified sediments accumulating in floodplain lakes are termed *limnic* or *lacustrine*. Greenish gray to black coloured clay, intercalated with silt lenses, is characteristic for floodplain lake deposits. A high content in organic matter combined with secondary minerals such as pyrite and vivianite, indicating an anoxic milieu, suggests eutrophic conditions. Due to the seasonally changing water level (and possibly complete dessication during the summer), the content of calcium carbonate is high. Limnic gastropods and freshwater ostracods (e.g., *Candona neglecta*) are common.

Residual lakes are a particular type of floodplain lakes. They differ from ordinary ones in that they originate from a marine embayment, which, after having been cut off through delta progradation, slowly turned into fresh water lake. These water bodies may be deeper than ordinary floodplain lakes, and their fine grained sediments include a continuous shift from marine to brackish microfossils at the bottom of the deposits to freshwater ones towards the top.

Appendix 2: Selected ISO and DIN Norms

DIN ISO 10390 Bestimmung des pH-Wertes (determination of pH)

DIN ISO 10693 Bestimmung des Carbonatgehalts (determination of carbonate content)

DIN ISO 11265 Bestimmung der spezifischen elektrischen Leitfähigkeit (determination of the specific electrical conductivity)

DIN 19684, T.3 Bestimmung der organischen Substanz als Glühverlust (determination of the organic matter content as loss-on-ignition)

Appendix 3: Radiocarbon age estimates

Sample	Lab. Code	Depth (b.s.)	Depth (b.s.l.)	Material	$\delta^{13}\text{C}$ (‰)	^{14}C Age	Calibrated Age (range $\pm 1\sigma$)
LIS 08/1H	Erl-10588	1.37-1.50	0.45-0.58	wood	-27.4	860 \pm 34 BP	1047-1259 cal AD
LIS 08/7T	Erl-10589	4.54-4.57	3.62-3.65	peat	-27.5	929 \pm 38 BP	1023-1205 cal AD
LIS 08/8H	Erl-10590	8.65	7.73	wood	-27.6	1010 \pm 37 BP	902-1153 cal AD
LIS 09/1Pf	Erl-10591	1.90-1.95	0.38-0.43	plant remains	-26.6	623 \pm 37 BP	1288-1401 cal AD
LIS 09/6H	Erl-10592	5.40-5.50	3.88-3.98	wood	-28	2865 \pm 30 BP	1128-930 cal BC
LIS 09/10H	Erl-10593	6.32-6.47	4.80-4.95	wood	-8	2865 \pm 34 BP	1189-926 cal BC
LIS 11/3T	Erl-10594	6.61	3.41	peat	-27.6	3512 \pm 39 BP	1941-1743 cal BC
LIS 11/5Pf	Erl-10595	8.82-8.90	5.62-5.70	plant remains	-27.2	4124 \pm 33 BP	2871-2580 cal BC
LIS 12/1H	Erl-10596	1.73	1.41	wood	-28.8	733 \pm 34 BP	1220-1377 cal AD
LIS 12/2H	Erl-10597	5.71	5.39	wood	-29.5	1003 \pm 38 BP	906-1154 cal AD
LIS 14/2T	Erl-10598	6.55-6.65	5.61-5.71	peat	-28.9	1108 \pm 38 BP	783-1018 cal AD
LIS 15/5H	Erl-10599	3.87	2.45	wood	-27.4	1196 \pm 63 BP	684-971 cal AD
LIS 17/2T	Erl-10601	3.56	2.25	peat	-23.7	1211 \pm 69 BP	670-969 cal AD
LIS 17/4T	Erl-10600	7.82-7.90	6.51-6.59	peat	-24	2046 \pm 67 BP	348 BC-112 cal AD
LIS 18/3T	Erl-10602	6.33-6.38	4.84-4.89	peat	-31.7	895 \pm 52 BP	1024-1251 cal AD
LIS 19/1T	Erl-10603	2.27	0.88	peat	-29.1	587 \pm 49 BP	1292-1421 cal AD
LIS 19/9H	Erl-10604	7.70-7.75	6.31-6.36	wood	-26.2	572 \pm 51 BP	1296-1430 cal AD
LIS 23/19H	Erl-12040	6.22	3.02	wood	-24.8	1289 \pm 41 BP	653-859 cal AD
LIS 23/24F	Erl-12129	8.40-8.45	5.20-5.25	shell	-6.9	5914 \pm 48 BP	4932-4691 cal BC
LIS 23/30H	Erl-12041	10.49	7.29	wood	-25	4599 \pm 42 BP	3518-3116 cal BC
LIS 24/14T	Erl-12042	6.61	3.28	peat	-26.5	3580 \pm 42 BP	2109-1775 cal BC
LIS 25/15H	Erl-12043	6.44	4.03	wood	-22.7	3569 \pm 42 BP	2030-1774 cal BC
LIS 25/20Pf	Erl-12044	9.42	7.01	plant remains	-24.2	4492 \pm 42 BP	3352-3029 cal BC
LIS 25/26H	Erl-12045	12.32	9.91	wood	-22.4	4795 \pm 42 BP	3655-3384 cal BC
LIS 26/8Pf	Erl-12046	3.47	1.69	plant remains	-21.7	932 \pm 41 BP	1021-1206 cal AD
LIS 26/11H	Erl-12047	5.50	3.72	wood	-20.3	967 \pm 42 BP	994-1161 cal AD
LIS 26/19H	Erl-12048	8.53	6.75	wood	-25.6	4216 \pm 42 BP	2908-2669 cal BC
LIS 28/18H	Erl-12049	5.89	4.41	wood	-27.8	4175 \pm 42 BP	2889-2629 cal BC
LIS 28/24H	Erl-12050	7.62	6.14	wood	-23.6	4185 \pm 42 BP	2893-2633 cal BC
LIS 29/8S	Erl-12051	2.50-2.54	0.84-0.88	grape seed	-25	2312 \pm 43 BP	508-209 cal BC
LIS 29/17H	Erl-12052	4.91	3.25	wood	-23.1	3411 \pm 41 BP	1877-1614 cal BC
LIS 29/21T	Erl-12053	5.76	4.10	peat	-22.2	3409 \pm 42 BP	1878-1612 cal BC
LIS 29/26T	Erl-12054	6.55-6.56	4.89-4.90	peat	-25.7	3548 \pm 42 BP	2014-1755 cal BC
LIS 29/29T	Erl-12055	7.42-7.52	5.76-5.86	peat	-24	3669 \pm 41 BP	2196-1938 cal BC
LIS 31/13Pf	4162	5.16	5.16	plant remains	-26.2	585 \pm 27 BP	1301-1414 cal AD
LIS 35/13T	Erl-12056	4.55	2.93	peat	-22.4	3890 \pm 42 BP	2474-2210 cal BC
LIS 35/23T	Erl-12057	5.63	4.01	peat	-23.4	3531 \pm 42 BP	1975-1746 cal BC
LIS 35/31T	Erl-12058	7.70	6.09	peat	-24.8	4096 \pm 42 BP	2870-2496 cal BC
LIS 35/35T	Erl-12059	8.83-8.90	7.21-7.28	peat	-25.9	4172 \pm 42 BP	2888-2627 cal BC
LIS 35/38H	Erl-12060	10.65	9.03	wood	-22.7	4145 \pm 42 BP	2878-2584 cal BC
LIS 38/23T	4163	7.80	3.86	peat	-26.1	3406 \pm 29 BP	1861-1624 cal BC
LIS 38/32T	4164	9.43-9.46	5.49-5.52	peat	-26.4	3454 \pm 28 BP	1878-1691 cal BC
LIS 38/35H	4165	10.63	6.69	wood	-23	3501 \pm 27 BP	1895-1746 cal BC
LIS 39/25T	4166	7.97-8.00	7.97-8.00	peat	-23.2	4560 \pm 28 BP	3485-3107 cal BC
LIS 40/13H	4167	5.63	2.67	wood	-26.3	4935 \pm 29 BP	3773-3653 cal BC
LIS 40/26H	4168	10.79	7.83	wood	-26	4497 \pm 29 BP	3345-3096 cal BC
LIS 42/19H	4169	8.45	4.52	wood	-26.7	4911 \pm 29 BP	3761-3643 cal BC
LIS 42/25T	4170	11.83-11.93	7.90-8.00	peat	-25.9	5226 \pm 31 BP	4224-3965 cal BC
LIS 43/12Pf	4171	7.85	5.27	plant remains	-26.7	1918 \pm 26 BP	23-132 cal AD
LIS 47/11F	4172	5.90	2.29	shell	-3.9	2472 \pm 27 BP	80-514 cal AD
LIS 47/18H	4173	8.70	5.09	wood	-24.8	2542 \pm 27 BP	797-549 cal BC
LIS 47/23T	4174	11.59	7.98	peat	-23.7	4490 \pm 29 BP	3348-3040 cal BC
LIS 48/16H	4175	7.44	5.12	wood	-25.8	4494 \pm 28 BP	3344-3095 cal BC

Sample	Lab. Code	Depth (b.s.)	Depth (b.s.l.)	Material	$\delta^{13}\text{C}$ (‰)	^{14}C Age	Calibrated Age (range $\pm 1\sigma$)
LIS 50/4H	4176	2.25	2.25	wood	-27.7	999 \pm 27 BP	986-1151 cal AD
LIS 51/17H	4177	8.53	5.52	wood	-26	2613 \pm 27 BP	822-771 cal BC
LIS 52/19H	4178	9.25	6.94	wood	-26.1	4372 \pm 28 BP	3088-2909 cal BC
LIS 53/13T	4179	6.67	4.51	peat	-26	2089 \pm 29 BP	192 BC-43 cal AD

Appendix 3: Radiocarbon age estimates. The radiocarbon measurements were carried out in the following laboratories: AMS Laboratory of the Department of Physics, Friedrich-Alexander-University of Erlangen-Nürnberg (lab code: "Erl"); Center for Applied Isotope Studies (CAIS), University of Georgia, Athens, USA. The conventional ^{14}C ages were calibrated according to the calibration program of Calib. Rev. 5.0.2 (Stuiver et al., 2006). Abbreviations; b.s. = below surface; b.s.l. = below present sea level.

Appendix 4: Macro- and microfossils as indicators of specific environmental conditions

Macrofossils

Marine species

Alvania sp.
Alvania mamillata (RISSE, 1826)
Arca sp.
Bittium latreillii (PAYRAUDEAU, 1826)
Bittium reticulatum (DA COSTA, 1778)
Cardita sp.
Cerithium vulgatum (BRUGUIÈRE, 1792)
Chamelea gallina (LINNAEUS, 1758)
Chlamys cf. *glabra* (LINNAEUS, 1758)
Chrysallida sp.
Cidaris sp.
Columbella rustica (LINNAEUS, 1758)
Corbula gibba (OLIVI, 1792)
Donax sp.
Donax trunculus (LINNAEUS, 1758)
Gastrana fragilis (LINNAEUS, 1758)
Gibbula sp.
Hinia sp.
Irus irus (LINNAEUS, 1758)
Jujubinus cf. *striatus* (LINNAEUS, 1758)
Lentidium sp.
Loripes lacteus (POLI, 1791)
Lucinella divaricata (LINNAEUS, 1758)
Modiolus sp.
Murex sp.
Mytilaster sp.
Mytilus sp.
Nassarius cf. *pygmaeus* (LAMARCK, 1822)
Nucula sp.
Nucula sulcata (BRONN, 1831)
Pirenella conica (BLAINWILL, 1829)
Pusillina sp.
Retusa sp.
Retusa semisulcata (BRUGUIÈRE, 1792)
Rissoa sp.
Rissoa variabilis (VON MÜHLFELDT, 1824)
Rissoa labiosa (MONTAGU, 1803)
Scrobicularia cottardi (PAYRAUDEAU, 1826)
Scrobicularia plana (DA COSTA, 1778)
Spisula sp.
Theodoxus sp.
Tricolia cf. *tenuis* (MICHAUD, 1829)
Tricolia pullus pullus (LINNAEUS, 1758)
Turbonilla cf. *lactea* (LINNAEUS, 1758)
Venus casina (LINNAEUS, 1758)
Venus verrucosa (LINNAEUS, 1758)

Brackish species

Cerastoderma glaucum (BRUGUIÈRE, 1789)
Hydrobia sp.
Lentidium mediterraneum (COSTA, 1829)

Freshwater species

Bithynia tentaculata (LINNAEUS, 1758)
Pisidium sp.
Stagnicola corvus (MÜLLER, 1774)

Microfossils**Ostracods****Marine species**

Aurila sp.
Aurila arborescens (BRADY, 1865)
Aurila woutersi (HORNE, 1986)
Callistocythere sp.
Callistocythere intricatoides (RUGGIERI, 1953)
Carinocythereis cf. *antiquata* (BAIRD, 1850)
Costa batei (BRADY, 1866)
Cytheretta adriatica (RUGGIERI, 1952)
Cytherois sp.
Cytheromorpha fuscata (BRADY, 1869)
Loxoconcha bairdi (MÜLLER, 1894)
Loxoconcha elliptica (BRADY, 1868)
Loxoconcha gibberosa (TERQUEM, 1878)
Loxoconcha stellifera (MÜLLER, 1894)
Pontocythere rubra (MÜLLER, 1894)
Paracypris sp.
Paracytherois cf. *rara* (MÜLLER, 1894)
Paradoxostoma cf. *fuscum* (MÜLLER, 1894)
Pontocypris sp.
Propontocypris cf. *dispar* (MÜLLER, 1894)
Pseudopsamocythere reniformis (BRADY, 1868)
Sclerochilus sp.
Semicytherura paradoxa (MÜLLER, 1894)
Semicytherura inversa (SEGUENZA, 1880)
Semicytherura psila (BARBEITO-GONZALES, 1971)
Semicytherura sulcata (MÜLLER, 1894)
Urocythereis margaritifera (MÜLLER, 1894)
Xestoleberis communis (MÜLLER, 1894)
Xestoleberis dispar (MÜLLER, 1894)

Brackish species

Cyprideis torosa (JONES, 1850)
Cyprideis torosa f. *littoralis* (JONES, 1850)
Cyprideis torosa f. *torosa* (JONES, 1850)
Leptocythere sp.
Leptocythere bacescoi (ROME, 1942)

Freshwater species

Candona sp.
Candona neglecta (SARS, 1887)
Candonopsis sp.
Cytherissa lacustris (SARS, 1863)
Darwinula sp.
Eucypris zenkeri (CHYZER & TOTH, 1858)
Iliocypris bradyi (SARS, 1890)
Potamocypris cf. *fallax* (FOX, 1967)
Pseudocandona cf. *parallela* (MÜLLER, 1900)

Foraminifers**Marine species**

Cibicides lobatulus (WALKER & JACOB, 1798)
Cycloforina sp.
Elphidium crispum (LINNAEUS, 1758)
Elphidium cuvillieri (LEVY, 1966)
Elphidium excavatum (TERQUEM, 1875)
Elphidium minutum (REUSS, 1865)

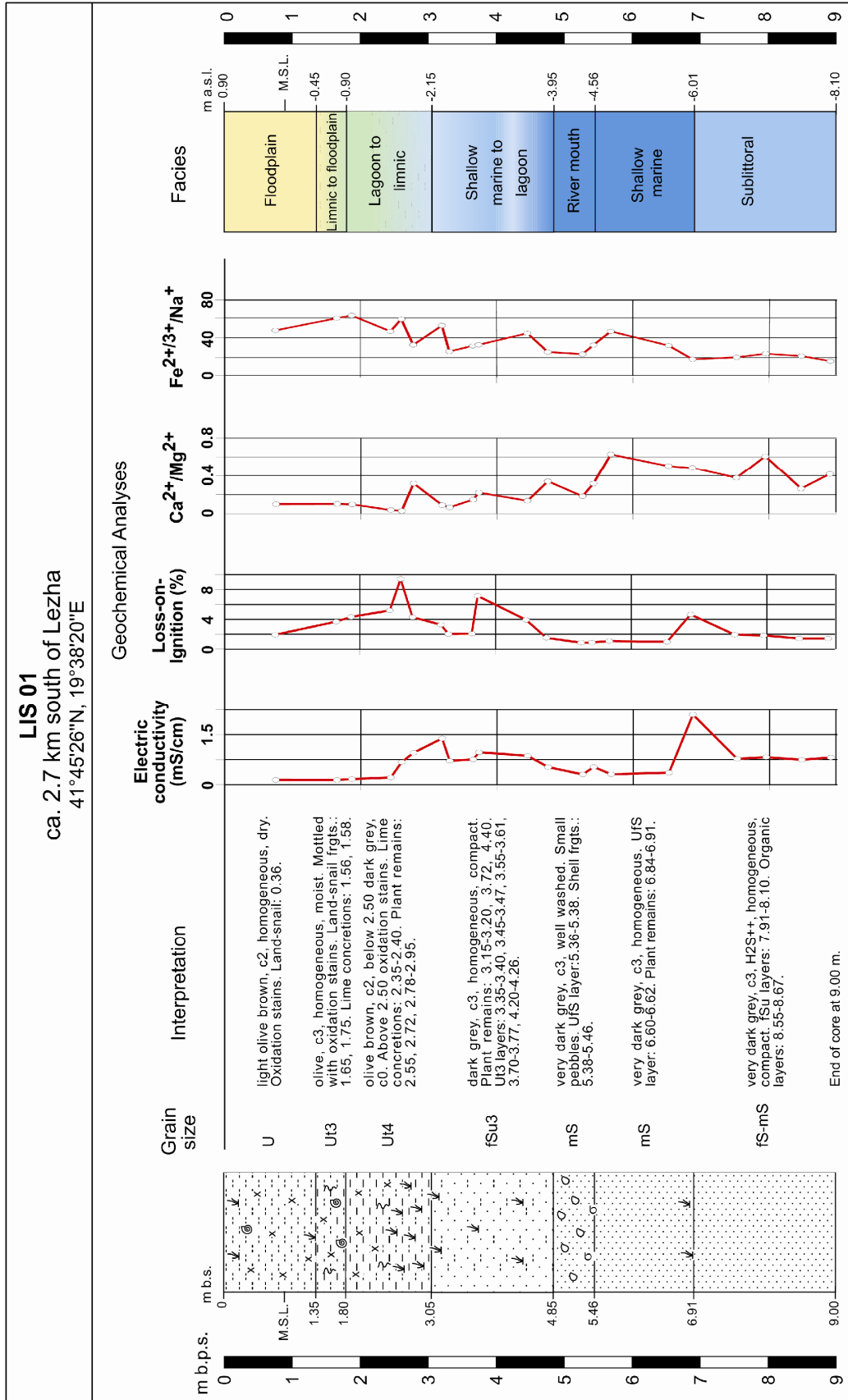
Hanzawaia sp.
Haynesina germanica (EHRENBERG, 1840)
Massilina sp.
Planorbulina mediterraneensis (D'ORBIGNY, 1826)
Polimorphina sp.
Rosalina globularis (D'ORBIGNY, 1826)
Rosalina macropora (HOFKER, 1951)
Spiroloculina depressa (D'ORBIGNY, 1826)
Quinqueloculina elegans (D'ORBIGNY, 1878)
Quinqueloculina cf. *striata* (D'ORBIGNY, 1843)
Quinqueloculina cf. *venusta* (KARRER, 1868)
Planorbulina mediterraneensis (D'ORBIGNY, 1826)
Sigmoilina sp.
Siphonaperta sp.
Triloculina sp.

Brackish species

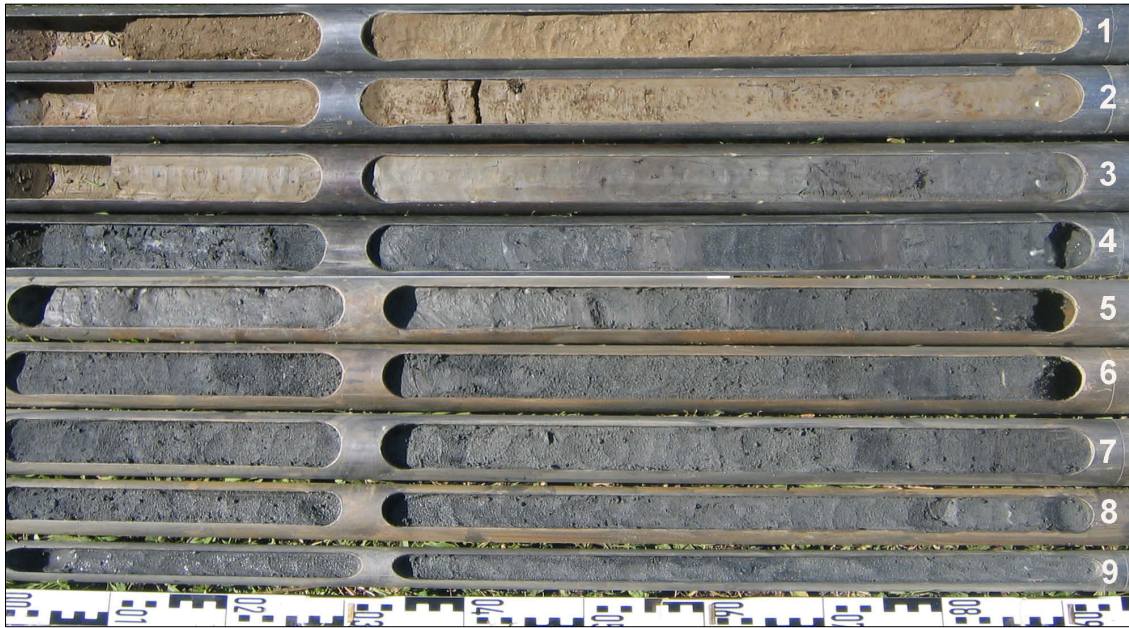
Ammonia beccarii (LINNAEUS, 1758)
Ammonia cf. *parkinsoniana* (D'ORBIGNY, 1838)
Ammonia cf. *tepida* (CUSHMAN, 1926)

Appendix 5: Geological profiles, photos and geochemical results

Appendix 5.1.1: Geological profile and selected geochemical results of LIS 01.



Appendix 5.1.2: Photo and geochemical results of LIS 01.

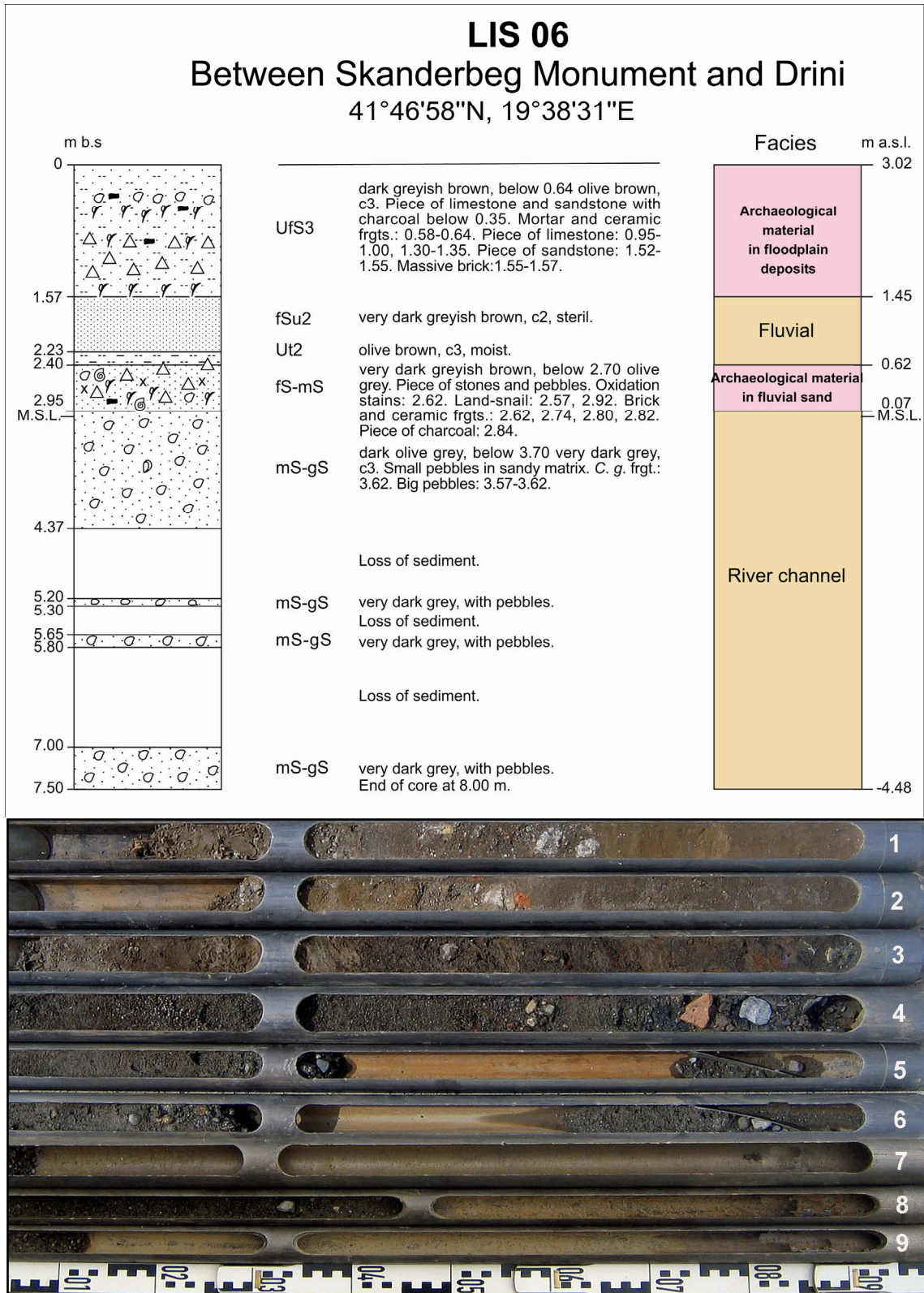


Sample - No.	Depth b.s. (cm)	pH (KCl) - value	Electric conductivity (mS/cm)	Loss-on-Ignition (%)	Carbonate content (%)	Orthophosphate (g/kg)	c(K ⁺) (g/kg)	c(Na ⁺) (g/kg)	c(Ca ²⁺) (g/kg)	c(Mg ²⁺) (g/kg)	c(Fe ^{2+/3+}) (g/kg)	c(Ca ²⁺)/c(Mg ²⁺)	c(Fe ^{2+/3+})/c(Na ⁺)
LIS 01/1	75	8.23	0.14	1.93	10.67	1.47	2.13	0.71	2.16	21.92	33.59	0.10	47.30
LIS 01/2	165	7.82	0.14	3.69	6.13	1.52	3.01	0.75	2.12	20.99	44.68	0.10	59.57
LIS 01/3	187	7.74	0.17	4.32	3.27	1.66	3.40	0.76	2.03	21.15	47.33	0.10	62.27
LIS 01/4	244	7.9	0.21	5.19	5.48	1.77	3.88	1.02	0.80	21.71	47.30	0.04	46.37
LIS 01/5	260	6.23	0.68	9.40	0.15	1.13	3.78	0.80	0.63	23.31	46.65	0.03	58.68
LIS 01/6	277.5	7.97	0.96	4.29	14.05	1.53	2.19	0.88	6.34	19.98	28.63	0.32	32.71
LIS 01/7	319.5	7.8	0.14	3.27	11.14	1.58	1.88	0.62	1.95	22.16	32.06	0.09	52.12
LIS 01/8	330.5	8.12	0.71	2.03	13.53	1.23	1.62	1.10	1.50	23.00	28.64	0.07	26.15
LIS 01/9	365	8.18	0.76	2.08	13.62	1.15	1.88	0.92	3.44	23.61	29.23	0.15	31.77
LIS 01/10	373.5	7.72	0.97	7.15	10.76	1.93	4.22	1.11	4.69	21.26	36.42	0.22	32.81
LIS 01/11	445	7.87	0.86	3.93	9.92	1.52	2.76	0.77	3.21	23.96	34.03	0.13	44.48
LIS 01/13	475	8.29	0.53	1.52	17.60	0.89	1.55	1.04	8.31	24.52	26.44	0.34	25.55
LIS 01/15	526	8.7	0.31	0.86	20.31	0.78	1.48	0.95	4.57	25.11	22.23	0.18	23.40
LIS 01/16	542	8.57	0.53	0.89	18.83	0.75	1.26	0.73	8.23	25.98	23.77	0.32	32.56
LIS 01/17	567.5	8.78	0.31	1.09	15.42	0.88	1.63	0.93	15.66	24.91	42.90	0.63	46.38
LIS 01/18	652.5	8.6	0.36	0.97	18.96	1.15	1.96	1.01	12.79	25.35	32.18	0.50	32.01
LIS 01/19	687.5	7.87	2.10	4.65	11.05	1.77	2.63	1.69	11.88	24.52	30.81	0.48	18.28
LIS 01/20	752.5	8.3	0.77	1.94	8.62	0.95	2.05	1.40	9.56	25.33	28.32	0.38	20.23
LIS 01/21	795	8.65	0.83	1.84	15.26	1.00	2.32	1.34	15.73	25.86	31.88	0.61	23.88
LIS 01/22	847.5	8.66	0.75	1.44	16.86	0.96	2.02	1.53	6.83	25.95	32.84	0.26	21.53
LIS 01/23	890	8.59	0.82	1.44	15.00	0.90	1.87	1.62	10.34	24.65	26.45	0.42	16.38

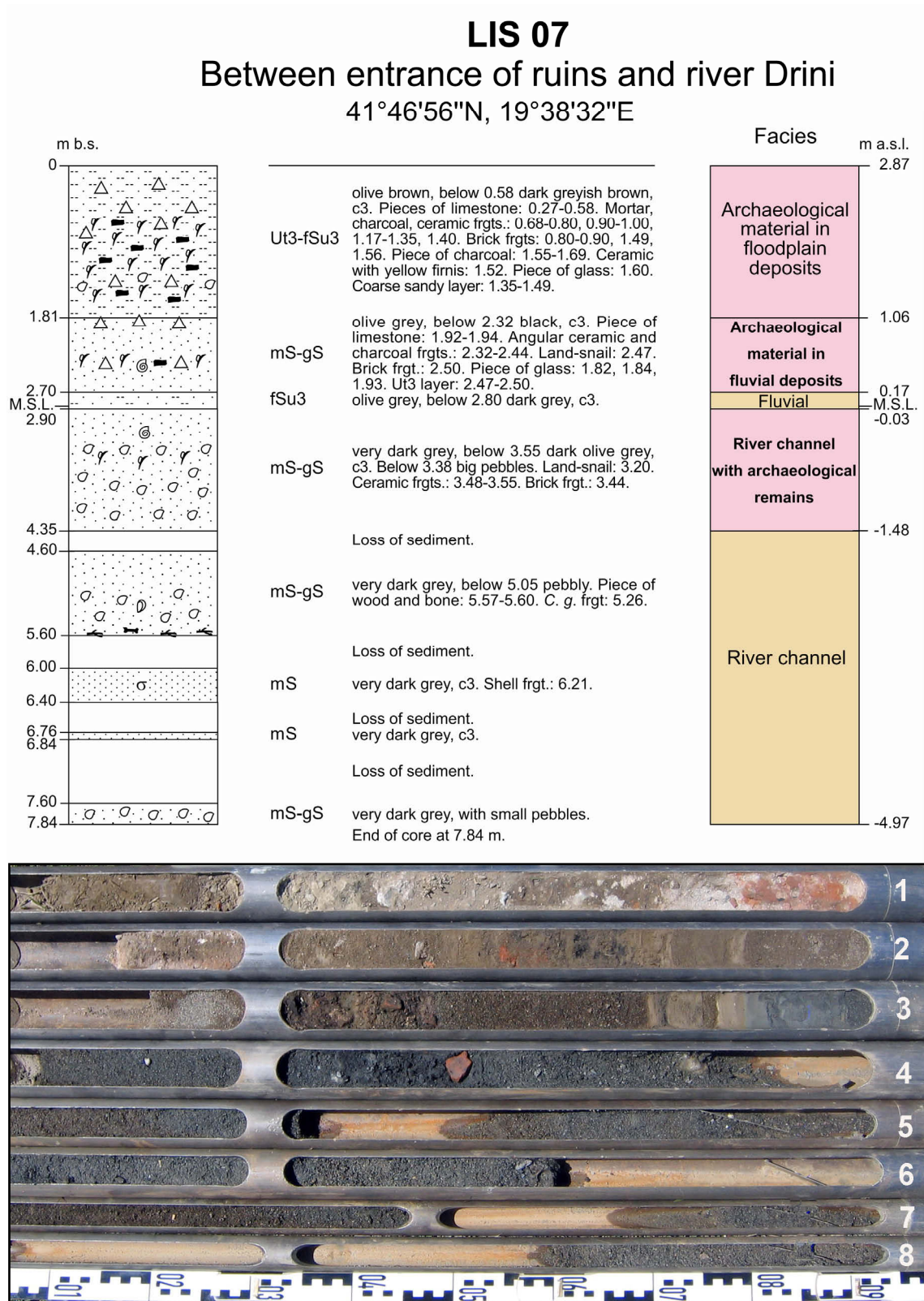
Appendix 5.2: Geochemical results of LIS 04.

Sample - No.	Depth b.s. (cm)	pH (KCl) - value	Electric conductivity (mS/cm)	Loss-on-Ignition (%)	Carbonate content (%)	Orthophosphate (g/kg)	c(K ⁺) (g/kg)	c(Na ⁺) (g/kg)	c(Ca ²⁺) (g/kg)	c(Mg ²⁺) (g/kg)	c(Fe ^{2+/3+}) (g/kg)	c(Ca ²⁺)/c(Mg ²⁺)	c(Fe ^{2+/3+})/c(Na ⁺)
LIS 04/1	65	7.53	0.08	2.68	4.68	1.25	2.31	0.97	14.26	18.02	29.90	0.79	30.98
LIS 04/2	130	7.31	0.12	3.01	3.19	0.78	2.95	1.13	8.40	19.25	36.94	0.44	32.84
LIS 04/3	140	7.36	0.04	2.18	6.03	0.66	1.96	1.48	20.85	21.87	31.92	0.95	21.57
LIS 04/5	185	7.49	0.12	3.05	7.59	2.75	2.05	1.88	23.29	23.48	33.60	0.99	17.92
LIS 04/6	245	7.5	0.10	1.93	6.08	1.07	1.44	0.65	15.57	23.56	36.11	0.66	55.55
LIS 04/7	255	7.53	0.05	0.88	7.38	0.67	1.07	1.00	21.36	24.03	30.08	0.89	30.23
LIS 04/8	280	7.73	0.12	1.45	8.97	0.88	0.49	1.73	34.08	27.40	28.08	1.24	16.23
LIS 04/10	378.5	7.78	0.07	1.58	6.70	0.84	0.80	1.67	27.66	27.03	28.26	1.02	16.97
LIS 04/11	570	8	0.09	1.40	8.08	0.62	0.65	0.95	27.65	26.14	26.48	1.06	28.02
LIS 04/12	675	7.44	0.87	6.48	1.93	1.77	3.95	4.61	3.39	25.64	60.85	0.13	13.21
LIS 04/13	693.5	7.81	0.20	1.96	7.57	0.92	1.26	1.51	23.39	22.46	31.00	1.04	20.53
LIS 04/14	772.5	7.7	0.12	1.70	7.95	0.92	0.95	0.68	24.10	22.35	27.70	1.08	41.03
LIS 04/19	987.5	7.93	0.09	0.87	14.66	0.40	0.11	0.81	58.90	23.67	20.84	2.49	25.73
LIS 04/20	1043	7.92	0.08	0.73	14.13	0.47	0.30	0.86	44.18	25.25	23.55	1.75	27.38

Appendix 5.3: Geological profile and photo of LIS 06.



Appendix 5.4: Geological profile and photo of LIS 07.



Appendix 5.5: Geochemical results of LIS 08.

Sample - No.	Depth b.s. (cm)	pH (KCl) - value	Electric conductivity (µS/cm)	Loss-on-Ignition (%)	Carbonate content (%)	Orthophosphate (g/kg)	c(K ⁺) (g/kg)	c(Na ⁺) (g/kg)	c(Ca ²⁺) (g/kg)	c(Mg ²⁺) (g/kg)	c(Fe ^{2+/3+}) (g/kg)	c(Ca ²⁺)/c(Mg ²⁺)	c(Fe ^{2+/3+})/c(Na ⁺)
LIS 08/1	70.0	7.67	0.33	5.96	2.99	1.59	1.59	4.32	5.90	16.90	35.51	0.35	8.23
LIS 08/2	90.0	8.1	0.35	2.13	8.08	0.91	0.77	2.49	24.20	19.36	27.86	1.25	11.21
LIS 08/3	143.5	7.68	1.36	3.34	5.91	0.49	1.19	3.11	20.40	20.68	23.79	0.99	7.65
LIS 08/4	177.5	8.2	0.63	2.09	12.51	0.71	0.81	2.28	44.05	22.13	27.75	1.99	12.20
LIS 08/5	257.5	7.94	1.56	1.75	11.63	0.55	0.76	2.00	40.20	20.93	18.85	1.92	9.45
LIS 08/6	285.0	7.83	1.72	1.44	10.66	0.50	0.89	1.72	35.85	21.43	24.19	1.67	14.10
LIS 08/7	336.0	7.47	2.11	10.98	9.51	0.70	1.33	2.26	33.10	19.77	19.90	1.67	8.80
LIS 08/8	355.0	7.88	1.27	3.09	11.38	0.78	1.58	0.50	36.05	21.43	23.93	1.68	47.86
LIS 08/9	385.0	8.25	0.64	1.33	13.37	0.88	2.21	0.85	42.05	20.86	27.13	2.02	32.10
LIS 08/10	447.0	8.65	0.30	1.54	15.05	0.95	1.00	0.79	44.70	20.94	28.15	2.13	35.63
LIS 08/11	485.0	8.49	0.23	1.49	14.00	0.82	0.85	0.80	46.70	21.00	28.35	2.22	35.44
LIS 08/12	557.5	8.62	0.21	1.48	15.27	0.79	0.95	0.65	49.95	21.93	27.40	2.28	42.47
LIS 08/13	677.5	8.8	0.16	1.50	17.01	0.74	0.71	1.32	50.25	22.01	25.36	2.28	19.21
LIS 08/14	780.0	8.67	0.20	1.56	15.03	0.71	0.87	0.50	47.50	21.96	26.77	2.16	54.08
LIS 08/15	875.0	8.64	0.24	1.38	15.53	0.72	1.01	1.06	50.20	22.29	26.86	2.25	25.45

Appendix 5.6: Geochemical results of LIS 09.

Sample - No.	Depth b.s. (cm)	pH (KCl) - value	Electric conductivity (mS/cm)	Loss-on-Ignition (%)	Carbonate content (%)	Orthophosphate (g/kg)	c(K ⁺) (g/kg)	c(Na ⁺) (g/kg)	c(Ca ²⁺) (g/kg)	c(Mg ²⁺) (g/kg)	c(Fe ^{2+/3+}) (g/kg)	c(Ca ²⁺)/c(Mg ²⁺)	c(Fe ^{2+/3+})/c(Na ⁺)
LIS 09/1	183.0	2.96	3.01	4.17	0.00	1.14	4.10	2.55	0.61	14.37	33.03	0.04	12.98
LIS 09/2	192.5	6.95	2.00	3.94	1.64	0.72	2.99	1.36	5.10	14.73	25.71	0.35	18.97
LIS 09/3	225.0	7.47	1.01	1.52	4.31	0.27	1.01	1.43	15.75	20.21	17.78	0.78	12.43
LIS 09/4	255.0	7.66	1.05	0.82	6.46	0.07	0.67	0.86	22.35	21.45	15.49	1.04	18.01
LIS 09/5	285.0	7.7	0.87	3.39	3.31	0.18	0.98	1.01	14.15	22.78	17.06	0.62	16.97
LIS 09/6	362.5	8.26	0.73	1.16	6.87	0.19	1.19	1.15	22.05	23.66	23.25	0.93	20.21
LIS 09/7	377.5	8.33	0.56	0.70	7.25	0.12	0.95	1.47	22.90	22.67	21.78	1.01	14.82
LIS 09/8	455.0	8.25	1.16	0.79	9.03	0.12	0.98	2.43	31.05	22.33	18.43	1.39	7.60
LIS 09/9	472.5	8.09	1.55	1.82	7.44	0.17	0.93	2.22	30.00	22.10	17.57	1.36	7.91
LIS 09/10	545.0	8.21	1.47	1.14	7.46	0.38	1.13	2.26	27.40	23.18	19.05	1.18	8.45
LIS 09/11	562.0	8.09	2.46	3.63	6.38	0.19	1.35	2.70	22.80	23.68	21.16	0.96	7.84
LIS 09/12	574.0	7.94	2.60	8.00	6.07	0.26	1.92	4.17	18.40	23.91	25.73	0.77	6.18
LIS 09/13	590.0	7.95	2.60	7.62	5.94	0.23	1.95	4.03	19.25	24.14	25.13	0.80	6.24
LIS 09/14	639.5	7.81	2.50	7.43	4.26	0.13	1.84	4.58	12.45	23.59	25.95	0.53	5.66
LIS 09/15	654.0	7.51	3.10	6.28	2.57	0.19	2.37	4.24	5.25	22.41	28.23	0.23	6.66
LIS 09/16	672.5	7.44	3.74	11.51	1.41	0.32	2.90	5.81	4.23	21.58	29.73	0.20	5.12
LIS 09/17	685.0	7.92	3.14	7.18	9.27	0.50	2.79	5.62	27.55	21.14	26.86	1.30	4.78
LIS 09/18	720.0	8.07	2.83	4.84	8.55	0.54	2.28	4.24	22.45	21.25	26.51	1.06	6.25
LIS 09/19	746	8.31	2.27	3.61	11.08	0.84	1.82	3.30	31.75	20.10	27.53	1.58	8.35
LIS 09/20	775	8.2	3.25	3.18	11.22	0.87	2.41	3.41	30.45	20.31	28.23	1.50	8.28
LIS 09/21	877.5	8.27	3.17	3.46	11.07	0.79	2.95	4.09	30.80	20.62	28.20	1.49	6.90
LIS 09/22	970	8.21	3.78	4.61	14.12	0.86	3.77	2.61	37.05	22.23	27.05	1.67	10.36
LIS 09/23	1074	8.25	3.43	3.40	13.18	0.75	5.64	6.35	32.10	21.28	26.84	1.51	4.23

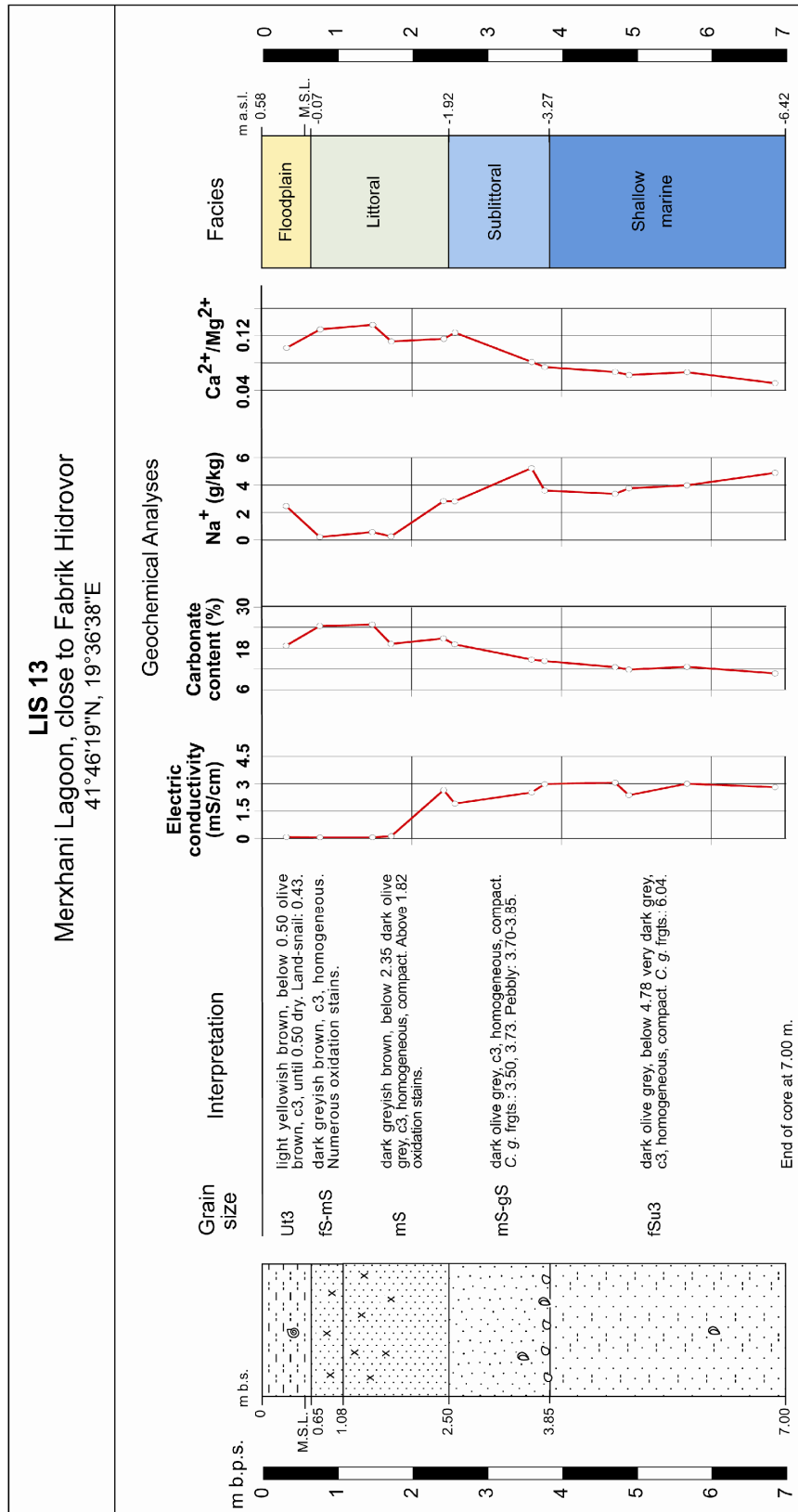
Appendix 5.7: Geochemical results of LIS 11.

Sample - No.	Depth b.s. (cm)	pH (KCl) - value	Electric conductivity (mS/cm)	Loss-on-Ignition (%)	Carbonate content (%)	Orthophosphate (g/kg)	c(K ⁺) (g/kg)	c(Na ⁺) (g/kg)	c(Ca ²⁺) (g/kg)	c(Mg ²⁺) (g/kg)	c(Fe ^{2+/3+}) (g/kg)	c(Ca ²⁺)/c(Mg ²⁺)	c(Fe ^{2+/3+})/c(Na ⁺)
LIS 11/1	75	7.34	0.23	5.66	0.95	1.35	3.79	1.61	2.33	10.20	36.98	0.23	23.04
LIS 11/2	120	6.88	0.16	7.59	0.00	1.28	4.26	3.45	0.87	12.58	49.06	0.07	14.22
LIS 11/3	144	7.3	0.53	10.79	2.24	1.08	4.15	2.64	4.06	10.98	43.10	0.37	16.36
LIS 11/4	175	4.24	1.53	10.73	0.15	0.91	4.52	1.66	0.42	10.35	33.22	0.04	20.01
LIS 11/5	265	5.18	0.49	4.60	0.31	0.74	5.69	2.74	0.78	10.87	46.33	0.07	16.94
LIS 11/6	285	6.67	0.09	4.63	0.00	0.83	4.82	1.66	0.86	11.14	58.55	0.08	35.27
LIS 11/7	312.5	7.38	0.16	4.63	0.47	0.61	5.13	1.45	1.48	12.46	40.19	0.12	27.71
LIS 11/8	325	8.29	0.09	1.27	14.11	0.33	1.25	1.40	55.50	20.52	23.83	2.71	17.02
LIS 11/9	375	8.69	0.09	0.68	13.47	0.43	0.83	1.20	51.00	23.35	27.13	2.18	22.61
LIS 11/10	445	8.63	0.09	0.93	13.50	0.33	0.80	1.29	46.35	23.13	23.30	2.00	18.06
LIS 11/11	487.5	8.63	0.08	1.08	11.85	0.33	1.14	2.61	42.05	22.79	23.15	1.85	8.88
LIS 11/12	570	8.63	0.08	0.68	18.03	0.29	0.61	1.02	61.00	21.29	22.55	2.87	22.10
LIS 11/13	640	8.62	0.08	0.64	11.59	0.35	1.14	1.56	43.40	22.81	22.83	1.90	14.68
LIS 11/14	672.5	8.56	0.08	0.75	12.67	0.31	1.07	1.42	42.80	23.34	24.00	1.83	16.96
LIS 11/15	736.5	8.55	0.09	0.77	14.29	0.36	1.01	1.36	48.35	23.57	23.49	2.05	17.34
LIS 11/16	749.5	8.69	0.19	1.44	12.91	0.39	1.16	1.54	53.50	24.35	23.98	2.20	15.57
LIS 11/17	760.5	8.5	0.28	1.61	13.25	0.78	1.15	0.79	44.90	22.79	29.52	1.97	37.37
LIS 11/18	767	8.05	0.64	2.34	12.23	0.77	2.55	0.79	41.25	24.19	29.50	1.71	37.34
LIS 11/19	773	8.03	0.92	2.41	11.68	0.62	1.15	1.02	37.60	24.83	31.03	1.51	30.42
LIS 11/20	785	8.27	0.34	1.95	14.53	0.80	1.11	0.72	44.85	24.08	29.62	1.86	41.14
LIS 11/21	847.5	8.36	0.35	1.85	14.58	0.80	1.40	0.68	28.90	23.81	29.73	1.21	44.04
LIS 11/22	880	7.68	1.46	4.72	11.96	1.02	2.40	1.37	39.20	22.67	26.58	1.73	19.40
LIS 11/23	897.5	7.56	1.84	6.56	14.06	0.79	1.68	1.44	41.00	23.94	26.83	1.71	18.70
LIS 11/24	967.5	8.51	0.48	1.22	14.94	0.74	1.46	1.32	51.50	24.32	29.12	2.12	22.06
LIS 11/25	990	8.47	0.72	0.86	15.51	0.74	1.15	0.89	52.00	23.90	25.42	2.18	28.56

Appendix 5.8: Geochemical results of LIS 12.

Sample - No.	Depth b.s. (cm)	pH (KCl) - value	Electric conductivity (mS/cm)	Loss-on-Ignition (%)	Carbonate content (%)	Orthophosphate (g/kg)	c(K ⁺) (g/kg)	c(Na ⁺) (g/kg)	c(Ca ²⁺) (g/kg)	c(Mg ²⁺) (g/kg)	c(Fe ^{2+/3+}) (g/kg)	c(Ca ²⁺)/c(Mg ²⁺)	c(Fe ^{2+/3+})/c(Na ⁺)
LIS 12/1	42.5	8.68	1.24	4.43	10.35	1.64	2.07	3.21	25.70	19.26	38.26	1.33	11.94
LIS 12/2	82.5	8.54	1.16	5.22	12.01	1.43	3.66	3.28	27.30	19.72	42.19	1.38	12.88
LIS 12/3	137.5	8.35	1.13	5.24	8.22	1.51	3.89	3.29	13.65	18.90	44.97	0.72	13.69
LIS 12/4	153	8.26	1.00	5.36	5.30	2.17	5.21	3.23	5.70	19.10	50.65	0.30	15.71
LIS 12/5	167.5	8.34	1.37	6.24	11.34	1.61	4.96	3.38	25.35	18.61	43.18	1.36	12.77
LIS 12/6	182.5	8.78	0.57	2.31	19.89	0.88	1.15	1.29	60.30	21.89	24.78	2.75	19.21
LIS 12/7	242.5	8.8	0.67	1.79	15.89	1.15	1.88	1.86	51.50	21.24	26.25	2.43	14.15
LIS 12/8	267.5	9.01	0.55	1.90	17.64	1.02	1.78	2.36	61.00	21.52	22.86	2.84	9.70
LIS 12/9	367	8.53	1.38	1.47	16.69	1.03	1.41	1.45	52.00	21.55	28.23	2.41	19.54
LIS 12/10	382.5	8.63	0.92	1.37	12.53	1.17	1.34	2.11	37.30	20.67	29.42	1.80	13.94
LIS 12/11	437	8.3	1.74	1.82	13.11	1.29	2.10	1.31	43.85	21.64	29.20	2.03	22.37
LIS 12/12	455	8.62	1.26	1.45	18.03	0.86	1.39	1.79	61.00	21.93	25.44	2.78	14.25
LIS 12/13	475	9.04	0.52	0.87	15.95	0.86	1.21	1.50	53.00	21.24	25.96	2.50	17.36
LIS 12/14	555	9.05	0.86	0.98	14.10	0.99	1.69	1.62	45.30	21.26	26.64	2.13	16.44
LIS 12/15	579	8.62	1.56	2.78	13.13	1.22	2.13	1.92	39.55	19.96	28.97	1.98	15.09
LIS 12/16	644.5	8.81	1.89	3.12	10.93	1.45	1.80	2.94	31.35	19.26	30.68	1.63	10.43
LIS 12/17	655	8.29	2.57	6.33	15.93	1.52	2.17	4.40	47.75	18.49	33.24	2.58	7.55
LIS 12/18	672.5	9	1.19	2.66	16.59	0.88	0.93	2.35	54.50	22.49	25.21	2.42	10.73
LIS 12/19	732.5	9.37	0.99	2.29	20.25	0.74	1.02	1.80	67.00	23.47	20.62	2.86	11.46
LIS 12/20	777.5	8.46	2.22	3.31	12.06	1.15	2.62	3.45	36.40	21.98	30.14	1.66	8.75
LIS 12/21	870	8.91	1.58	1.94	20.19	0.77	1.04	2.49	71.00	23.06	21.62	3.08	8.70
LIS 12/22	985	8.94	1.67	2.44	17.28	0.92	1.18	2.85	52.50	21.93	24.89	2.39	8.75

Appendix 5.9.1: Geological profile and selected geochemical results of LIS 13.



Appendix 5.9.2: Photo and geochemical results of LIS 13.

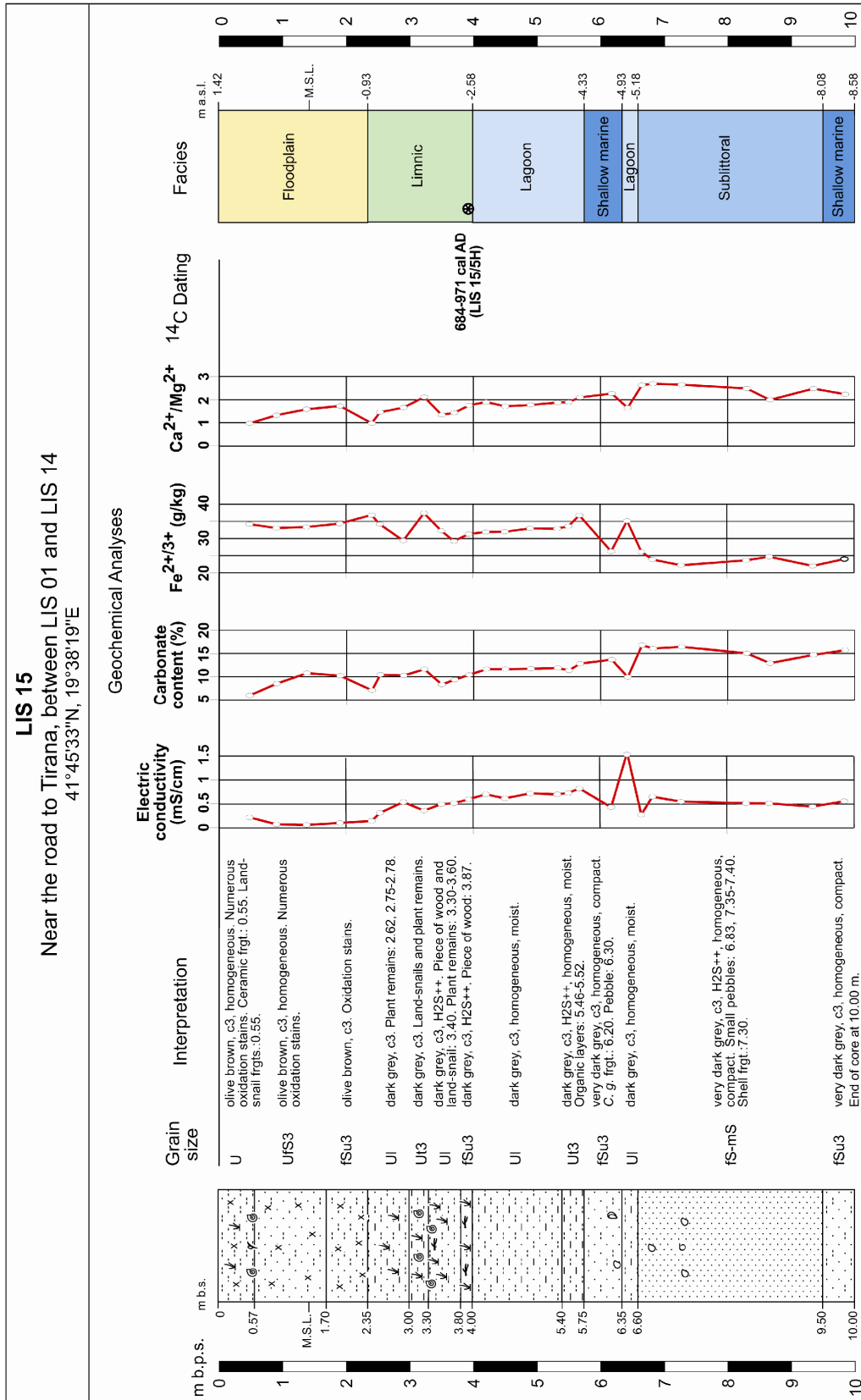


Sample - No.	Depth b.s. (cm)	pH (KCl) - value	Electric conductivity (mS/cm)	Loss-on-Ignition (%)	Carbonate content (%)	Orthophosphate (g/kg)	c(K ⁺) (g/kg)	c(Na ⁺) (g/kg)	c(Ca ²⁺) (g/kg)	c(Mg ²⁺) (g/kg)	c(Fe ^{2+/3+}) (g/kg)	c(Ca ²⁺)/c(Mg ²⁺)	c(Fe ^{2+/3+})/c(Na ⁺)
LIS 13/1	32.5	8.37	0.07	1.23	18.7	0.65	0.68	2.48	2.58	25.27	26.18	0.10	10.55
LIS 13/2	77.5	8.88	0.06	0.63	24.4	0.69	0.38	0.22	3.46	26.75	23.24	0.13	108.09
LIS 13/3	147.5	8.30	0.06	0.73	24.8	0.58	0.46	0.58	3.69	27.10	22.89	0.14	39.80
LIS 13/4	172.5	8.93	0.12	0.69	19.2	0.64	0.75	0.26	3.08	27.54	27.09	0.11	104.17
LIS 13/5	242.5	9.02	2.65	2.70	20.8	0.72	0.45	2.84	3.00	25.99	20.63	0.12	7.26
LIS 13/6	257.5	9.26	1.91	2.20	19.1	0.73	0.39	2.82	2.65	21.24	19.79	0.12	7.02
LIS 13/7	360	9.18	2.52	2.34	14.7	0.86	1.23	5.24	2.14	26.26	27.26	0.08	5.20
LIS 13/8	377.5	9.16	2.98	2.50	14.3	0.76	0.98	3.61	1.83	24.73	21.67	0.07	6.00
LIS 13/9	471.5	9.02	3.06	2.16	12.5	0.85	0.93	3.37	1.66	24.84	23.67	0.07	7.02
LIS 13/10	490	8.92	2.37	2.03	11.8	0.67	1.18	3.77	1.60	25.59	26.02	0.06	6.90
LIS 13/11	567.5	8.96	3.00	1.94	12.6	0.82	1.06	3.99	1.73	25.95	26.43	0.07	6.63
LIS 13/12	685	8.78	2.81	2.45	10.7	0.85	1.61	4.90	1.35	26.70	26.99	0.05	5.51

Appendix 5.10: Geochemical results of LIS 14.

Sample - No.	Depth b.s. (cm)	pH (KCl) - value	Electric conductivity (mS/cm)	Loss-on-Ignition (%)	Carbonate content (%)	Orthophosphate (g/kg)	c(K ⁺) (g/kg)	c(Na ⁺) (g/kg)	c(Ca ²⁺) (g/kg)	c(Mg ²⁺) (g/kg)	c(Fe ^{2+/3+}) (g/kg)	c(Ca ²⁺)/c(Mg ²⁺)	c(Fe ^{2+/3+})/c(Na ⁺)
LIS 14/1	40	8.06	0.15	2.99	7.78	1.37	2.03	2.66	1.00	24.06	43.97	0.04	16.53
LIS 14/2	87.5	7.97	0.14	2.37	7.62	1.41	2.11	3.99	0.97	23.36	40.92	0.04	10.27
LIS 14/3	120	8.66	0.09	0.75	11.51	1.42	0.73	0.35	1.95	24.60	29.67	0.08	84.77
LIS 14/4	147.5	8.7	0.09	0.84	10.97	1.56	0.63	0.51	1.72	23.35	24.83	0.07	49.17
LIS 14/5	222.5	8.92	0.15	0.44	12.74	1.26	0.54	0.47	2.08	24.39	26.93	0.09	57.90
LIS 14/6	260	8.9	0.12	0.42	14.27	1.09	0.52	0.21	2.07	23.87	25.72	0.09	122.45
LIS 14/7	338.5	8.98	0.13	1.13	15.44	0.98	0.60	0.23	2.27	26.01	24.65	0.09	109.56
LIS 14/8	354	8.62	0.19	1.49	10.92	0.74	1.00	1.12	1.58	24.60	24.73	0.06	22.08
LIS 14/9	430	8.93	0.11	1.17	14.88	1.01	0.58	0.38	2.13	26.36	24.90	0.08	66.40
LIS 14/10	464	8.94	0.10	1.11	16.00	0.95	0.69	0.72	2.33	26.75	24.77	0.09	34.64
LIS 14/11	480	8.82	0.13	1.34	12.15	0.76	0.54	0.16	1.75	24.74	25.18	0.07	157.34
LIS 14/12	525	8.88	0.12	1.21	12.33	0.64	0.70	0.63	1.93	24.70	24.01	0.08	38.11
LIS 14/13	546.5	8.88	0.12	0.91	14.71	1.40	0.47	1.53	2.15	25.91	25.70	0.08	16.80
LIS 14/14	646.5	9.04	0.10	0.85	16.45	0.71	0.63	0.27	2.41	26.47	25.39	0.09	95.79
LIS 14/15	660	8.09	0.98	3.88	12.30	0.82	2.16	1.61	1.74	25.60	31.26	0.07	19.41
LIS 14/16	674	8.43	0.71	0.75	18.06	0.76	0.60	0.27	2.71	25.48	23.42	0.11	86.74
LIS 14/17	692.5	8.77	0.37	0.65	18.88	0.82	0.56	0.33	2.82	25.59	23.70	0.11	72.92
LIS 14/18	737.5	8.58	0.51	0.61	17.65	0.70	0.42	0.32	2.71	25.78	24.97	0.11	78.02
LIS 14/19	762.5	8.36	0.81	0.68	13.15	0.70	0.47	1.32	2.08	26.54	25.72	0.08	19.56
LIS 14/20	780	8.5	1.13	1.56	17.57	0.87	0.58	0.41	2.60	26.03	23.17	0.10	57.21
LIS 14/21	865	8.51	1.10	1.69	17.15	0.64	0.58	1.78	2.61	26.41	23.88	0.10	13.45
LIS 14/22	972.5	8.53	1.56	3.78	15.30	0.57	0.80	1.36	1.90	23.68	27.25	0.08	20.03
LIS 14/23	992.5	8.73	1.05	3.07	17.29	0.44	0.67	1.36	2.38	26.08	24.19	0.09	17.85

Appendix 5.11.1: Geological profile and selected geochemical results of LIS 15

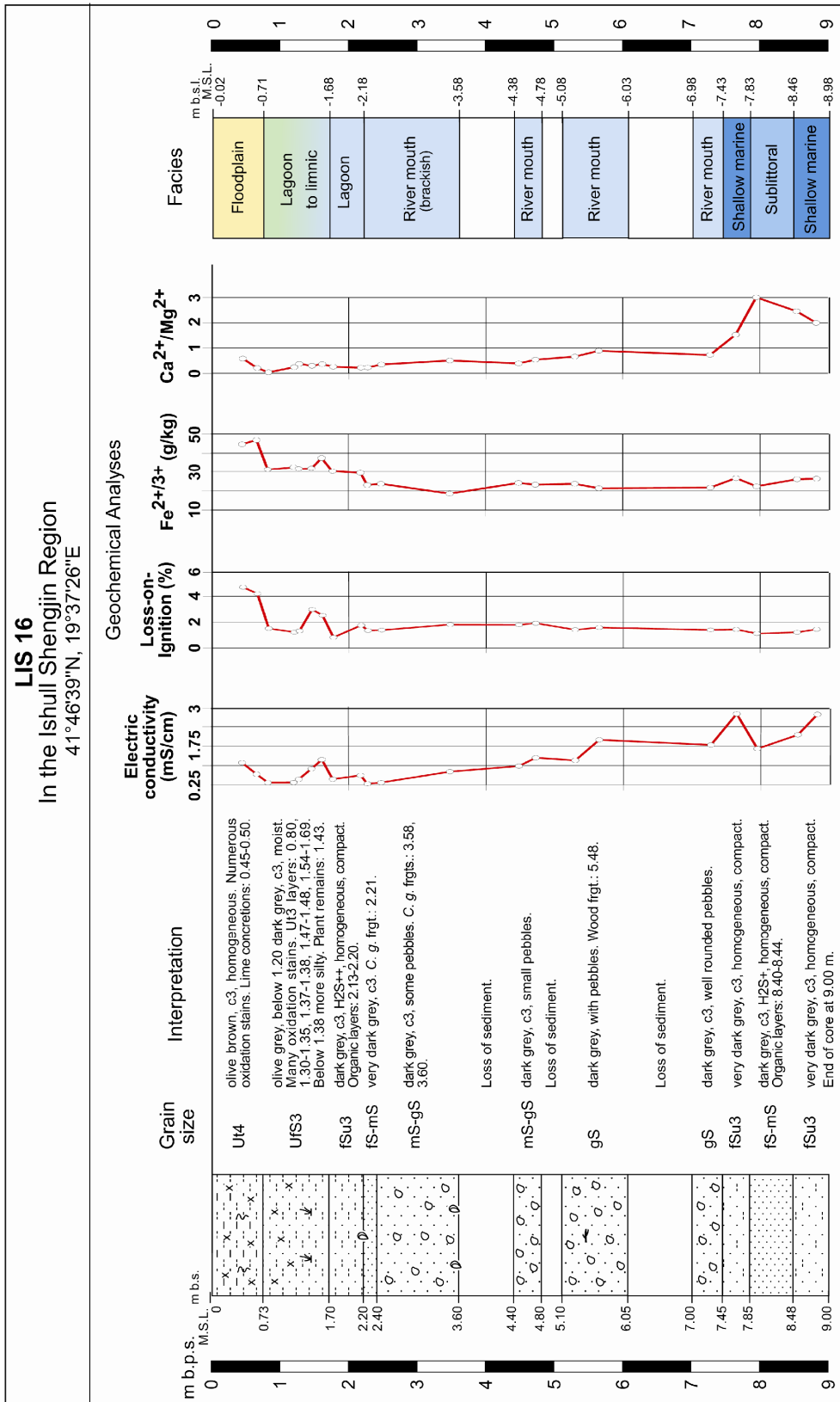


Appendix 5.11.2: Photo and geochemical results of LIS 15.



Sample - No.	Depth b.s. (cm)	pH (KCl) - value	Electric conductivity (mS/cm)	Loss-on-Ignition (%)	Carbonate content (%)	Orthophosphate (g/kg)	c(K ⁺) (g/kg)	c(Na ⁺) (g/kg)	c(Ca ²⁺) (g/kg)	c(Mg ²⁺) (g/kg)	c(Fe ^{2+/3+}) (g/kg)	c(Ca ²⁺)/c(Mg ²⁺)	c(Fe ^{2+/3+})/c(Na ⁺)
LIS 15/1	47.5	7.62	0.22	2.33	5.97	1.64	2.07	1.68	19.80	20.41	34.20	0.97	20.35
LIS 15/2	90	8.12	0.08	1.67	8.52	1.45	1.81	1.10	26.95	20.37	33.04	1.32	30.17
LIS 15/3	137.5	8.16	0.06	1.54	10.78	1.17	1.54	1.06	35.75	22.59	33.34	1.58	31.60
LIS 15/4	190	8.11	0.11	3.16	10.23	1.27	1.83	1.08	34.30	19.91	34.36	1.72	31.96
LIS 15/5	240	8.02	0.15	4.18	7.06	1.21	2.53	0.90	21.25	21.89	36.85	0.97	41.17
LIS 15/6	253	8.1	0.31	3.77	10.43	1.30	1.81	0.77	28.25	19.42	34.19	1.46	44.69
LIS 15/7	290	8.04	0.54	3.95	10.27	1.13	1.82	1.02	35.55	21.50	29.40	1.65	28.96
LIS 15/8	322.5	8.26	0.36	4.02	11.62	1.16	1.29	1.02	43.00	20.37	37.41	2.11	36.68
LIS 15/9	350	8.05	0.50	3.20	8.32	1.31	1.65	0.98	29.70	22.18	32.28	1.34	32.93
LIS 15/10	370	8.05	0.52	2.70	9.37	1.40	1.65	1.50	28.70	20.08	29.24	1.43	19.56
LIS 15/11	393	7.97	0.60	3.49	10.41	1.16	1.45	1.07	34.60	19.75	31.33	1.75	29.41
LIS 15/12	420	8.03	0.71	3.28	11.61	1.28	1.51	0.77	41.15	21.72	31.91	1.90	41.44
LIS 15/13	450	8.01	0.62	3.18	11.62	1.56	2.61	1.12	32.90	19.28	31.99	1.71	28.69
LIS 15/14	490	8.02	0.72	3.33	11.72	1.57	2.18	1.86	33.90	19.16	32.97	1.77	17.72
LIS 15/15	532.5	8.02	0.70	3.58	11.87	1.55	2.52	1.59	36.10	19.27	32.87	1.87	20.67
LIS 15/16	550	8.02	0.73	2.78	11.37	1.71	2.16	0.86	33.95	17.95	33.58	1.89	39.27
LIS 15/17	567.5	8.03	0.83	2.82	12.81	1.84	2.48	1.14	35.35	16.87	36.76	2.10	32.24
LIS 15/18	617.5	8.5	0.43	1.85	13.67	0.97	1.38	2.72	47.80	21.10	26.23	2.27	9.64
LIS 15/19	642.5	7.73	1.57	4.94	9.92	1.74	3.03	0.86	29.80	18.16	35.17	1.64	40.89
LIS 15/20	665	8.6	0.28	1.64	16.81	1.03	1.55	1.17	58.00	22.05	26.14	2.63	22.34
LIS 15/21	682.5	8.31	0.65	1.54	16.09	0.82	1.35	1.11	59.00	21.94	23.91	2.69	21.54
LIS 15/22	727.5	8.47	0.55	1.49	16.44	0.68	1.04	0.93	58.50	22.13	22.19	2.64	23.86
LIS 15/23	830	8.47	0.52	1.64	15.05	0.79	0.97	0.81	54.00	21.74	23.66	2.48	29.21
LIS 15/24	866.5	8.47	0.51	1.45	12.91	0.93	1.55	1.73	44.15	22.21	24.71	1.99	14.32
LIS 15/25	935	8.58	0.45	1.14	14.70	0.77	1.54	1.45	55.50	22.40	22.01	2.48	15.23
LIS 15/26	985	8.52	0.56	1.46	15.72	0.97	1.84	1.16	50.00	22.41	24.04	2.23	20.72

Appendix 5.12.1: Geological profile and selected geochemical results of LIS 16.



Appendix 5.12.2: Photo and geochemical results of LIS 16.

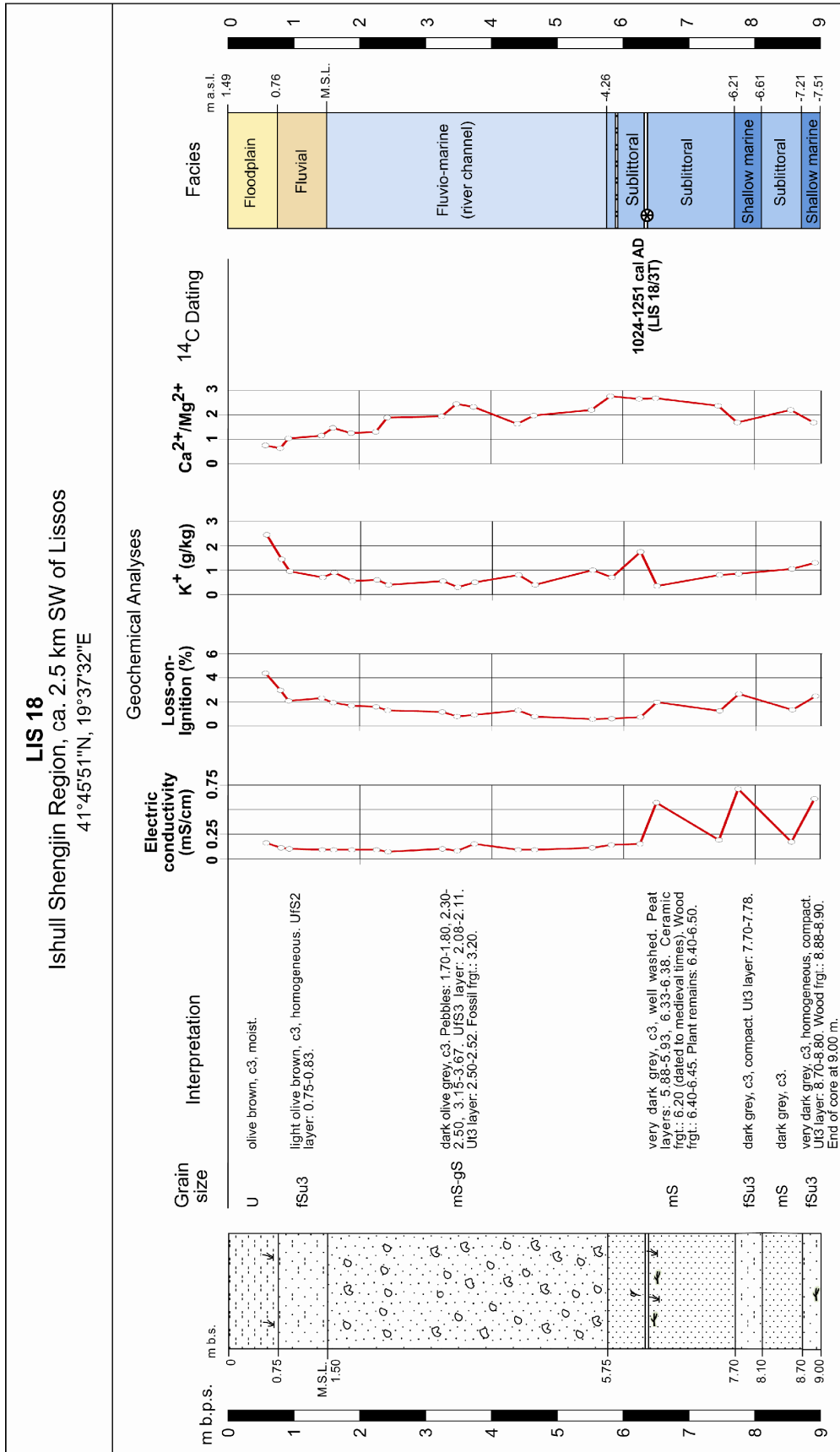


Sample - No.	Depth b.s. (cm)	pH (KCl) - value	Electric conductivity (mS/cm)	Loss-on-Ignition (%)	Carbonate content (%)	Orthophosphate (g/kg)	c(K ⁺) (g/kg)	c(Na ⁺) (g/kg)	c(Ca ²⁺) (g/kg)	c(Mg ²⁺) (g/kg)	c(Fe ^{2+/3+}) (g/kg)	c(Ca ²⁺)/c(Mg ²⁺)	c(Fe ^{2+/3+})/c(Na ⁺)
LIS 16/1	45	8.87	1.10	4.70	9.37	1.49	3.29	3.77	12.69	21.84	44.68	0.58	11.87
LIS 16/2	66	8.67	0.66	4.21	9.69	1.44	4.30	2.55	4.46	21.42	46.87	0.21	18.38
LIS 16/3	82.5	8.71	0.33	1.51	9.76	1.40	1.37	1.06	0.76	20.35	31.29	0.04	29.66
LIS 16/4	120	8.79	0.34	1.22	8.76	1.25	1.32	1.42	5.18	21.38	32.63	0.24	22.98
LIS 16/5	127.5	8.56	0.46	1.33	9.09	1.29	1.46	1.15	7.81	20.96	31.72	0.37	27.70
LIS 16/6	146	8.34	0.87	2.99	6.38	1.31	2.01	1.33	6.52	21.95	31.90	0.30	24.07
LIS 16/7	161	8.23	1.22	2.53	12.62	1.51	2.49	1.25	6.92	19.01	37.45	0.36	29.96
LIS 16/8	177	8.67	0.47	0.83	10.02	1.19	1.07	0.67	5.84	22.56	30.35	0.26	45.30
LIS 16/9	217.5	8.71	0.62	1.76	10.90	1.19	1.62	1.03	5.02	22.55	29.40	0.22	28.54
LIS 16/10	227.5	8.85	0.29	1.36	13.59	0.96	1.49	0.90	5.08	22.67	22.99	0.22	25.68
LIS 16/11	247.5	8.98	0.34	1.39	13.08	0.94	1.32	0.85	7.40	21.29	23.62	0.35	27.95
LIS 16/12	347.5	9.03	0.76	1.82	15.04	0.84	1.24	1.23	9.32	18.56	18.54	0.50	15.13
LIS 16/13	448	9.1	0.97	1.79	13.60	0.86	1.51	1.45	8.61	22.04	24.08	0.39	16.61
LIS 16/14	472.5	9.23	1.30	1.92	14.74	0.82	1.22	2.30	12.78	23.83	23.16	0.54	10.09
LIS 16/15	530	9.18	1.19	1.41	13.74	0.65	1.13	1.62	15.15	22.95	23.61	0.66	14.62
LIS 16/16	565	9.11	1.99	1.59	14.41	0.66	1.55	2.22	21.31	23.92	21.33	0.89	9.61
LIS 16/17	727.5	9.12	1.79	1.40	14.25	0.52	1.03	2.66	17.78	24.51	21.62	0.73	8.13
LIS 16/18	765	8.91	2.99	1.43	12.84	0.84	1.34	3.12	33.99	22.22	26.57	1.53	8.53
LIS 16/19	795	9.09	1.64	1.12	17.70	0.87	1.16	2.31	68.85	22.88	22.30	3.01	9.67
LIS 16/20	854	8.92	2.18	1.21	14.27	0.90	1.44	3.11	57.75	23.50	26.01	2.46	8.38
LIS 16/21	882.5	8.67	2.97	1.44	11.44	0.93	1.30	3.00	45.38	22.72	26.30	2.00	8.78

Appendix 5.13: Geochemical results of LIS 17.

Sample - No.	Depth b.s. (cm)	pH (KCl) - value	Electric conductivity (mS/cm)	Loss-on-Ignition (%)	Carbonate content (%)	Orthophosphate (g/kg)	c(K ⁺) (g/kg)	c(Na ⁺) (g/kg)	c(Ca ²⁺) (g/kg)	c(Mg ²⁺) (g/kg)	c(Fe ^{2+/3+}) (g/kg)	c(Ca ²⁺)/c(Mg ²⁺)	c(Fe ^{2+/3+})/c(Na ⁺)
LIS 17/1	55	7.6	0.21	4.05	4.08	1.38	2.27	1.10	16.75	19.58	41.14	0.86	37.57
LIS 17/2	82.5	8.6	0.06	1.22	20.39	0.88	0.74	1.21	79.00	23.78	32.35	3.32	26.73
LIS 17/3	145	8.74	0.06	1.14	24.78	0.80	1.07	1.58	88.50	22.46	24.28	3.94	15.42
LIS 17/4	155	8.79	0.06	1.08	26.41	0.79	0.95	1.42	93.00	23.44	25.41	3.97	17.89
LIS 17/5	175	8.78	0.06	0.90	23.82	0.88	1.01	1.46	89.50	23.39	24.92	3.83	17.07
LIS 17/6	245	8.78	0.09	0.96	18.32	0.95	1.06	1.01	65.50	23.12	25.13	2.83	24.88
LIS 17/7	277.5	8.65	0.11	0.96	16.99	0.79	0.75	0.83	64.00	23.03	23.83	2.78	28.88
LIS 17/8	292.5	8.37	0.20	1.17	11.49	0.86	1.18	4.69	40.00	22.60	27.33	1.77	5.83
LIS 17/9	332.5	8.4	0.21	1.12	12.98	0.67	1.07	1.27	50.00	22.34	25.20	2.24	19.84
LIS 17/10	346.5	8.75	0.13	0.76	18.37	0.69	0.89	1.51	68.00	23.16	24.45	2.94	16.25
LIS 17/11	365	8.5	0.15	1.27	12.48	0.93	1.08	3.79	47.85	22.63	27.95	2.11	7.37
LIS 17/12	380	8.26	0.26	2.02	10.11	0.97	1.53	2.89	40.70	22.48	28.48	1.81	9.87
LIS 17/13	392.5	8.15	0.35	2.06	10.35	1.18	1.55	1.64	41.85	22.26	28.17	1.88	17.18
LIS 17/15	435	7.99	0.60	3.24	9.80	1.18	1.77	1.39	39.25	21.55	27.11	1.82	19.50
LIS 17/16	448	8.64	0.22	1.15	16.72	0.73	0.98	1.03	62.00	22.89	22.94	2.71	22.27
LIS 17/17	465	8.67	0.29	1.11	18.18	0.69	1.73	0.66	67.00	23.06	22.82	2.91	34.84
LIS 17/18	485	8.36	0.45	1.53	12.00	0.97	1.06	1.26	48.50	22.73	24.81	2.13	19.69
LIS 17/19	545	8.44	0.42	1.51	12.29	0.93	1.21	1.57	52.50	22.84	24.89	2.30	15.90
LIS 17/20	557.5	8.4	0.57	1.25	14.55	0.76	0.85	1.36	59.00	22.85	22.74	2.58	16.72
LIS 17/22	592.5	8.65	0.14	1.07	14.78	0.89	1.00	1.22	54.00	23.13	26.15	2.34	21.43
LIS 17/23	645	8.69	0.16	1.13	13.70	0.77	0.99	1.07	53.00	23.13	25.27	2.29	23.72
LIS 17/24	695	8.7	0.14	1.32	14.84	0.84	0.82	0.85	54.00	23.25	25.52	2.32	30.02
LIS 17/25	755	8.85	0.14	0.91	15.27	0.94	1.40	1.05	57.00	23.18	26.46	2.46	25.32
LIS 17/26	775	8.52	0.16	0.67	15.54	0.89	1.40	3.06	55.00	22.89	25.91	2.40	8.48
LIS 17/27	786	8.22	0.63	1.87	12.43	0.90	1.51	1.41	46.20	22.80	26.55	2.03	18.83
LIS 17/28	855	8.6	0.27	1.03	14.53	0.92	1.24	1.00	53.50	22.64	26.11	2.36	26.11
LIS 17/29	965	8.48	0.52	1.74	13.69	1.01	2.29	2.16	49.85	22.11	26.04	2.26	12.08

Appendix 5.14.1: Geological profile and selected geochemical results of LIS 18.

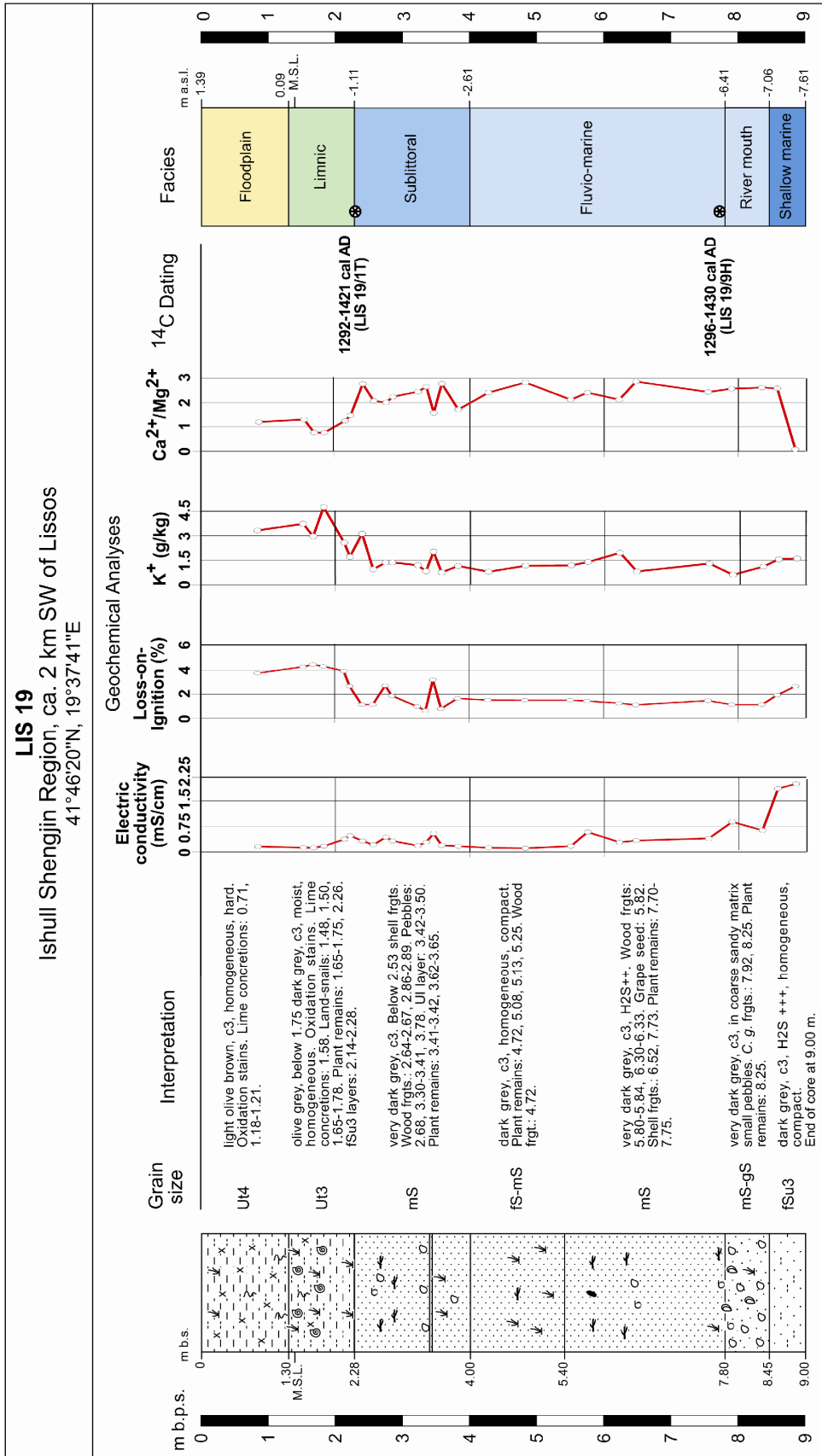


Appendix 5.14.2: Photo and geochemical results of LIS 18.



Sample - No.	Depth b.s.l. (cm)	pH (KCl) - value	Electric conductivity (mS/cm)	Loss-on-Ignition (Mass - %)	Carbonate content (%)	Orthophosphate (g/kg)	c(K ⁺) (g/kg)	c(Na ⁺) (g/kg)	c(Ca ²⁺) (g/kg)	c(Mg ²⁺) (g/kg)	c(Fe ^{2+/3+}) (g/kg)	c(Ca ²⁺)/c(Mg ²⁺)	c(Fe ^{2+/3+})/c(Na ⁺)
LIS 18/1	57.5	7.66	0.16	4.38	5.69	1.60	2.45	0.65	14.45	19.20	43.55	0.75	67.00
LIS 18/2	80	7.86	0.11	2.97	4.25	1.42	1.45	0.70	12.85	20.35	37.25	0.63	53.21
LIS 18/3	92.5	8.03	0.10	2.08	5.47	1.11	0.95	0.75	20.10	19.40	30.80	1.04	41.07
LIS 18/4	142.5	8.03	0.09	2.31	0.56	0.91	0.70	0.55	23.10	20.05	30.10	1.15	54.73
LIS 18/5	160	8.10	0.09	1.93	9.40	0.87	0.90	1.00	30.60	20.85	29.45	1.47	29.45
LIS 18/6	187.5	8.24	0.09	1.69	7.27	0.78	0.55	0.60	27.30	21.75	29.45	1.26	49.08
LIS 18/7	225	8.43	0.09	1.59	8.07	1.00	0.60	0.95	28.00	21.45	27.60	1.31	29.05
LIS 18/8	242.5	8.63	0.07	1.29	5.00	0.65	0.40	0.65	42.45	22.45	24.95	1.89	38.38
LIS 18/9	325	8.82	0.10	1.17	13.54	0.77	0.55	0.60	42.20	21.75	25.00	1.94	41.67
LIS 18/10	347.5	8.80	0.08	0.79	14.66	0.74	0.30	0.65	49.80	20.35	21.05	2.45	32.38
LIS 18/11	373.5	8.76	0.15	0.92	13.57	1.02	0.50	1.00	50.30	21.60	22.90	2.33	22.90
LIS 18/12	440	8.46	0.09	1.29	9.52	0.89	0.80	0.60	35.35	21.65	26.15	1.63	43.58
LIS 18/13	465	8.56	0.09	0.78	13.16	0.81	0.40	0.65	41.60	21.10	22.90	1.97	35.23
LIS 18/14	552.5	8.74	0.11	0.57	12.77	0.60	1.00	1.20	48.10	21.85	21.40	2.20	17.83
LIS 18/15	581.5	8.77	0.14	0.61	17.00	0.71	0.70	0.65	62.15	22.50	23.25	2.76	35.77
LIS 18/17	625	8.78	0.15	0.73	17.25	0.56	1.75	0.95	60.75	22.90	24.75	2.65	26.05
LIS 18/18	650	8.13	0.57	1.98	12.45	0.76	0.35	0.90	58.35	21.75	21.85	2.68	24.28
LIS 18/19	745	8.52	0.19	1.25	13.06	0.69	0.80	4.95	48.60	20.50	21.45	2.37	4.33
LIS 18/20	774	8.05	0.71	2.66	10.36	1.07	0.85	0.60	35.45	21.00	30.00	1.69	50.00
LIS 18/22	855	8.50	0.17	1.34	13.10	0.78	1.05	1.00	47.30	21.45	23.75	2.21	23.75
LIS 18/24	890	8.22	0.61	2.47	9.41	1.12	1.30	1.15	34.50	20.45	28.35	1.69	24.65

Appendix 5.15.1: Geological profile and selected geochemical results of LIS 19

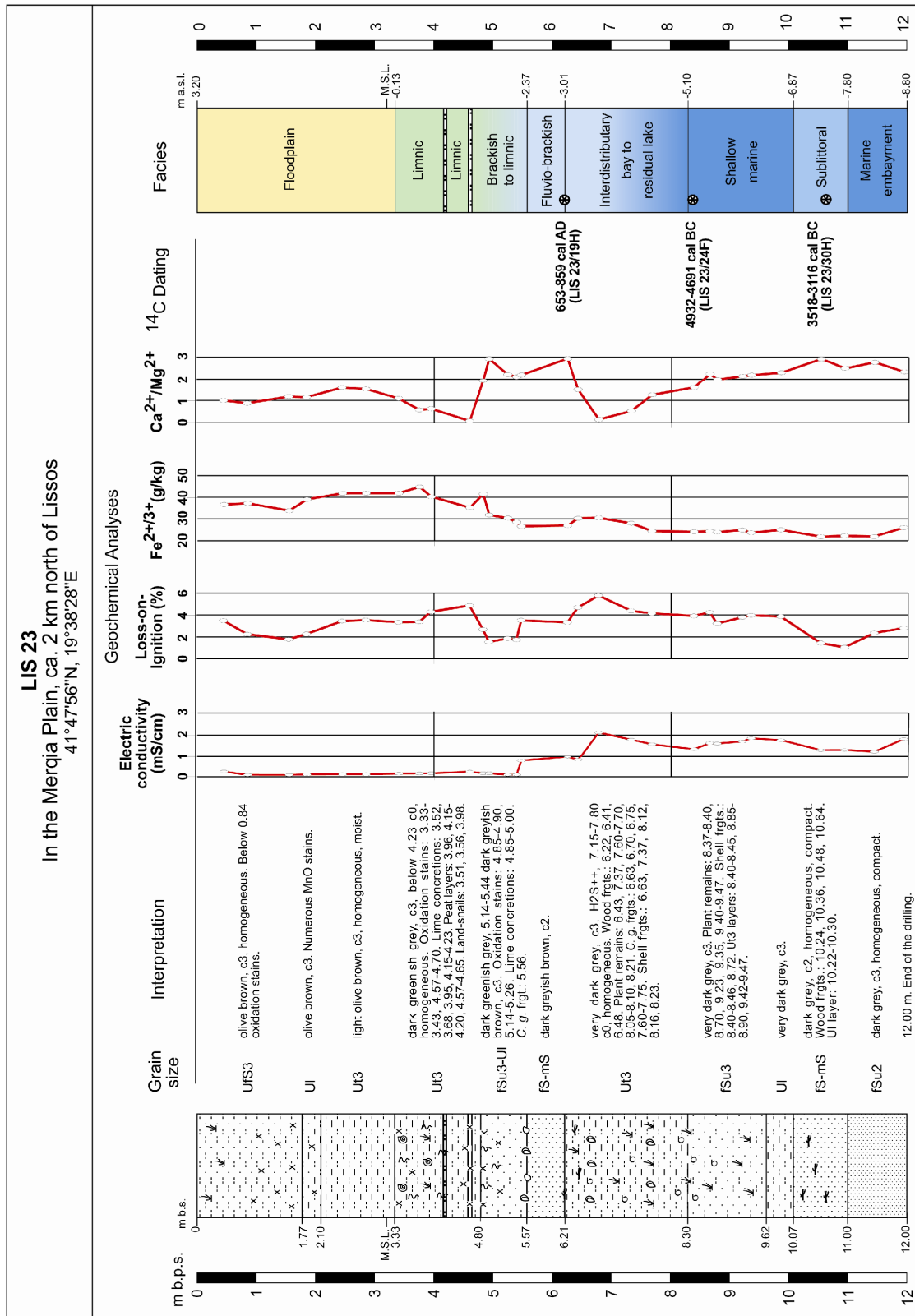


Appendix 5.15.2: Photo and geochemical results of LIS 19.

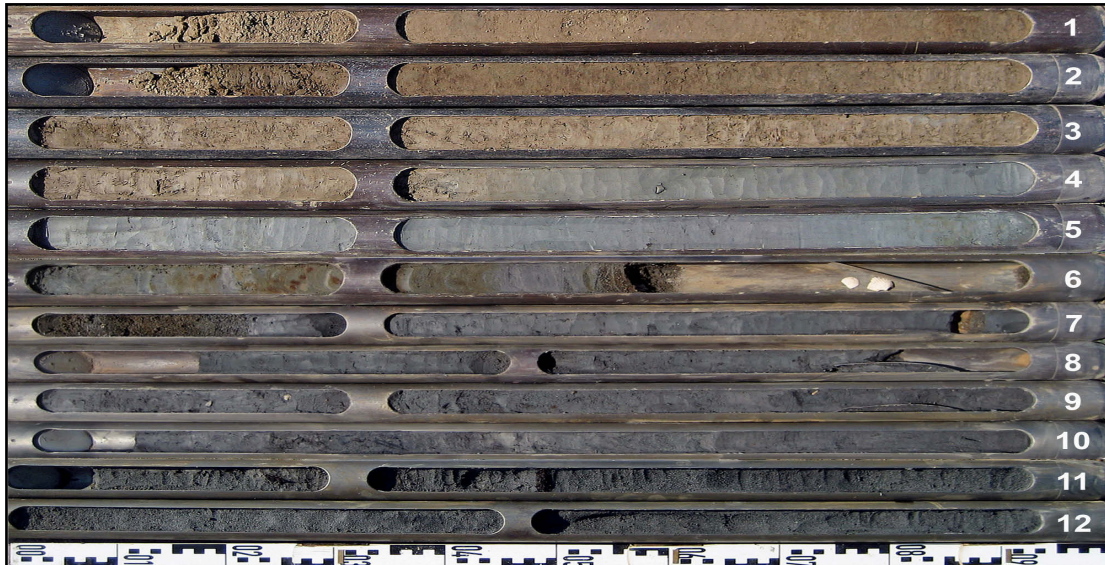


Sample - No.	Depth b.s. (cm)	pH (KCl) - value	Electric conductivity (mS/cm)	Loss-on-Ignition (%)	Carbonate content (%)	Orthophosphate (g/kg)	c(K ⁺) (g/kg)	c(Na ⁺) (g/kg)	c(Ca ²⁺) (g/kg)	c(Mg ²⁺) (g/kg)	c(Fe ^{2+/3+}) (g/kg)	c(Ca ²⁺)/c(Mg ²⁺)	c(Fe ^{2+/3+})/c(Na ⁺)
LIS 19/1	85	8.42	0.16	3.74	8.27	1.42	3.33	2.29	23.95	19.90	39.32	1.20	17.21
LIS 19/2	152.5	8.18	0.13	4.28	9.41	1.46	3.74	1.36	25.70	19.72	40.62	1.30	29.87
LIS 19/3	167.5	8.02	0.12	4.47	6.24	1.47	2.98	1.20	14.65	19.03	42.87	0.77	35.87
LIS 19/4	183	8.01	0.17	4.31	6.61	1.60	4.77	1.38	14.90	19.49	40.66	0.76	29.57
LIS 19/5	213.5	8.07	0.37	3.93	9.09	1.31	2.59	1.32	26.80	21.42	36.94	1.25	28.09
LIS 19/6	222	8.23	0.47	2.67	8.72	1.13	1.72	0.70	32.10	21.74	28.11	1.48	40.15
LIS 19/7	240	8.72	0.32	1.12	17.43	1.02	3.13	1.02	64.50	23.26	24.11	2.77	23.75
LIS 19/8	256.5	8.82	0.21	1.12	12.86	0.78	0.95	0.78	46.80	22.60	22.03	2.07	28.24
LIS 19/9	275	8.2	0.43	2.70	12.07	1.04	1.37	1.30	45.25	22.49	29.65	2.01	22.89
LIS 19/10	285	8.45	0.32	1.87	14.36	0.99	1.37	2.00	51.50	23.00	27.55	2.24	13.81
LIS 19/11	322.5	8.86	0.18	0.97	16.66	0.81	1.20	1.56	56.50	23.04	22.86	2.45	14.70
LIS 19/12	335	8.91	0.28	0.63	17.92	0.69	0.84	0.71	62.00	23.36	23.67	2.65	33.33
LIS 19/13	346	8.09	0.54	3.20	10.38	1.43	2.03	1.12	34.00	21.57	33.98	1.58	30.47
LIS 19/14	358	8.76	0.19	0.78	17.72	0.76	0.76	0.80	65.00	23.37	24.98	2.78	31.42
LIS 19/15	382.5	8.82	0.17	1.64	7.51	0.87	1.16	1.40	40.35	23.50	25.49	1.72	18.27
LIS 19/16	427.5	8.92	0.12	1.50	11.11	0.80	0.80	0.93	56.50	23.39	25.51	2.42	27.42
LIS 19/17	482.5	8.88	0.11	1.49	14.55	0.87	1.17	0.86	66.00	23.31	26.35	2.83	30.82
LIS 19/18	550	9.02	0.17	1.49	10.71	0.75	1.19	0.83	50.00	23.52	22.54	2.13	27.16
LIS 19/19	575	8.45	0.58	1.43	13.14	0.74	1.40	1.13	56.50	23.43	21.64	2.41	19.24
LIS 19/20	622.5	8.74	0.28	1.23	12.85	0.91	1.96	1.85	50.00	23.52	22.18	2.13	11.99
LIS 19/21	647.5	8.92	0.33	1.09	16.46	0.68	0.81	0.78	67.50	23.54	19.87	2.87	25.47
LIS 19/22	755	8.65	0.39	1.46	15.00	0.62	1.31	2.25	57.00	23.38	22.81	2.44	10.16
LIS 19/23	790	8.48	0.88	1.11	14.26	0.49	0.61	0.94	59.00	22.92	17.63	2.57	18.86
LIS 19/24	835	8.45	0.63	1.12	13.85	0.57	1.11	1.47	62.00	23.66	19.69	2.62	13.44
LIS 19/25	858	8.44	1.85	1.92	16.56	1.05	1.57	1.55	59.00	22.77	22.83	2.59	14.73
LIS 19/26	885	8.32	2.00	2.66	13.29	1.04	1.62	1.96	1.86	25.00	25.02	0.07	12.76

Appendix 5.16.1: Geological profile and selected geochemical results of LIS 23.

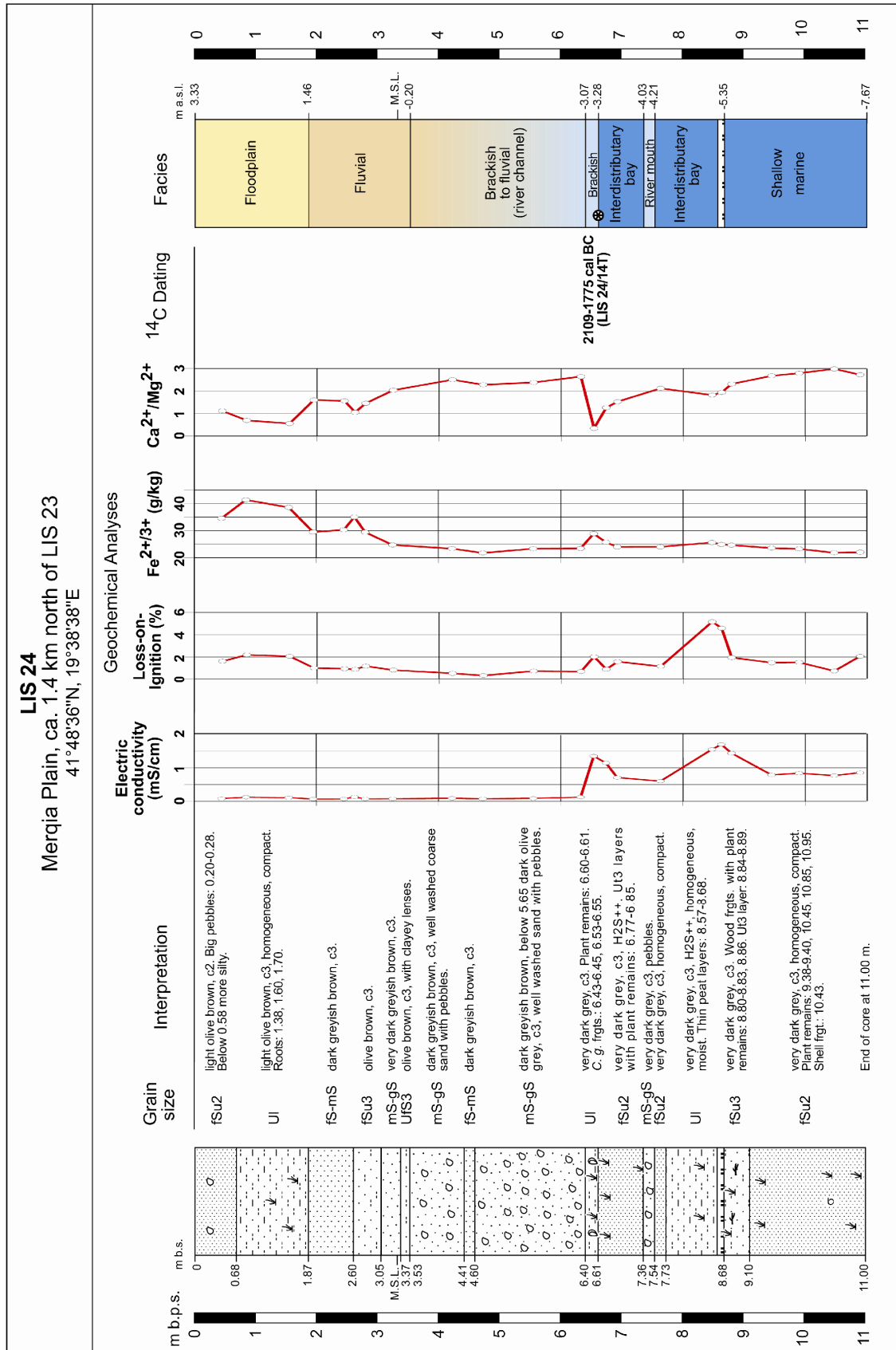


Appendix 5.16.2: Photo and geochemical results of LIS 23.

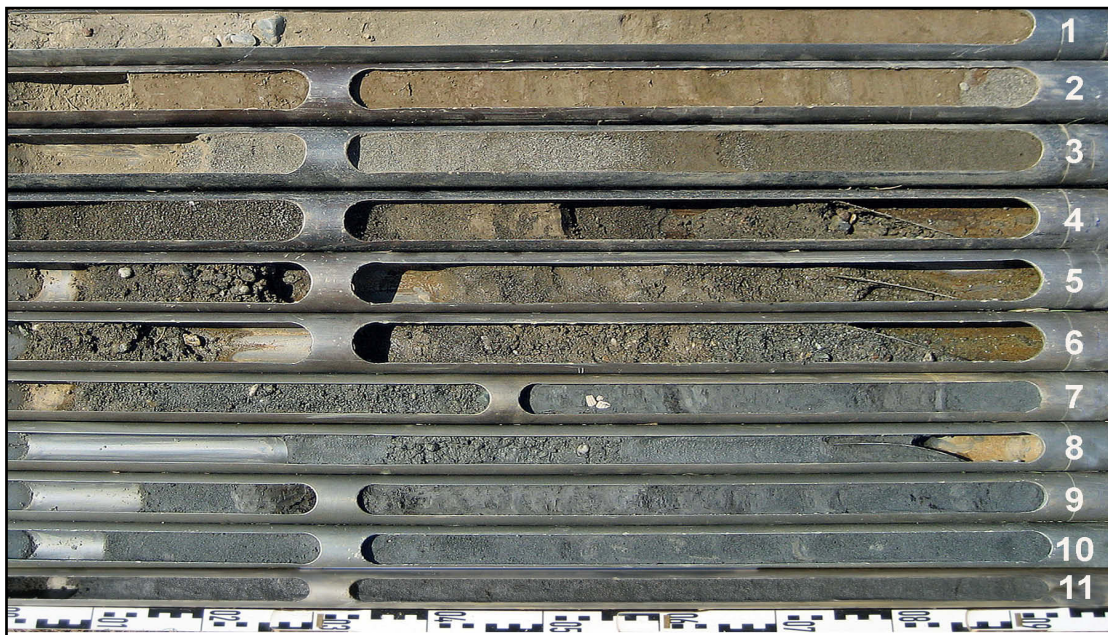


Sample - No.	Depth b.s. (cm)	pH (KCl) - value	conductivity (mS/cm)	Loss-on-Ignition (%)	Carbonate content (%)	Orthophosphate (g/kg)	c(K ⁺) (g/kg)	c(Na ⁺) (g/kg)	c(Ca ²⁺) (g/kg)	c(Mg ²⁺) (g/kg)	c(Fe ^{2+/3+}) (g/kg)	c(Ca ²⁺)/c(Mg ²⁺)	c(Fe ^{2+/3+})/c(Na ⁺)
LIS 23/1	45	7.62	0.24	3.49	5.60	1.51	1.58	1.86	20.73	20.62	36.70	1.01	19.78
LIS 23/2	85	7.66	0.08	2.24	6.13	1.10	1.18	1.87	20.95	23.74	37.27	0.88	19.98
LIS 23/3	155	7.83	0.08	1.78	7.25	1.13	0.80	2.07	25.67	21.77	33.83	1.18	16.38
LIS 23/4	185	7.78	0.10	2.26	7.41	1.42	2.53	1.77	23.65	20.49	39.06	1.15	22.06
LIS 23/5	245	7.72	0.11	3.44	10.04	1.50	2.65	1.89	33.42	21.01	41.91	1.59	22.17
LIS 23/6	285	7.74	0.11	3.54	11.57	1.30	1.67	2.05	33.47	21.88	41.96	1.53	20.52
LIS 23/8	340	7.73	0.14	3.34	8.68	1.71	2.88	2.13	22.28	20.29	41.96	1.10	19.70
LIS 23/9	375	7.68	0.15	3.37	5.70	1.77	2.84	1.93	11.82	20.49	44.77	0.58	23.26
LIS 23/10	395	7.75	0.16	4.30	5.43	1.57	3.66	2.05	12.92	20.53	40.31	0.63	19.66
LIS 23/11	460	7.24	0.23	4.87	0.00	1.87	2.29	2.34	1.36	19.18	35.26	0.07	15.07
LIS 23/12	482.5	7.71	0.16	2.68	15.29	2.11	1.97	4.69	40.82	21.24	41.58	1.92	8.87
LIS 23/13	492.5	7.78	0.16	1.54	20.16	1.36	1.37	0.89	66.30	22.63	31.81	2.93	35.94
LIS 23/14	524	7.95	0.09	1.86	14.47	1.30	0.97	0.69	48.85	22.05	30.41	2.22	44.39
LIS 23/15	539	8.06	0.09	1.74	14.20	1.14	1.17	0.93	47.39	22.54	28.55	2.10	30.69
LIS 23/16	547	7.82	0.77	3.52	12.42	1.08	1.30	1.00	46.03	21.01	26.62	2.19	26.62
LIS 23/19	625	7.73	0.95	3.33	18.66	1.30	1.20	1.38	61.60	20.96	27.01	2.94	19.64
LIS 23/20	642.5	7.73	0.81	4.69	10.38	1.10	1.85	1.63	33.58	22.37	30.33	1.50	18.61
LIS 23/21	677.5	7.32	2.13	5.78	1.18	0.71	2.74	1.16	3.10	22.26	30.49	0.14	26.40
LIS 23/22	732.5	7.45	1.80	4.38	3.92	0.82	3.25	1.30	11.07	21.01	28.03	0.53	21.56
LIS 23/23	767.5	7.55	1.57	4.16	7.55	1.04	2.51	1.47	25.44	20.19	24.47	1.26	16.65
LIS 23/24	838.5	7.83	1.34	3.91	10.23	0.88	1.48	1.60	36.21	22.59	24.17	1.60	15.10
LIS 23/25	865	7.75	1.63	4.25	13.57	1.01	1.51	1.82	48.46	21.64	24.37	2.24	13.42
LIS 23/26	877.5	7.72	1.61	3.22	13.72	0.88	1.39	1.98	44.45	22.37	24.00	1.99	12.15
LIS 23/27	920	7.72	1.71	3.80	12.45	0.89	1.15	2.24	46.03	21.57	24.95	2.13	11.14
LIS 23/28	935	7.61	1.86	3.97	12.46	0.72	1.31	1.77	47.59	21.75	23.70	2.19	13.39
LIS 23/29	985	7.86	1.77	3.86	15.43	0.98	1.74	2.17	53.30	23.20	25.03	2.30	11.56
LIS 23/30	1053	8.09	1.30	1.43	19.12	0.50	0.63	1.76	73.65	25.19	21.85	2.92	12.41
LIS 23/31	1093	8.21	1.30	1.05	17.99	0.44	0.63	2.01	61.80	24.76	22.24	2.50	11.09
LIS 23/32	1143	8.22	1.22	2.35	21.05	0.62	0.76	1.54	69.15	24.96	21.91	2.77	14.22
LIS 23/33	1193	8.25	1.82	2.80	16.02	0.66	1.22	2.47	60.05	25.69	26.05	2.34	10.57

Appendix 5.17.1: Geological profile and selected geochemical results of LIS 24.



Appendix 5.17.2: Photo and geochemical results of LIS 24.



Sample - No.	Depth b.s. (cm)	pH (KCl) - value	Electric conductivity (mS/cm)	Loss-on-Ignition (%)	Carbonate content (%)	Orthophosphate (g/kg)	c(K ⁺) (g/kg)	c(Na ⁺) (g/kg)	c(Ca ²⁺) (g/kg)	c(Mg ²⁺) (g/kg)	c(Fe ^{2+/3+}) (g/kg)	c(Ca ²⁺)/c(Mg ²⁺)	c(Fe ^{2+/3+})/c(Na ⁺)
LIS 24/1	45	7.82	0.08	1.63	6.38	0.92	1.61	0.68	23.88	21.39	34.53	1.12	50.78
LIS 24/2	85	7.66	0.12	2.20	4.54	1.22	2.97	0.65	14.79	21.22	41.35	0.70	64.11
LIS 24/3	155	7.67	0.11	2.08	3.42	1.44	3.05	0.59	10.91	19.62	38.57	0.56	65.93
LIS 24/4	195	7.91	0.07	1.02	8.97	0.53	0.85	0.55	36.06	22.49	29.46	1.60	54.06
LIS 24/5	245	7.87	0.07	0.96	7.40	0.61	0.75	1.18	34.15	21.84	30.28	1.56	25.66
LIS 24/6	262.5	7.72	0.13	0.90	7.08	1.20	1.46	0.82	23.20	22.01	35.03	1.05	42.71
LIS 24/7	280	7.84	0.07	1.19	8.01	0.67	1.12	0.99	31.97	21.95	29.40	1.46	29.85
LIS 24/8	325	8.02	0.07	0.84	11.64	0.43	0.62	0.89	46.44	22.82	24.69	2.04	27.90
LIS 24/9	422	8.24	0.09	0.54	15.58	0.43	0.63	1.14	55.75	22.26	23.37	2.50	20.59
LIS 24/10	472.5	8.28	0.07	0.34	15.61	0.59	0.68	1.34	53.75	23.59	21.75	2.28	16.23
LIS 24/11	555	8.22	0.09	0.74	13.65	0.57	1.12	1.90	56.25	23.64	23.33	2.38	12.28
LIS 24/13	632.5	8.24	0.12	0.71	17.68	0.53	0.54	0.84	63.40	23.99	23.42	2.64	27.88
LIS 24/14	654	7.52	1.36	2.04	3.18	0.64	2.93	1.58	7.33	21.48	28.87	0.34	18.27
LIS 24/15	674	7.55	1.15	0.91	8.30	0.95	1.79	1.30	26.59	21.12	25.71	1.26	19.85
LIS 24/17	692.5	7.76	0.71	1.60	9.70	0.63	1.43	0.94	30.92	20.23	23.98	1.53	25.51
LIS 24/19	763	8.04	0.60	1.17	12.79	0.48	1.06	0.85	49.11	23.17	23.98	2.12	28.38
LIS 24/21	847.5	7.52	1.55	5.17	11.03	1.03	2.16	0.99	40.98	22.53	25.61	1.82	25.86
LIS 24/22	863	7.5	1.70	4.58	12.41	1.05	2.12	1.39	42.99	22.19	24.91	1.94	17.99
LIS 24/23	879.5	7.54	1.44	1.95	13.51	0.90	2.03	1.33	53.30	23.05	24.64	2.31	18.60
LIS 24/24	945	7.88	0.79	1.49	17.64	0.84	1.34	0.90	65.35	24.39	23.55	2.68	26.31
LIS 24/25	990	8.05	0.84	1.53	19.09	0.75	1.42	1.02	68.80	24.64	23.24	2.79	22.78
LIS 24/26	1048	8.16	0.77	0.75	19.27	0.57	0.73	1.02	73.40	24.61	21.82	2.98	21.49
LIS 24/27	1090	8.08	0.86	2.08	12.36	0.77	0.99	0.97	66.75	24.51	22.01	2.72	22.81

Appendix 5.18: Geochemical results of LIS 25.

Sample - No.	Depth b.s. (cm)	pH (KCl) - value	Electric conductivity (mS/cm)	Loss-on-Ignition (%)	Carbonate content (%)	Orthophosphate (g/kg)	c(K ⁺) (g/kg)	c(Na ⁺) (g/kg)	c(Ca ²⁺) (g/kg)	c(Mg ²⁺) (g/kg)	c(Fe ^{2+/3+}) (g/kg)	c(Ca ²⁺)/c(Mg ²⁺)	c(Fe ^{2+/3+})/c(Na ⁺)
LIS 25/1	55	7.95	0.21	2.71	8.83	1.49	4.05	2.12	32.94	21.43	38.67	1.54	18.24
LIS 25/2	95	7.83	0.18	2.02	9.11	1.61	3.04	1.22	31.13	21.22	36.32	1.47	29.89
LIS 25/3	165	7.88	0.11	1.14	8.48	1.27	2.18	3.29	29.64	22.92	34.47	1.29	10.48
LIS 25/4	255	7.82	0.47	3.57	7.27	2.31	3.03	0.99	20.92	21.57	43.04	0.97	43.69
LIS 25/5	267	7.61	0.41	4.06	3.81	1.82	3.96	1.15	9.48	20.85	43.64	0.45	37.95
LIS 25/6	297.5	7.62	0.59	4.40	7.81	2.43	3.28	0.64	15.08	22.43	50.60	0.67	79.06
LIS 25/7	335	7.85	0.28	3.65	11.99	2.22	2.55	0.90	31.05	20.21	41.97	1.54	46.63
LIS 25/8	397.5	7.73	0.87	4.27	20.03	1.50	2.49	1.25	65.85	20.96	30.93	3.14	24.84
LIS 25/9	425	7.57	0.89	5.14	15.05	1.45	2.13	0.96	48.90	21.94	32.11	2.23	33.62
LIS 25/10	445	7.54	0.85	4.05	16.15	1.47	1.47	1.42	52.40	21.49	29.76	2.44	20.96
LIS 25/11	473.5	7.69	0.82	3.18	28.47	1.94	2.20	0.56	60.40	23.05	31.15	2.62	56.12
LIS 25/12	488	7.62	0.68	4.42	18.18	1.47	1.90	0.68	91.00	24.57	32.66	3.70	48.03
LIS 25/13	545	7.4	1.24	4.42	2.06	0.82	4.62	1.19	4.69	21.31	30.12	0.22	25.41
LIS 25/14	565	7.37	0.97	3.77	5.66	0.96	2.60	0.94	18.67	20.48	25.11	0.91	26.85
LIS 25/15	637.5	7.43	0.91	4.46	6.54	1.06	4.05	1.02	17.39	18.94	27.07	0.92	26.54
LIS 25/17	692.5	7.57	0.61	4.59	17.79	1.48	2.61	0.78	59.65	22.78	30.94	2.62	39.92
LIS 25/19	767.5	7.75	1.01	5.10	4.32	1.37	4.59	1.14	29.72	20.18	29.87	1.47	26.20
LIS 25/20	866.5	7.93	1.30	4.43	11.10	1.27	6.57	4.32	31.54	20.05	28.49	1.57	6.60
LIS 25/21	960	8.26	0.93	0.91	16.84	0.78	1.26	1.56	73.20	25.50	20.44	2.87	13.14
LIS 25/22	985	8.08	1.96	3.73	15.07	0.98	1.67	2.22	55.05	24.27	25.48	2.27	11.50
LIS 25/23	1047	7.87	2.25	3.62	14.34	0.96	1.71	2.22	49.41	24.89	27.64	1.99	12.45
LIS 25/24	1078	8.06	2.39	3.07	14.77	1.09	2.07	2.52	49.44	22.79	26.38	2.17	10.47
LIS 25/25	1175	8.06	3.73	4.75	16.12	1.38	2.62	4.18	56.35	23.08	25.35	2.44	6.07
LIS 25/26	1233	8.02	3.88	5.88	16.07	1.38	2.85	8.72	55.05	22.66	25.89	2.43	2.97
LIS 25/27	1290	7.87	2.72	5.42	13.30	1.25	3.04	2.94	44.90	23.18	28.28	1.94	9.62

Appendix 5.19: Geochemical results of LIS 26.

Sample - No.	Depth b.s. (cm)	pH (KCl) - value	Electric conductivity (mS/cm)	Loss-on-Ignition (%)	Carbonate content (%)	Orthophosphate (g/kg)	c(K ⁺) (g/kg)	c(Na ⁺) (g/kg)	c(Ca ²⁺) (g/kg)	c(Mg ²⁺) (g/kg)	c(Fe ^{2+/3+}) (g/kg)	c(Ca ²⁺)/c(Mg ²⁺)	c(Fe ^{2+/3+})/c(Na ⁺)
LIS 26/1	72.5	7.46	1.11	4.08	7.92	1.51	2.77	1.13	20.81	20.77	42.25	1.00	37.38
LIS 26/2	92.5	7.52	2.01	3.23	7.77	1.36	2.76	1.75	21.17	20.83	39.81	1.02	22.75
LIS 26/3	182.5	7.59	1.00	4.80	8.24	1.45	3.10	1.51	21.56	20.68	42.04	1.04	27.84
LIS 26/5	272.5	7.68	0.50	5.27	2.68	1.63	3.49	1.75	4.85	21.61	46.20	0.22	26.47
LIS 26/9	377.5	7.73	1.16	4.21	13.08	1.25	2.09	1.75	40.52	21.24	30.47	1.91	17.46
LIS 26/10	472.5	7.73	0.99	2.76	13.91	1.52	2.50	1.81	42.97	22.11	30.77	1.94	17.00
LIS 26/11	515	7.67	1.52	4.94	8.85	0.99	3.31	2.78	21.93	21.93	33.03	1.00	11.90
LIS 26/12	577.5	7.68	1.55	4.32	6.13	0.85	3.75	2.65	13.98	22.56	32.27	0.62	12.20
LIS 26/14	670	7.89	1.54	3.70	10.83	1.11	4.83	2.71	23.54	18.48	36.06	1.27	13.33
LIS 26/16	722.5	8.14	1.25	1.26	13.85	0.77	2.40	2.14	44.35	24.25	26.42	1.83	12.35
LIS 26/17	757	8.01	1.70	2.64	13.65	0.79	2.31	2.52	46.24	24.65	26.71	1.88	10.62
LIS 26/18	776	7.72	2.15	2.61	12.46	0.83	2.44	1.77	45.87	25.50	28.14	1.80	15.90
LIS 26/19	845	7.72	1.83	1.81	17.60	0.73	1.55	1.39	67.60	25.12	23.84	2.69	17.15
LIS 26/20	877.5	7.95	1.29	0.64	20.38	0.70	1.49	1.35	68.80	25.18	22.14	2.73	16.46
LIS 26/22	950	7.98	1.64	1.90	19.52	0.59	2.09	1.95	75.10	25.86	21.99	2.90	11.31
LIS 26/23	990	8.02	1.50	1.84	23.17	0.65	1.23	1.40	79.30	25.63	21.57	3.09	15.41

Appendix 5.20: Geochemical results of LIS 27.

Sample - No.	Depth b.s. (cm)	pH (KCl) - value	Electric conductivity (mS/cm)	Loss-on-Ignition (%)	Carbonate content (%)	Orthophosphate (g/kg)	c(K ⁺) (g/kg)	c(Na ⁺) (g/kg)	c(Ca ²⁺) (g/kg)	c(Mg ²⁺) (g/kg)	c(Fe ^{2+/3+}) (g/kg)	c(Ca ²⁺)/c(Mg ²⁺)	c(Fe ^{2+/3+})/c(Na ⁺)
LIS 27/1	75	7.58	0.14	2.46	0.00	0.75	4.22	0.48	2.95	12.97	31.66	0.23	65.95
LIS 27/2	155	6.96	0.09	3.69	0.00	1.30	5.09	0.55	0.97	14.67	40.24	0.07	73.83
LIS 27/3	185	6.79	0.08	3.85	0.00	1.14	4.70	0.51	0.88	14.28	38.86	0.06	76.95
LIS 27/4	250	6.27	0.15	6.12	0.00	1.66	5.73	0.59	0.77	13.94	39.24	0.06	66.51
LIS 27/5	264	6.28	0.14	4.81	0.00	1.66	5.00	0.96	0.67	12.56	36.55	0.05	38.07
LIS 27/6	290	6.85	0.09	3.10	0.00	1.16	4.80	0.91	0.77	11.84	31.63	0.06	34.94
LIS 27/7	355	6.83	0.08	2.73	0.00	1.09	3.77	1.75	0.63	12.01	34.09	0.05	19.48
LIS 27/8	375	6.44	0.07	3.65	0.00	0.93	4.91	0.67	1.01	12.76	39.57	0.08	59.05
LIS 27/9	475	6.16	0.06	3.63	0.00	1.39	5.07	0.61	1.01	13.06	38.42	0.08	62.98
LIS 27/10	565	5.84	0.09	3.51	0.00	1.69	6.24	0.64	0.66	13.65	40.25	0.05	62.89
LIS 27/11	670	6.03	0.11	4.02	0.00	1.10	6.17	0.73	0.79	13.22	41.75	0.06	57.59
LIS 27/12	735	5.86	0.10	3.36	0.00	1.15	5.65	0.89	0.50	11.24	38.66	0.04	43.68
LIS 27/13	762.5	5.87	0.09	2.88	0.00	1.10	4.74	0.73	0.43	11.20	38.67	0.04	53.34
LIS 27/14	778.5	5.9	0.10	2.24	0.00	0.76	5.21	0.63	0.39	11.02	34.57	0.04	55.31
LIS 27/15	861	6.18	0.07	2.52	0.00	1.29	4.75	0.46	0.59	12.25	39.05	0.05	84.88
LIS 27/16	877.5	6.32	0.07	2.75	0.00	0.96	4.42	0.92	0.51	11.64	31.12	0.04	34.01
LIS 27/18	960	6.04	0.08	4.98	0.00	1.20	3.32	0.51	0.82	10.19	28.76	0.08	56.94
LIS 27/19	981	6.05	0.07	3.82	0.00	1.19	5.34	1.10	0.65	11.57	31.56	0.06	28.82
LIS 27/20	1045	6	0.06	3.18	0.00	1.11	4.33	0.78	0.83	12.12	35.78	0.07	45.87
LIS 27/21	1090	6.06	0.07	2.57	0.00	1.06	2.72	0.57	0.93	22.12	34.98	0.04	61.90

Appendix 5.21: Geochemical results of LIS 28.

Sample - No.	Depth b.s. (cm)	pH (KCl) - value	Electric conductivity (mS/cm)	Loss-on-Ignition (%)	Carbonate content (%)	Orthophosphate (g/kg)	c(K ⁺) (g/kg)	c(Na ⁺) (g/kg)	c(Ca ²⁺) (g/kg)	c(Mg ²⁺) (g/kg)	c(Fe ^{2+/3+}) (g/kg)	c(Ca ²⁺)/c(Mg ²⁺)	c(Fe ^{2+/3+})/c(Na ⁺)
LIS 28/3	180.5	7.04	0.23	2.75	9.16	6.64	5.23	1.54	29.93	18.58	31.15	1.61	20.23
LIS 28/4	219	7.18	0.21	2.09	10.10	4.34	4.30	1.45	27.76	19.04	34.52	1.46	23.81
LIS 28/5	242.5	7.66	0.18	1.64	31.50	1.60	1.28	0.89	129.95	16.11	19.70	8.07	22.13
LIS 28/6	267.5	7.59	0.18	1.66	36.05	1.71	1.26	1.12	148.70	20.49	18.52	7.26	16.54
LIS 28/13	464.5	7.5	0.32	1.27	14.12	0.92	0.48	1.17	51.65	28.02	26.73	1.84	22.85
LIS 28/15	492.5	7.2	0.46	0.73	18.83	1.03	0.61	1.26	58.90	28.09	27.66	2.10	22.04
LIS 28/16	564	7.51	0.52	1.67	17.40	0.85	0.70	1.28	61.35	28.93	33.57	2.12	26.33
LIS 28/17	574	7.52	0.75	2.07	13.36	0.57	0.56	1.25	44.85	28.43	32.09	1.58	25.78
LIS 28/18	587.5	7.06	2.34	4.38	13.18	0.65	0.96	1.35	23.14	26.92	22.72	0.86	16.89
LIS 28/20	647.5	7.25	1.52	5.90	9.25	0.95	2.24	1.69	18.09	26.12	23.97	0.69	14.23
LIS 28/21	665	7.31	1.58	8.10	8.87	0.86	2.27	1.39	26.60	26.25	25.74	1.01	18.58
LIS 28/22	689	7.36	1.61	6.51	9.71	0.83	1.74	1.12	11.19	27.71	26.70	0.40	23.94
LIS 28/24	760	7.19	2.32	6.41	8.12	0.82	1.78	1.80	6.04	28.25	27.07	0.21	15.08
LIS 28/26	792.5	7.29	1.56	1.05	8.40	0.35	0.38	0.96	4.78	30.10	35.00	0.16	36.64
LIS 28/27	875	7.29	1.55	1.69	16.61	0.26	0.37	1.42	7.42	29.93	32.48	0.25	22.87

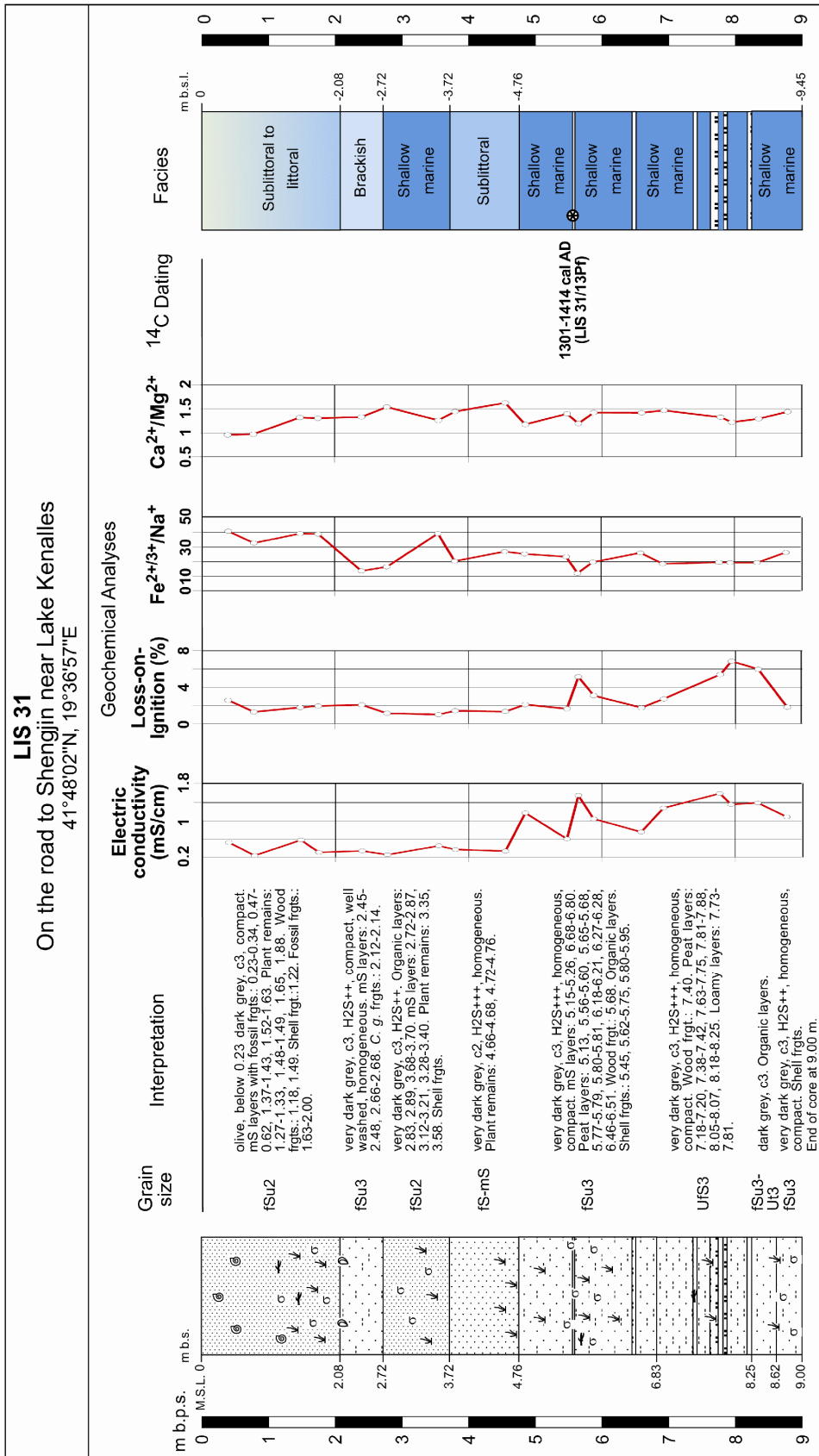
Appendix 5.22: Geochemical results of LIS 29.

Sample - No.	Depth b.s. (cm)	pH (KCl) - value	Electric conductivity (mS/cm)	Loss-on-Ignition (%)	Carbonate content (%)	Orthophosphate (g/kg)	c(K ⁺) (g/kg)	c(Na ⁺) (g/kg)	c(Ca ²⁺) (g/kg)	c(Mg ²⁺) (g/kg)	c(Fe ^{2+/3+}) (g/kg)	c(Ca ²⁺)/c(Mg ²⁺)	c(Fe ^{2+/3+})/c(Na ⁺)
LIS 29/1	55	7.44	0.22	3.45	11.85	7.61	2.53	0.93	47.65	20.59	33.01	2.31	35.49
LIS 29/2	77.5	7.44	0.15	1.68	9.39	4.33	1.60	0.81	33.41	19.46	31.88	1.72	39.60
LIS 29/3	95	7.51	0.13	1.65	10.78	2.74	0.87	2.44	26.86	18.53	29.86	1.45	12.26
LIS 29/4	122.5	7.51	0.15	1.98	7.08	3.68	1.68	2.16	29.93	20.68	33.00	1.45	15.31
LIS 29/6	175	7.32	0.17	2.22	8.61	7.63	4.18	1.13	32.86	17.79	29.57	1.85	26.16
LIS 29/8	251	7.25	0.20	4.52	5.43	4.55	3.70	1.02	23.79	17.40	25.85	1.37	25.34
LIS 29/9	266.5	7.45	0.10	1.29	7.27	2.08	1.15	1.06	26.28	21.93	21.99	1.20	20.74
LIS 29/12	357.5	7.47	0.12	1.20	8.35	1.55	0.87	0.75	32.02	22.60	23.17	1.42	30.89
LIS 29/13	370.5	7.51	0.14	1.11	9.60	3.46	1.05	0.99	36.22	22.16	29.54	1.63	29.83
LIS 29/15	395.5	7.38	0.17	1.28	7.54	1.95	1.58	0.62	33.16	23.79	26.80	1.39	43.57
LIS 29/16	480	7.56	0.20	1.79	6.70	1.77	1.61	3.23	36.90	22.27	24.66	1.66	7.63
LIS 29/23	593.5	7.22	1.49	6.58	8.67	1.00	2.08	0.76	31.46	20.96	21.41	1.50	28.16
LIS 29/24	641	7.36	1.36	3.29	11.29	0.84	1.53	1.56	39.74	22.68	19.65	1.75	12.63
LIS 29/28	674	7.5	0.68	1.83	13.98	0.76	2.45	1.24	48.88	25.13	23.24	1.94	18.82
LIS 29/29	737	7.51	0.68	5.31	12.38	1.21	2.78	0.97	38.69	21.11	29.92	1.83	31.00
LIS 29/31	865.5	7.2	2.20	8.66	7.08	0.95	2.33	0.99	33.28	25.05	25.28	1.33	25.53
LIS 29/32	881.5	7.21	2.16	9.57	8.85	0.99	2.67	1.53	28.42	25.14	25.97	1.13	17.03
LIS 29/34	993.5	7.46	1.49	3.66	11.73	1.17	3.20	0.88	36.58	25.08	28.90	1.46	33.03
LIS 29/35	1050	7.57	1.35	1.67	11.01	0.68	0.93	0.78	45.23	28.52	28.50	1.59	36.77
LIS 29/36	1070	7.94	0.63	1.61	8.13	0.54	0.83	0.97	34.00	28.52	31.44	1.19	32.41
LIS 29/37	1090	8.01	0.27	1.29	8.58	0.51	0.76	1.02	39.12	28.55	33.91	1.37	33.25

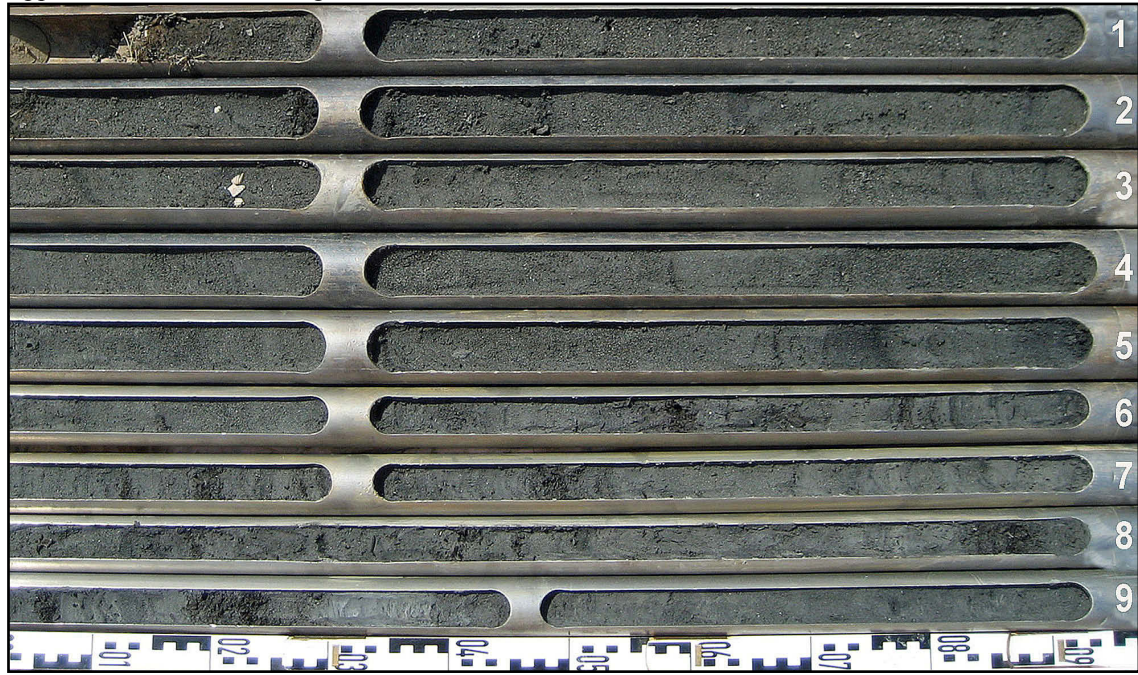
Appendix 5.23: Geochemical results of LIS 30.

Sample - No.	Depth b.s. (cm)	pH (KCl) - value	Electric conductivity (mS/cm)	Loss-on-Ignition (%)	Carbonate content (%)	Orthophosphate (g/kg)	c(K ⁺) (g/kg)	c(Na ⁺) (g/kg)	c(Ca ²⁺) (g/kg)	c(Mg ²⁺) (g/kg)	c(Fe ^{2+/3+}) (g/kg)	c(Ca ²⁺)/c(Mg ²⁺)	c(Ca ²⁺)/c(Fe ^{2+/3+})	c(Fe ^{2+/3+})/c(Na ⁺)
LIS 30/1	75	8.04	0.12	0.95	7.85	0.91	0.26	0.14	5.11	4.48	5.70	1.14	0.90	41.33
LIS 30/2	175	8.04	0.16	1.74	7.74	0.86	0.23	0.13	4.79	4.60	5.79	1.04	0.83	45.27
LIS 30/3	185	8.04	0.18	1.89	6.90	0.77	0.21	0.13	3.98	4.80	6.08	0.83	0.65	46.06
LIS 30/4	255	8.06	0.20	1.45	9.29	0.90	0.20	0.18	5.23	4.52	5.49	1.16	0.95	30.84
LIS 30/6	290	8.06	0.21	1.06	8.63	0.96	0.20	0.12	5.25	4.50	5.62	1.17	0.94	46.80
LIS 30/7	337.5	7.72	0.82	3.39	9.72	0.97	0.25	0.19	5.71	4.71	6.05	1.21	0.94	31.65
LIS 30/9	365	8.11	0.27	1.35	12.43	0.87	0.16	0.14	7.93	4.60	5.20	1.72	1.53	36.87
LIS 30/10	380	8.16	0.20	0.99	10.48	1.26	0.16	0.13	6.52	4.30	5.48	1.52	1.19	41.79
LIS 30/12	462.5	8.01	0.55	1.20	11.95	0.87	0.19	0.14	6.54	4.54	5.17	1.44	1.27	36.63
LIS 30/14	495	7.81	0.73	1.21	15.21	0.26	0.10	0.18	11.28	5.05	4.08	2.23	2.76	22.55
LIS 30/16	547.5	7.76	1.35	2.35	11.22	0.38	0.20	0.21	7.72	4.83	4.74	1.60	1.63	22.81
LIS 30/17	590	7.78	1.40	1.58	16.83	0.53	0.14	0.19	10.82	4.63	3.79	2.34	2.85	19.64
LIS 30/18	667.5	7.83	1.41	1.02	16.33	0.34	0.13	0.23	10.39	4.98	4.12	2.09	2.52	18.13
LIS 30/19	692.5	7.78	2.10	2.53	11.00	0.50	0.23	0.27	6.42	4.87	4.62	1.32	1.39	17.12
LIS 30/20	757.5	7.89	2.02	2.24	10.53	0.36	0.20	0.51	6.97	4.81	4.76	1.45	1.47	9.42
LIS 30/21	792.5	7.78	2.02	2.47	11.54	0.90	0.31	0.31	7.19	4.22	4.76	1.70	1.51	15.41
LIS 30/22	857.5	7.81	1.94	1.44	10.39	0.76	0.25	0.29	6.56	4.47	5.20	1.47	1.26	17.70
LIS 30/23	870	7.73	2.65	4.10	10.66	1.07	0.49	0.46	6.31	3.82	5.69	1.65	1.11	12.47

Appendix 5.24.1: Geological profile and selected geochemical results of LIS 31.

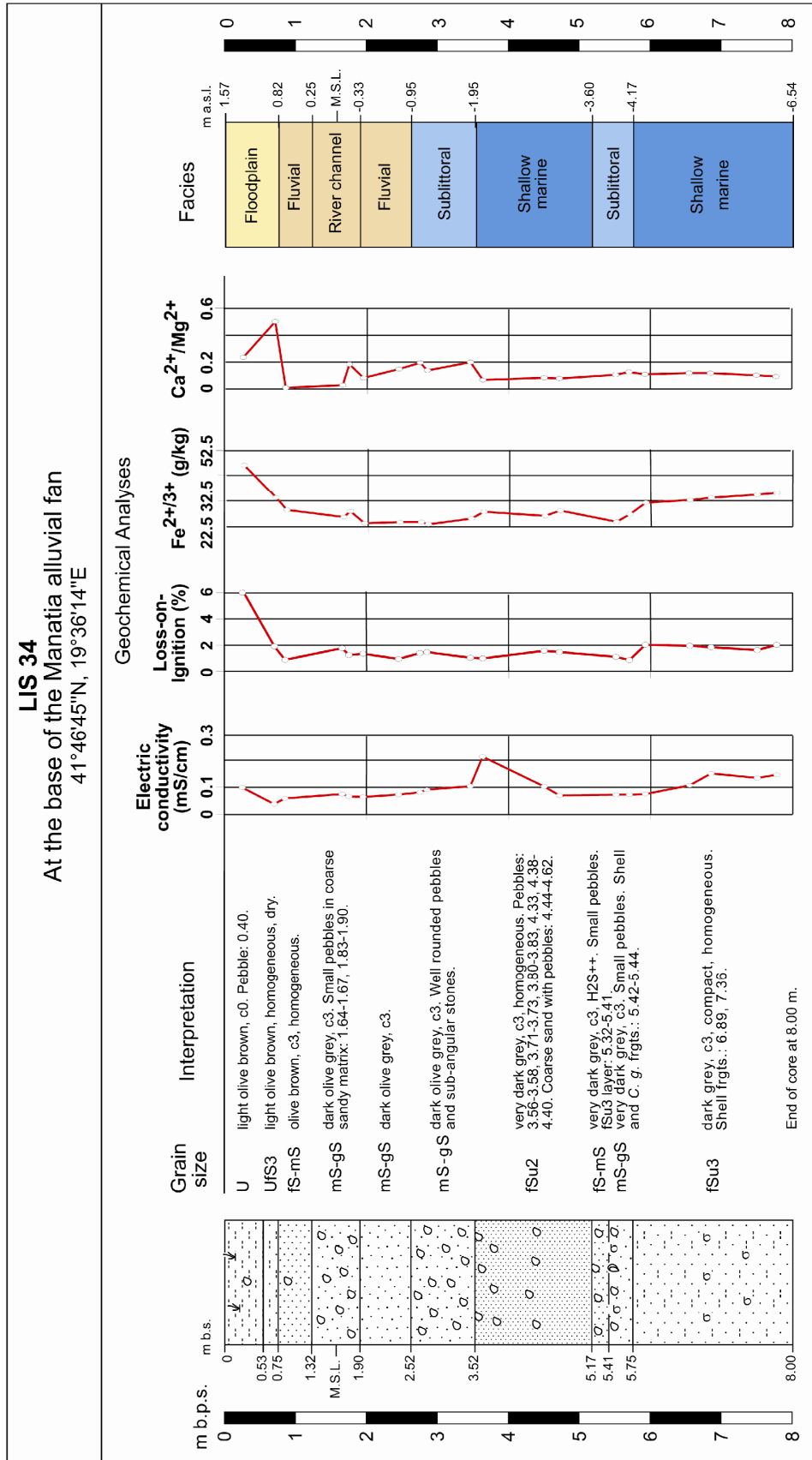


Appendix 5.24.2: Photo and geochemical results of LIS 31.

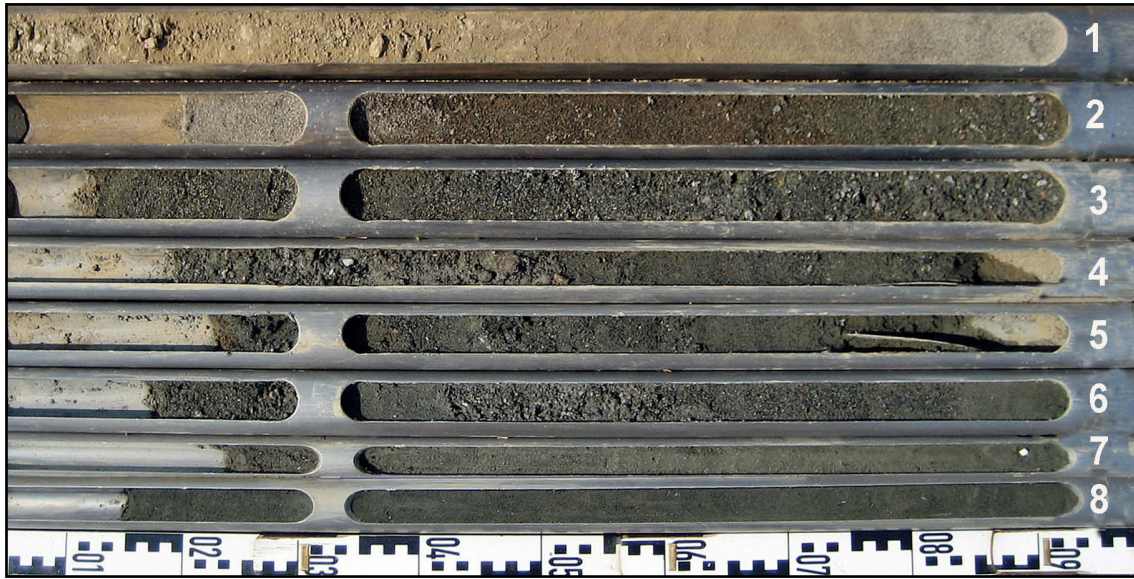


Sample - No.	Depth b.s. (cm)	pH (KCl) - value	Electric conductivity (mS/cm)	Loss-on-Ignition (%)	Carbonate content (%)	Orthophosphate (g/kg)	c(K ⁺) (g/kg)	c(Na ⁺) (g/kg)	c(Ca ²⁺) (g/kg)	c(Mg ²⁺) (g/kg)	c(Fe ^{2+/3+}) (g/kg)	c(Ca ²⁺)/c(Mg ²⁺)	c(Fe ^{2+/3+})/c(Na ⁺)
LIS 31/1	40	7.54	0.52	2.56	6.28	0.64	1.08	0.71	21.87	22.85	29.01	0.96	40.85
LIS 31/2	78.5	7.76	0.23	1.28	6.78	0.57	0.96	0.84	21.54	22.15	27.38	0.97	32.78
LIS 31/4	148	7.61	0.58	1.77	8.33	0.31	0.90	0.72	27.89	21.12	28.31	1.32	39.32
LIS 31/6	175	8.02	0.31	1.93	3.72	0.55	1.30	0.76	27.35	20.99	29.63	1.30	38.98
LIS 31/7	240	8.1	0.34	2.04	4.82	0.52	1.33	2.07	27.43	20.58	28.29	1.33	13.67
LIS 31/8	278	8.14	0.25	1.13	6.93	0.48	0.72	1.35	30.99	20.13	22.15	1.54	16.46
LIS 31/9	355	8.03	0.45	0.98	6.37	0.63	1.28	0.68	25.21	20.01	26.72	1.26	39.29
LIS 31/10	380	8.12	0.37	1.42	7.10	0.60	1.28	1.20	30.38	21.02	24.45	1.45	20.38
LIS 31/11	455	8.2	0.33	1.32	8.79	0.70	1.21	0.92	33.87	20.82	24.75	1.63	26.90
LIS 31/12	485	7.82	1.17	2.08	6.60	0.77	1.36	1.06	24.51	20.87	26.65	1.17	25.26
LIS 31/14	547.5	8.02	0.60	1.62	6.37	0.45	0.90	1.10	28.31	20.25	25.63	1.40	23.40
LIS 31/16	564.5	7.69	1.56	5.14	4.97	0.76	1.18	2.24	23.73	19.88	26.95	1.19	12.06
LIS 31/19	587.5	7.88	1.04	3.08	7.20	0.93	1.39	1.37	27.92	19.59	27.01	1.42	19.72
LIS 31/23	659	8.02	0.75	1.73	7.50	0.88	1.31	1.11	29.30	20.63	28.77	1.42	26.03
LIS 31/24	692.5	7.82	1.28	2.71	9.47	1.11	1.66	1.56	28.12	19.13	29.02	1.47	18.60
LIS 31/26	777	7.73	1.60	5.38	8.61	1.04	1.79	1.52	25.45	19.17	29.56	1.33	19.51
LIS 31/28	794	7.77	1.36	6.85	9.02	0.96	1.68	1.62	24.38	19.96	31.30	1.22	19.32
LIS 31/30	834	7.7	1.40	5.96	10.07	1.07	2.69	1.87	22.15	17.13	36.11	1.29	19.36
LIS 31/31	877.5	7.92	1.09	1.79	8.23	0.87	1.37	1.13	30.13	20.89	29.60	1.44	26.31

Appendix 5.25.1: Geological profile and selected geochemical results of LIS 34.



Appendix 5.24.2: Photo and geochemical results of LIS 34.



Sample - No.	Depth b.s. (cm)	pH (KCl) - value	Electric conductivity (mS/cm)	Loss-on-Ignition (%)	Carbonate content (%)	Orthophosphate (g/kg)	c(K ⁺) (g/kg)	c(Na ⁺) (g/kg)	c(Ca ²⁺) (g/kg)	c(Mg ²⁺) (g/kg)	c(Fe ^{2+/3+}) (g/kg)	c(Ca ²⁺)/c(Mg ²⁺)	c(Fe ^{2+/3+})/c(Na ⁺)
LIS 34/1	25	7.15	0.10	6.21	0.00	0.84	5.24	0.91	4.18	17.72	46.36	0.24	50.95
LIS 34/2	70	7.11	0.04	1.91	0.00	0.13	1.39	1.87	12.51	24.90	33.80	0.50	18.12
LIS 34/3	85	7.46	0.06	0.88	4.91	0.01	0.49	0.99	0.22	25.93	29.05	0.01	29.34
LIS 34/4	165.5	7.7	0.08	1.77	2.31	0.03	0.51	1.48	0.76	26.71	26.31	0.03	17.83
LIS 34/5	175	7.93	0.07	1.24	5.78	0.01	0.38	1.78	4.70	25.42	28.48	0.18	16.05
LIS 34/6	195	7.93	0.06	1.35	2.65	0.09	0.65	1.32	2.18	26.68	23.89	0.08	18.17
LIS 34/7	245	8.05	0.07	0.95	4.90	0.25	0.49	1.70	3.88	26.17	24.33	0.15	14.35
LIS 34/8	275	8.05	0.08	1.39	4.98	0.04	0.53	1.36	4.83	24.70	24.34	0.20	17.90
LIS 34/9	285	8.05	0.09	1.47	5.30	0.17	0.51	1.55	3.55	25.70	23.47	0.14	15.14
LIS 34/10	346	8.16	0.10	1.03	6.29	0.24	0.50	1.60	4.79	23.98	25.68	0.20	16.10
LIS 34/11	363.5	7.65	0.21	0.99	5.65	0.00	1.00	1.03	1.79	26.81	28.30	0.07	27.60
LIS 34/12	450	7.6	0.10	1.58	4.33	0.14	0.83	1.34	2.21	26.50	26.74	0.08	20.03
LIS 34/13	471.5	7.74	0.07	1.48	6.17	0.22	0.95	1.21	2.08	26.72	28.77	0.08	23.88
LIS 34/14	551	7.69	0.07	1.11	4.15	0.12	0.57	1.34	2.69	25.55	24.45	0.11	19.56
LIS 34/15	570	7.79	0.07	0.85	3.56	0.13	0.84	1.21	3.35	26.49	27.41	0.13	14.24
LIS 34/16	592.5	7.71	0.08	2.03	3.16	0.15	0.96	1.25	2.89	26.53	31.82	0.11	28.04
LIS 34/17	655	7.73	0.11	1.95	0.00	0.19	1.31	1.93	3.10	26.20	32.86	0.12	23.06
LIS 34/18	685	7.87	0.15	1.85	0.00	0.16	1.30	1.14	3.07	26.06	33.76	0.12	25.01
LIS 34/19	750	7.76	0.13	1.62	3.66	0.18	1.27	1.43	2.67	26.11	34.93	0.10	24.51
LIS 34/20	777.5	7.89	0.15	2.02	3.52	0.22	1.51	1.35	2.42	26.03	35.59	0.09	26.36

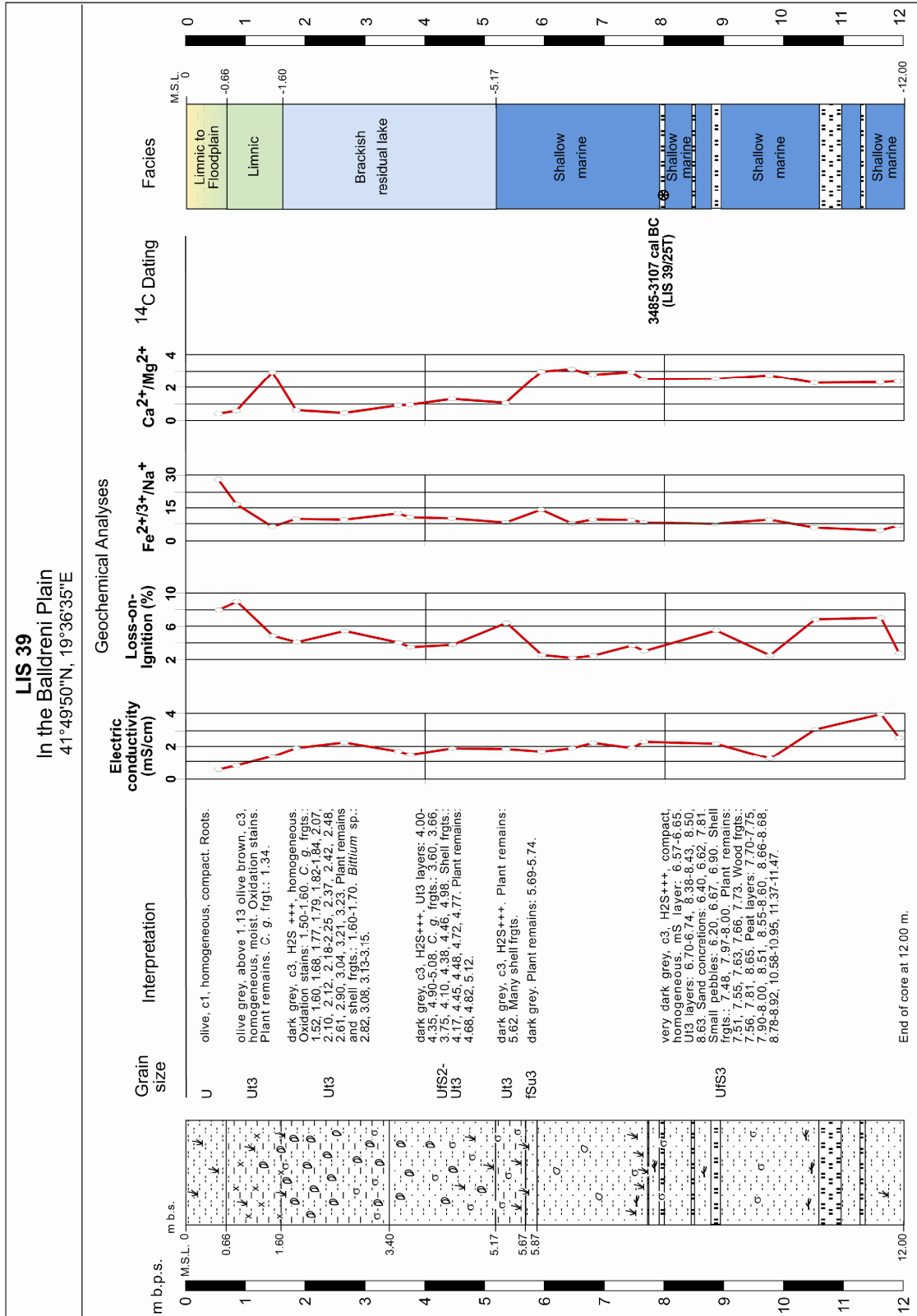
Appendix 5.26: Geochemical results of LIS 35.

Sample - No.	Depth b.s. (cm)	pH (KCl) - value	Electric conductivity (mS/cm)	Loss-on-Ignition (%)	Carbonate content (%)	Orthophosphate (g/kg)	c(K ⁺) (g/kg)	c(Na ⁺) (g/kg)	c(Ca ²⁺) (g/kg)	c(Mg ²⁺) (g/kg)	c(Fe ^{2+/3+}) (g/kg)	c(Ca ²⁺)/c(Mg ²⁺)	c(Fe ^{2+/3+})/c(Na ⁺)
LIS 35/1	75	7.54	0.15	2.43	6.60	4.51	2.02	0.69	19.38	21.57	33.42	0.90	48.43
LIS 35/4	155	7.46	0.60	2.09	16.47	6.79	3.40	0.91	60.90	17.93	25.14	3.40	27.77
LIS 35/6	195	7.51	0.10	0.91	8.11	2.37	1.48	0.77	33.01	21.53	23.94	1.53	31.08
LIS 35/7	225	7.6	0.11	1.16	6.32	1.45	1.08	0.96	30.36	22.26	22.38	1.36	23.43
LIS 35/8	275	7.55	0.10	1.21	6.38	1.18	0.96	0.98	26.96	22.98	22.83	1.17	23.42
LIS 35/9	347	7.51	0.10	1.05	9.78	1.11	1.02	0.94	35.86	23.04	22.44	1.56	24.00
LIS 35/10	360	7.42	0.12	0.85	8.35	1.75	1.22	1.73	31.93	22.92	24.02	1.39	13.88
LIS 35/11	385	7.46	0.13	1.80	11.12	1.73	1.06	0.78	39.15	22.51	28.92	1.74	37.32
LIS 35/12	449	7.53	0.13	1.76	10.45	1.24	1.02	0.58	39.68	22.60	22.23	1.76	38.32
LIS 35/20	545	7.11	1.60	3.52	8.15	0.92	1.96	0.75	30.21	21.73	22.16	1.39	29.74
LIS 35/24	570	7.17	1.63	3.01	19.72	0.55	1.14	0.80	94.30	24.29	18.82	3.88	23.53
LIS 35/25	586.5	7.36	1.21	2.55	13.88	0.48	1.80	1.03	45.60	25.44	25.62	1.79	24.87
LIS 35/27	664	7.27	1.56	4.87	16.01	0.61	1.99	1.32	69.35	24.27	22.00	2.86	16.66
LIS 35/28	675	7.23	1.09	5.45	12.33	1.03	3.59	1.57	43.98	22.31	23.99	1.97	15.33
LIS 35/32	788	7.22	1.83	3.87	9.42	0.80	1.71	1.08	37.98	24.94	22.39	1.52	20.73
LIS 35/33	845	7.22	1.53	1.70	18.06	0.70	0.94	1.47	66.00	25.96	22.60	2.54	15.37
LIS 35/34	857.5	7.03	2.60	8.41	7.32	0.82	1.84	0.90	33.87	25.37	25.13	1.33	27.92
LIS 35/36	951.5	7.1	2.90	13.01	6.20	0.87	2.10	0.98	21.67	24.31	25.14	0.89	25.65
LIS 35/37	981.5	7.19	2.11	5.06	9.03	0.97	3.03	1.24	26.02	25.22	30.91	1.03	25.03
LIS 35/38	1072	7.55	1.18	1.81	7.13	0.55	0.82	0.90	31.22	28.32	30.98	1.10	34.42
LIS 35/39	1092	7.72	0.61	1.54	5.68	0.38	0.64	0.87	34.39	28.20	32.16	1.22	37.18

Appendix 5.27: Geochemical results of LIS 38.

Sample - No.	Depth b.s. (cm)	pH (KCl) - value	Electric conductivity (mS/cm)	Loss-on-Ignition (%)	Carbonate content (%)	Orthophosphate (g/kg)	c(K ⁺) (g/kg)	c(Na ⁺) (g/kg)	c(Ca ²⁺) (g/kg)	c(Mg ²⁺) (g/kg)	c(Fe ^{2+/3+}) (g/kg)	c(Ca ²⁺)/c(Mg ²⁺)	c(Fe ^{2+/3+})/c(Na ⁺)
LIS 38/3	65	7.2	0.19	3.68	1.41	5.12	4.17	1.87	1.23	13.96	28.98	0.09	15.54
LIS 38/6	155	7.56	0.24	2.82	6.77	5.19	3.84	1.49	23.75	15.73	27.03	1.51	18.20
LIS 38/10	245	7.69	0.15	2.26	12.40	5.97	3.80	0.69	46.06	14.05	23.84	3.28	34.80
LIS 38/12	275	7.56	0.15	2.12	13.82	6.26	3.69	0.59	46.70	13.24	24.30	3.53	41.19
LIS 38/17	445	7.78	0.13	1.28	5.97	0.96	0.88	1.03	21.93	19.18	17.38	1.14	16.87
LIS 38/18	475	7.92	0.07	1.03	7.69	0.96	0.76	0.63	28.05	19.80	17.07	1.42	27.30
LIS 38/19	587	7.96	0.09	1.02	5.71	0.75	1.01	1.51	17.84	19.21	18.65	0.93	12.35
LIS 38/20	655	7.97	0.12	0.70	6.32	0.63	0.88	0.73	20.85	18.98	18.16	1.10	25.05
LIS 38/21	755	7.7	0.12	2.39	7.14	0.82	1.26	0.85	24.50	20.45	23.91	1.20	28.13
LIS 38/23	780	8.04	0.11	1.74	12.00	0.87	1.02	0.45	38.64	16.05	22.47	2.41	49.93
LIS 38/24	790	7.41	1.52	1.93	10.90	0.77	0.93	0.84	36.23	17.18	17.53	2.11	20.99
LIS 38/25	855	7.15	2.23	6.26	10.36	0.72	0.91	0.70	34.18	16.54	16.14	2.07	23.05
LIS 38/27	870	7.2	2.02	3.70	9.76	0.73	1.02	0.69	31.77	17.10	16.71	1.86	24.21
LIS 38/30	930	7.49	1.82	1.82	11.66	0.76	0.99	0.72	36.75	17.21	16.28	2.14	22.76
LIS 38/33	953.5	7.61	0.84	4.68	12.36	1.46	2.62	0.84	30.24	16.82	26.85	1.80	32.16
LIS 38/34	977.5	7.61	1.01	4.21	9.96	1.40	3.06	0.63	25.98	16.95	30.35	1.53	48.17
LIS 38/35	1055	7.6	1.38	7.21	9.40	1.07	2.12	1.67	26.85	18.77	25.32	1.43	15.20
LIS 38/37	1088	7.7	1.51	3.07	9.26	0.48	0.87	1.24	37.93	26.02	23.37	1.46	18.85
LIS 38/38	1150	8.1	1.15	1.34	14.23	0.34	0.53	0.63	48.97	26.00	21.68	1.88	34.40
LIS 38/39	1180	7.92	1.61	0.88	17.98	0.37	0.50	1.06	69.90	26.86	25.98	2.60	24.51

Appendix 5.28.1: Geological profile and selected geochemical results of LIS 39.

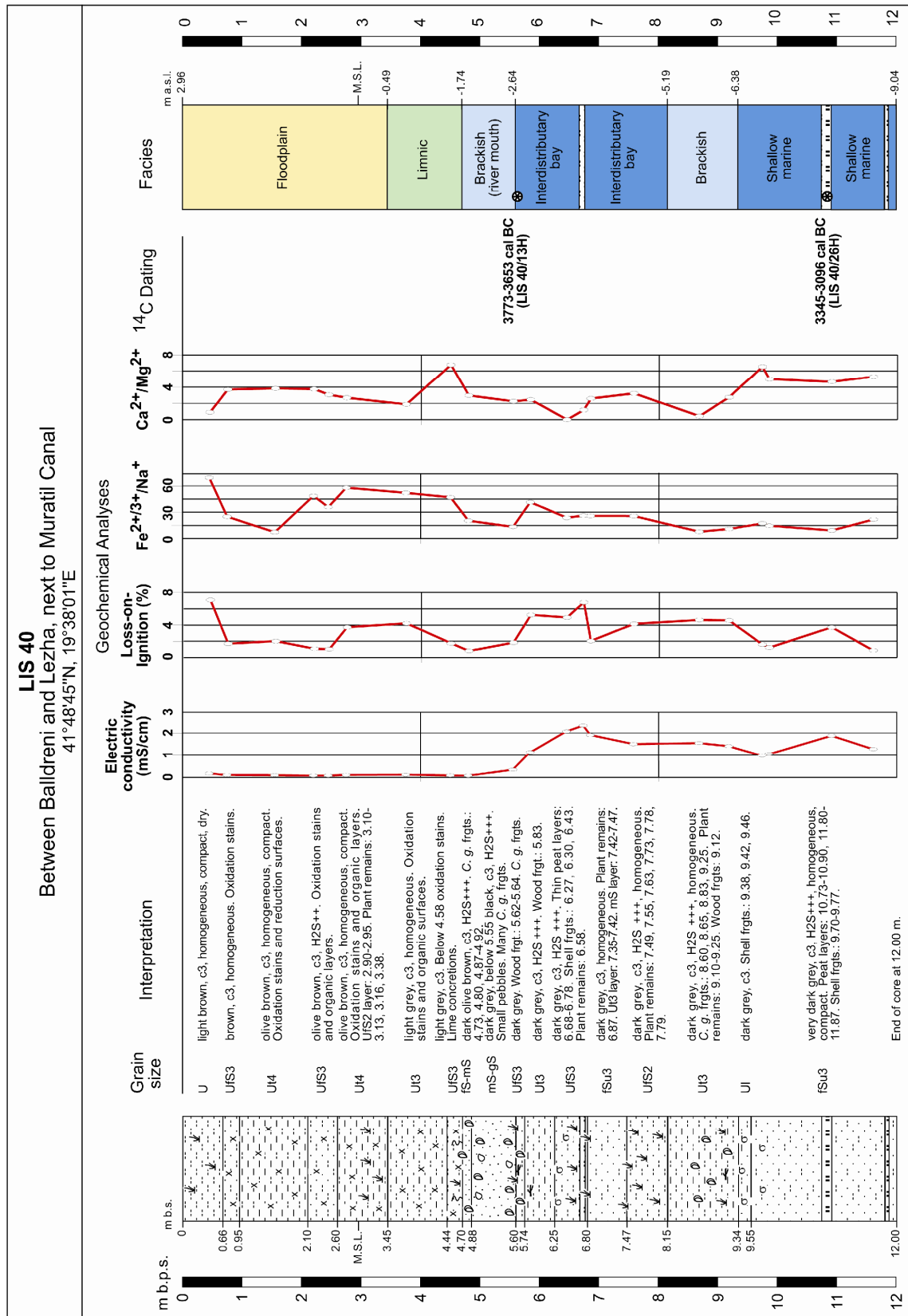


Appendix 5.28.1: Photo and geochemical results of LIS 39.

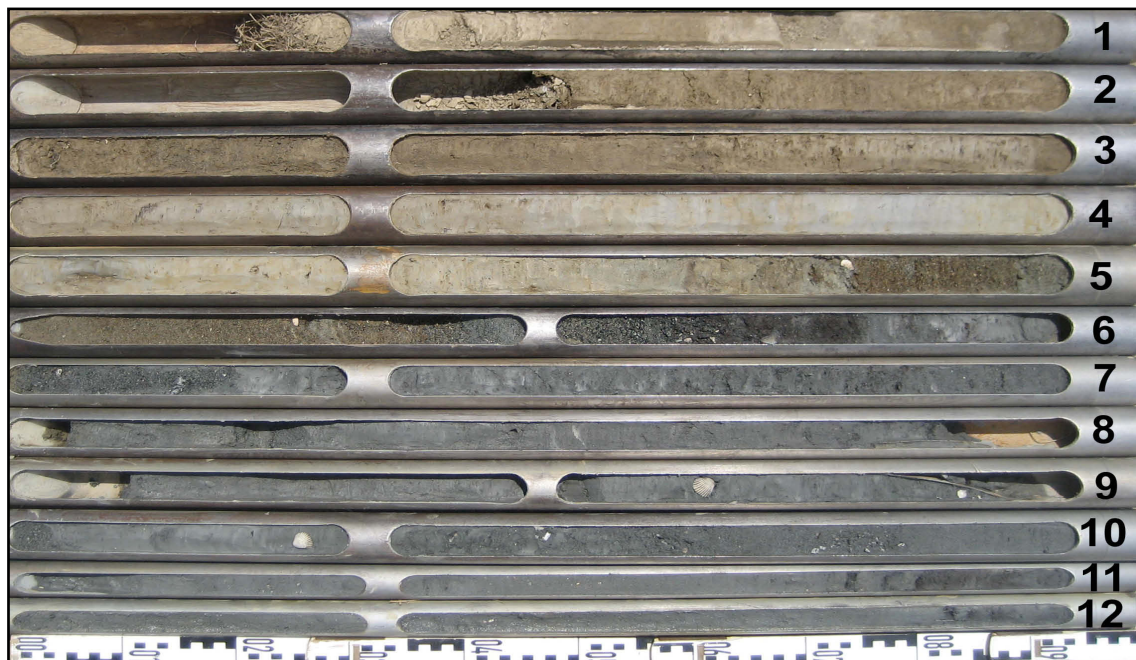


Sample - No.	Depth b.s. (cm)	pH (KCl) - value	Electric conductivity (mS/cm)	Loss-on-Ignition (%)	Carbonate content (%)	Orthophosphate (g/kg)	c(K ⁺) (g/kg)	c(Na ⁺) (g/kg)	c(Ca ²⁺) (g/kg)	c(Mg ²⁺) (g/kg)	c(Fe ^{2+/3+}) (g/kg)	c(Ca ²⁺)/c(Mg ²⁺)	c(Fe ^{2+/3+})/c(Na ⁺)
LIS 39/1	55	7.14	0.58	7.96	5.52	1.65	2.69	1.32	7.10	17.15	37.01	0.41	28.04
LIS 39/2	85	7.27	0.82	8.99	4.80	1.46	2.52	2.15	9.32	15.93	35.86	0.58	16.68
LIS 39/4	145	7.53	1.39	4.85	16.92	1.16	1.60	3.85	47.89	16.34	24.67	2.93	6.42
LIS 39/6	185	7.45	1.90	4.08	4.74	1.03	2.97	2.65	11.77	18.79	26.47	0.63	9.99
LIS 39/8	265	7.51	2.24	5.43	4.34	1.02	3.45	2.76	8.51	18.68	26.52	0.46	9.62
LIS 39/11	355	7.62	1.70	4.01	6.42	0.99	2.23	1.90	16.51	18.05	23.68	0.91	12.50
LIS 39/12	375	7.62	1.50	3.47	6.55	0.89	1.83	2.04	16.39	17.26	21.80	0.95	10.71
LIS 39/14	445	7.76	1.88	3.77	9.27	1.13	2.05	2.22	22.55	17.34	22.67	1.30	10.21
LIS 39/16	535	7.77	1.85	6.41	9.54	0.81	3.97	3.47	21.68	20.34	28.79	1.07	8.30
LIS 39/18	594	8.01	1.69	2.54	18.49	0.79	1.14	1.28	62.35	20.96	18.20	2.97	14.22
LIS 39/19	645	8.16	1.90	2.17	23.69	0.56	0.66	2.08	67.55	21.62	16.47	3.12	7.92
LIS 39/20	680	8.04	2.22	2.46	20.97	0.81	1.02	1.95	60.25	21.64	18.98	2.78	9.73
LIS 39/21	745	8.2	1.91	3.68	19.30	0.92	1.14	2.32	59.90	20.36	21.98	2.94	9.49
LIS 39/23	765	8.13	2.28	3.01	16.45	0.79	1.19	2.50	49.44	19.72	20.77	2.51	8.31
LIS 39/28	885	7.96	2.17	5.50	16.49	0.78	1.06	2.52	49.94	19.68	19.51	2.54	7.76
LIS 39/30	975	8.41	1.25	2.48	21.06	0.64	0.78	1.97	60.85	22.17	19.00	2.74	9.64
LIS 39/32	1050	8.13	3.02	6.83	16.34	0.95	1.07	3.45	48.85	21.40	20.84	2.28	6.04
LIS 39/35	1160	8.2	3.95	7.02	16.76	1.34	1.28	5.06	48.16	20.75	23.70	2.32	4.69
LIS 39/36	1190	8.3	2.53	2.76	16.43	0.92	0.99	3.42	53.20	22.50	23.65	2.36	6.93

Appendix 5.29.1: Geological profile and selected geochemical results of LIS 40

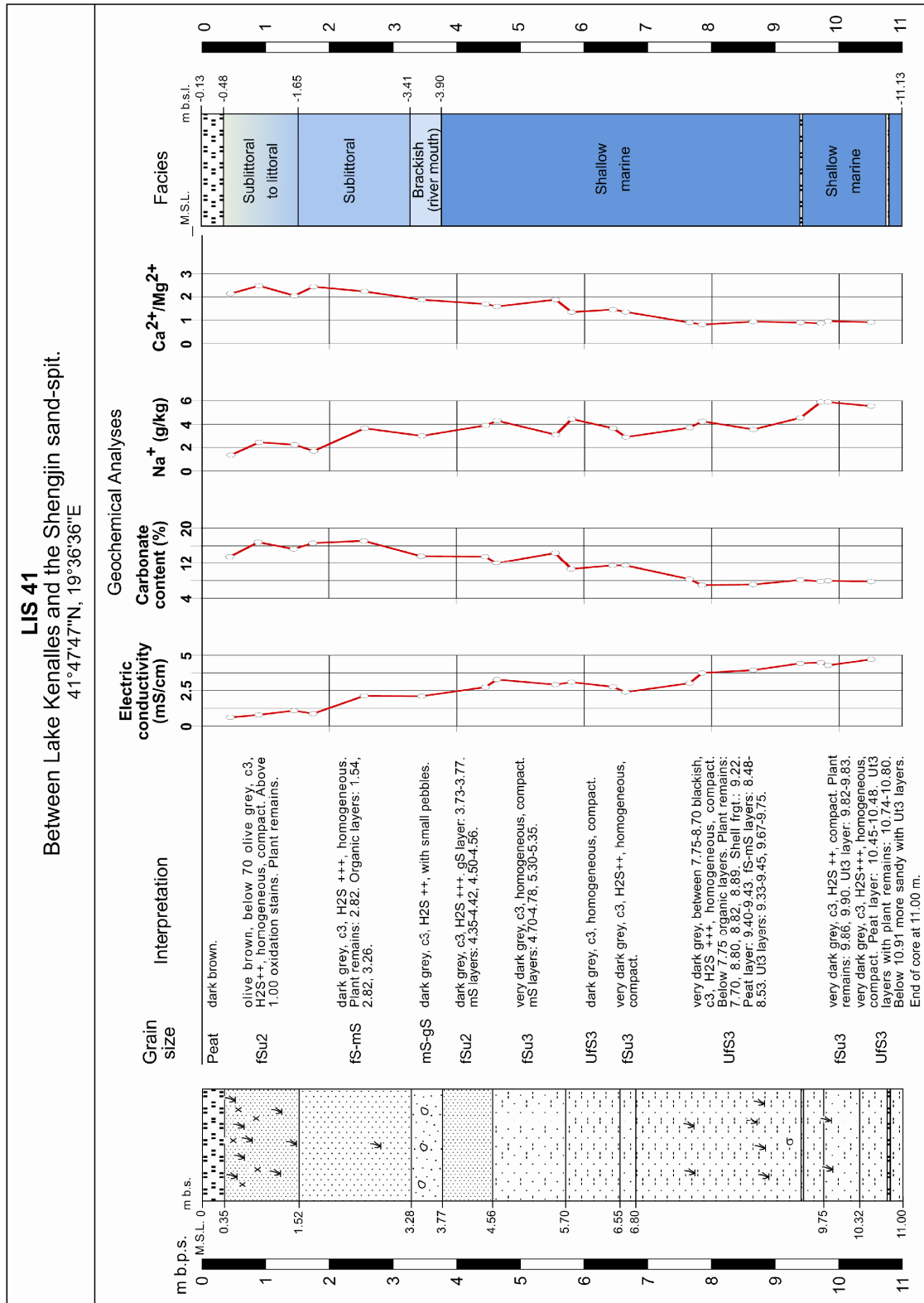


Appendix 5.29.2: Photo and geochemical results of LIS 40.

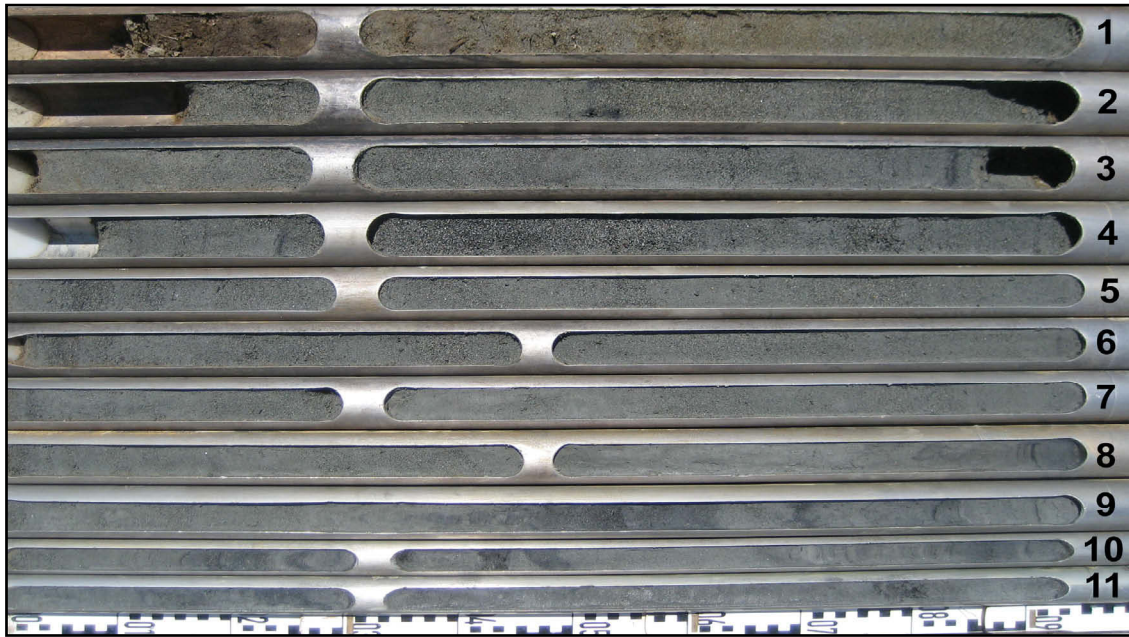


Sample - No.	Depth b.s. (cm)	pH (KCl) - value	Electric conductivity (mS/cm)	Loss-on-Ignition (%)	Carbonate content (%)	Orthophosphate (g/kg)	c(K ⁺) (g/kg)	c(Na ⁺) (g/kg)	c(Ca ²⁺) (g/kg)	c(Mg ²⁺) (g/kg)	c(Fe ²⁺³⁺) (g/kg)	c(Ca ²⁺)/c(Mg ²⁺)	c(Fe ²⁺³⁺)/c(Na ⁺)
LIS 40/1	45	7.37	0.18	7.08	4.17	2.48	1.40	0.48	7.40	16.34	33.30	0.45	69.38
LIS 40/2	75	7.84	0.10	1.71	10.75	1.10	0.55	1.05	33.37	18.00	26.12	1.85	24.99
LIS 40/3	155	7.85	0.10	2.01	11.74	1.15	0.93	3.54	34.47	18.00	31.16	1.92	7.15
LIS 40/4	220	7.94	0.08	1.09	12.27	0.60	0.30	0.56	35.85	19.09	25.33	1.88	48.54
LIS 40/5	245	7.91	0.08	1.03	9.74	0.85	0.61	0.93	29.12	19.02	27.19	1.53	35.93
LIS 40/6	275	7.81	0.11	3.74	9.79	1.02	1.00	0.58	22.51	16.70	33.42	1.35	57.97
LIS 40/8	375	7.85	0.12	4.21	8.79	1.32	1.48	0.49	16.78	17.84	33.62	0.94	52.08
LIS 40/9	450	8.13	0.09	1.75	19.87	1.12	0.53	0.58	56.70	16.75	25.26	3.39	46.97
LIS 40/10	480	8.4	0.08	0.81	14.17	0.30	0.31	1.39	38.25	25.75	27.01	1.49	20.40
LIS 40/12	555	8.05	0.35	1.84	9.82	0.55	0.40	2.02	29.26	25.99	28.26	1.13	13.34
LIS 40/15	584	8.07	1.14	5.25	10.09	1.12	1.83	0.65	23.32	18.92	26.95	1.23	41.52
LIS 40/16	645	7.67	2.07	4.92	0.69	0.72	2.81	0.91	0.00	18.93	26.78	0.00	23.62
LIS 40/17	673	6.96	2.33	6.79	4.75	0.85	1.72	0.77	10.29	17.30	21.38	0.59	26.20
LIS 40/18	685	7.33	1.91	2.04	8.90	0.63	0.93	0.86	24.38	18.75	20.05	1.30	25.82
LIS 40/19	757.5	7.51	1.50	4.14	9.65	0.91	1.37	1.05	27.97	17.29	22.08	1.62	25.71
LIS 40/20	867.5	7.59	1.55	4.63	4.30	0.94	2.65	3.76	4.08	19.10	26.87	0.21	7.70
LIS 40/21	917.5	7.41	1.41	4.57	11.81	1.02	3.08	1.72	27.43	19.81	28.96	1.38	10.78
LIS 40/23	973.5	7.98	0.98	1.60	23.37	0.69	0.86	1.07	70.20	21.49	18.54	3.27	17.33
LIS 40/24	985	8.22	1.05	1.23	17.17	0.82	0.79	1.44	53.65	21.48	20.95	2.50	14.55
LIS 40/26	1090	7.82	1.87	3.72	15.89	0.80	0.69	1.99	43.95	18.86	18.07	2.33	9.10
LIS 40/27	1160	8.29	1.28	0.87	19.17	0.68	0.54	0.92	53.50	20.18	19.99	2.65	21.84

Appendix 5.30.1: Geological profile and selected geochemical results of LIS 41.

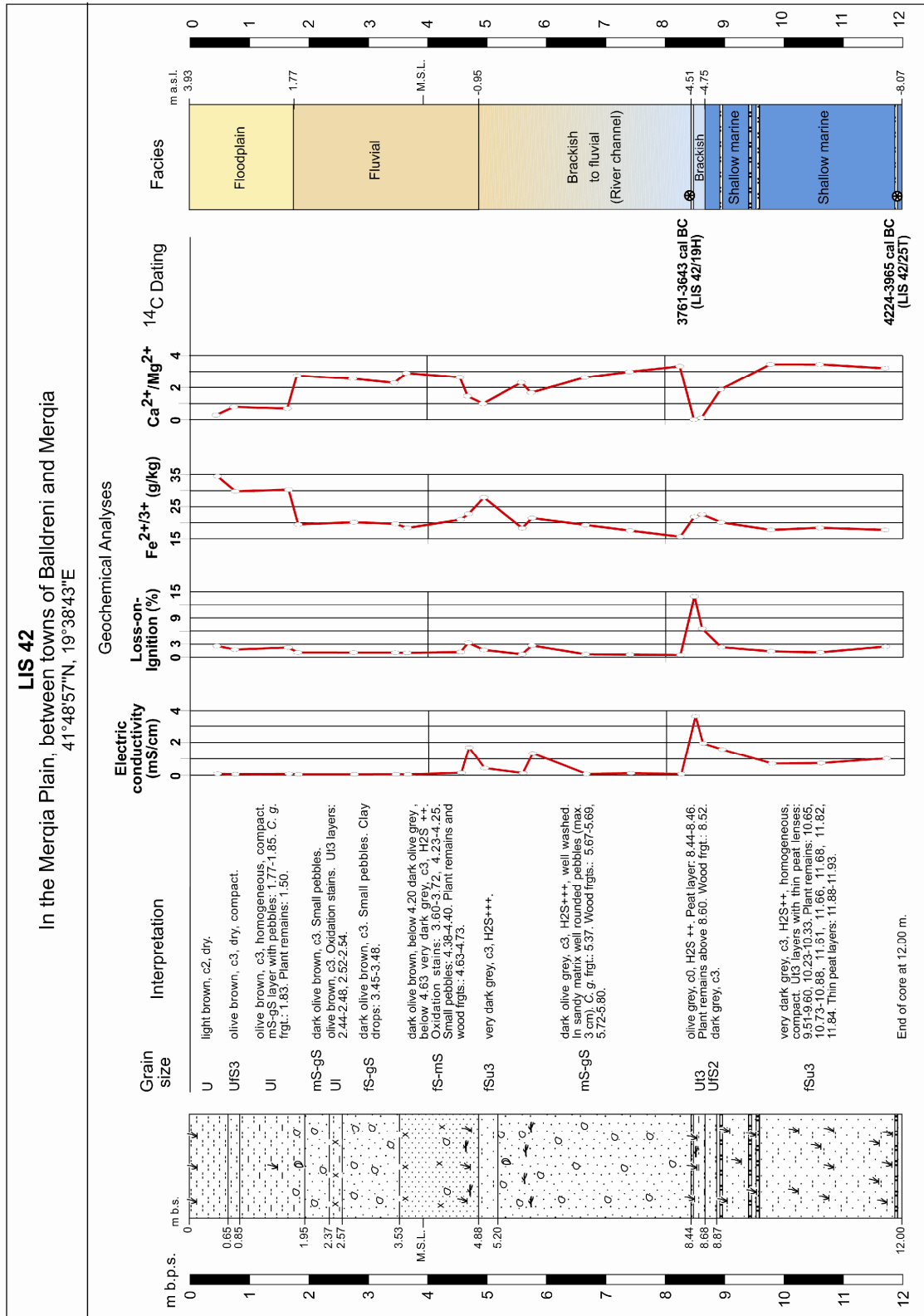


Appendix 5.30.2: Photo and geochemical results of LIS 41.



Sample - No.	Depth b.s. (cm)	pH (KCl) - value	Electric conductivity (mS/cm)	Loss-on-Ignition (%)	Carbonate content (%)	Orthophosphate (g/kg)	c(K ⁺) (g/kg)	c(Na ⁺) (g/kg)	c(Ca ²⁺) (g/kg)	c(Mg ²⁺) (g/kg)	c(Fe ^{2+/3+}) (g/kg)	c(Ca ²⁺)/c(Mg ²⁺)	c(Fe ^{2+/3+})/c(Na ⁺)
LIS 41/1	45	8.37	0.61	2.44	13.54	0.71	0.50	1.35	48.70	22.65	22.45	2.15	16.63
LIS 41/2	89.5	8.54	0.79	1.37	16.82	0.70	0.20	2.45	57.30	23.05	24.00	2.49	9.80
LIS 41/3	145	8.47	1.09	0.96	15.28	0.89	1.25	2.25	46.10	22.40	24.05	2.06	10.69
LIS 41/4	175	8.55	0.87	2.28	16.61	0.71	0.85	1.70	55.70	22.80	22.10	2.44	13.00
LIS 41/5	255	8.52	2.13	2.36	17.12	0.79	0.85	3.65	52.45	23.40	24.55	2.24	6.73
LIS 41/7	345	8.45	2.10	1.38	13.65	0.66	0.50	3.00	46.20	24.50	18.15	1.89	6.05
LIS 41/8	445	8.56	2.75	1.10	13.57	0.78	2.20	3.90	38.30	22.55	22.45	1.70	5.76
LIS 41/9	463	8.47	3.28	2.60	12.06	1.07	1.90	4.30	36.20	22.70	25.85	1.59	6.01
LIS 41/10	555	8.62	2.92	2.17	14.37	0.92	0.70	3.10	43.60	23.05	22.80	1.89	7.35
LIS 41/11	580	8.42	3.10	1.79	10.61	1.24	1.75	4.45	30.65	22.65	27.05	1.35	6.08
LIS 41/12	645	8.48	2.77	1.06	11.42	0.88	0.50	3.65	33.00	22.60	26.25	1.46	7.19
LIS 41/13	665	8.50	2.40	2.31	11.43	0.65	0.60	2.90	32.00	23.50	23.60	1.36	8.14
LIS 41/14	765	8.31	3.02	2.94	8.31	1.22	1.60	3.70	21.95	24.25	28.55	0.91	7.72
LIS 41/15	785	8.02	3.75	3.56	6.98	1.17	1.50	4.25	20.65	25.25	31.45	0.82	7.40
LIS 41/16	865	8.07	3.95	3.34	7.09	0.82	0.70	3.55	21.20	22.45	28.50	0.94	8.03
LIS 41/18	939	8.00	4.43	5.02	8.13	1.10	1.40	4.55	20.10	22.20	28.45	0.91	6.25
LIS 41/19	971	7.95	4.48	5.25	7.81	1.45	1.60	5.90	18.70	21.35	32.60	0.88	5.53
LIS 41/20	982.5	8.05	4.29	3.57	7.95	1.19	3.30	5.90	23.20	24.10	30.00	0.96	5.08
LIS 41/21	1050	7.94	4.71	6.19	7.77	1.23	1.35	5.55	21.45	23.30	29.65	0.92	5.34

Appendix 5.31.1: Geological profile and selected geochemical results of LIS 42.

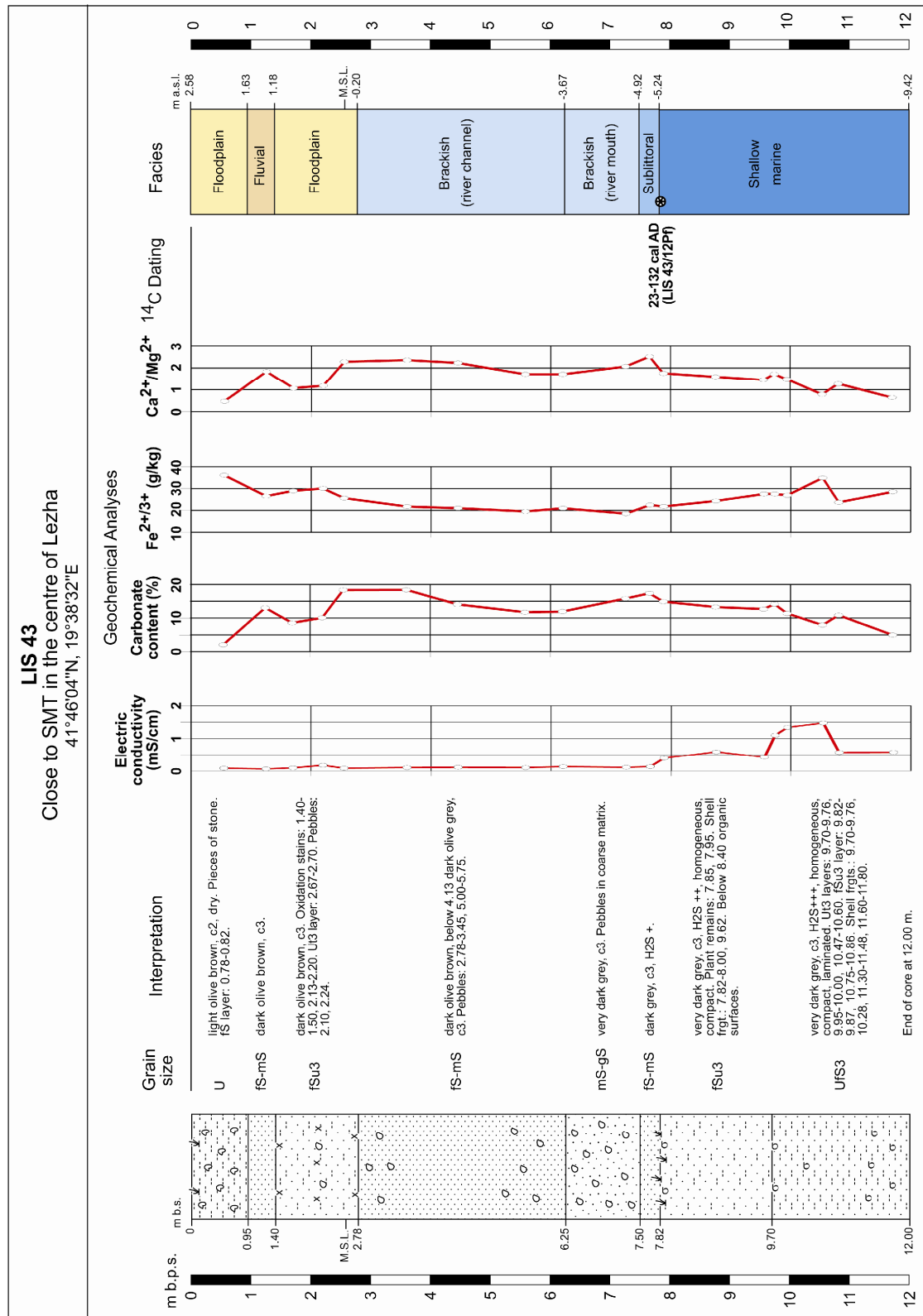


Appendix 5.31.2: Photo and geochemical results of LIS 42.

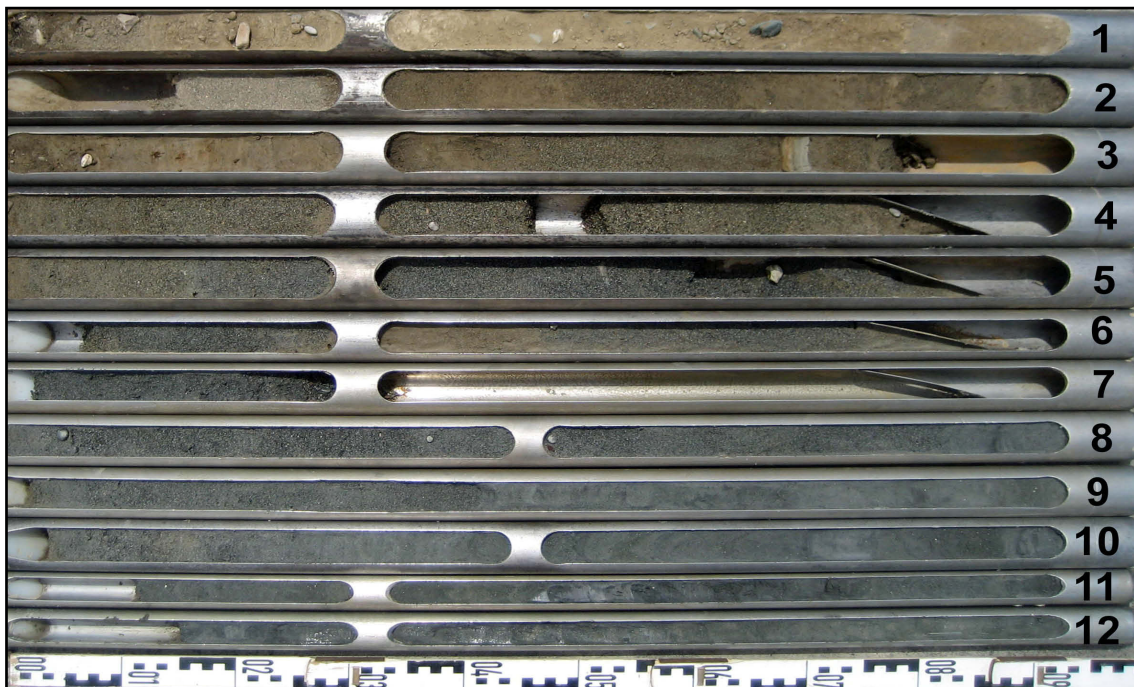


Sample - No.	Depth b.s. (cm)	pH (KCl) - value	Electric conductivity (mS/cm)	Loss-on-Ignition (%)	Carbonate content (%)	Orthophosphate (g/kg)	c(K ⁺) (g/kg)	c(Na ⁺) (g/kg)	c(Ca ²⁺) (g/kg)	c(Mg ²⁺) (g/kg)	c(Fe ^{2+/3+}) (g/kg)	c(Ca ²⁺)/c(Mg ²⁺)	c(Fe ^{2+/3+})/c(Na ⁺)
LIS 42/1	45	7.62	0.09	2.61	3.22	1.43	1.05	1.45	9.44	19.00	34.49	0.50	23.87
LIS 42/2	75	7.88	0.07	1.75	7.98	0.98	0.72	0.61	23.31	19.37	29.82	1.20	49.28
LIS 42/3	165	7.8	0.08	2.24	8.03	1.64	2.17	1.58	20.73	19.40	30.30	1.07	19.18
LIS 42/4	181	8.49	0.05	1.07	15.19	0.67	0.30	0.69	53.25	19.66	19.45	2.71	28.18
LIS 42/6	275	8.49	0.05	1.05	14.41	0.76	0.48	0.51	51.25	19.28	20.13	2.66	39.86
LIS 42/7	345	8.5	0.06	1.03	14.10	0.74	0.30	0.99	44.80	20.12	19.64	2.23	19.93
LIS 42/8	365	8.53	0.05	0.99	18.98	0.62	0.36	0.85	53.25	19.97	18.32	2.67	21.55
LIS 42/9	455	8.38	0.15	1.16	19.07	0.98	0.72	10.41	55.40	20.62	20.98	2.69	2.02
LIS 42/10	468	7.41	1.70	3.34	10.86	0.76	0.43	0.68	33.19	18.61	22.77	1.78	33.73
LIS 42/12	494	7.92	0.43	1.67	11.45	1.29	0.72	4.31	27.52	19.07	27.90	1.44	6.48
LIS 42/13	558.5	8.63	0.13	0.65	16.23	0.80	0.30	0.80	42.10	21.32	18.26	1.97	22.97
LIS 42/15	575	7.73	1.33	2.71	11.09	0.87	0.32	0.67	35.72	19.73	21.45	1.81	32.25
LIS 42/16	665	8.62	0.08	0.67	17.34	0.94	0.38	1.07	50.60	20.31	19.28	2.49	18.02
LIS 42/17	740	8.61	0.12	0.58	17.61	0.62	0.15	0.54	52.35	20.22	17.52	2.59	32.44
LIS 42/18	825	8.77	0.08	0.49	18.14	1.02	0.24	0.76	52.05	20.10	15.62	2.59	20.55
LIS 42/19	848.5	4.81	3.60	13.94	0.00	1.05	1.39	0.49	0.00	13.34	21.84	0.00	44.57
LIS 42/20	861.5	6.24	1.95	6.52	0.67	1.21	1.73	0.69	2.29	16.88	22.59	0.14	32.97
LIS 42/21	893.5	7.42	1.58	2.30	12.93	0.95	0.74	0.57	37.42	20.61	20.09	1.82	35.25
LIS 42/22	977.5	8.08	0.71	1.32	21.00	0.76	0.31	0.08	61.40	20.77	17.73	2.96	221.63
LIS 42/23	1060	8.13	0.73	1.09	21.34	0.78	0.49	0.86	63.55	21.13	18.40	3.01	21.52
LIS 42/24	1170	8.03	1.02	2.46	19.14	0.86	0.50	0.61	56.85	20.65	17.72	2.75	29.29

Appendix 5.32.1: Geological profile and selected geochemical results of LIS 43.

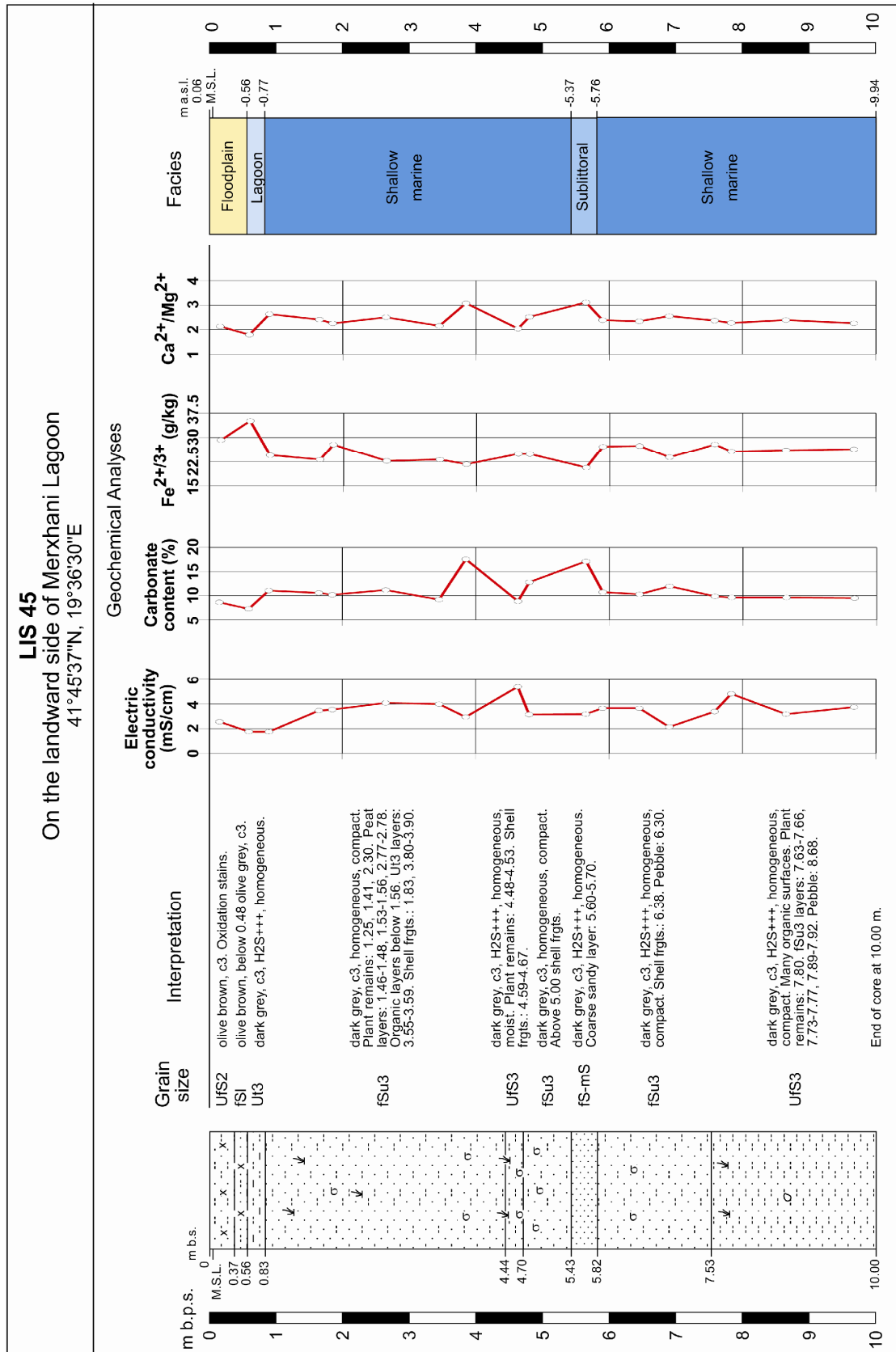


Appendix 5.32.2: Photo and geochemical results of LIS 43.

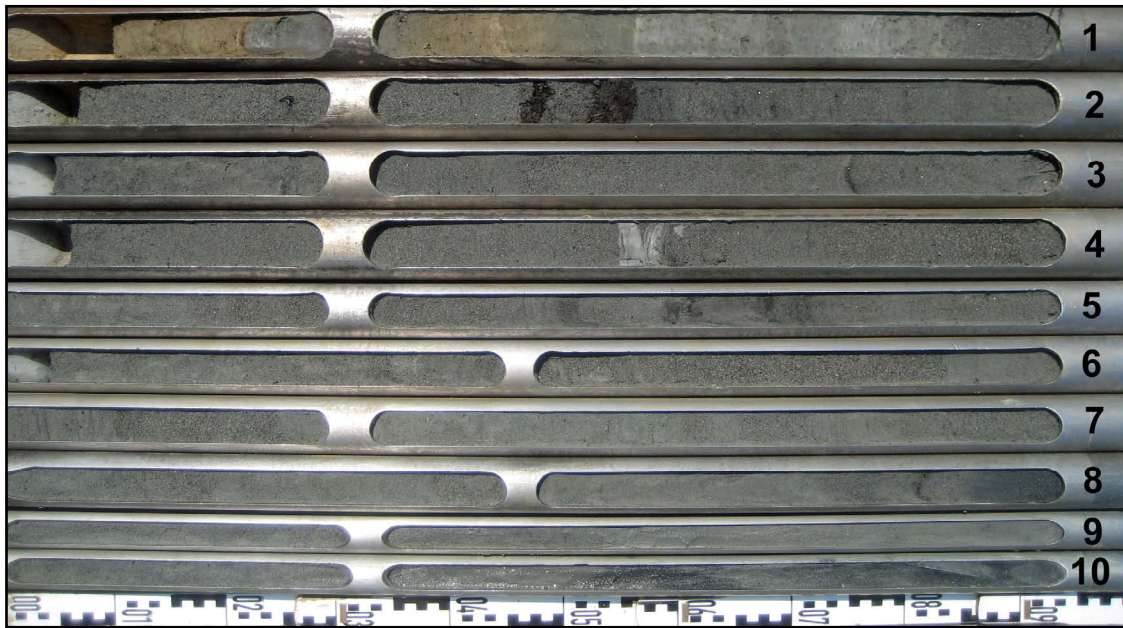


Sample - No.	Depth b.s. (cm)	pH (KCl) - value	Electric conductivity (mS/cm)	Loss-on-Ignition (%)	Carbonate content (%)	Orthophosphate (g/kg)	c(K ⁺) (g/kg)	c(Na ⁺) (g/kg)	c(Ca ²⁺) (g/kg)	c(Mg ²⁺) (g/kg)	c(Fe ^{2+/3+}) (g/kg)	c(Ca ²⁺)/c(Mg ²⁺)	c(Fe ^{2+/3+})/c(Na ⁺)
LIS 43/1	55	7.72	0.08	2.87	2.09	0.94	1.55	1.75	11.55	24.60	36.10	0.47	20.63
LIS 43/2	125	8.33	0.06	1.50	13.07	1.24	0.55	0.60	39.95	21.80	26.50	1.83	44.17
LIS 43/3	170	7.90	0.09	1.99	8.57	1.46	0.60	0.55	23.90	22.40	28.95	1.07	52.64
LIS 43/4	220	7.73	0.17	2.64	10.12	1.52	0.55	0.60	25.85	21.95	30.05	1.18	50.08
LIS 43/5	255	8.34	0.08	1.19	18.39	1.06	1.20	0.60	51.30	22.45	25.60	2.29	42.67
LIS 43/6	360	8.50	0.10	0.79	18.44	0.98	0.80	2.25	52.70	22.35	21.70	2.36	9.64
LIS 43/7	445	8.52	0.11	0.74	14.09	0.97	0.70	0.90	51.20	22.95	21.00	2.23	23.33
LIS 43/8	557	8.40	0.10	1.04	11.75	0.97	0.45	0.80	35.55	20.80	19.50	1.71	24.38
LIS 43/9	620	8.38	0.13	0.71	11.96	1.02	0.25	1.55	36.95	21.65	20.95	1.71	13.52
LIS 43/10	725	8.56	0.11	0.59	15.85	0.88	0.20	0.70	48.15	23.25	18.50	2.07	26.43
LIS 43/11	765	8.61	0.13	0.53	17.43	1.08	0.85	1.60	60.30	23.95	22.45	2.52	14.03
LIS 43/12	788	8.14	0.39	1.16	14.91	1.00	0.60	0.60	41.55	23.75	21.75	1.75	36.25
LIS 43/13	875	7.79	0.59	2.12	13.30	1.06	1.10	0.95	38.20	24.00	24.30	1.59	25.58
LIS 43/14	955	8.01	0.42	2.07	12.68	1.04	3.10	2.05	36.55	25.20	27.50	1.45	13.41
LIS 43/15	973	7.82	1.10	2.68	14.18	0.98	1.40	1.35	39.60	23.05	27.50	1.72	20.37
LIS 43/16	994	7.76	1.34	2.22	11.40	1.13	1.90	2.00	35.20	23.90	26.90	1.47	13.45
LIS 43/17	1053	7.82	1.48	4.29	7.94	1.26	1.95	2.15	20.95	26.65	34.85	0.79	16.21
LIS 43/18	1080	8.25	0.57	1.74	10.86	0.72	0.95	1.65	32.60	25.75	23.65	1.27	14.33
LIS 43/20	1170	8.50	0.58	1.70	4.96	0.59	1.70	3.05	16.75	26.30	28.55	0.64	9.36

Appendix 5.33.1: Geological profile and selected geochemical results of LIS 45.

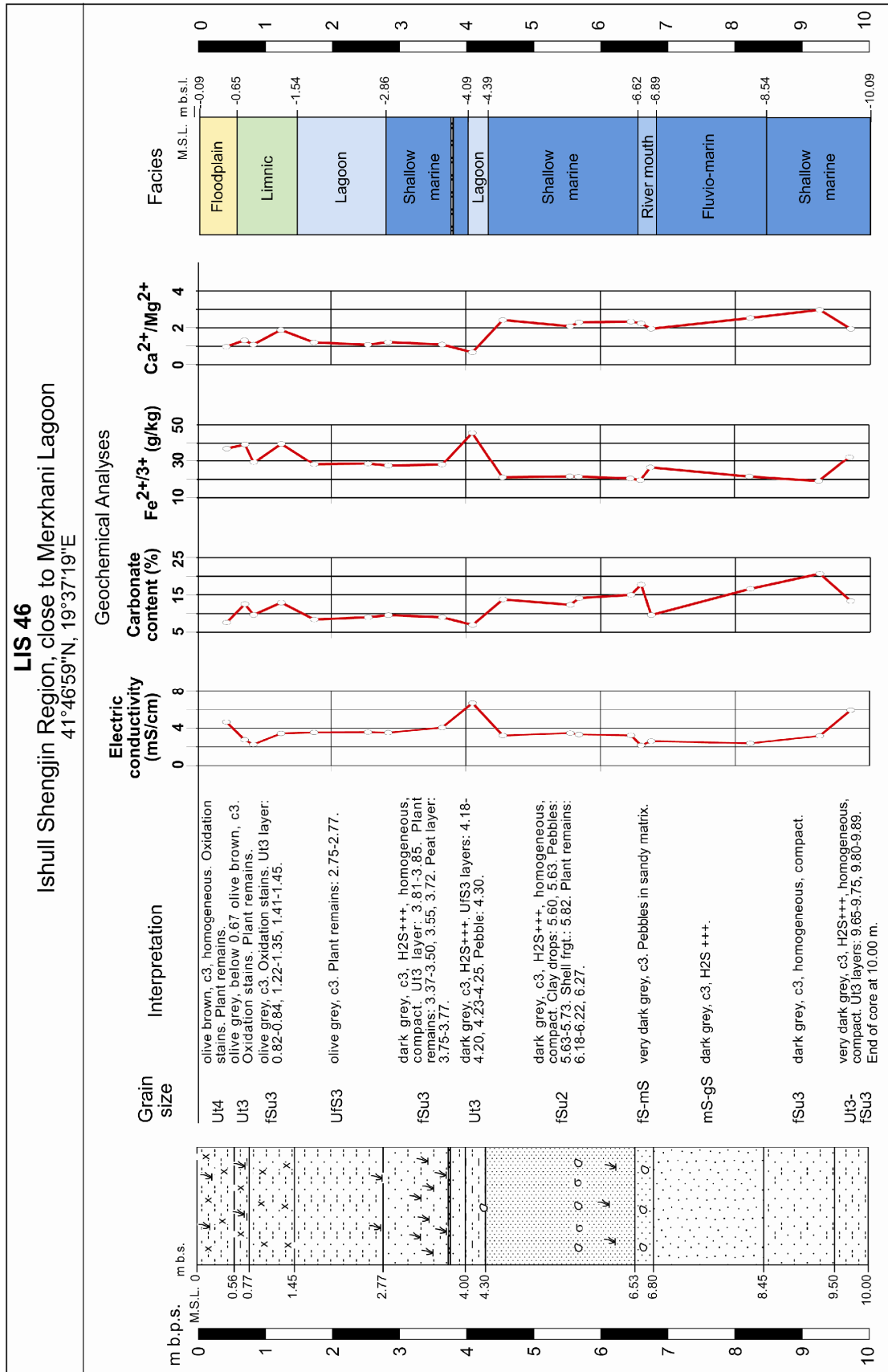


Appendix 5.33.2: Photo and geochemical results of LIS 45.

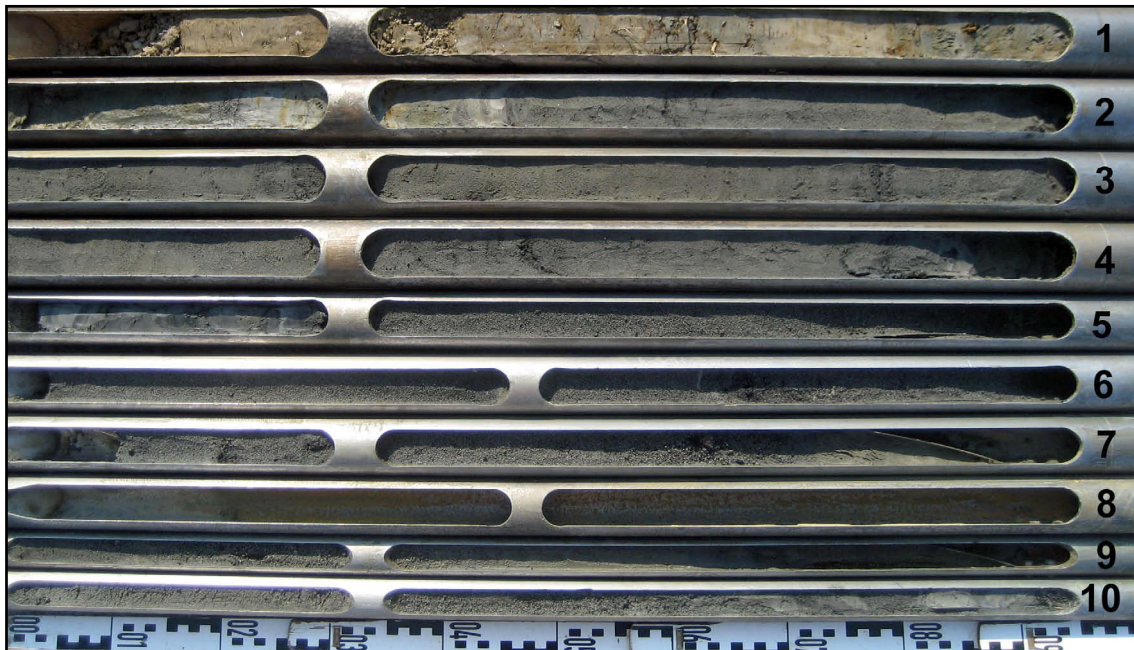


Sample - No.	Depth b.s. (cm)	pH (KCl) - value	Electric conductivity (mS/cm)	Loss-on-Ignition (%)	Carbonate content (%)	Orthophosphate (g/kg)	c(K ⁺) (g/kg)	c(Na ⁺) (g/kg)	c(Ca ²⁺) (g/kg)	c(Mg ²⁺) (g/kg)	c(Fe ^{2+/3+}) (g/kg)	c(Ca ²⁺)/c(Mg ²⁺)	c(Fe ^{2+/3+})/c(Na ⁺)
LIS 45/1	16	8.38	2.56	3.42	8.63	2.04	1.30	3.40	26.00	22.95	29.25	1.13	8.60
LIS 45/2	60	8.05	1.76	3.64	7.26	1.62	1.20	2.50	17.15	21.65	35.15	0.79	14.06
LIS 45/3	90	8.20	1.75	1.97	11.06	1.01	0.55	3.45	34.90	21.35	24.50	1.63	7.10
LIS 45/6	165	7.96	3.47	2.30	10.57	1.06	0.40	3.35	32.25	22.85	23.15	1.41	6.91
LIS 45/7	185	8.09	3.55	2.74	10.18	0.83	0.80	3.85	29.25	23.25	27.80	1.26	7.22
LIS 45/8	265	8.24	4.09	1.94	11.18	0.63	1.40	5.35	32.00	21.20	22.70	1.51	4.24
LIS 45/9	345	8.26	4.00	1.50	9.19	0.81	0.95	4.15	23.55	20.40	23.15	1.15	5.58
LIS 45/10	385	8.49	2.95	1.29	17.56	0.64	0.40	3.45	48.80	23.45	21.70	2.08	6.29
LIS 45/11	463	7.92	5.41	3.84	8.84	0.93	1.05	5.45	22.05	21.10	24.90	1.05	4.57
LIS 45/12	480	8.46	3.15	1.19	12.81	0.84	0.60	3.50	33.35	21.90	24.85	1.52	7.10
LIS 45/13	565	8.54	3.18	0.87	17.13	0.68	0.65	3.65	48.95	23.15	20.65	2.11	5.66
LIS 45/14	590	8.45	3.66	0.99	10.73	1.27	1.10	3.95	30.85	22.20	27.20	1.39	6.89
LIS 45/15	645	8.42	3.66	1.22	10.29	1.18	1.30	4.00	30.05	22.40	27.40	1.34	6.85
LIS 45/16	690	8.57	2.14	2.48	11.96	1.01	1.15	4.40	34.75	22.30	23.85	1.56	5.42
LIS 45/17	758	8.42	3.39	2.59	9.85	1.36	1.25	3.95	30.00	21.90	27.85	1.37	7.05
LIS 45/18	783	7.98	4.83	2.93	9.63	0.94	0.75	4.65	27.80	21.80	25.70	1.28	5.53
LIS 45/19	865	8.45	3.18	1.19	9.62	0.85	0.75	3.95	31.65	22.70	26.10	1.39	6.61
LIS 45/20	967	8.28	3.75	2.75	9.51	1.08	1.30	4.30	29.50	23.35	26.40	1.26	6.14

Appendix 5.34.1: Geological profile and selected geochemical results of LIS 46.



Appendix 5.34.2: Photo and geochemical results of LIS 46.

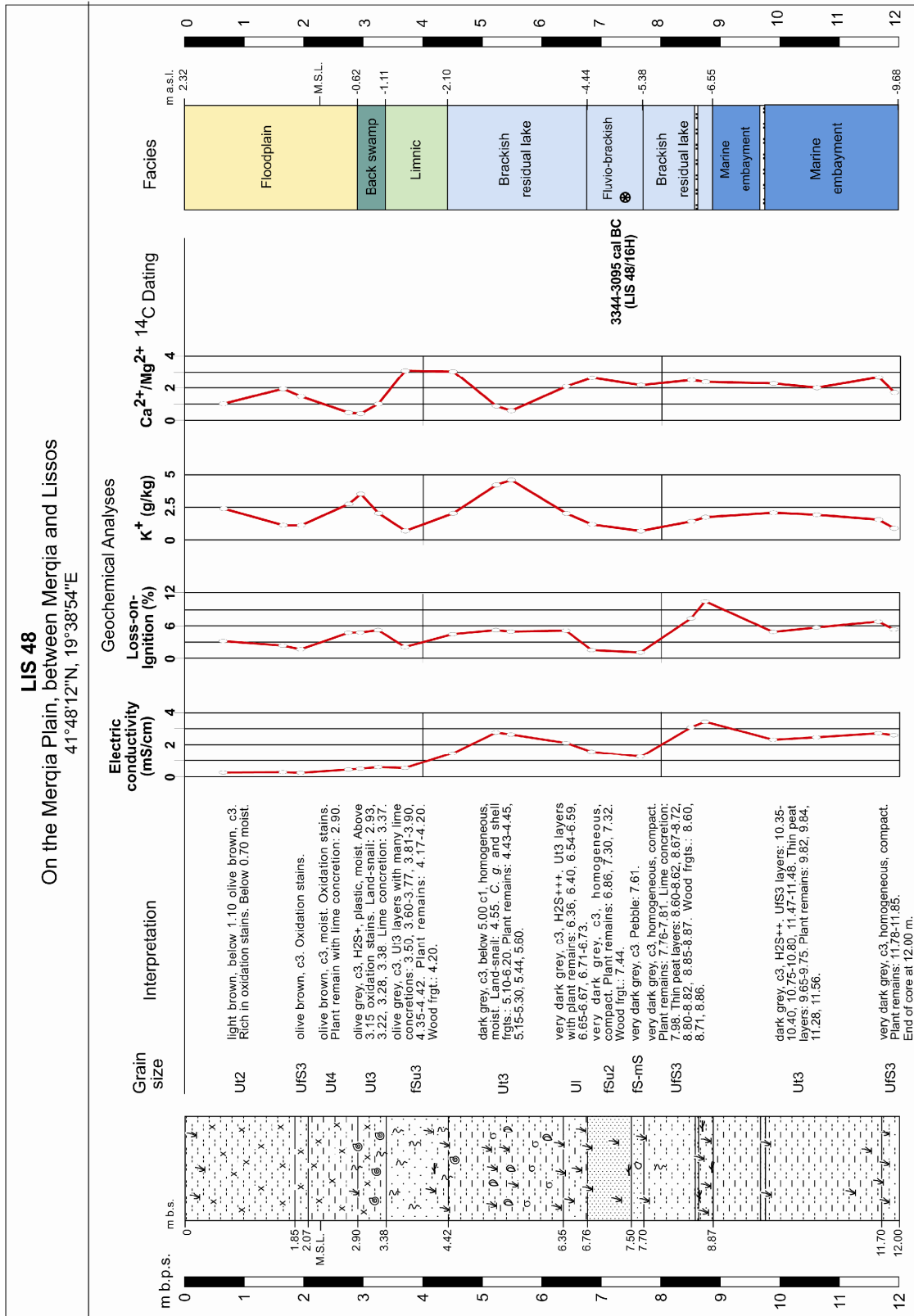


Sample - No.	Depth b.s. (cm)	pH (KCl) - value	Electric conductivity (mS/cm)	Loss-on-Ignition (%)	Carbonate content (%)	Orthophosphate (g/kg)	c(K ⁺) (g/kg)	c(Na ⁺) (g/kg)	c(Ca ²⁺) (g/kg)	c(Mg ²⁺) (g/kg)	c(Fe ^{2+/3+}) (g/kg)	c(Ca ²⁺)/c(Mg ²⁺)	c(Fe ^{2+/3+})/c(Na ⁺)
LIS 46/1	45	7.68	4.67	5.63	7.60	1.75	3.50	4.45	20.35	20.95	37.05	0.97	8.33
LIS 46/2	72	8.02	2.76	3.83	12.55	1.79	3.90	4.90	28.15	21.30	39.30	1.32	8.02
LIS 46/3	85	8.17	2.26	3.49	9.62	1.44	1.15	2.80	23.20	21.40	29.25	1.08	10.45
LIS 46/4	126	8.15	3.44	4.45	12.94	1.61	1.75	5.10	40.90	21.70	39.65	1.88	7.77
LIS 46/5	175	8.16	3.55	2.18	8.40	1.20	0.50	3.75	27.20	22.60	28.15	1.20	7.51
LIS 46/6	255	8.26	3.58	1.29	8.99	1.35	1.25	3.90	24.60	22.80	28.50	1.08	7.31
LIS 46/8	285	8.23	3.52	2.73	9.57	1.18	0.75	3.85	26.75	21.95	27.40	1.22	7.12
LIS 46/9	365	8.22	4.07	2.83	8.99	1.34	0.95	4.45	23.85	21.90	28.00	1.09	6.29
LIS 46/11	410	7.88	6.70	6.36	6.93	2.60	2.35	9.80	14.45	21.70	45.55	0.67	4.65
LIS 46/12	455	8.46	3.22	1.19	13.79	1.04	0.60	3.10	40.40	16.70	21.00	2.42	6.77
LIS 46/13	555	8.50	3.48	2.34	12.33	0.97	0.80	4.25	36.90	17.75	21.55	2.08	5.07
LIS 46/14	568	8.12	3.33	2.31	14.13	1.09	0.75	3.75	42.60	18.55	21.35	2.30	5.69
LIS 46/15	645	8.56	3.24	1.38	14.98	0.87	0.55	3.30	43.85	18.80	20.45	2.33	6.20
LIS 46/16	660	8.70	2.17	0.74	17.74	0.82	0.40	2.25	49.10	21.95	19.45	2.24	8.64
LIS 46/17	675	8.29	2.62	3.04	9.59	1.26	0.85	3.10	35.85	18.45	26.45	1.94	8.53
LIS 46/18	822	8.63	2.39	2.28	16.62	0.97	0.40	2.15	48.45	19.15	21.45	2.53	9.98
LIS 46/19	925	8.60	3.18	2.63	20.68	0.85	0.45	4.05	63.65	21.40	19.00	2.97	4.69
LIS 46/20	971	8.22	5.94	7.14	13.36	1.83	3.50	10.60	31.30	16.15	32.40	1.94	3.06

Appendix 5.35: Geochemical results of LIS 47.

Sample - No.	Depth b.s. (cm)	pH (KCl) - value	Electric conductivity (mS/cm)	Loss-on-Ignation (%)	Carbonate content (%)	Orthophosphate (g/kg)	c(K ⁺) (g/kg)	c(Na ⁺) (g/kg)	c(Ca ²⁺) (g/kg)	c(Mg ²⁺) (g/kg)	c(Fe ^{2+/3+}) (g/kg)	c(Ca ²⁺)/c(Mg ²⁺)	c(Fe ^{2+/3+})/c(Na ⁺)
LIS 47/1	55	7.42	0.13	4.11	3.42	1.21	3.34	1.97	5.59	17.52	36.57	0.32	18.56
LIS 47/2	165	7.94	0.10	1.42	9.78	1.06	0.80	0.97	31.89	19.23	27.20	1.66	28.04
LIS 47/3	185	7.83	0.11	1.79	8.24	1.33	1.19	0.89	25.31	17.73	28.35	1.43	31.85
LIS 47/4	265	7.85	0.11	2.13	10.36	1.75	1.49	0.80	31.04	16.94	27.97	1.83	34.96
LIS 47/5	320	7.73	0.14	2.18	8.87	1.83	1.66	0.70	23.72	17.83	30.19	1.33	43.13
LIS 47/6	345	7.72	0.39	2.39	8.48	1.96	2.47	1.84	24.87	19.85	32.55	1.25	17.69
LIS 47/7	375	6.69	0.22	4.88	0.45	1.78	4.05	1.00	0.00	14.75	34.15	0.00	34.15
LIS 47/8	465	7.39	0.23	4.11	0.89	1.62	2.89	0.78	0.00	15.58	34.15	0.00	43.78
LIS 47/9	520	7.85	0.20	2.46	3.03	0.99	1.22	1.16	7.59	24.42	30.76	0.31	26.52
LIS 47/10	550	7.24	0.17	2.96	0.30	0.89	1.96	1.00	0.72	23.25	28.49	0.03	28.49
LIS 47/11	580	6.57	1.61	3.43	0.28	0.65	1.98	1.12	1.32	25.45	31.89	0.05	28.47
LIS 47/12	660	7.33	1.78	4.84	2.89	0.83	3.17	1.60	5.38	22.78	27.17	0.24	16.98
LIS 47/13	690	7.44	1.90	5.09	4.72	0.88	2.50	1.17	12.33	22.82	25.11	0.54	21.46
LIS 47/14	720	7.48	1.55	4.85	5.00	0.93	2.18	1.10	13.10	22.05	24.13	0.59	21.94
LIS 47/15	756.5	7.41	1.81	4.98	5.60	0.99	3.18	1.23	12.21	21.29	25.01	0.57	20.33
LIS 47/16	837.5	7.38	1.66	4.51	1.64	1.12	4.18	1.08	1.19	19.56	28.36	0.06	26.26
LIS 47/17	860	7.26	1.85	6.47	1.20	1.11	5.45	1.38	0.00	19.94	28.19	0.00	20.43
LIS 47/18	915	7.6	1.71	3.83	5.75	0.98	2.88	1.15	16.30	24.14	26.52	0.68	23.06
LIS 47/19	967.5	7.51	1.60	5.21	2.48	1.27	4.81	1.47	2.16	17.62	28.38	0.12	19.31
LIS 47/20	1050	7.55	1.67	3.86	6.90	1.31	4.11	1.01	15.59	20.28	28.41	0.77	28.13
LIS 47/21	1075	7.93	1.18	2.73	14.78	1.19	1.18	0.78	51.05	20.68	20.97	2.47	26.88
LIS 47/22	1145	8.07	1.03	2.13	16.21	1.24	1.21	0.87	54.60	21.44	21.43	2.55	24.63
LIS 47/23	1168	7.84	1.57	5.21	12.52	1.28	1.11	1.47	44.68	20.88	20.70	2.14	14.08
LIS 47/24	1185	8.01	1.57	3.49	11.92	1.77	1.83	1.73	37.19	20.60	26.03	1.81	15.05

Appendix 5.36.1: Geological profile and selected geochemical results of LIS 48.



Appendix 5.36.2: Photo and geochemical results of LIS 48.



Sample - No.	Depth b.s. (cm)	pH (KCl) - value	Electric conductivity (mS/cm)	Loss-on-Ignition (%)	Carbonate content (%)	Orthophosphate (g/kg)	c(K ⁺) (g/kg)	c(Na ⁺) (g/kg)	c(Ca ²⁺) (g/kg)	c(Mg ²⁺) (g/kg)	c(Fe ^{2+/3+}) (g/kg)	c(Ca ²⁺)/c(Mg ²⁺)	c(Fe ^{2+/3+})/c(Na ⁺)
LIS 48/1	65	8.02	0.26	3.20	9.73	1.36	2.40	1.12	17.94	17.59	32.25	1.02	28.79
LIS 48/2	165	8.2	0.28	2.35	12.95	1.39	1.13	1.02	34.94	17.99	31.86	1.94	31.39
LIS 48/3	195	8.24	0.23	1.65	11.26	1.31	1.12	1.39	27.63	18.78	30.35	1.47	21.83
LIS 48/4	275	8.07	0.44	4.73	7.15	1.47	2.77	1.97	8.62	18.29	39.31	0.47	20.00
LIS 48/5	295	8.13	0.49	4.77	6.02	1.79	3.53	2.26	7.46	18.16	40.98	0.41	18.17
LIS 48/6	325	8.26	0.59	5.24	8.81	1.69	2.05	1.81	17.82	17.56	35.94	1.01	19.91
LIS 48/7	370	8.34	0.54	2.09	22.65	0.99	0.69	1.58	63.80	20.65	24.82	3.09	15.71
LIS 48/10	450	7.96	1.46	4.47	18.58	1.26	2.05	16.80	54.35	17.87	27.05	3.04	1.61
LIS 48/11	522	7.49	2.75	5.23	6.85	0.67	4.23	3.00	15.68	17.91	27.81	0.88	9.27
LIS 48/12	547	7.63	2.63	4.95	5.65	0.76	4.61	3.08	10.53	17.97	29.40	0.59	9.54
LIS 48/13	640	7.82	2.11	5.14	14.13	1.22	2.04	2.21	42.32	20.22	23.49	2.09	10.63
LIS 48/15	683	7.87	1.57	1.52	16.98	0.85	1.19	1.44	56.50	21.46	25.55	2.63	17.80
LIS 48/17	765	8.32	1.24	1.08	14.80	0.51	0.69	2.41	48.79	22.51	18.04	2.17	7.50
LIS 48/19	850	7.86	3.07	7.40	13.69	1.31	1.43	3.49	48.59	19.50	22.58	2.49	6.48
LIS 48/20	873	7.86	3.42	10.58	15.27	1.13	1.75	3.70	44.43	18.69	20.77	2.38	5.62
LIS 48/22	987	8.15	2.31	4.88	14.62	1.55	2.09	3.06	45.88	20.23	27.71	2.27	9.06
LIS 48/23	1060	8.24	2.46	5.71	20.15	1.58	1.94	3.79	47.51	23.73	33.96	2.00	8.96
LIS 48/25	1164	8.14	2.71	6.81	21.98	1.44	1.56	3.70	59.30	22.27	27.65	2.66	7.47
LIS 48/26	1190	8.12	2.59	5.35	13.19	1.01	0.89	3.10	39.27	22.90	27.98	1.72	9.03

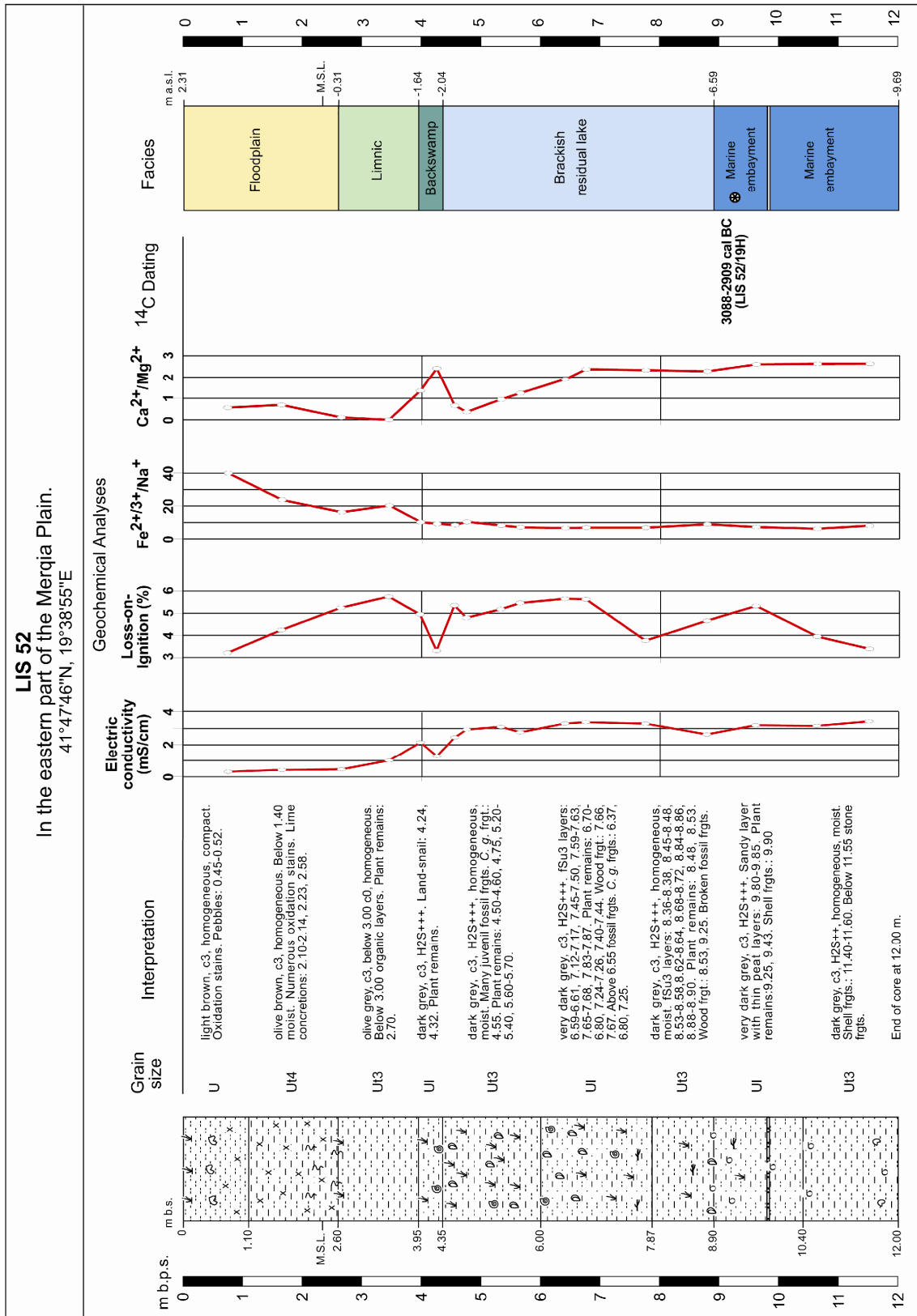
Appendix 5.37: Geochemical results of LIS 50.

Sample - No.	Depth b.s. (cm)	pH (KCl) - value	Electric conductivity (mS/cm)	Loss-on-Ignition (%)	Carbonate content (%)	Orthophosphate (g/kg)	c(K ⁺) (g/kg)	c(Na ⁺) (g/kg)	c(Ca ²⁺) (g/kg)	c(Mg ²⁺) (g/kg)	c(Fe ^{2+/3+}) (g/kg)	c(Ca ²⁺)/c(Mg ²⁺)	c(Fe ^{2+/3+})/c(Na ⁺)
LIS 50/1	75	8.22	4.30	1.57	7.99	1.10	1.95	7.45	23.55	23.45	26.50	1.00	3.56
LIS 50/4	220	6.63	15.52	40.05	0.15	1.57	1.45	18.60	8.40	14.70	13.45	0.57	0.72
LIS 50/5	265	8.06	2.82	2.28	17.43	0.94	0.80	4.60	60.70	24.10	19.40	2.52	4.22
LIS 50/6	355	8.33	3.86	1.71	14.40	0.99	0.75	3.25	47.20	20.80	19.10	2.27	5.88
LIS 50/7	460	8.12	3.87	1.16	15.63	1.05	0.60	2.85	47.85	21.45	21.55	2.23	7.56
LIS 50/9	560	8.10	4.18	4.41	11.60	1.10	0.90	4.15	30.15	22.15	24.80	1.36	5.98
LIS 50/10	580	8.31	3.33	2.51	12.76	1.16	0.70	2.80	37.60	22.20	25.00	1.69	8.93
LIS 50/12	655	8.33	2.73	1.35	14.10	1.11	0.70	2.75	48.40	23.00	20.10	2.10	7.31
LIS 50/13	670	8.37	3.06	0.88	14.71	1.14	0.65	2.55	34.80	19.85	18.65	1.75	7.31
LIS 50/14	765	8.36	2.34	2.22	14.99	1.29	0.65	2.95	48.10	23.60	21.15	2.04	7.17
LIS 50/15	870	8.41	2.33	2.26	16.67	1.10	0.25	2.50	52.25	23.55	21.35	2.22	8.54
LIS 50/16	890	8.16	2.92	2.64	10.42	1.26	1.05	4.25	32.10	22.90	25.50	1.40	6.00

Appendix 5.38: Geochemical results of LIS 51.

Sample - No.	Depth b.s. (cm)	pH (KCl) - value	Electric conductivity (mS/cm)	Loss-on-Ignition (%)	Carbonate content (%)	Orthophosphate (g/kg)	c(K ⁺) (g/kg)	c(Na ⁺) (g/kg)	c(Ca ²⁺) (g/kg)	c(Mg ²⁺) (g/kg)	c(Fe ^{2+/3+}) (g/kg)	c(Ca ²⁺)/c(Mg ²⁺)	c(Fe ^{2+/3+})/c(Na ⁺)
LIS 51/1	45	7.01	0.13	5.13	0.00	0.66	1.90	0.65	0.75	11.40	38.95	0.07	59.92
LIS 51/2	65	7.29	0.13	3.35	0.15	0.77	2.50	0.50	1.00	9.40	32.10	0.11	64.20
LIS 51/3	85	7.35	0.11	2.90	0.68	0.57	2.00	0.55	2.10	8.15	27.65	0.26	50.27
LIS 51/4	165	7.36	0.13	4.34	1.00	0.53	2.20	0.60	1.65	10.50	36.35	0.16	60.58
LIS 51/5	190	7.05	0.08	3.28	0.00	0.62	2.05	1.20	0.35	9.20	31.40	0.04	26.17
LIS 51/6	220	6.46	0.06	5.58	0.15	1.17	3.40	0.85	0.60	11.25	43.15	0.05	50.76
LIS 51/7	265	6.08	0.07	5.29	0.00	0.91	3.80	1.15	0.70	11.70	40.10	0.06	34.87
LIS 51/8	295	6.46	0.06	2.33	0.00	0.43	2.40	1.05	1.80	15.70	34.85	0.11	33.19
LIS 51/9	365	8.01	0.16	1.05	5.26	0.30	0.70	1.00	21.45	21.25	24.35	1.01	24.35
LIS 51/10	420	8.27	0.13	0.81	4.60	0.16	0.50	0.90	19.80	20.20	21.35	0.98	23.72
LIS 51/11	532	8.55	0.09	0.84	3.38	0.23	0.70	1.40	14.50	20.10	20.45	0.72	14.61
LIS 51/12	559	8.08	0.09	1.43	3.83	0.32	0.90	0.85	15.70	22.25	25.30	0.71	29.76
LIS 51/13	590	8.39	0.08	0.84	4.09	0.23	0.40	0.90	13.45	20.65	22.00	0.65	24.44
LIS 51/14	663	8.05	0.09	1.12	5.32	0.34	2.00	0.80	16.30	22.30	26.30	0.73	32.88
LIS 51/15	755	8.64	0.08	0.67	5.41	0.29	0.55	0.95	17.85	21.05	19.55	0.85	20.58
LIS 51/16	782	8.16	0.20	1.29	5.66	0.28	0.80	0.80	18.70	23.65	25.90	0.79	32.38
LIS 51/18	870	8.20	0.17	2.10	4.81	0.40	1.15	0.75	13.75	22.15	30.00	0.62	40.00
LIS 51/20	880	8.30	0.18	1.77	4.66	0.37	0.95	1.30	16.70	21.95	26.55	0.76	20.42

Appendix 5.39.1: Geological profile and selected geochemical results of LIS 52.

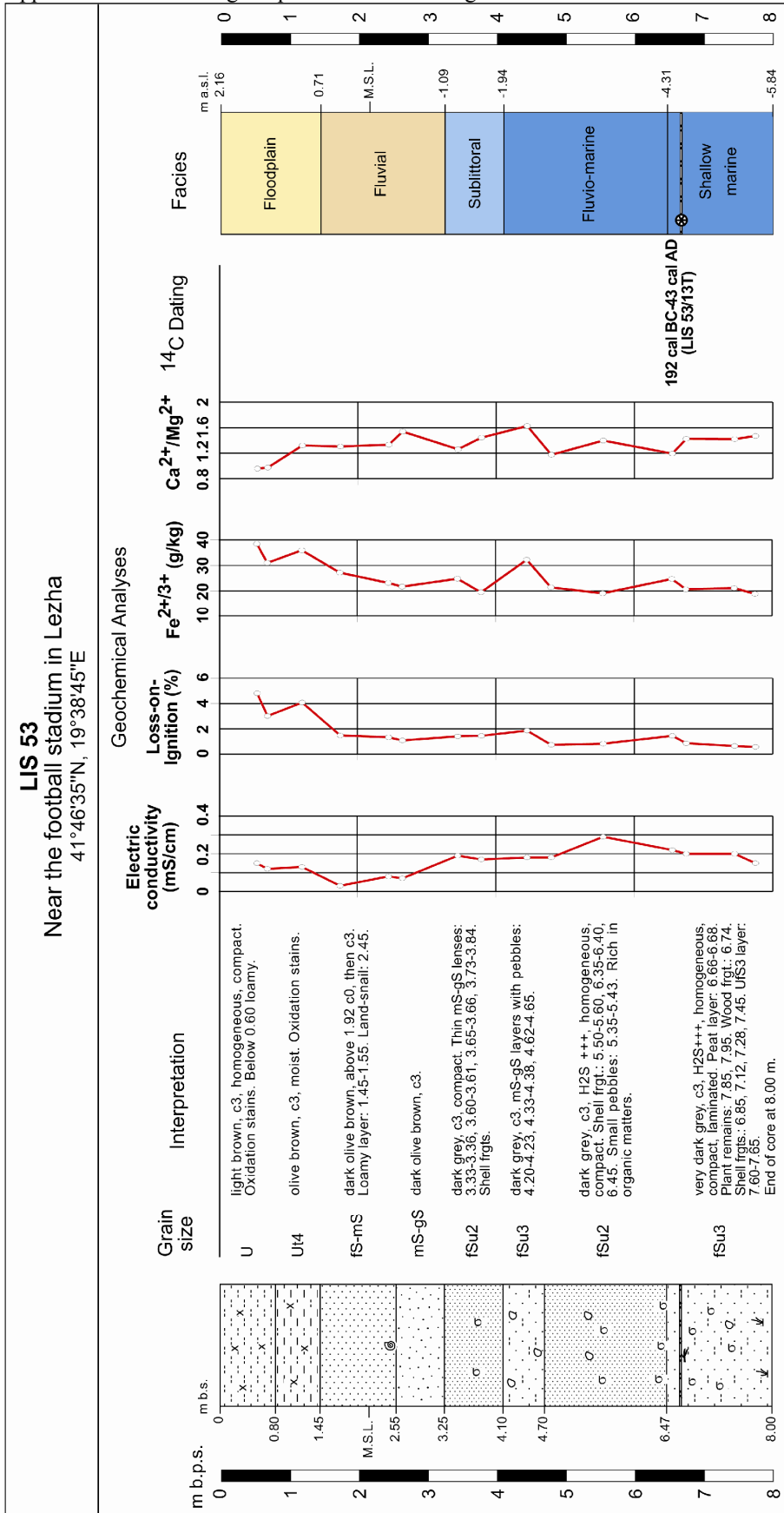


Appendix 5.39.2: Photo and geochemical results of LIS 52.

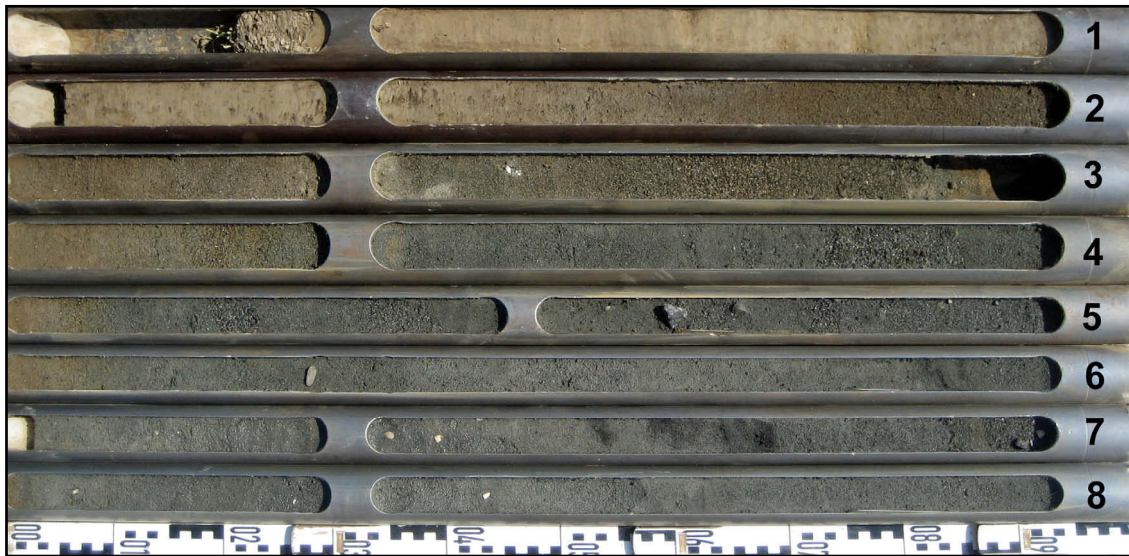


Sample - No.	Depth b.s. (cm)	pH (KCl) - value	Electric conductivity (mS/cm)	Loss-on-Ignition (%)	Carbonate content (%)	Orthophosphate (g/kg)	c(K ⁺) (g/kg)	c(Na ⁺) (g/kg)	c(Ca ²⁺) (g/kg)	c(Mg ²⁺) (g/kg)	c(Fe ^{2+/3+}) (g/kg)	c(Ca ²⁺)/c(Mg ²⁺)	c(Fe ^{2+/3+})/c(Na ⁺)
LIS 52/1	75	7.56	0.31	3.21	5.30	0.73	2.18	0.95	9.81	17.34	37.97	0.57	39.97
LIS 52/2	165	7.78	0.42	4.25	6.52	1.04	2.85	1.40	11.38	16.34	33.15	0.70	23.68
LIS 52/3	265	7.56	0.46	5.25	2.08	1.16	4.00	2.33	1.75	16.44	37.84	0.11	16.24
LIS 52/4	345	7.4	1.01	5.75	0.00	1.45	6.38	2.25	0.00	18.16	45.74	0.00	20.33
LIS 52/5	397	7.45	2.14	4.95	8.94	1.47	1.50	2.37	22.45	16.54	24.26	1.36	10.24
LIS 52/6	425	8.05	1.29	3.31	14.88	0.83	2.77	2.27	49.83	20.63	20.93	2.42	9.22
LIS 52/7	455	7.4	2.45	5.35	5.87	1.02	4.31	2.85	11.29	16.94	24.25	0.67	8.51
LIS 52/8	475	7.38	2.94	4.79	2.63	0.76	4.00	2.67	1.38	16.70	27.76	0.36	10.40
LIS 52/9	532	7.54	3.11	5.18	4.51	0.82	3.50	2.99	6.09	17.40	24.75	0.95	8.28
LIS 52/10	565	7.75	2.77	5.46	8.36	0.92	2.90	3.29	16.57	16.48	23.31	1.24	7.09
LIS 52/12	640	7.7	3.32	5.65	7.57	0.91	2.90	3.48	20.47	21.68	23.15	1.90	6.65
LIS 52/13	675	7.71	3.40	5.63	13.52	1.19	2.06	3.15	41.22	19.34	21.83	2.37	6.93
LIS 52/15	775	7.96	3.31	3.76	14.99	1.25	2.02	3.20	45.89	21.20	22.07	2.33	6.90
LIS 52/18	878	8.12	2.64	4.66	15.07	1.58	1.54	2.74	49.44	21.07	24.53	2.28	8.95
LIS 52/20	960	7.9	3.21	5.33	14.94	1.32	1.83	3.09	48.00	20.38	22.51	2.61	7.28
LIS 52/23	1063	7.91	3.17	3.95	15.60	1.62	2.02	4.20	53.10	20.03	25.98	2.63	6.19
LIS 52/24	1150	7.9	3.45	3.39	16.77	1.50	2.65	3.65	52.65	19.96	29.56	2.64	8.10

Appendix 5.40.1: Geological profile and selected geochemical results of LIS 53.

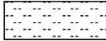
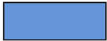

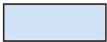


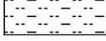

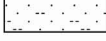

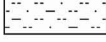


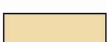

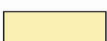




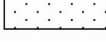


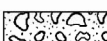
















Appendix 5.40.2: Photo and geochemical results of LIS 53.



Sample - No.	Depth b.s. (cm)	pH (KCl) - value	Electric conductivity (mS/cm)	Loss-on-Ignition (%)	Carbonate content (%)	Orthophosphate (g/kg)	c(K ⁺) (g/kg)	c(Na ⁺) (g/kg)	c(Ca ²⁺) (g/kg)	c(Mg ²⁺) (g/kg)	c(Fe ^{2+/3+}) (g/kg)	c(Ca ²⁺)/c(Mg ²⁺)	c(Fe ^{2+/3+})/c(Na ⁺)
LIS 53/1	55	7.53	0.15	4.81	5.35	2.16	2.60	1.10	12.25	16.65	38.45	0.96	40.85
LIS 53/2	70	7.64	0.12	3.01	9.34	1.78	1.10	0.45	22.65	15.95	31.00	0.97	32.78
LIS 53/3	120	7.54	0.13	4.08	7.23	1.81	2.25	0.60	16.90	14.60	35.95	1.32	39.32
LIS 53/4	175	7.15	0.03	1.48	0.00	0.75	0.70	1.00	3.20	20.90	27.20	1.30	38.98
LIS 53/5	245	8.02	0.08	1.33	5.30	0.45	0.55	0.90	21.05	20.00	23.15	1.33	13.67
LIS 53/6	265	8.16	0.07	1.08	4.40	0.49	0.45	1.20	18.10	22.10	21.70	1.54	16.46
LIS 53/7	345	8.00	0.19	1.41	5.04	0.50	0.85	1.10	17.30	22.85	24.85	1.26	39.29
LIS 53/8	379	8.11	0.17	1.44	3.63	0.49	0.60	1.20	14.80	21.70	19.50	1.45	20.38
LIS 53/9	445	7.76	0.18	1.86	4.14	0.51	1.20	1.15	13.65	23.90	32.25	1.63	26.90
LIS 53/10	480	8.28	0.18	0.73	7.32	0.50	0.50	0.90	25.65	22.20	21.45	1.17	25.26
LIS 53/11	555	7.94	0.29	0.82	6.42	0.41	0.55	0.95	23.30	21.05	19.10	1.40	23.40
LIS 53/12	655	7.79	0.22	1.44	5.82	0.37	1.00	1.15	20.40	23.20	24.75	1.19	12.06
LIS 53/15	675	8.19	0.20	0.86	9.80	0.44	0.50	1.00	29.40	22.60	20.70	1.42	19.72
LIS 53/16	745	8.20	0.20	0.64	8.29	0.56	0.50	0.95	26.85	22.80	21.15	1.42	26.03
LIS 53/17	775	8.16	0.15	0.57	5.42	0.48	0.55	0.95	21.85	22.05	18.90	1.47	18.60

Appendix 6: Key to the corings profiles

Granulometry		Facies	
	Silt		Shallow marine
	Loamy silt		Brackish
	Sandy silt		Sublittoral
	Clayey silt		Littoral
	Silty fine sand		Limnic
	Silty loam		Swamp
	Loamy sand		Fluvial
	Loamy fine sand		Floodplain
	Fine sand		Terrestrial (Pre-Holocene)
	Medium sand		Former river channel (Pre-Holocene)
	Coarse sand		Archaeological layer
	Peat		Layer of set limestone (Anthropogenic)
	Angular stone		
	Pebble		
	Lime concretions		
	Oxidation stains		
	Marine shell		
	Cerastoderma glaucum		
	Terrestrial fossil		
	Ceramic		
	Piece of bone		
	Piece of wood		
	Plant remains		
	Charcoal		
	Seed		
	Dated material		

Appendix 7: List of abbreviations

BC Before Christ
 AD Anno Domini
 BP Before Present
 cal calibrated (^{14}C) age
 kyr thousand years

M.S.L. Mean Sea Level
 a.s.l. above sea level
 b.s.l. below sea level
 a.p.s.l. above present sea level
 b.p.s.l. below present sea level
 b.s. below surface
 m metre

opp. opposite
 approx. approximately
 cf. (lat.: *confer*) compare
 e.g. (lat.: *exempli gratia*) for example
 et al. (lat.: *et aliae*) and others
 i.e. (lat.: *id est*) that is
 ca. circa
 f. form
 sp. species (singular)
 spp. species (plural)
 fig. figure
 ed. editor
 eds. editors
 Hrsg. (in German: Herausgeber) editor

ASI Advanced Science Institutes
 CIESM Commission Internationale pour l'Exploration Scientifique de la mer Méditerranée
 FAO Food and Agriculture Organization of the United Nations
 IAG International Association of Geomorphologists
 MAP Mediterranean Action Plan
 UNEP United Nations Environment Programme

AMS Accelerator Mass Spectrometry
 OSL Optically Stimulated Luminescence

Grain size

T, t	clay
U, u	silt
L, l	loam
S	sand
fS	fine sand
mS	medium sand
gS	coarse sand

Additional component

2	slight
3	medium
4	strong

e.g., fSu2 means: slightly silty fine sand

¹⁴C-AMS dated material

T	peat
H	wood
Pf.	plant remains
F	fossil
S	seed